

University of Windsor

Scholarship at UWindor

Electronic Theses and Dissertations

Theses, Dissertations, and Major Papers

2017

Load Distribution Factors for Skewed Composite Steel I-Girder Bridges

MUHAMMAD KASHIF RAZZAQ

University of Windsor

Follow this and additional works at: <https://scholar.uwindsor.ca/etd>

Recommended Citation

RAZZAQ, MUHAMMAD KASHIF, "Load Distribution Factors for Skewed Composite Steel I-Girder Bridges" (2017). *Electronic Theses and Dissertations*. 7392.

<https://scholar.uwindsor.ca/etd/7392>

This online database contains the full-text of PhD dissertations and Masters' theses of University of Windsor students from 1954 forward. These documents are made available for personal study and research purposes only, in accordance with the Canadian Copyright Act and the Creative Commons license—CC BY-NC-ND (Attribution, Non-Commercial, No Derivative Works). Under this license, works must always be attributed to the copyright holder (original author), cannot be used for any commercial purposes, and may not be altered. Any other use would require the permission of the copyright holder. Students may inquire about withdrawing their dissertation and/or thesis from this database. For additional inquiries, please contact the repository administrator via email (scholarship@uwindsor.ca) or by telephone at 519-253-3000ext. 3208.

Load Distribution Factors for Skewed Composite Steel I-Girder Bridges

By

Muhammad Kashif Razzaq

A Dissertation

Submitted to the Faculty of Graduate Studies
through the Department of **Civil and Environmental Engineering**
in Partial Fulfillment of the Requirements for
the Degree of **Doctor of Philosophy**
at the University of Windsor

Windsor, Ontario, Canada

2017

© 2017 Muhammad Kashif Razzaq

Load Distribution Factors for Skewed Composite Steel I-Girder Bridges

by

Muhammad Kashif Razzaq

APPROVED BY:

K. Galal, External Examiner
Department of Building, Civil and Environmental Engineering
Concordia University

N. Zamani
Department of Mechanical, Automotive & Materials Engineering

S. Cheng
Department of Civil and Environmental Engineering

A. El Ragaby
Department of Civil and Environmental Engineering

F. Ghrib, Advisor
Department of Civil and Environmental Engineering

K. Sennah, Co-Advisor
Department of Civil Engineering
Ryerson University

December 8, 2017

DECLARATION OF ORIGINALITY

I hereby certify that I am the sole author of this thesis and that no part of this thesis has been published or submitted for publication.

I certify that, to the best of my knowledge, my thesis does not infringe upon anyone's copyright nor violate any proprietary rights and that any ideas, techniques, quotations, or any other material from the work of other people included in my thesis, published or otherwise, are fully acknowledged in accordance with the standard referencing practices. Furthermore, to the extent that I have included copyrighted material that surpasses the bounds of fair dealing within the meaning of the Canada Copyright Act, I certify that I have obtained a written permission from the copyright owner(s) to include such material(s) in my thesis and have included copies of such copyright clearances to my appendix.

I declare that this is a true copy of my thesis, including any final revisions, as approved by my thesis committee and the Graduate Studies office, and that this thesis has not been submitted for a higher degree to any other University or Institution.

ABSTRACT

The concept of load distribution factors have been used in bridge design for many decades as a simplified method to estimate load effects on bridge members. It enables bridge engineers to consider the transverse and longitudinal effects of truck wheel loads as two separate phenomena and thus simplifying the analysis and design of new bridges as well as for the evaluation of the load carrying capacity of existing bridges. Existing bridge design codes do not provide sufficient guidance to bridge engineers regarding the accurate assessment of load distribution factors for skew composite bridges. Thus leads to an extremely conservative design in some cases and to unsafe design in others, since these factors do not represent the actual behavior of the bridge structure.

The presence of skew angle makes the analysis and design of composite slab-on-girder bridges much more complex in comparison to straight bridges. Over the past decade, several authors have drawn attention toward the steel I-girder twisting placed over highly skewed supports. These rotations are larger at the obtuse corners and difficult to predict due to the uneven load distribution across the bridge superstructure. In addition to girder twisting, skewed bridges can also lead to increased lateral flange bending stresses as well as increased shear and end reactions at girder obtuse corners that subsequently results in the reduction of girder shear and end reactions, and even possibly undesirable uplift in girders at the acute corners of the bridge.

Recently mandated North American bridge code specifications include provisions considering angle of skew for slab-on-girder bridges applicable within certain ranges of the design parameters. These ranges are often found too narrow and thus frequently exceeded in routine design check. When one of the design parameter exceeds its corresponding limit, refined analysis is suggested. Unfortunately many bridge design engineers are not fully aware or adequately skillful with these refined analysis techniques. In addition, the analysis equations in current design code specifications are developed using the regression of grillage analysis results that is not always recommended for skewed bridges. Further, these design guidelines are developed by ignoring the contribution of diaphragms in a skewed bridge structure, which may not be realistic and leads to inaccurate prediction of load distribution for a skewed bridge structure.

In order to address the shortcomings in the current code specifications, this research was initiated to address these concerns by better understanding the skew bridge behavior and developing design guidelines for rational and accurate assessment of load distribution factors for composite skewed slab-on steel I-girder bridges. For this purpose, a parametric study was conducted using three-dimensional finite element modeling of a composite bridge structure under dead and CHBDC live loads for ultimate, serviceability and fatigue limit states by considering different design parameters including: skew angles, girder stiffness and cross-frame layout, span length, girder spacing, number of girders, and number of design lanes. Based on the results obtained from a parametric study, a set of empirical expressions were developed for the girder moment and shear distribution factors for rational prediction of the girder load distribution. Further, the load distribution factors for girder moment and shear obtained by FEA for both straight and skewed bridge was correlated with the proposed empirical equations and the CHBDC design guidelines. The results showed that the proposed equations for girder moment and shear distribution factors were in good agreement with the FEA results for both straight and skewed bridge configuration. However for straight bridge, the CHBDC equations proved to be ineffective to capture the behavior of most of the straight slab-on-girder bridge geometries. For skewed bridges, the CHBDC equations gave conservative response for certain bridge configurations and for others it produced highly under estimated response, yielding to an unsafe design. Finally, the applicability of the proposed equations for moment and shear distribution factors developed for simply supported straight and skewed slab-on-girder bridge geometry under dead and live load conditions to the multi-span continuous bridge structures was also investigated. The results showed that both the proposed equations and the CHBDC simplified equations proved to be unsafe for some cases, and for other situations resulted in conservative estimates. Based on the limited set of data selected for this study, a new set of design equations for a skewed continuous bridge were proposed, adequately conforming the results obtained from finite element analysis. Design guidelines for bridge engineers were proposed to treat a skewed bridge as an equivalent straight bridge. The findings of this design-oriented dissertation would enable bridge engineers to design composite skewed slab-on steel I-girder bridges more reliably and economically.

DEDICATION

Alhumdulillah (Praise to Allah) for this important achievement of my life.

I am very thankful to my wife for her continuous moral support and encouragement not only throughout this thesis work but also throughout our lives. This achievement would not have been possible without her. I am grateful to my parents for their prayers and well wishes. And last but not the least, I would like to thank my two precious and perfect kids Reyan and Manal for being incredibly understanding and patient during my work.

ACKNOWLEDGEMENTS

I would like to express my deepest appreciation and gratitude to my research advisors, Dr. Khaled Sennah and Dr. Faouzi Ghrib for their patient guidance, fruitful discussions, and kind support during the course of this study. I believe such a technical research would not have been possible without their kind supervision. The advice and comments made by Dr. Amr El Ragaby are also valuable assets for me to complete this project. I would like to thank Dr. Khaled Galal from Concordia University for accepting to review my dissertation. Drs. Zamani and Cheng kindly accepted to be on the defence committee. I would like to thank Mr. Mark Gryn, the systems administrator for his help for all the computer related issues. Lastly, I would also like to thank my colleagues, Drs. Javaid Ahmed and Ali Mohammadi for their incredible help and support.

TABLE OF CONTENTS

DECLARATION OF ORIGINALITY	iii
ABSTRACT	iv
DEDICATION	vi
ACKNOWLEDGEMENTS	vii
LIST OF TABLES	xiv
LIST OF FIGURES	xviii
LIST OF ABBREVIATIONS	xxix

Chapter 1 Introduction

1.1 Background	1
1.2 Problem Statement	2
1.3 Research Objectives	4
1.4 Dissertation Organization	5

Chapter 2 Literature Review

2.1 General	6
2.2 Procedures for Evaluating Distribution Factors in North America	8
2.2.1 Canadian Highway Bridge Design Code (CSA 2006a)	8
2.2.1.1 Limitations of CHBDC (CSA 2006a)	11
2.2.2 Canadian Highway Bridge Design Code (CSA 2014a)	12
2.2.2.1 Limitations of CHBDC (CSA 2014a)	13
2.2.3 AASHTO Standard Specifications	14
2.2.3.1 Limitations of AASHTO Standard Specifications	14
2.2.4 AASHTO-LRFD Specifications	16
2.2.4.1 Limitations of AASHTO-LRFD Specifications	18

2.3	Literature Review on Methods for Evaluating Load Distribution Factors	19
2.3.1	Analytical Studies	20
2.3.2	Field Studies	24
2.4	Effects of Bridge Parameters on Live Load Distribution Factors	28
2.4.1	Span Length	28
2.4.2	Girder Spacing	29
2.4.3	Girder Stiffness	29
2.4.4	Deck Thickness	30
2.4.5	Skew Angle	30
2.4.6	Length-to-Width Ratio	31
2.4.7	Cross-frame Layout and Spacing	31
2.4.8	Deck Overhang	32
2.4.9	Secondary Stiffening Elements	32
2.5	Conclusions	33

Chapter 3 Development of Finite Element Models for Straight and Skew Bridges

3.1	General	34
3.2	Finite Element Method	35
3.3	Finite Element Program	37
3.4	Finite Element Bridge Modeling	38
3.4.1	Material Modeling	39
3.4.2	Geometric Modeling	40
3.4.3	Boundary Condition	42
3.4.4	Aspect Ratio	42
3.4.5	Live Load Modeling	43
3.5	Validation of Finite Element Modeling	44
3.5.1	Validation of Skewed Slab-on-Girder Bridge	44
3.5.1.1	Instrumentation	45
3.5.1.2	Load Truck	46
3.5.1.3	Truck Runs	47
3.5.1.4	Comparison of Results	48

3.6	Evaluation of Skewed Bridge Parameters by Sensitivity Study	49
3.6.1	Cross-frame Design	50
3.6.1.1	Cross-frame Layout	50
3.6.1.2	Cross-frame Spacing	59
3.6.2	Sequence of Construction	63
3.6.2.1	Un-shored Construction.....	63
3.6.2.2	Shored Construction	66
3.6.3	Effect of CHBDC Vehicular Load Type	69
3.6.4	Estimation of Longitudinal Flexural Stiffness of Steel I-Girder	79
3.6.5	Assessment of Multi-lane Truck Loading Condition.....	82
3.7	Conclusions.....	91

Chapter 4 Dead Load Distribution in Straight and Skewed Bridges

4.1	General.....	92
4.2	Behavior of Skewed I-girder Bridge at Construction Stage	93
4.3	Non-composite I-girder Bridge at Construction Stage	94
4.4	Composite I-girder Bridge at Construction Stage.....	95
4.4.1	Parametric Study.....	95
4.4.2	Description of Bridge Prototypes.....	96
4.4.3	Finite Element Modeling	98
4.4.4	Loading Condition	99
4.4.5	Evaluation of Distribution Factors.....	99
4.4.5.1	Effect of Skew Angle	100
4.4.5.2	Effect of Span Length.....	107
4.4.5.3	Effect of Girder Spacing, Number of Girders and Number of Lanes.....	113
4.4.6	Empirical Formula for Distribution Factors	120
4.4.7	Correlation of FEA Results and Proposed Equations with CHBDC	123
4.5	Conclusions.....	127

Chapter 5 Live Load Distribution in Straight and Skewed Bridges

5.1	General.....	129
5.2	Composite Steel I-girder Bridge.....	130
5.2.1	Parametric Study.....	131
5.2.2	Evaluation of Load Distribution Factors.....	132
5.2.2.1	Load Distribution Factors for Longitudinal Bending Moment .	135
5.2.2.2	Load Distribution Factors for Shear.....	136
5.2.3	Description of Bridge Prototypes.....	137
5.2.4	Finite Element Modeling.....	138
5.2.5	Loading Condition.....	139
5.2.6	Results from the Parametric Study.....	146
5.2.6.1	Effect of Skew Angle.....	147
5.2.6.2	Effect of Span Length.....	160
5.2.6.3	Effect of Girder Spacing, Number of Girders and Number of Lanes.....	172
5.2.7	Load Distribution Factors for Straight Bridges at ULS and SLS.....	183
5.2.7.1	Correlation of FEA Results and Proposed Equations with CHBDC.....	191
5.2.8	Load Distribution Factors for Straight Bridges at FLS.....	194
5.2.8.1	Correlation of FEA Results and Proposed Equations with CHBDC.....	197
5.2.9	Load Distribution Factors for Skewed Bridges at ULS and SLS.....	200
5.2.9.1	Correlation of FEA Results and Proposed Equations with CHBDC.....	204
5.2.10	Load Distribution Factors for Skewed Bridges at FLS.....	208
5.2.10.1	Correlation of FEA Results and Proposed Equations with CHBDC.....	211
5.3	Correlation of Data with Bridge Code Specifications in North America	214
5.3.1	AASHTO-LRFD (2014) for Straight Slab-on-Girder Bridges.....	214
5.3.2	AASHTO-LRFD (2014) for Skewed Slab-on-Girder Bridges.....	219
5.3.3	CHBDC (CSA 2006b) – Jaeger and Smith (1997).....	224

5.4	Correlation of Data with Previous Research.....	235
5.5	Conclusions.....	240
Chapter 6 Skew Limitations for Composite Slab-on-Girder Bridges		
6.1	General.....	243
6.2	Parametric Study.....	246
6.2.1	Evaluation of Magnification Factors	247
6.2.2	Results from the Parametric Study	248
6.2.2.1	Effect of Skew Angle	249
6.2.2.2	Effect of Span Length.....	255
6.2.2.3	Effect of Bridge Width and Number of Lanes	255
6.2.3	Empirical Expression for Magnification Factors.....	255
6.2.4	Empirical Expression for Skew Limitation.....	256
6.2.5	Correlation of Proposed Equation with CHBDC (CSA 2006a).....	257
6.3	Conclusions.....	259
Chapter 7 Load Distribution in Continuous Skewed Bridges		
7.1	General.....	260
7.2	Parametric Study.....	261
7.2.1	Loading Condition	262
7.2.2	Boundary Condition.....	263
7.2.3	Results from the Parametric Study	264
7.2.4	Correlation of FEA Results and Proposed Equations with CHBDC	274
7.3	Conclusions.....	290
Chapter 8 Summary and Conclusions		
8.1	Dissertation Summary.....	292
8.2	Principal Contributions	293
8.3	Future Directions	298
References.....		299

Appendix A	Illustrative Example for Moment and Shear Distribution Factors for Skewed Slab-on Steel I-girder Bridges at Dead Load	308
Appendix B	Illustrative Example for Moment and Shear Distribution Factors for Straight Slab-on Steel I-girder Bridges at ULS and SLS.....	310
Appendix C	Illustrative Example for Moment and Shear Distribution Factors for Straight Slab-on Steel I-girder Bridges at FLS.....	317
Appendix D	Illustrative Example for Moment and Shear Distribution Factors for Skewed Slab-on Steel I-girder Bridges at ULS and SLS.....	325
Appendix E	Illustrative Example for Moment and Shear Distribution Factors for Skewed Slab-on Steel I-girder Bridges at FLS.....	330
Appendix F	Illustrative Example for Moment and Shear Distribution Factors for Straight Two-span Continuous Slab-on Steel I-girder Bridges at Dead Load.....	335
Appendix G	Illustrative Example for Moment and Shear Distribution Factors for Straight Two-span Continuous Slab-on Steel I-girder Bridges at ULS and SLS	338
Appendix H	Illustrative Example for Moment and Shear Distribution Factors for Straight Two-span Continuous Slab-on Steel I-girder Bridges at FLS	352
Appendix I	Illustrative Example for Moment and Shear Distribution Factors for Skewed Two-span Continuous Slab-on Steel I-girder Bridges at Dead Load.....	367
Appendix J	Illustrative Example for Moment and Shear Distribution Factors for Skewed Two-span Continuous Slab-on Steel I-girder Bridges at ULS and SLS.....	370
Appendix K	Illustrative Example for Moment and Shear Distribution Factors for Skewed Two-span Continuous Slab-on Steel I-girder Bridges at FLS	378
Vita Auctoris.....		386

LIST OF TABLES

Table 3.1	Missouri bridge A-6101 truck run positions.....	48
Table 3.2	Parameters considered for cross-frame layout.....	51
Table 3.3	Parameters considered for cross-frame spacing.....	60
Table 3.4	Parameters considered for un-shored construction.....	64
Table 3.5	Parameters considered for shored construction.....	67
Table 3.6	Parameters considered for effect of CHBDC vehicular load type.....	70
Table 3.7	Parameters considered for assessment of multi-lane truck loading condition.....	83
Table 4.1	Geometry of prototype bridges.....	97
Table 4.2	Moment distribution factors for shored sequence of construction under dead loads.....	121
Table 4.3	Shear distribution factors for shored sequence of construction under dead loads.....	122
Table 4.4	Comparison of moment distribution factors for skewed slab-on steel I-girder bridges at dead load.....	125
Table 4.5	Comparison of shear distribution factors for skewed slab-on steel I-girder bridges at dead load.....	125
Table 5.1	Geometry of prototype bridges for ULS and SLS analysis.....	133
Table 5.2	Geometry of prototype bridges for FLS analysis.....	134
Table 5.3	Exterior girder moment distribution factors for straight bridge at ULS & SLS under live loading.....	189
Table 5.4	Interior girder moment distribution factors for straight bridge at ULS & SLS under live loading.....	189
Table 5.5	Exterior girder shear distribution factors for straight bridge at ULS & SLS under live loading.....	190
Table 5.6	Interior girder shear distribution factors for straight bridge at ULS & SLS under live loading.....	190
Table 5.7	Comparison of moment distribution factors for straight slab-on steel I-girder bridges at ULS and SLS.....	191
Table 5.8	Comparison of shear distribution factors for straight slab-on steel I-girder bridges at ULS and SLS.....	191

Table 5.9	Exterior girder moment distribution factors for straight bridge at FLS underlive loading	195
Table 5.10	Interior girder moment distribution factors for straight bridge at FLS under live loading.....	196
Table 5.11	Exterior girder shear distribution factors for straight bridge at FLS under live loading.....	196
Table 5.12	Interior girder shear distribution factors for straight bridge at FLS under live loading.....	197
Table 5.13	Comparison of moment distribution factors for straight slab-on steel I-girder bridges at FLS	198
Table 5.14	Comparison of shear distribution factors for straight slab-on steel I-girder bridges at FLS	198
Table 5.15	Exterior girder moment distribution factors for skewed bridge at ULS & SLS under live load.....	202
Table 5.16	Interior girder moment distribution factors for skewed bridge at ULS & SLS under live load.....	203
Table 5.17	Shear distribution factors at girder obtuse corner for skewed bridge at ULS and SLS under live load.....	203
Table 5.18	Shear distribution factors at girder acute corner for skewed bridge at ULS and SLS under live load.....	204
Table 5.19	Shear distribution factors at interior girder for skewed bridge at ULS and SLS under live load.....	204
Table 5.20	Comparison of moment distribution factors for skewed slab-on steel I-girder bridges at ULS and SLS.....	205
Table 5.21	Comparison of shear distribution factors for skewed slab-on steel I-girder bridges at ULS and SLS.....	205
Table 5.22	Exterior girder moment distribution factors for skewed bridge at FLS under live load.....	209
Table 5.23	Interior girder moment distribution factors for skewed bridge at FLS under live load.....	209
Table 5.24	Shear distribution factors at girder obtuse corner for skewed bridge at FLS under live load.....	210
Table 5.25	Shear distribution factors at girder acute corner for skewed bridge at FLS under live load.....	210

Table 5.26	Shear distribution factors at interior girder for skewed bridge at FLS under live load.....	210
Table 5.27	Comparison of moment distribution factors for skewed slab-on steel I-girder bridges at FLS	211
Table 5.28	Comparison of shear distribution factors for skewed slab-on steel I-girder bridges at FLS	211
Table 5.29	LRFD load distribution factors for straight slab-on-girder bridges (Customary U.S. Units)	216
Table 5.30	LRFD Correction factors for skewed slab-on-girder bridges (Customary U.S. Units).....	220
Table 5.31	Geometry of prototype bridges considered by Al-Hashimy (2005)	234
Table 6.1	Magnification factor equation for live load at ULS & SLS.....	256
Table 6.2	Proposed skew limitations based on $\pm 5\%$ tolerance in design parameters .	257
Table 6.3	Correlation of proposed equation with CHBDC equation for skew limitation	258
Table 7.1	Geometry of prototype bridges	262
Table 7.2	Span distribution factors under dead loads for straight continuous two-span bridge	269
Table 7.3	Support distribution factors under dead loads for straight continuous two-span bridge	269
Table 7.4	Span distribution factors at ULS and SLS for straight continuous two-span bridge	270
Table 7.5	Support distribution factors at ULS and SLS for straight continuous two-span bridge	270
Table 7.6	Span distribution factors at FLS for straight continuous two-span bridge .	271
Table 7.7	Support distribution factors at FLS for straight continuous two-span bridge	271
Table 7.8	Span distribution factors under dead loads for skewed continuous two-span bridge	272
Table 7.9	Support distribution factors under dead loads for skewed continuous two-span bridge	272
Table 7.10	Span distribution factors at ULS and SLS for skewed continuous two-span bridge	273

Table 7.11	Support distribution factors at ULS and SLS for skewed continuous two-span bridge	273
Table 7.12	Span distribution factors at FLS for skewed continuous two-span bridge	274
Table 7.13	Support distribution factors at FLS for skewed continuous two-span bridge	274

LIST OF FIGURES

Figure 1.1	Load Path on a Skewed Bridge.....	2
Figure 2.1	Distribution factor illustrations.....	6
Figure 2.2	Transverse moment distribution using simplified method of analysis for ULS and SLS	8
Figure 2.3	AASHTO Standard vs. AASHTO-LRFD moment distribution factors (Reproduced from Sotelino et al. 2004)	16
Figure 2.4	AASHTO Standard vs. AASHTO-LRFD shear distribution factors (Reproduced from Cross et al. 2006)	16
Figure 3.1	Four node shell element.....	38
Figure 3.2	Cross-section diagram of a concrete slab over steel I-girder bridge for: (a) two-lane, and (b) four-lane	39
Figure 3.3	Details of the three-dimensional finite element modeling for: (a) bridge structure, and (b) composite girder with cross-frame	41
Figure 3.4	Boundary condition for single-span bridge model for: (a) two-lane, and (b) four-lane.....	42
Figure 3.5	CHBDC truck loading: (a) CL-W truck clearance, (b) CL-W truck load, and (c) CL-W lane load. (Reproduced from CHBDC (CSA, 2014))	43
Figure 3.6	Elevation view of Missouri A-6101 bridge. (Reproduced from Wu 2003)..	44
Figure 3.7	Missouri bridge A-6101 cross-section. (Reproduced from Wu 2003)	45
Figure 3.8	Missouri bridge A-6101 framing plan. (Reproduced from Wu 2003).....	45
Figure 3.9	Missouri bridge A-6101: (a) load truck, and (b) truck dimensions with wheel loads (Reproduced from Wu 2003).....	47
Figure 3.10	Missouri bridge A-6101 truck run scheme.(Reproduced from Wu 2003)....	48
Figure 3.11	Validation of live load field testing with finite element modeling results....	49
Figure 3.12	Cross-frame layouts for bridges with skewed supports for (a) parallel configuration, (b) perpendicular-continuous configuration, and (c) perpendicular-discontinuous configuration	51
Figure 3.13	Moment magnification factor for interior girders for: (a) one-lane, and (b) four-lane	53
Figure 3.14	Moment magnification factor for exterior girders for: (a) one-lane, and (b) four-lane	54

Figure 3.15	Reaction magnification factor at obtuse corners for: (a) one-lane, and (b) four-lane	56
Figure 3.16	Reaction magnification factor at acute corners for: (a) one-lane, and (b) four-lane	57
Figure 3.17	Differential displacement of cross-frame end members: (a) one-lane, and (b) four-lane	58
Figure 3.18	Moment magnification factor for interior girders for: (a) one-lane, and (b) four-lane	61
Figure 3.19	Reaction magnification factor at obtuse corners for: (a) one-lane, and (b) four-lane	62
Figure 3.20	M_d - Moment magnification factor for exterior and interior girders for: (a) two-lane, and (b) four-lane	65
Figure 3.21	(M_s+M_{sd}) - Moment magnification factor for exterior and interior girders for: (a) two-lane, and (b) four-lane	68
Figure 3.22	Live loading cases for two-lane bridge configuration for: (a) Exterior girder-partial load (b) Exterior girder-full load, and (c) Interior girder-full load	70
Figure 3.23	Live loading cases for four-lane bridge configurations for: (a) Exterior girder one-partial load (b) Exterior girder two-partial load (c) Exterior girder-full load (d) Interior girder two-partial load, and (e) Interior girder-full load	72
Figure 3.24	Exterior girder bending stress for two-lane bridge configuration at skew angle= 0° for: (a) Span =15 m, and (b) Span = 40 m	72
Figure 3.25	Exterior girder bending stress for two-lane bridge configuration at skew angle= 60° for: (a) Span =15 m, and (b) Span = 40 m	73
Figure 3.26	Exterior girder bending stress for four-lane bridge configuration at skew angle= 0° for: (a) Span =15 m, and (b) Span = 40 m	74
Figure 3.27	Exterior girder bending stress for four-lane bridge configuration at skew angle= 60° for: (a) Span =15 m, and (b) Span = 40 m	75
Figure 3.28	Interior girder bending stress for two-lane bridge configuration at skew angle= 0° for: (a) Span =15 m, and (b) Span = 40 m	76
Figure 3.29	Interior girder bending stress for two-lane bridge configuration at skew angle= 60° for: (a) Span =15 m, and (b) Span = 40 m	77
Figure 3.30	Interior girder bending stress for four-lane bridge configuration at skew angle= 0° for: (a) Span =15 m, and (b) Span = 40 m	78
Figure 3.31	Interior girder bending stress for four-lane bridge configuration at skew angle= 60° for: (a) Span =15 m, and (b) Span = 40 m	79

Figure 3.32	Relationship between span and longitudinal flexural rigidity per unit width (Reproduced from Bakht and Moses 1988)	81
Figure 3.33	Relationship between span length and longitudinal flexural rigidity per unit width	82
Figure 3.34	Truck loading conditions on a skew aligned bridge for (a) truck moves side-by-side, (b) truck moves side-by-side with time lag, and (c) one truck in each lane at a time and by superposition of results	85
Figure 3.35	Moment magnification factor for two-lane bridge for: (a) exterior girder, and (b) interior girder	86
Figure 3.36	Shear magnification factor for two-lane bridge for: (a) obtuse corner (b) acute corner, and (c) interior girder	88
Figure 3.37	Moment magnification factor for four-lane bridge for: (a) exterior girder, and (b) interior girder	89
Figure 3.38	Shear magnification factor for four-lane bridge for: (a) obtuse corner (b) acute corner, and (c) interior girder	90
Figure 4.1	Effect of skew angle on F_m of exterior girders for: (a) two-lane, and (b) four-lane	102
Figure 4.2	Effect of skew angle on F_m of interior girders for: (a) two-lane, and (b) four-lane	103
Figure 4.3	Effect of skew angle on F_v at bridge obtuse corners for: (a) two-lane, and (b) four-lane	104
Figure 4.4	Effect of skew angle on F_v at bridge acute corners for: (a) two-lane, and (b) four-lane	105
Figure 4.5	Effect of skew angle on F_v of interior girders for: (a) two-lane, and (b) four-lane	106
Figure 4.6	Effect of span length on F_m of exterior girders for: (a) two-lane, and (b) four-lane	109
Figure 4.7	Effect of span length on F_m of interior girders for: (a) two-lane, and (b) four-lane	110
Figure 4.8	Effect of span length on F_v at bridge obtuse corners for: (a) two-lane, and (b) four-lane	111
Figure 4.9	Effect of span length on F_v at bridge acute corners for: (a) two-lane, and (b) four-lane	112
Figure 4.10	Effect of span length on F_v of interior girders for: (a) two-lane, and (b) four-lane	113

Figure 4.11	Effect of girder spacing on F_m of exterior girders for: (a) two-lane, and (b) four-lane	115
Figure 4.12	Effect of girder spacing on F_m of interior girders for: (a) two-lane, and (b) four-lane	116
Figure 4.13	Effect of girder spacing on F_v at bridge obtuse corners for: (a) two-lane, and (b) four-lane.....	117
Figure 4.14	Effect of girder spacing on F_v at bridge acute corners for: (a) two-lane, and (b) four-lane.....	118
Figure 4.15	Effect of girder spacing on F_v of interior girders for: (a) two-lane, and (b) four-lane	119
Figure 4.16	Correlation between moment distribution factors obtained from FEA results with proposed equations	123
Figure 4.17	Correlation between shear magnification factors obtained from FEA results with CHBDC and proposed equations for; (a) obtuse corner, (b) acute corner, and (c) interior girder.	125
Figure 5.1	Cross-frame arrangements at (a) support level, and (b) between span lengths	138
Figure 5.2	Live loading case for one-lane bridge for ULS and SLS for exterior and interior girder-partial load.....	140
Figure 5.3	Live loading cases for two-lane bridge for ULS and SLS for; (a) exterior girder-partial load, (b) exterior girder-full load, and (c) Interior girder-full load.....	141
Figure 5.4	Live loading cases for three-lane bridge for ULS and SLS for; (a) exterior girder-partial load, (b) exterior girder-partial load, (c) exterior girder-full load, (d) Interior girder-partial load, and (e) Interior girder-full load	142
Figure 5.5	Live loading cases for four-lane bridge for ULS and SLS for; (a) exterior girder-partial load, (b) exterior girder-partial load, (c) exterior girder-partial load, (d) exterior girder-full load, (e) interior girder-partial load, (f) interior girder-partial load, (g) interior girder-partial load, (h) interior girder-full load, (i) interior girder-full load, and (j) interior girder-full load	144
Figure 5.6	Live loading case for one-lane bridge for FLS	144
Figure 5.7	Live loading case for two-lane bridge for FLS	145
Figure 5.8	Live loading case for three-lane bridge for FLS for; (a) exterior girder-fatigue load, and (b) interior girder-fatigue load.....	145
Figure 5.9	Live loading case for four-lane bridge for FLS for; (a) exterior girder-fatigue load, and (b) interior girder-fatigue load.....	146

Figure 5.10	Effect of skew angle on F_{T_m} of an exterior girder at ULS & SLS for: (a) two-lane, and (b) four-lane.....	148
Figure 5.11	Effect of skew angle on F_{T_m} of an interior girder at ULS & SLS for: (a) two-lane, and (b) four-lane.....	149
Figure 5.12	Effect of skew angle on F_{T_m} of an exterior girder at FLS for: (a) two-lane, and (b) four-lane	150
Figure 5.13	Effect of skew angle on F_{T_m} of an interior girder at FLS for: (a) two-lane, and (b) four-lane	151
Figure 5.14	Effect of skew angle on F_{T_v} of the girder at obtuse corner at ULS & SLS for: (a) two-lane, and (b) four-lane	152
Figure 5.15	Effect of skew angle on F_{T_v} of the girder at acute corner at ULS & SLS for: (a) two-lane, and (b) four-lane	153
Figure 5.16	Effect of skew angle on F_{T_v} of the interior girder at ULS & SLS for: (a) two-lane, and (b) four-lane.....	154
Figure 5.17	Effect of skew angle on F_{T_v} of the girder at obtuse corner at FLS for: (a) two-lane, and (b) four-lane.....	155
Figure 5.18	Effect of skew angle on F_{T_v} of the girder at acute corner at FLS for: (a) two-lane, and (b) four-lane.....	156
Figure 5.19	Effect of skew angle on F_{T_v} of the interior girder at FLS for: (a) two-lane, and (b) four-lane	157
Figure 5.20	Effect of span length on F_{T_m} of the exterior girder at ULS & SLS for: (a) two-lane, and (b) four-lane.....	162
Figure 5.21	Effect of span length on F_{T_m} of the interior girder at ULS & SLS for: (a) two-lane, and (b) four-lane.....	163
Figure 5.22	Effect of span length on F_{T_m} of the exterior girder at FLS for: (a) two-lane, and (b) four-lane	164
Figure 5.23	Effect of span length on F_{T_m} of the interior girder at FLS for: (a) two-lane, and (b) four-lane	165
Figure 5.24	Effect of skew angle on F_{T_v} of the girder at obtuse corner at ULS and SLS for: (a) two-lane, and (b) four-lane	166

Figure 5.25	Effect of skew angle on F_{T_v} of the girder at acute corner at ULS and SLS for: (a) two-lane, and (b) four-lane	167
Figure 5.26	Effect of skew angle on F_{T_v} of the interior girder corner at ULS and SLS for: (a) two-lane, and (b) four-lane	168
Figure 5.27	Effect of skew angle on F_{T_v} of the girder at obtuse corner at FLS for: (a) two-lane, and (b) four-lane.....	169
Figure 5.28	Effect of skew angle on F_{T_v} of the girder at acute corner at FLS for: (a) two-lane, and (b) four-lane.....	170
Figure 5.29	Effect of skew angle on F_{T_v} of the interior girder corner at FLS for: (a) two-lane, and (b) four-lane.....	171
Figure 5.30	Effect of girder spacing on F_{T_m} of the exterior girder at ULS and SLS for: (a) two-lane, and (b) four-lane	173
Figure 5.31	Effect of girder spacing on F_{T_m} of the interior girder at ULS and SLS for: (a) two-lane, and (b) four-lane	174
Figure 5.32	Effect of girder spacing on F_{T_v} of the girder at obtuse corner at ULS & SLS for: (a) two-lane, and (b) four-lane	175
Figure 5.33	Effect of girder spacing on F_{T_v} of the girder at acute corner at ULS & SLS for: (a) two-lane, and (b) four-lane	176
Figure 5.34	Effect of girder spacing on F_{T_v} of the interior girder corner at ULS & SLS for: (a) two-lane, and (b) four-lane	177
Figure 5.35	Effect of girder spacing on F_{T_m} of the exterior girder at FLS for: (a) two-lane, and (b) four-lane	178
Figure 5.36	Effect of girder spacing on F_{T_m} of the interior girder at FLS for: (a) two-lane, and (b) four-lane	179
Figure 5.37	Effect of girder spacing on F_{T_v} of the girder at obtuse corner at FLS for: (a) two-lane, and (b) four-lane	180
Figure 5.38	Effect of girder spacing on F_{T_v} of the girder at acute corner at FLS for: (a) two-lane, and (b) four-lane	181
Figure 5.39	Effect of girder spacing on F_{T_v} of the interior girder corner at FLS for: (a) two-lane, and (b) four-lane	182

Figure 5.40	Effect of span length on “R” for an exterior girder moment at ULS and SLS for: (a) two-lane, and (b) four-lane	185
Figure 5.41	Effect of girder spacing on “R” for an exterior girder moment at ULS and SLS for: (a) two-lane, and (b) four-lane	185
Figure 5.42	Effect of span length on “R” for an interior girder moment at ULS and SLS for: (a) two-lane, and (b) four-lane	186
Figure 5.43	Effect of girder spacing on “R” for an interior girder moment at ULS and SLS for: (a) two-lane, and (b) four-lane	186
Figure 5.44	Effect of span length on “R” for an exterior girder shear at ULS and SLS for: (a) two-lane, and (b) four-lane	186
Figure 5.45	Effect of girder spacing on “R” for an exterior girder shear at ULS and SLS for: (a) two-lane, and (b) four-lane	187
Figure 5.46	Effect of span length on “R” for an interior girder shear at ULS and SLS for: (a) two-lane, and (b) four-lane	187
Figure 5.47	Effect of girder spacing on “R” for an interior girder shear at ULS and SLS for: (a) two-lane, and (b) four-lane	187
Figure 5.48	Correlation between moment distribution factors at ULS & SLS obtained from FEA results with proposed equations and CHBDC for straight slab-on-girder bridges for; (a) exterior girder, and (b) interior girder	192
Figure 5.49	Correlation between shear distribution factors at ULS & SLS obtained from FEA results with proposed equations and CHBDC for straight slab-on-girder bridges for; (a) exterior girder, and (b) interior girder	193
Figure 5.50	Correlation between moment distribution factors at FLS obtained from FEA results with proposed equations and CHBDC for straight slab-on-girder bridges for; (a) exterior girder, and (b) interior girder	199
Figure 5.51	Correlation between shear distribution factors at FLS obtained from FEA results with proposed equations and CHBDC for straight slab-on-girder bridges for; (a) exterior girder, and (b) interior girder	200
Figure 5.52	Correlation between moment distribution factors at ULS & SLS obtained from FEA results with proposed equations and CHBDC for skewed slab-on-girder bridges for; (a) exterior girder, and (b) interior girder	206
Figure 5.53	Correlation between shear distribution factors at ULS & SLS obtained from FEA results with proposed equations and CHBDC for skewed slab-on-girder bridges for girders at;(a) obtuse corner, (b) acute corner, and (c) interior..	208

Figure 5.54	Correlation between moment distribution factors at FLS obtained from FEA results with proposed equations and CHBDC for skewed slab-on-girder bridges for; (a) exterior girder, and (b) interior girder.....	212
Figure 5.55	Correlation between shear distribution factors at FLS obtained from FEA results with proposed equations and CHBDC for skewed slab-on-girder bridges for girders at;(a) obtuse corner, (b) acute corner, and (c) interior..	214
Figure 5.56	Correlation between moment distribution factors obtained from FEA results with proposed equations and AASHTO-LRFD for straight slab-on-girder bridges for; (a) interior girder, and (b) exterior girder.....	217
Figure 5.57	Correlation between shear distribution factors obtained from FEA results with proposed equations and AASHTO-LRFD for straight slab-on-girder bridges for; (a) interior girder, and (b) exterior girder.....	218
Figure 5.58	Correlation between interior girder moment distribution factors obtained from FEA results with proposed equations and AASHTO-LRFD for skewed slab-on-girder bridges at skew angle of; (a) 40°, and (b) 60°	221
Figure 5.59	Correlation between exterior girder moment distribution factors obtained from FEA results with proposed equations and AASHTO-LRFD for skewed slab-on-girder bridges at skew angle of; (a) 40°, and (b) 60°	222
Figure 5.60	Correlation between shear distribution factors at obtuse corners obtained from FEA results with proposed equations and AASHTO-LRFD for skewed slab-on-girder bridges at skew angle of; (a) 40°, and (b) 60°	223
Figure 5.61	Correlation between shear distribution factors at obtuse corners obtained from FEA results with proposed equations and Jaeger and Smith (1997) at ULS & SLS for skewed slab-on-girder bridges at skew angle of; (a) 20° ,(b) 40°, and (c) 60°	226
Figure 5.62	Correlation between shear distribution factors at acute corners obtained from FEA results with proposed equations and Jaeger and Smith (1997) at ULS & SLS for skewed slab-on-girder bridges at skew angle of; (a) 20° ,(b) 40°, and (c) 60°	228
Figure 5.63	Correlation between shear distribution factors at interior girder obtained from FEA results with proposed equations and Jaeger and Smith (1997) at ULS & SLS for skewed slab-on-girder bridges at skew angle of; (a) 20° ,(b) 40°, and (c) 60°	229
Figure 5.64	Correlation between shear distribution factors at obtuse corners obtained from FEA results with proposed equations and Jaeger and Smith (1997) at FLS for skewed slab-on-girder bridges at skew angle of; (a) 20° ,(b) 40°, and (c) 60°	231

Figure 5.65	Correlation between shear distribution factors at acute corners obtained from FEA results with proposed equations and Jaeger and Smith (1997) at FLS for skewed slab-on-girder bridges at skew angle of; (a) 20° ,(b) 40°, and (c) 60°	232
Figure 5.66	Correlation between shear distribution factors at interior girder obtained from FEA results with proposed equations and Jaeger and Smith (1997) at FLS for skewed slab-on-girder bridges at skew angle of; (a) 20° ,(b) 40°, and (c) 60°	234
Figure 5.67	Correlation between moment distribution factors obtained from FEA results with proposed equations and Al-Hashimy (2005) equations for ULS & SLS for straight slab-on-girder bridges for; (a) exterior girder, and (b) interior girder	237
Figure 5.68	Correlation between moment distribution factors obtained from FEA results with proposed equations and Al-Hashimy (2005) equations for FLS for straight slab-on-girder bridges for; (a) exterior girder, and (b) interior girder	238
Figure 5.69	Correlation between shear distribution factors obtained from FEA results with proposed equations and Al-Hashimy (2005) equations for ULS & SLS for straight slab-on-girder bridges for; (a) exterior girder, and (b) interior girder	239
Figure 5.70	Correlation between shear distribution factors obtained from FEA results with proposed equations and Al-Hashimy (2005) equations for FLS for straight slab-on-girder bridges for; (a) exterior girder, and (b) interior girder	240
Figure 6.1	Magnification factor with limiting skew angle at dead load condition for: (a) moment for exterior girder, (b) moment for interior girder, (c) shear at obtuse corner, (d) shear at acute corner, (e) shear at interior girder, and (f) flexural frequency.....	250
Figure 6.2	Magnification factor with limiting skew angle at ULS and SLS for: (a) moment for exterior girder, (b) moment for interior girder, (c) shear at obtuse corner, (d) shear at acute corner, (e) shear at interior girder, and (f) flexural frequency.....	251
Figure 6.3	Magnification factor with limiting skew angle at FLS for: (a) moment for exterior girder, (b) moment for interior girder, (c) shear at obtuse corner, (d) shear at acute corner, (e) shear at interior girder, and (f) flexural frequency.....	252
Figure 6.4	Effect of skew angle and bridge width on the flexural frequency of slab-on-girder bridge at: (a) dead load, (b) ULS and SLS, and (c) FLS	253

Figure 6.5	Effect of span length on the flexural frequency of slab-on-girder bridge at: (a) dead load, (b) ULS and SLS, and (c) FLS	254
Figure 6.6	Correlation of proposed equation with CHBDC equation for skew limitation	258
Figure 7.1	Boundary condition for two-span bridge model	264
Figure 7.2	Correlation between load distribution factors at dead load obtained from FEA results with proposed equations and CHBDC equations for straight bridges for; (a) interior girder span moment, and (b) obtuse girder span shear	265
Figure 7.3	Correlation between load distribution factors at dead load obtained from FEA results with proposed equations and CHBDC equations for skewed bridges for; (a) interior girder span moment, and (b) obtuse girder span shear	266
Figure 7.4	Correlation between load distribution factors at ULS and SLS obtained from FEA results with proposed equations and CHBDC equations for straight bridges for; (a) interior girder span moment, and (b) obtuse girder span shear	266
Figure 7.5	Correlation between load distribution factors at ULS and SLS obtained from FEA results with proposed equations and CHBDC equations for skewed bridges for; (a) interior girder span moment, and (b) obtuse girder span shear	267
Figure 7.6	Correlation between load distribution factors at FLS obtained from FEA results with proposed equations and CHBDC equations for straight bridges for; (a) interior girder span moment, and (b) obtuse girder span shear	267
Figure 7.7	Correlation between load distribution factors at FLS obtained from FEA results with proposed equations and CHBDC equations for skewed bridges for; (a) interior girder span moment, and (b) obtuse girder span shear	268
Figure 7.8	Correlation between span load distribution factors at dead load obtained from FEA results with proposed equations and CHBDC equations for straight bridges for; (a) exterior girder moment, (b) interior girder moment, (c) obtuse girder shear, (d) acute girder shear, and (e) interior girder shear	276
Figure 7.9	Correlation between support load distribution factors at dead load obtained from FEA results with proposed equations and CHBDC equations for straight bridges for; (a) exterior girder moment, (b) interior girder moment, (c) obtuse girder shear, (d) acute girder shear, and (e) interior girder shear	277
Figure 7.10	Correlation between span load distribution factors at ULS and SLS obtained from FEA results with proposed equations and CHBDC equations for straight bridges for; (a) exterior girder moment, (b) interior girder moment, (c) exterior girder shear, and (d) interior girder shear	278

Figure 7.11	Correlation between support load distribution factors at ULS and SLS obtained from FEA results with proposed equations and CHBDC equations for straight bridges for; (a) exterior girder moment, (b) interior girder moment, (c) exterior girder shear, and (d) interior girder shear.	279
Figure 7.12	Correlation between span load distribution factors at FLS obtained from FEA results with proposed equations and CHBDC equations for straight bridges for; (a) exterior girder moment, (b) interior girder moment, (c) exterior girder shear, and (d) interior girder shear	280
Figure 7.13	Correlation between support load distribution factors at FLS obtained from FEA results with proposed equations and CHBDC equations for straight bridges for; (a) exterior girder moment, (b) interior girder moment, (c) exterior girder shear, and (d) interior girder shear	281
Figure 7.14	Correlation between span load distribution factors at dead load obtained from FEA results with proposed equations and CHBDC equations for skewed bridges for; (a) exterior girder moment, (b) interior girder moment, (c) obtuse girder shear, (d) acute girder shear, and (e) interior girder shear	283
Figure 7.15	Correlation between support load distribution factors at dead load obtained from FEA results with proposed equations and CHBDC equations for skewed bridges for; (a) exterior girder moment, (b) interior girder moment, (c) obtuse girder shear, (d) acute girder shear, and (e) interior girder shear	284
Figure 7.16	Correlation between span load distribution factors at ULS and SLS obtained from FEA results with proposed equations and CHBDC equations for skewed bridges for; (a) exterior girder moment, (b) interior girder moment, (c) obtuse girder shear, (d) acute girder shear, and (e) interior girder shear	286
Figure 7.17	Correlation between support load distribution factors at ULS and SLS obtained from FEA results with proposed equations and CHBDC equations for skewed bridges for; (a) exterior girder moment, (b) interior girder moment, (c) exterior girder shear, and (d) interior girder shear.	287
Figure 7.18	Correlation between span load distribution factors at FLS obtained from FEA results with proposed equations and CHBDC equations for skewed bridges for; (a) exterior girder moment, (b) interior girder moment, (c) obtuse girder shear, (d) acute girder shear, and (e) interior girder shear	288
Figure 7.19	Correlation between support load distribution factors at FLS obtained from FEA results with proposed equations and CHBDC equations for skewed bridges for; (a) exterior girder moment, (b) interior girder moment, (c) exterior girder shear, and (d) interior girder shear	289

LIST OF ABBREVIATIONS

B	bridge width
b	length of the shorter side of a rectangular section as shown in Figure 5.7 of CHBDC (CSA 2014a)
b_e	reduced value of b as shown in Figure 5.7 of CHBDC (CSA 2014a)
C_e	correction factor used to adjust the F value for longitudinal moment to account for the vehicle edge distance
C_f	correction factor used to adjust the F value for longitudinal moment and longitudinal vertical shear
DLA	dynamic load allowance
D_T	truck load distribution width
D_{VE}	vehicle edge distance for slab-on-girder bridges
D_x	longitudinal flexural stiffness of the bridge superstructure per unit width
D_y	transverse flexural stiffness of the bridge superstructure per unit length
E	modulus of elasticity
e	eccentricity between centroids of girder and slab
E_c	modulus of elasticity of concrete
E_s	modulus of elasticity of steel
EI	flexural rigidity of a longitudinal beam representing a strip of width S
F	width dimension that characterizes load distribution for a bridge as per CHBDC (CSA 2006a)
F_m	longitudinal moment distribution factors under dead loads
F_{m_2006}	moment distribution factor from finite element analysis as per CHBDC (CSA 2006a)
$F_{refined}$	maximum bending moment or shear force determined from refined analysis
F_s	skew factor
$F_{simple\ beam}$	maximum bending moment or shear force determined from simple beam-line analysis

f_{Skew}	maximum fundamental flexural frequencies obtained from the finite element modeling for a skewed bridge
$f_{Straight}$	maximum fundamental flexural frequencies obtained from the finite element modeling for a straight bridge
F_T	truck load fraction as calculated by the simplified method of analysis and used to generate the design longitudinal load effects
F_{T_m}	longitudinal moment distribution factors under live loads
F_{T_v}	shear distribution factor from finite element analysis as per CHBDC (CSA 2014a)
F_v	shear distribution factors under dead loads
$F_{v_{2006}}$	shear distribution factor from finite element analysis as per CHBDC (CSA 2006a)
F_y	specified minimum yield stress, yield point, or yield strength
$I_{Composite}$	moment of inertia of a composite deck slab
K_g	longitudinal stiffness
L	span length
LDF	load distribution factor
L_e	equivalent span length specified for the uses of the beam analogy method in clause 5.6 (CSA 2014a)
L_1, L_2	span lengths used in determining the equivalent span in Figure 5.1(a) (CSA 2014a)
M_d	bending moment in the beam or girder at serviceability limit state (SLS) due to dead load
M_{Sd}	bending moment in the beam or girder at SLS due to the superimposed dead load
M_T	maximum longitudinal moment for one lane width of truck or lane loading, as applicable, including dynamic load allowance
M_g	maximum longitudinal moment per girder due to live load
M_{gavg}	average moment per girder due to live load
M_D	longitudinal moment due to the dead load

M_L	longitudinal moment per girder due to the CL-W loading
N	number of girders
n	number of design lanes
R_L	modification factor based on actual number of design lanes as per clause 3.8.4.2 (CSA 2014a)
R'_L	modification factor based on actual number of loaded lanes as per clause 3.8.4.2 (CSA 2014a)
S	centre-to-centre spacing of longitudinal girders
S_n, S_{3n}	elastic section modulus comprising the steel beam or girder and the concrete slab, calculated using a modular ratio of n or $3n$, respectively
ts	thickness of the deck slab
V_D	longitudinal shear due to the dead load
V_{FEA}	maximum shear stress obtained from a three-dimensional simply supported structure under the effect of truck live load at ULS and SLS, and FLS
V_g	maximum longitudinal vertical shear per girder due to live load
V_{gavg}	average shear per girder due to live load
V_L	longitudinal shear per girder due to the CL-W loading
V_{Skew}	maximum shear force obtained from the finite element modeling for a skewed bridge
$V_{Straight}$	maximum shear force obtained from the finite element modeling for a straight bridge
V_T	maximum longitudinal vertical shear for one lane width of truck or lane loading, as applicable, including dynamic load allowance
W_e	width of a design lane
ε	skew parameter for slab-on-girder bridges
γ_c	truck load modification factor for slab-on-girder bridges
γ_e	truck load modification factor for the exterior girder of slab-on-girder bridges
λ	lane width parameter

μ	lane width modification factor
ψ	skew angle
σ_{FEA}	maximum flexural stress obtained from a three-dimensional simply supported structure under the effect of truck live load at ULS and SLS, and FLS.
σ_{Skew}	maximum bending stresses obtained from the finite element modeling for a skewed bridge
$\sigma_{Straight}$	maximum bending stresses obtained from the finite element modeling for a straight bridge
σ_T	maximum flexural stress from a simple two-dimensional beam-line model under the effect of truck live load at ULS and SLS, and FLS.

CHAPTER 1

Introduction

1.1 Background

Composite slab-on steel I-girder bridges are among the most common short-to-medium span bridges built in the North America (Cao 1996). This was mainly due to the reduction in the structure's dead weight, better load carrying capacity, and a considerable reduction in the bridge depth (Ebeido 1995). Moreover, the use of steel built-up girders which directly support the slab formwork avoids the expensive shoring needed to support the wet cast-in-place concrete slab, and this makes construction easy and rapid with minimum traffic disruptions (Khan 1996).

The presence of skew angle makes the analysis and design of a composite bridge much more complex in comparison to a straight bridge. In modern transportation network, skewed bridges are indispensable where natural or existing man-made obstacles prevent a perpendicular crossing and consequently they are commonly found in mountainous areas. In many cases, the lack of space at complex intersections and in congested urban areas may also require bridges to be built on skew alignment (Huang et al. 2004, Menassa et al. 2007). In North America about 40% of the total bridge deck area is on skew alignment and about 10% of the total area is on high skew angles (Helba and Kennedy 1994, Deng 1998). Over the past decade, several authors have drawn attention to the potential for steel I-girder twisting on highly skewed supports (AASHTO/NSBA 2003, Beckman et al. 2005, Coletti and Yadlosky 2005, 2007). These rotations are larger at the obtuse corners and they are difficult to predict due to the uneven distribution of loads across the superstructure that increase the skew effects (Choo et al. 2005). In addition to girder twisting, skewness can also lead to an increased flange lateral bending stresses in the girders as well as increased girder shears and end reactions at the obtuse corners of the bridge that subsequently results in a reduction of girder shear and end reactions, and even possibly undesirable uplift in girders at the acute corners of the bridge (Fisher 2006, Ozgur et al. 2011, Krupicka and Poellot 1993). Further as the aspect ratio (length to width ratio) of a bridge structure decreases, a skewed bridge behaves more as a plate than a beam. Depending on the

transverse stiffness of a skewed bridge, part of the load travels transversely to the obtuse corners choosing the shorter path, rather than travelling along the longitudinal girders, as shown in Figure 1.1. This shift in load transfer reduces the longitudinal bending moments and increases the shear at the girder obtuse corners (Menassa et al. 2007).

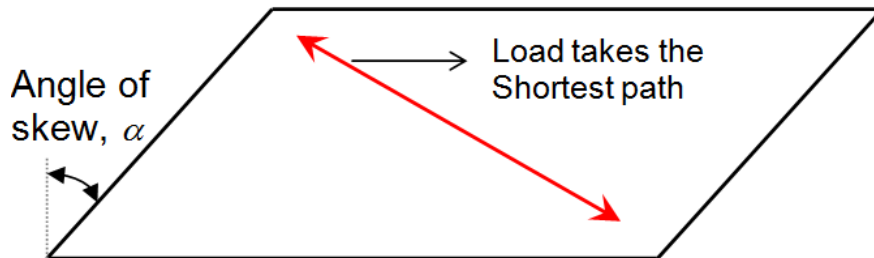


Figure 1.1 Load path on a skewed bridge

Alternate load paths and different load distributions are two complications that arises when designing a bridge with a skew angle (Coletti et al. 2011). Load distribution factors have been used in bridge design for many decades as a simple method to estimate load effects on bridge members. It allows bridge designers to predict structural responses by treating the longitudinal and transverse effects of dead and live loads as uncoupled phenomena without requiring special skills and analytical tools. With the specified formulas for distribution factors and simplified beam line analyses, the load effect on each girder can be evaluated for design and evaluation purposes. However, using inappropriate load distribution factors may lead to extremely conservative design forces or sometimes makes the design of the bridge unsafe. Therefore, an accurate assessment of load distribution throughout the bridge system is desired.

1.2 Problem Statement

The research work dedicated to the evaluation of load distribution factors has indicated that the behavior of a skewed bridge is quite different from their straight bridge counterparts (*e.g.*, Bishara et. al. 1993, Menassa et al. 2007, Mergel and Almansour 2010). These efforts have shown that previous bridge code specifications (CSA 2000, 2006a; AASHTO 1996) were unable to adequately predict the skewed bridge behavior including maximum mid span moment and the shear force at the girder obtuse corner.

Recently, based on the parametric study analysis by Theoret and Massicotte (2011), CHBDC (CSA 2014a) has specified equations considering skew for slab-on-girder bridges applicable within certain ranges of design parameters, such as, skew angle, span length, girder spacing etc. These ranges are often found too narrow and thus frequently exceeded in routine design (Razzaq et al. 2015, 2016). When one of the design parameter exceeds its corresponding limit, refined analysis is suggested by the code specifications (CSA 2014a-clause 5.9). Unfortunately many bridge design engineers are not familiar or adequately equipped with these refined analysis techniques. Further, the design equations in current design code specifications (CSA 2014a) are developed using the regression of grillage analysis results, however for skewed bridges it results inaccurate assessment of the bridge responses and is not always recommended (Coletti and Puckett 2012, Vayas et al. 2011). Also, these design guidelines are developed by considering simplifying assumptions that impose restrictions upon their applicability to the skewed slab-on-girder bridges under dead and live load conditions: (i) contribution of diaphragms should not be considered, and (ii) diaphragms and intermediate cross-frame should be placed parallel to the line of support (CSA, 2014b; clause 5.6.3). Previous studies revealed that the arrangement of internal diaphragms in skewed bridge has a significant effect on the load distribution pattern and should not be ignored (Khaloo and Mirzabozorg 2003, Nouri and Ahmadi 2012). Also under the application of loads, diaphragms resist girder lateral torsional buckling and stabilizes compression flange (Keating and Alan 1992, Helwig and Wang 2003). A recent study has demonstrated that parallel cross-frame layout can be employed for a skew angle up to 30° (Razzaq et al. 2015). It was also found in that study that beyond that skew limit and up to 60° , a perpendicular staggered cross-frame layout enhances the performance of the bridge structure due to three facts: (i) reduction of the cross-frame forces at the supports, (ii) limitation of the differential vertical displacement of cross-frame at obtuse corners, and (iii) reduction of girder longitudinal bending moment and vertical support reactions.

With developments in computer technology, the finite element method proves to be the most powerful, versatile and flexible approach for the analysis of composite steel girder bridges (AASHTO/NSBA 2011). Further, literature survey conducted by Sotelino et al. (2004) indicated that more previous researchers adopted finite element method as an analysis tool over the grillage analysis or other simplified methods. This finding is in

agreement with other's research work when analyzing new bridges or evaluating the load carrying capacity of existing skewed bridges (Bishara et. al. 1993, Mabsout et al. 1997b).

The current research was initiated to address these concerns by better understanding skew bridge behavior and developing design guidelines for rational and accurate assessment of load distribution factors for skewed slab-on steel I-girder bridges by adopting three-dimensional finite element analysis.

1.3 Research Objectives

Although CHBDC (CSA 2014a) has given relatively simple empirical equations for calculation of distribution factors for slab-on-girder bridges applicable within certain ranges of the design parameters, such as, skew angle, span length, girder spacing etc. These ranges are often found too narrow and thus frequently exceeds in routine design (Razzaq et al. 2016). When one of the design parameter exceeds its corresponding limit, refined analysis is suggested by the code specifications (CHBDC-clause 5.9.1). Unfortunately many bridge design engineers are not familiar or adequately proficient with these refined analysis techniques. In addition, the analysis equations in current design code specifications (CSA 2014a) are developed using the regression of grillage analysis results, however for skewed bridges it results inaccurate assessment of the bridge responses and is not always recommended (Coletti and Puckett 2012, Vayas et al. 2011). To address the shortcomings in the current bridge design code the objectives of this study were:

1. Evaluate load distribution factors for simply supported straight and skewed composite slab-on-steel I-girder bridges for dead and live load conditions using 3-dimentional finite element analysis (FEA). The results were correlated with the available CHBDC equations to determine their level of accuracy.
2. Based on the data generated from the parametric study analysis, reliable expressions for the moment and shear distribution factors were developed for the accurate prediction of skewed bridge behavior.
3. Assessment of skew limitations for slab-on-girder bridges by treating skew bridge as an equivalent straight bridge in structural analysis and design.

4. To check the applicability of the proposed equations for moment and shear distribution factors for simply supported straight and skewed slab-on-girder bridge under dead and live load conditions to the multi-span continuous bridge structures.

1.4 Dissertation Organization

Following this introductory chapter, chapter 2 describes the main methods used in North American bridge design codes along with the previous research efforts used to determine the load distribution factors for composite slab-on steel I-girder bridge systems. Further the effect of various bridge design parameters on the girder load distribution factor is also discussed. Chapter 3 presents the structural model developed for the analysis of composite slab-on-girder bridge prototypes using the 3-dimensional finite element method. In this chapter, the calibration of finite element model with actual field test data results of existing bridges are also presented. The results of sensitivity studies to estimate the effect of bridge design parameters on the load distribution of skewed composite steel I-girder bridges are included herein. Chapter 4 presents the effect of sequence of construction in skewed slab-on-girder bridges by conducting a three-dimensional finite element modeling under dead loads, and new empirical expressions for the evaluation of girder moment and shear distribution factors are proposed, and presented herein. Chapter 5 includes the proposed equations for the girder moment and shear distribution factors for straight and skewed slab-on-girder bridges under CHBDC truck loading for ultimate, serviceability and fatigue limit states. The correlation of the proposed equations with the current and previous bridge design codes are evaluated along with the design equations presented in previous literature available. In chapter 6, the skew limitations of composite slab-on-girder bridges are investigated using 3-dimensional finite element modeling in-order to treat the skewed slab-over steel I-girder bridge as an equivalent straight bridge for structural analysis and design purposes. Chapter 7 discusses the applicability of the proposed equations for moment and shear distribution factors for simply supported straight and skewed slab-on-girder composite bridge under the dead and live load conditions to the multi-span continuous bridge structure. Finally, Chapter 8 contains a brief summary, conclusions of this research study and suggestions for future research involving composite slab-on steel I-girder bridges.

CHAPTER 2

Literature Review

2.1 General

The concept of live load distribution factors have been used in bridge design for many decades as a simplified method to estimate live load effects on bridge members. Live load distribution is important for the design of new bridges as well as for the evaluation of the load carrying capacity of existing bridges. With specified formulas for distribution factors, bridge engineers can conveniently determine the maximum response in the girders by multiplying the live load distribution factor by the maximum responses obtained from a single beam line (one-dimensional) analysis under live load, as illustrated in Figure 2.1. In other words, the live load distribution factor (LDF) is defined in equation 2.1 as:

$$F_{refined} = LDF \times F_{simple\ beam} \quad (2.1)$$

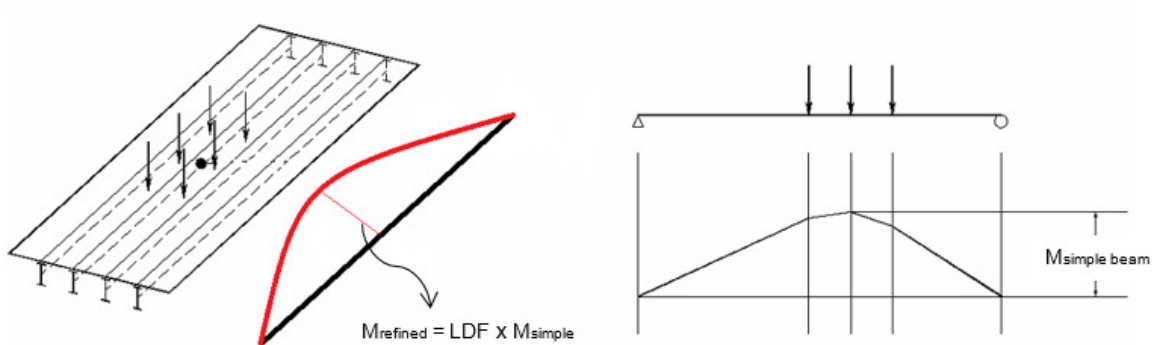


Figure 2.1 Distribution factor illustrations

$F_{refined}$ corresponds to the largest bending moment or shear force distributed to the girder for all of the load combinations from the refined analysis. $F_{simple\ beam}$ corresponds to the maximum bending moment or shear force determined from a simple beam-line analysis of one lane of traffic. The live load distribution factors allows bridge designers to predict structural responses by treating the longitudinal and transverse effects of vehicular live loads as uncoupled phenomena. Another advantage of live load distribution factors is that bridge engineers and researchers can predict the maximum responses without special skills and analytical tools.

Based on finite element analysis (FEA), the research work dedicated to the evaluation of load distribution factors has indicated that the behavior of a skewed bridge is quite different from their straight bridge counterparts (*e.g.*, Bishara et. al. 1993, Menassa et al. 2007, Mergel and Almansour 2010). These efforts have shown that the previous bridge code specifications (CSA 2000, 2006a; AASHTO 1996) were unable to adequately predict the skewed bridge behavior including maximum mid span moment and the shear force at the girder obtuse corner.

Recently mandated North American bridge code specifications (CSA 2014a, AASHTO-LRFD 2014) include provisions considering skew for slab-on-girder bridges applicable within certain ranges of the design parameters, such as, skew angle, span length, girder spacing etc. These ranges are often found too narrow and thus frequently exceeded in routine design. When one of the design parameter exceeds its corresponding limit, refined analysis is suggested by the code specifications. Unfortunately many bridge design engineers are not familiar or adequately proficient with these refined analysis techniques. In addition, the analysis equations in current design code specifications are developed using the regression of grillage analysis results, which may not be realistic for some cases. This short coming has convinced many bridge engineers and designers to adopt three-dimensional finite element modeling technique when analyzing new bridges or evaluating the load carrying capacity of existing bridges (Bishara et. al. 1993, Mabsout et al. 1997b). However few studies have recommended the usage of three-dimensional finite element analysis when the skew angle is greater than 20° (Menassa et al. 2007, Nouri and Ahmadi 2012).

The current research was initiated to address these concerns by better understanding skew bridge behavior and developing design guidelines and tools to facilitate design practice in North America, particularly in Canada. The literature review presented in this chapter covers the main methods used in North American codes to determine live load distribution factors and discuss previous research efforts particularly related to live load distribution in composite slab-on steel I-girder bridge systems.

2.2 Procedures for Evaluating Distribution Factors in North America

The procedures to evaluate the load distribution factors specified in North American bridge design specifications, particularly Canadian Highway Bridge Design Specification (CSA 2006a, 2014a), AASHTO Standard Specification (AASHTO 1996) and, AASHTO-LRFD (2014) Bridge Design Specification are briefly discussed herein. Moreover, the limitations involved for these bridge code specifications applicability are also discussed.

2.2.1 Canadian Highway Bridge Design Code (CSA 2006a)

The Canadian Highway Bridge Code (CSA 2006a) adopted the work of Bakht (1988), Bakht and Moses (1988), and Bakht and Jaeger (1990). The Canadian Highway Bridge Design Code (CHBDC) (CSA 2006a), describes a method for computing the live load distribution factors that is based on equal distribution of live loads to all girders as shown in Figure 2.2. A modification factor is applied to the value computed by the equal distribution, which is dependent on the bridge type, geometry, action, and limit state (ULS, SLS and FLS).

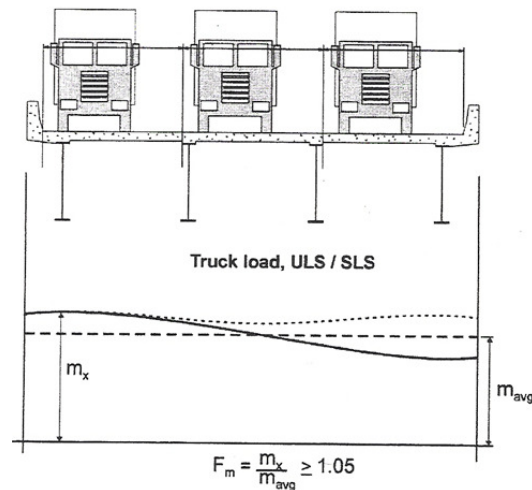


Figure 2.2 Transverse moment distribution using simplified method of analysis for ULS and SLS

Several conditions must be met in order to use the Canadian method for live load distribution calculations for slab-on-girder bridges (clause 5.6.1.1 for dead load analysis, and clause 5.7.1.1 for live load analysis). If these conditions are not fully met, the code

states that engineering judgment shall be used to determine whether the bridge satisfies these conditions to an extent sufficient for the appropriate simplified method to apply.

The Simplified Method of Analysis specified in clause 5.7.1 of the Canadian Highway Bridge Design Code (CSA 2006a) allows a bridge to be treated as a beam for live load analysis. The total load applied to the bridge will be n lanes, reduced by the multiple presence factor, R_L , as stipulated in Section 3. For girder-type bridges, the total moment M_T on the cross-section at any point along the span can be averaged by sharing the total moment equally among all girders. Hence, average moment per girder due to live load (M_{gavg}) for ultimate and serviceability limit states (ULS and SLS) can be calculated from equation 2.2 as follows:

$$M_{gavg} = \frac{nM_T R_L}{N} \quad (2.2)$$

The variation of maximum force intensity across the width of the bridge depends on the transverse position of the lane loads, the torsional stiffness of the cross-section, the span length, and the transverse and longitudinal stiffnesses. This transverse variation of force intensity can best be visualized by the introduction of an amplification factor, F_m , which represents the ratio of the true force intensity to the average force intensity, and expressed in equation 2.3 as follows:

$$F_m = \frac{M_g}{M_{gavg}} \quad (2.3)$$

where, M_g is the longitudinal moment per girder, and, M_{gavg} is the average moment per girder due to live load determined by sharing equally the total moment on the bridge cross-section among all girders in the cross-section. It is shown in equation 2.3 that F_m is a measure of how much the extreme load distribution deviates from the average distribution. Lower values of F_m indicate less deviation, thus greater ability of the bridge to transfer load across its width (CSA 2006b).

For slab-on-girder bridges at ULS and SLS, the amplification factor to account for the transverse variation in maximum longitudinal moment intensity, as compared to the average longitudinal moment intensity (clause 5.7.1.2.1.2-a) can be expressed as follow:

$$F_m = \frac{SN}{F \left(1 + \frac{\mu C_f}{100} \right)} \geq 1.05 \quad (2.4)$$

$$\mu = \frac{W_e - 3.3}{0.6} \leq 1.0$$

For fatigue limit states (FLS), the traffic load includes one CL-W truck, that causes maximum effects only, increased by the dynamic load allowance and placed at the center of one travelled lane (clause 3.8.4.1). Thus, for slab-on-girder bridges at FLS the amplification factors (clause 5.7.1.2.2.2-c) can be expressed as follows:

$$M_{gavg} = \frac{M_T}{N}$$

$$F_m = \frac{SN}{F \left(1 + \frac{\mu C_f}{100} + \frac{C_e}{100} \right)} \geq 1.05 \quad (2.5)$$

In equations 2.4 and 2.5, S is the center-to-center girder spacing, and N is the number of girders. Parameter F is a width dimension that characterizes the load distribution for a bridge (CSA 2006a clause 5.7.1.2.1.2-a for ULS and SLS, and clause 5.7.1.2.2.2-c for FLS). It depends on many factors, including bridge type, highway class, span length, number of design lanes, and girder position. Parameter W_e is width of design lane calculated in accordance with clause 3.8.2, C_f is the percentage correction factor obtained from Table 5.3 and 5.4 for ULS and SLS, and FLS respectively, and C_e is the percentage correction factor for vehicle edge distance obtained from Table 5.5 of CHBDC (CSA 2006a).

The longitudinal vertical shear per girder, V_g , at ultimate, serviceability and fatigue limit states (ULS, SLS and FLS) can be defined as:

$$V_g = F_v \cdot V_{gavg} \quad (2.6)$$

where V_{gavg} is the average shear per girder and F_v is the amplification factor for the transverse variation in maximum longitudinal vertical shear intensity.

$$V_{gavg} = \frac{nV_T R_L}{N} \tag{2.7}$$

$$F_v = \frac{SN}{F} \geq 1.05$$

where V_T is the maximum shear per design lane.

Extensive comparative analyses of skew and equivalent right bridges conducted by Bakht (1988), and Jaeger and Bakht (1989) showed that the angle of skew of bridge is not the only measure of its skewness; the span length and girder spacing also affect the load distribution. In particular, it has been shown that a dimensionless parameter characterizing the skewness of a slab-on-girder bridge is, $\varepsilon = S \tan \psi/L$. To allow the analysis of a skew bridge as an equivalent right bridge, the 2006 version of CHBDC (CSA 2006a) has imposed the upper limits of 1/18 for ε . In the current version of the code that limit has been removed.

2.2.1.1 Limitations of CHBDC (CSA 2006a)

Previous studies noticed the following discrepancies in the CHBDC (CSA 2006a):

- i. Mergel and Almansour (2010), examined the accuracy of the load distribution method specified in CHBDC (CSA 2006a). For this purpose, the analytical results of the live load distribution factors obtained by three dimensional finite element model of a two lane single span bridge were compared by the simplified method of analysis specified in CHBDC (CSA 2006a). Results showed that the simplified method of analysis leads an over-estimation from 7% to 17% for the longitudinal moment and shear.
- ii. The Canadian Highway Bridge Design Code (CSA 2006a) follows the concept of equal distribution and applies modification factors of the bridge type, the geometry of the structure, and the limit state in order to improve the accuracy. Equivalent Orthotropic plate theory is the basis for the modification made to equal distribution, which may not be realistic for some cases.

2.2.2 Canadian Highway Bridge Design Code (CSA 2014a)

To address the shortcoming in the previous bridge code (CSA 2006a), new provisions based on extensive analysis of simply supported single-span bridge was introduced to further simplify the procedure of distributing live load effects in slab, voided-slab, slab-on-girder and multi-spine box girder bridges. The new provisions are based on a parametric study done by grillage analysis of more than 3000 slab-on-girder bridges that represents a wide variety of geometries and loading conditions (Theoret and Massicotte 2011). As per clause 5.6.4.1, the longitudinal moment and vertical shear shall be calculated as follows:

$$\begin{aligned} M_L &= F_T F_S M_T \\ V_L &= F_T F_S V_T \end{aligned} \quad (2.8)$$

where F_T is the truck load fraction represents the load effects per girder due to highway traffic, and F_S accounts for the effects of skew geometry. Therefore, equation 2.8 specifies that the maximum load effect (M_L or V_L) can be determined by multiplying the one-lane loading case load effects (M_T or V_T) by two factors i.e. F_T and F_S .

The truck load fraction depends on the girder spacing, superstructure dimensions, highway class, vehicle edge distance and deck overhang length beyond the exterior girder. For Slab-on-girder bridges, the truck load fraction, F_T , shall be calculated from equation 2.9 and 2.10 for ULS and SLS, and FLS respectively as follows:

$$F_T = \frac{S}{D_T \gamma_C (1 + \mu \lambda)} \geq 1.05 \frac{nR_L}{N} \quad \text{for ULS \& SLS} \quad (2.9)$$

$$F_T = \frac{S}{D_T \gamma_C (1 + \mu \lambda + \gamma_e)} \geq 1.05 \frac{1}{N} \quad \text{for FLS} \quad (2.10)$$

where S is the centre-to-centre spacing of longitudinal girders of a deck-on-girder bridge, m; D_T is the truck load distribution width, m; γ_C is the truck load modification factor for slab-on-girder bridges; γ_e is the truck load modification factor for the exterior girder of slab-on-girder bridges, μ is lane width modification factor; and, λ is the lane width parameter.

The refined analysis was conducted to obtain D_T factors (F in previous edition of CSA 2006a) to consider the critical number of loaded lanes out of all possible combinations (Theoret and Massicotte 2011).

2.2.2.1 Limitations of CHBDC (CSA 2014a)

CHBDC design guidelines (CSA 2006a, 2014a) are developed by considering specific assumptions that limit their applicability to skewed slab-on-girder bridges i.e.

- i. Both CHBDC specifications (CSA 2006a, 2014a) are based on the orthotropic plate theory and consider the equivalent stiffness of the bridge structure and thereby ignore the effect of transverse intermediate diaphragms when developing the equations for moment and shear. The presence of such diaphragms has a significant effect on the load distribution pattern and lead to better load distribution and hence significant reductions in both the span and support moments (Khaloo and Mirzabozorg 2003, Nouri and Ahmadi 2012).
- ii. In both versions of CHBDC (CSA 2006a, 2014a), the LDF equations do not differentiate between slab-on concrete girders or braced steel girders; the same set of equations are specified for both bridge structures resulting in erroneous design parameters.
- iii. CHBDC (CSA 2014b), clause 5.6.3 specifies the placement of diaphragms and intermediate cross-frame parallel to the line of support. A study by Razzaq et al. (2015) has demonstrated that the parallel cross-frame layout can be employed up to a 30° skew angle and when the skew angle increases from 30° to 60° , perpendicular staggered cross-frame layout enhances the performance of a skewed bridge.
- iv. CHBDC (CSA 2014a) clause 5.6.3 and clause 5.6.6.2 stipulate the use of the same skew factor to magnify the longitudinal vertical shear forces V_L without any discrimination for the forces at acute and obtuse corners. However, finite element based results demonstrated that the obtuse corners are very much affected by the variation of skew angle in comparison to the acute corners (Razzaq et al. 2016).
- v. The simplified procedure for evaluating the moment in CHBDC (CSA 2014a) is silent on the effect of skew for the exterior and the interior girders. Whereas, a skew

correction factor is specified for the shear force at the girder obtuse corner (clause 5.6.3-b for dead load analysis, and clause 5.6.6.2 for live load analysis). Previous research revealed that interior girders is substantially affected by the skew angle than exterior girders (Ebeido and Kennedy 1996a). For this reason, the moments predicted using the current CHBDC (CSA 2014a) could results in conservative results for the interior girder of a skew bridge.

2.2.3 AASHTO Standard Specifications

The current distribution factor in the AASHTO Standard Specifications (AASHTO 1996) for composite steel I-beam bridges with two or more traffic lanes was developed by Newmark and Seiss (1943). This distribution factor was derived by considering a portion of the slab to act as a beam on an elastic foundation, and then using moment distribution methods to determine the beam response. The wheel load distribution factor from the “S-over” equation for concrete slab on steel girder bridges for straight bridges with two or more design lanes loaded is:

$$LDF = \frac{S}{D} \quad (2.11)$$

where S is girder spacing (ft), and D is a constant based on the bridge type that depends on the superstructure type (e.g., $D = 5.5$ for concrete slab on steel girders). No other parameters are considered.

2.2.3.1 Limitations of AASHTO Standard Specifications

Based on research review, the following limitation in AASHTO Standard Specifications (1996) are observed:

- i. Equation 2.11 allows the designer to simply calculate the part of the live load to be transferred to the girders without any consideration for the bridge deck, girder stiffness and span length resulting in a substantial conservative design. Furthermore, some bridge designers extend the application of the above mentioned formula even to more complicated bridge structures such as skewed, curved, continuous and large span with

- wide and different geometry compromising bridge service life and safety (Yousif 2005).
- ii. Previous research shows that for long span bridges, S-over equations result in values that are over-conservative. However for short span bridges with small girder spacing, they lead to underestimated results in comparison with AASHTO-LRFD, as shown in Figure 2.3 (Reproduced from Sotelino et al. 2004.) and Figure 2.4 (Reproduced from Cross et al. 2006).
 - iii. Nutt et al. (1988) summarized the weaknesses in the AASHTO standard specifications that have led to inconsistencies in the load distribution criteria, as follows:
 - a) Inconsistent changes in distribution factors to reflect the changes in design lane width. For-example, at the time the “s-over” equation was developed, the standard design lane was 10 ft. (3.05 m) wide, while today according to AASHTO-geometric design of highways and streets, 12 ft. (3.66 m) design lanes are customary (AASHTO 2001).
 - b) Inconsistent consideration of a reduction in load intensity for multiple lane loading (Zokaie and Imbsen 1992).
 - iv. Zokaie (2000) reported that the *S/D* formulas were acceptable for bridges having girder spacing near 6 ft. (1.83 m) and span length close to 60 ft. (18.30 m), whereas the formulas were unable to predict the accurate response when the properties of a bridge vary.
 - v. Kocsis (2004) also reported the inaccuracy of the AASHTO standard method by using a structural analysis program, *SECAN*, based on semi-continuum method (Mufti et al. 1992). This study showed that the standard AASHTO formulas for live load in some cases underestimate the live load moments by as much as 40%.

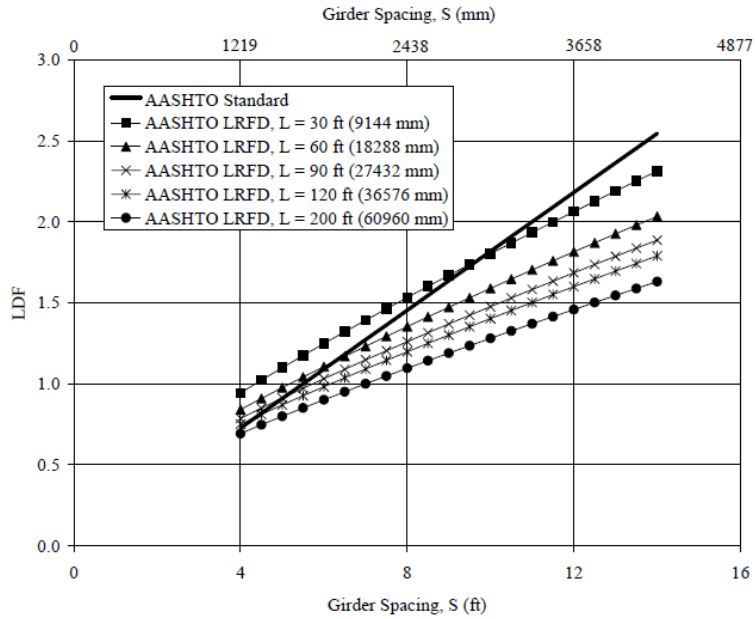


Figure 2.3 AASHTO Standard vs. AASHTO-LRFD moment distribution factors
(Reproduced from Sotelino et al. 2004)

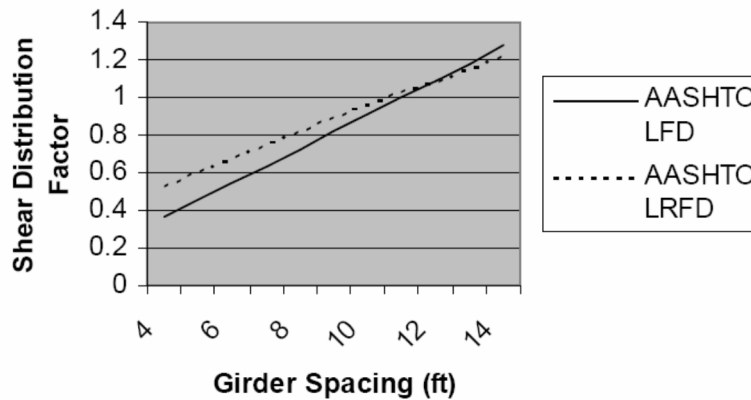


Figure 2.4 AASHTO Standard vs. AASHTO-LRFD shear distribution factors
(Reproduced from Cross et al. 2006)

2.2.4 AASHTO-LRFD Specifications

In-order to address the weakness and limitations in the AASHTO Standard specifications, the National Cooperative Highway Research Program (NCHRP) Project 12-26 was initiated in the mid-1980s in order to develop comprehensive specification provisions for distribution of wheel loads in highway bridges. The study was performed in two phases:

Phase-I concentrated on beam-and-slab and box girder bridges; Phase-II concentrated on slab, multibox beam, and spread box beam bridges. Three levels of analysis were considered for each bridge type. Level-1 used simple formulas to predict lateral load distribution. Level-2 included either graphical methods, nomographs and influence surfaces, or simplified computer programs, such as, SALOD based on influence surface method. The most accurate level, level-3, involves detailed modeling of the bridge superstructure using computer analysis programs, such as, for the beam-and-slab bridges finite element analysis software GENDEK-S was found to be very accurate (Zokaie and Imbsen 1992).

The first edition of AASHTO-LRFD (1994) specification was based on NCHRP Project 12-26 (Zokaie and Imbsen 1992). The LRFD equations were developed based on a parametric study developed from a set of 364 existing bridges located in ten different states comprised of three different types of bridges i.e. prestressed T-beam, concrete I-girder, and steel I-girder. After analyzing the sensitivity of the distribution factors, the critical parameters used in the parametric study were girder spacing, span length, girder stiffness, and slab thickness. Based on the results of the sensitivity studies, two sets of equations were developed for moment and shear with one and bridges with two or more design lanes. For example, the wheel load distribution factor equation from AASHTO-LRFD (2014) for concrete slab on steel girder bridges with two or more design lanes loaded is:

$$LDF = 0.15 + \left(\frac{S}{3}\right)^{0.6} \cdot \left(\frac{S}{L}\right)^{0.2} \cdot \left(\frac{K_g}{12Lt_s^3}\right)^{0.1} \quad (US \text{ customary unit})$$

$$LDF = 0.15 + \left(\frac{S}{914}\right)^{0.6} \cdot \left(\frac{S}{L}\right)^{0.2} \cdot \left(\frac{K_g}{12Lt_s^3}\right)^{0.1} \quad (SI \text{ unit})$$
(2.12)

where S is girder spacing (ft, mm), L is span length (ft, mm), $K_g = n(I+ Ae^2)$ is the longitudinal stiffness (in^4 , mm^4), t_s is the slab thickness (in, mm), n is the modular ratio between steel and concrete, I is the girder stiffness (in^4 , mm^4), A is the girder area (in^2 , mm^2), and e is the eccentricity between centroids of girder and slab (in, mm).

The equations recommended by AASHTO-LRFD are generally more complex than AASHTO standard specifications, but they also present a great degree of accuracy. The

formulas previously presented in the AASHTO standard specifications are although simpler but do not present the degree of accuracy demanded by today's bridge engineers. In many cases these formulas can result in highly unconservative results (more than 40%); and in other cases they may be highly conservative (more than 50%). However, AASHTO-LRFD equations of wheel load distribution factors are within 5% of the results of an accurate analysis, used for its development (Zokaie and Imbsen 1992).

2.2.4.1 Limitations of AASHTO-LRFD Specifications

The most obvious advantage of the AASHTO-LRFD equations is their simplicity. They do not require any special tools other than a calculator. No special computers or computer programs are needed, and no special knowledge of finite element modeling techniques is required. If the simplified equations are applied within their applicable range and the bridge has a regular geometry, accurate results can be obtained with ease (Zokaie and Imbsen 1992). However, simplified equations have limitations which should be understood. These limitations are briefly described below:

- i. The AASHTO-LRFD equations are assumed to be representative of the actual behavior of bridges (Zokaie 2000, Zokaie and Imbsen 1992). However, the FE model used in developing the AASHTO-LRFD LDF equation did not include some important features of bridges which may affect lateral load distribution. First, despite the presence of the secondary elements such as cross bracing, diaphragms, and parapets in bridges, these elements were not considered in the development of the LDF equation. Parametric studies, such as, Nouri and Ahmadi (2012), Chung et al. (2006) and, Khaloo and Mirzabozorg (2003) have showed that consideration of secondary elements has a significant effect on lateral load distribution. Consequently, the AASHTO-LRFD equation often provides overly conservative results.
- ii. Shahawy and Huang (2001), demonstrated that AASHTO-LRFD showed good agreement with test results for bridges with two or more loaded design lanes, provided that girder spacing and overhang deck did not exceed 2.4 m and 0.9 m, respectively. Outside these ranges, the error could be as much as 30%. For one loaded design lane,

- the relative error was less than 10% for interior girders and could be as high as 100% for exterior girders.
- iii. AASHTO-LRFD equation requires an iterative procedure for the selection of certain parameters that are not known until girder selection. These parameters are the longitudinal stiffness, K_g , and the slab thickness, t_s . Therefore, the third term in the AASHTO-LRFD equation (i.e. $K_g/12Lt_s^3$ for US customary units and K_g/Lt_s^3 for SI units) is assumed to be equal to unity as recommended for a first trial in design. For most bridges, this term ranges from 0.85 to 1.10 (Sotelino et al. 2004).
 - iv. Since its inception, the new LDF design equations have faced a significant amount of skepticism regarding their adoption. Although, LDF equations takes into account additional bridge parameters than the AASHTO standard specifications (Zokaie 2000). Designers have found the equations more complex and difficult to use. As a result, the calculation of live-load distribution factors is still not settled (Barr and Amin 2006).
 - v. Chen and Aswad (1996) found that the LRFD distribution factors results in conservative design for bridges with large span-to-depth ratios. Based on the results of finite element analysis, Chen and Aswad found that this conservatism could be as much as 23% for interior girders and 12% for exterior girders.
 - vi. For slab-on-girder bridges, AASHTO-LRFD clause 4.6.2.2 specify the ranges of applicability of LDF equations include spacing not less than 3.5 ft. (1.07 m) while not greater than 16 ft. (4.88 m), slab thickness not less than 4.5 in. (11.43 cm) while not greater than 12 in. (30.48 cm), span length not less than 20 ft. (6.10 m) while not larger than 240 ft. (73.15 m) and so on. The equations are most accurate when applied to bridges within the range of applicability. Outside this range, a refined analysis such as grillage analysis and finite element analysis must be considered. In such case, engineers have to make certain assumption and work on a case-by-case basis.

2.3 Literature Review on Methods for Evaluating Load Distribution Factors

This section presents the state of the art and practice related to skewed bridge behavior and design practice, based on a literature review conducted in the present research project. It has been observed hereby that all research efforts identified and reviewed have employed numerical approaches assisted by limited physical testing in investigating skewed bridge

behavior. Research has been conducted by several investigators focused on examining the accuracy of the bridge code specifications for the evaluation of distribution factors. These efforts have included both analytical studies using finite element analysis and field studies of existing bridges. Regression analysis based on the data produced using the numerical and experimental approaches was also common to identify the trend of skew effect as a function of design parameters such as skew angle, girder spacing, span length, etc. Research efforts have also been focused on assessing the influence of various parameters on the load distribution behavior of bridge superstructures. Although this topic has been a point of interest of many researchers and engineers since the mid of last century, however this section will encompass and summarize the research efforts dedicated in the last three decade.

2.3.1 Analytical Studies

By adopting finite element analysis (FEA) method, many researchers have devoted efforts towards developing new and simplified equations for live load moment and shear distribution factors for skewed bridges (Zokaie 2000, Hue et al. 2004, 2005). Most of the proposed methods are applicable to one or two particular types of bridges (Tarhini and Fredrick 1992, Bishara et al. 1993, Barr et al. 2001, Barr and Amin 2006). Whereas, few studies proposed moderate changes to the bridge design code specifications by assessing the accuracy of these bridge code specifications with respect to variation of one or more specific parameters, such as sidewalk and railings, diaphragms and secondary bracing elements, skewed alignment, structural continuity, girder longitudinal stiffness and aspect ratio, load applications and nontraditional designs on the load distribution behavior of bridge superstructures (Mabsout et al. 1997a, Chung et al. 2006, Nouri and Ahmadi 2012, Bishara et al. 1993, Khaloo and Mirzabozorg 2003, Diab et al. 2011, Mabsout et al. 1998, Zokaie 2000, Yousif and Hindi 2006, Gheitasi and Harris 2015). A summary of selected studies are presented herein.

Khaleel and Itani (1990) conducted finite element analyses to determine moments in continuous straight and skewed slab-on-girder bridge subjected to the AASHTO HS20-44 truck live loads. This research considered bridge configurations with span lengths ranging

from 24.4 m (80 ft.) to 36.6 m (120 ft.) and girder spacing from 1.8 m (6 ft.) to 2.7 m (9 ft.). Skew angles varying between 0° to 60° were considered. Results of this research were compared to distribution factors obtained from the AASHTO Standard equations. The results showed that the increase of skew angle resulted in a reduction of design moments. The reduction of maximum positive and negative moments in interior girders is less than 6% for a skew angle less than 30° and as much as 29% when skew angle approached 60° . The reduction of the maximum positive or negative bending moments in the exterior girders is less than 10% for angles of skew less than 45° and as much as 20% when skew angle is 60° .

Ebeido and Kennedy (1996a, b) performed laboratory tests on three continuous composite skewed bridges. Finite element analyses were conducted and had good agreement with the test results. A parametric study on more than 600 prototype bridges was conducted to investigate the influence of all major parameters affecting the moment, shear, and reaction distribution factors. Empirical formulas of load distribution factors for continuous, skewed composite bridges were developed, based on different girder types and loading cases. Results showed that both the span and the support girder moments decrease significantly with the increase in the skew angle. The effect of skew on design of interior girder is more significant than for exterior girders. Moreover, the increase in the skew angle reduces the shear distribution factor for the girder close to the obtuse corner, and increases the shear distribution factor for the girder close to the acute corner and for interior girders. Furthermore, the influence of skew on the shear and moment distribution factors becomes more significant for skew angles greater than 30° .

Mabsout et al. (1997b) compared four finite element modeling techniques, available in the literature, to determine load distribution factors for a simply supported composite steel girder bridge. In the first method, the concrete slab was modeled with quadrilateral shell elements, and the steel girders were idealized as space frame members. In the second method, the concrete slab was modeled with quadrilateral shell elements and rigidly connected to girders represented by space frame members. In the third method, the concrete slab and steel girder web were modeled with quadrilateral shell elements and girder flanges as space frame elements. The connection between the girder flange and deck was modeled

by imposing a rigid link. In the fourth method, the concrete slab was modeled with isotropic, eight-node brick elements; the steel girder flanges and webs were modeled with quadrilateral shell elements. The results of these modeling techniques were compared with AASHTO-LRFD load distribution factors and published experimental results. The results showed that the four finite element models produced similar load distribution factors for the AASHTO-LRFD equations.

Using three-dimensional finite element analysis method, Khaloo and Mirzabozorg (2003) analyzed simply supported skewed slab-on-girder bridges. The main parameters of his study were: girder spacing (1.8–2.7 m), span length (25–35 m), skew angle (0° – 60°), and four different arrangements of internal transverse diaphragms. They showed that for a skew angle of 60° , the load distribution factor of exterior girders was reduced by 24% as compared with the right bridges. Moreover, the study concluded that decks with internal transverse diaphragms perpendicular to the longitudinal girders are the best arrangement for load distribution in skew bridges. Furthermore, it was concluded that the load distribution factors of the AASHTO standard specifications were highly conservative and resulted up to 43.1% higher results than those found by FEA.

Yousif and Hindi (2007) performed a comparison between the distribution factors of simple span slab-on-girder bridge due to live load calculated in accordance with the AASHTO-LRFD equations and the finite element analysis. The range of applicability limits specified in the AASHTO-LRFD in terms of span length, slab thickness, girder spacing, and longitudinal stiffness were investigated. A total of 886 bridge superstructures were modeled by adopting several finite elements linear elastic models to accurately assess structures. The vehicular load plus the standard lane load as specified by AASHTO-LRFD was used to represent the live load in the analysis. The study concluded that for most of the cases, AASHTO-LRFD equations overestimated the live load distribution when compared to finite elements analysis results that reached a maximum of about 55%. However, in some cases it was also noticed that the AASHTO-LRFD underestimates live load distribution factors by 20% when compared to finite elements analysis.

Jingjuan and Chen (2011) adopted the beam-on-elastic-spring-supports model proposed by Hu (1996) to calculate the live and dead load reaction at each supporting girder. A standard

live load including single and multilane loads and a permit truck with four wheel axle, was considered. The validity of the model was assessed by comparing the spring model results with LRFD equations, finite element analysis, and field tests data. The results demonstrated that in most cases, the model results were close to the results using the LRFD equations. However, the spring model analysis results were proved to be conservative than field-test data and finite element analysis results. Thus the study concluded that the spring model provides load-distribution factors that can be used in bridge design.

Nouri and Ahmadi (2012) studied the effect of the skew angle and other design parameters on the bending moment, shear force, and distribution factor of two-span continuous composite steel-concrete bridges using three-dimensional finite element analysis (FEA) subjected to AASHTO HS20-44 loading. The results of the FEA for skewed bridges were compared with the straight bridges as well as the AASHTO standard specifications and AASHTO-LRFD specifications. The results showed that the AASHTO standard specifications overestimate the maximum bending moment and shear force by 50% and 10% respectively for a skew angle of 45°. Moreover, the study concluded that AASHTO-LRFD specifications overestimate the longitudinal bending moment and shear force for a skew angle larger than or equal to 20° and in some cases the overestimation reached the 45% value.

Bae and Oliva (2012) focused on modifying the current design specifications and proposing modification factors to better accommodate the effect of oversized, overweight trucks on the lateral load distribution behavior of slab-on-girder bridges. Three-dimensional finite element analyses of 118 girder type bridges with 16 different loading configurations of overload vehicles were performed. Various configurations of the vehicles, number of bridge spans, girder spacing, deck depth, girder type, skew angles of the bridge and diaphragms were considered in developing the load distribution factor equations for the multi-girder bridges. The results showed that the load distribution factors decrease as the skew angle increases and this trend was more evident for the shear load distribution factor with dual-lane trailer loading case. Moreover, the study revealed that the positive moment distribution factors for two-span bridges were comparable to those of single-span bridges. Whereas, the negative moment distribution factors of two-span

bridges were found to follow a different pattern than the positive moment distribution factors for single-span bridges. Based on those findings, the study concluded that the modified empirical equations can be used for single and continuous span bridges and bridges with skew angles.

Gheitasi and Harris (2015) studied two in-service composite steel girder bridge superstructures in the state of Michigan to investigate variations in lateral distribution behavior over the entire loading history up to failure. The first bridge (i.e. Stanley Bridge) selected for this study was a simply supported straight three-span bridge with a total length of 86.8 m operating on Stanley Road over I-75 in Flint, Michigan. However, simply supported skewed (i.e. 15°) single span bridge (i.e. Huron Bridge) with a total length of 42.6 m operating on M-36 over the Huron River in Livingston County, Michigan was selected as a second bridge for this study. Both composite bridges had been previously subjected to a live-load testing. An extensive parametric study analysis using three-dimensional finite element analysis (FEA) method was conducted to study the effect of boundary condition, loading position, and load configuration on the overall structural response and the girder distribution behavior of the selected bridges. Comparing the results obtained from nonlinear FEA with those proposed by the AASHTO-LRFD specifications demonstrated that the code-specified values for the distribution factors are overly conservative.

2.3.2 Field Studies

Great efforts have been conducted to assess the accuracy of the live load distribution equations stipulated in existing bridge code specifications by performing field testing. By adopting field testing, many researchers have devoted efforts to determine live load distribution among the girders of simple and continuous bridges at different stages of loading (Bakht and Jaeger 1992, Razaqpur and Esfandiari 2006). Few studies also focused to estimate the mechanical causes of the reinforced concrete deck cracking under heavy truck loadings, and service load stresses (Castaneda 1997). A summary of selected studies are presented herein.

Fu et al. (1996) conducted live load tests on four steel I-girder bridges of which three were straight bridges and one had a skewed configuration. Comparison of the field test results to the LRFD distribution factors showed that for three non-skewed bridges the LRFD equations were found to be conservative anywhere from 7% to 42%. However, for the skewed aligned bridge the LRFD equations underestimated the load effects by 13%.

Kim and Nowak (1997) performed field tests on two simply supported steel I-girder bridges. One bridge, designated as M50/GR had a span length of 14.63 m and a girder spacing of 1.45 m. The second bridge, referred to as US23/HR, had a span length of 23.77 m and a girder spacing of 1.91 m. The girders measured static strain data, after removing the dynamic components, was used to develop equations for girder distribution factors and compared with AASHTO Standard and LRFD Specifications. The study concluded that AASHTO Standard Specification was found to be more conservative as compared to LRFD Specification. It was shown that the LRFD distribution factors overestimated the actual distribution by 28% and 19% in the two bridges tested. Furthermore, the distribution factors obtained from the Standard Specifications were 16% and 24% greater than the load distribution factors that resulted from field-testing results.

Eom and Nowak (2001) study involved the field-testing of seventeen steel I-girder bridges having span lengths ranging from 9.75 m to 42.67 m and girder spacing from 1.22 m to 2.82 m. The majority of the bridges selected were not skewed, but some moderately skewed bridges (10° to 30°) were also included in this study. It was found that the actual distribution factors evaluated from field tests were lower than those given by the bridge code specifications in all cases. It was also noticed that the AASHTO Standard Specifications were very conservative for short spans with small girder spacing, and even more conservative for other situations. Moreover, the LRFD distribution factors were found to be more accurate than those from the AASHTO Standard Specifications, although were still considered to be conservative.

Huang et al. (2004) study involved both a field test of a recently constructed two-span continuous slab-on-steel composite highway bridge with a skew angle of 60° located in Delaware, and a numerical analysis using finite element modeling. A field test was conducted to measure the strain in the girders at various locations under controlled load

conditions. For this purpose, two fully loaded three-axle dump trucks having a gross vehicle weights of 255 kN and 271 kN were used. A finite element model was developed and calibrated by the field test results. An extensive parametric study was conducted using finite element analyses to investigate the influence of model mesh, transverse stiffness, diaphragms, and modeling of the supports on the load distribution factors. The resulting field test and FEA analytical results were compared with LRFD load distribution equations to assess the accuracy of the current empirical formulas. The study concluded that the LRFD equations for transverse load distribution found to be conservative for positive bending.

Cross et al. (2009) performed field testing on twelve interstate bridges that most typically represent the bridge inventory in Illinois to determine the validity of AASHTO-LRFD shear distribution factors used in bridge design. For this purpose, six bridges along Interstate I-55 and six along Interstate I-270/70 in Illinois were selected for monitoring. All the bridges were instrumented on their girder webs to measure shear stresses caused by static, slow-moving, and dynamic load tests. Finite element models were also generated to verify both the field test results and the validity of the LRFD shear distribution factors. The study showed that the LRFD distribution factors closely approximate the shear distribution factors determined by both the finite element modeling and field testing.

Fu et al. (2011) investigated the behavior of skewed concrete bridge decks on steel superstructure subjected to truck wheel loads. For this purpose, full-scale bridge field testing of a steel highway bridge located in Michigan interstate I-94 highway in Washtenaw County that was scheduled for rehabilitation was selected. The tested bridge was skewed by an angle of 49.1° . The bridge superstructure consists of 10 plate girders spaced at 2.13 m, with a composite concrete deck through studs of two rows at 0.203 m spacing. For understanding the behavior of the concrete deck under truck wheel loads, the deck was instrumented by strain transducers at four locations. After the deck concrete hardened, a loaded six-axle truck was slowly driven on the deck across the test bridge span. The strain gauges were read using a data acquisition system. The field testing results were further verified by performing a linear analysis using finite element method. It was noticed that because AASHTO-LRFD bridge design specifications provide skew factors for girders but

not for the deck, hence the current design approach can reasonably estimate the local effect but unable to capture the global effect of truck wheel load. Moreover, the study concluded that the total strain/stress effects due to truck load increase slightly because of skew angle.

Razaqpur et al. (2013) study focused on experimentally investigating a 1/3 scale model of a hypothetical composite bridge to failure with the objective to understand the load distribution characteristics of concrete slab on steel girder composite bridges with the initiation of yielding and inelasticity. The bridge model was 6 m long and was constructed using three W250x39 steel sections spaced at 620 mm and a 70 mm thick reinforced concrete deck slab. The model was loaded with three point loads, representing the load due to the wheels of an idealized 1/3 scaled truck. Extensive measurements, including girder deflections and strains in steel and concrete were recorded during the test to allow better understanding of the structural response of slab-on-girder bridges as well as their live load distribution characteristics. The experimentally determined distribution factors for the tested bridge model were compared with the calculated values based on the Canadian Highway Bridge Design Code (CSA 2000). It was observed that the CHBDC (CSA 2000) gave conservative estimate, on average of 27%, of the moment carried by the loaded girder when compared with the recorded strain values during the test.

Seo et al. (2014) studied the effect of agricultural vehicles on lateral load distribution characteristics of girder bridges on rural roadways in the United States. Five simply supported short-span steel girder bridges with zero skew, which are located on a rural roadway in Iowa, were selected for field tests with four agricultural vehicles and a highway-type truck. Strain sensors were mounted on the bottom flanges of girders at mid-span of all five bridges. Strain data resulting from the test vehicles were measured and used to capture the field responses and to determine experimental distribution factors. Finite element models were calibrated with the field test data by considering agricultural vehicles as live loads. From FEA results analytical distribution factors were computed by performing vehicle-induced model simulations. The analytical distribution factors were compared with those of the field test results and the AASHTO standard and LRFD code equations. Findings revealed that the analytical and experimental distribution factors were

in most cases smaller than code-specified values. However, these factors exceeded code values in some of the cases also.

2.4 Effects of Bridge Parameters on Live Load Distribution Factors

Several previous researchers (Newmark and Siess 1942, Walker 1987, Nutt et al. 1988, Tarhini and Frederick 1992, Kim and Nowak 1997, Mabsout et al. 1997a, Eom and Nowak 2001) have investigated the effect of numerous parameters on live load distribution in slab-and-girder bridges. As a result of these research efforts, girder spacing, span length, and girder stiffness have been determined to be the most significant parameters affecting the distribution characteristics of bridges. The effect of skewed support on the wheel load distribution factor was studied by a number of investigators: (Khaleel and Itani 1990, Bishara et al. 1993, Barr et al. 2001, Menassa et al. 2007, Nouri and Ahmadi 2012, Diab et al. 2011). In-addition to parameters mentioned above, numerous other parameters have also been considered.

2.4.1 Span Length

Bishara et al. (1993) evaluated the distribution factor expressions for the interior and exterior girders of composite slab-on-girder bridges of medium span length. These expressions were derived from finite element analysis of 36 bridges. The results showed that for interior girders, the bridge span length had a slight effect on the distribution of wheel loads. The effect of span length on the load distribution was found more pronounced in bridge geometries with smaller deck widths and skew angles larger than 40° . However, for exterior girders the distribution factor increases with span length, especially for highly skewed bridges. For-example for skew angles of 20° , 40° and 60° resulted in 12%, 20% and 100% increase respectively, of distribution factors.

Khaloo and Mirzabozorg (2003) showed that the load distribution factor of external girders increases with the increase in span length. However, the load distribution factors of internal girders are not very sensitive to span length.

2.4.2 Girder Spacing

Since early work by Newmark (1938), girder spacing has been considered to be the most influential parameter affecting the live load distribution. Newmark and Siess (1942) originally developed simple, empirical equations expressing distribution factors as a function of transverse spacing of beams, span length, and beam stiffness relative to the stiffness of the slab. In a later research (Newmark 1949), the effects of span length and beam stiffness on live load distribution were neglected, and the distribution factors were expressed as a linear function of girder spacing only. These relationships are still incorporated in the AASHTO Standard Specifications with minimal changes since their adoption.

Khaloo and Mirzabozorg (2003) utilized finite element method to analyze the conventional simply supported bridges and concluded that the load distribution factors of external girder increases with the girder spacing. In contrast to the behavior in external girders, the effects of skew angle and girder spacing on load distribution factors of internal girders do not have any co-relations.

2.4.3 Girder Stiffness

Nutt et al. (1988) found there was a significant relationship between girder stiffness and live load distribution. The study concluded that the effect of increase in girder stiffness resulted in increased distribution factor, whereas the increase in span length caused the distribution factor to decrease. The effects of varying torsional stiffness were also evaluated in this study and it was noticed that it had a marginal effect on girder distribution factors (3% difference).

On the basis of FEA results, Yousif and Hindi (2006) demonstrated that the effect of bridge stiffness represented by girder type and slab thickness had a significant impact on bridge distribution factors using both the CHBDC and AASHTO-LRFD simplified methods, therefore it is useful for bridge engineers to understand the effect of selecting the optimum girder type and slab thickness for a specific bridge geometry.

2.4.4 Deck Thickness

Conflicting information exists regarding the effect of the thickness of concrete decks on live load distribution. Newmark (1949) states that deck thickness will affect wheel load distribution as deck thickness will have a direct influence on the relative stiffness.

Although, in the research done by Tarhini and Frederick (1992) bridges with varying slab thickness of 5.5 in. (13.97 cm) to 11.5 in. (29.21 cm) were analyzed and it was found that these changes had a negligible effect on live load distribution.

Nutt et al. (1988) also found that bridge deck thickness had a minimal effect on the load distribution characteristics of the slab-on-girder bridges i.e. about 10% difference was observed in the load effect by changing the bridge slab thickness from 6 in. (15.24 cm) to 9 in. (22.86 cm). This finding was in agreement with Tarhini and Frederick (1992), and among others.

2.4.5 Skew Angle

The skew angle of the deck is the most significant factor affecting the load distribution. Various research studies have demonstrated the influence of skew angle on girder moments and shear forces. For space limitations and brevity purposes, the summary of few previous studies will be presented herein.

- i. Nutt et al. (1988) observed that skew did affect live load distribution. Specifically, increasing skew tends to decrease the wheel load distribution for moment and increase the shear distributed to the obtuse corner of the bridge.
- ii. Bakht (1988) presented a simplified methods of analysis for skew slab-on-girder bridges. The study recommended to ignore the angle of skew and analyze the bridge as a right bridge for skew angle less than 20° .
- iii. Khaleel and Itani (1990) conducted finite element analyses to determine moments in continuous normal and skewed slab-on steel bridges under live loads. The analyses results showed that the maximum moment in the girder of a skewed bridge were found less than that of a normal bridge by approximately 20%.

- iv. Khaloo and Mirzabozorg (2003) demonstrated that the load distribution factors of skew bridges were always less than those of right bridges. This finding is in agreement with the investigations of Bishara et al. (1993), Diab et al. (2011) among others.
- v. Menassa et al. (2007) performed FEA on a simply supported one-span multilane skew reinforced concrete slab bridge. They concluded that the ratio between the FEA longitudinal moments for skewed and straight bridges was almost one for bridges with a skew angle less than 20° . This ratio decreased to 0.75 for bridges with skew angles between 30° and 40° , and further decreased to 0.5 as the skew angle of the bridge increased to 50° .
- vi. Diab et al. (2011) conducted a FEA and the results indicated that the maximum longitudinal bending moment decrease with the increase in skew angle as compared to straight bridges regardless of the number of lanes, span length, and girder spacing. The decrease was trivial for skew angles less than 20° , and increases significantly with the skew angle beyond 30° .
- vii. Nouri and Ahmadi (2012) found that an increase in skew angle caused a reduction in both the exterior and interior support moment girders. The reduction was about 10% for skew angles less than 20° and it reached 33% for a skew angle of 45° .

2.4.6 Length-to-Width Ratio

Diab et al. (2011) reported that the extent of reduction in moment due to skew angle in case of high aspect ratio (long span with fewer lanes) was found significant as compared to the lower aspect ratio (short span with more lanes) which resulted in higher reduction of moment.

2.4.7 Cross-frame Layout and Spacing

Nouri and Ahmadi (2012) found that bridges with transverse diaphragm perpendicular to the longitudinal girders were the best and most economical solution for the design of continuous composite skewed bridges and resulted in significant reduction in moment ratio.

Dilger et al. (1988) studied the effect of diaphragms on the support reactions and internal forces by considering three different arrangements of diaphragms. The study concluded that orthogonal diaphragms performed well for skew aligned bridges. Moreover, in the absence of diaphragms relatively high transverse moments were developed in the vicinity of the obtuse corners, which required an increase in slab thickness in the end zones.

Khaloo and Mirzabozorg (2003) conducted a parametric study and noticed that for bridges with large skew angles, concrete deck with internal transverse diaphragms perpendicular to the longitudinal girders enhance load distribution.

Razzaq et al. (2015) performed a sensitivity study by using three-dimensional finite element modeling for evaluating the most efficient cross-frame layout that provides better load distribution among girders by considering three commonly used cross-frame layouts. The results showed that for high skew angles perpendicular-discontinuous cross-frame layout provided better load distribution among girders by reducing girder displacement significantly.

Kim and Nowak (1997) on the basis of field studies indicated that relatively widely spaced diaphragms lead to more uniform load distribution among girders.

2.4.8 Deck Overhang

For exterior girders, deck overhang showed a linear effect on load distribution (Nutt et al. 1988). This finding has already been incorporated into the LRFD Specifications (AASHTO-LRFD 2014) in the form of a correction factor applied to exterior girders when two or more design lanes are considered. The effect deck overhang width on interior girder was considered negligible.

Barr and Amin (2006) concluded that deck overhang length effected the exterior girder shear distribution factor significantly in comparison to the interior girder.

2.4.9 Secondary Stiffening Elements

Chung et al. (2006) modeled secondary elements such as lateral bracing and parapet using the finite element method, and the calculated load distribution factors were compared with

the LRFD equations. The study concluded that secondary elements enhance the distribution of transverse moment. It was found that the inclusion of secondary elements in the analysis can result in a reduction of LDF of about 39% compared to code specified values.

Mabsout et al. (1997a) concluded that the presence of sidewalks and railings or parapets acting integrally with the bridge deck had the effect of stiffening the exterior girders by attracting more load while reducing the load effects in the interior girders.

2.5 Conclusions

The load distribution factor concept allows the bridge engineers and designers to consider the longitudinal and transverse effects of wheel loads as two separate phenomena and thus simplifying the analysis and design of the bridge. Current North American codes of practice follow simplified methods to determine the forces transferred to individual bridge girders by the use of load distribution factors. These specifications do not provide the design engineers with sufficient guidance regarding load distribution factors for skew composite bridges, resulting in an extremely conservative design in some cases and to unsafe design in other cases. Secondly, the simplified equations recommended in the code specifications are based on simplified model analysis that do not represent the actual behavior of the structure. Based on research efforts and results, many bridge engineers are convinced to adopt three-dimensional finite element modeling to adequately predict stresses at the exterior and interior girders of a skewed bridge. The current research addresses these concerns by better understanding skew bridge behavior and developing design guidelines to facilitate design practice in North America, particularly in Canada. The literature review presented in this chapter covers the main methods used in North American codes to determine load distribution factors in a skewed composite slab-on-girder bridges, and discuss previous research efforts in this regards.

CHAPTER 3

Development of Finite Element Models for Straight and Skew Bridges

3.1 General

The responses of a bridge under dead and live loads are important for both design and evaluation purposes, because they enable the bridge engineer to find the strength and serviceability of a given superstructure with sufficient accuracy. However, predicting the accurate maximum responses and girder load distributions is a difficult task because of the complexity of the bridge structures. The addition of skewness to the bridge geometry further complicates the behavior of slab-on steel I-girder bridges by introducing alternate load paths and causing complex interaction between the main girders and secondary framing members that can lead to significant construction and design problems (Coletti et al. 2011).

Several methods are available for the analysis of bridge structures. In each method some assumptions usually exist in order to facilitate analysis. The accuracy of the analysis obtained by a given method depends on the accuracy of representation of the structure and the extent of the approximations involved in the method. Three most popular computer-aided modelling method for the analysis of steel-concrete composite bridges, as reported in literature are: semi-continuum method, the grillage analogy method, and the finite element method (Jaeger and Bakht 1982, Jaeger and Bakht 1989, Hambly 1990, Zeinkiewicz and Taylor 1989). The semi-continuum method of load distribution analysis of bridges involves representation of wheel loads by harmonic series and the idealization of deck structure by discrete members with torsional stiffness in both longitudinal and transverse directions (Bakht and Jaeger 1985). However, this method proves to be incapable of modeling the diaphragms and orthotropic deck slab for a bridge structure (Bell 1998). In grillage method of analysis, the structure is idealized by means of a series of beam elements. Each element is assigned an equivalent bending and torsion stiffness to represent the associated portion of the deck. The longitudinal composite girders are represented by beam elements with equivalent cross sectional properties that include the steel beam and the concrete flange, while the deck slab is idealized by a series of transverse

beams (Hambly 1990). Although this analysis technique is generally accepted as sufficiently accurate for the most common design situations as well as for the construction stages, however for skewed bridges it results inaccurate assessment of the bridge responses and is not always recommended (Coletti and Puckett 2012, Vayas et al. 2011). With recent developments in computer technology and modern finite element (FE) programs with user friendly graphical interfaces, the finite element method (FEM) proves to be most powerful, versatile and flexible approach for the analysis of composite steel girder bridges (AASHTO/NSBA 2011). Further, literature survey conducted by Sotelino et al. (2004) indicated that more previous researchers adopted finite element method as an analysis tool over the grillage analysis or other simplified methods. For this reason, finite element method was selected as the refined method of analysis to model the three dimensional bridge system using a generalized discretization scheme available in CSiBridge v17.2.0 (CSI 2015) in this study.

3.2 Finite Element Method

The finite element method (FEM) for the analysis of bridge structures is one of the refined methods recognized by the CHBDC (CSA 2014a, 2006a) clause 5.9, for short and medium span bridges, and it is considered to be the most powerful and multipurpose technique. Finite element analyses (FEA) enables bridge engineers to determine the distribution of wheel loads more accurately than empirical formulas specified by bridge codes. Few studies focusing the importance of FEM while dealing with cumbersome and complicated bridge systems related to the evaluation of load distribution factors are presented below:

- i. Mabsout et al. (1997b) carried out an investigation to assess the accuracy and the performance of four different finite element modeling techniques of common use in evaluating the wheel load distribution factors of a straight steel girder bridges. The first model consisted of quadrilateral shell elements with five degrees of freedom per node for the deck slab and space frame elements with six degrees of freedom per node for the girders. The centroid of the concrete deck was coincided with the centroid of the girder cross section. In the second model, the concrete deck and girders were modeled by the same elements used for the first method, however rigid links were imposed to

account for the eccentricity of the girders with respect to the deck slab. For the third model, the concrete deck slab and steel girder web were idealized as quadrilateral shell elements, girder flanges were modeled as space frame elements, while girder flange to deck eccentricity was modeled by imposing a rigid link. The concrete slab was idealized using isotropic eight node brick elements with three degrees of freedom at each node for the fourth model, while the steel girders were modeled using quadrilateral shell elements. Results indicated that when dealing with straight bridges the use of quadrilateral shell elements for modeling the concrete deck and concentric space frame elements for modeling the girders is encouraged. The other FEA cases could be adopted to accurately idealize the more complex bridge geometries.

- ii. In order to analyze the bridge superstructure under working load conditions, Fu and Lu (2003) simulated the composite deck girder interaction by using a finite element model. The girders were discretized with traditional eight-node isoparametric quadrilateral elements adopted from Cook et al. (1989), while the flanges of the girder were modeled using plate elements and the web with plane stress elements. To simulate the shear studs, bar elements were used to provide a dimensionless link between the concrete deck and the top flange of the girders. With the help of the computer program RESIDU and with the results from previous experimental studies (Yam and Chapman 1972) the numerical model was evaluated. The deflections along a test bridge were compared to those obtained using classical transformed area method. The FEM results were found very close to the experimental study results but considerably far from those obtained with the transformed area method.
- iii. Huang et al. (2004) conducted research to estimate the transverse load distribution for highly skewed steel girder bridges by means of both experimental and numerical analysis. The field test was conducted to measure strains at different points along a 60° skewed bridge by passing two fully loaded trucks over it. The three dimensional analytical finite element model was implemented by using ANSYS software package. Four node three dimensional elastic shell elements with six degrees of freedom per node were used to model the concrete slab and the girders, while the crossframes were modeled with two node three dimensional elastic beam elements with six degrees of freedom per node. The boundary constraints at both the end supports were imposed to

restrict translational displacements except for the longitudinal direction. However, for the intermediate support all the displacements were restrained. No rotational constraint was considered. The overhangs and parapets were ignored. The FEA results were compared with AASHTO-LRFD design formulas for live load distribution to assess the accuracy of the current empirical formulas. The results showed that AASHTO-LRFD formulation tends to be safely conservative for positive bending and for negative bending they are accurate but not conservative.

3.3 Finite Element Program

There are many commercial finite element software programs for structural engineering applications. The specialized FEA program, CSiBridge (CSI 2015), was used to generate the 3D finite element models. CSiBridge is an object-based interface that converts bridge objects to a finite element model to be analyzed using SAP2000 (CSI 2007). It is capable of analyzing structures in static and dynamic modes. The various element types available are:

- i. *Frame element*: The frame element is a two-node three-dimensional element, which includes the effect of biaxial bending, tension, axial deformation and biaxial shear deformation.
- ii. *Shell element*: The shell element is a four-node three-dimensional element, which combines both bending and membrane characteristics. The four-node shell element has six degrees of freedom at each node that are the three displacements (U_1, U_2, U_3) and three rotations (ϕ_1, ϕ_2, ϕ_3). A detailed diagram of the shell element is presented in Figure 3.1. The membrane behaviour includes translational in-plane stiffness components and rotational stiffness component in the direction normal to plane of the element. The plate bending behaviour includes two-way, out of plane, plate rotational stiffness component in the direction normal to the plane of the element. The program allows using pure membrane, pure plate or full shell behaviour.
- iii. *Solid element*: The available solid element is an eight-node three-dimensional element which includes nine optional incompatible bending modes. The solid element

contributes stiffness in all three translational degrees of freedom at each of its connected joints.

- iv. *Nlink element*: A NLink element is one-dimensional element with structural nonlinearities. A NLink element may be either a one-joint grounded spring or a two-joint link and is assumed to be composed of six separate springs, one for each degree of deformational degrees of freedom including axial, shear, torsion and pure bending. Non-linear behaviour can be supported by NLink during nonlinear time-history analyses or nonlinear static analyses.

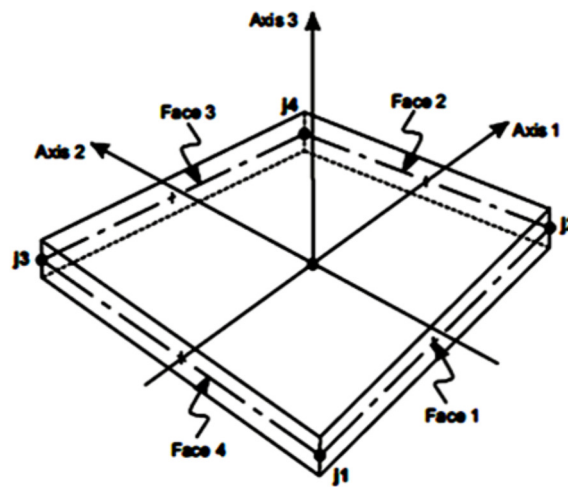


Figure 3.1 Four node shell element

3.4 Finite Element Bridge Modeling

The finite element technique was adopted to model composite skewed concrete over steel I-girder bridges. Three-dimensional finite element models were constructed in a way to represent the actual physical structural geometry, boundary conditions, load locations, and material properties of the bridge components, namely: reinforced concrete for the deck slab and steel for the webs, bottom flange, diaphragms and cross bracings. The following subsections explain the element type selected for each component, the material modeling, and the boundary conditions used in the developed finite element models (FEM) were described below.

3.4.1 Material Modeling

The material properties are very important component in developing FEM to define in order to get accurate results. The bridge slab is made of reinforced concrete while the rest of the I-girder and angle section diaphragms is made of steel. The elastic material properties of these materials are defined and used throughout this study.

The bridge structure was idealized using the following assumptions: (1) all materials were elastic and homogeneous; (2) the effects of road super-elevation and curbs were ignored; and (3) the reinforced-concrete deck slab and the supporting steel I-girders were in full composite action; (4) both the deck slab and the supporting I-girders were simply supported at the abutments; (5) intermediate cross-braces were moment-connected to the longitudinal girders. The typical cross-section of a two-lane and four-lane composite steel I-girder bridge is shown in Figure 3.2.

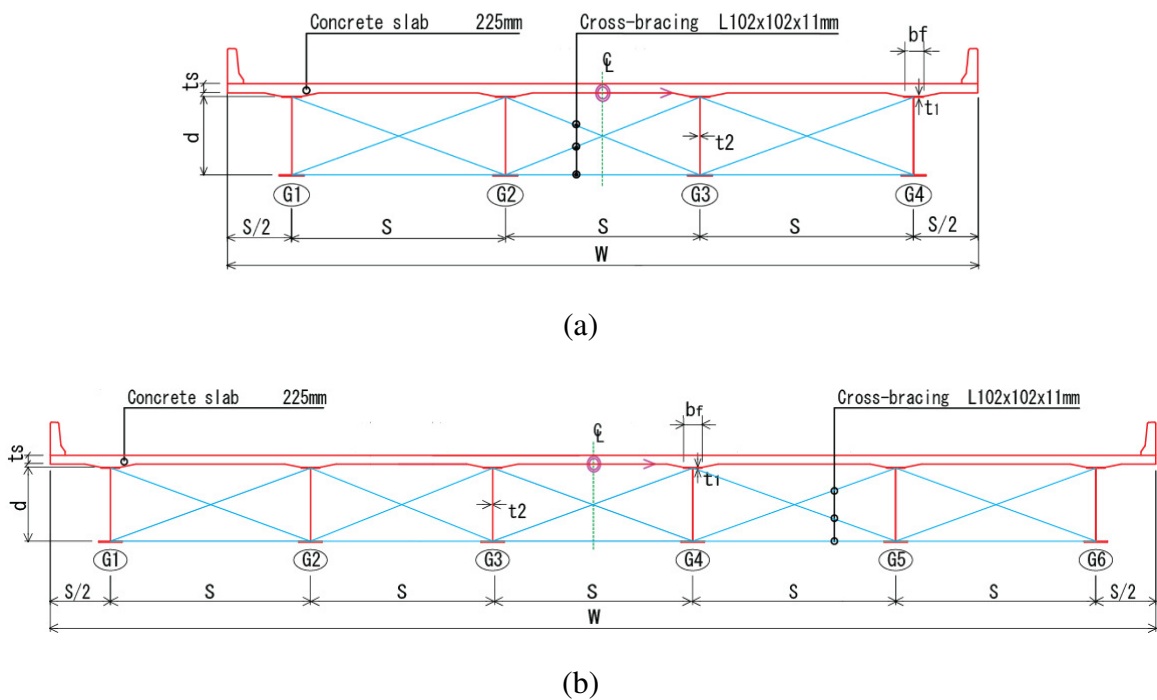


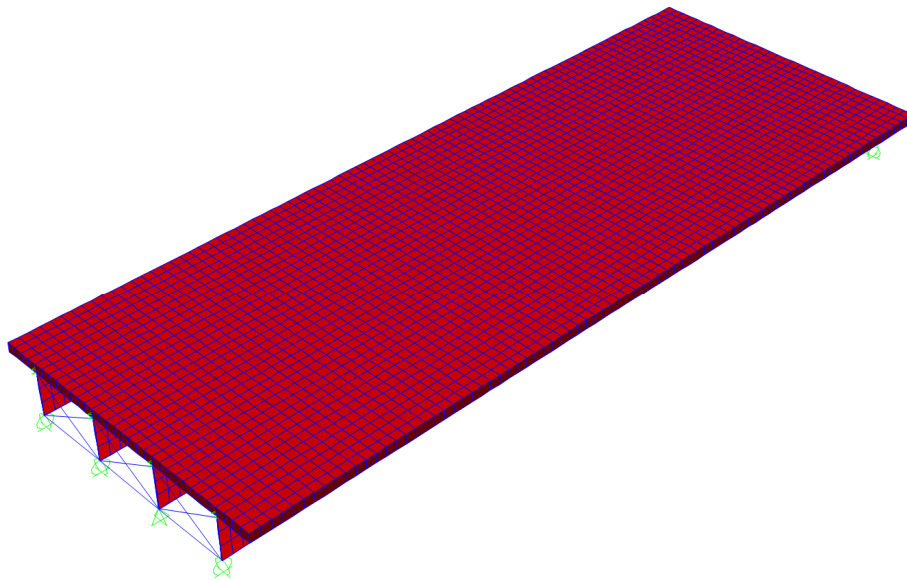
Figure 3.2 Cross-section diagram of a concrete slab over steel I-girder bridge for: (a) two-lane, and (b) four-lane

The concrete deck slab thickness was 225 mm. The over-hanged slab length was equal to half the girder spacing. The steel I-girders and X-type cross-frames at the support and between the span was provided in accordance with the specification stipulated in the manual of standard short-span steel bridges (Theodor and Al-Bazi 1997). Based on a sensitivity study discussed in section 3.6.1.2, cross-frame members were spaced at equal intervals between the support lines and were made of L102x102x11 steel angles. Moreover, cross-frames were oriented in a parallel layout for the skew angle less than 30°, however for higher skew angles (from 30° to 60°) perpendicular discontinuous layout was used (Razzaq et al. 2015).

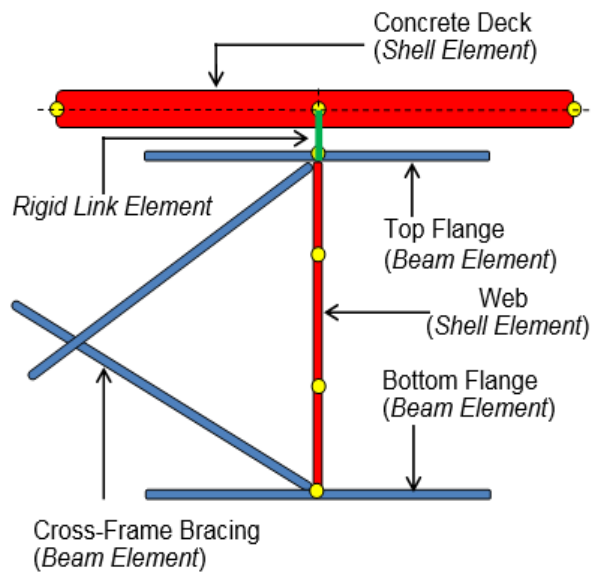
Cracking of concrete was not considered. The reason for assuming linear elastic properties of the concrete and steel was that the stresses due to temperature changes were not high as suggested by CHBDC (CSA 2014a). Thus, it was not necessary to consider the material nonlinearity. The modulus of elasticity of the concrete material was 25 GPa with a Poisson's ratio of 0.20, whereas these design values for the steel material were 200 GPa and 0.30, respectively.

3.4.2 Geometric Modeling

A three-dimensional finite element model was developed to simulate each of the bridges considered in this study. The concrete deck slab and web of steel girders were modeled using four-node three-dimensional elastic shell elements with six degrees of freedom at each node. The top and bottom flanges of longitudinal steel girders were modeled using two-node three-dimensional elastic beam elements with six degrees of freedom at each node. The transverse diaphragm cross-frames were simplified and modeled using the same beam elements. Rigid link elements were used to model the composite action between the deck slab and the girders by connecting the nodal degrees of freedom of the beam to those of the shell element. Thus the displacements in the beam element are dictated by those in the shell element. There is one incompatibility in the form of shear slip at the beam-slab interface in this model. Marx et al. (1986) claimed that this incompatibility is not important in a slab-on-girder bridges. Details of the finite element modeling of composite girder with cross-frame are shown in Figure 3.3.



(a)



(b)

Figure 3.3 Details of the three-dimensional finite element modeling for: (a) bridge structure, and (b) composite girder with cross-frame

3.4.3 Boundary Condition

One of the crucial parameters for the success of structural analysis is the proper characterization of the boundary conditions of the system. Behavior of abutments at the support point must be examined and properly implemented into the structural analysis model. For the static analysis, it is common to use a simple representation of support (e.g., fixed, pinned, roller) without characterizations of the soil-structure interaction. Each bearing support was assumed to be located at the centroid of the beam element representing the bottom flange of the girder in such way to simulate temperature-free bridge superstructure (Lee 1994). For a single span bridge, one of the middle supports on the right end of the bridge was restrained against all possible translations (longitudinal, vertical and lateral), and on the left side, one of the middle supports was restrained against vertical and lateral translations. However, the rest of supports at both ends were restrained against vertical translations only. Figure 3.4 shows typical boundary conditions considered for two-lane and four-lane bridges respectively.

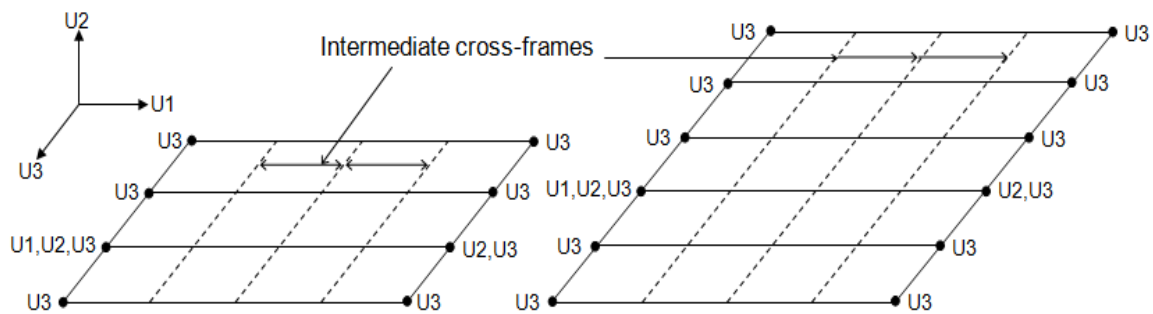


Figure 3.4 Boundary condition for single-span bridge model for: (a) two-lane, and (b) four-lane

3.4.4 Aspect Ratio

The aspect ratio is defined as the ratio of the longest dimension to the shortest dimension of a quadrilateral element. In many cases, as the aspect ratio increases, the inaccuracy of the solution increases (Logan 2002). To improve the accuracy of the finite element modeling and to make the design more efficient and cost-effective, the aspect ratio of the shell elements was adjusted less than 4. Logan (2002) proved that as the aspect ratio rises above 4, the inaccuracy of the solution increases.

3.4.5 Live Load Modeling

The live load, as specified in CHBDC (CSA 2014a), consists of CL-W truck and CL-W lane loading. The CL-W truck consists of idealized five axles with total load of 625 kN as shown in Figure 3.5. The CL-W lane loading consists of CL-W truck loading with each axle load reduced to 80% of its original value and superimposed within uniformly distributed load of 9 kN/m over 3 m width. The selection between two different CHBDC types of live loads i.e. CL-W truck and CL-W lane, depends on whichever gives the greatest design values. Both CL-W loadings were considered in an extensive sensitivity study, mentioned in the forthcoming section 3.6.3. The study revealed that the CL-W truck loading increased the girder response as compared to CL-W lane load, and accordingly considered in parametric study analysis thereafter.

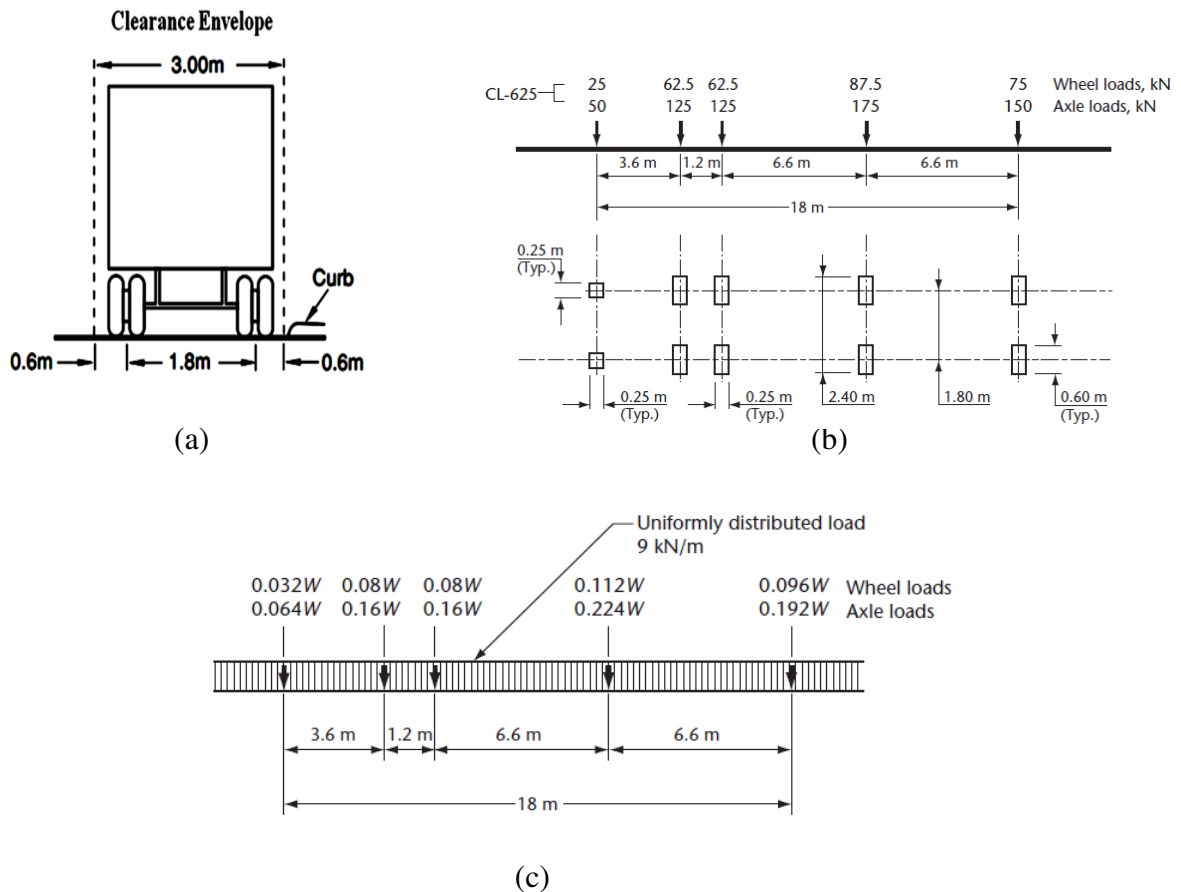


Figure 3.5 CHBDC truck loading: (a) CL-W truck clearance, (b) CL-W truck load, and (c) CL-W lane load. (Reproduced from CHBDC (CSA 2014a))

3.5 Validation of Finite Element Modeling

To verify the validity of the finite element modeling technique presented in this chapter, physical load test data from the field testing was compared against the results of a finite element model of the traditional and integral abutment bridges using the described modeling technique. Contained herein is a brief description of this bridge and its field testing as well as the comparison of the finite element data and the field test data.

3.5.1 Validation of Skewed Slab-on-Girder Bridge

For validation purposes, the first high-performance steel (HPS) two-span skewed continuous bridge (Missouri Bridge A-6101) built in Missouri, constructed by Missouri Department of Transportation (MoDOT) in 2002 as part of the Federal Highway Administration's (FHWA) innovative bridge research and construction program was considered. The bridge is located on Route 224 in Lafayette County, Missouri. On August 20, 2002, field testing of Missouri Bridge A-6101 was conducted by the University of Missouri–Columbia and West Virginia University in cooperation with the Missouri Department of Transportation (MoDOT) (Wu 2003).



Figure 3.6 Elevation view of Missouri A-6101 bridge (Reproduced from Wu 2003)

Figure 3.6 shows an elevation view of this bridge. The design calculations and dimensions presented in the plans for Missouri Bridge A-6101 are in metric units. Figure 3.7 shows

the cross-sectional view of the Bridge A-6101 with information regarding bridge width, girder spacing, number of girders, deck slab thickness and deck overhang length. Also, the bridge's framing plan can be seen in Figure 3.8. For brevity purposes only the details related to calibration of the finite element model is presented herein, however more details about the Missouri Bridge A-6101 can be found elsewhere (Davis 2003, Wu 2003).

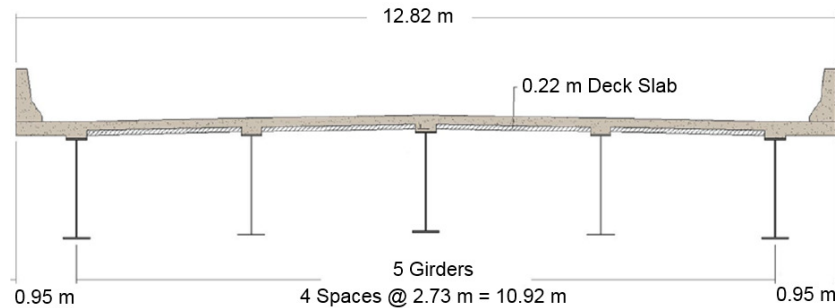


Figure 3.7 Missouri bridge A-6101 cross-section (Reproduced from Wu 2003)

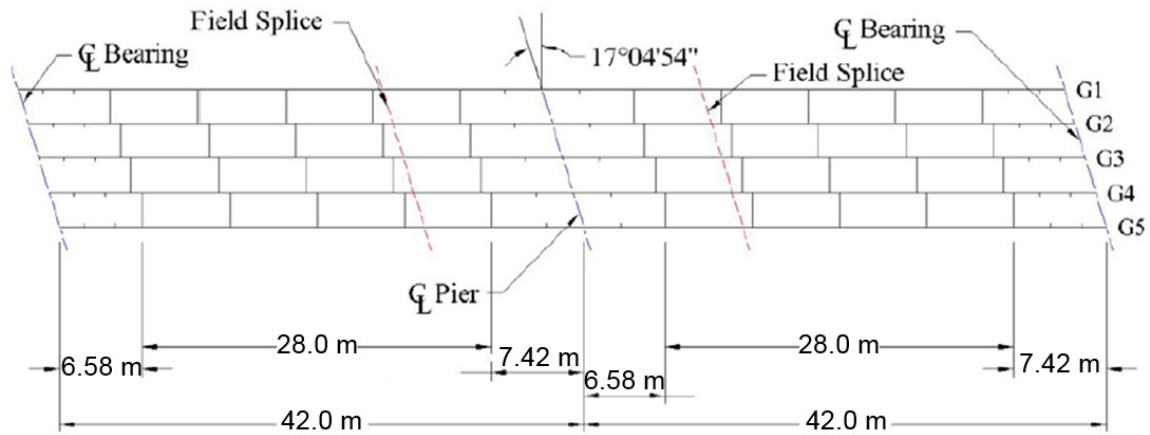


Figure 3.8 Missouri bridge A-6101 framing plan (Reproduced from Wu 2003)

3.5.1.1 Instrumentation

For the purposes of verifying the finite element modeling technique presented in this Chapter, only instruments pertaining to measuring deflection values are discussed herein.

Two different devices for measuring vertical displacements were employed during this field test. The first was a set of string potentiometers, or “string pots”, placed directly below

each girder at the 0.4L point of each girder or 16.8 m (55.1 ft.) from the east bearing. These were used in lieu of conventional linear variable differential transformers (or LVDTs) due to the height of the girder from the ground. However, after interpreting the data from the string pots after the field test, the team concluded that the string pots were malfunctioning during the field test and any data derived from these were not used.

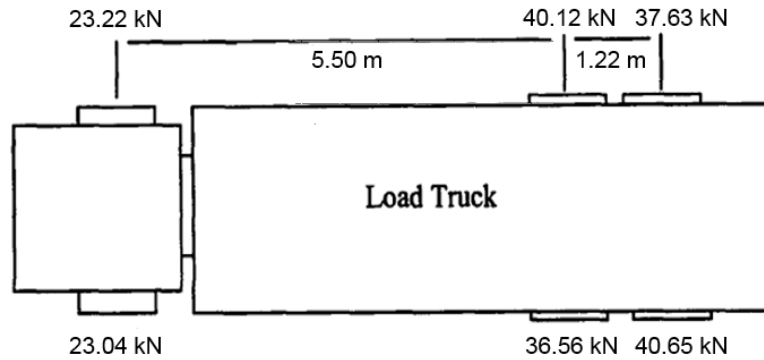
The second device was a laser deflection system developed by the Civil Engineering Department at the University of Missouri–Columbia. The live load deflection of girder 2 was measured using a set of laser devices with a helium neon laser installed on a tripod and a deflection device installed on girder 2 of the second span. The laser was aimed at a deflection device attached to girder 2 at 0.4L of the respective girder, which acted as a reference point as the bridge deflected. Relative deflections were measured and recorded for girder 2 during the field test. After subsequent analysis by the field test team, it was determined that the laser deflection device performed very well. However, after the eighth truck run, the laser device stopped taking measurements. This was reasonable, as the laser needed to be precisely aimed at the deflection device on the girder. As can be seen from Figure 3.6, conditions on the ground on the day of field testing were quite muddy; this could have possibly caused the tripod to go out of a level position and, therefore, cause defective operation.

3.5.1.2 Load Truck

The vehicle used to load the bridge was a 1984 Freighliner block and brick truck owned by the Civil Engineering Department of the University of Missouri (Davis 2003). Steel blocks were used to load the test truck to increase its weight for the load testing. After the static deflection testing procedure was completed, weighing pads were used to determine the truck's individual wheel weights. A photograph of the load truck is shown in Figure 3.9, along with pertinent truck dimensions and each wheel's individual weights.



(a)



(b)

Figure 3.9 Missouri bridge A-6101: (a) Load truck, and (b) truck dimensions with wheel loads (Reproduced from Wu 2003)

3.5.1.3 Truck Runs

To obtain deflection values that were representative of static loading, the load truck was run across the bridge as slow as possible to reduce impact. For each run, the truck began on the east approach, traveled completely across the bridge, then made the same pass in reverse back to the east side. This process was completed twelve times. For each run, the truck maintained a constant distance transversely across the bridge. These distances are illustrated in Figure 3.10, and tabulated in Table 3.1.

Table 3.1 Missouri bridge A-6101 truck run positions

Distance from center of driver's side wheel to curb	
Truck Run	Distance (m)
1	2.13
2	3.27
3	4.78
4	5.18
5	6.00
6	6.32
7	7.51
8	7.83
9	8.65
10	9.05
11	10.56
12	Face of South Parapet

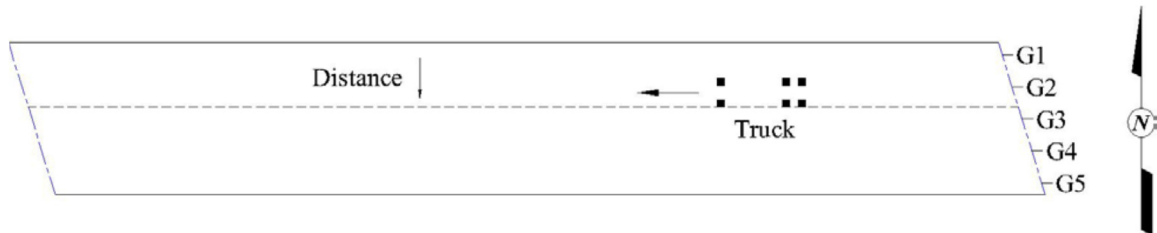


Figure 3.10 Missouri bridge A-6101 truck run scheme (Reproduced from Wu 2003)

3.5.1.4 Comparison of Results

Presented in Figure 3.11 is a comparison of both the physical data from the field test of Missouri Bridge A-6101 along with the data from the bridge's finite element model. Out of the twelve different truck positions on the bridge span, the girder deflection values for eight truck positions were reported as they were determined by the test team to be the most accurate (Wu 2003). The comparison indicates that this finite element modeling technique is quite accurate in predicting bridge system behavior and girder response with the largest difference in values is only 0.4 mm, equivalent to a 5% difference.

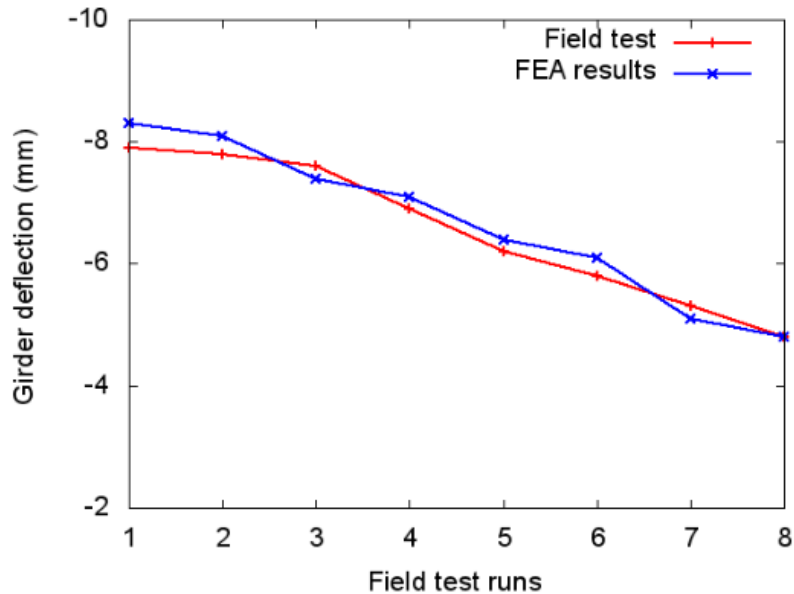


Figure 3.11 Validation of live load field testing with finite element modeling results

3.6 Evaluation of Skewed Bridge Parameters by Sensitivity Study

The following section describes the effect of the various design parameters using finite element analysis to determine their sensitivity on the load distribution of steel I-girder bridges. A description of the procedures used to develop the parametric bridges is presented. Finally, the results of the sensitivity study are discussed, focusing the influence of the varied parameters.

The following sensitivity studies are carried out to estimate the effect of the following parameters on the load distribution of skewed composite concrete over steel I-girder bridges.

1. Cross-frame Design
 - i. Cross-frame Layout
 - ii. Cross-frame Spacing
2. Sequence of Construction
 - i. Un-shored Construction
 - ii. Shored Construction.
3. Effect of CHBDC vehicular load type

4. Estimation of Longitudinal Flexural Stiffness of Steel I-girder.
5. Assessment of Multi-lane Truck Loading Condition.

3.6.1 Cross-frame Design

Behavior of skewed bridges is much more complicated than straight aligned bridges with normal supports due to the complex interaction between the steel girders and the cross-frames. This interaction generate large forces in the cross-frames under the truck live loads, thereby augment fatigue cracks commonly found around locations of cross-frames during routine maintenance inspections (Yura et al. 1992, Helwig et al. 1993, Helwig and Wang 2003). The severity of the fatigue problem is dependent on the layouts that are used for the cross-framing. In-addition, cross-frames provide stability to the girders as well as improving the lateral or torsional stiffness of the bridge system. Depending on the geometry of the bridge, in many situations the removal or inadequate cross-frame spacing can result in a partial or complete collapse of the structure. This module provides an overview of the design requirements of the braces so that engineers can properly size the members to ensure adequate strength and stiffness.

3.6.1.1 Cross-frame Layout

The CHBDC (CSA 2014a) and AASHTO-LRFD Bridge Design Specifications (AASHTO-LRFD 2014) allow cross-frames to be parallel to the support line when the skew angle is less than 20° . However, for skew angles greater than 20° , both design specifications require the cross-frames to be perpendicular to the longitudinal axis of the girders. Previous studies reported that the evaluation of the effect of cross-frames layout in skew composite concrete slab-over steel I-girder bridges on load distribution among girders is as yet to be assessed (Fraser et al. 2000, Barth and Bowman 2001, Hartman et al. 2010).

In order to estimate the effectiveness of the cross-frame layout with the variation of the skew angle three cross-frame layouts, shown in Figure 3.12, commonly used in skewed bridges are considered, namely: parallel cross frames to the skew support lines (parallel layout), perpendicular cross-frames to the longitudinal girder axes (perpendicular-

continuous layout), and perpendicular cross-frames to the longitudinal girder axes with staggered arrangement between girders (perpendicular-discontinuous layout).

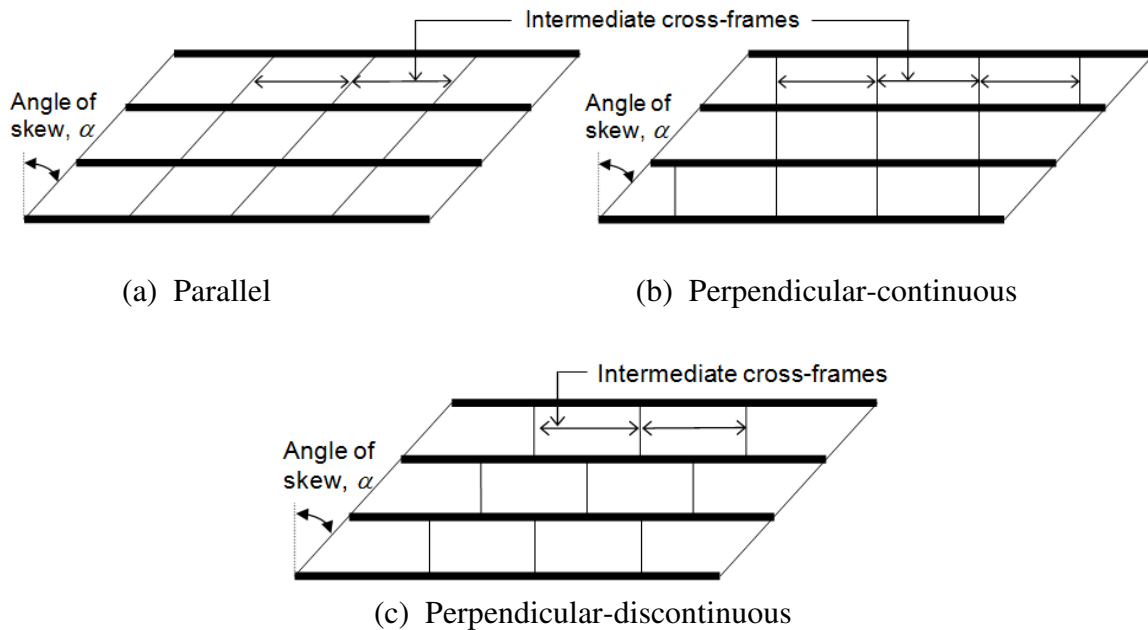


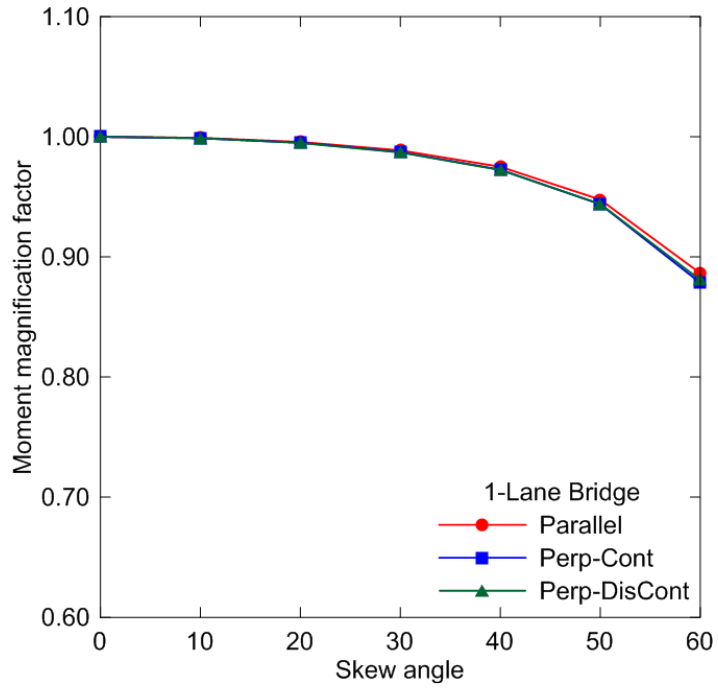
Figure 3.12 Cross-frame layouts for bridges with skewed supports for (a) parallel configuration, (b) perpendicular-continuous configuration, and (c) perpendicular-discontinuous configuration

Table 3.2 Parameters considered for cross-frame layout

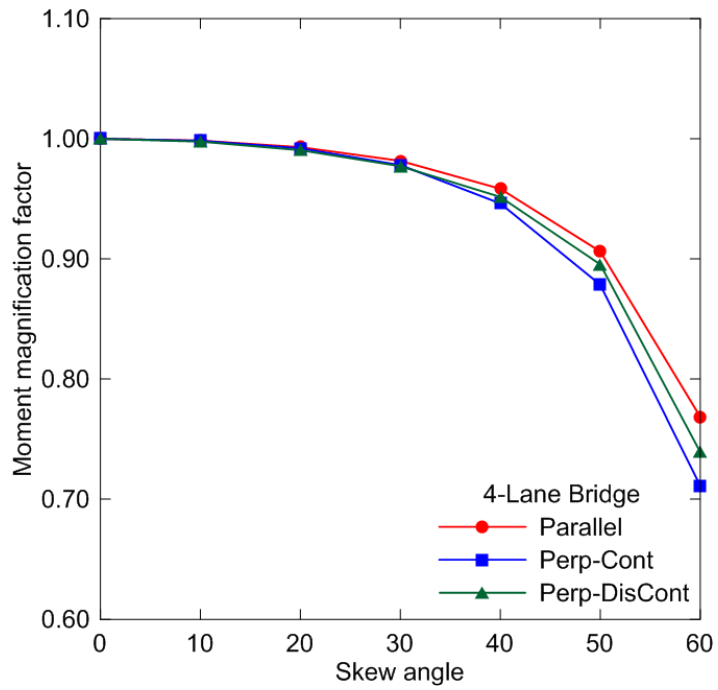
Parameters considered	Range of Parameters
No. of Lanes	1-Lane (6 m) & 4-Lane (18 m)
Cross-frame Layouts	<ul style="list-style-type: none"> • Parallel • Perpendicular-continuous • Perpendicular-discontinuous
Skew angle	0, 10, 20, 30, 40, 50 and 60°
Girder spacing (m)	1.5 m & 3 m

Previous research attempts regarding cross-frames layout perpendicular to the girder line (continuous and discontinuous) is not conclusive as to which layout performs better with respect to effective load sharing among girders and curbing differential vertical displacement at the two ends of the cross-frame. The objective of the current study was to investigate the effectiveness of cross-frame layout in skew composite concrete deck-over steel I-girder bridges under a uniform distributed load of 10 kN/m^2 by conducting three-dimensional (3D) finite element modeling. For brevity purposes, the finite element results in terms of magnification factors for girder longitudinal bending moment and vertical support reactions are presented herein. Further details and parameters considered in this study can be seen elsewhere (Razzaq et al. 2015). Table 3.2 presents the basic cross-sectional configurations considered.

The longitudinal bending moments for the interior and exterior girders of multi-lane bridges were evaluated and the corresponding magnification factors (M_o/M_o) are presented in Figure 3.13 and 3.14, respectively. The FEA results of an interior girder of multi-lane bridges shows that for one-lane bridge, all cross-frame layouts resulted in about 12% decrease in longitudinal internal girder moment with a skew angle varying between 0° to 60° . Whereas, for four-lane bridge, all cross-frame layouts experienced a similar trend of 2% decrease of internal girder moment up to a skew angle of 30° . Subsequently for a skew angle between 30° to 60° , this reduction in the internal girder moment was found more prominent and resulted in a decrease of 23%, 29% and 25% for parallel, perpendicular-continuous and perpendicular-discontinuous cross-frame layouts respectively. However for exterior girder moment, FEA results showed a marginal effect for different cross-frame layouts for skew angle between 0° to 60° .

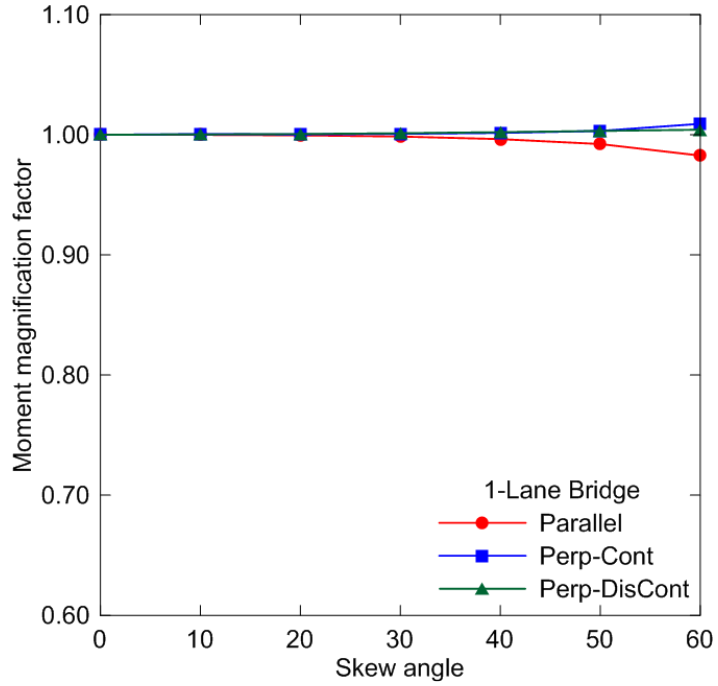


(a)

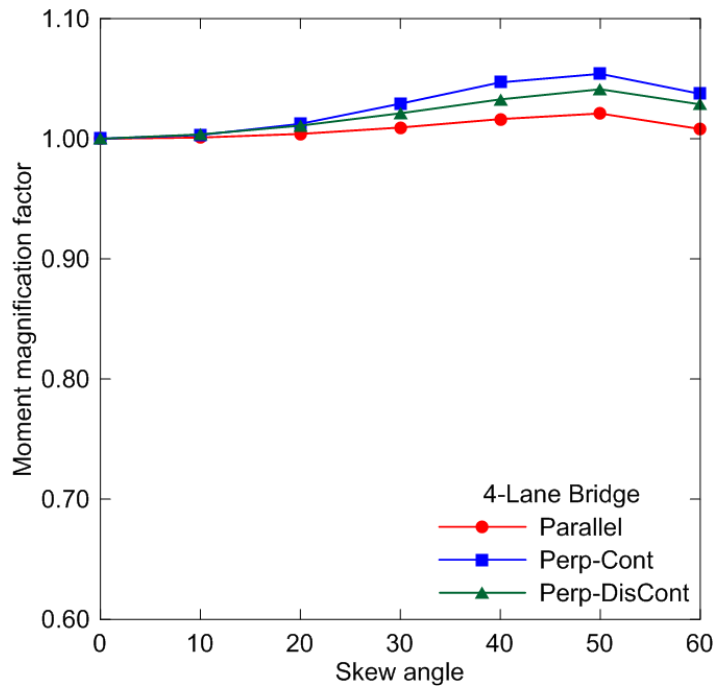


(b)

Figure 3.13 Moment magnification factor for interior girders for: (a) one-lane, and (b) four-lane



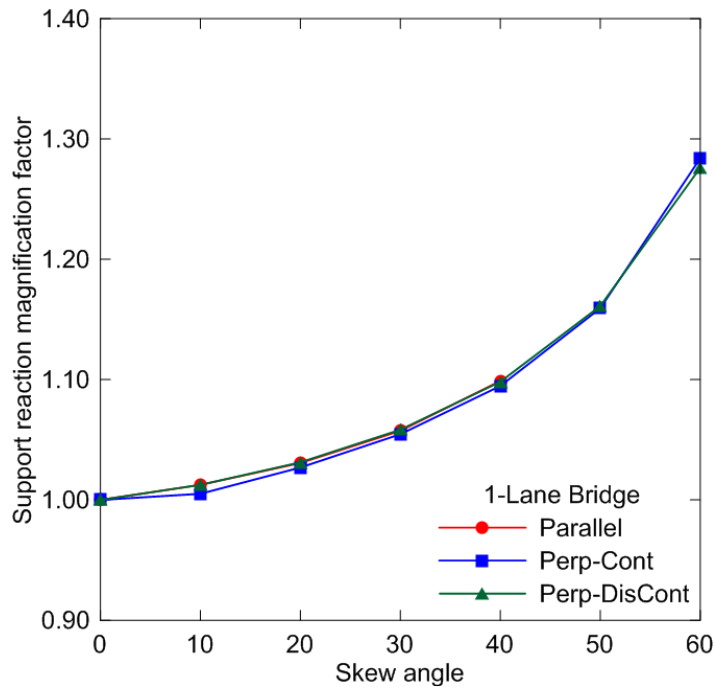
(a)



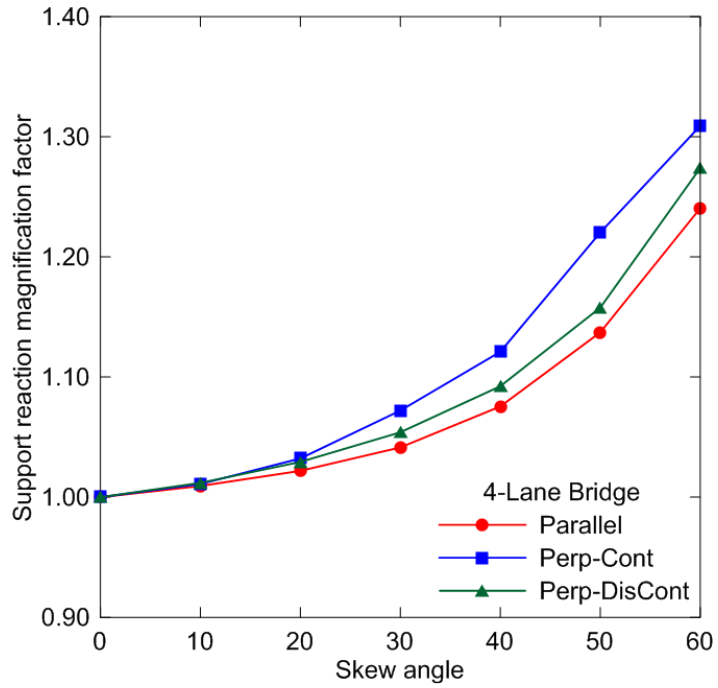
(b)

Figure 3.14 Moment magnification factor for exterior girders for: (a) one-lane, and (b) four-lane

In skewed bridges the behavior of the structure near the bearings particularly at the obtuse corner requires special consideration. Figure 3.15 shows the support reaction at obtuse corners for one-lane and four-lane bridge system in term of magnification factor (R_a/R_o). The results showed that for one-lane bridge system, all cross-frame layouts resulted in a 6% increase in exterior girder support reaction at obtuse corner for skew angle up to 30°. However, an increase of 22% is obtained beyond 30° up to 60° skew angles. For four-lane bridge system, a maximum of 7% increase in support reaction was observed at 30° skew angle for perpendicular-continuous cross-frame layout. However for skew angles in the interval of 30° to 60°, the support reactions resulted in an increase of 21%, 26% and 23% for parallel, perpendicular-continuous and perpendicular-discontinuous cross-frame layouts respectively. Figure 3.16 revealed that cross-frame layouts have insignificant effect on acute corner support reaction with the variation of skew angle for both bridge configurations.

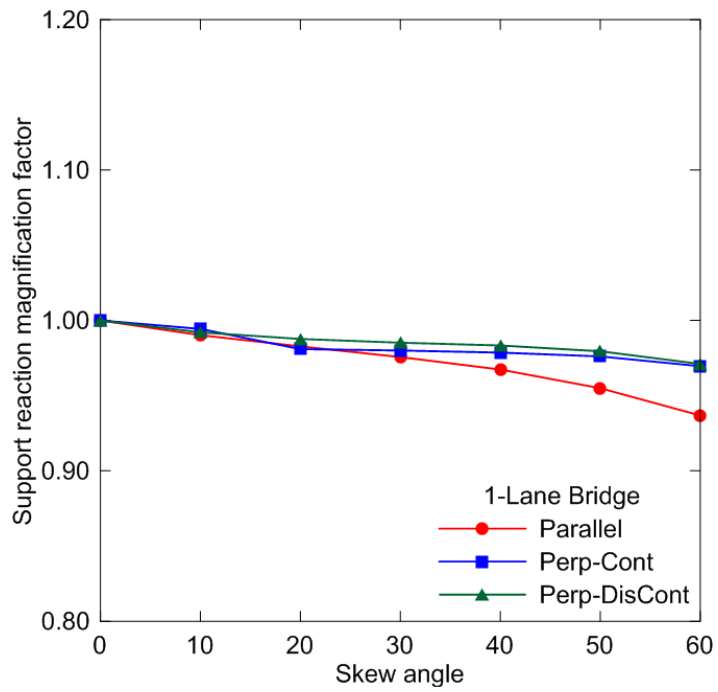


(a)

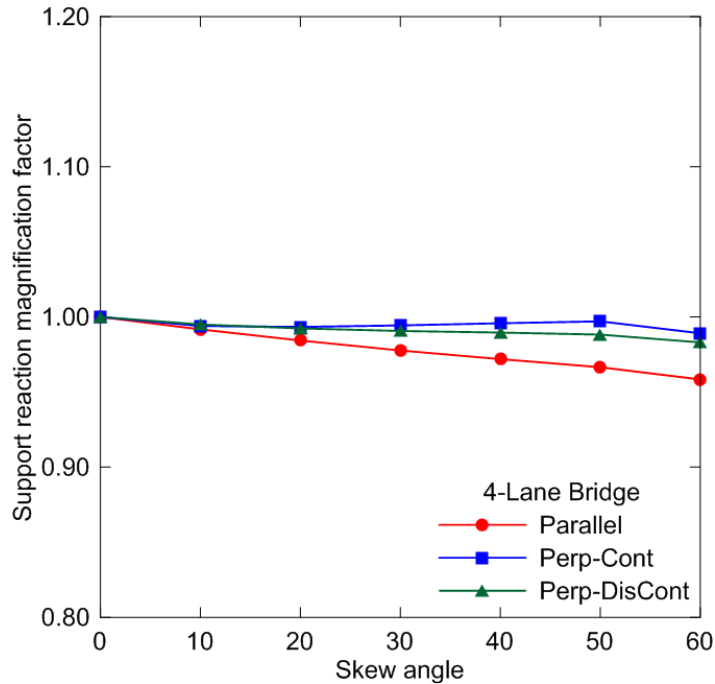


(b)

Figure 3.15 Reaction magnification factor at obtuse corners for: (a) one-lane, and (b) four-lane



(a)



(b)

Figure 3.16 Reaction magnification factor at acute corners for: (a) one-lane, and (b) four-lane

Moreover, the FEA results revealed that the differential vertical displacement at the obtuse corners of the intermediate cross-frame members increased significantly in case of perpendicular-continuous cross-frame layout in comparison with parallel and perpendicular-discontinuous layouts for multi-lane bridges, as shown in Figure 3.17. Furthermore, the result showed that at high skew angle, perpendicular-discontinuous layout performed well in reducing the differential vertical displacement at the cross-frame ends significantly.

By varying the parameters of bridge geometry i.e. number of lanes or bridge width, number of girders, girder spacing and skew angles, the responses of a skewed bridge were computed and compared to the reference three-dimensional FEA straight bridges. The FEA results showed that the computed responses have insignificant effect with the change of skew angle up to 30°. For that reason, parallel cross-frame layout can be employed for skew angles up to 30°. However, for high skew angles (between 30° to 60°) perpendicular-

discontinuous cross-frame layout provides better load distribution among girders by significantly reducing the girder displacement.

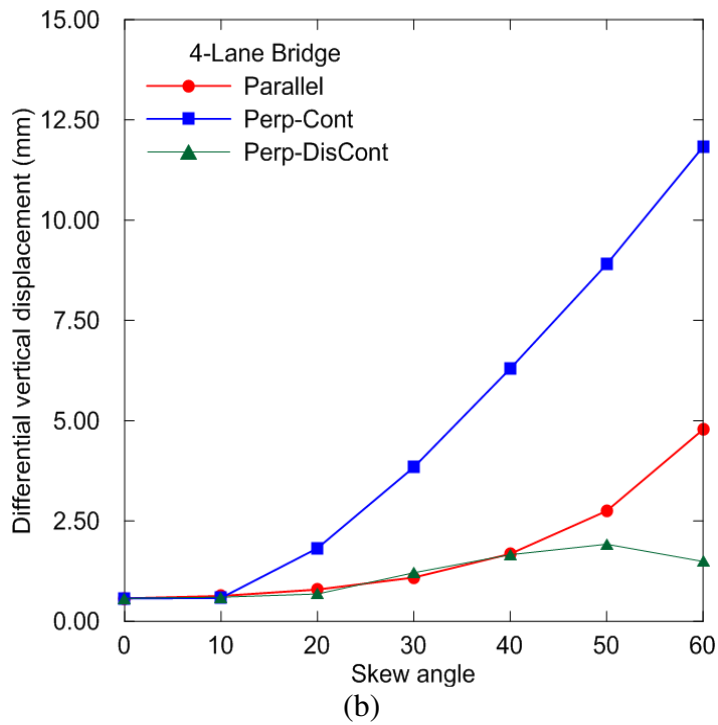
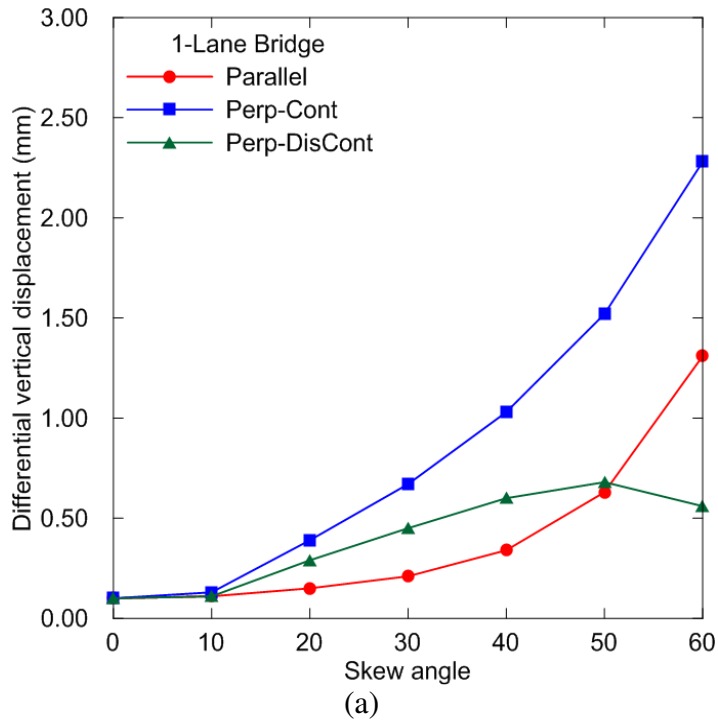


Figure 3.17 Differential displacement of cross-frame end members: (a) one-lane, and (b) four-lane

3.6.1.2 Cross-frame Spacing

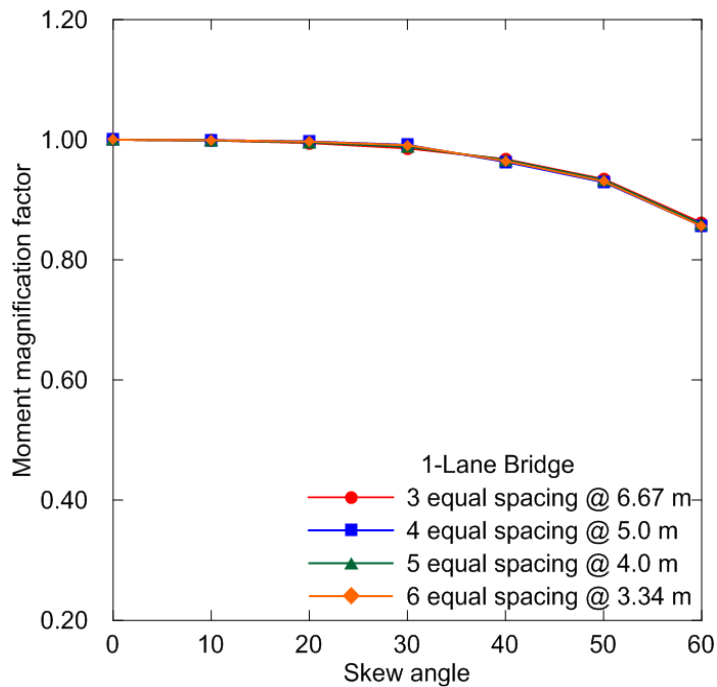
Cross-frames and diaphragms are relatively costly structural components in steel bridges from the perspective of both fabrication and erection. The braces can be difficult to install in bridges due to fit-up problems and may also attract significant live load forces, particularly in bridges with large support skews. Therefore, minimizing the number of cross frames in bridges can be an objective for better overall bridge behavior as well as for reduced cost effectiveness. The typical practice in steel bridge construction is to place cross-frames between each of the girders at a uniform spacing along the length (Helwig and Yura 2012).

The CHBDC (CSA 2014a), clause 8.18.5 states: “Steel I-girder supporting deck slabs designed in accordance with the Empirical Design Method of clause 8.18.4 shall have intermediate cross-frames or diaphragms at a spacing not greater than 8.0 m center-to-center”. Although cross-frames and diaphragms are critical elements for girder stability, the current AASHTO specifications do not provide guidelines for the basic bracing requirements. For several decades, the AASHTO specifications limited the maximum cross-frame spacing to 7.6 m (25 ft.). This spacing limit is still in effect in the AASHTO Standard Specification (AASHTO 1996); however the limit was removed from the AASHTO-LRFD specifications (AASHTO-LRFD 2014) due to fatigue concerns associated with the bracing details. The commentary in the LRFD code specifications (AASHTO-LRFD 2014) instead specifies that engineers need to design the braces by rational analysis, however no guidance is provided for the requirements of such an analysis.

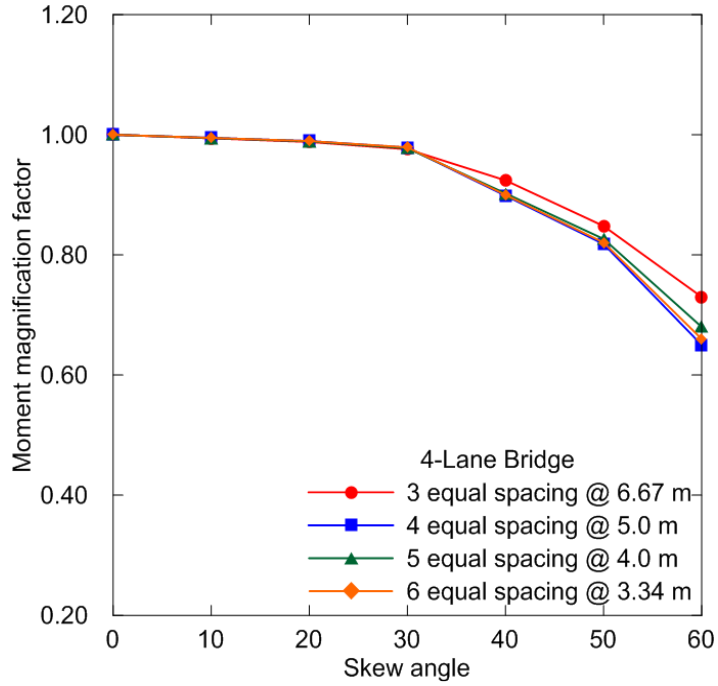
The objective of the current study aims at investigating the effectiveness of cross-frame spacing in skew composite concrete deck-over steel I-girder bridges under a uniform distributed load of 10 kN/m^2 by conducting three-dimensional finite element modeling. The finite element results are presented in terms of magnification factors for girder longitudinal bending moment and vertical support reactions for skew angle ranging from 0° to 60° . Table 3.3 presents the basic cross-sectional configurations considered in the analysis.

Table 3.3 Parameters considered for cross-frame spacing

Parameters considered	Range of Parameters
Span length	20 m
No. of Lanes	1-Lane (6 m) & 4-Lane (18 m)
Cross-frame spacing	3 equal spacing @ 6.667 m 4 equal spacing @ 5.0 m 5 equal spacing @ 4.0 m 6 equal spacing @ 3.334 m
Cross-frame Layouts	<ul style="list-style-type: none"> • Parallel for skew angle < 30° • Perpendicular-discontinuous for skew angle > 30°
Skew angle	0, 10, 20, 30, 40, 50 and 60°
Girder spacing (m)	1.5 m & 3 m

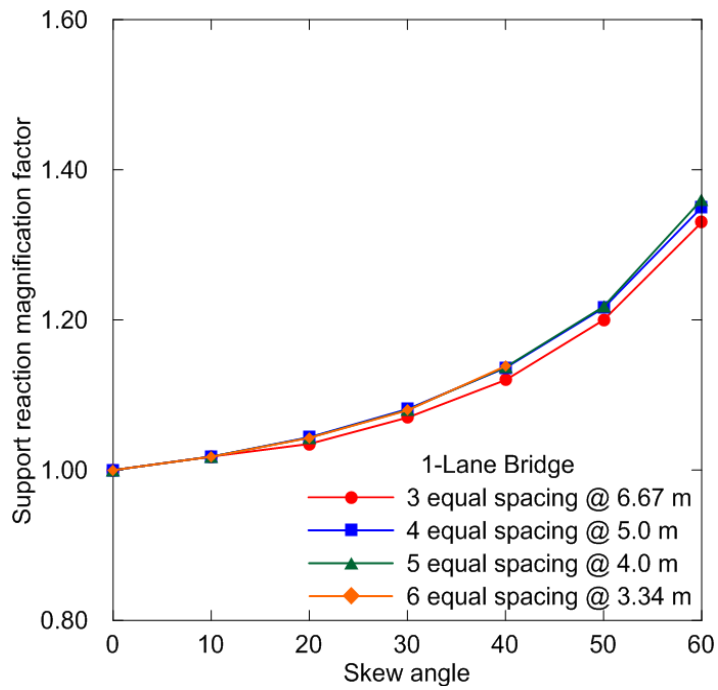


(a)

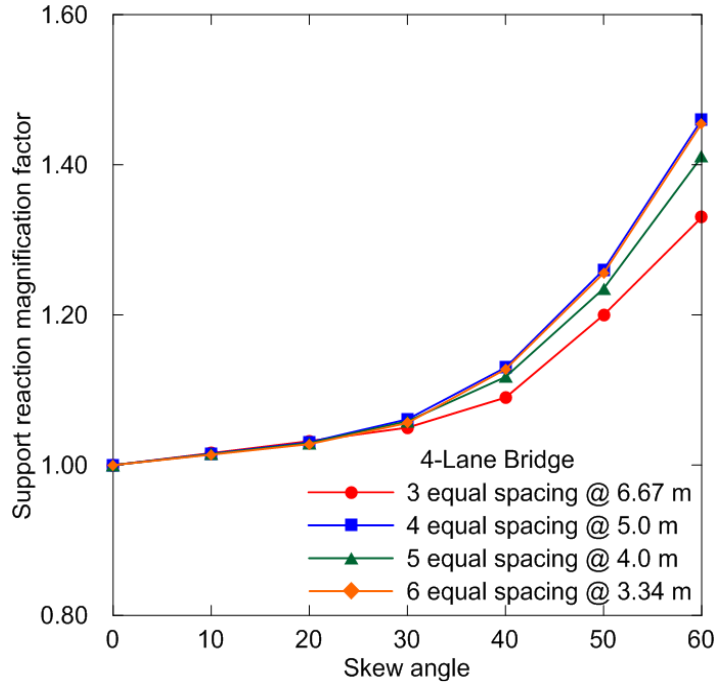


(b)

Figure 3.18 Moment magnification factor for interior girders for: (a) one-lane, and (b) four-lane



(a)



(b)

Figure 3.19 Reaction magnification factor at obtuse corners for: (a) one-lane, and (b) four-lane

The longitudinal bending moments for interior girders of multi-lane bridges were evaluated and the corresponding magnification factors (M_a/M_o) are presented in Figure 3.18. For exterior girders moment, the FEA results showed an insignificant effect of different cross-frame spacing arrangements with the variation of skew angle from 0° to 60°. Only interior girder responses are discussed and presented herein.

Figure 3.19 shows the support reaction at obtuse corners for one-lane and four-lane bridge system in term of magnification factor (R_a/R_o). The results showed that for one-lane bridge system, all cross-frame spacing arrangements resulted in similar increasing trend of exterior girder support reaction at obtuse corner with an increase of skew angle up to 60°. However, for four-lane bridge system a maximum difference of 10% is observed at 60° skew angle when cross-frames were arranged between the maximum and minimum permitted equal spacing limits i.e. 6.67 m and 3.34 m, respectively.

From this study it was concluded that for highly skewed bridges, keeping the maximum cross-frame spacing within the prescribed code limitations (CSA 2014a), relatively widely

spaced diaphragms lead to a better load distribution among girders by reducing the support reactions at the obtuse corners. This finding is in agreement with the research work conducted by Kim and Nowak (1997).

3.6.2 Sequence of Construction

In skewed composite steel I-girder bridges, the sequence of loading during construction influences the magnitude of stresses developed in the girders and it is usually not considered in the design. Many designers and contractors have demonstrated their limited experience to comprehend the structural behaviour during different phases of skewed bridge construction. The Canadian Highway Bridge Design Code (CSA 2014a) and AASHTO-LRFD Bridge Design Specifications (AASHTO-LRFD 2014) permits shored composite construction. However, design guidelines to estimate the accumulation of girder flexural stresses due to different moment distribution among girders (i) before the concrete hardening, (ii) after placing the asphalt layer and the barrier wall, and (iii) when trucks move over the bridge are as yet unavailable. To assess load distribution at different stages of construction, as described earlier, the sequence of construction is categorized in two classes, i.e. (a) un-shored construction, and (b) shored construction.

3.6.2.1 Un-shored Construction

According to CHBDC (CSA 2014a) clause 10.11.4 for composite beams and girders in the positive moment regions, the normal stress in either flange of the steel section due to serviceability dead and live loads (to control permanent deformation) shall not exceed $0.90 F_y$. The following requirements shall also be satisfied:

$$\frac{M_d}{S} + \frac{M_{Sd}}{S_{3n}} + \frac{M_L}{S_n} \leq 0.90 F_y \quad (3.1)$$

where, M_d is the bending moment in the beam or girder at serviceability limit state (SLS) due to dead load (N-mm); M_{Sd} is the bending moment in the beam or girder at SLS due to the superimposed dead load (N-mm); M_L is the bending moment in the beam or girder at SLS due to live load (N-mm); S is the elastic section modulus of steel section (mm^3), and

S_n , S_{3n} are the elastic section modulus comprising the steel beam or girder and the concrete slab, calculated using a modular ratio of n or $3n$, respectively (mm^3).

The CHBDC (CSA 2014a) simplified method of analysis has specified the modification factor to account total girder moment at SLS under live load condition as follows:

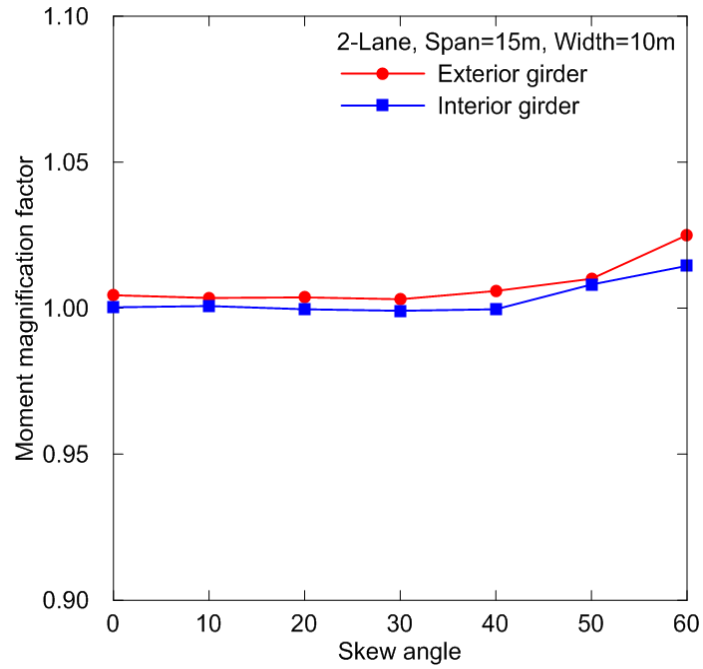
$$M_L = (F_T F_S) \times M_T \quad (3.2)$$

No moment magnification factor is considered under the dead load conditions. In order to check that whether separate moment magnification factors are required for the shored and un-shored construction a three-dimensional finite element modeling was conducted to determine the moment magnification factor in bridge girders by considering different parameters including: skew angles, girder stiffness and cross-frame layout, span length and number of design lanes under dead load conditions. Table 3.4 presents the basic cross-sectional configurations considered.

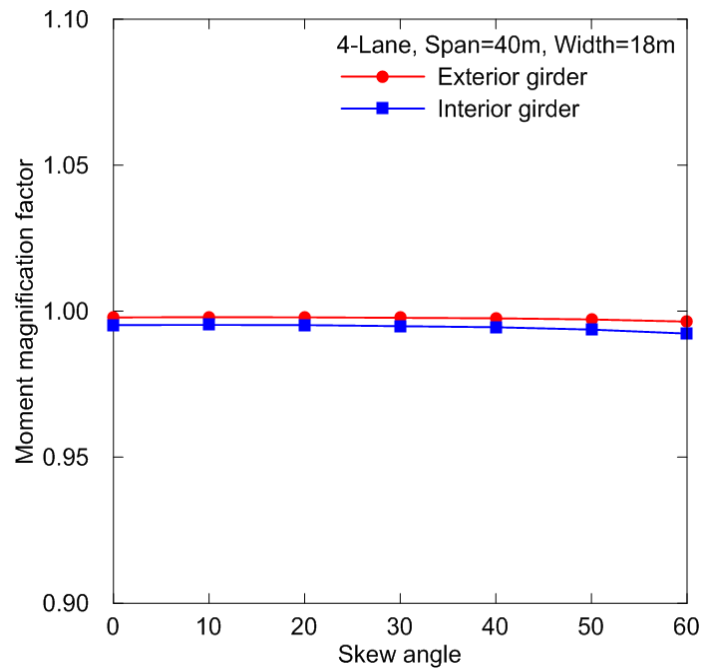
Table 3.4 Parameters considered for un-shored construction

Parameters considered	Range of Parameters	
Span length	15 m	40 m
No. of Lanes	2-Lane (10 m), and	4-Lane (18 m)
Cross-frame spacing	2 equal spacing @ 7.5 m	5 equal spacing @ 8 m
Cross-frame Layouts	<ul style="list-style-type: none"> • Parallel for skew angle < 30° • Perpendicular-discontinuous for skew angle > 30° 	
Skew angle	0, 10, 20, 30, 40, 50 and 60°	
Girder spacing (m)	2.5 m	2.25 m

The finite element analysis was conducted for the non-composite braced steel girder system under self-weight and weight of the concrete slab before hardening (M_d). FEA results are shown in Figure 3.20.



(a)



(b)

Figure 3.20 M_d - Moment magnification factor for exterior and interior girders for: (a) two-lane, and (b) four-lane

Finally the results showed that with the change of skew angle from 0° to 60°, the effect of un-shored sequence of construction (i.e. before concrete hardening) was found insignificant on the moment magnification factors. Therefore, it can be considered equal to 1 for M_d calculation in equation 3.1.

3.6.2.2 Shored Construction

In the shored construction of a skewed steel I-girder bridge, the bridge girders are supported at intermediate points by temporary shores placed at close intervals. The temporary shores supposedly keep the girders in a state that closely approaches zero stress, termed herein as the no-load condition. When the deck concrete is poured, the beams support the dead load due to their own weight as well as the weight of the freshly poured deck concrete. Because the beams are supported at close intervals, it is assumed that they do not develop any stresses due either to their own dead weight or the fresh concrete. The temporary shores are removed after sufficient hardening of concrete occurs, following which the beam develops composite action, and all loads (self-weight, superimposed loads and the live load) are assumed to be resisted by the composite girder section. If the no-load condition is not achieved in the field, a skewed I-girder will deflect and rotate out of plane, due to its self-weight, as a direct result of its geometry.

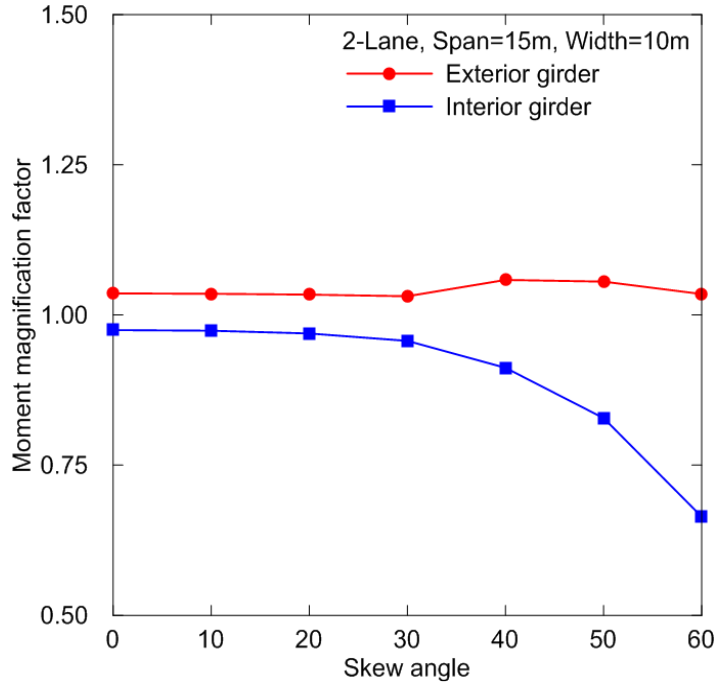
While shored construction is permitted according to bridge code specifications (CSA 2014a, AASHTO-LRFD 2014), no design procedure to predict the moment magnification factors is specified under the dead load conditions. In order to check the adequacy of the moment magnification factors for the shored construction a three-dimensional finite element modeling was conducted to determine the moment magnification factor in bridge girders by considering different parameters including: skew angles, girder stiffness and cross-frame layout, span length and number of design lanes under dead load conditions. Table 3.5 presents the basic cross-sectional configurations considered. For shored construction, the following SLS condition need to be satisfied;

$$\frac{(M_d + M_{sd})}{S_{3n}} + \frac{M_L}{S_n} \leq 0.90F_Y \quad (3.3)$$

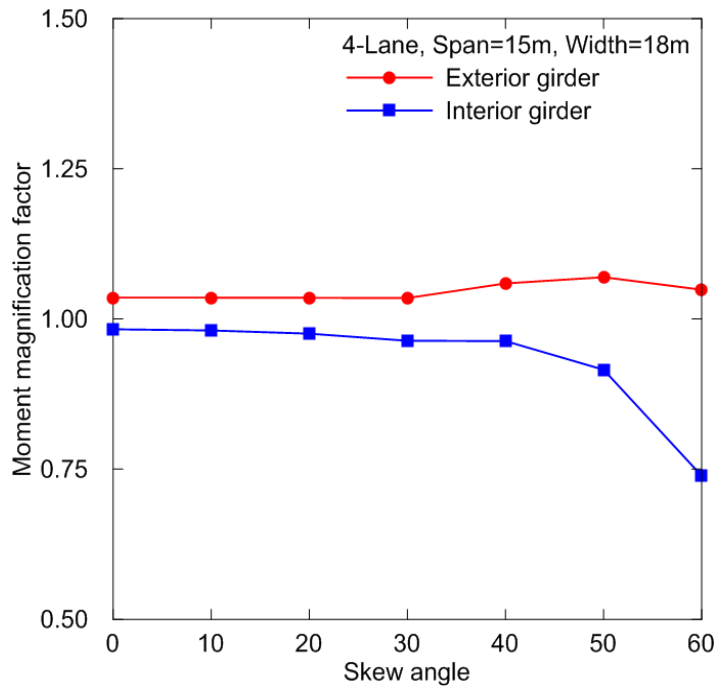
Table 3.5 Parameters considered for shored construction

Parameters considered	Range of Parameters	
Span length	15 m	40 m
No. of Lanes	2-Lane (10 m), and	4-Lane (18 m)
Cross-frame spacing	2 equal spacing @ 7.5 m	5 equal spacing @ 8 m
Cross-frame Layouts	<ul style="list-style-type: none"> • Parallel for skew angle < 30° • Perpendicular-discontinuous for skew angle > 30° 	
Skew angle	0, 10, 20, 30, 40, 50 and 60°	
Girder spacing (m)	2.5 m	2.25 m

In equation 3.3, the composite girder in shored construction supports the combined effect of : (i) dead load due to their own weight as well as the weight of the freshly poured deck concrete (M_d), and (ii) superimposed loading coming over the structure in-terms of weight of asphalt layer and the weight of the barrier wall (M_{sd}). The sensitivity study result shows that shored sequence of construction has substantial effect on the load distribution of girder, particularly on the interior girders, and needs to be considered to develop more realistic design guidelines. The FEA results of a composite braced steel girder ($M_d + M_{sd}$) subjected to self-weight of the structure in-addition to the super-imposed dead load (i.e. weight of asphalt layer and the weight of the barrier wall) are presented in Figure 3.21.



(a)



(b)

Figure 3.21 (M_s+M_{sd}) - Moment magnification factor for exterior and interior girders for: (a) two-lane, and (b) four-lane

3.6.3 Effect of CHBDC Vehicular Load Type

For normal traffic, the CHBDC (CSA 2014a) clause 3.8.4.1 states that for SLS combination-1 and for ULS, the traffic load shall be the CL-W truck load increased by the dynamic load allowance or CL-W lane load, whichever produces the maximum load effect. The objectives of this sensitivity study was to assess the critical loading conditions out of CL-W truck and lane load that can develop the dominating girder bending stresses for a bridge configurations considered in this study when the skew angle changes from 0° to 60°. Table 3.6 presents the bridge cross-sectional configurations considered for this study. Different live load cases considered to evaluate the extreme effect of girder bending stress using CL-W truck load and lane load for two- and four-lane bridge configurations are presented in Figure 3.22 and 3.23, respectively. Under linear elastic conditions, stresses are proportional to the bending moments in the girders. Hence, maximum stresses at the extreme fiber of the bottom flanges obtained from finite element results were used. The expressions used to evaluate the girder bending stress in case of the CL-W truck load and CL-W lane load are presented below:

$$\text{For CL-W Truck load: } \sigma = R_L \times \sigma_{FEA@bottom\ flange} \times (1 + DLA) \quad (3.4)$$

$$\text{For CL-W Lane load: } \sigma = R_L \times \sigma_{FEA@bottom\ flange} \quad (3.5)$$

The exterior girder bending stress for two- and four-lane bridge system at 0° and 60° skew angle for the CL-W truck and lane load are presented in Figure 3.24 to 3.27, respectively. Similarly, the interior girder bending stress for two- and four-lane bridge configurations for the CL-W truck and lane load are presented in Figure 3.28 to 3.31, respectively for 0° and 60° skew angles. FEA results by using sensitivity study on a prototype bridge structure aims at evaluating the girder bending stresses due to the CL-W truck load and lane load to investigate the severity of CL-W loading that produces maximum load effect. Results showed that the stresses produced by truck load were found higher than those obtained from the lane load for all the load case for short span bridge configurations ranging from 15 m to 40 m span length. Consequently, the parametric study for the evaluation of load distribution factors for composite slab-on steel I-girder bridges were initiated using the CL-W five-axle truck load, shown in Figure 3.5(b).

Table 3.6 Parameters considered for effect of CHBDC vehicular load type

Skew angle	No. of Lanes (n)	Span (L), m	Width (B), m	No. of Girders (N)	Girder spacing (S), m	Cross-frame spacing
0°	2	15	10	4	2.5	2 equal spacing @ 7.5m
	4	15	18	8	2.25	2 equal spacing @ 7.5m
	2	40	10	4	2.5	5 equal spacing @ 8m
	4	40	18	8	2.25	5 equal spacing @ 8m
60°	2	15	10	4	2.5	2 equal spacing @ 7.5m
	4	15	18	8	2.25	2 equal spacing @ 7.5m
	2	40	10	4	2.5	5 equal spacing @ 8m
	4	40	18	8	2.25	5 equal spacing @ 8m

Cross-frame Layouts: Parallel for skew angle < 30°

Perpendicular-discontinuous for skew angle > 30°

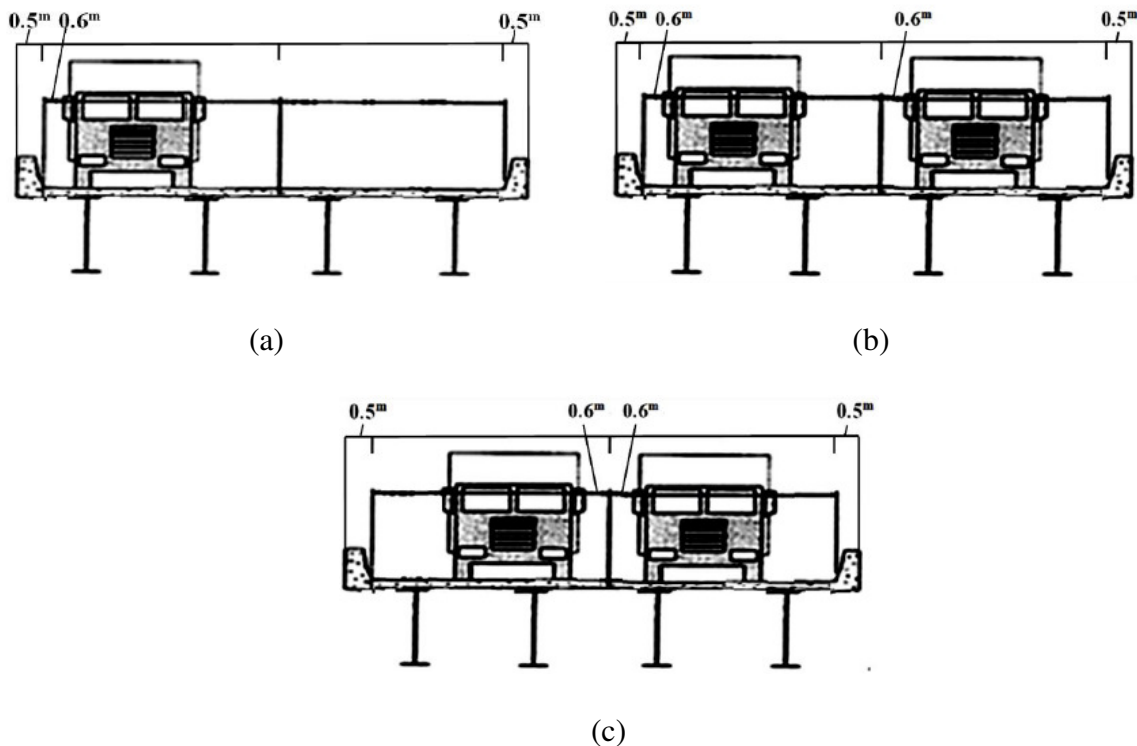
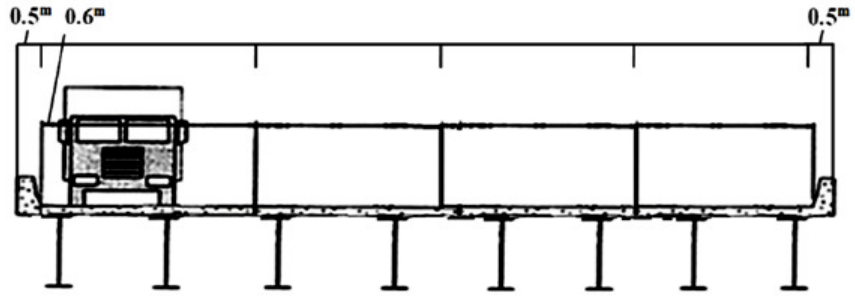
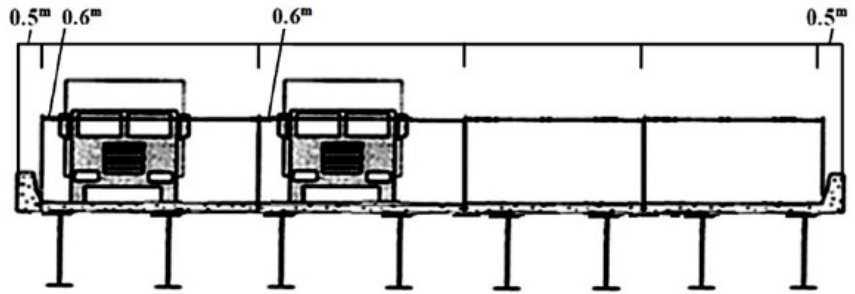


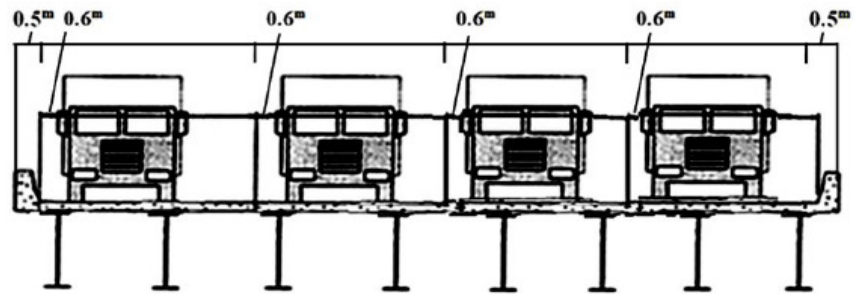
Figure 3.22 Live loading cases for two-lane bridge configuration for: (a) Exterior girder-partial load (b) Exterior girder-full load, and (c) Interior girder-full load



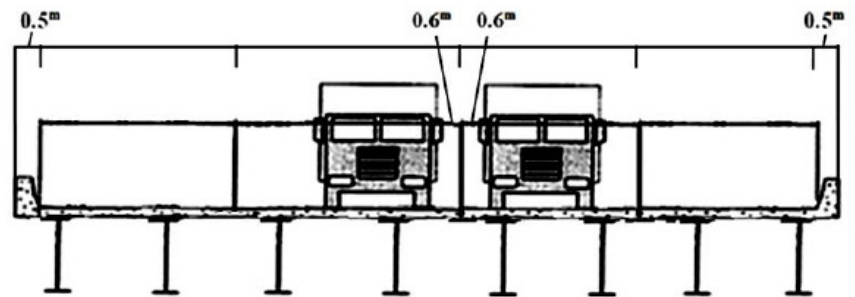
(a)



(b)



(c)



(d)

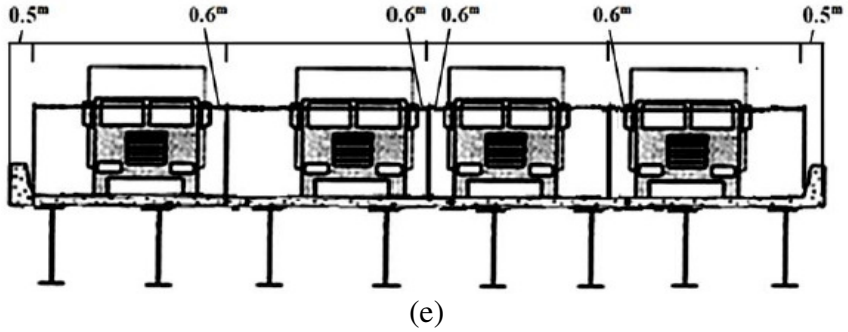


Figure 3.23 Live loading cases for four-lane bridge configurations for: (a) Exterior girder one-partial load (b) Exterior girder two-partial load (c) Exterior girder-full load (d) Interior girder two-partial load, and (e) Interior girder-full load

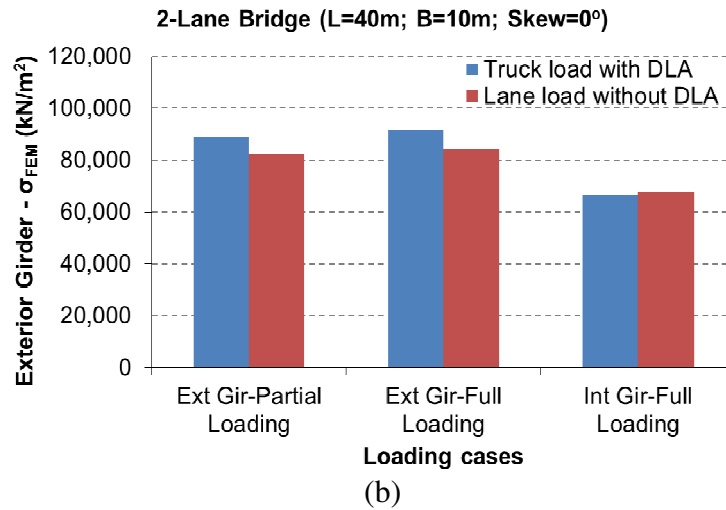
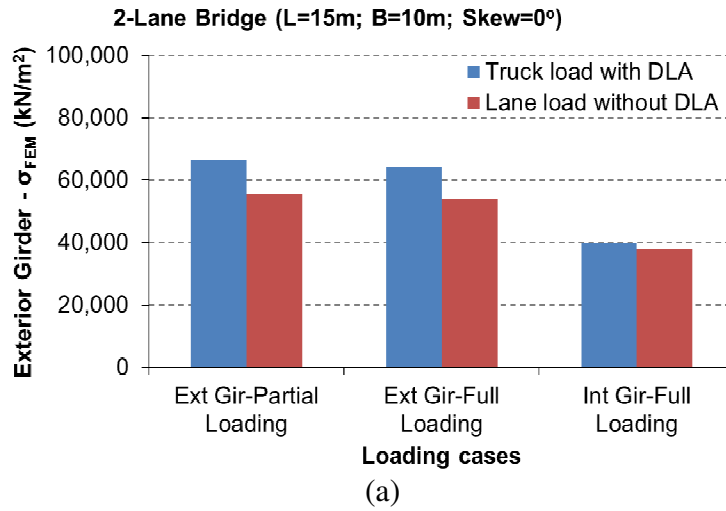


Figure 3.24 Exterior girder bending stress for two-lane bridge configuration at skew angle=0° for: (a) Span =15 m, and (b) Span = 40 m

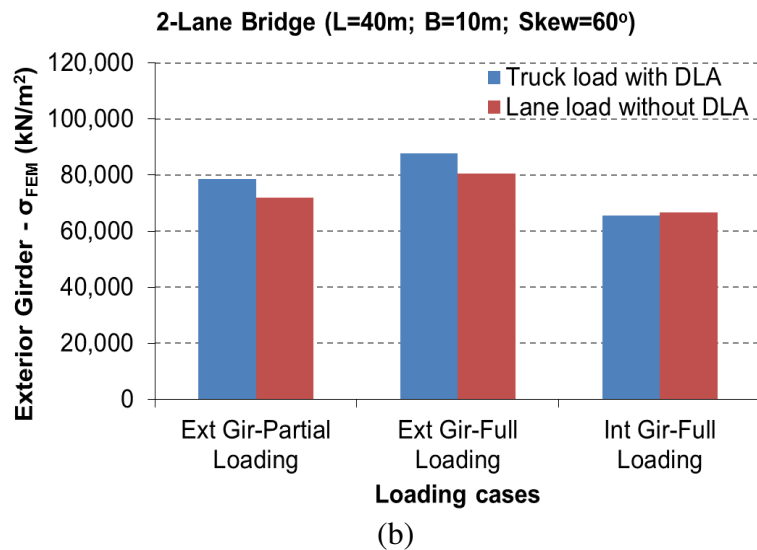
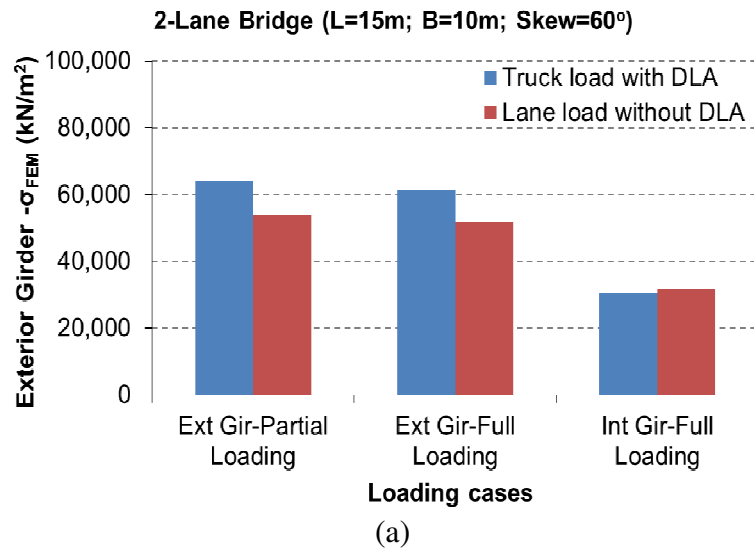


Figure 3.25 Exterior girder bending stress for two-lane bridge configuration at skew angle=60° for: (a) Span =15 m, and (b) Span = 40 m

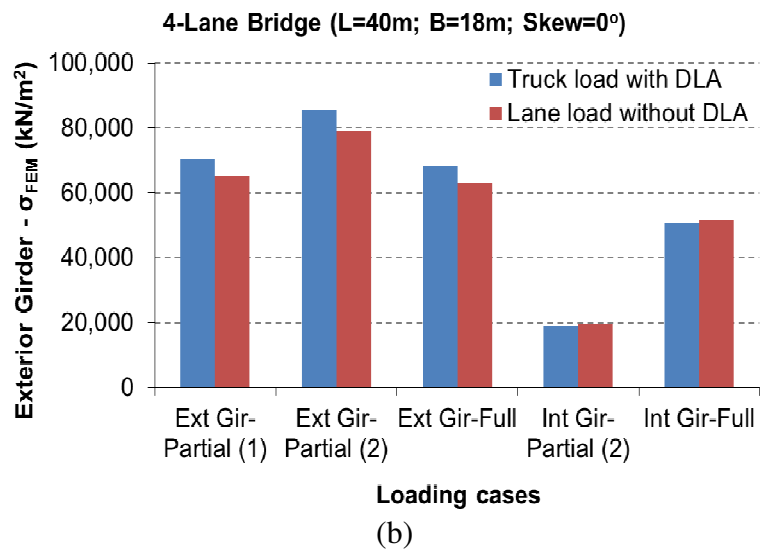
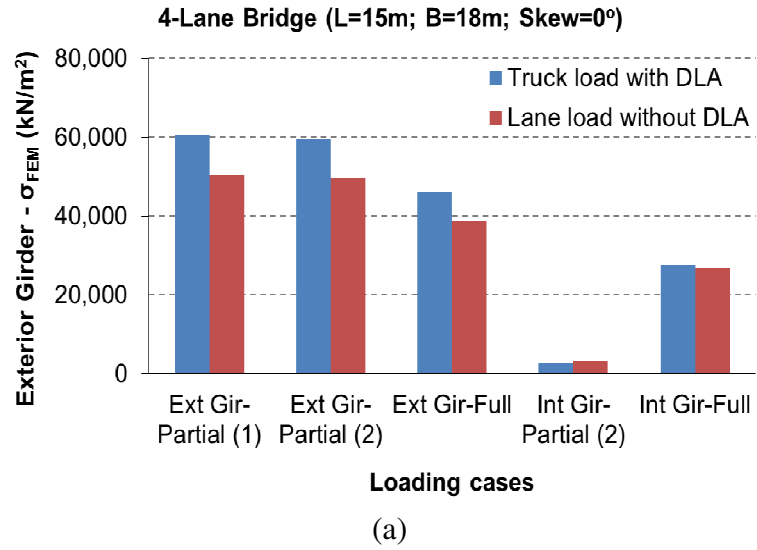


Figure 3.26 Exterior girder bending stress for four-lane bridge configuration at skew angle=0° for: (a) Span =15 m, and (b) Span = 40 m

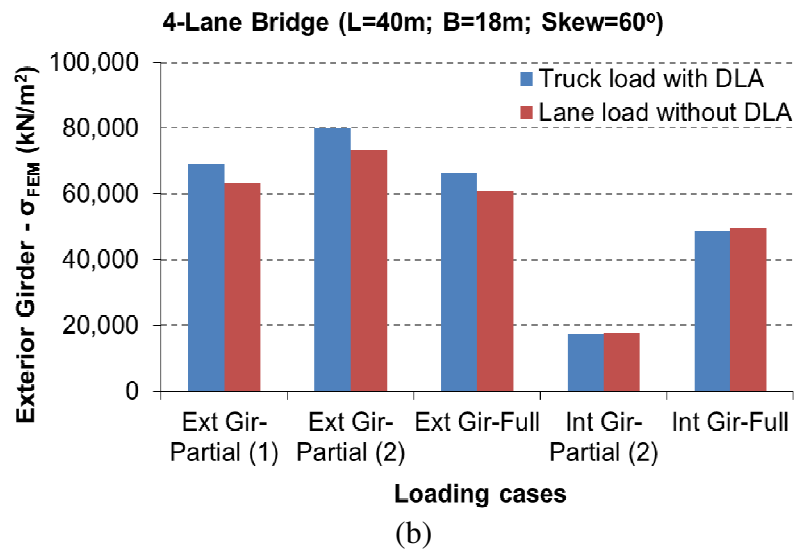
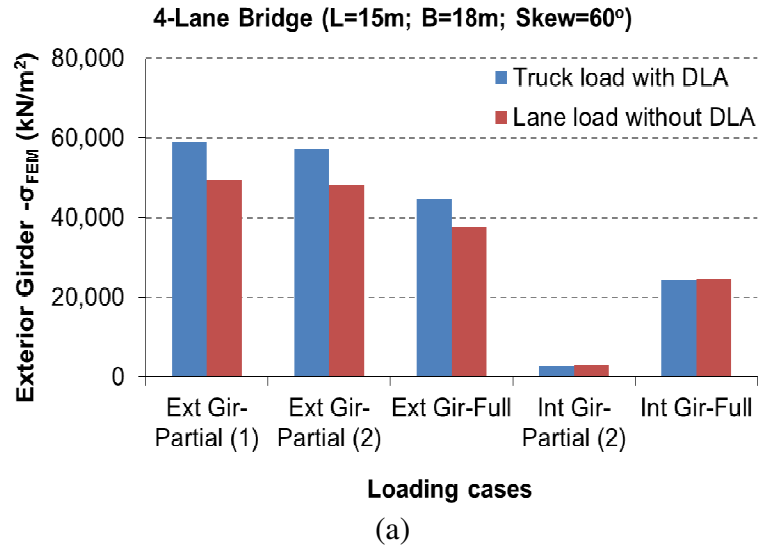


Figure 3.27 Exterior girder bending stress for four-lane bridge configuration at skew angle=60° for: (a) Span =15 m, and (b) Span = 40 m

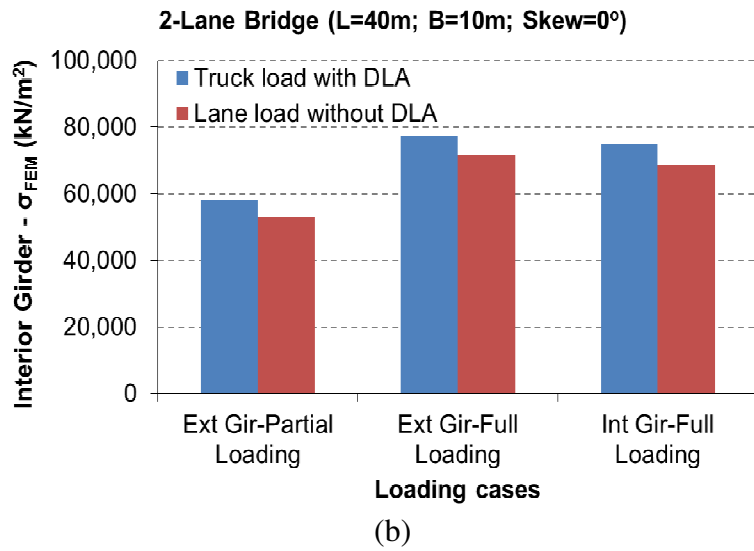
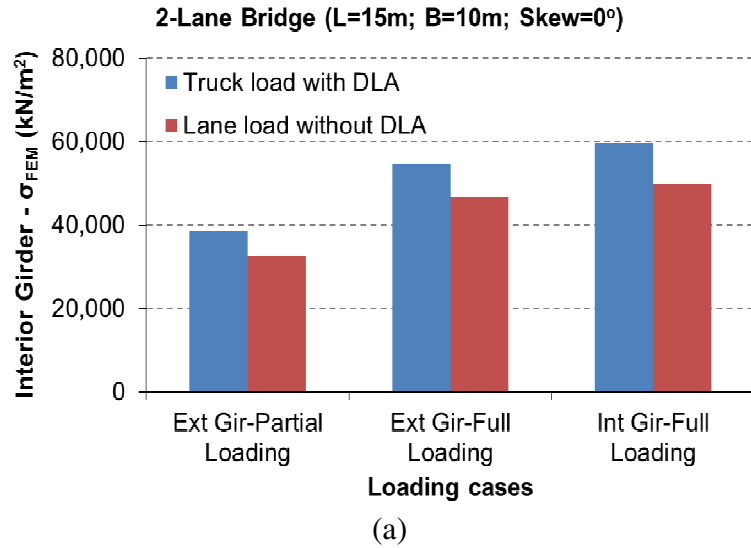


Figure 3.28 Interior girder bending stress for two-lane bridge configuration at skew angle=0° for: (a) Span =15 m, and (b) Span = 40 m

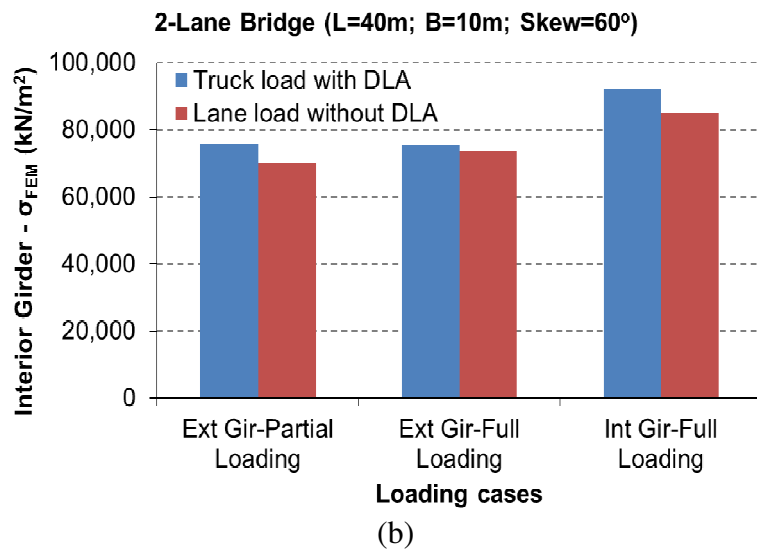
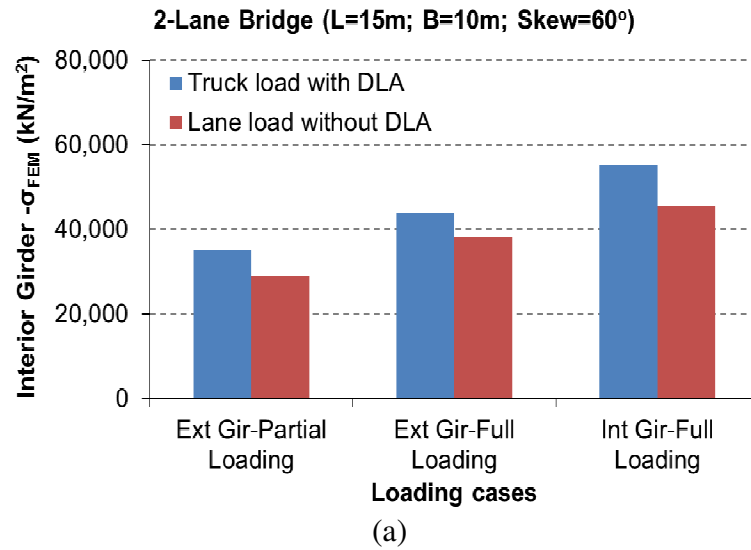


Figure 3.29 Interior girder bending stress for two-lane bridge configuration at skew angle=60° for: (a) Span =15 m, and (b) Span = 40 m

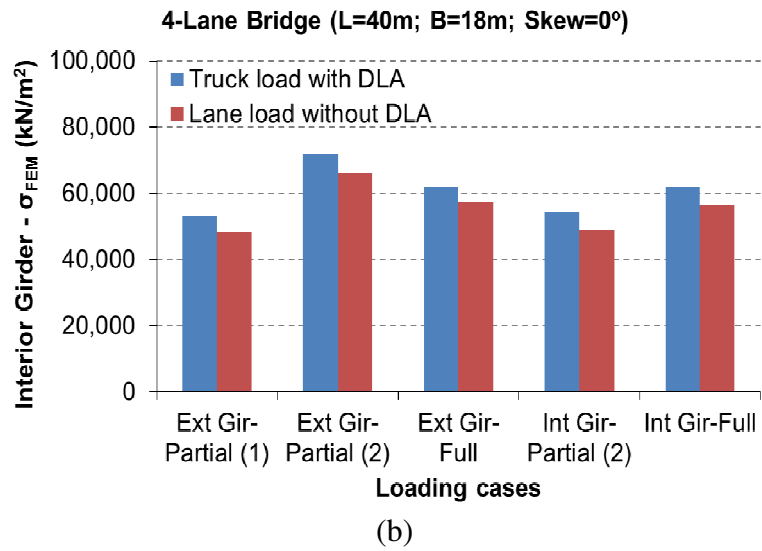
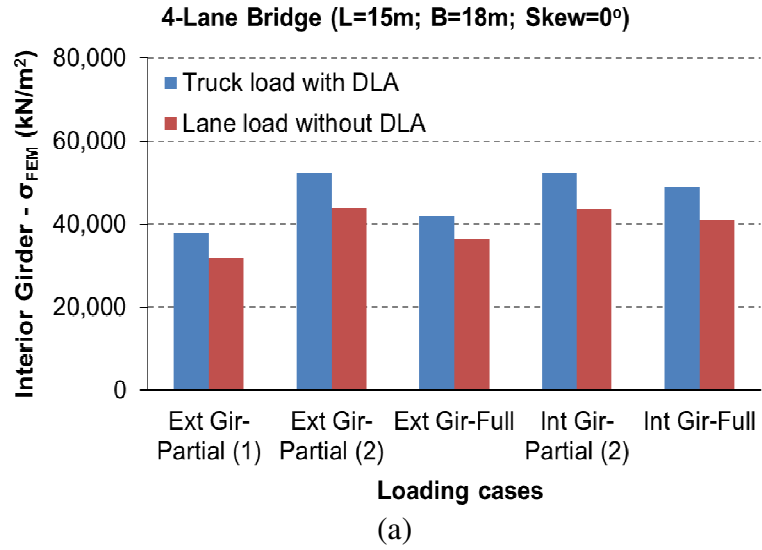


Figure 3.30 Interior girder bending stress for four-lane bridge configuration at skew angle=0° for: (a) Span = 15 m, and (b) Span = 40 m

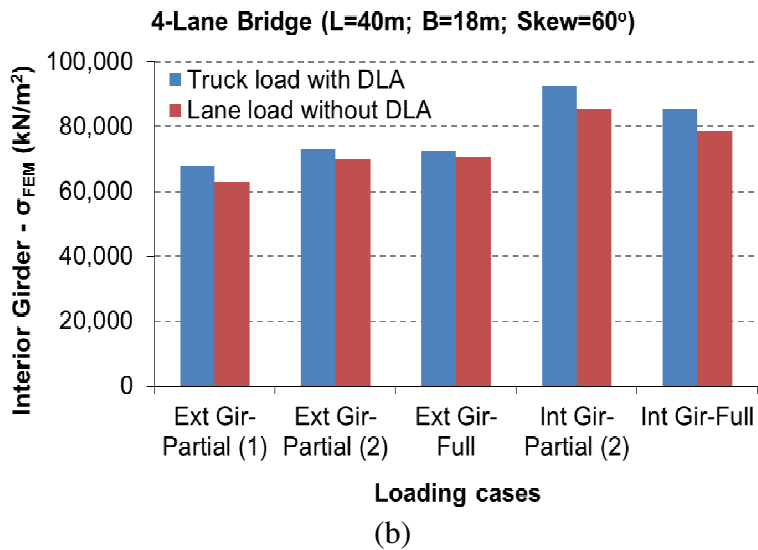
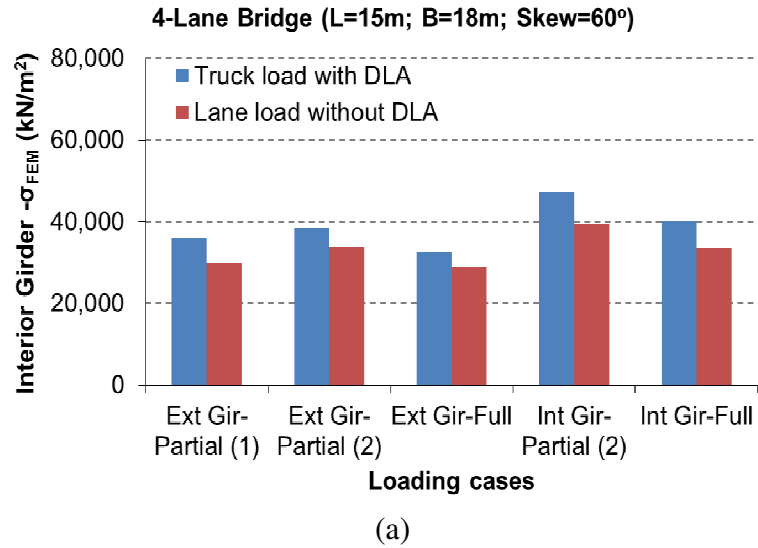


Figure 3.31 Interior girder bending stress for four-lane bridge configuration at skew angle=60° for: (a) Span =15 m, and (b) Span = 40 m

3.6.4 Estimation of Longitudinal Flexural Stiffness of Steel I-Girder

The load causes the slab-girder system to displace. As one can expect, the girder near the location of the load application carries more load than those away from the applied load. If linear behavior is assumed, the load transferred to each girder is proportional to the displacement. Equilibrium requires that the summation of the load carried by all the girders equals the total applied load. The load carried by each girder is a function of the relative

stiffness of the components that comprise the slab-girder system (Barker and Puckett 1997).

To account for the relative stiffness of the bridge system, Bakht and Moses (1988) on the basis of detailed study of some 30 slab-on-girder highway bridges of different spans in North America presented a relationship for the upper and lower bound limit between the longitudinal flexural rigidity per unit width (D_x) and the span length (L). It was concluded that the upper-bound values of D_x can be represented as a function of the span length L , by the following equation:

$$D_x = 59,575L + 2,257L^2 \quad (3.6)$$

Similarly, the equation for the lower-bound values:

$$D_x = 9,250L + 1,790L^2 \quad (3.7)$$

In the above equations, L is in “meter” and D_x in “kN-m”. The two bounds of D_x , together with the values for specific bridges studied by Bakht and Moses (1988) are plotted in Figure 3.32. Equation 3.6 and 3.7 shown above formed the basis for estimating the flexural stiffness of I-girders for the evaluation of load distribution formulas specified in Ontario Highway Bridge Design Code (OMTC 1992).

In order to compute the longitudinal flexural rigidity per unit width, D_x , of the girder bridges adopted the semi-continuum idealization approach (Jaeger and Bakht 1989), where a bridge is conceptually divided into strips of equal widths represented by a longitudinal beam. The flexural rigidity EI of a longitudinal beam representing a strip of width S is given by:

$$EI = S.D_x$$
$$D_x = \frac{EI}{S} \quad (3.8)$$

For slab-on-girder bridges, a database of steel girder sections adopted from the manual of short span steel bridge (Theodor and Al-bazi 1997) was generated for the evaluation of the longitudinal bending stiffness (D_x) by considering the composite deck-girder section, and represented in equations 3.9:

$$D_x = \frac{E.I_{Composite}}{S} \quad (3.9)$$

Subsequently, for the detailed parametric study all the selected bridge geometries were plotted by considering the upper and lower bound limits as specified by Bakht and Moses (1988) and represented in Figure 3.33. The results indicated that the calculated bending stiffness of all the selected girders satisfied the prescribed limits as mentioned above in equations 3.6 and 3.7 respectively.

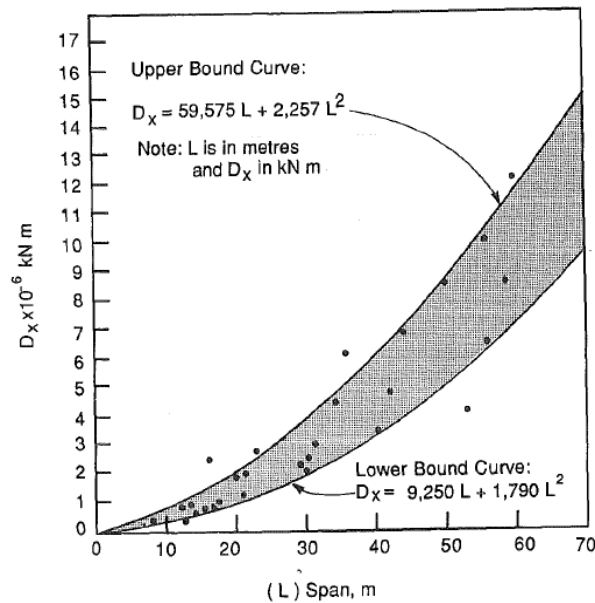


Figure 3.32 Relationship between span and longitudinal flexural rigidity per unit width (Reproduced from Bakht and Moses 1988)

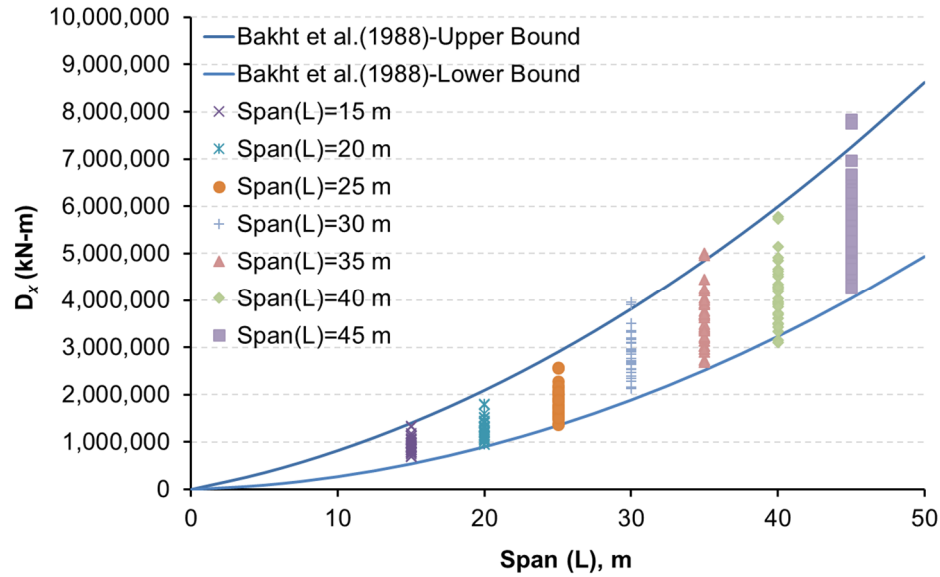


Figure 3.33 Relationship between span length and longitudinal flexural rigidity per unit width

3.6.5 Assessment of Multi-lane Truck Loading Condition

The current study involves the assessment of multi-lane truck loading condition on the load distribution among girders in skewed composite steel I-girder bridges. The analysis of the multi-lane loading involves the distribution of truck load to girders. Accurate knowledge of the load carrying capacity and load distribution among girders are vital for satisfactory performance of the bridge. Adding skew to a straight girder bridge complicates the behavior and the associated analysis required to capture it. For this purpose, a three-dimensional finite element modeling was conducted to determine the magnification factor for moment and shear force in bridge girders by considering different parameters including: skew angles, girder stiffness and cross-frame layout, number of design lanes, span length and girder spacing under various truck positions. Three truck loading scenarios were considered for this study, namely: (i) side-by-side trucks entering the bridges simultaneously, (ii) multi trucks running over the bridge with time lag between them, and (iii) one truck in each lane at a time and with superposition of results. For all loading conditions, moving load technique available in CSiBridge (CSI 2015) software was utilized to obtain the maximum moment and shear in girders. Table 3.7 presents the bridge configurations considered for this study. The CHBDC (CSA 2014a) specified five-axle

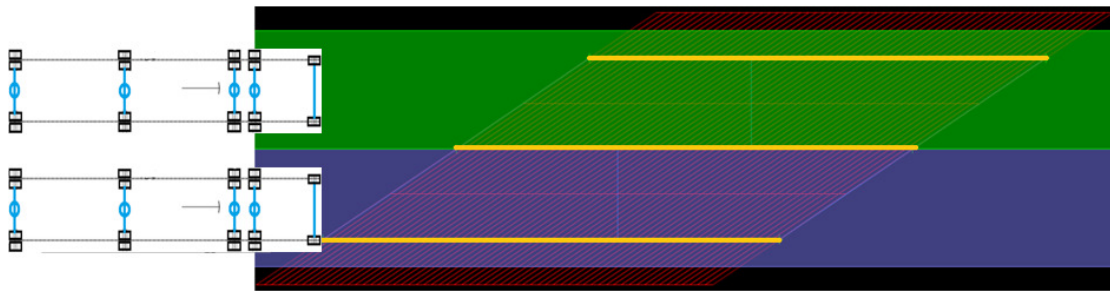
CL-W truck load was used to get the extreme effect of girder bending and shear stresses for three loading conditions mentioned previously.

Table 3.7 Parameters considered for assessment of multi-lane truck loading condition

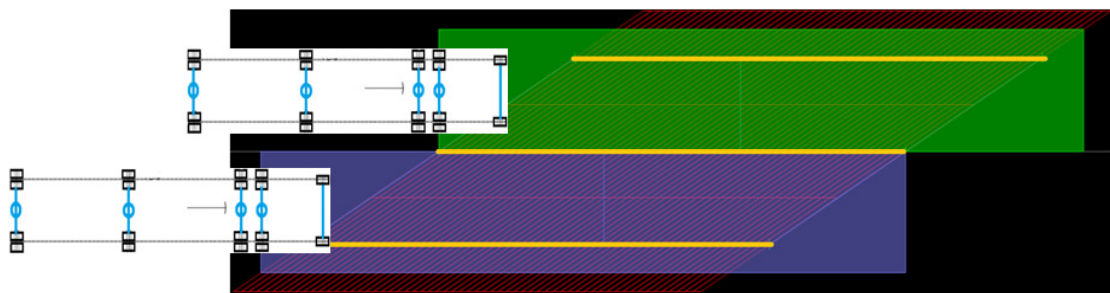
No. of Lanes (n)	Span Length (L), m	Bridge Description
Two-lane	15	<ul style="list-style-type: none"> • Bridge Width (B) = 7.6 m • Deck Width (W_c) = 6.6 m • Design Lane Width (W_e) = 3.3 m • No. of Girders (N) = 3 • Girder Spacing (S) = 2.533 m • Skew Angle (α) = 0°, 10°, 20°, 30°, 40°, 50° and 60°.
Four-lane	30	<ul style="list-style-type: none"> • Bridge Width (B) = 18.0 m • Deck Width (W_c) = 17.0 m • Design Lane Width (W_e) = 4.25 m • No. of Girders (N) = 6 • Girder Spacing (S) = 3.0 m • Skew Angle (α) = 0°, 10°, 20°, 30°, 40°, 50° and 60°.

In case of straight or curved bridges, it is common practice to allow the truck to enter the bridge at the same time. However, in case of a skew bridge this approach will predict inaccurate assessment about the load effects due to the fact that the behavior of a skew plate is anti-symmetrical with obtuse angle facing the acute angle at the other side of the bridge on the same free edge. In order to capture the variation in the load effect under CL-W truck load condition on a skew aligned bridge three different possibilities were considered. For this purpose, the location of the maximum stress values (bending and shear) for each bridge configuration was evaluated first under dead load condition. Subsequently, the stress values under truck live loads were determined for the three load scenarios (i.e. side-by-side, side-by-side with time lag, and by superposition) at the same location where previously assessed the maximum dead load stresses were determined. The three loading conditions considered are as follows:

- i. Truck moves side-by-side in a multi-lane bridge with the front and rear bumper aligned, as shown in Figure 3.34(a). The number of trucks positioned transversely on bridge deck was the same as the number of lanes (Diab et al. 2011, Tian 1999).
- ii. Truck moves side-by-side in a multi-lane bridge with a time lag between them i.e. trucks placed parallel to support line, as shown in Figure 3.34(b) (Huo et al. 2005, Tian 1999).
- iii. In a multi-lane skewed bridge, one truck was allowed to move in each lane at a time and final response was evaluated by superposition of results, as shown in Figure 3.34(c) (Turer 1997, 2000).



(a)



(b)

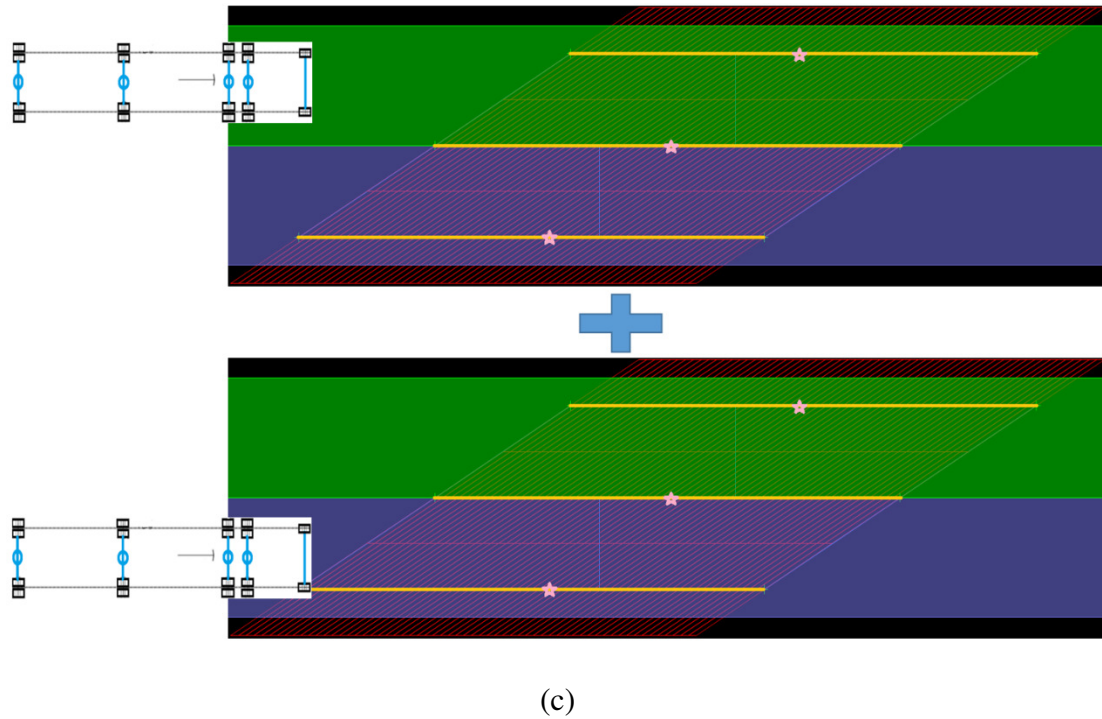


Figure 3.34 Truck loading conditions on a skew aligned bridge for (a) truck moves side-by-side, (b) truck moves side-by-side with time lag, and (c) one truck in each lane at a time and by superposition of results

The FEA results are presented in term of moment and shear magnification factors for the two- and four-lane bridge configurations considered in this study. The moment and shear magnification factors for a two-lane bridge are presented in Figure 3.35 and 3.36, respectively. Whereas, Figure 3.37 and 3.38 shows the moment and shear magnification factors for a four-lane bridge system. The result shows that for short span bridges all the three loading scenarios demonstrated an insignificant effect on girder bending and shear responses. For the detailed parametric study analysis presented in coming chapters, the girder responses were estimated by the superposition of results as presented in option-3 for the evaluation of load distribution factors.

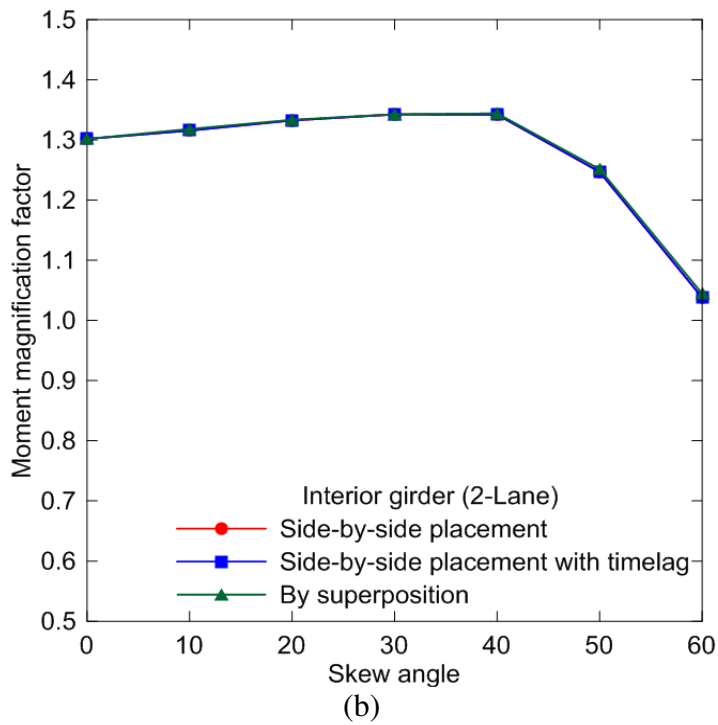
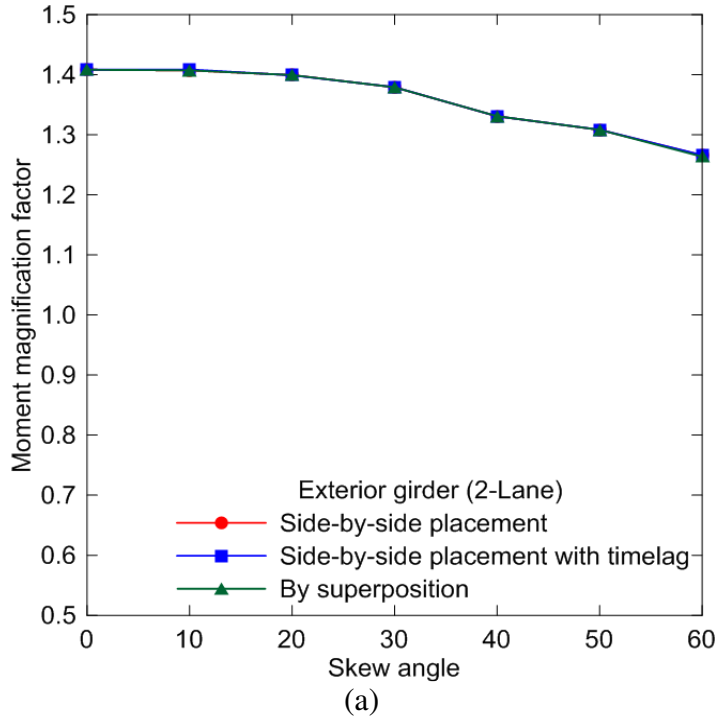
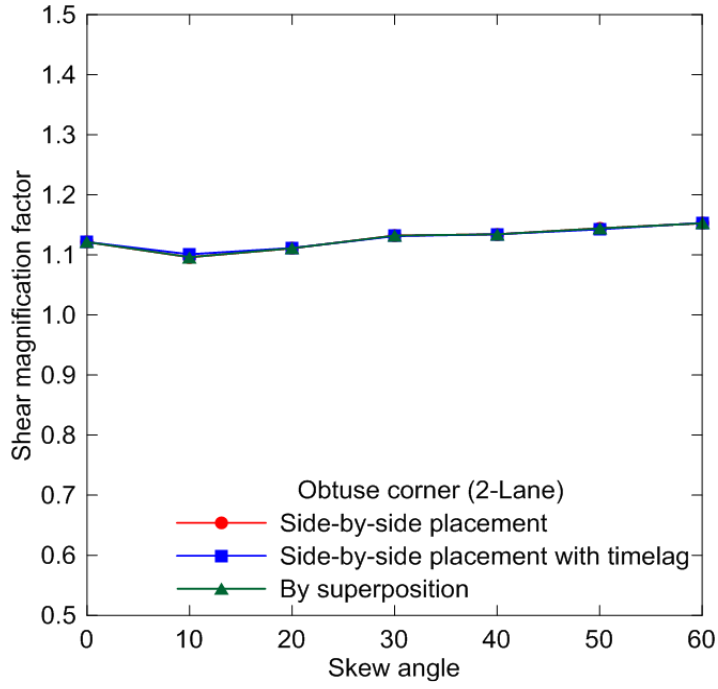
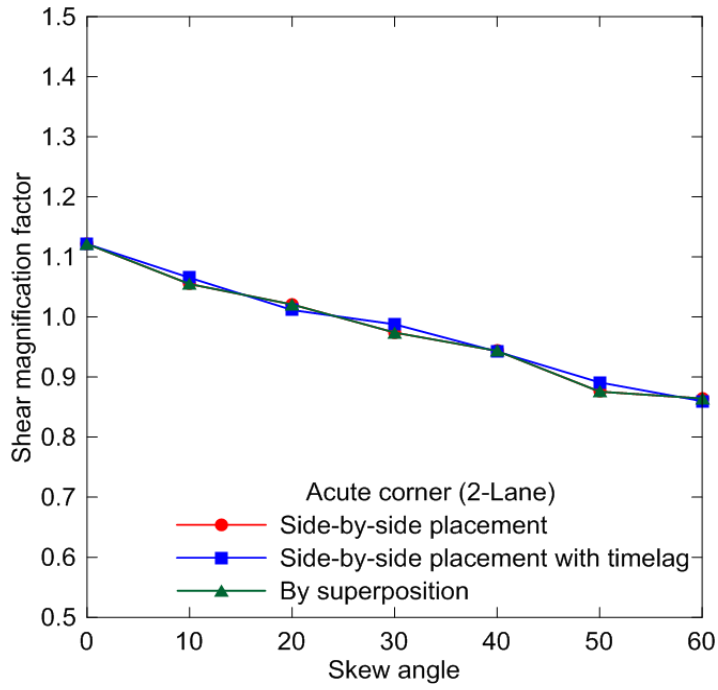


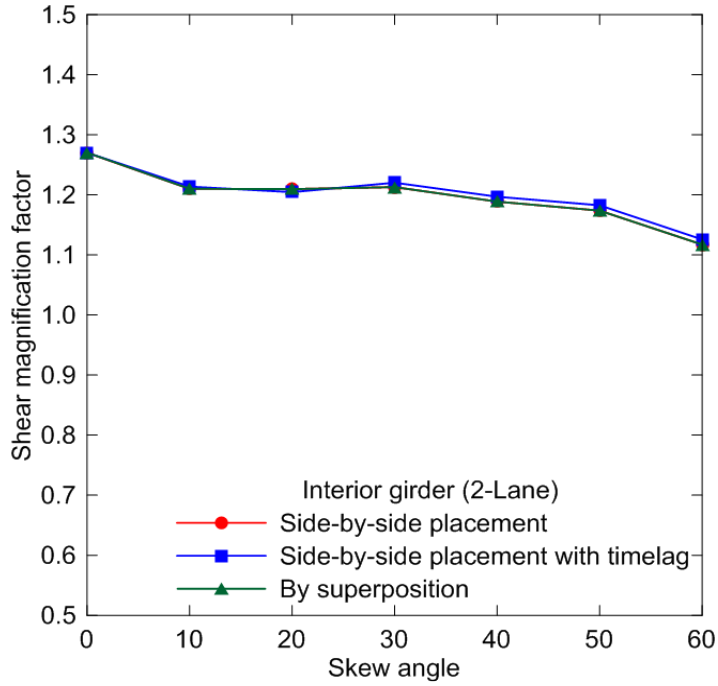
Figure 3.35 Moment magnification factor for two-lane bridge for: (a) exterior girder, and (b) interior girder



(a)

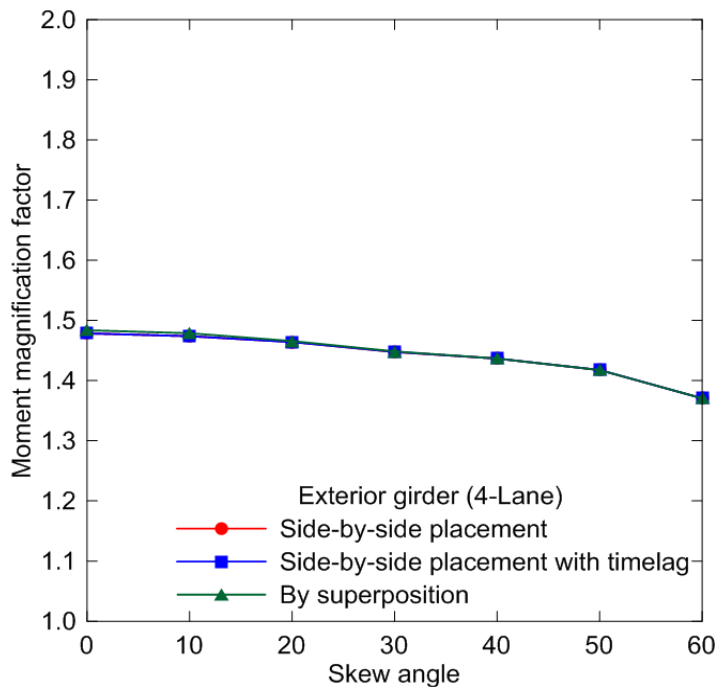


(b)

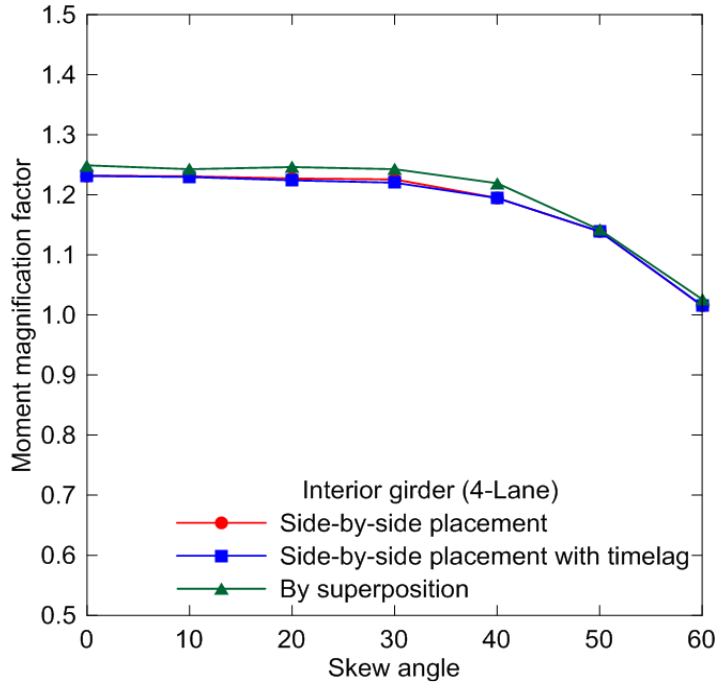


(c)

Figure 3.36 Shear magnification factor for two-lane bridge for: (a) obtuse corner (b) acute corner, and (c) interior girder

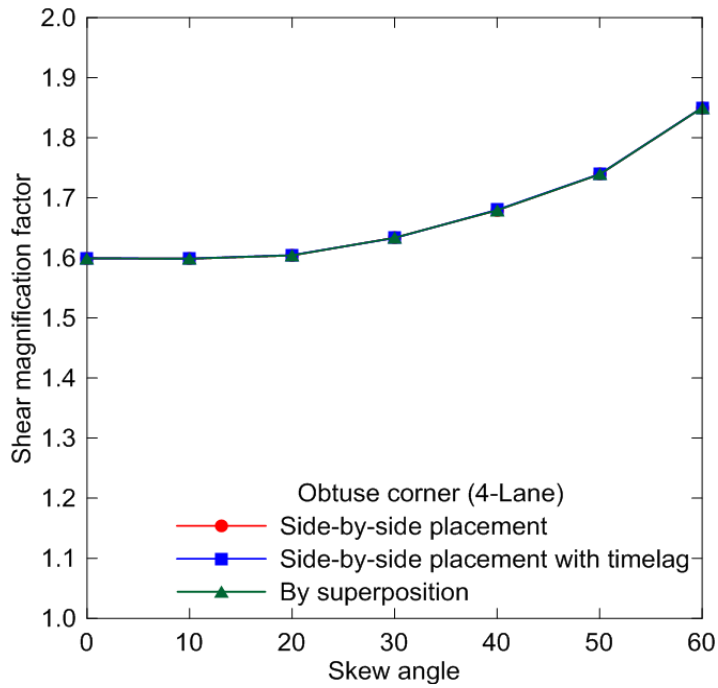


(a)

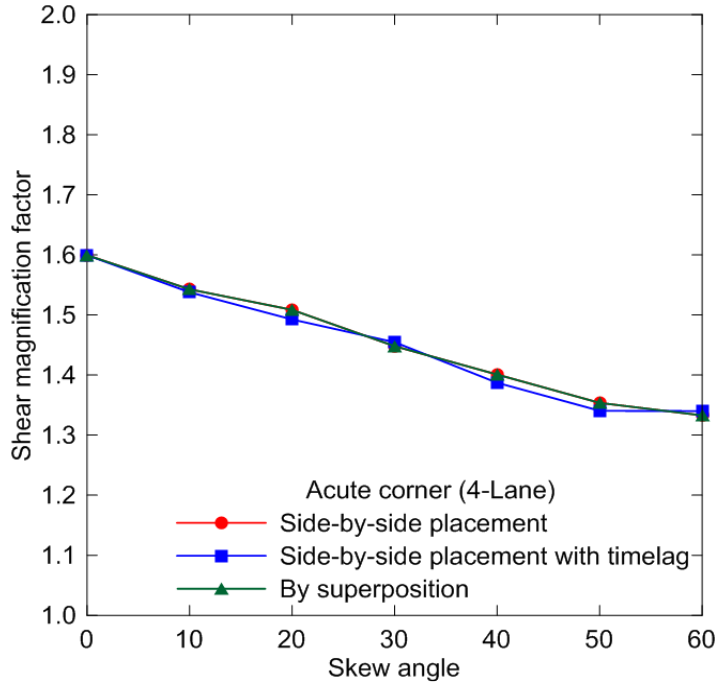


(b)

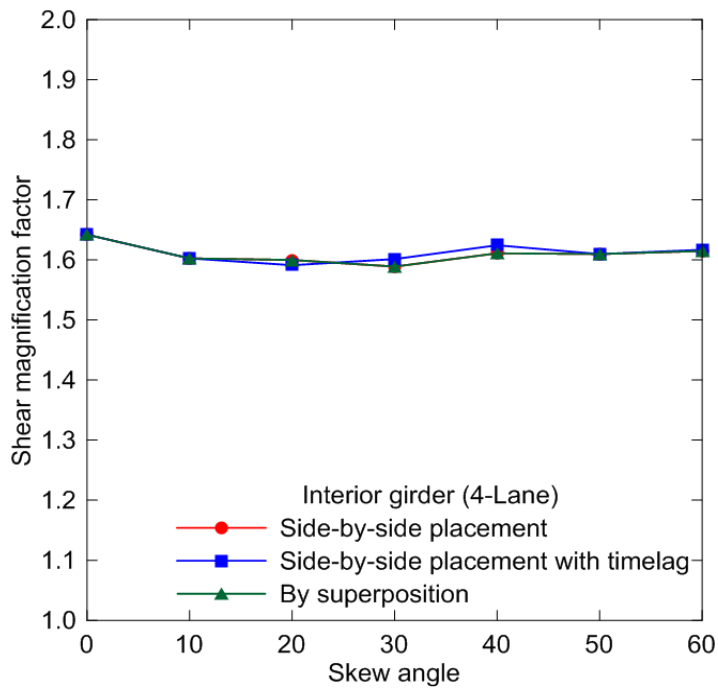
Figure 3.37 Moment magnification factor for four-lane bridge for: (a) exterior girder, and (b) interior girder



(a)



(b)



(c)

Figure 3.38 Shear magnification factor for four-lane bridge for: (a) obtuse corner (b) acute corner, and (c) interior girder

3.7 Conclusions

This chapter presents a brief description of the finite element approach, modeling methodology, structural geometry, boundary conditions and loads acting on the structure. The available commercial finite element program, CSiBridge v17.2.0, was used to investigate the most probable responses of a modeled bridge structure. Calibration of the finite element modeling technique was done by correlating the available physical load test data from the field testing of a highway bridge against the results of a finite element model of the same bridge. Sensitivity studies were also carried out to estimate the effect of composite bridge design parameters on the load distribution of skewed composite concrete over steel I-girder bridges.

CHAPTER 4

Dead Load Distribution in Straight and Skewed Bridges

4.1 General

In skewed bridges, the sequence of loading during construction influences the magnitude of stresses developed in the girders and is usually not considered in the design. Many designers and contractors have demonstrated their limited experience to comprehend the structural behavior during different phases of skewed bridge construction. The Canadian Highway Bridge Design Code and AASHTO-LRFD Bridge Design Specifications permits shored construction. However, design guidelines to estimate the accumulation of girder stresses due to different load conditions i.e. (i) before the concrete hardening, and (ii) after placing the asphalt layer and the barrier wall are as yet unavailable. Such discrepancies in design specifications results inappropriate load distribution factors that may lead to extremely conservative design forces or sometimes makes the design of the bridge unsafe. Thus an accurate assessment of load distribution throughout the bridge system is desired. Therefore there is a need for the generation of a database for both moment and shear distribution factors leading to the formation of empirical formulas for the rational design of a skewed composite slab-on I-girder bridges.

In this chapter, the influence of various parameters on the moment and shear distribution factors in a simply supported skewed bridge are studied. For this purpose, a three-dimensional finite element analysis were conducted to determine the moment and shear distribution factors by considering different parameters including: skew angles, girder stiffness, cross-frame layout, span length and number of design lanes under dead load conditions. The finite element modeling of the prototype bridges was calibrated by means of a physical load test data from the field testing of a two-span continuous skewed slab-on-girder bridge described in chapter-3. Based on this study empirical formulas for the moment and shear distribution factors under dead loading were generated to develop more realistic design guidelines for shored and unshored sequence of construction.

4.2 Behavior of Skewed I-girder Bridge at Construction Stage

In modern transportation system, skewed bridges are becoming increasingly common due to ever more restrictive site and geometric constraints. Skew greatly complicates the behavior of slab-on steel I-girder bridges by introducing alternate load paths and causing complex interaction between the main girders and secondary framing members that can lead to significant construction and design problems (Coletti et al. 2011). In skewed bridges, under the influence of live loads, longitudinal girders undergo torsional rotation at the supports (Surana and Humar 1984). These rotations are larger at the obtuse corners and difficult to predict during the construction stage due to the uneven distribution of wet concrete dead loads across the superstructure that increase the skew effects (Choo et al. 2005). Over the past decade, several authors have drawn attention to the potential for steel I-girder twisting on highly skewed supports (AASHTO/NSBA 2003, Beckman et al. 2005, Coletti and Yadlosky (2005, 2007). In addition to girder twisting, skewed bridges can also lead to increased flange lateral bending stresses in the girders, as well as increased girder shears and end reactions for girders framing into the obtuse corners of the bridge and results in subsequent reductions in girder shears and end reactions, and even possibly undesirable uplift in girders, framing into the acute corners of the bridge (Fisher 2006, Ozgur et al. 2011, Krupicka and Poellot 1993).

Unlike in-service skewed bridges, there are limited studies that focus on the behavior of these structures during the construction stage (Norton et al. 2003, Linzell et al. 2010, Sharafbayani et al. 2011). Similar research dealing with the development of load distribution factors for girder moment and shear at construction stage is scarce. Recently, based on the parametric study analysis by Theoret and Massicotte (2011), CHBDC (CSA 2014a) has specified equations to compute the shear magnification factor for skewed slab-on-girder bridges due to dead loads for shored sequence of construction. These design guidelines are developed by considering some assumptions that impose restrictions upon its applicability to the skewed slab-on-girder bridges under shored sequence of construction: (i) contribution of diaphragms should not be considered, and (ii) diaphragms and intermediate cross-frame should be placed parallel to the line of support (CSA, 2014b; clause 5.6.3). Previous studies revealed that the arrangement of internal diaphragms in

skewed bridge has a significant effect on the load distribution pattern and should not be ignored (Khaloo and Mirzabozorg 2003, Nouri and Ahmadi 2012). Also, during the construction stage diaphragms resist girder lateral torsional buckling and stabilizes compression flange (Keating and Alan 1992, Helwig and Wang 2003). A recent study has demonstrated that parallel cross-frame layout can be employed for a skew angle up to 30° (Razzaq et al. 2015). It was also found that beyond that skew limit and up to 60°, a perpendicular staggered cross-frame layout enhances the performance of the bridge structure due to three facts: (i) reduction of the cross-frame forces at the supports, (ii) limitation of the differential vertical displacement of cross-frame at obtuse corners, and (iii) reduction of girder longitudinal bending moment and vertical support reactions.

4.3 Non-composite I-girder Bridge at Construction Stage

According to CHBDC (CSA 2014a) clause 10.11.4, for composite beams and girders in the positive moment regions, the normal stress in either flange of the steel section due to serviceability dead and live loads (to control permanent deflection) shall not exceed 0.90 F_y .

$$\frac{M_d}{S} + \frac{M_{Sd}}{S_{3n}} + \frac{M_L}{S_n} \leq 0.9F_y \quad (4.1)$$

where, M_d is the bending moment in beams or girders at SLS due to dead load, M_{Sd} is the bending moment in beams or girders at SLS due to superimposed dead load, M_L is the bending moment in beams or girders at SLS due to live load, S is the elastic section modulus of the steel section, and S_n , S_{3n} are the elastic section modulus comprising the steel beam or girder and the concrete slab, calculated using a modular ratio of n or $3n$, respectively.

In-order to evaluate the effect of sequence of construction on the load distribution of skewed steel I-girder bridge, a sensitivity study explained in chapter-3 was conducted to predict the influence of M_d and M_{Sd} on the moment magnification factor. The results showed that the moment magnification factors have negligible effect on non-composite braced steel girder superstructure with different skew angles (i.e. before concrete hardening), so that it can be considered equal to 1 for M_d calculation in equation 4.1.

4.4 Composite I-girder Bridge at Construction Stage

The CHBDC (CSA 2014a) and AASHTO-LRFD (AASHTO 2014) bridge design specifications permits shored sequence of construction. This form of construction keeps the steel girders in a load free condition until the concrete has cured and allows the steel girders to work together with the bridge concrete deck above and form a composite section, which increases the girder strength as well as its stability. Based on the sensitivity study presented in chapter-3, it has been demonstrated that for modeling the composite braced steel girder system under dead load after hardening the moment magnification factor changes with the skew angle. So, it has to be calculated for the determination of M_{sd} in equation 4.1. In case of shored construction, the composite section carries all dead load available in the structure so that equation 4.1 can be re-written as;

$$\frac{M_d + M_{sd}}{S_{3n}} + \frac{M_L}{S_n} \leq 0.9F_y \quad (4.2)$$

In equation 4.2, the composite girder in shored construction supports the combined effect of: (i) dead load due to their own weight as well as the weight of the freshly poured deck concrete (M_d), and (ii) superimposed loading coming over the structure in-terms of weight of asphalt layer and the weight of the barrier wall (M_{sd}). The sensitivity study results showed that shored sequence of construction has substantial effect on the load distribution of girder, particularly on the interior girders, and needs to be considered to develop more realistic slab-on-girder design guidelines.

4.4.1 Parametric Study

The objective of current research was to investigate the effect of shored sequence of construction on the girder response in a skewed slab-on-girder bridge by conducting three-dimensional finite element modeling. The study examined: (i) flexural stresses in the interior and exterior girders, and (ii) shear stresses at the obtuse, acute and interior girder corners of the bridge to ascertain influences of various parameters including: span length, girder spacing, number of girders, number of design lanes and skew angle; on behavior and corresponding shear and moment distribution factors were computed. The parametric study

was based on the following assumptions: (1) all materials were elastic and homogeneous; (2) the effects of road super-elevation and curbs were ignored; and (3) the reinforced-concrete deck slab and the supporting steel I-girders were in full composite action; (4) both the deck slab and the supporting I-girders were simply supported at the abutments; (5) transverse intermediate cross-braces were moment-connected to the longitudinal girders. Subsequently, based on the data generated from this parametric study, sets of empirical expressions were developed to accurately calculate the girder shear and moment distribution factors.

4.4.2 Description of Bridge Prototypes

To avoid repetition, Figure 3.2 shows typical details of a two-lane and a four-lane single span steel-concrete composite I-girder bridges as an examples of bridges considered in this study. The basic bridge cross-sectional configurations considered in this study are presented in Table 4.1. The modulus of elasticity of the concrete material was 25 GPa with a Poisson's ratio of 0.20, whereas these design values for the steel material were 200 GPa and 0.30, respectively. Six different span lengths ranging from 15 m to 40 m were considered with an increment of 5 m, and girder response was evaluated for nine different skew angles from 0° to 60°. The concrete deck slab thickness was 225 mm. The cantilever slab length was equal to half the girder spacing. The X-type cross-frames at the support and between the span was provided in accordance with the specification stipulated in the manual of standard short-span steel bridges (Theodor and Al-Bazi 1997). Cross-frame members were spaced at equal intervals between the support lines and were made of L102x102x11 steel angles. Based on a sensitivity study presented in chapter-3, parallel cross-frame layout was used for bridge configurations up to 30° skew angle, and perpendicular staggered cross-frame layout was adopted for skew angles between 30° and 60° (Razzaq et al. 2015). In total, 594 bridge cases were analyzed and assessed using finite element analyses (FEA).

Table 4.1 Geometry of prototype bridges

Span (L), m	Design lanes (n)	Bridge width (W), m	Number of girders (N)	Girder spacing (S), m	Girder cross-sectional dimensions, mm			
					Girder depth (d)	Flange width (b _f)	Flange thickness (t ₁)	Web thickness (t ₂)
15	1	6	3	2.00	1000	300	20	14
			4	1.50	1000	300	20	14
	2	7.6	3	2.53	1000	300	20	14
			4	1.90	1000	300	20	14
			5	1.52	1000	300	20	14
	3	11.2	4	2.80	1000	300	20	14
			5	2.24	1000	300	20	14
			6	1.87	1000	300	20	14
	4	14.6	5	2.92	1000	300	20	14
			6	2.43	1000	300	20	14
			7	2.09	1000	300	20	14
	20	1	6	3	2.00	1100	300	25
4				1.50	1100	300	25	14
2		7.6	3	2.53	1100	300	25	14
			4	1.90	1100	300	25	14
			5	1.52	1100	300	25	14
3		11.2	4	2.80	1100	300	25	14
			5	2.24	1100	300	25	14
			6	1.87	1100	300	25	14
4		14.6	5	2.92	1100	300	25	14
			6	2.43	1100	300	25	14
			7	2.09	1100	300	25	14
25		1	6	3	2.00	1200	400	25
	4			1.50	1200	400	25	16
	2	7.6	3	2.53	1200	400	25	16
			4	1.90	1200	400	25	16
			5	1.52	1200	400	25	16
	3	11.2	4	2.80	1200	400	25	16
			5	2.24	1200	400	25	16
			6	1.87	1200	400	25	16
	4	14.6	5	2.92	1200	400	25	16
			6	2.43	1200	400	25	16
			7	2.09	1200	400	25	16
	30	1	6	3	2.00	1200	550	40
4				1.50	1200	550	40	16
2		7.6	3	2.53	1200	550	40	16
			4	1.90	1200	550	40	16
			5	1.52	1200	550	40	16
3		11.2	4	2.80	1200	550	40	16

			5	2.24	1200	550	40	16
			6	1.87	1200	550	40	16
	4	14.6	5	2.92	1200	550	40	16
			6	2.43	1200	550	40	16
			7	2.09	1200	550	40	16
35	1	6	3	2.00	1400	550	35	16
			4	1.50	1400	550	35	16
	2	7.6	3	2.53	1400	550	35	16
			4	1.90	1400	550	35	16
			5	1.52	1400	550	35	16
	3	11.2	4	2.80	1400	550	35	16
			5	2.24	1400	550	35	16
			6	1.87	1400	550	35	16
	4	14.6	5	2.92	1400	550	35	16
			6	2.43	1400	550	35	16
			7	2.09	1400	550	35	16
40	1	6	3	2.00	1600	500	30	16
			4	1.50	1600	500	30	16
	2	7.6	3	2.53	1600	500	30	16
			4	1.90	1600	500	30	16
			5	1.52	1600	500	30	16
	3	11.2	4	2.80	1600	500	30	16
			5	2.24	1600	500	30	16
			6	1.87	1600	500	30	16
	4	14.6	5	2.92	1600	500	30	16
			6	2.43	1600	500	30	16
			7	2.09	1600	500	30	16

4.4.3 Finite Element Modeling

The concrete slab and web of steel girders were modeled using four-node 3D elastic shell elements with six degrees of freedom at each node. The top and bottom flanges of longitudinal steel girders were modeled using two-node 3D elastic beam elements with six degrees of freedom at each node. The transverse diaphragm cross-frames were simplified and modeled using the same beam elements. The shell and beam elements were connected by rigid link elements. These elements were used to model the composite action between the deck and the girders by connecting the nodes of the deck elements with the beam and shell elements. The connections between the girder and cross-frame elements were fixed. Further details about the finite element modeling of composite slab-on I-girder bridges can be found in chapter-3.

4.4.4 Loading Condition

For the purpose of comparing the results of a skewed bridge with a straight configuration, in-addition to the self-weight of the structure, the superimposed loading was applied over the girders in the form of line loads assuming that each girder carried the equal weight of the two barrier walls and the asphalt layer. The thickness of the asphalt layer was taken as 90 mm, and CHBDC performance level-3 bridge barriers (CSA 2014a) were considered on both sides of the bridge deck as applied loads without any contribution to bridge cross-section flexural stiffness.

4.4.5 Evaluation of Distribution Factors

A practical design oriented parametric study was conducted on selected bridge configurations, shown in Table 4.1, to determine the longitudinal moment (F_m) and shear distribution factors (F_v). Since under the linear elastic conditions, stresses are proportional to the bending moments in the girders. Hence, instead of computing the girder moment, maximum stresses at the extreme fiber of the girder bottom flange was obtained from finite element analyses. For this purpose, the maximum flexural stress (σ_{3D}) and the maximum shear force (V_{3D}) of a three-dimensional simply supported structure under the effect of dead load were first calculated for each prototype bridge. Subsequently, the maximum flexural stress (σ_{2D}) and the maximum shear force (V_{2D}) from a simple two-dimensional beam-line model (Barker and Puckett 1997) were evaluated for each prototype bridge in the parametric study. The F_m and F_v , thus calculated is represented as;

$$F_m = \frac{\sigma_{3D}}{\sigma_{2D}} \quad (4.3)$$

$$F_v = \frac{V_{3D}}{V_{2D}} \quad (4.4)$$

To precisely determine the parameters affecting the previously mentioned distribution factors, a sensitivity study was undertaken. As a result, it was found that the key parameters that affect the structural response of a skewed bridge system are: (1) skew angle (ψ), (2)

girder spacing (S), and (3) span length (L). The study revealed that the slab thickness has insignificant effects on the skewed girder behavior. This result is in agreement with the investigations of Huo et al. (2004) and Phuvoravan et al. (2004), among others. For this reason, slab thickness is taken constant i.e. 225 mm, for all bridge configurations considered in this study. To account for the relative stiffness of the bridge system, Bakht and Moses (1988) on the basis of detailed study of some 30 slab-on-girder bridges of different spans in North America presented a relationship for the upper and lower bound limit between the longitudinal flexural rigidity per unit width (D_x) and the span length (L). All girder geometries, mentioned in Table 4.1, selected from the manual of standard short-span steel bridges (Theodor and Al-Bazi 1997) falls well within the practical upper and lower bound limits.

Based on sensitivity study findings, the effect of above-mentioned superstructure variables on girder F_m and F_v were examined in the parametric study, and discussed in the following sub-section. Only the response of girders in a two-lane and four-lane bridge configuration are presented whereas the equations for F_m and F_v were developed for all the bridge design matrix.

4.4.5.1 Effect of Skew Angle

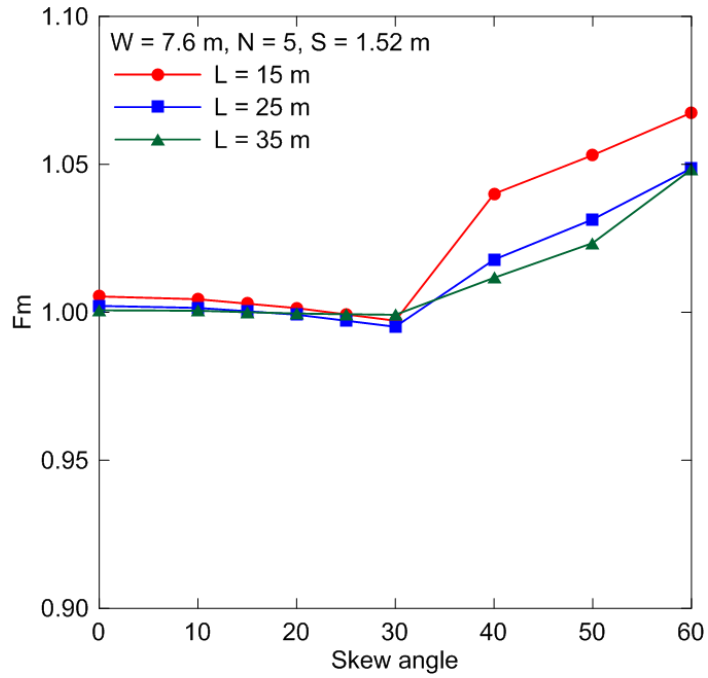
Skew angle of the deck is the most critical factor that influences the moment and shear distribution among girders. Figure 4.1 and 4.2, shows the FEA results of an exterior and interior girder of skewed bridges under shored sequence of construction quantified in terms of F_m as follows;

- 1) It was observed that skew has no significant effect on the exterior and interior girder moment distribution factor for skew angles between 0° and 30° .
- 2) For skew angle between 30° to 60° , exterior girder showed an increase of F_m value with the increase skew angle. As shown in Figure 4.1(a), this increase in F_m was more prominent in small span lengths for up to two-lane bridge configuration. However, with the increase in the number of lanes up to four, as can be seen in Figure 4.1(b), large span lengths resulted in greater increase of F_m value.

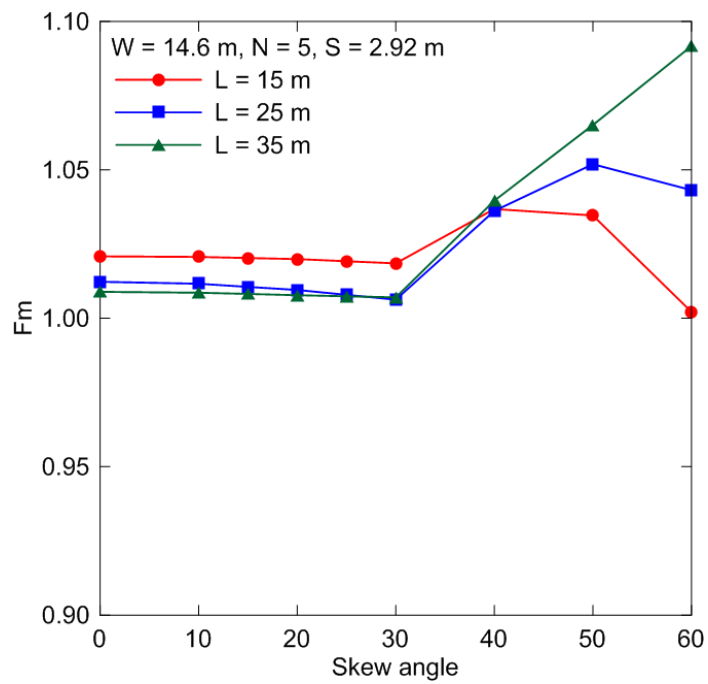
- 3) For one-lane and two-lane bridges at skew angle between 30° to 60° , interior girder showed a decrease of F_m value with the increase of skew angle. As illustrated in Figure 4.2(a), this reduction was more significant at high skew angles ($> 50^\circ$) for span length of 15 m and beyond 20 m span length, the effect of skew angle on the F_m value was found insignificant. Whereas three-lane and four-lane bridge configurations, as shown in Figure 4.2(b), resulted in considerable reduction of F_m value with the increase of skew angle up to 20 m span length and beyond 20 m span length up to 40 m, the increase of F_m value with the increase of skew angle between 30° to 60° was experienced.

Figure 4.3, 4.4 and 4.5, shows the FEA results of F_v at obtuse corner, acute corner and interior girder respectively for shored skewed bridge under dead loading;

- 1) For a multi-lane bridge configuration, it was observed that at the obtuse corner between 0° and 30° skew angle, F_v value was increased to a maximum of about 12%. With further increase in skew angles from 30° to 60° , as presented in Figure 4.3, the obtuse corner showed a substantial raise in F_v value. This increase in the response of F_v value was more pronounced in bridge structures having small girder spacing and reached about 35% within that skew range.
- 2) Figure 4.4 demonstrates the behavior of girder shear distribution factor at acute corners with the variation of skew angle. The results showed insignificant effect on the response of F_v value with the increase of skew angle between 0° to 60° .
- 3) At the interior girders, the value of F_v remains unaffected with the variation of skew angle between 0° and 30° (Figure 4.5). However, when the skew angle is in the range of 30° to 60° , a reduction of F_v value at interior girders were noticed. This decrease in the response of F_v value was more pronounced in bridge structures having equal number of lanes with large girder spacing.

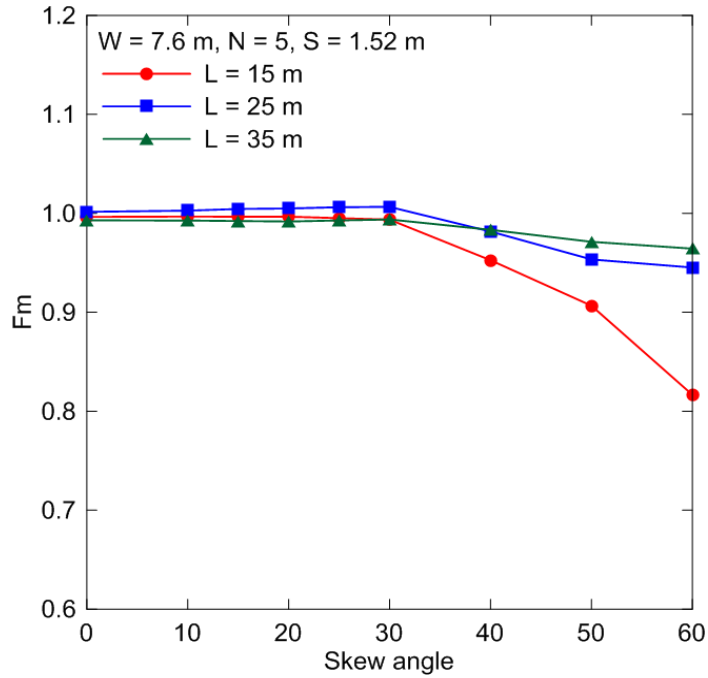


(a)

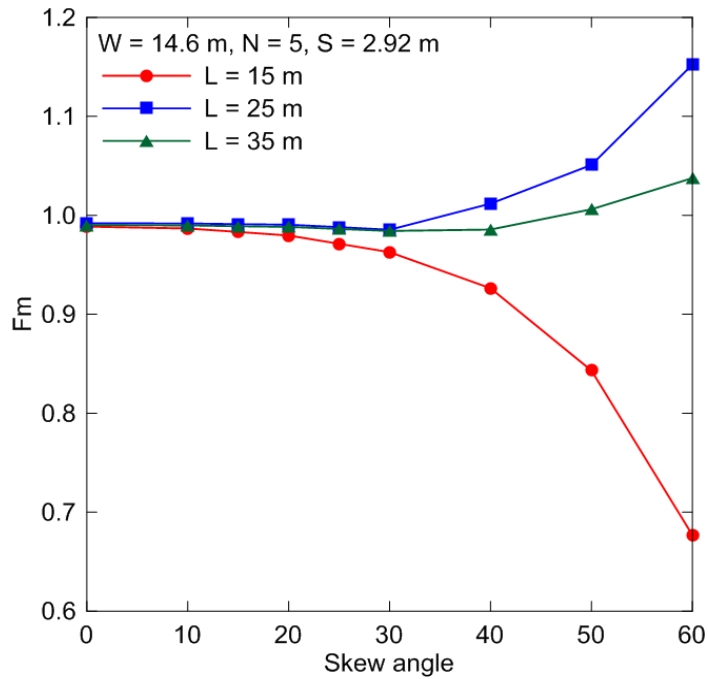


(b)

Figure 4.1 Effect of skew angle on F_m of exterior girders for: (a) two-lane, and (b) four-lane

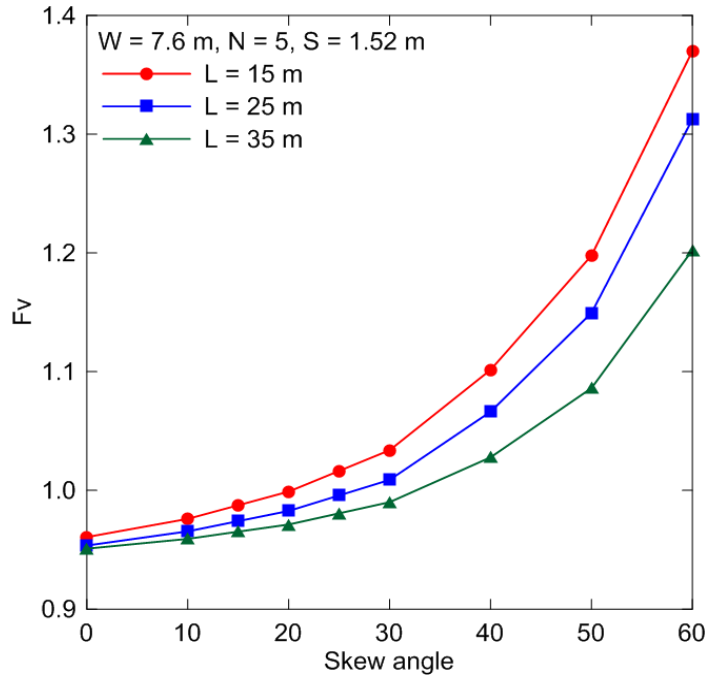


(a)

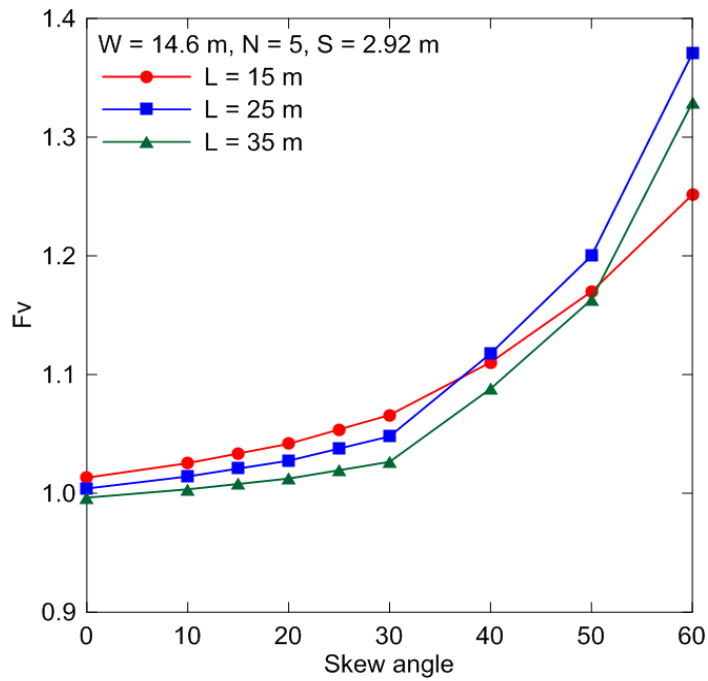


(b)

Figure 4.2 Effect of skew angle on F_m of interior girders for: (a) two-lane, and (b) four-lane

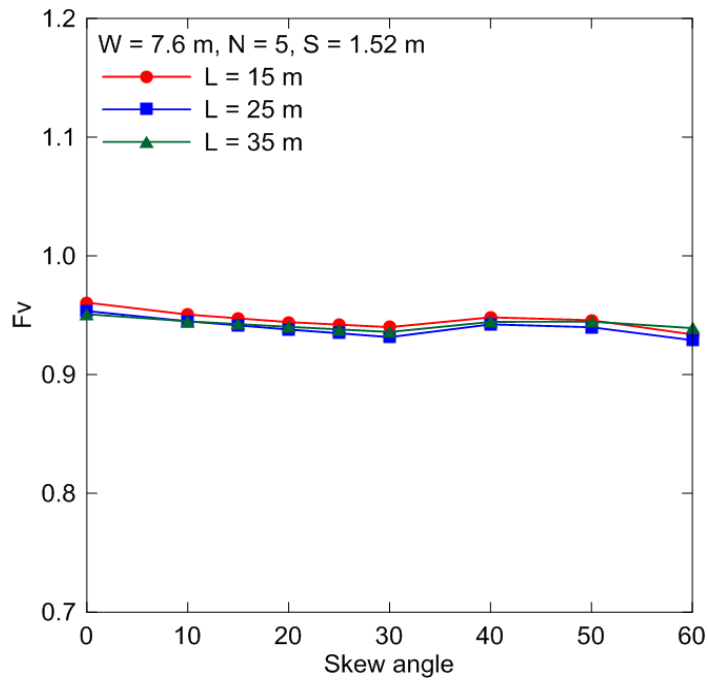


(a)

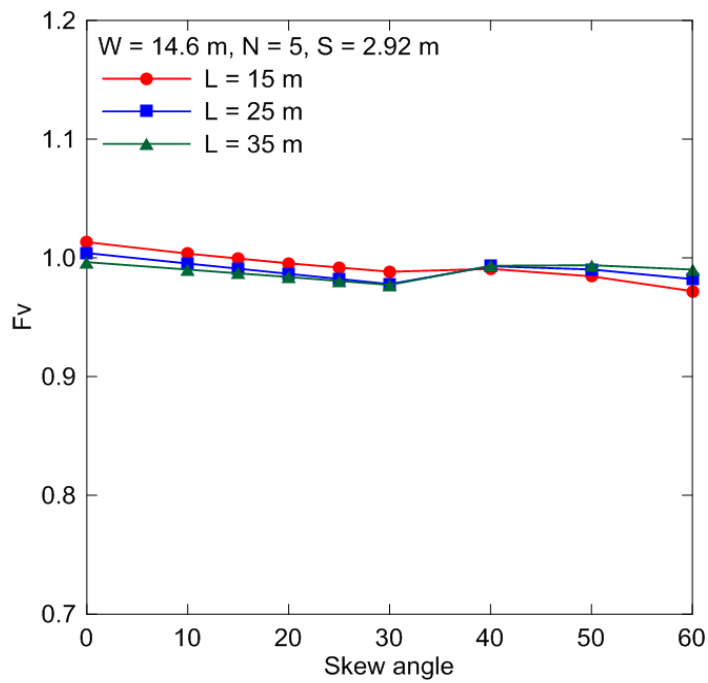


(b)

Figure 4.3 Effect of skew angle on Fv at bridge obtuse corners for: (a) two-lane, and (b) four-lane

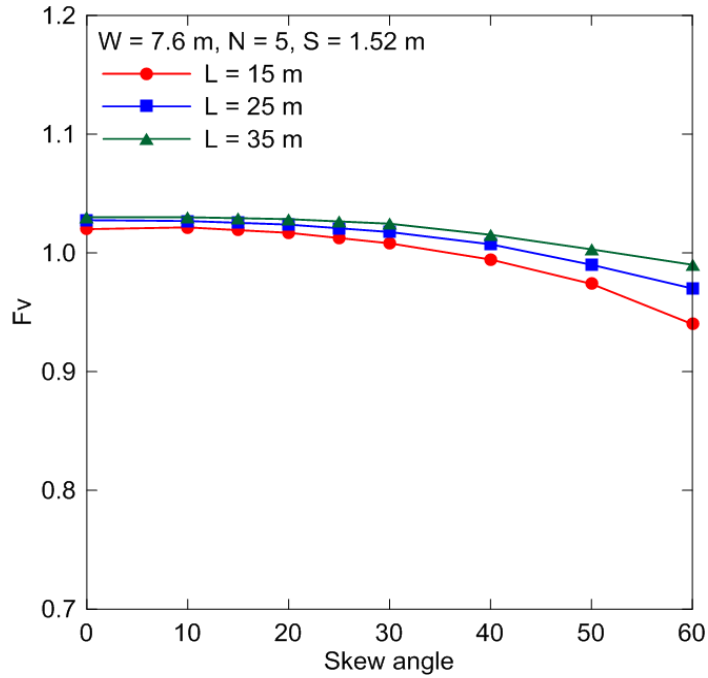


(a)

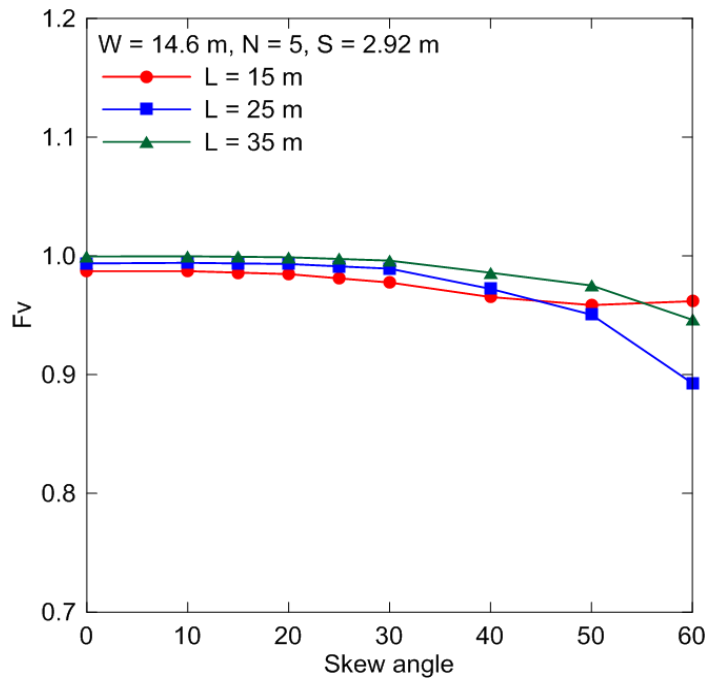


(b)

Figure 4.4 Effect of skew angle on Fv at bridge acute corners for: (a) two-lane, and (b) four-lane



(a)



(b)

Figure 4.5 Effect of skew angle on F_v of interior girders for: (a) two-lane, and (b) four-lane

4.4.5.2 Effect of Span Length

The moment and shear distribution factors for the multi-lane skewed bridges were evaluated and their effects with the variation of span lengths are summarized below;

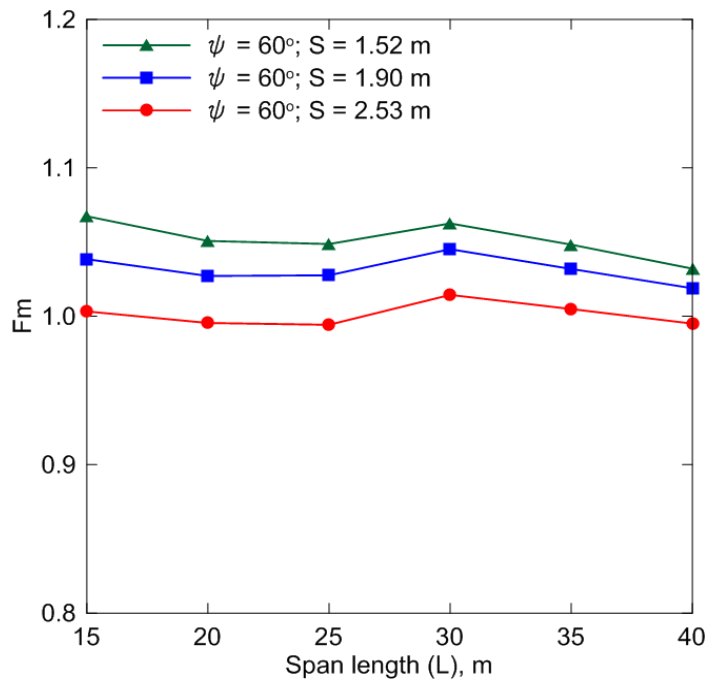
- 1) For skew angle up to 30° , F_m values for both the exterior and interior girder remains unaffected with the increase of span length.
- 2) Between 30° to 60° skew angles, the response of a one-lane and two-lane exterior girders showed a marginal increase in F_m value with the increase of span length up to 30 m and subsequently a declining trend in the response of F_m experienced between 30 m to 40 m span lengths, as can be seen in Figure 4.6(a). However, for the same skew angle range, the three-lane and four-lane bridge structure showed a considerable increase in F_m value up to 30 m span length, as shown in Figure 4.6(b).
- 3) The effect of span length on the F_m value of interior girder is presented in Figure 4.7. The results showed that for up to two-lane bridge configuration, the interior girder response increases with the span length for skew angles between 30° to 60° . For a three-lane and four-lane bridge a substantial increases of about 45% in F_m value was experienced when the span length varied from 15 m to 25 m, followed by an average of 12% reduction in F_m response for different girder spacing up to 40 m span length.

Figure 4.8, 4.9 and 4.10, shows the FEA results of an obtuse corner, acute corner and interior girder respectively of skewed bridges under shored sequence of construction and their effect on span length are summarized below;

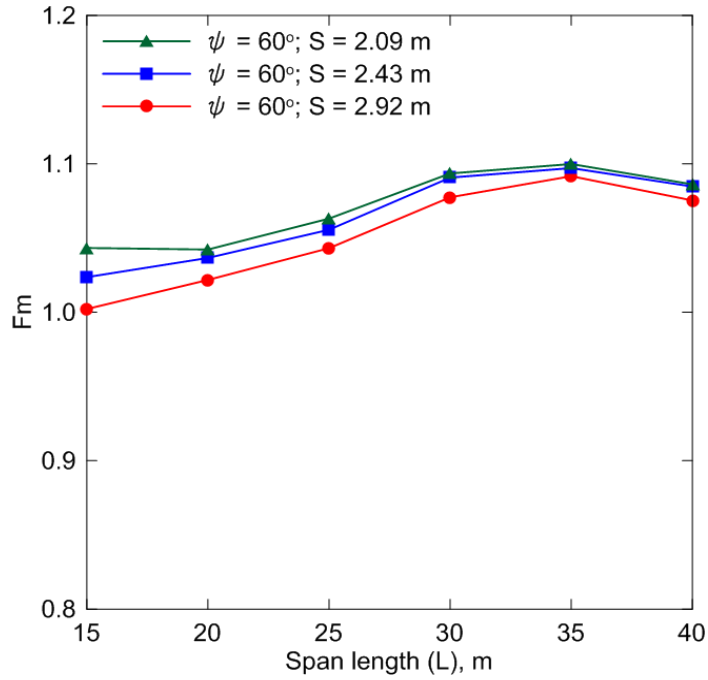
- 1) For multi-lane bridge configurations up to 30° skew angle, F_v values at the bridge obtuse corners were not significantly affected with the increase of the span length. A variation of about 5% was observed within that skew range. However, when the skew angle changes from 30° to 60° , F_v value decreases with the increase of span length and a maximum reduction of about 20% was experienced in two-lane bridge configuration, as shown in Figure 4.8(a). However, this reduction in the response of F_v value between 30° to 60° skew angles at the obtuse corners were found less prominent in case of one-lane and three-lane bridge structures i.e. 9% and 8% decrease respectively. Whereas, four-lane bridge arrangement showed a maximum of 12% increase in the F_v value with

the increase of span length from 15 m to 25 m, and subsequently a reduction of about 8% was noticed when the span length changes from 25 m to 40 m, as can be seen in Figure 4.8(b).

- 2) The girder shear distribution factor at acute corners were found not sensitive with the variation of span length, as presented in Figure 4.9.
- 3) Figure 4.10, shows the variation of the skewed bridge shear distribution factor for interior girders with the span length changes from 15 m to 40 m. For different number of lanes ($n=1$ to 4), the effect of shear distribution factor at interior girders resulted in the maximum of 5% increase with the variation of span length when the skew angle changes from 0° to 30° . However, between 30° to 60° skew angles, the interior girder reflected a significant increase in F_v value with the increase of span length from 15 m to 40 m for two-lane bridge geometry shown in Figure 4.10(a). Whereas, for bridge configuration having number of lanes greater than two, this increase in F_v value for 15 m to 40 m span length was found marginal.

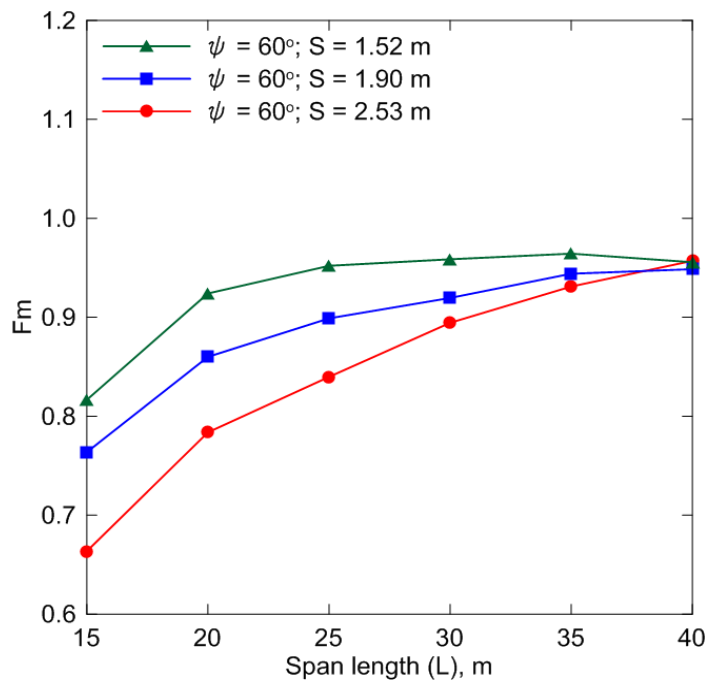


(a)

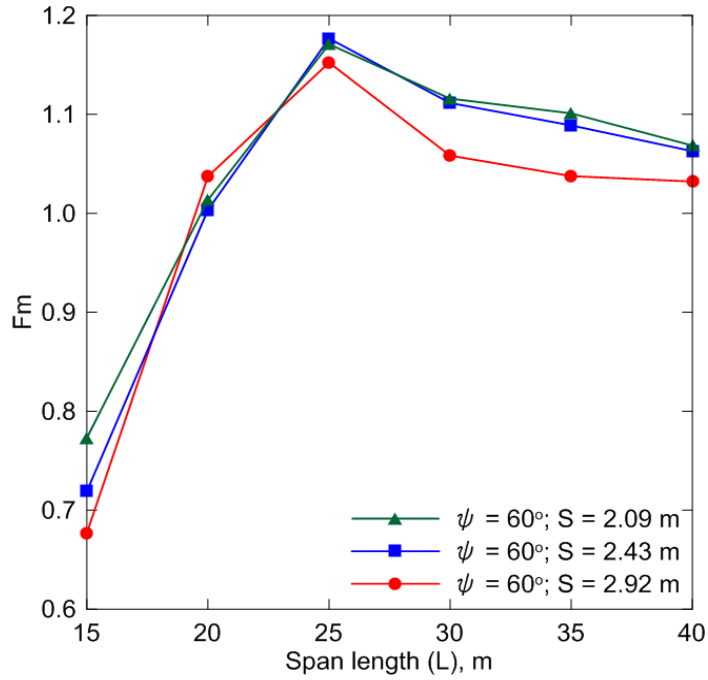


(b)

Figure 4.6 Effect of span length on Fm of exterior girders for: (a) two-lane, and (b) four-lane

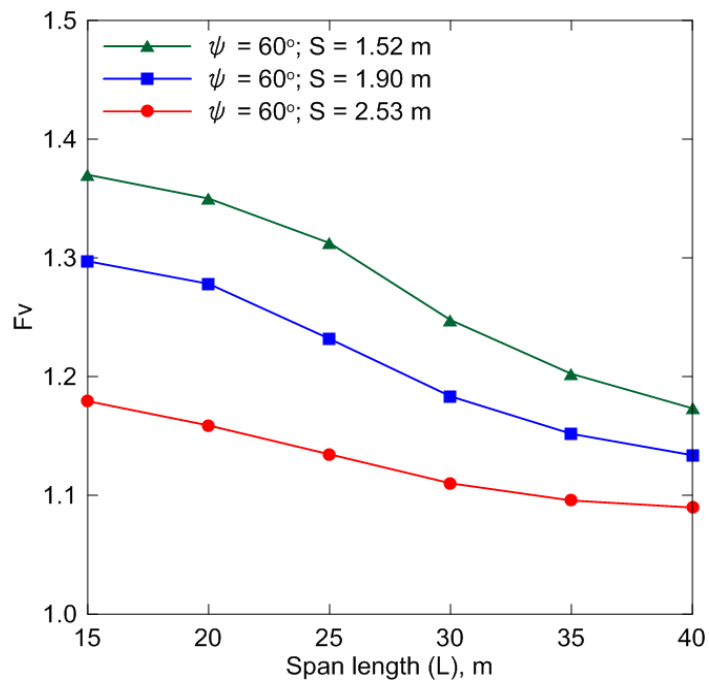


(a)

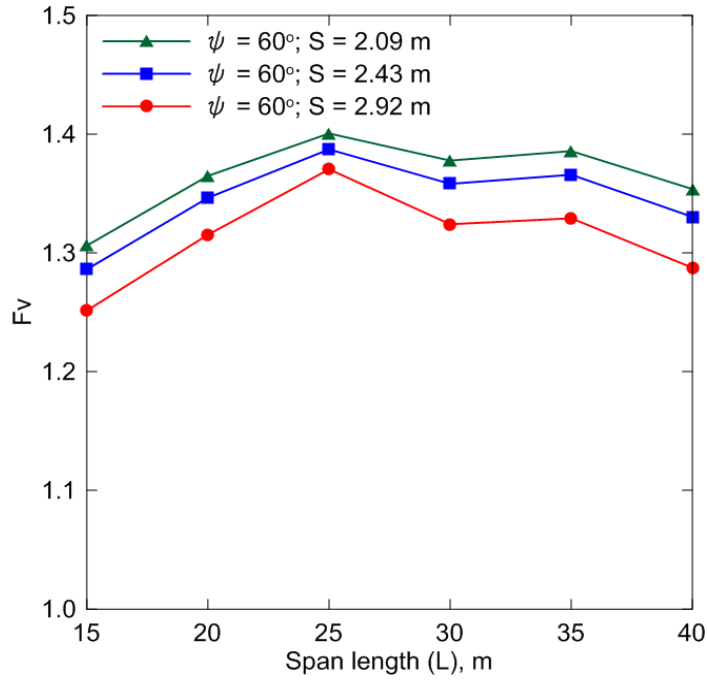


(b)

Figure 4.7 Effect of span length on F_m of interior girders for: (a) two-lane, and (b) four-lane

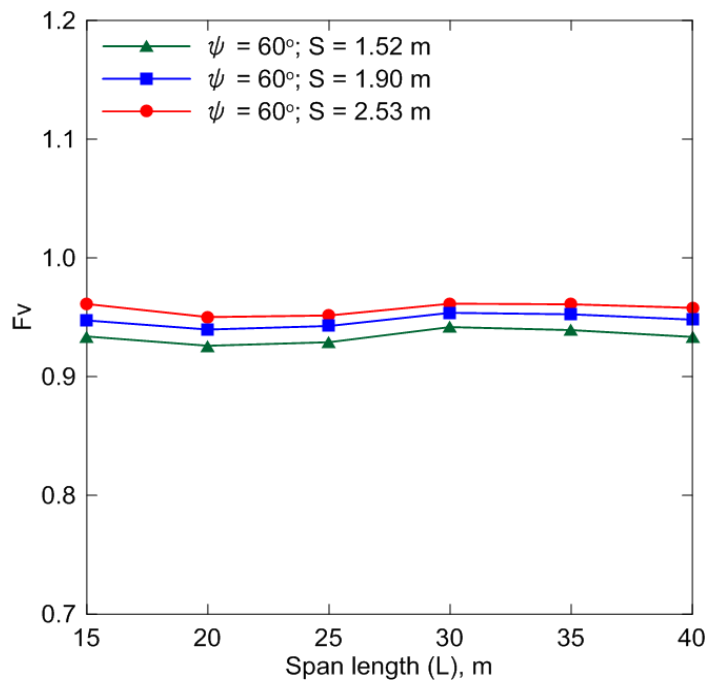


(a)

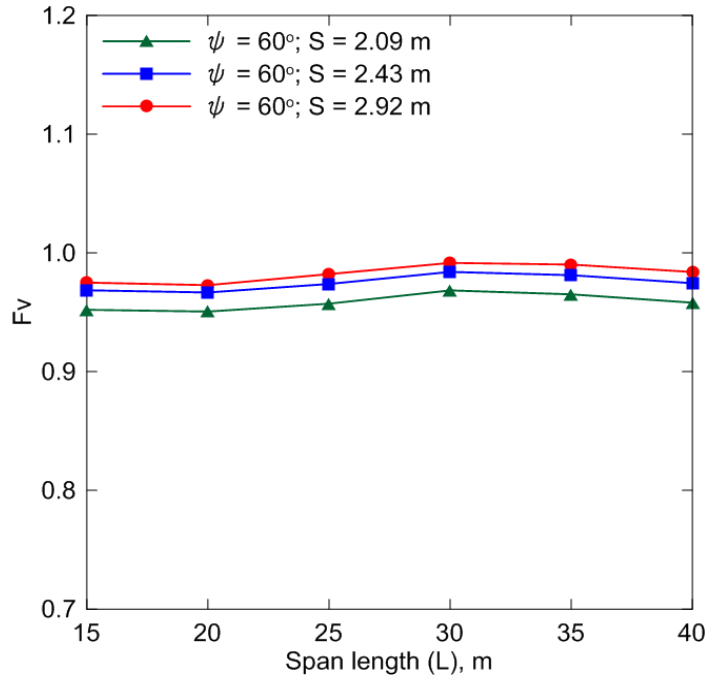


(b)

Figure 4.8 Effect of span length on Fv at bridge obtuse corners for: (a) two-lane, and (b) four-lane

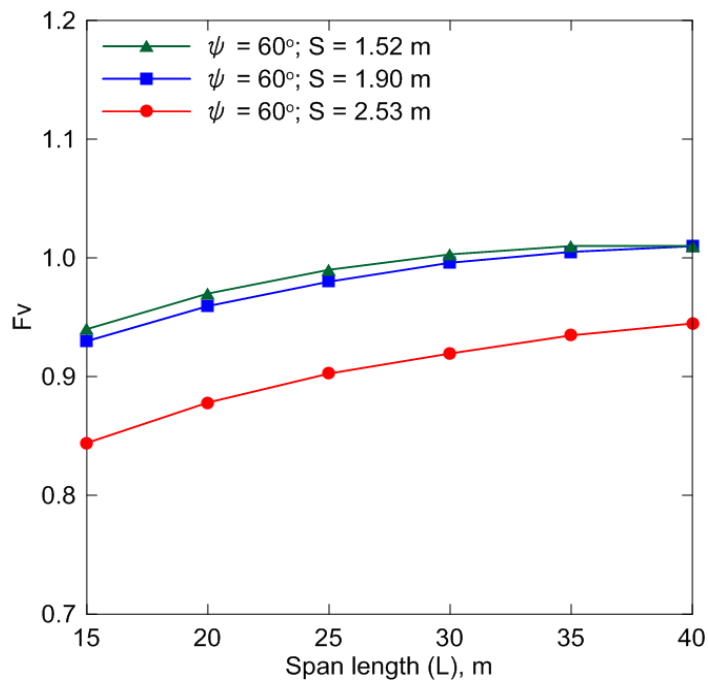


(a)

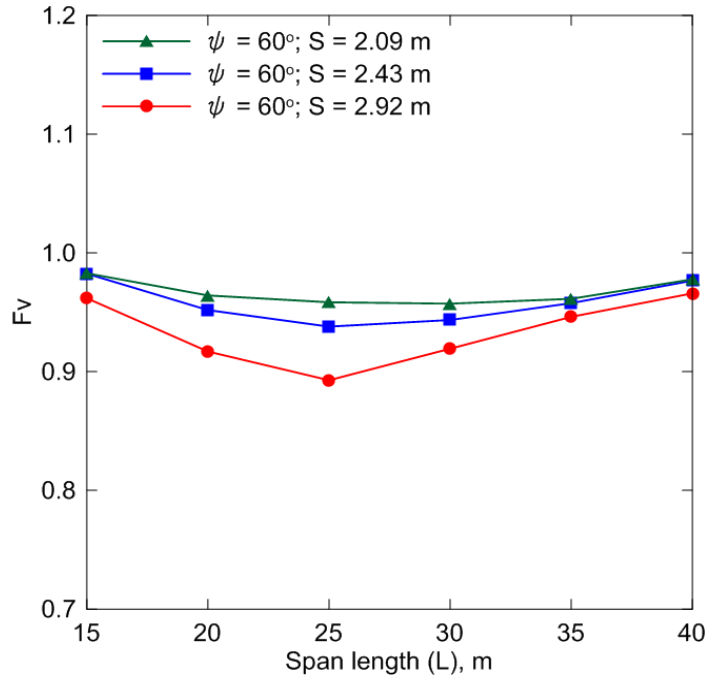


(b)

Figure 4.9 Effect of span length on Fv at bridge acute corners for: (a) two-lane, and (b) four-lane



(a)



(b)

Figure 4.10 Effect of span length on Fv of interior girders for: (a) two-lane, and (b) four-lane

4.4.5.3 Effect of Girder Spacing, Number of Girders and Number of Lanes

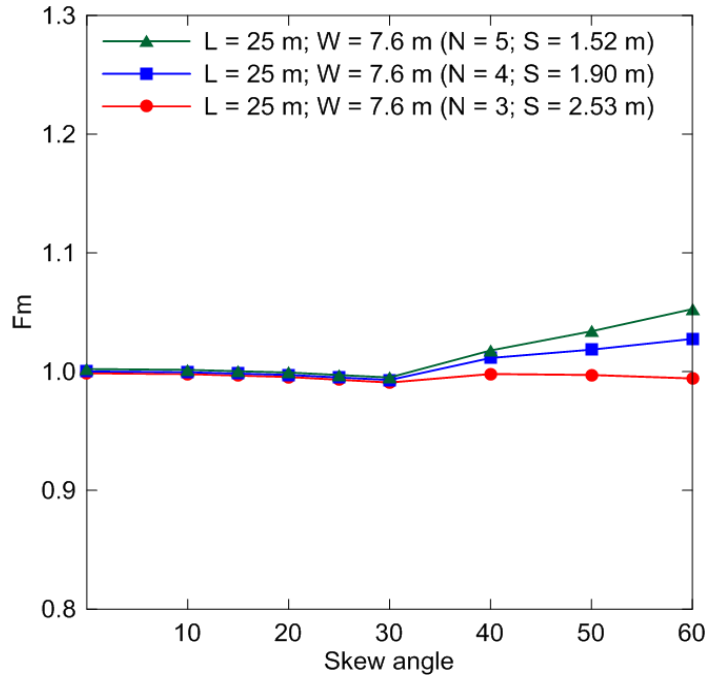
The girder spacing is dependent on the bridge width and the number of longitudinal girders. The bridge width can be considered to be the number of lanes multiplied by the lane width, which can be assumed to be constant for a given bridge configuration. Therefore the girder spacing could be related to the number of girders and the number of lanes. The effect of girder spacing on the moment distribution factors of the exterior and the interior girder are presented in Figure 4.11 and 4.12, and summarized below;

- 1) For the skew angle up to 30° , Fm values for both the exterior and interior girders were found insensitive to girder spacing.
- 2) As demonstrated in Figure 4.11, the increase in girder spacing causes reduction in the exterior girder Fm value for 30° to 60° skew angles.
- 3) Contrary to the behavior of external girders, the effect of girder spacing on the interior girder moment distribution factors did not present any clear pattern. For-example for the two-lane bridge, between 30° to 60° skew angle, increase in girder spacing resulted

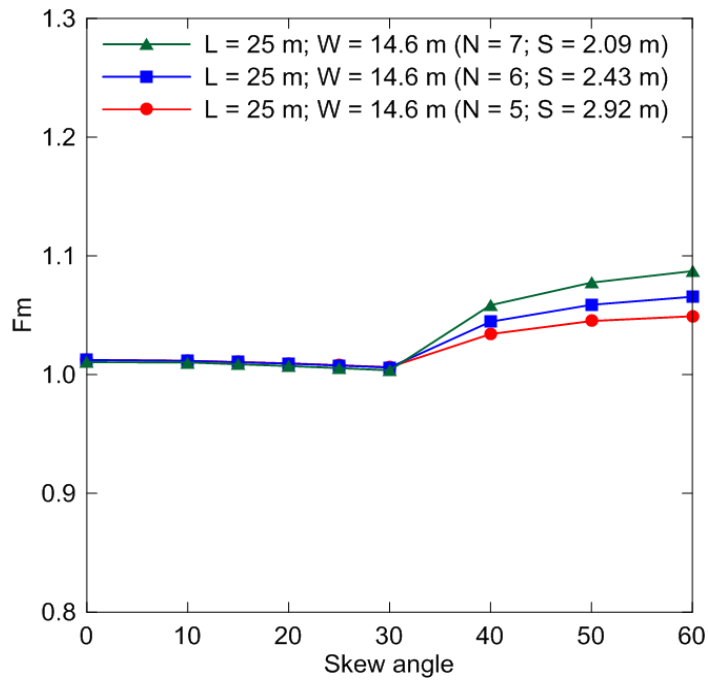
in the reduction of F_m value. However, for the three-lane and four-lane bridge geometries for the span length less than 20 m, it resulted in the reduction of F_m value and beyond 20 m span length it caused the F_m value to increase, as can be seen in Figure 4.12.

The effect of girder spacing on the shear distribution factors at bridge obtuse corner, acute corner and interior girder are presented in Figure 4.13, 4.14 and 4.15 respectively and discussed below;

- 1) For skew angle up to 30° , F_v value for the obtuse girder supports was found not sensitive to girder spacing. A minimal increase of about 5% was noticed within that skew range.
- 2) For higher skew angles ($> 30^\circ$), increase in girder spacing resulted in the reduction of the obtuse corner F_v value. This reduction in the response of F_v at bridge obtuse corners with the increase of girder spacing is much more pronounced up to three-lane bridge configurations. However for four-lane bridge, the influence of different girder spacing at high skew angles ($> 30^\circ$) found negligibly small, as shown in Figure 4.13(b).
- 3) The influence of girder spacing on F_v for a multi-lane bridge configuration at acute edges, shown in Figure 4.14, were found marginal with the variation of skew angle from 0° to 60° .
- 4) For skew angle between 30° to 60° , interior girder showed a reduction of F_v value with the increase of skew angle. This reduction is more pronounced in bridge configuration with larger girder spacing.

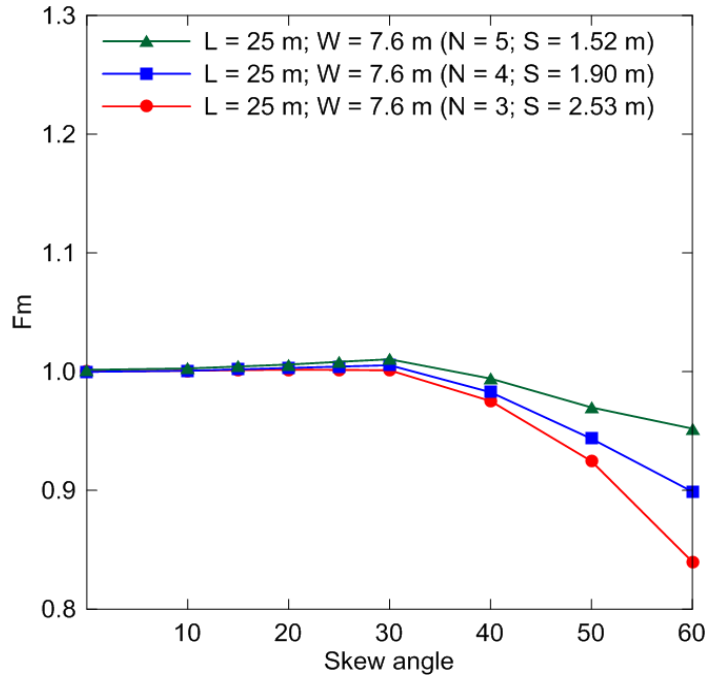


(a)

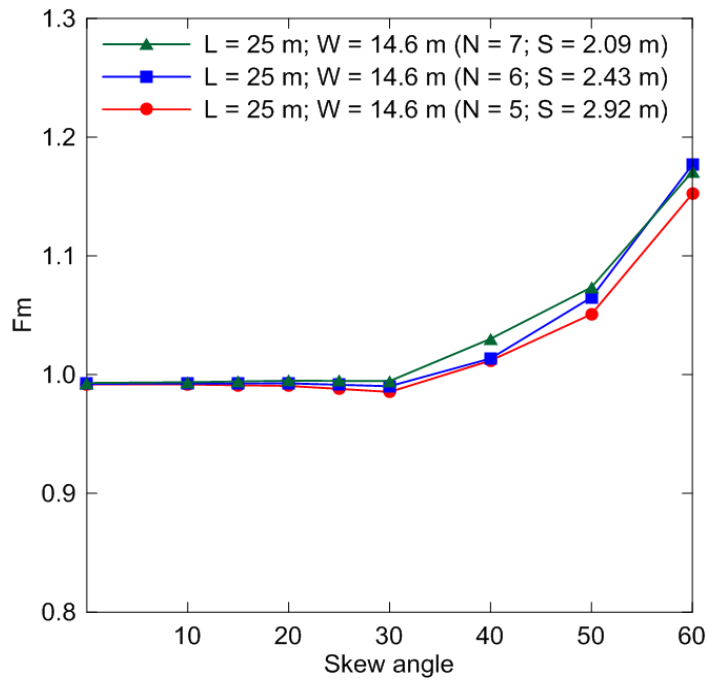


(b)

Figure 4.11 Effect of girder spacing on F_m of exterior girders for: (a) two-lane, and (b) four-lane

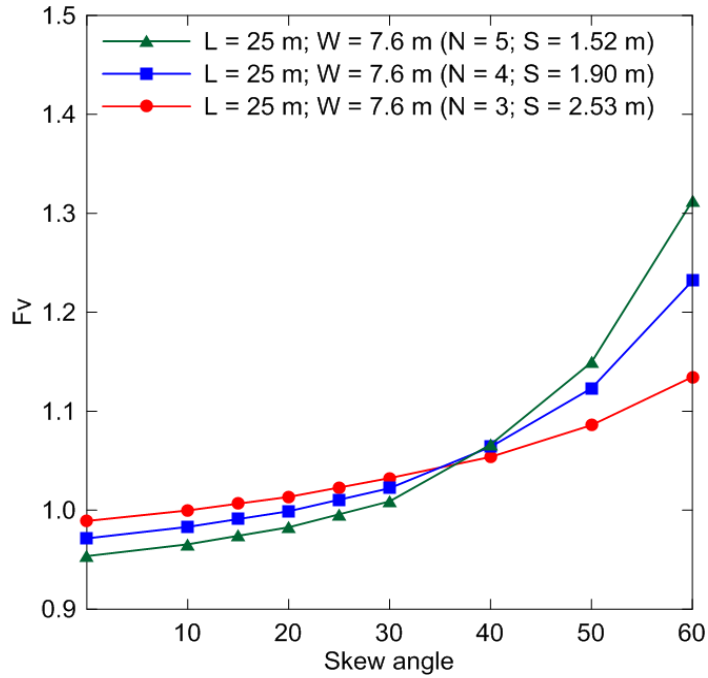


(a)

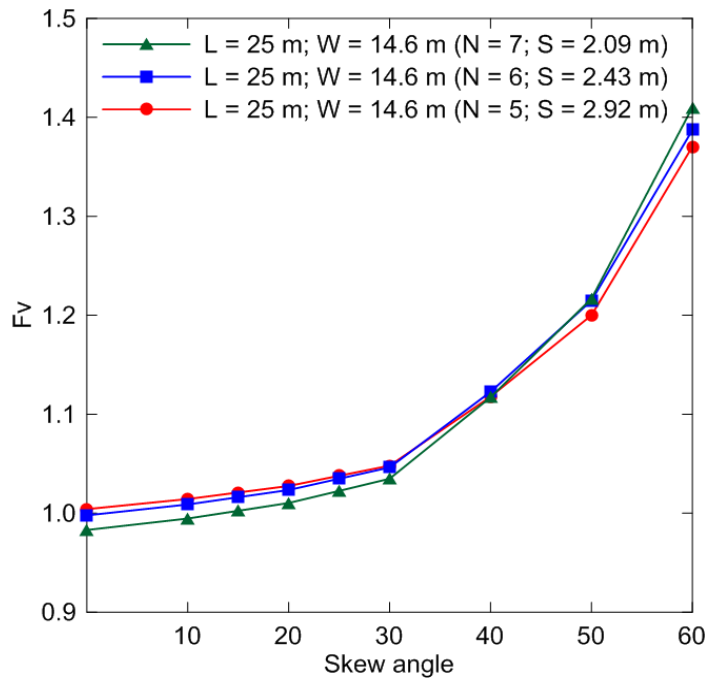


(b)

Figure 4.12 Effect of girder spacing on F_m of interior girders for: (a) two-lane, and (b) four-lane

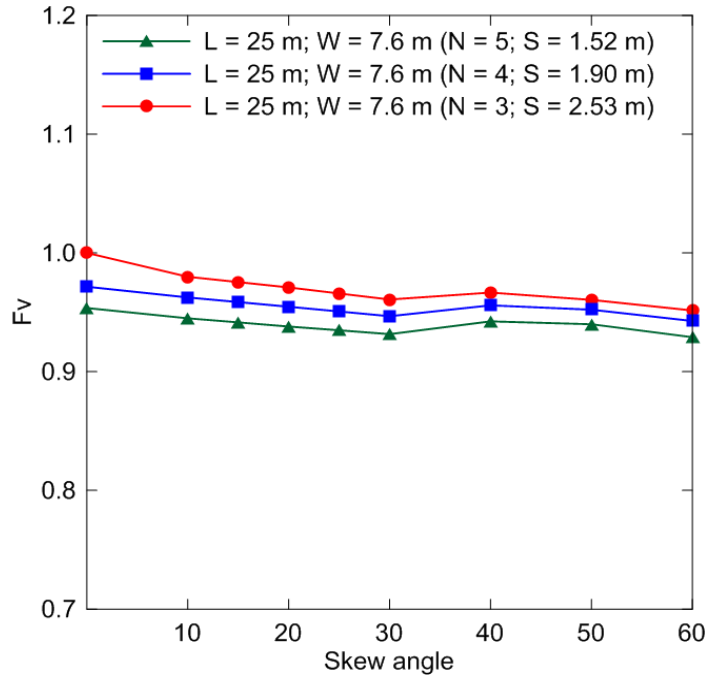


(a)

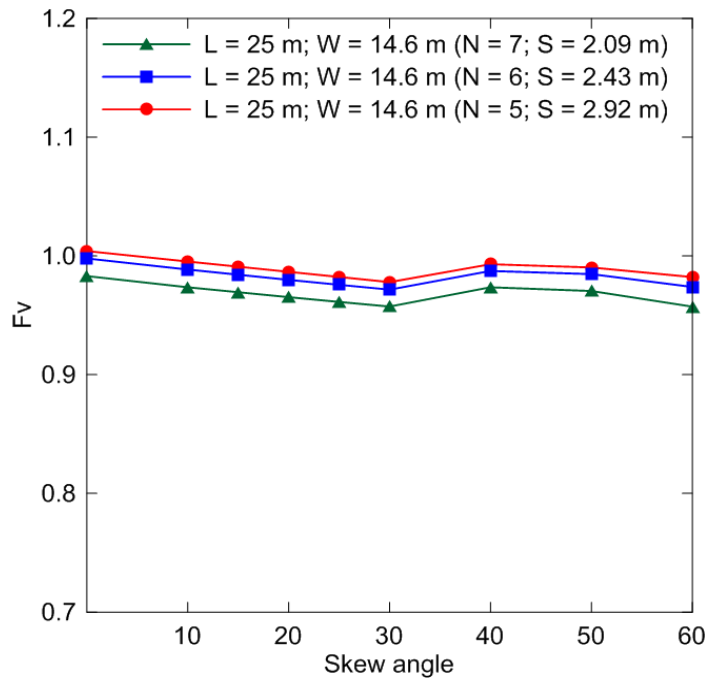


(b)

Figure 4.13 Effect of girder spacing on F_v at bridge obtuse corners for: (a) two-lane, and (b) four-lane

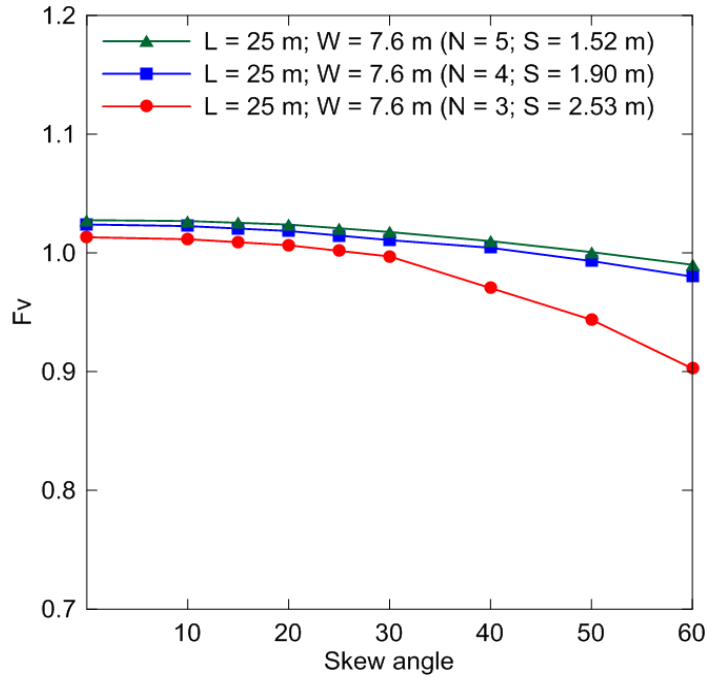


(a)

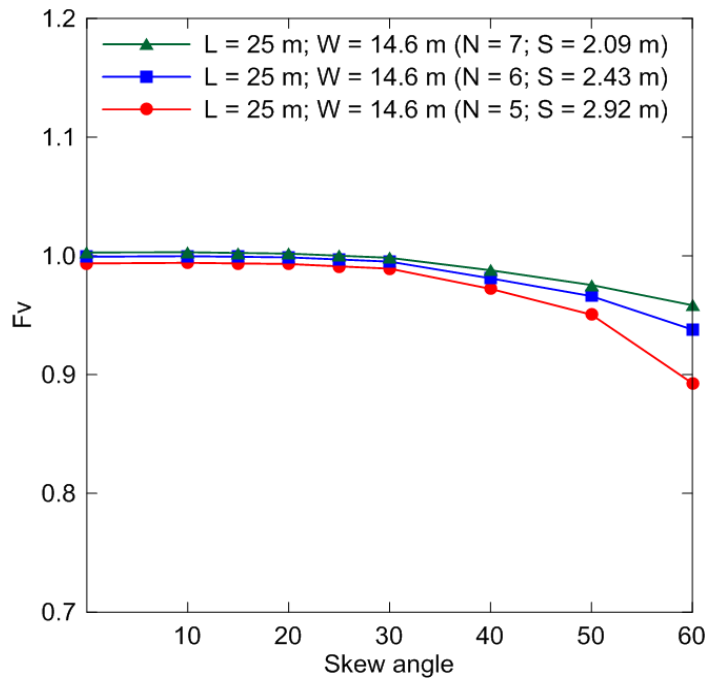


(b)

Figure 4.14 Effect of girder spacing on F_v at bridge acute corners for: (a) two-lane, and (b) four-lane



(a)



(b)

Figure 4.15 Effect of girder spacing on F_v of interior girders for: (a) two-lane, and (b) four-lane

4.4.6 Empirical Formula for Distribution Factors

Recently CHBDC (CSA 2014a) has specified equations to compute the shear distribution factor for the skewed slab-on-girder bridges due to dead loads for shored sequence of construction;

$$F_s = 1.2 - \frac{2.0}{(\varepsilon + 10)} \quad (4.5)$$

where,

$$\varepsilon = \left(\frac{L}{S} \right) \cdot \tan \psi \quad (4.6)$$

However, no such equation for the moment distribution factor is available in highway bridge codes (CSA 2014a). Such discrepancies in design specifications demands an accurate assessment of load distribution factors by developing modified equations based on a parametric study by considering three-dimensional finite element analysis. Using the data generated from the parametric study, it was found that moment and shear distribution factors were mainly influenced by few critical parameters, namely: skew angle, span length, girder spacing, number of girders and number of design lanes. So, in-order to keep uniformity and simplicity in understanding the distribution factors for bridge designers and engineers, it was decided to keep the format of equation 4.5 the same as proposed in the code (CSA 2014a), and develop a new equation for the “ ε ” factor that replaces equation 4.6, based on the parametric study results. Hence, the general empirical equation for the moment and shear “ ε ” factor took the following form, respectively;

$$\varepsilon = a \times L^b \times S^c \times N^d \times n^e \times \tan \psi \quad (4.7)$$

$$\varepsilon = a \times L^b \times S^c \times N^d \times n^e \times \cos \psi \quad (4.8)$$

where, a, b, c, d and e are equation variables, L is the bridge span length in meters; S is the girder spacing in meters; N is the number of girders, and n is the number of design lanes. Using regression analyses, the two sets of empirical equations for moment and shear distribution factor for the girders under dead loading of a skewed slab-on girder bridge were deduced and presented in Tables 4.2 and 4.3, respectively.

Table 4.2 Moment distribution factors for shored sequence of construction under dead loads

Load effect	Skew angle (ψ), deg.	Span (L), m	Fm	ϵ
Moment -exterior	$0 \leq \psi \leq 40$	$15 \leq L \leq 40$	$1.2 - \frac{2.0}{(\epsilon + 10)}$	$0.75L^{-1.2} S^{1.3} N^{0.75} n^{1.5} \tan \psi$
	$40 < \psi \leq 60$			$0.30L^{1.25} S^{-4.6} N^{-2.5} n^{4.85} \tan \psi$
Moment -interior	$0 \leq \psi \leq 30$	$15 \leq L \leq 40$	$1.2 - \frac{2.0}{(\epsilon + 10)}$	$-3.50L^{-0.9} S^{1.25} N^{-0.75} n^{1.25} \tan \psi$
	$30 < \psi \leq 40$			$-2.0L^{-1.4} S^{4.0} N^{1.7} n^{-2.0} \tan \psi$
	$40 < \psi \leq 50$	$L \leq 25$	$1.71 - \frac{19.0}{(\epsilon + 10)}$	$0.10L^{0.56} S^{2.0} N^{2.22} n^{-1.83} \tan \psi$
		$L \leq 40$	$1.10 - \frac{13.60}{(\epsilon + 10)}$	$0.23L^{0.7} S^{1.95} N^{2.48} n^{-1.75} \tan \psi$
	$50 < \psi \leq 60$	$L \leq 15$	$1.40 - \frac{14.90}{(\epsilon + 10)}$	$0.12L^{0.54} S^{1.42} N^{2.27} n^{-1.97} \tan \psi$
		$L \leq 25$	$5.37 - \frac{60.0}{(\epsilon + 10)}$	$0.15L^{0.28} S^{1.04} N^{1.16} n^{-0.82} \tan \psi$
		$L \leq 40$	$2.0 - \frac{20.33}{(\epsilon + 10)}$	$0.10L^{0.20} S^{2.0} N^{2.23} n^{-1.62} \tan \psi$

Table 4.3 Shear distribution factors for shored sequence of construction under dead loads

Load Effect	Span (L), m	Fv	Skew angle (ψ), deg.	ϵ
Shear - Obtuse	$15 \leq L \leq 40$	$1.2 - \frac{2.0}{(\epsilon + 10)}$	$0 \leq \psi \leq 20$	$\epsilon = -0.14L^{0.38} S^{-1.58} N^{1.72} n^{-1.14} \cos \psi$
			$20 < \psi \leq 40$	$\epsilon = 2.38L^{-1.46} S^{3.60} N^{2.66} n^{-1.50} \cos \psi$
			$40 < \psi \leq 50$	$\epsilon = 10.0L^{-1.58} S^{1.50} N^{3.50} n^{0.20} \cos \psi$
			$50 < \psi \leq 60$	$\epsilon = 6.77L^{-1.0} S^{-1.0} N^{2.48} n^{1.61} \cos \psi$
Shear - Acute	$15 \leq L \leq 40$	$1.2 - \frac{2.0}{(\epsilon + 10)}$	$0 \leq \psi \leq 20$	$\epsilon = -0.14L^{0.38} S^{-1.58} N^{1.72} n^{-1.14} \cos \psi$
			$20 < \psi \leq 40$	$\epsilon = -6.5L^{0.35} S^{-2.05} N^{-0.92} n^{0.74} \cos \psi$
			$40 < \psi \leq 60$	$\epsilon = -35.0L^{-0.16} S^{-1.70} N^{-0.72} n^{0.38} \cos \psi$
Shear - Interior	$15 \leq L \leq 40$	$1.2 - \frac{2.0}{(\epsilon + 10)}$	$0 \leq \psi \leq 20$	$\epsilon = 0.57L^{0.41} S^{-0.67} N^{1.19} n^{-2.85} \cos \psi$
			$20 < \psi \leq 40$	$\epsilon = -0.52L^{-1.64} S^{5.75} N^{1.14} n^{-2.10} \cos \psi$
			$40 < \psi \leq 50$	$\epsilon = -2.0L^{-1.11} S^{4.70} N^{1.17} n^{-2.20} \cos \psi$
			$50 < \psi \leq 60$	$\epsilon = 0.25L^{1.15} S^{-1.0} N^{1.95} n^{-0.35} \cos \psi$

4.4.7 Correlation of FEA Results and Proposed Equations with CHBDC

The effect of sequence of construction in a skewed slab-on-girder bridge was investigated by conducting a three-dimensional finite element modeling under dead loads. Based on the results obtained from the parametric study, set of empirical expressions were developed for the girder moment and shear distribution factors for rational prediction of the girder load distribution. Finally, the correlation between the CHBDC (CSA 2014a) equations and the proposed equations based on the parametric study for the moment and shear distribution factors are obtained and compared with the F_m and F_v values from the finite element analysis due to dead loads, as presented in Figure 4.16 and 4.17 respectively. The figure shows good correlation between the values obtained from the proposed equations and those calculated from FEA, and all data points fall within 5% over and under-estimation region, shown by dotted lines in Figure 4.16 and 4.17.

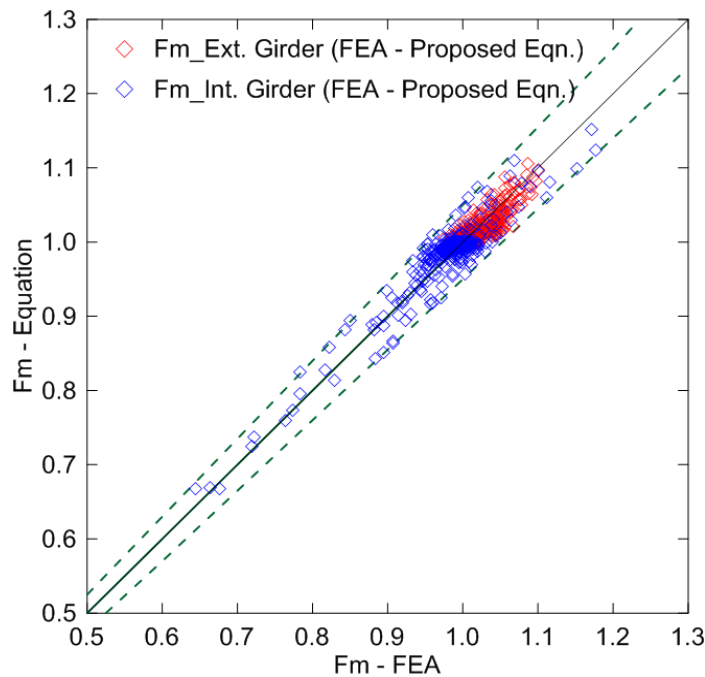
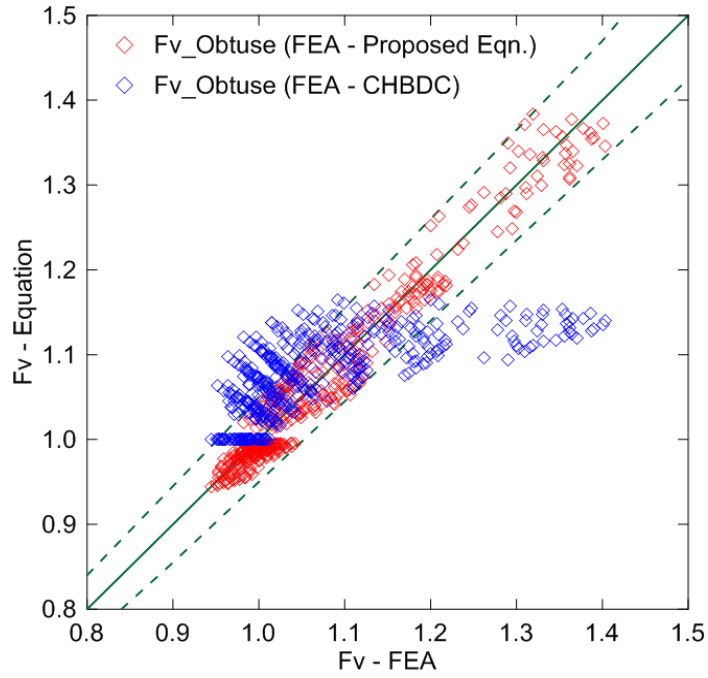
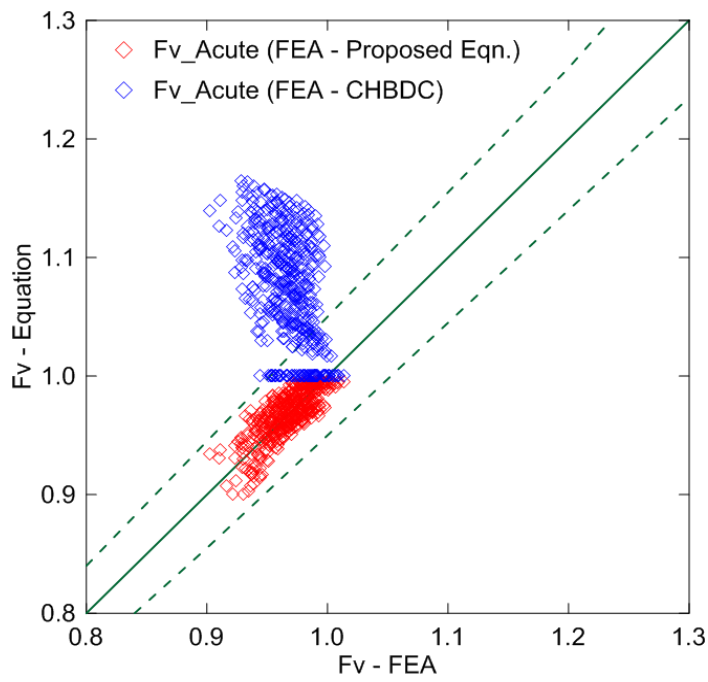


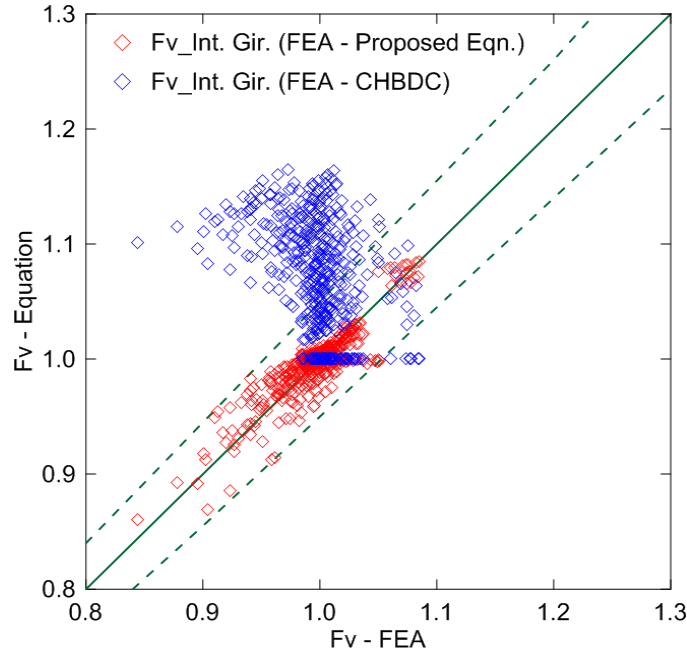
Figure 4.16 Correlation between moment distribution factors obtained from FEA results with proposed equations



(a)



(b)



(c)

Figure 4.17 Correlation between shear magnification factors obtained from FEA results with CHBDC and proposed equations for; (a) obtuse corner, (b) acute corner, and (c) interior girder

The illustrative example to calculate the moment and shear distribution factors using FEA, proposed equation and the CHBDC (CSA 2014a) for skewed slab-on steel I-girder bridges at dead loads are described in Appendix A. The comparison of results for the moment and shear distribution factors evaluated using FEA, proposed equation and the CHBDC (CSA 2014a) equation are presented in Table 4.4 and 4.5, respectively.

Table 4.4 Comparison of moment distribution factors for skewed slab-on steel I-girder bridges at dead load

Location of girder	FEA results	Proposed equation
Exterior	1.08	1.08
Interior	1.17	1.15

Table 4.5 Comparison of shear distribution factors for skewed slab-on steel I-girder bridges at dead load

Location of girder	FEA results	Proposed equation	CHBDC (CSA 2014a)
Obtuse corner	1.39	1.37	1.13
Acute corner	0.96	0.97	1.13
Interior girders	0.96	0.98	1.13

The result showed that the proposed equations were sufficiently accurate in predicting the response of a skewed bridge behavior. The CHBDC design equation was found conservative for shear at the acute corner and at the interior girders, whereas the code specifications resulted in an unsafe design for the girder shear at the obtuse corners. The main reasons for the inadequacy of the design equation to represent the actual behavior of a skewed bridge are highlighted below:

- 1) Based on the parametric study using grillage method of analysis for slab-on-girder bridges, Theoret and Massicotte (2011) introduced a new parameter F_s to modify the values of F_T to account for skew effects for shear at the obtuse corner. Although this analysis technique is generally accepted as sufficiently accurate for the most common design situations as well as for the construction stages, however for skewed bridges it results inaccurate assessment of the bridge responses and is not always recommended (Coletti and Puckett 2012, Vayas et al. 2011).
- 2) These design guidelines (CSA 2014a) are developed by considering some assumptions that impose restrictions upon its applicability to the skewed slab-on-girder bridges under shored sequence of construction: (i) contribution of diaphragms should not be considered, and (ii) diaphragms and intermediate cross-frame should be placed parallel to the line of support (CSA, 2014b; clause 5.6.3).
- 3) To represent skewed bridge behavior, the design equation is comprised of three design parameters i.e. span length (L), girder spacing (S) and skew angle (ψ). The parametric study results showed that behavior of skewed bridge is also affected by the width of the bridge represented by number of lanes (n) and number of girders (N).
- 4) It has already been reported that the presence of skew angle greatly complicates the bridge behavior (AASHTO/NSBA 2003, Beckman et al. 2005, Fisher 2006). Whereas, a single equation (clause 5.6.3b) to represent the girder shear at the obtuse corner, acute corner and at the interior girder location is specified in CHBDC design code. Further, it is also noticed that the presence of skew reduces the longitudinal moment in the girders in comparison with straight bridges because the effective span is reduced (Ozgur et al. 2011), but no design equations to calculate the moment distribution factors are available yet, resulting in erroneous results.

4.5 Conclusions

The effect of sequence of construction in skewed slab-on-girder bridges is investigated by conducting a three-dimensional finite element modeling under dead loads. Based on the results obtained from a parametric study, a set of two empirical expressions were developed for the girder moment and shear distribution factors for rational prediction of the girder load distribution. Finally, the F_m and F_v values obtained by FEA were correlated with the proposed empirical equations. The F_v values obtained from FEA were compared with CHBDC design guidelines. The results showed that the proposed equations for F_m and F_v showed good agreement with the FEA results. However, CHBDC equations given in clause 5.6.3 for slab-on-girder bridges for estimating the shear distribution factors under the shored sequence of construction proved to be ineffective to capture the behavior of most of the skewed slab-on-girder bridge geometries. Furthermore, the comparison showed that CHBDC design equations gives conservative response for certain bridge configurations and for some other bridge cross-sections it produces highly under-estimated response, yielding unsafe design. Based on this study, the equations specified in CHBDC needs to be modified to comprehend the shear stresses developing at girder supports during construction under the influence of dead loads. Also, it is recommended to include moment distribution equations proposed in this study for accurate assessment of girder flexural stresses. The following conclusions can also be drawn from the current study:

- 1) The FEA results showed that as the angle of skew increased, more reaction was transferred towards girder obtuse corners and less on the acute corners. The increase was marginal for skew angle less than 30° , and tends to be significant when the skew angle exceeded 30° .
- 2) At high skew angles ($>30^\circ$) with larger number of girders having smaller girder spacing resulted in significant increase of exterior girder F_m and obtuse corner F_v value, in comparison to bridge configuration with less number of girders and large spacing between them.
- 3) Increase in the number of lanes resulted in the increase of exterior girder moment and shear distribution factors at the obtuse corners particularly in bridge geometries having;

- (i) high skew angles ($>30^\circ$) with long span length ($L \geq 25$ m), and (ii) more number of girders with less girder spacing.
- 4) The shear distribution factor at girder acute corner was practically found insensitive to the skew angle and girder spacing when the span length changes from 15 m to 40 m.
 - 5) Exterior girders are affected less than interior girders by the skew angle effect. This tendency is more obvious in bridges with large skew angles and long spans.

CHAPTER 5

Live Load Distribution in Straight and Skewed Bridges

5.1 General

The main objective of this research is to provide the simplest, yet sufficiently accurate equation for calculation of load distribution for skewed bridges. North American bridge code specifications do not provide the design engineers with sufficient guidance regarding load distribution factors of simply supported skewed composite bridge. Despite being less conservative than the AASHTO Standard specifications, previous research suggests that the newly adopted AASHTO-LRFD equations are still too conservative when compared with field data and finite element analysis for slab-on-girder bridges (Chen and Aswad 1996, Sotelino et al. 2004, Barr and Amin 2006, Cross et al. 2006). The AASHTO-LRFD live load distribution equations have more parameters as compared to AASHTO standard specifications and a different computation philosophy, which complicates the design process. Furthermore, the LRFD formulas do not reflect today's bridges because they neglect important factors such as bridge continuity and the presence of the secondary elements such as cross bracing, diaphragms, and parapets in bridges that reduces the distribution factors. Recently, based on a parametric study analysis, the Canadian Highway Bridge Design Code (CSA 2014a) has specified equations to compute the shear magnification factor for the skewed slab-on-girder bridges due to live loads, and for the sake of simplicity the same equation is applied to all the girders (CSA 2014b clause 5.6.6.2).

In this chapter, the influence of several parameters on the shear and moment distribution factors in simply supported skewed composite steel-concrete bridges are presented. These parameters are: span length, girder spacing, number of girders, number of design lanes and skew angle. A detailed parametric study was conducted on prototype composite steel-concrete bridges subjected to CHBDC truck loading for ultimate, serviceability and fatigue limit states (ULS, SLS and FLS). Here in this thesis for the application of live loading as per CHBDC clause 3.8.4, the serviceability limit states means the limit state other than the superstructure vibrations (SLS-2). Whereas, fatigue limit state that comprise the formation

of cracks as a result of the repeated application of loads also includes the serviceability limit state due to superstructure vibrations (SLS-2). The ULS and SLS (combination 1) correspond to the most critical loading pattern that can occur during a bridge design life cycle. Accordingly, CL-W truck load increased by the dynamic load allowance or the CL-W lane load, whichever produces the maximum load effect needs to be positioned longitudinally and transversely within a design lane at a location and in the direction that produces maximum load effect. However for the FLS and for the superstructure vibration serviceability limit state (combination 2), the traffic load that includes one CL-W truck that causes maximum effects only, increased by the dynamic load allowance and placed at the center of one travelled lane needs to be considered, and lane load are not considered. The parametric study included more than 3200 load cases. The finite element modeling of the prototype bridges was verified and substantiated by means of a field test data results on a simply supported two-span skewed composite steel-concrete bridge described in chapter 3. Based on this study empirical equations for shear and moment distribution factors under CHBDC truck loading were generated to develop new equations that are more realistic and effective for designing skewed simply supported bridges.

5.2 Composite Steel I-girder Bridge

Composite steel I-girder bridges are among the most common short-to-medium span bridges built in the North America (Cao 1996). For designing these bridges under truck live load, a bridge engineer must account for safety, serviceability, and economy. Therefore, an accurate assessment of the load distribution throughout the bridge system is desired. However, in skewed bridges, due to the complex structural behavior certain simplifications are generally used in the design procedure which result in a conservative design.

The concept of live-load distribution factor simplifies the analysis and design of bridges and has been used by several design codes for many years (e.g., CSA 2014a, AASHTO-LRFD 2014). The CHBDC (CSA 2014a) specifies equations for the simplified method of analysis to define the longitudinal bending moments and vertical shear in slab-on-girder bridges due to live load for ULS, SLS and FLS using load distribution factors. The CHBDC

(CSA 2014a) simplified method of analysis is based on the beam analogy method in which the bridge is considered as a beam for determining the longitudinal distribution of load effects. The transverse distribution of the load effects across the bridge width is obtained by multiplying the one-lane longitudinal load effect by the truck load fraction, F_T , to be determined with the formulas provided in CHBDC (CSA 2014a) clause 5.6. In the current CHBDC (CSA 2014a), the main improvement by using simplified method of analysis is the consideration of skewed slab-on-girder bridge geometries for dead and live load conditions. Skewed bridges up to 45° can now be analyzed using the simplified method.

Generally, the presence of skew reduces the longitudinal moment in the girders in comparison with straight bridges because the effective span is reduced. However, it also causes high concentration of shear in the girder closest to the obtuse corner and it reduces it in the girder closest to the acute corner as well in the interior girders. Such complex behavior of a skewed bridge demands an accurate assessment of load distribution factors by developing modified equations based on a parametric study by considering three-dimensional finite element analysis. Therefore there was a need for the generation of a database for both the shear and moment distribution factors leading to the formation of empirical equations for the design of skewed composite steel I-girder bridges. For this reason, a detailed parametric study was conducted described below in the following subsection.

5.2.1 Parametric Study

The objectives of the parametric study were: (i) to investigate the influence of all major parameters affecting the moment and shear distribution among composite girder; (ii) to generate a database for moment and shear distribution factors including more than 1600 bridge cases; and (iii) to develop empirical equations for moment and shear distribution factors corresponding to CHBDC truck loading for three limit states i.e. ULS and SLS, and FLS as specified in CHBDC (CSA 2014a). The parameters chosen for this study were: angle of skew, span length, girder stiffness, girder spacing, number of lanes and number of girders. The parametric study was based on the following assumptions: (i) all materials were elastic and homogeneous; (ii) the effects of road super-elevation and curbs were

ignored; and (iii) the reinforced-concrete deck slab and the supporting steel I-girders were in full composite action; (iv) both the deck slab and the supporting I-girders were simply supported at the abutments; (v) transverse intermediate cross-braces were moment-connected to the longitudinal girders. Subsequently, based on the data generated from this parametric study, sets of empirical expressions were developed to accurately calculate the girder shear and moment distribution factors.

5.2.2 Evaluation of Load Distribution Factors

In order to calculate the live load carried by each girder, lateral load distribution factor is a vital element in analyzing existing bridges and designing new ones. To simplify the design process, North American bridge codes, such as CHBDC (CSA 2014a) and AASHTO-LRFD (2014) bridge design specifications, treat the longitudinal and transverse effects of wheel loads as uncoupled phenomena.

The formulas for the calculation of distribution factors for longitudinal bending stress (F_{T_m}) and shear (F_{T_v}) were evaluated for the bridge configurations presented in Table 5.1 and Table 5.2 for ULS and SLS, and FLS respectively. Since under the linear elastic conditions, stresses are proportional to the bending moments in the girders. Hence, instead of computing the girder moment, maximum stresses at the extreme fiber of the girder bottom flange was obtained from finite element analyses. For this purpose, the maximum flexural stress (σ_{3D}) and the maximum shear force (V_{3D}) of a three-dimensional simply supported structure under the effect of truck live load at ULS and SLS, and FLS were first calculated for each prototype bridge. Subsequently, the maximum flexural stress (σ_{2D}) and the maximum shear force (V_{2D}) from a simple two-dimensional beam-line model (Barker and Puckett 1997) were evaluated for each prototype bridge in the parametric study. The distribution factor for moment and shear, thus calculated is represented as;

$$F_{T_m} = \frac{\sigma_{3D}}{\sigma_{2D}} \quad (5.1)$$

$$F_{T_v} = \frac{V_{3D}}{V_{2D}} \quad (5.2)$$

Table 5.1 Geometry of prototype bridges for ULS and SLS analysis

Design lanes (n)	Bridge width (W), m	Deck width (Wc), m	Design lane width (We), m	Number of girders (N)	Girder spacing (S), m
1	4.5	3.5	3.5	3	1.5
1	6.0	5.0	5.0	3	2.00
				4	1.50
2	7.6	6.6	3.3	3	2.53
				4	1.90
				5	1.52
2	8.8	7.8	3.9	3	2.93
				4	2.20
				5	1.76
2	10.0	9.0	4.5	3	3.33
				4	2.50
				5	2.00
2	11.2	10.2	5.1	4	2.80
				5	2.24
				6	1.87
2	12.4	11.4	5.7	4	3.10
				5	2.48
				6	2.07
2	13.6	12.6	6.3	4	3.40
				5	2.72
				6	2.27
3	11.2	10.2	3.4	4	2.80
				5	2.24
				6	1.87
3	12.4	11.4	3.8	4	3.10
				5	2.48
				6	2.07
3	13.6	12.6	4.2	4	3.40
				5	2.72
				6	2.27
4	14.6	13.6	3.4	5	2.92
				6	2.43
				7	2.09
4	16.2	15.2	3.8	6	2.70
				7	2.31
				8	2.025
4	18.0	17.0	4.25	6	3.00
				7	2.57
				8	2.25

Table 5.2 Geometry of prototype bridges for FLS analysis

Design lanes (n)	Bridge width (W), m	Deck width (Wc), m	Design lane width (We), m	Shoulder width, m	Number of girders (N)	Girder spacing (S), m
1	4.5	3.5	3.5	0.0	3	1.5
1	6.0	5.0	3.3	0.85	3	2.00
					4	1.50
2	7.6	6.6	3.3	0.0	3	2.53
					4	1.90
					5	1.52
2	8.8	7.8	3.3	0.6	3	2.93
					4	2.20
					5	1.76
2	10.0	9.0	3.3	1.2	3	3.33
					4	2.50
					5	2.00
2	11.2	10.2	3.3	1.8	4	2.80
					5	2.24
					6	1.87
2	12.4	11.4	3.3	2.4	4	3.10
					5	2.48
					6	2.07
2	13.6	12.6	3.3	3.0	4	3.40
					5	2.72
					6	2.27
3	11.2	10.2	3.4	0.0	4	2.80
					5	2.24
					6	1.87
3	12.4	11.4	3.3	0.75	4	3.10
					5	2.48
					6	2.07
3	13.6	12.6	3.3	1.35	4	3.40
					5	2.72
					6	2.27
4	14.6	13.6	3.4	0.0	5	2.92
					6	2.43
					7	2.09
4	16.2	15.2	3.3	3.3	6	2.70
					7	2.31
					8	2.025
4	18.0	17.0	3.3	3.3	6	3.00
					7	2.57
					8	2.25

To calculate the moment of inertia of the idealized girder, the effective concrete slab width (b_e) was calculated based on the following two equations specified in the CHBDC (CSA 2014a) clause 5.8.1;

$$\begin{aligned} \frac{b_e}{b} &= 1 - \left[1 - \frac{L}{15b} \right]^3 \quad \text{for } \frac{L}{b} \leq 15 \\ &= 1 \quad \text{for } \frac{L}{b} > 15 \end{aligned} \quad (5.3)$$

where, b_e and b are the dimensions shown in Figure 5.7 of CHBDC (CSA 2014a) clause 5.8.1 for the applicable type of bridge cross-section, and L is the span length (m).

5.2.2.1 Load Distribution Factors for Longitudinal Bending Moment

To determine the load distribution factor for the longitudinal bending moment for exterior and interior girders, longitudinal stresses in girder at the extreme fiber at bottom surface of the flange resulting from the 3D finite element analysis due to truck loading were identified. The maximum stress at the bottom surface of the bottom flange was identified from average stress results for elements adjacent to the chosen section. Thus, the girder stress can be calculated from the obtained stresses using the following equation:

For ULS and SLS:

$$\begin{aligned} F_{T-m} &= F_{m-2006} \times \left(\frac{n.R_L}{N} \right) \\ F_{T-m} &= \frac{\sigma_{FEA} \times R'_L}{\left(\frac{n.\sigma_T.R_L}{N} \right)} \times \left(\frac{n.R_L}{N} \right) \end{aligned} \quad (5.4)$$

For FLS:

$$\begin{aligned} F_{T-m} &= F_{m-2006} \times \left(\frac{1}{N} \right) \\ F_{T-m} &= \frac{\sigma_{FEA}}{\left(\frac{\sigma_T}{N} \right)} \times \left(\frac{1}{N} \right) \end{aligned} \quad (5.5)$$

where,

F_{T_m} = Moment distribution factor from finite element analysis as per CHBDC (CSA 2014a).

F_{m_2006} = Moment distribution factor from finite element analysis as per CHBDC (CSA 2006a).

n = number of design lanes on a bridge.

R_L = modification factor based on actual number of design lanes as per clause 3.8.4.2 (CSA 2014a).

R'_L = modification factor based on actual number of loaded lanes as per clause 3.8.4.2 (CSA 2014a).

N = number of girders.

σ_{FEA} = maximum flexural stress obtained from a three-dimensional simply supported structure under the effect of truck live load at ULS and SLS, and FLS.

σ_T = maximum flexural stress from a simple two-dimensional beam-line model under the effect of truck live load at ULS and SLS, and FLS.

5.2.2.2 Load Distribution Factors for Shear

The maximum shear forces were determined from the finite element modeling for straight and skewed bridge due to truck loading for ULS and SLS, and FLS, respectively. Consequently, the shear distribution factor was calculated as follows:

For ULS and SLS:

$$\begin{aligned} F_{T_v} &= F_{V_2006} \times \left(\frac{n.R_L}{N} \right) \\ F_{T_v} &= \frac{V_{FEA} \times R'_L}{\left(\frac{n.V_T.R_L}{N} \right)} \times \left(\frac{n.R_L}{N} \right) \end{aligned} \quad (5.6)$$

For FLS:

$$F_{T_v} = F_{V_{2006}} \times \left(\frac{1}{N} \right)$$
$$F_{T_v} = \frac{V_{FEA}}{\left(\frac{V_T}{N} \right)} \times \left(\frac{1}{N} \right) \quad (5.7)$$

where,

F_{T_v} = Shear distribution factor from finite element analysis as per CHBDC (CSA 2014a).

$F_{V_{2006}}$ = Shear distribution factor from finite element analysis as per CHBDC (CSA 2006a).

n = number of design lanes on a bridge.

R_L = modification factor based on actual number of design lanes as per clause 3.8.4.2 (CSA 2014a).

R'_L = modification factor based on actual number of loaded lanes as per clause 3.8.4.2 (CSA 2014a).

N = number of girders.

V_{FEA} = maximum shear stress obtained from a three-dimensional simply supported structure under the effect of truck live load at ULS and SLS, and FLS.

V_T = maximum shear stress from a simple two-dimensional beam-line model under the effect of truck live load at ULS and SLS, and FLS.

5.2.3 Description of Bridge Prototypes

Figure 3.2 shows typical details of two-lane and four-lane single span steel-concrete composite I-girder bridges as examples of bridges considered in this study. The basic bridge cross-sectional configurations considered in this study, based on CHBDC (CSA 2014a) clause 3.8.2, are presented in Table 5.1 and Table 5.2 for ULS and SLS-1; and, FLS and SLS-2 respectively. The modulus of elasticity of the concrete material was 25 GPa with a Poisson's ratio of 0.20, whereas these design values for the steel material were 200

GPa and 0.30, respectively. Six different span lengths ranging from 15 m to 40 m were considered with an increment of 5 m, and girder response was evaluated for seven different skew angles from 0° to 60° with an increment of 10° skew angle. The concrete deck slab thickness was 225 mm. The cantilever slab length was equal to half the girder spacing. The X-type cross-frames at the support and between the span was provided in accordance with the specification stipulated in the manual of standard short-span steel bridges (Theodor and Al-Bazi 1997). Cross-frame members were spaced at equal intervals between the support lines and were made of L102x102x11 steel angles. The arrangement of the cross-frames at the support and between the span is shown in Figure 5.1. Based on a sensitivity study presented in chapter-3, parallel cross-frame layout was used for bridge configurations up to 30° skew angle and for skew angles in the interval 30° and 60° skew angle perpendicular staggered cross-frame layout was adopted for this study (Razzaq et al. 2015). In total, 3276 bridge cases (i.e. 1638 cases each for ULS and SLS, and for FLS) were analyzed and assessed using finite element analyses (FEA).

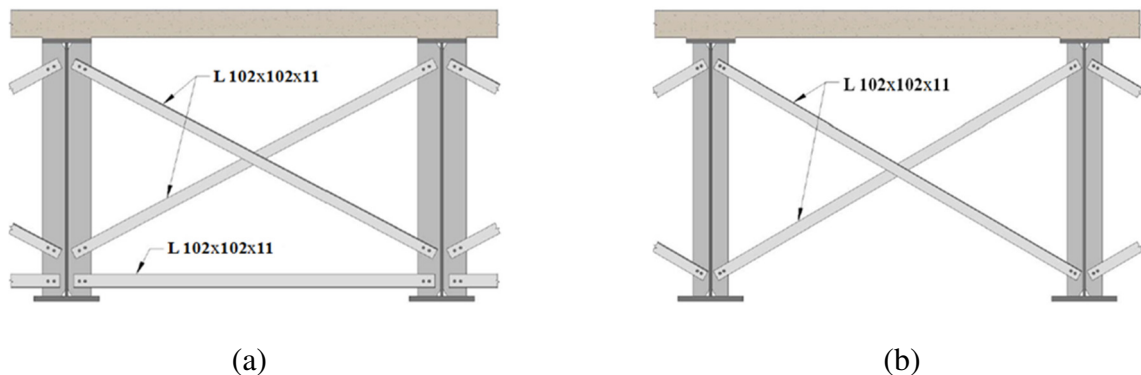


Figure 5.1 Cross-frame arrangements at (a) support level, and (b) between span lengths

5.2.4 Finite Element Modeling

The general FEA program, CSiBridge (CSI 2015), was used to generate the 3D finite element models.

The concrete slab and web of steel girders were modeled using four-node 3D elastic shell elements with six degrees of freedom at each node. The top and bottom flanges of longitudinal steel girders were modeled using two-node 3D elastic beam elements with six degrees of freedom at each node. The transverse diaphragm cross-frames were simplified

and modeled using the same beam elements. The shell and beam elements were connected by rigid link elements. These elements were used to model the composite action between the deck and the girders by connecting the nodes of the deck elements with the beam and shell elements. The connections between the girder and cross-frame elements were fixed. Further details about the finite element modeling of composite slab-on I-girder bridge can be seen in chapter-3.

5.2.5 Loading Condition

The live load, specified in the CHBDC, consists of CL-W truck and CL-W lane loading. The CL-W truck consists of idealized five axles with total load of 625 kN. The CL-W lane loading consists of CL-W truck loading with each axle load reduced to 80% of its original value and superimposed within uniformly distributed load of 9 kN/m over 3 m width. The selection between two different CHBDC types of live loads (CL-W truck and CL-W lane) depends on whichever gives the maximum design values. A sensitivity study which was carried out, presented in chapter-3, showed that the CL-W truck loading governs the extreme design values. Consequently, the CL-W truck loading was utilized as a live loading in finite element modeling.

The CSiBridge software has the ability to run a moving load along a bridge. For moving load analysis, the number of lanes, vehicle and vehicle class were modeled and defined. The lane width was specified in the program as well as the distance between the vehicles, and the distance of the vehicle from the curb or barrier wall was also identified. CL-W truck loading was represented in the program by number of concentrated forces. Each truck axle was represented by single or double loads with defined axle width. The minimum or the maximum distances between each CL-W truck axle was specified in the program.

Truck loading conditions for the three limit states (ULS, SLS and FLS), as specified in CHBDC were defined. For ULS and SLS, two different loading cases i.e. full and partial CL-W truck loadings, were considered for each bridge prototype. In each loading cases, the wheel loads close to the curbs were applied at a distance of 0.6 m from the inside edge of the curb. Additionally for the FLS, only one CL-W truck was placed at the center of one travelling lane. For fatigue limit state and superstructure vibration, the vehicle edge

distance (the distance from the center of the outer wheel load to the edge of the bridge) of 3 m was maintained, as specified in clause 5.6.6 of CHBDC. For one-lane to four-lane bridge configurations, Figure 5.2 to 5.5 and Figure 5.6 to 5.9 schematically indicate all possible CL-W truck positions considered for the ultimate and fatigue limit states, respectively. The exterior girder was the one closest to bridge curb or barrier wall while the interior girder was any girder between the exterior girders. The modification factors for multi-lane loading as specified in CHBDC clause 3.8.4.2 was also considered while applying the truck live loads using FEA modelling.

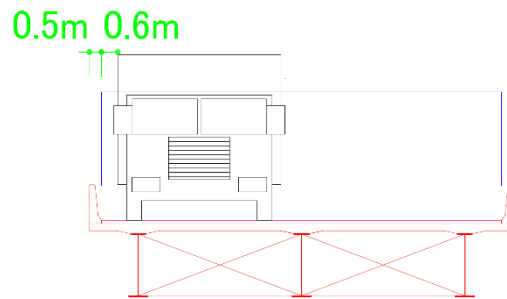
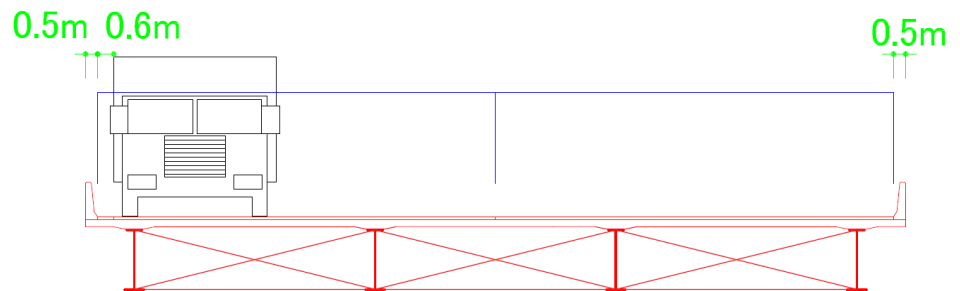
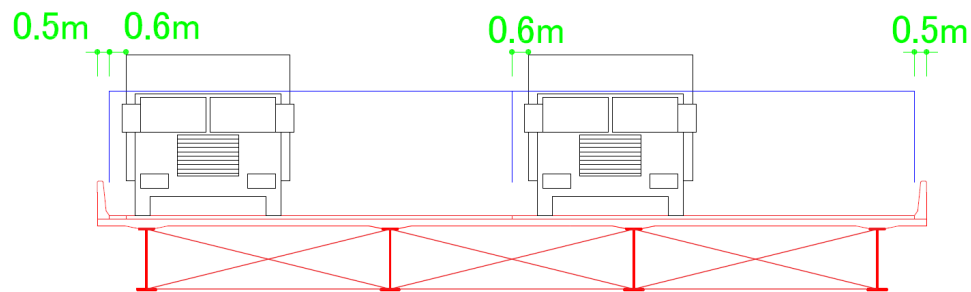


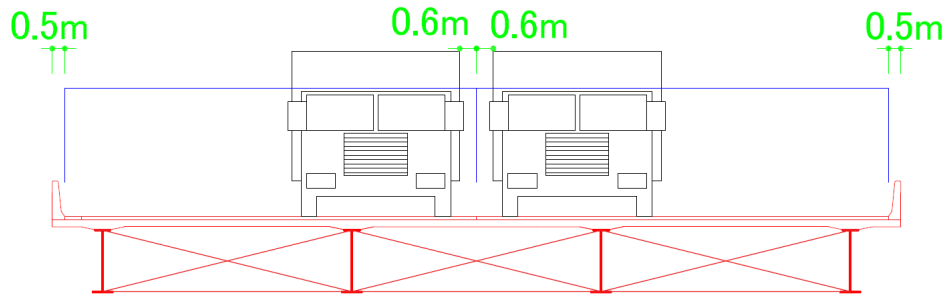
Figure 5.2 Live loading case for one-lane bridge for ULS and SLS for exterior and interior girder-partial load



(a)

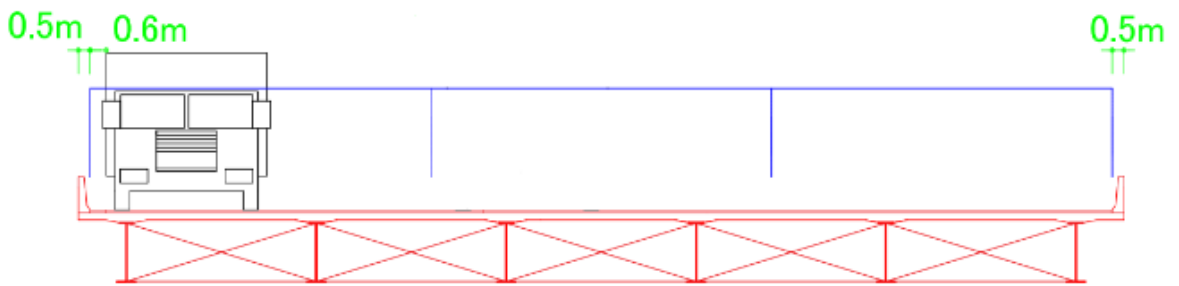


(b)

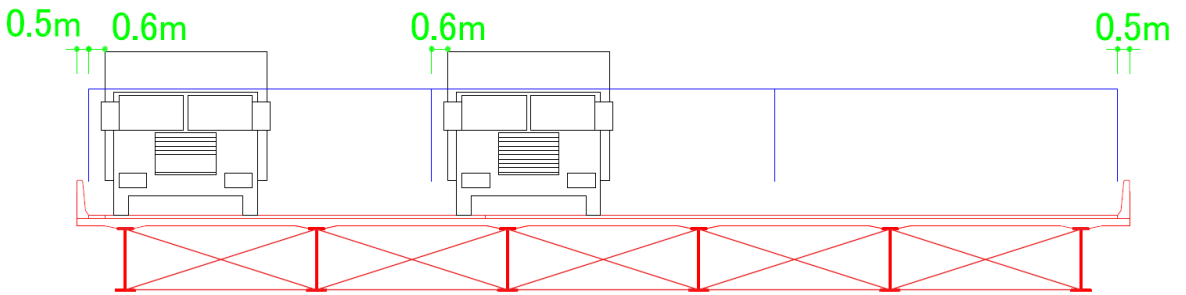


(c)

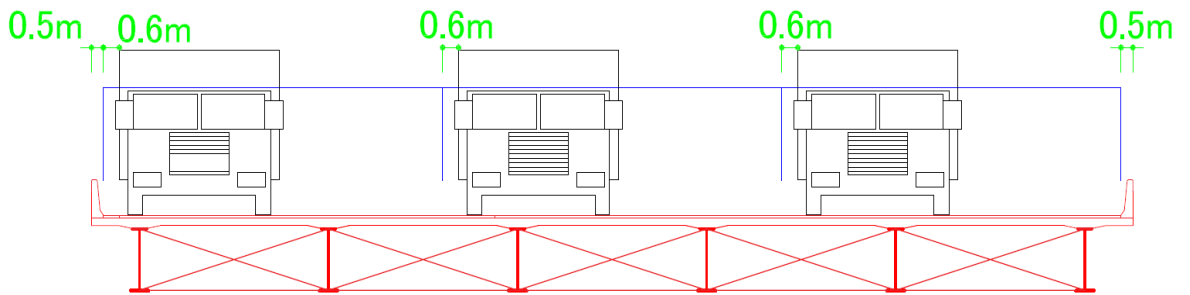
Figure 5.3 Live loading cases for two-lane bridge for ULS and SLS for; (a) exterior girder-partial load, (b) exterior girder-full load, and (c) Interior girder-full load



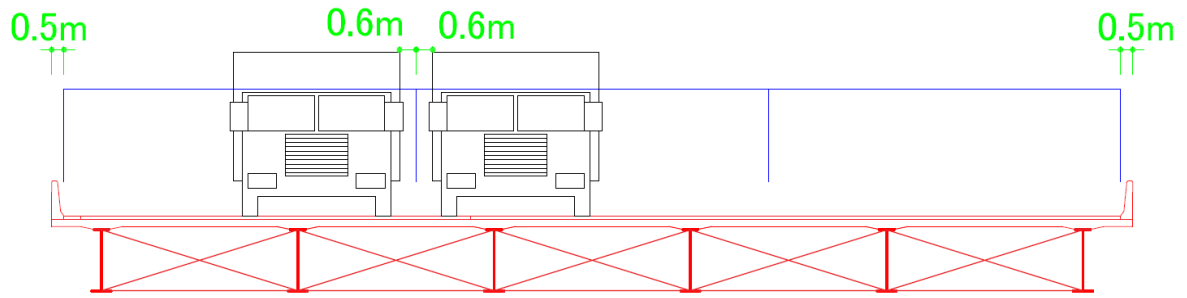
(a)



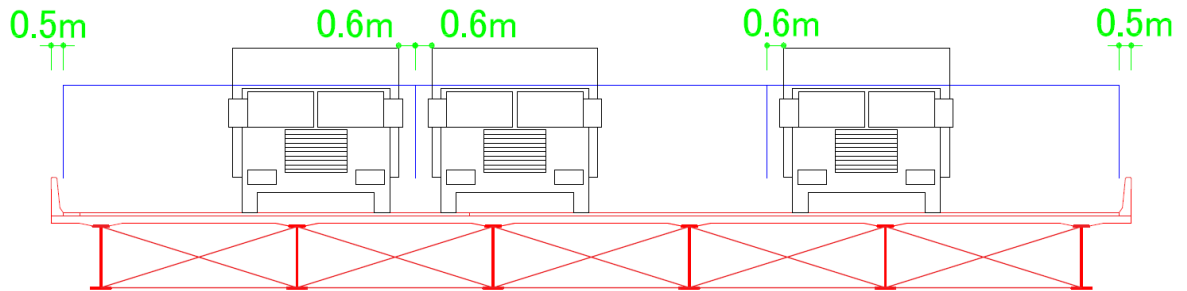
(b)



(c)

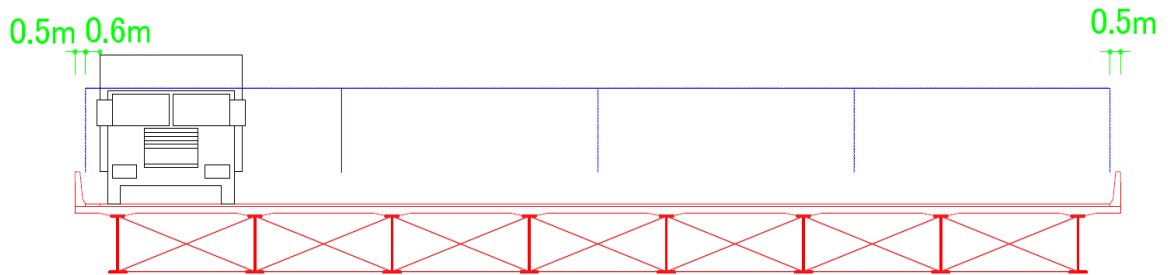


(d)

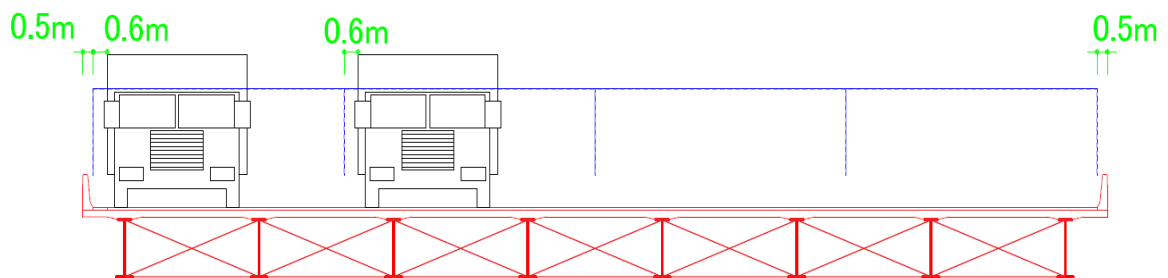


(e)

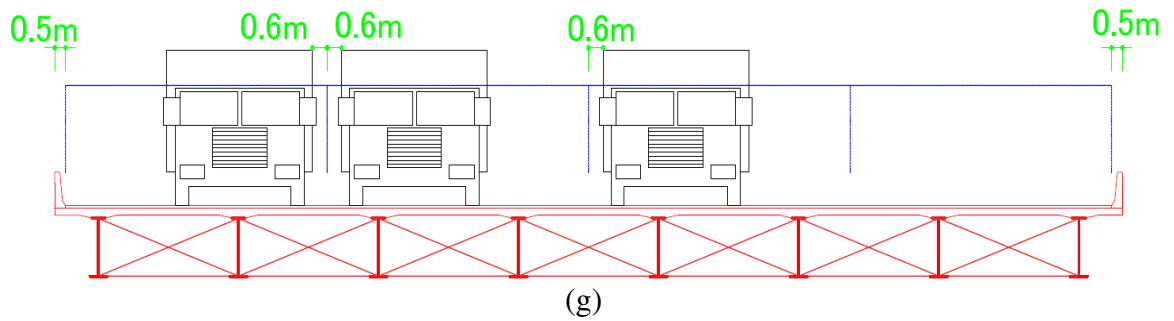
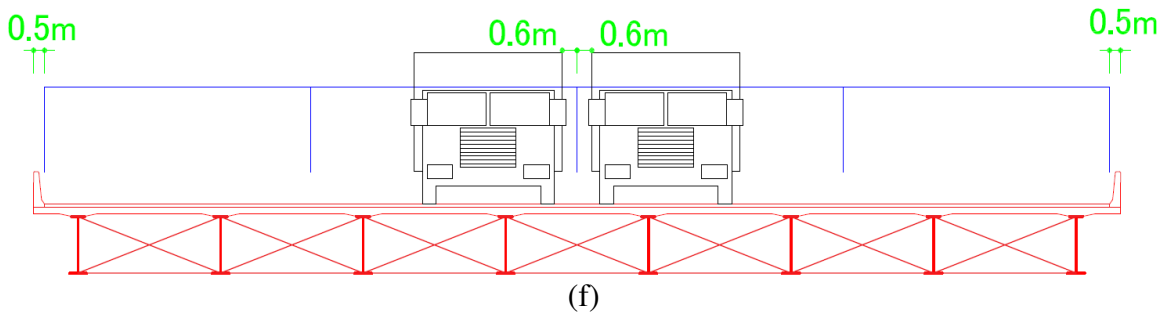
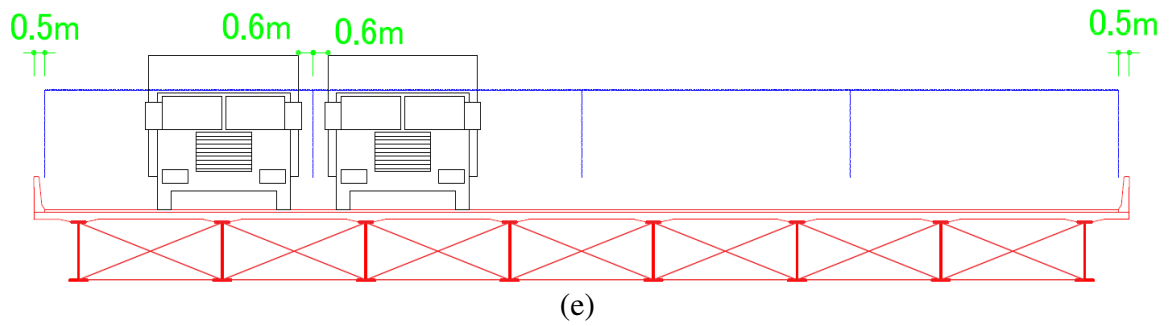
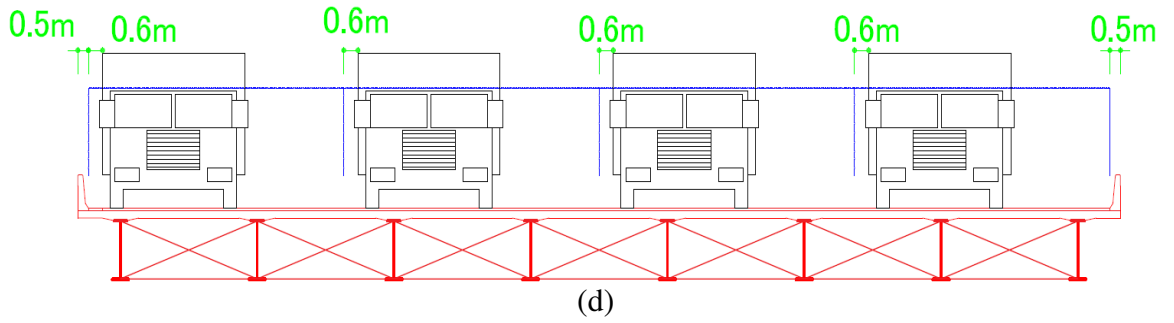
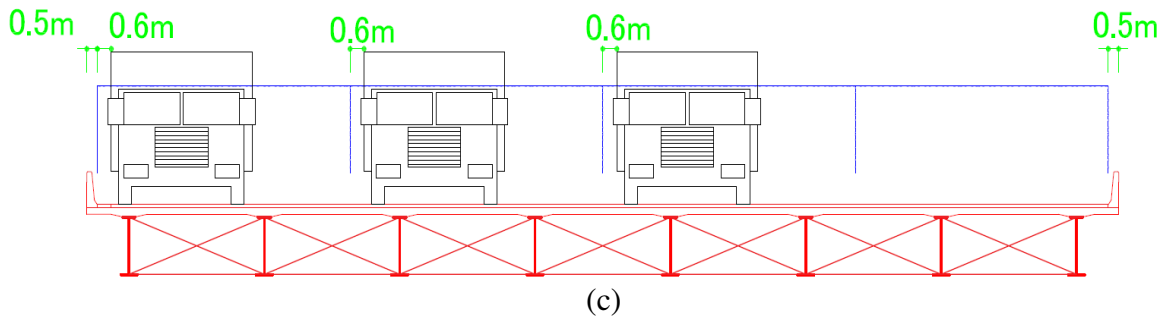
Figure 5.4 Live loading cases for three-lane bridge for ULS and SLS for; (a) exterior girder-partial load, (b) exterior girder-partial load, (c) exterior girder-full load, (d) Interior girder-partial load, and (e) Interior girder-full load



(a)



(b)



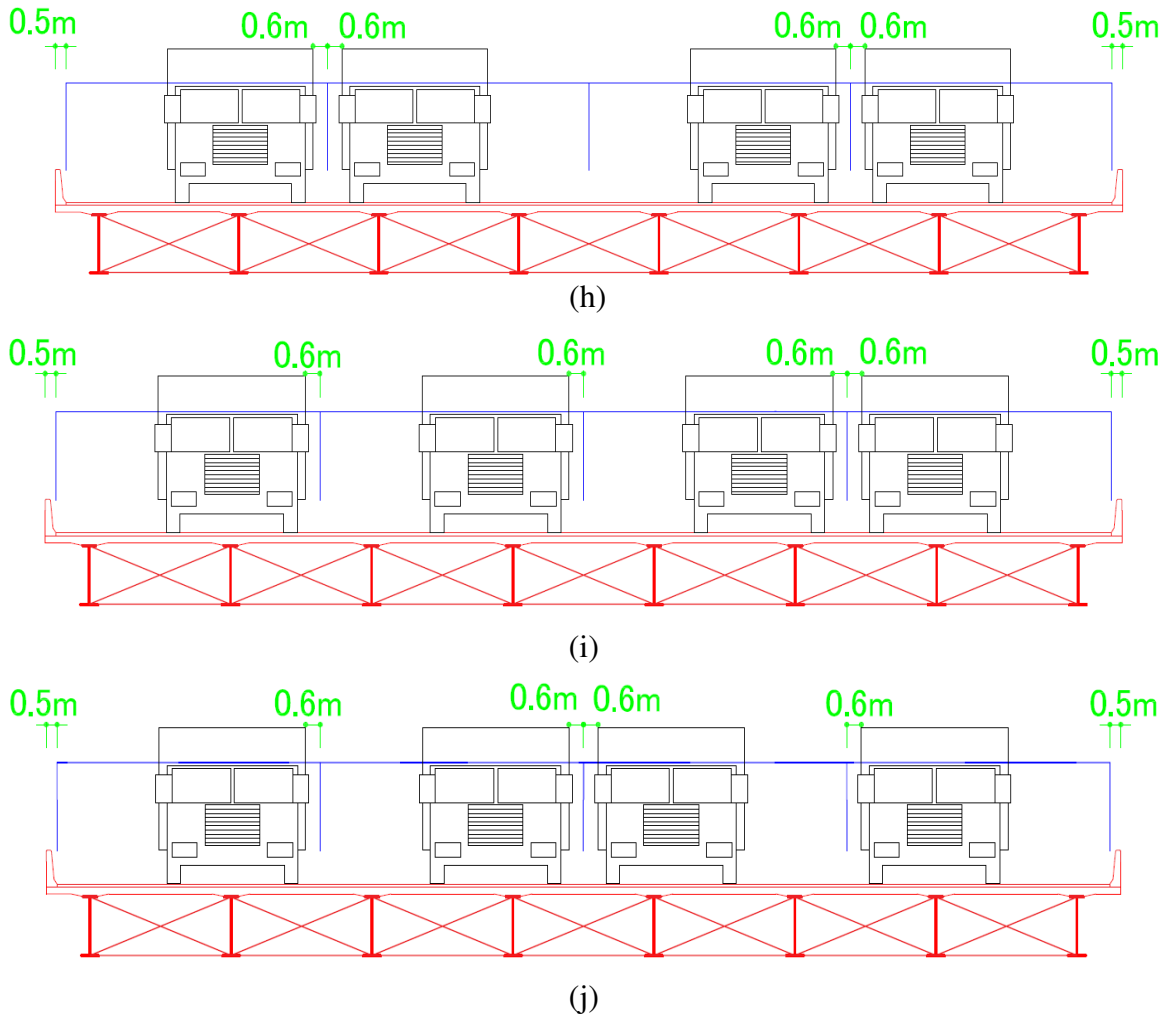


Figure 5.5 Live loading cases for four-lane bridge for ULS and SLS for; (a) exterior girder-partial load, (b) exterior girder-partial load, (c) exterior girder-partial load, (d) exterior girder-full load, (e) interior girder-partial load, (f) interior girder-partial load, (g) interior girder-partial load, (h) interior girder-full load, (i) interior girder-full load, and (j) interior girder-full load

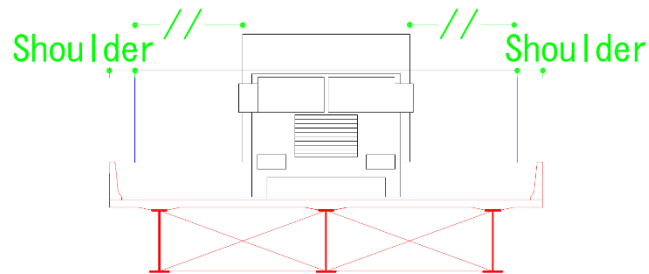


Figure 5.6 Live loading case for one-lane bridge for FLS

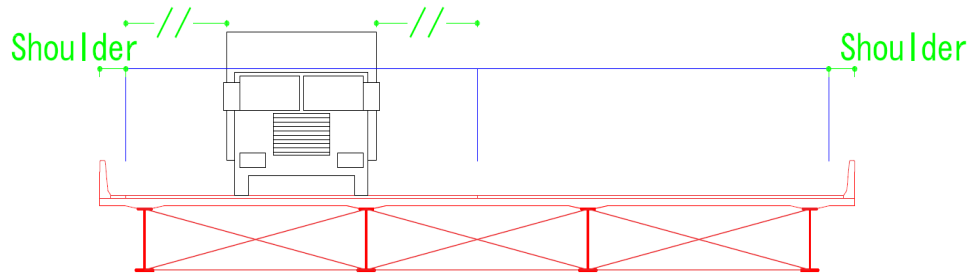


Figure 5.7 Live loading case for two-lane bridge for FLS

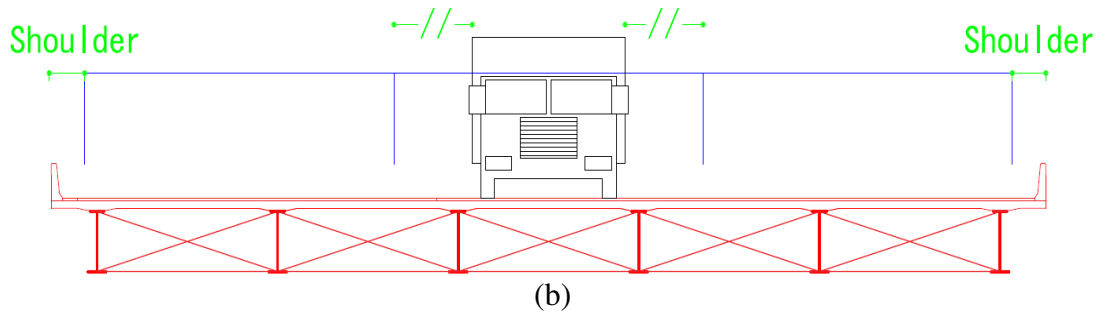
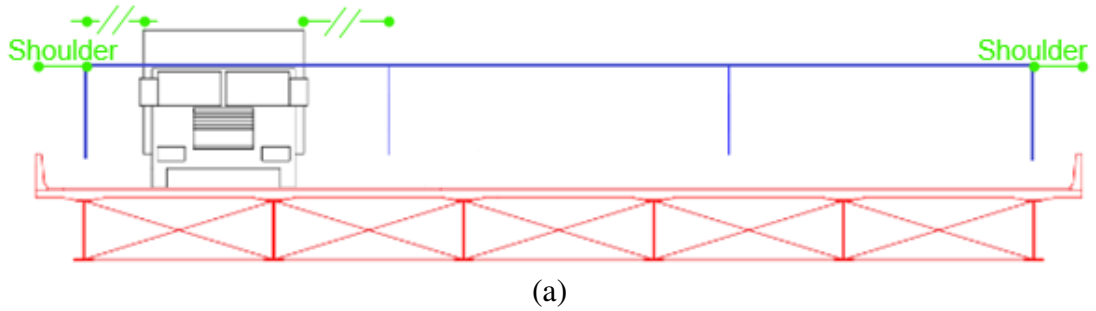
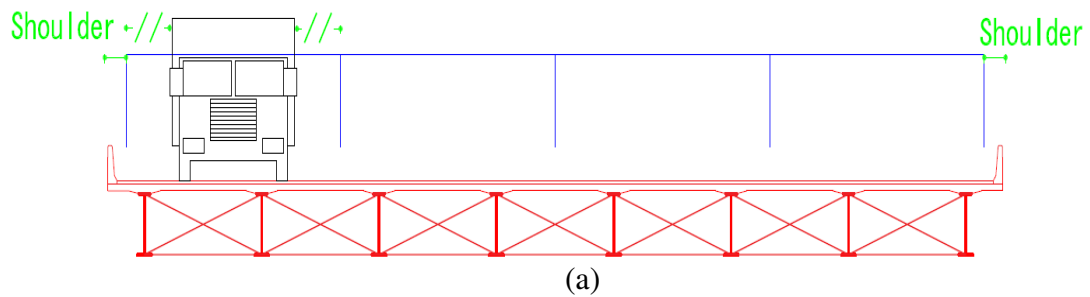


Figure 5.8 Live loading case for three-lane bridge for FLS for; (a) exterior girder-fatigue load, and (b) interior girder-fatigue load



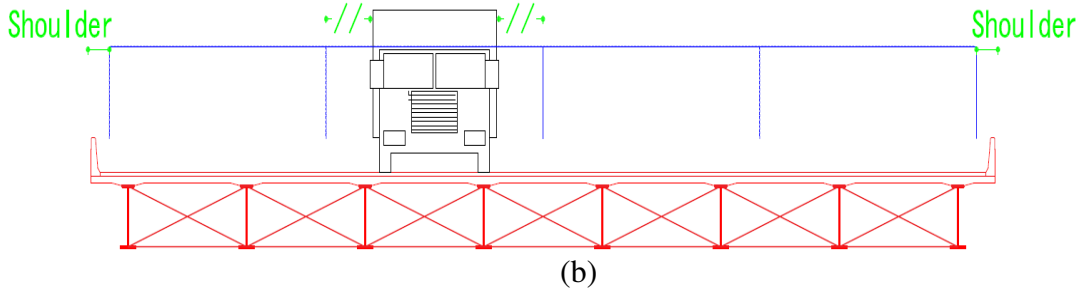


Figure 5.9 Live loading case for four-lane bridge for FLS for; (a) exterior girder-fatigue load, and (b) interior girder-fatigue load

5.2.6 Results from the Parametric Study

This section presents an extensive parametric study in which more than 3200 composite straight and skewed slab-on-girder bridge prototypes were considered for three limit states (ULS, SLS and FLS) using three-dimensional finite element analysis. In order to precisely determine the parameters affecting the load distribution factors, a sensitivity study was first undertaken to determine the influence of the different parameters that may affect these distribution factors. As a result, it was found that the key parameters that affect the structural response of a skewed bridge system were: (1) skew angle (ψ), (2) span length (L), (3) girder spacing (S), (4) number of girders (N), and (5) number of lanes (n). Based on the guidelines stipulated in the manual of standard short-span steel bridges (Theodor and Al-Bazi 1997), slab thickness was taken constant i.e. 225 mm, for all bridge configurations considered in this study. To account for the relative stiffness of the bridge system, a relationship for the upper and lower bound limits specified by Bakht and Moses (1988) in terms of the longitudinal flexural rigidity per unit width (D_x) and the span length (L) was adopted. For each span length considered in this study, steel I-girder geometries were selected from the manual of standard short-span steel bridges (Theodor and Al-Bazi 1997) falls well within the practical upper and lower bound limits.

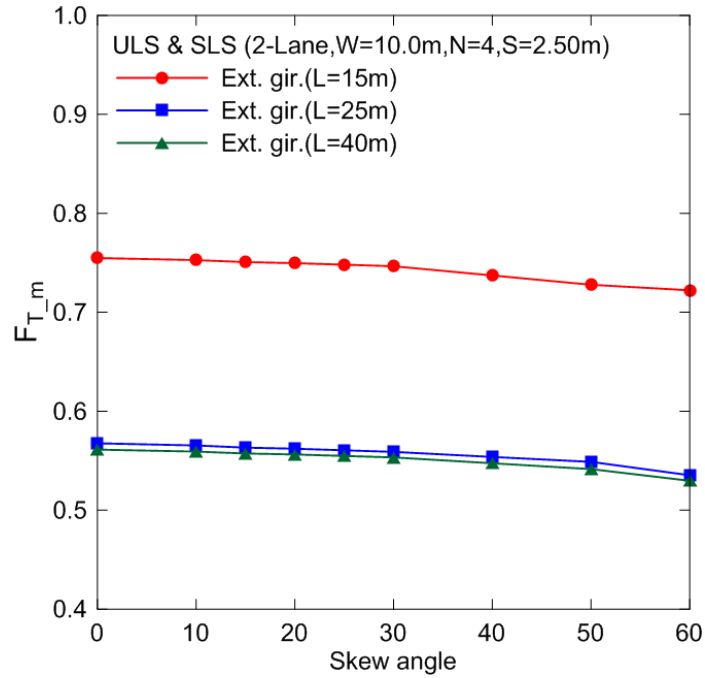
Based on sensitivity study findings, the effect of above-mentioned superstructure variables on girder F_{T_m} and F_{T_v} were examined in the parametric study, and discussed in the following sub-section. Only response of girders in a two-lane and four-lane bridge configuration are presented and discussed herein.

5.2.6.1 Effect of Skew Angle

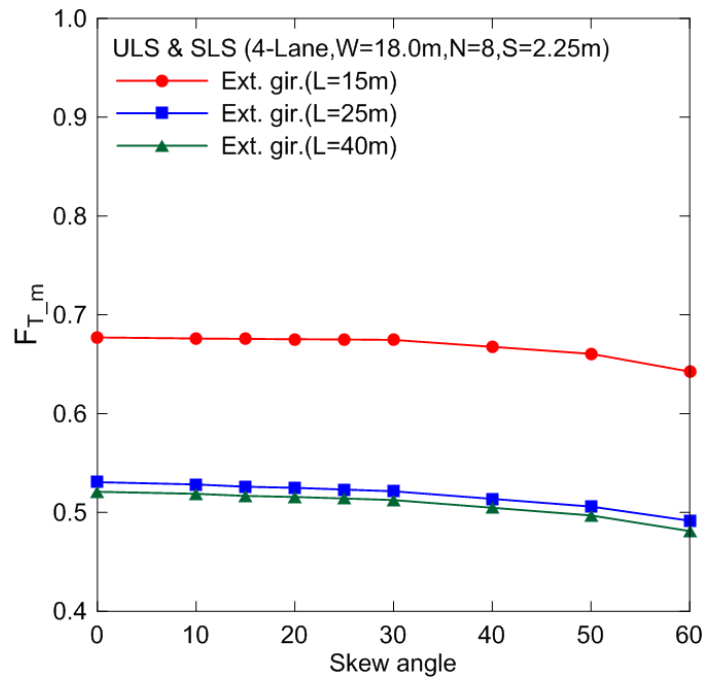
Skew angle of the deck is the most critical factor that influences the moment and shear distribution among girders. The present study showed that the exterior and interior girder moment distribution factors of skew bridges were always less than those of right bridges. This finding is in agreement with the investigations of Khaloo and Mirzabozorg (2003) and Nouri and Ahmadi (2012), among others. Also, the increase in skew resulted in high concentration of shear in the girder closest to the obtuse corner and reduced shear concentration in the closest girder to the acute corner as well as in the interior girders (Nutt et al. 1988, Ebeido and Kennedy 1995).

Figure 5.10 and 5.11, shows the FEA results of an exterior and interior girder moment distribution factors of a skewed bridge under live load conditions for ULS and SLS in terms of F_{T_m} as follows:

- 1) The value of the moment distribution factor for a right bridge, $\psi = 0^\circ$, was higher in exterior girder in comparison to interior girder.
- 2) For two and four-lane bridge configuration, the effect of exterior girder moment distribution factor with the increase of skew angle was found insignificant. The load distribution factor of external girder reduces by 5% for a skew angle of 60° , as compared with the straight aligned bridge.
- 3) For two and four-lane bridge geometry, for a span length less than 20 m the sensitivity of load distribution factors of internal girders with respect to skew angle was high, such that, for bridge with a skew angle of 60° , these factors decrease by 25% and 27% respectively as compared with right bridges. However for a span length of 40 m, the effect of interior girder moment distribution factor with the increase of skew angle was found less sensitive, such that, for bridge with a skew angle of 60° , these factors decrease by 9% and 11% respectively as compared with right bridges.
- 4) For both external and internal girders, the effect of skew angle on the moment distribution factor decreases when span length increases. This structural behavior in a skew bridge was more pronounced when span length was less than 20 m, and became less sensitive as the span length increases up to 40 m.

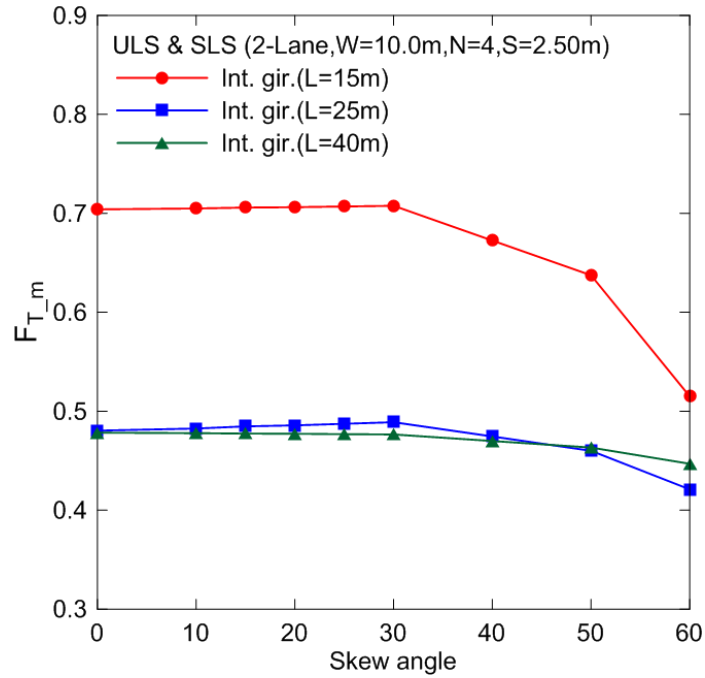


(a)

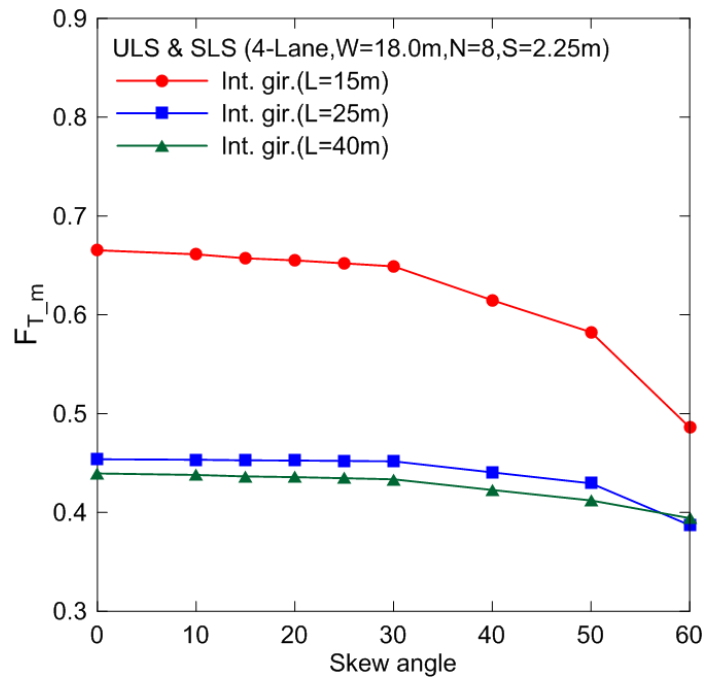


(b)

Figure 5.10 Effect of skew angle on $F_{T,m}$ of an exterior girder at ULS & SLS for: (a) two-lane, and (b) four-lane

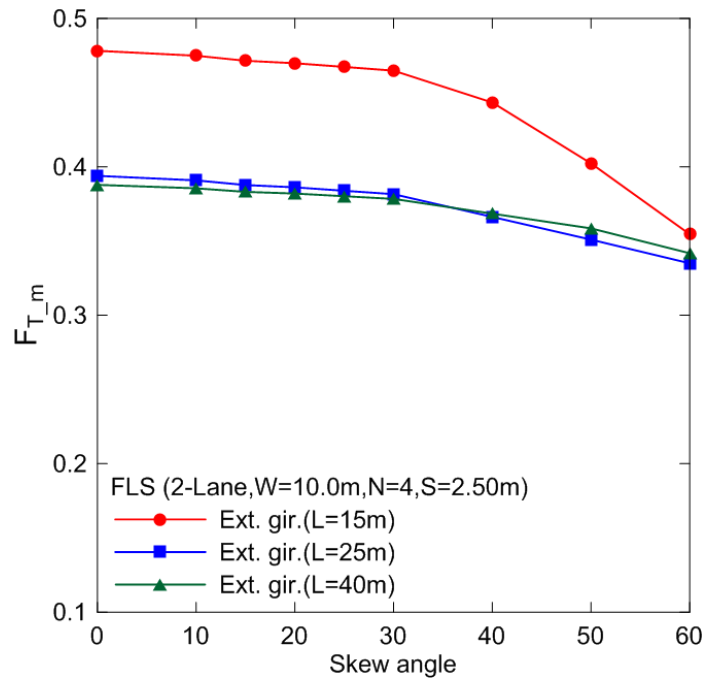


(a)

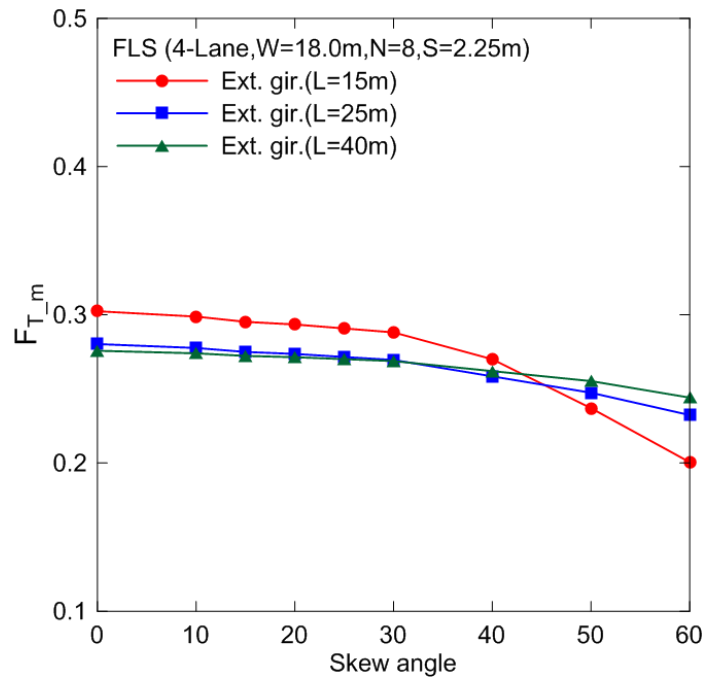


(b)

Figure 5.11 Effect of skew angle on $F_{T,m}$ of an interior girder at ULS & SLS for: (a) two-lane, and (b) four-lane

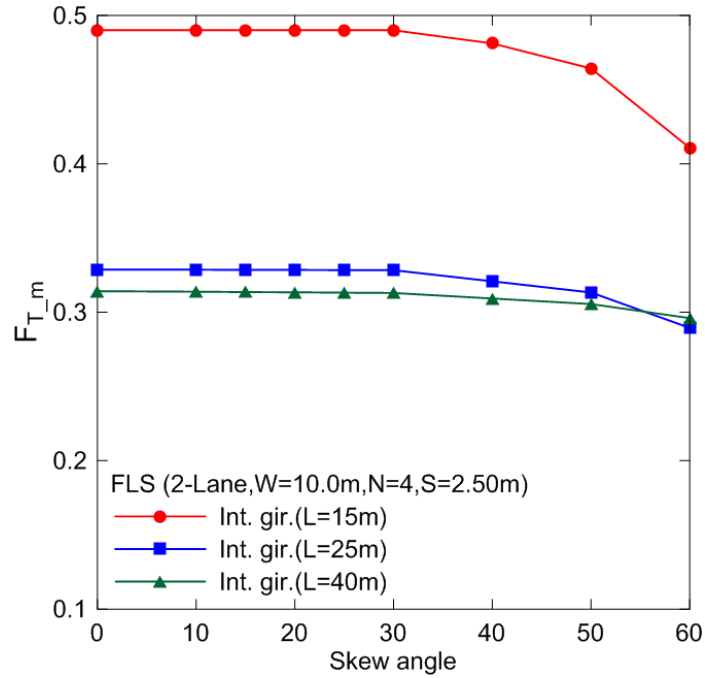


(a)

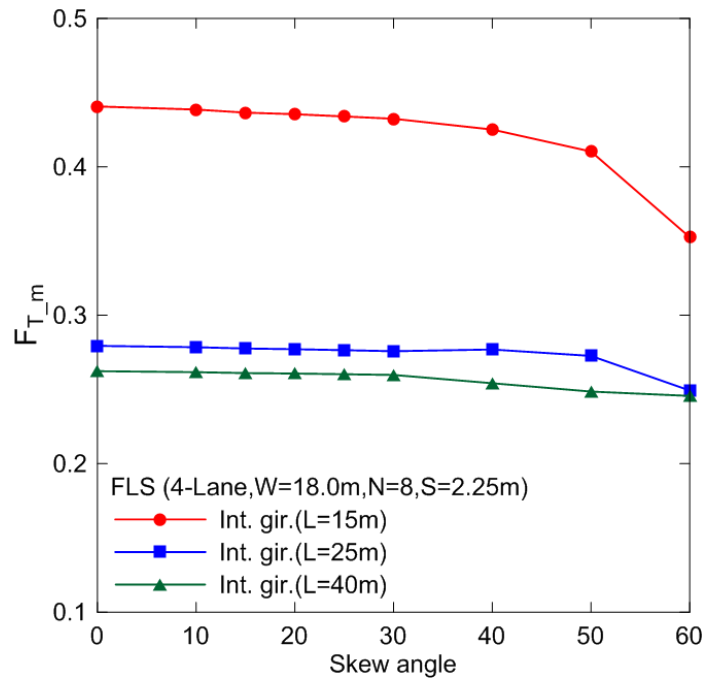


(b)

Figure 5.12 Effect of skew angle on $F_{T,m}$ of an exterior girder at FLS for: (a) two-lane, and (b) four-lane

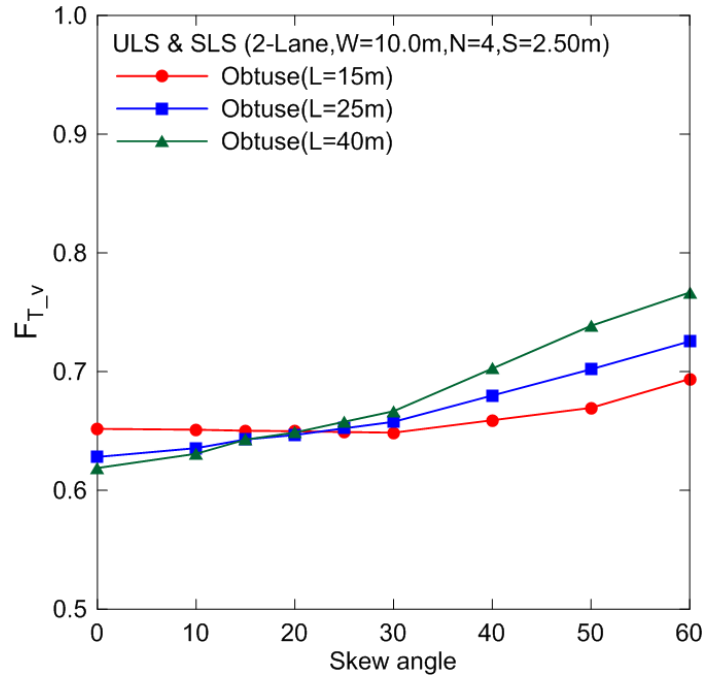


(a)

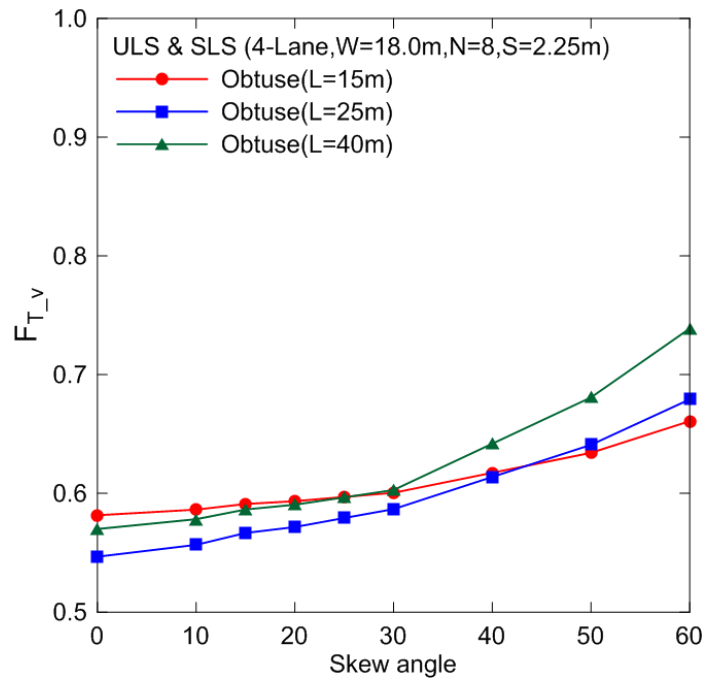


(b)

Figure 5.13 Effect of skew angle on $F_{T,m}$ of an interior girder at FLS for: (a) two-lane, and (b) four-lane

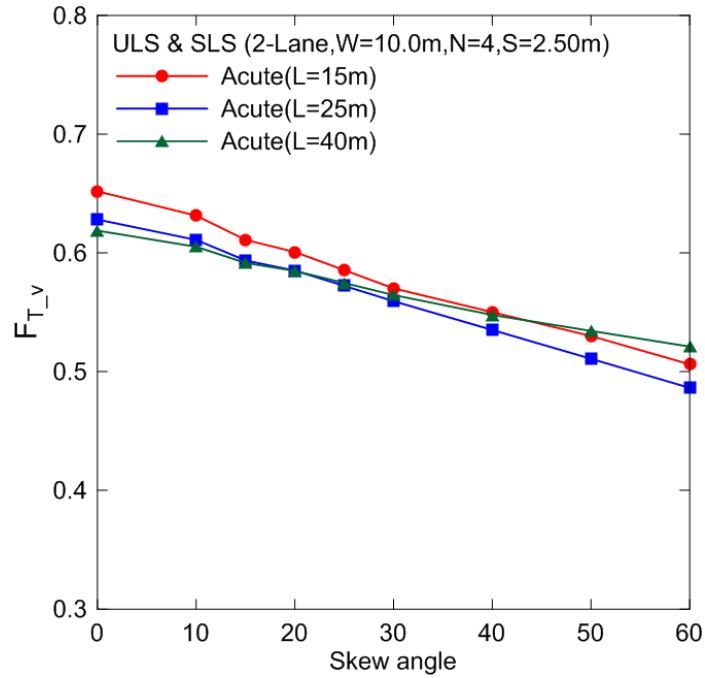


(a)

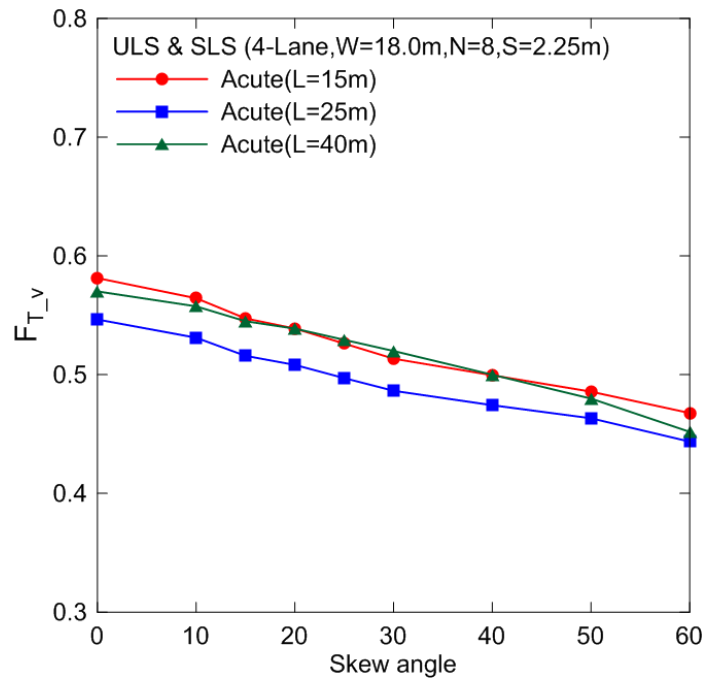


(b)

Figure 5.14 Effect of skew angle on F_{T_v} of the girder at obtuse corner at ULS & SLS for:
 (a) two-lane, and (b) four-lane

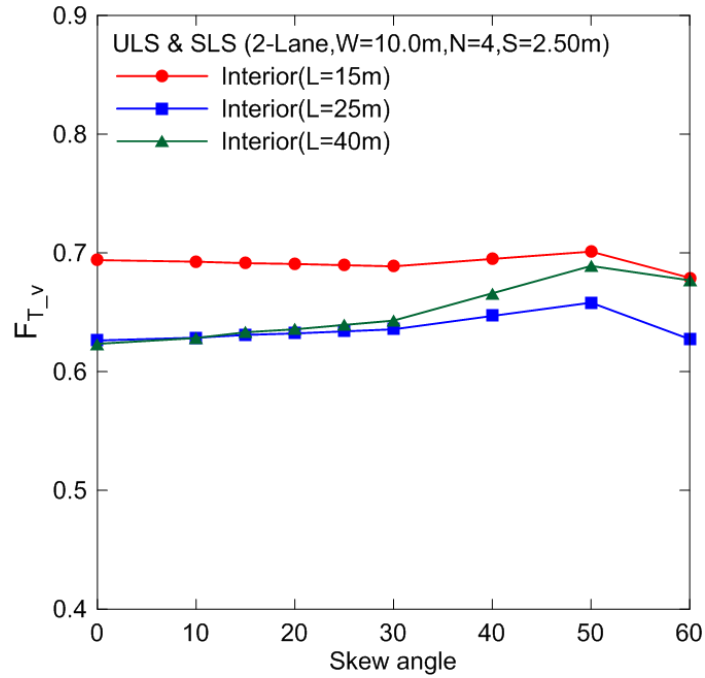


(a)

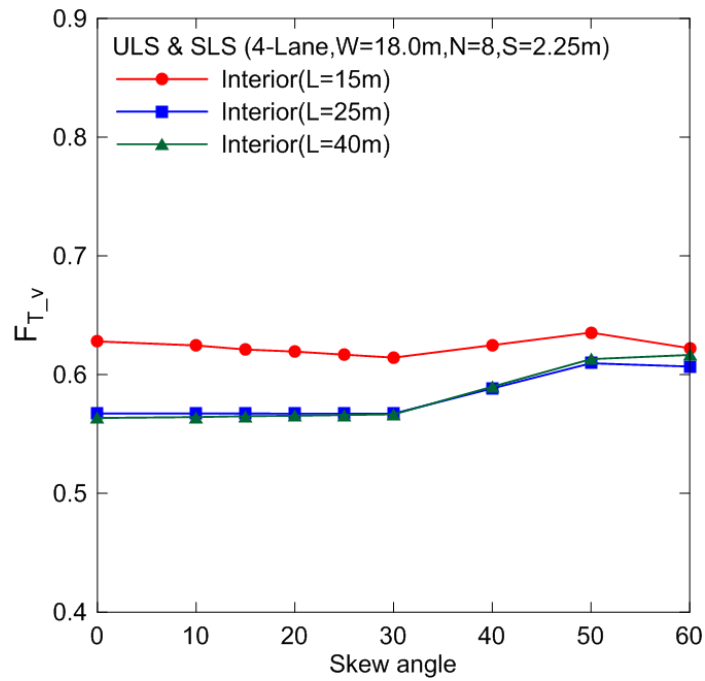


(b)

Figure 5.15 Effect of skew angle on F_{T_v} of the girder at acute corner at ULS & SLS for:
 (a) two-lane, and (b) four-lane

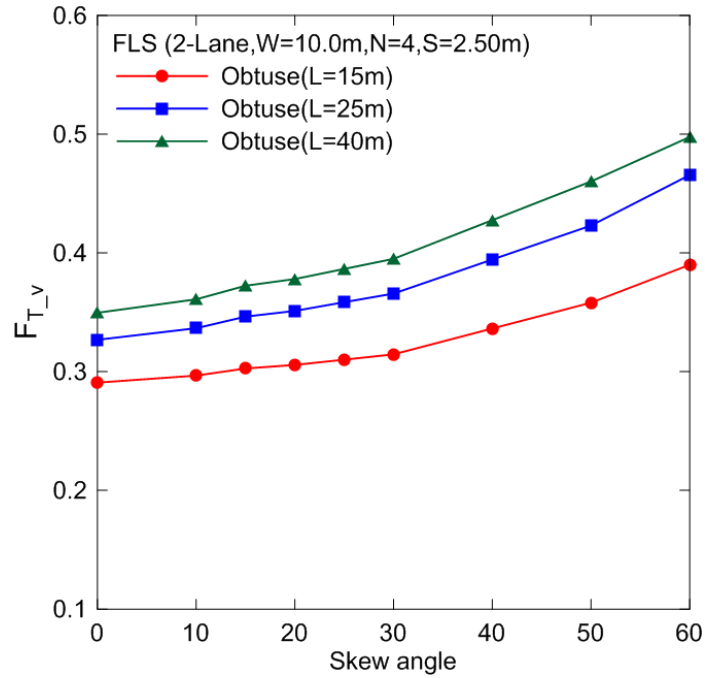


(a)

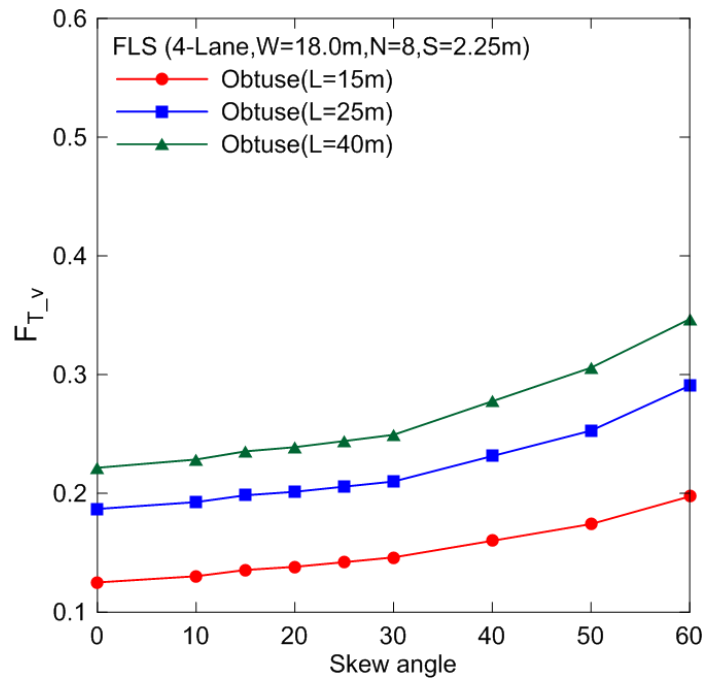


(b)

Figure 5.16 Effect of skew angle on F_{T_v} of the interior girder at ULS & SLS for: (a) two-lane, and (b) four-lane

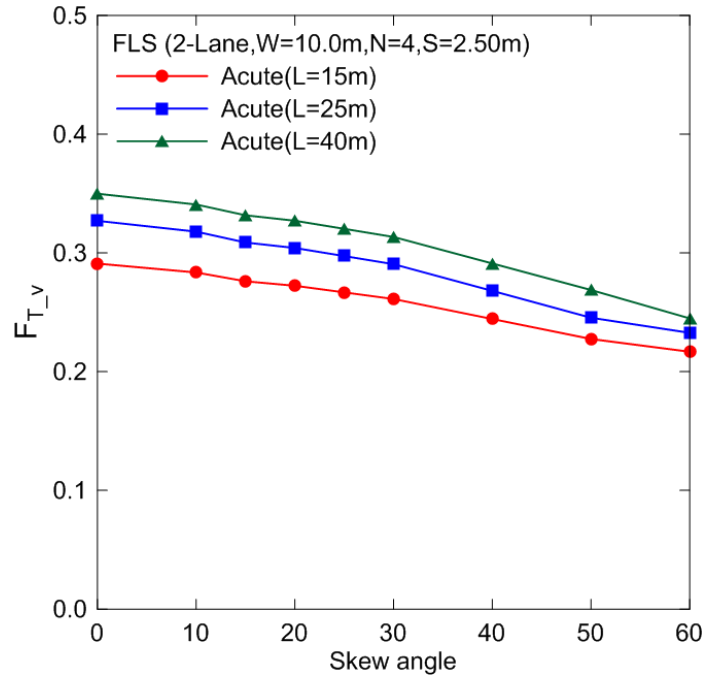


(a)

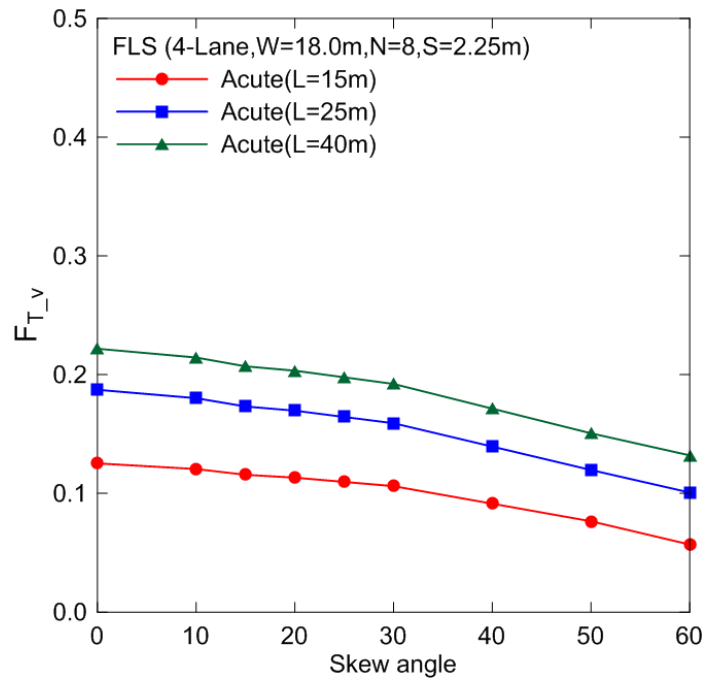


(b)

Figure 5.17 Effect of skew angle on F_{T_v} of the girder at obtuse corner at FLS for: (a) two-lane, and (b) four-lane

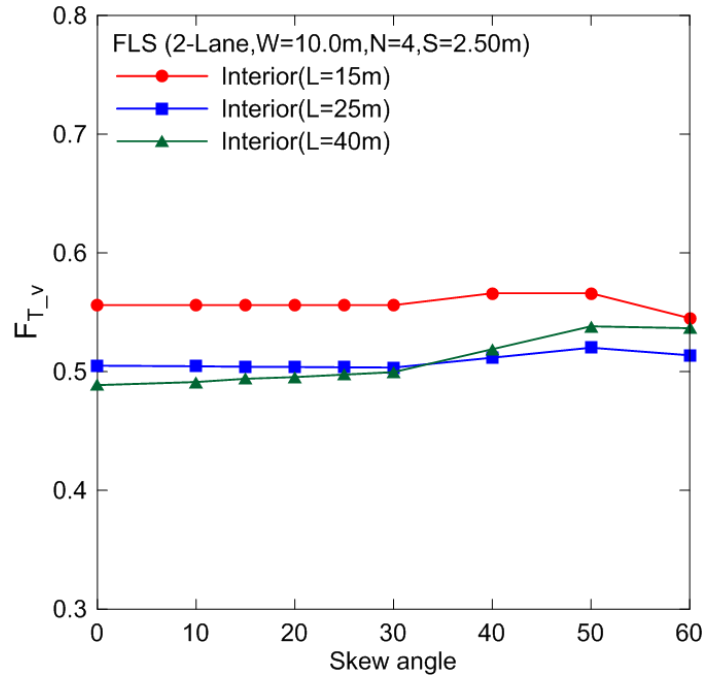


(a)

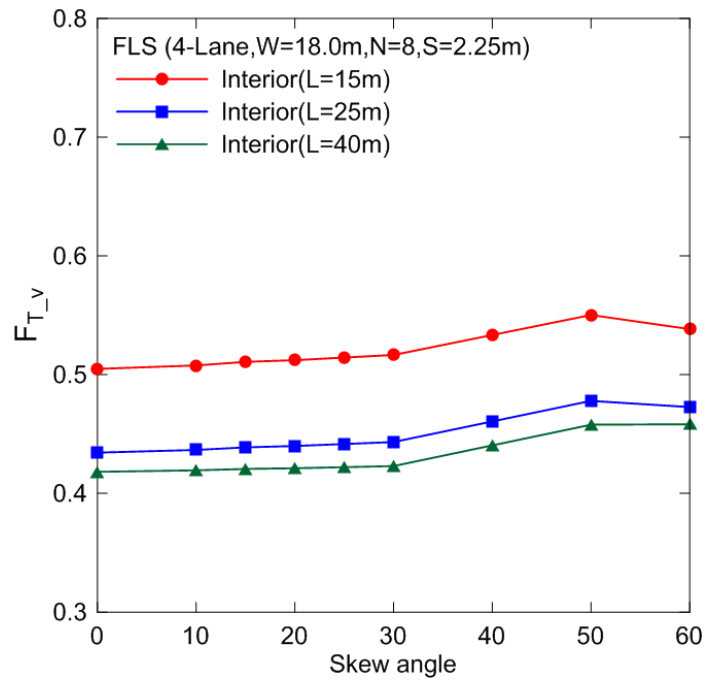


(a)

Figure 5.18 Effect of skew angle on F_{T_v} of the girder at acute corner at FLS for: (a) two-lane, and (b) four-lane



(a)



(b)

Figure 5.19 Effect of skew angle on F_{T_v} of the interior girder at FLS for: (a) two-lane, and (b) four-lane

Figure 5.12 and 5.13, shows the FEA results of an exterior and interior girder moment distribution factors of a skewed bridge under live load conditions for FLS quantified in terms of F_{T_m} . The main conclusions derived from these results are:

- 1) The effect of skew angle on the moment distribution factor of external and internal girder was insignificant up to 30° skew angle for both two and four-lane bridge geometry.
- 2) For high skew angle ($>30^\circ$), the sensitivity of load distribution factors of external and internal girders with respect to skew angle was predominantly high when span length was less than 20 m. For-example for bridge decks with a skew angle of 60° , exterior girder showed a decrease of about 27% and 33% for two and four-lane bridge system, respectively. Like-wise a reduction of about 18% and 20% was noticed in the moment distribution factor of interior girder for the two and four-lane bridge, respectively.
- 3) For high skew angle ($>30^\circ$), the effect of exterior and interior girder moment distribution factor with the increase of skew angle was found less sensitive when span length exceeds 20 m. For-example, for a 40 m span bridge with a skew angle of 60° , these factors for the exterior girder decreases by 12% and 14% for two and four-lane bridge respectively, and like-wise a 3% reduction was noticed in the interior girder distribution factor as compared with right bridge.

Figure 5.14, 5.15 and 5.16, shows the FEA results of a girder shear distribution factor of a skewed bridge at obtuse, acute and interior girder corner under live load conditions for ULS and SLS presented in terms of F_{T_v} as follows:

- 1) For skewed bridges up to 60° , two-lane bridge geometry resulted in high value of the shear distribution factors at the obtuse, acute and interior girder as compared with four-lane bridge configuration.
- 2) It was observed that the shear distribution factor at the girder obtuse corner increases with increase in the angle of skew. The rate of this increase for skew angle between 30° and 60° was greater than for skew angle between 0° and 30° .

The shear distribution factor at the acute girder location decreases with the increase of the angle of skew, such that, for bridge decks with a skew angle of 60° , the shear

distribution factor of acute girder corner reduced by 22% and 21% for two and four-lane bridge respectively, as compared with right bridge.

Figure 5.16 shows that the effect of shear distribution factor of interior girders with respect to skew angle was insignificant. For high skew angle, such as, 30° to 60° interval, a marginal increase in these factors were noticed for span length greater than 20 m for two and four-lane bridge configuration.

- 3) It was noticed that the effect of skew angle on the shear distribution factor at the obtuse girder corner was more sensitive to the width of the bridge. For-example, for a bridge with a skew angle of 60°, these factors increased by 14%, 23% and 31% for a four-lane bridge when a span length of 15 m, 25 m and 40 m, respectively was considered. On the contrary, a two-lane bridge resulted in 6%, 15% and 24% increase in the obtuse girder shear distribution factor for 15 m, 25 m and 40 m, respectively span lengths. From the aforesaid finding also, we concluded that the effect of skew angle on the shear distribution factor at the obtuse girder corner increases when the span length increases. It was worth noting that the shear distribution factor at the girder obtuse corner was sensitive to the aspect ratio i.e. length/width ratio, of the bridge.

Figure 5.17, 5.18 and 5.19, shows the FEA results of a girder shear distribution factor of a skewed bridge at obtuse, acute and interior girder corner under live load conditions for FLS described in terms of F_{T_v} as follows:

- 1) High value of the shear distribution factors at the obtuse, acute and interior girder were observed for two-lane bridge geometry as compared with four-lane bridge configuration for a skewed bridges up to 60°.
- 2) It was observed that the shear distribution factor at the girder obtuse corner increases with the increase in the angle of skew. The rate of this increase for skew angle between 30° and 60° was greater than for skew angle between 0° and 30°. For example, for a skew angle up to 30° a maximum increase of 12% was observed, and further increase in skew angle from 30° to 60° resulted in 31% increase of shear distribution factor at the girder obtuse corner for two-lane bridge configuration. Likewise, for a four-lane bridge geometry 13% increase in these factors was observed for a skew angle up to 30° that further augmented to 45% when skew angle increases from 30° to 60°.

The shear distribution factor at the acute girder location decreases with the increase of the angle of skew, such that, for bridge decks with a skew angle of 60° , the shear distribution factor of acute girder corner reduced by 31% and 47% for two and four-lane bridge respectively, as compared with right bridge for three different span lengths as shown in Figure 5.18.

Figure 5.19 shows that the effect of shear distribution factor of interior girders with respect to skew angle was insignificant. For high skew angle ($> 30^\circ$) up to 60° , a marginal increase in these factors were noticed for two and four-lane bridge configuration.

5.2.6.2 Effect of Span Length

The moment distribution factors for the multi-lane skewed bridges were evaluated and their effects with the variation of span lengths are presented in Figure 5.20 and 5.21 for ULS and SLS, and in Figure 5.22 and 5.23 for FLS, and briefly summarized in terms of F_{T_m} as follows:

- 1) For both exterior and interior girders, the effect of span length on the moment distribution factors decreases when skew angle increases from 0° to 60° .
- 2) For span length up to 25 m, the sensitivity of moment distribution factors for the exterior and interior girders with respect to span length was high. For example, for exterior girder at ULS and SLS these factor decreased by 25% in two and four-lane bridges, whereas 31% and 34% decrease was noticed in the interior girders of a two and four lane bridge configuration respectively. Similarly for FLS, these factors for an exterior girder decreased by 19% and 6% for two and four-lane bridges respectively, and a decrease of about 38% and 41% in the moment distribution factor of interior girder was noticed for the two and four-lane bridges respectively. Hence it can be inferred from the above finding that the moment distribution factor of an interior girder was more sensitive with the increase of span length up to 25 m for all three limit states.
- 3) For span length greater than 25 m up to 40 m, the effect of span length on the moment distribution factors of exterior and interior girders was insignificant.

The effect of shear distribution factors of a skewed bridge at obtuse, acute and interior girder corners with the variation of span length are presented in Figure 5.24, 5.25 and 5.26 for ULS and SLS, and in Figure 5.27, 5.28 and 5.29 for FLS, and discussed in terms of F_{T_v} as follows:

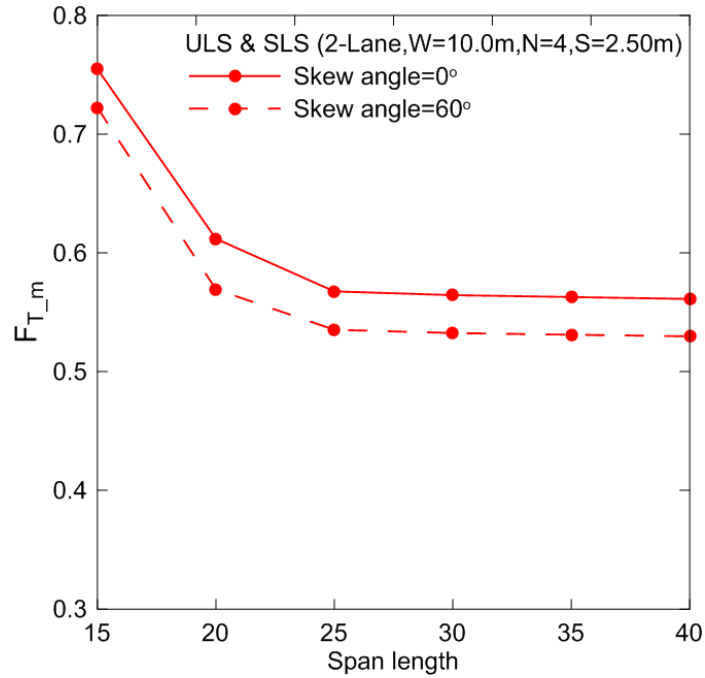
- 1) For right bridges (i.e. skew angle= 0°) at ULS and SLS, the shear distribution factors at the obtuse girder corner were found not very sensitive to span length. A marginal decrease in these factors were noticed with the increase of span length from 15 m to 40 m. However, Figure 5.24 shows that the sensitivity of shear distribution factor of obtuse girder corner with respect to span length was high, such that, for a skew angle of 60° , these factors increased by 12% as the span length increases from 15 m to 40 m for two and four-lane bridge.

Figure 5.27 shows that for FLS the increase of span length resulted in the increase of shear distribution factors at the obtuse girder corner. This effect was more pronounced in skewed bridges as compared to right bridges.

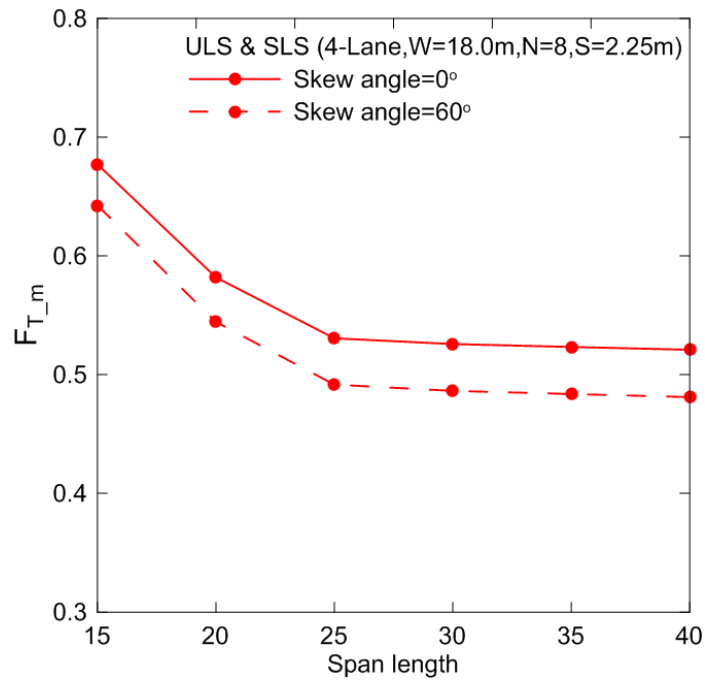
- 2) Figure 5.25 shows that for ULS and SLS, the shear distribution factors at the acute girder corner were found not sensitive to the span length. A marginal decrease in these factors were noticed with the increase of span length between 15 m to 40 m.

For FLS, the increase of the span length resulted in the increase of shear distribution factors at the acute girder corner. Figure 5.28 shows that this effect was more pronounced in skewed bridges as compared to right bridges.

- 3) As shown in Figure 5.26 and 5.29, the shear distribution factor of an interior girder decreases with the increase of span length up to 25 m for ULS and SLS, and FLS. However, as the span length increases from 25 m to 40 m, a marginal increase of these factors were noticed in a two-lane skewed bridge behavior, whereas for a four-lane bridge this effect was insignificant when the span length increases from 25 m to 40 m.

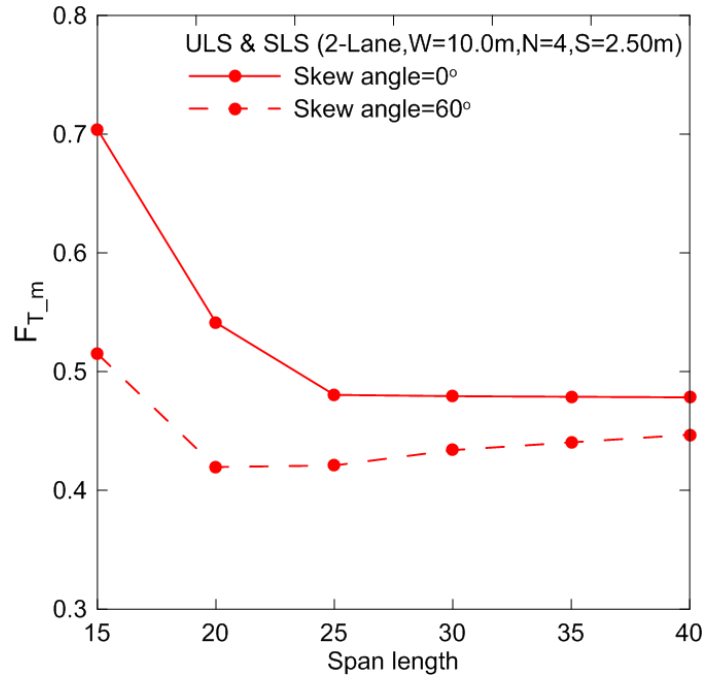


(a)

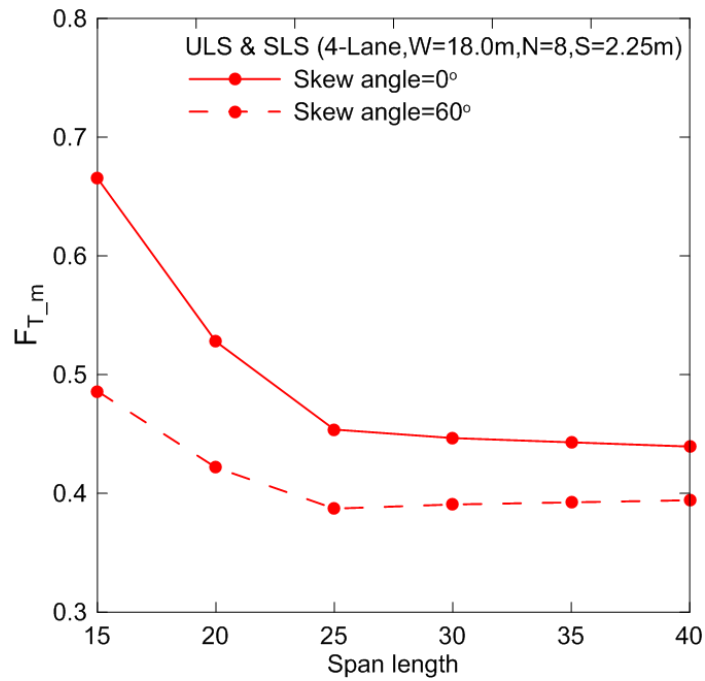


(b)

Figure 5.20 Effect of span length on $F_{T,m}$ of the exterior girder at ULS & SLS for: (a) two-lane, and (b) four-lane

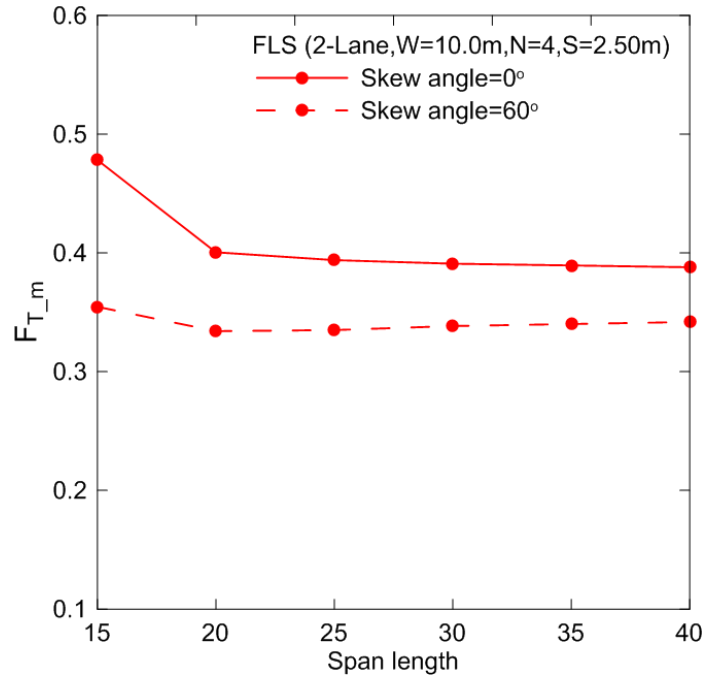


(a)

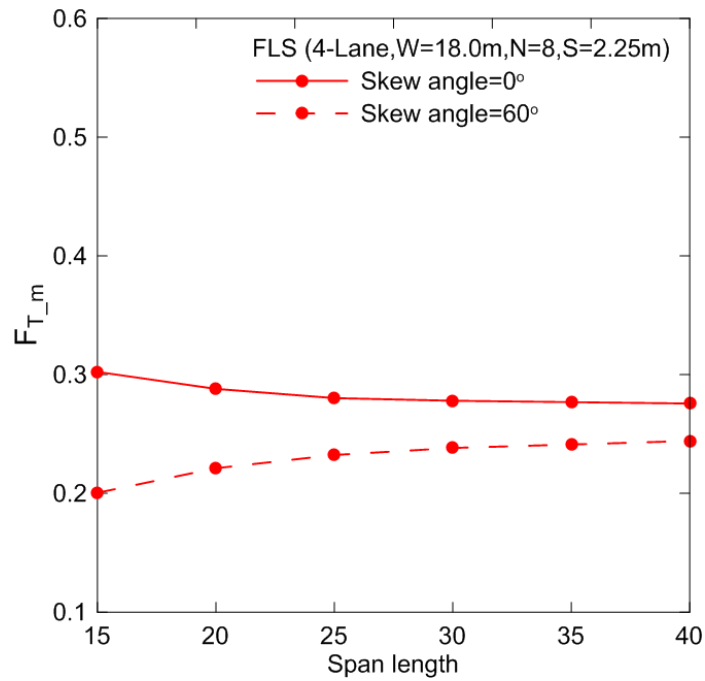


(b)

Figure 5.21 Effect of span length on $F_{T,m}$ of the interior girder at ULS & SLS for: (a) two-lane, and (b) four-lane

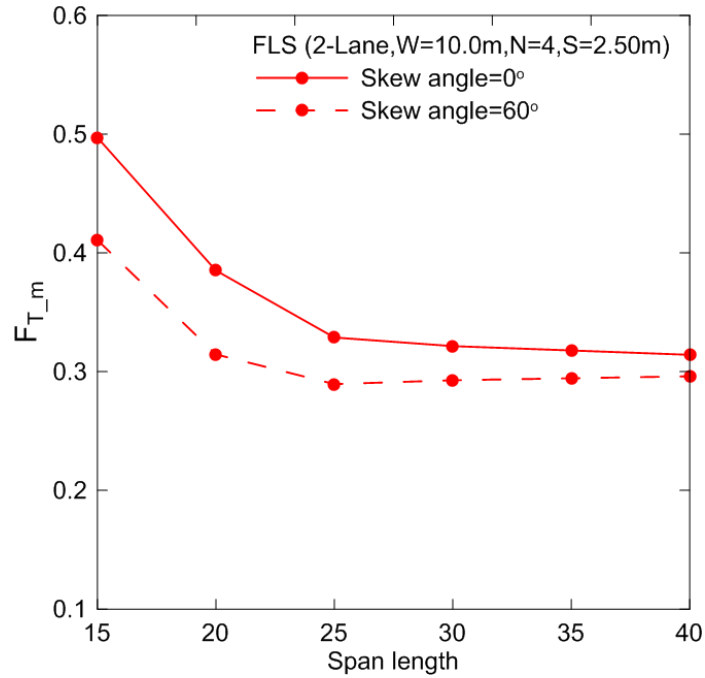


(a)

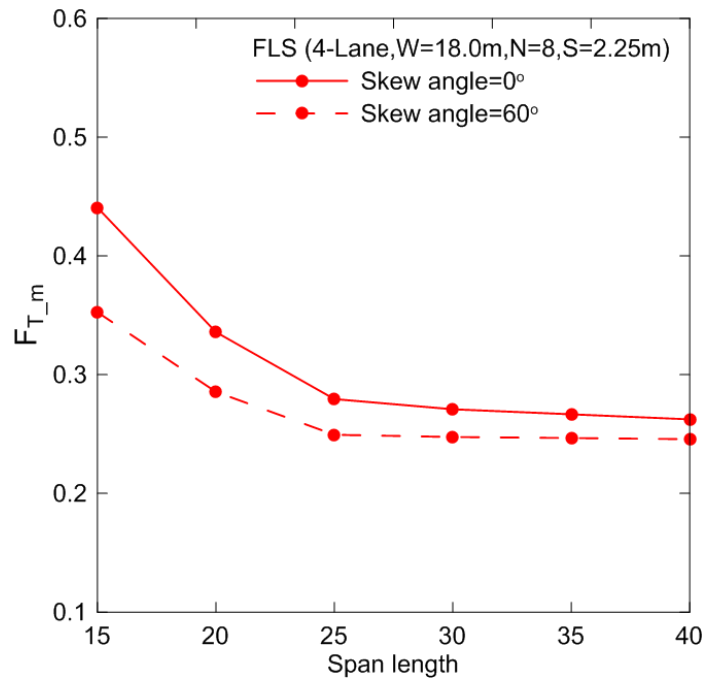


(b)

Figure 5.22 Effect of span length on F_{T_m} of the exterior girder at FLS for: (a) two-lane, and (b) four-lane

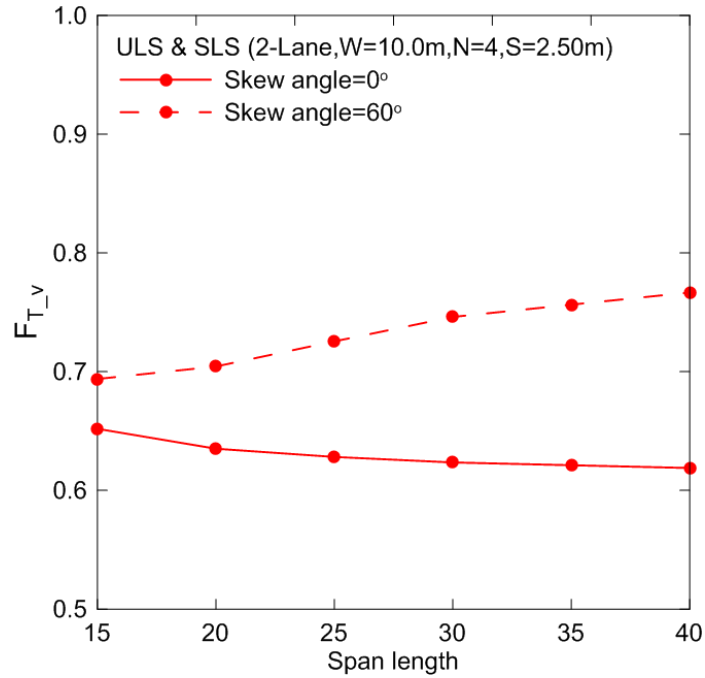


(a)

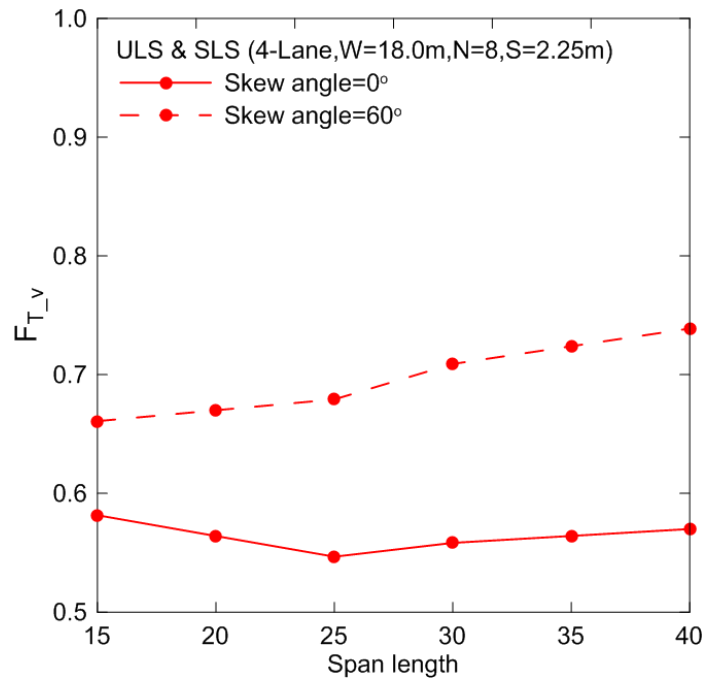


(b)

Figure 5.23 Effect of span length on F_{T_m} of the interior girder at FLS for: (a) two-lane, and (b) four-lane

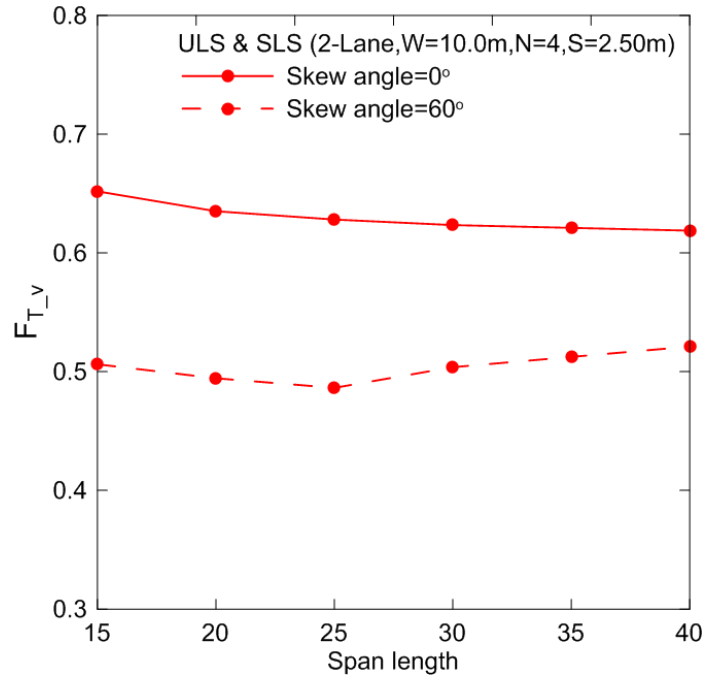


(a)

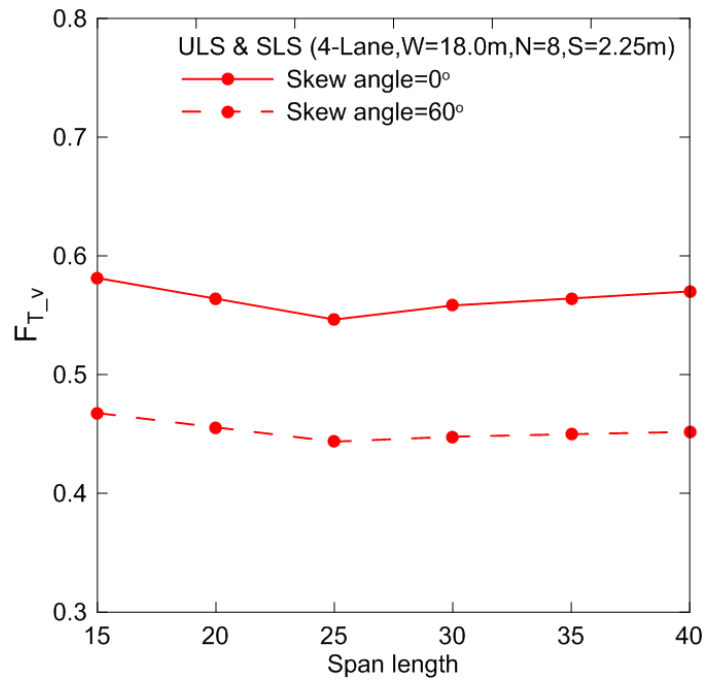


(b)

Figure 5.24 Effect of skew angle on F_{T_v} of the girder at obtuse corner at ULS and SLS for: (a) two-lane, and (b) four-lane

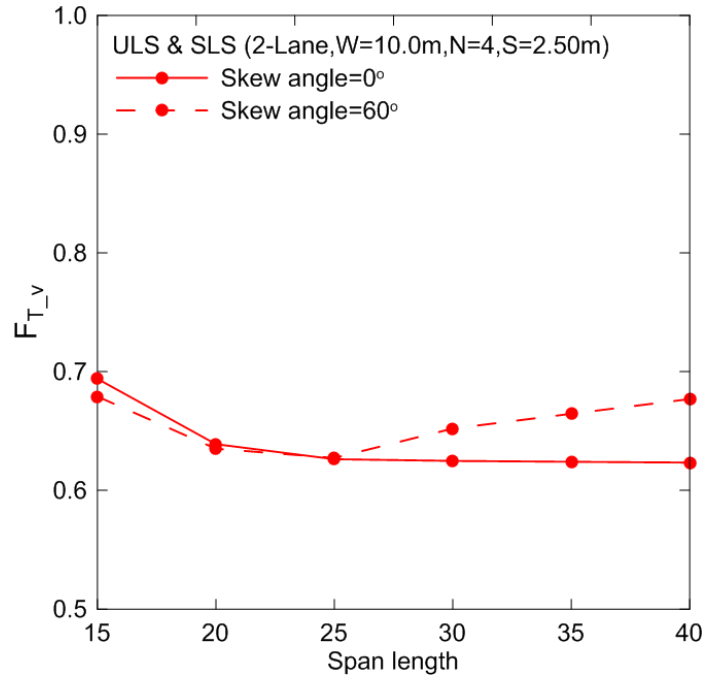


(a)

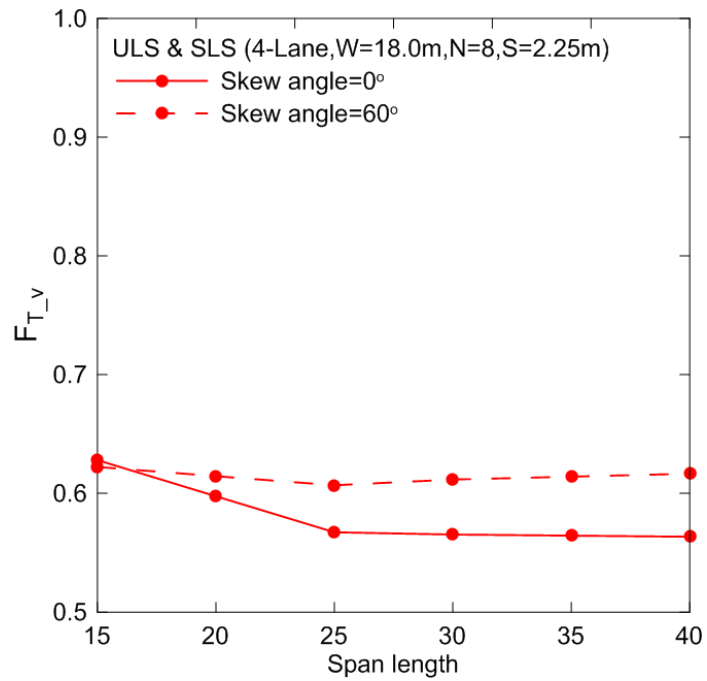


(b)

Figure 5.25 Effect of skew angle on F_{T_v} of the girder at acute corner at ULS and SLS for: (a) two-lane, and (b) four-lane

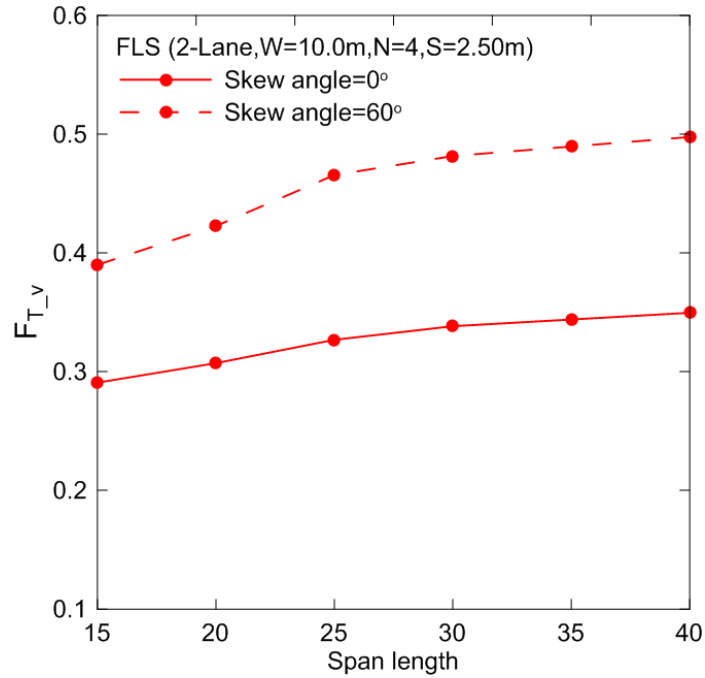


(a)

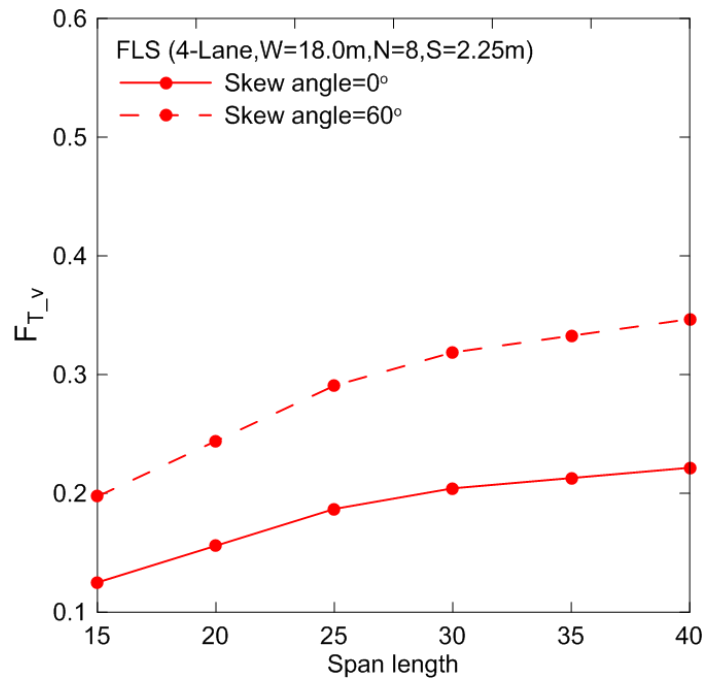


(b)

Figure 5.26 Effect of skew angle on F_{T_v} of the interior girder corner at ULS and SLS for:
 (a) two-lane, and (b) four-lane

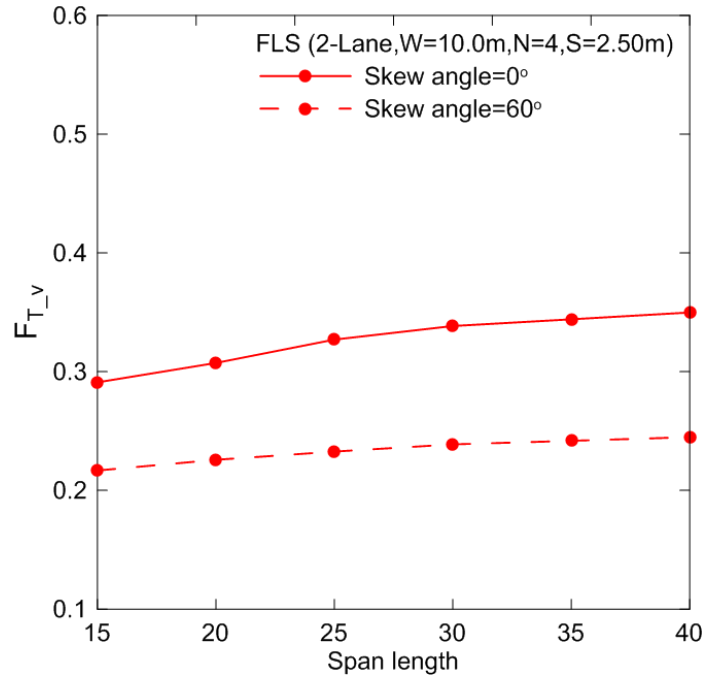


(a)

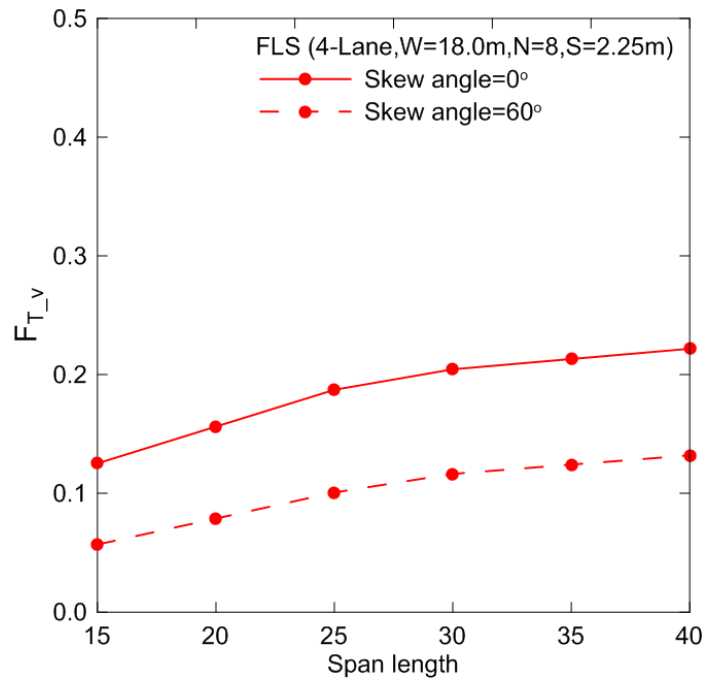


(b)

Figure 5.27 Effect of skew angle on F_{T_v} of the girder at obtuse corner at FLS for: (a) two-lane, and (b) four-lane

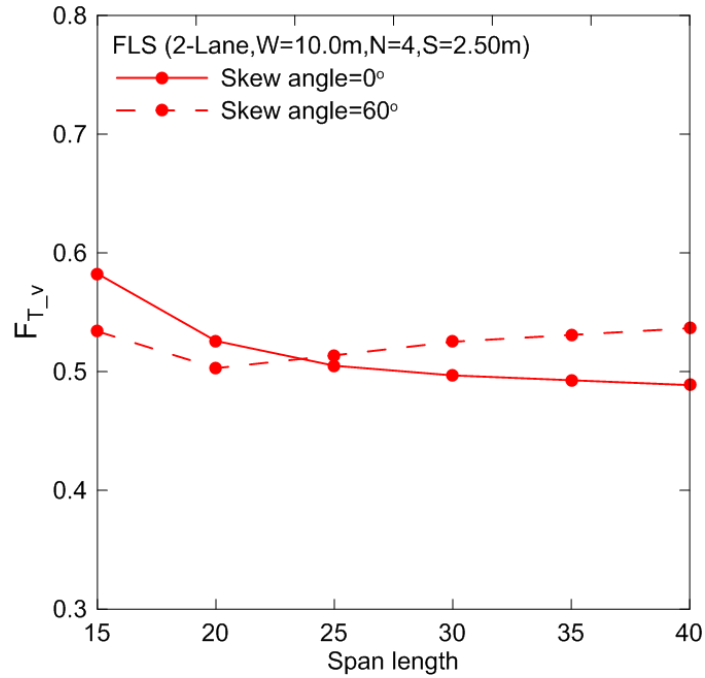


(a)

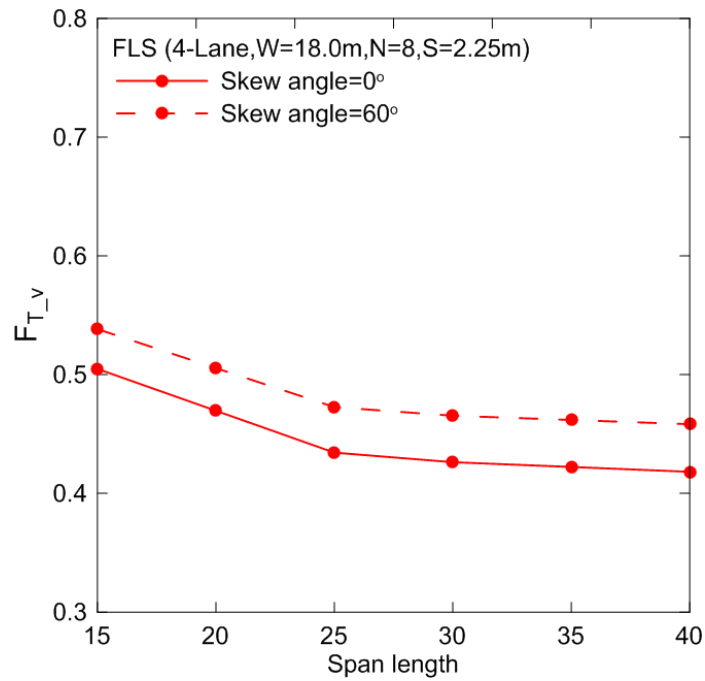


(b)

Figure 5.28 Effect of skew angle on F_{T_v} of the girder at acute corner at FLS for: (a) two-lane, and (b) four-lane



(a)



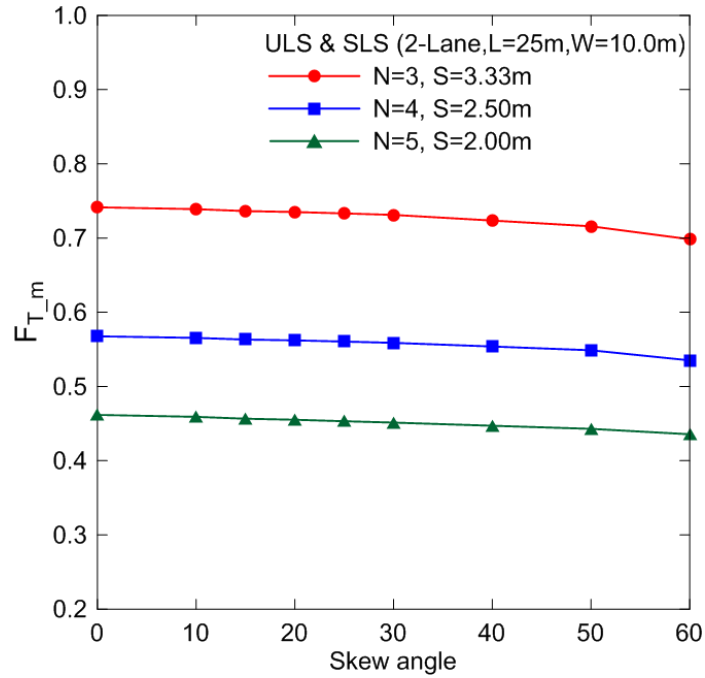
(b)

Figure 5.29 Effect of skew angle on F_{T_v} of the interior girder corner at FLS for: (a) two-lane, and (b) four-lane

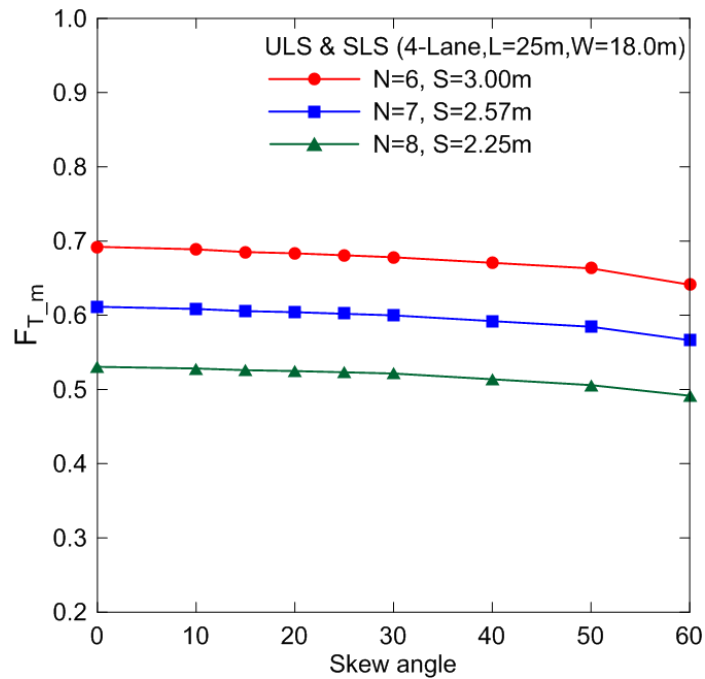
5.2.6.3 Effect of Girder Spacing, Number of Girders and Number of Lanes

The effect of girder spacing on the moment distribution factors of the exterior and the interior girder are presented in Figure 5.30 and 5.31 for ULS and SLS, and in Figure 5.35 and 5.36 for FLS, and summarized in terms of F_{T_m} as follows:

- 1) The bridge configuration having less number of girders arranged at greater spacing results in higher value of moment distribution factor for both exterior and interior girder at both ULS and SLS, and FLS, as compared to the bridge geometry comprised of more number of girders positioned at less spacing among them.
- 2) For ULS and SLS, the effect of girder spacing on the moment distribution factor of exterior girder with the increase of skew angle was less sensitive, such that, a marginal decrease of about 6% was noticed. However for FLS, a maximum decrease of about 17% was observed for two and four-lane bridge structures having more number of girders arranged at less spacing between them.
- 3) For ULS and SLS, and FLS, the sensitivity of load distribution factor of interior girder with respect to girder spacing was high when the skew angle increases from 30° to 60°. Also it was noticed that within that skew angle range, the bridge structure having less number of girders with wide girder spacing resulted in greater reduction of moment distribution factor. For-example for decks with a skew angle of 60°, these factors decreased by 17% and 22% when a two and four-lane bridge geometry was considered for ULS and SLS. Also the effect of girder spacing on the load distribution factor of interior girder resulted in the reduction of about 17% in case of FLS for a highly skewed bridge (i.e. skew angle=60°) as compared to the right bridge. However, for decks with a skew angle up to 30°, this effect was insignificant for both ULS and SLS, and FLS.

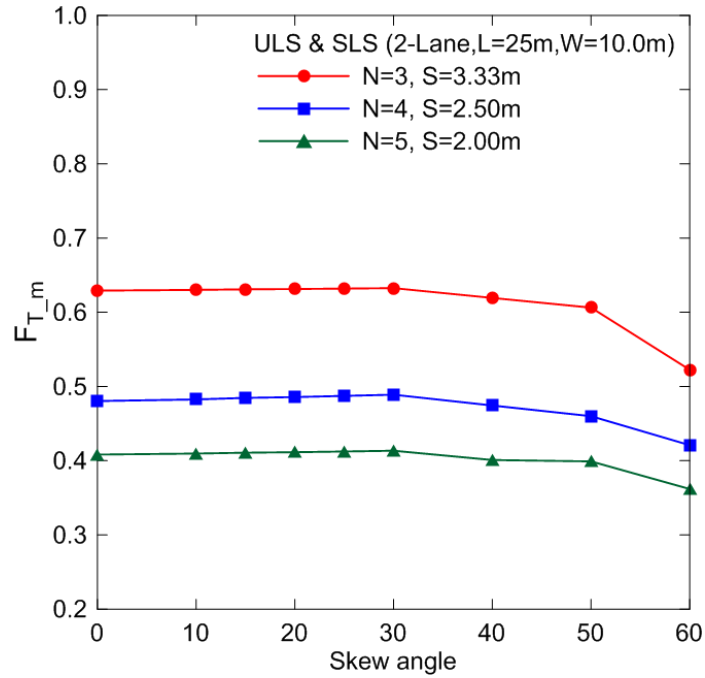


(a)

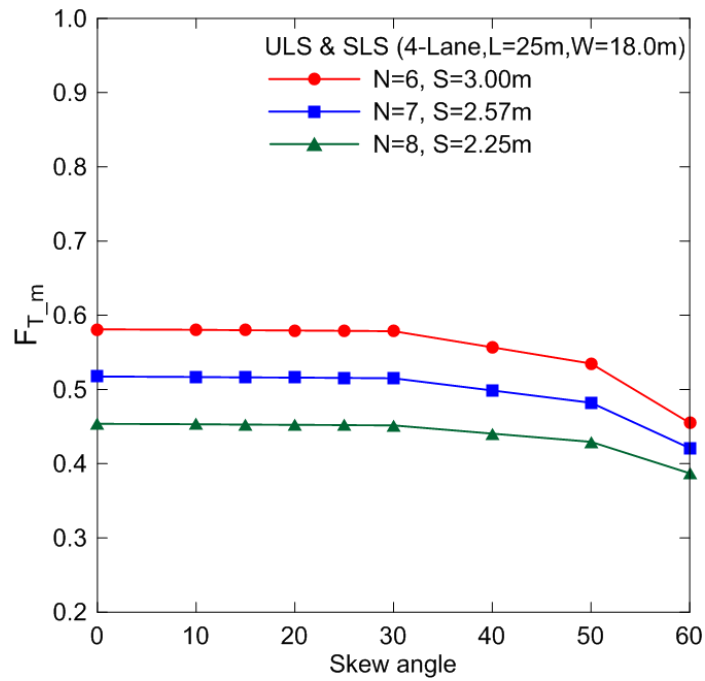


(b)

Figure 5.30 Effect of girder spacing on $F_{T,m}$ of the exterior girder at ULS and SLS for: (a) two-lane, and (b) four-lane

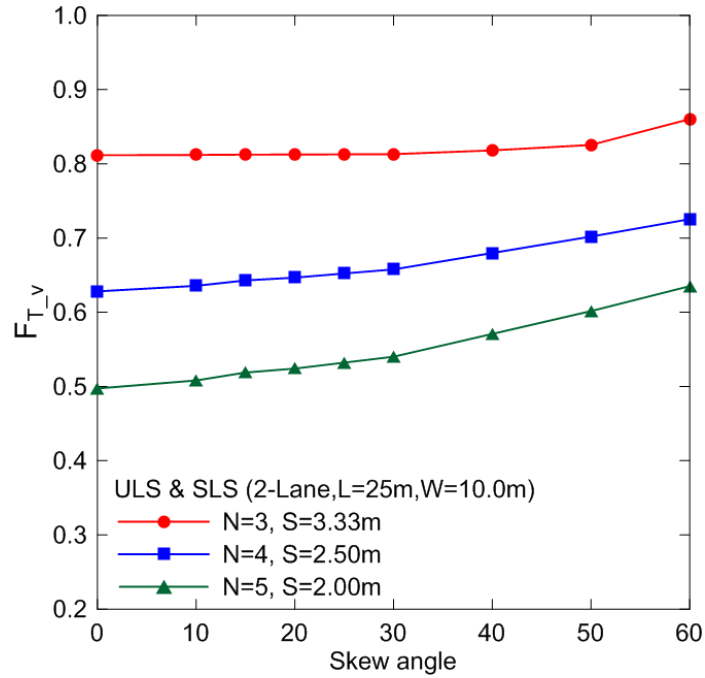


(a)

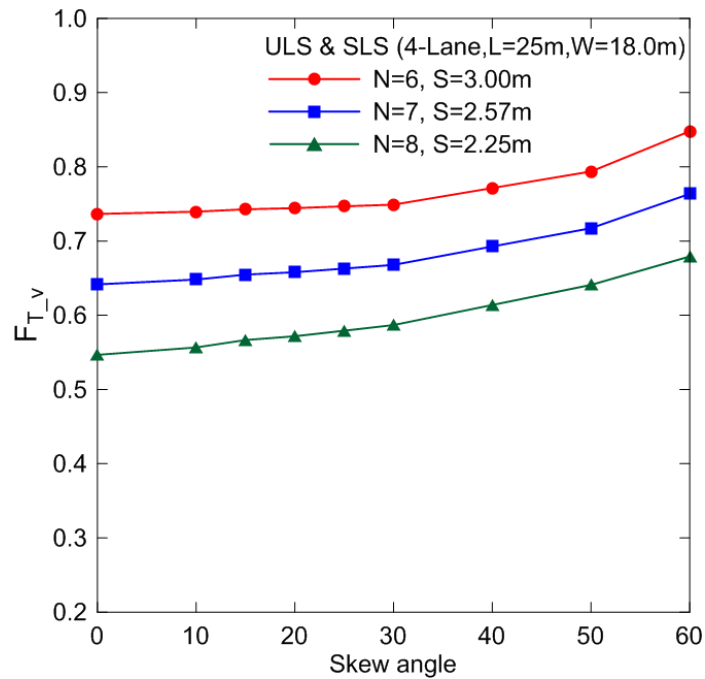


(b)

Figure 5.31 Effect of girder spacing on $F_{T,m}$ of the interior girder at ULS and SLS for: (a) two-lane, and (b) four-lane

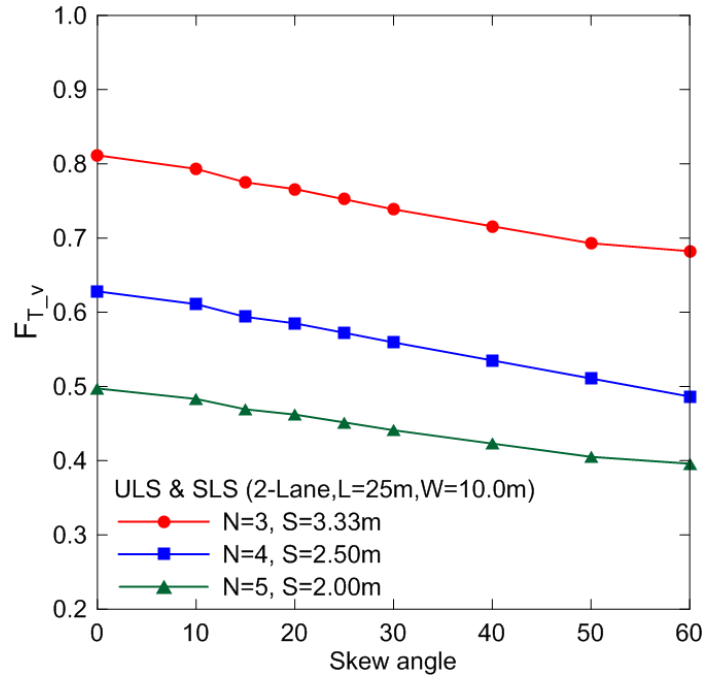


(a)

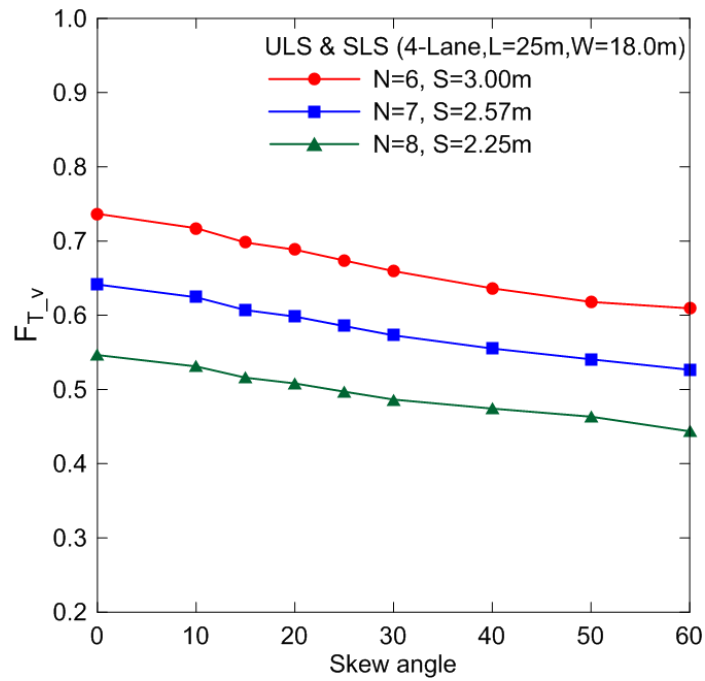


(b)

Figure 5.32 Effect of girder spacing on F_{T_v} of the girder at obtuse corner at ULS & SLS for: (a) two-lane, and (b) four-lane

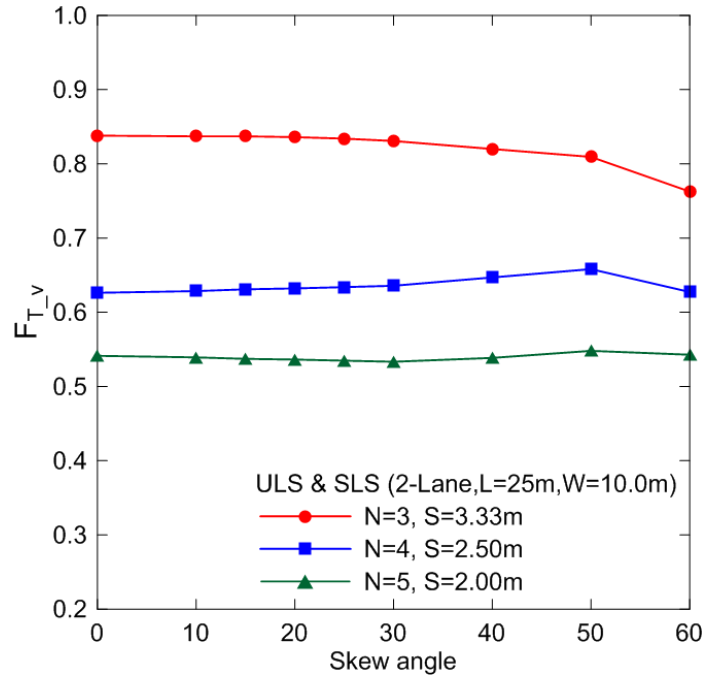


(a)

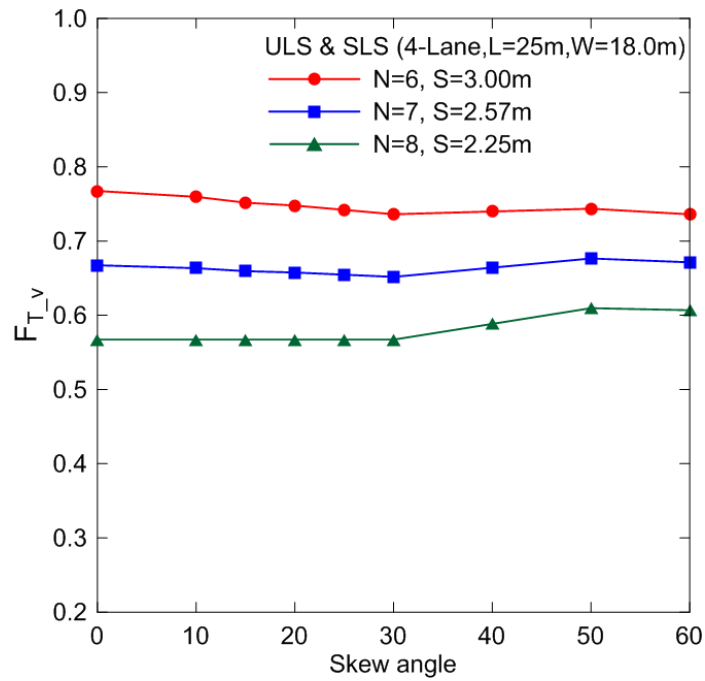


(b)

Figure 5.33 Effect of girder spacing on $F_{T,v}$ of the girder at acute corner at ULS & SLS for: (a) two-lane, and (b) four-lane

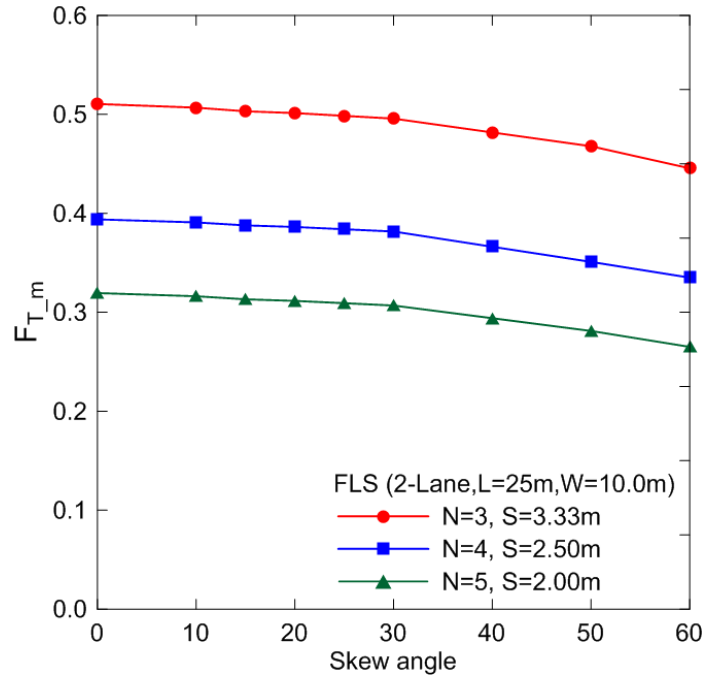


(a)

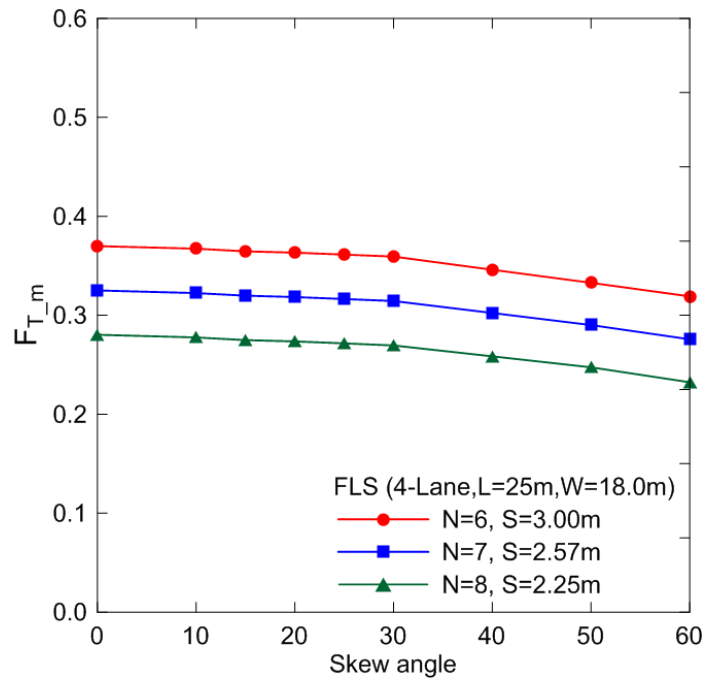


(b)

Figure 5.34 Effect of girder spacing on F_{T_v} of the interior girder corner at ULS & SLS for: (a) two-lane, and (b) four-lane

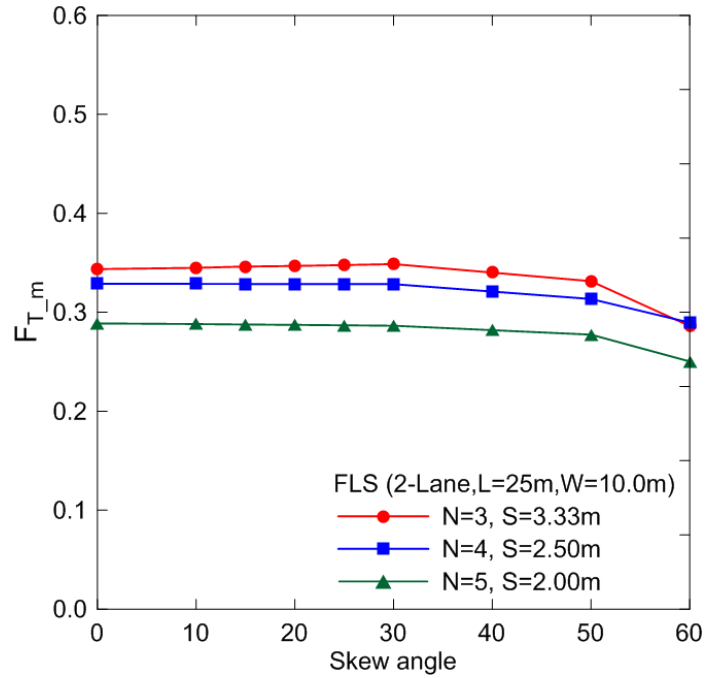


(a)

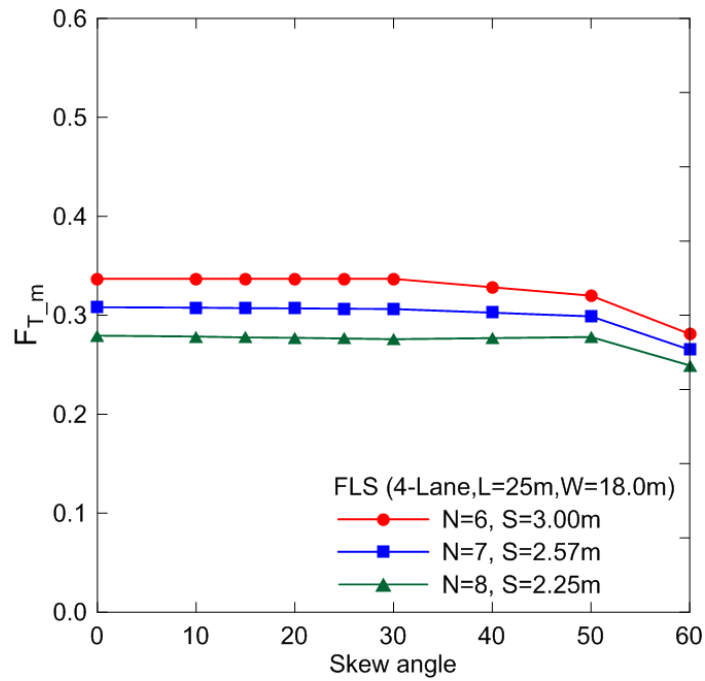


(b)

Figure 5.35 Effect of girder spacing on $F_{T,m}$ of the exterior girder at FLS for: (a) two-lane, and (b) four-lane

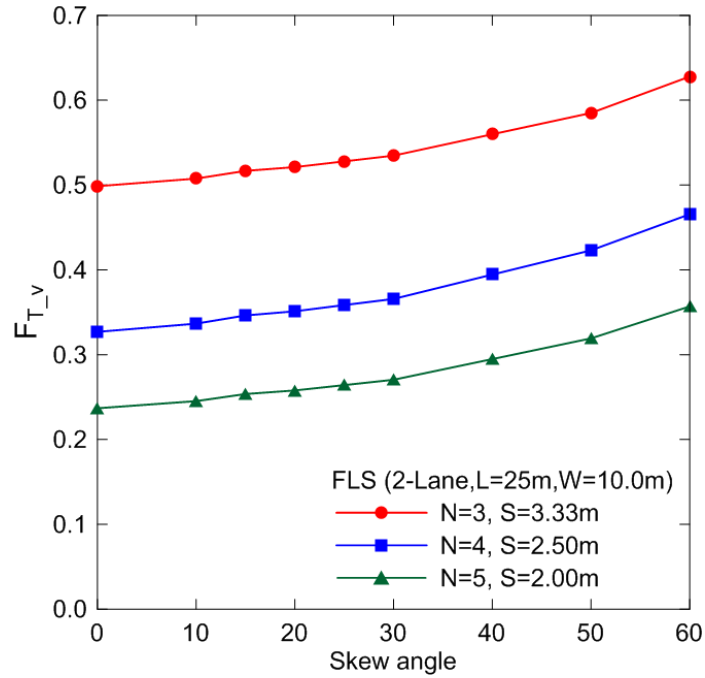


(a)

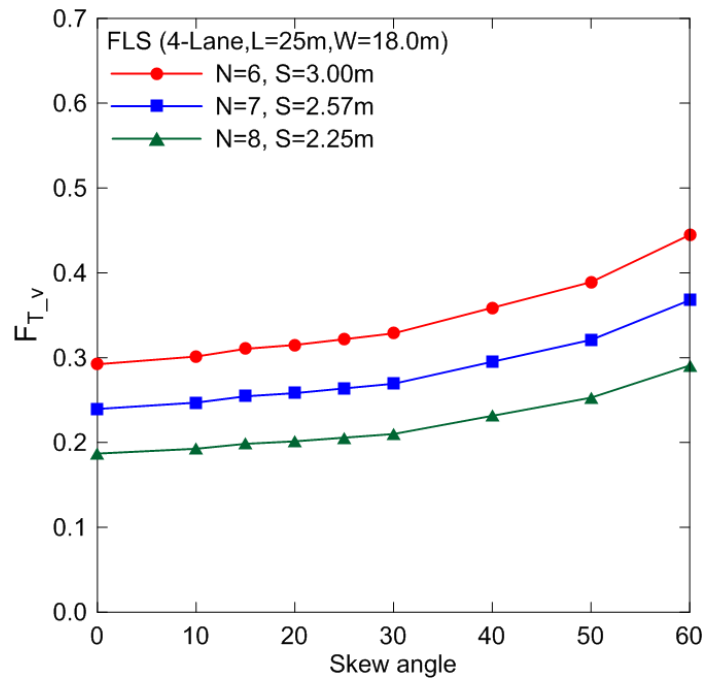


(b)

Figure 5.36 Effect of girder spacing on $F_{T,m}$ of the interior girder at FLS for: (a) two-lane, and (b) four-lane

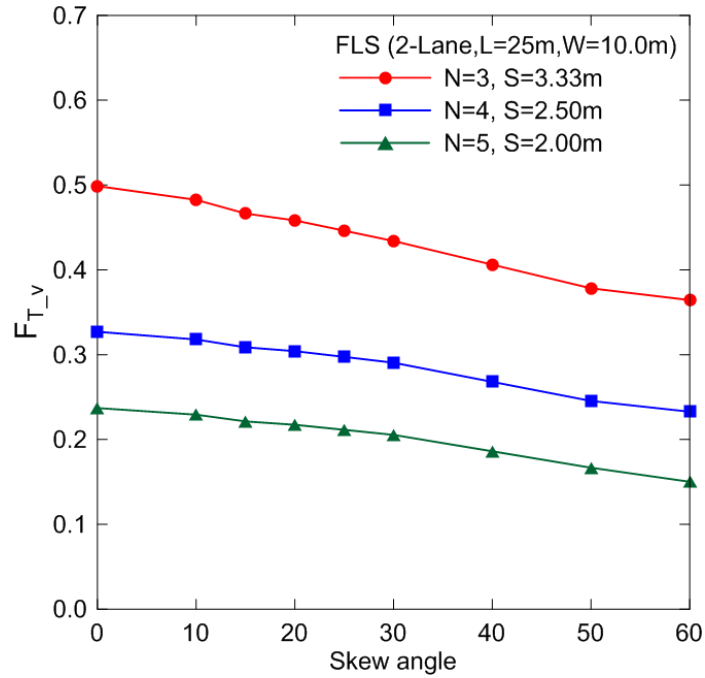


(a)

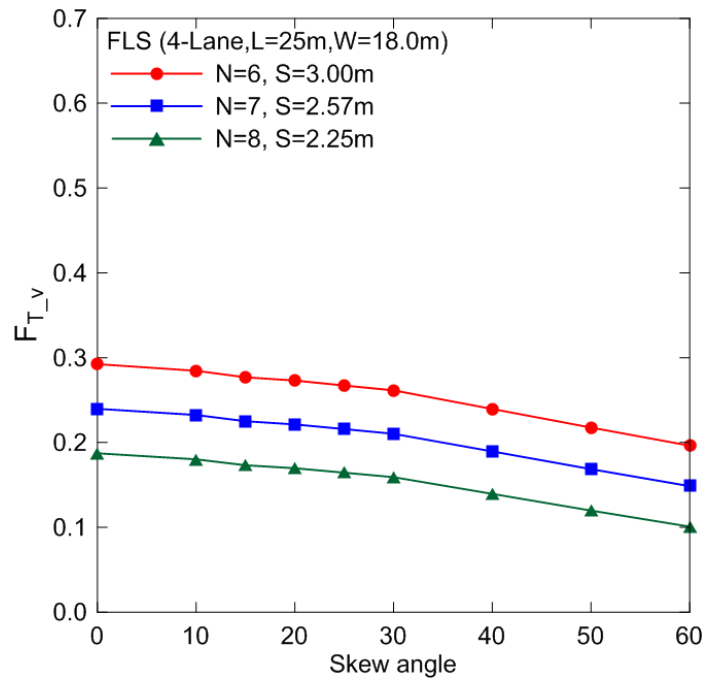


(b)

Figure 5.37 Effect of girder spacing on F_{T_v} of the girder at obtuse corner at FLS for: (a) two-lane, and (b) four-lane

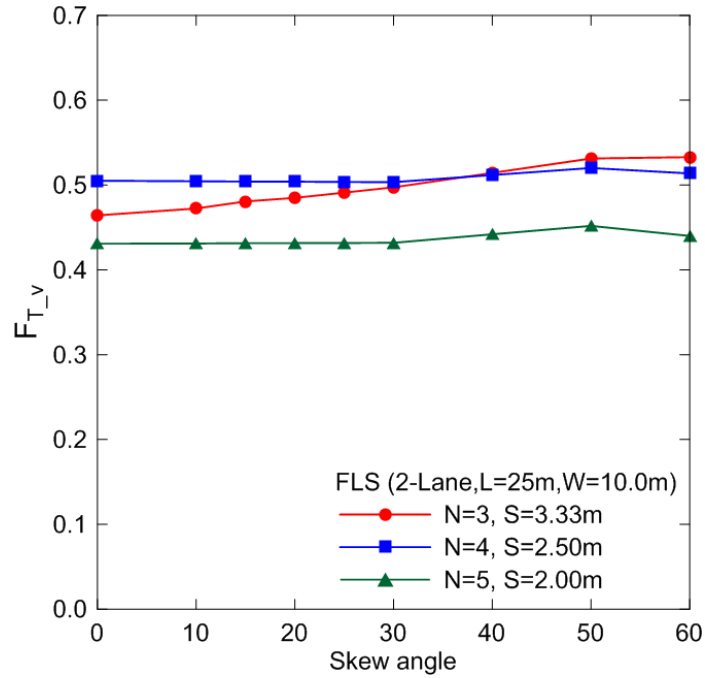


(a)

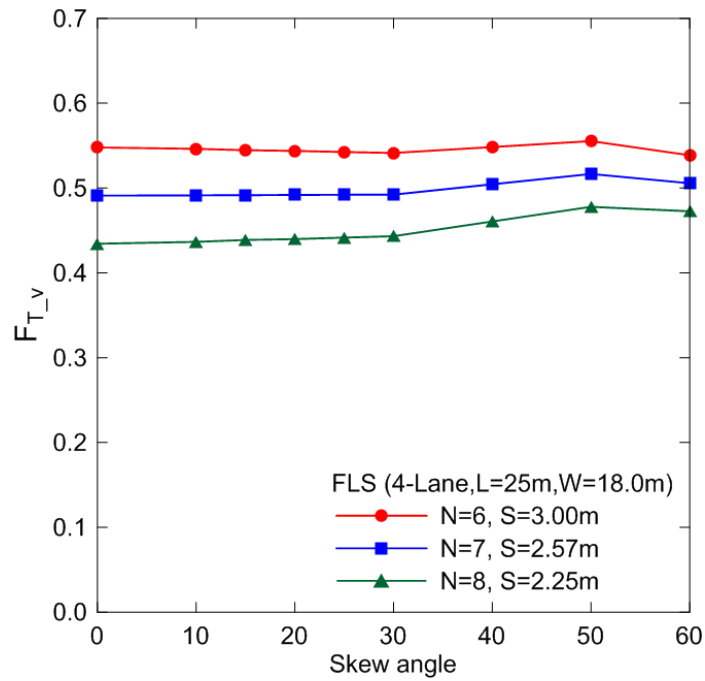


(b)

Figure 5.38 Effect of girder spacing on F_{T_v} of the girder at acute corner at FLS for: (a) two-lane, and (b) four-lane



(a)



(b)

Figure 5.39 Effect of girder spacing on F_{T_v} of the interior girder corner at FLS for: (a) two-lane, and (b) four-lane

The effect of girder spacing on the shear distribution factors at bridge obtuse corner, acute corner and interior girder are presented in Figure 5.32, 5.33 and 5.34 for ULS and SLS, and in Figure 5.37, 5.38 and 5.39 for FLS respectively, and discussed below:

- 1) Less number of girders with greater girder spacing results in higher value of shear distribution factor for the obtuse, acute and interior girder location at both ULS and SLS, and FLS, as compared with the bridge geometry having smaller spacing between girders.
- 2) For ULS and SLS, and FLS at obtuse girder corner, the effect of girder spacing resulted an increase of shear distribution factor with the increase of skew angle for two and four-lane bridges. This effect was more pronounced in bridge configurations having more number of girders with less spacing between them. For example, decks with a skew angle of 60° , these factors increased by 28% and 24% for ULS and SLS, and resulted in 50% and 55% increase for FLS, when two and four-lanes bridge geometry was considered, respectively.
- 3) For ULS and SLS, and FLS, the effect of girder spacing resulted in the decrease of shear distribution factor at acute girder corner with the increase of skew angle for two and four-lanes bridge. For example, decks with a skew angle of 60° , these factors decreased by 23% and 19% for ULS and SLS, and resulted in 37% and 46% decrease for FLS, when two and four-lanes bridge geometry was considered, respectively.
- 4) The effect of girder spacing on the shear distribution factors of interior girders at ULS and SLS, and at FLS for both two and four-lanes bridge structure was considered insignificant.

5.2.7 Load Distribution Factors for Straight Bridges at ULS and SLS

Recently CHBDC (CSA 2014a) has specified simplified method of analysis to define the longitudinal bending moments and vertical shear in slab-on-girder bridges due to live load for ULS and SLS, and FLS using load distribution factors. The Simplified Method of Analysis specified in clause 5.6.4 of the current CHBDC allows a bridge to be treated as a beam for live load analysis. The CHBDC distribution factor equations for slab-on-girder bridges have already been explained in chapter-2.

From the results of the parametric study it became evident that the moment and shear distribution factor was governed by the following parameters: (i) skew angle, (ii) span length, (iii) girder spacing, (iv) number of girders, and (v) number of lanes. However, for straight bridge the effect of skew angle on the moment and shear distribution factors was considered irrelevant. In-order to estimate the correlation between the distribution factors calculated from the current CHBDC code in comparison with the factors from FEA analysis, a sensitivity study was performed with the purpose to evaluate a factor R to compare the CHBDC design equations with FEA results. The factor R is defined as follow:

$$R = \frac{F_{T_CHBDC}}{F_{T_FEA}} \quad (5.8)$$

For ULS and SLS, and FLS the results of factor R with respect to span and girder spacing for two and four-lanes bridge structures were evaluated. Only results of ULS and SLS are presented and discussed herein. Figure 5.40 and 5.41 represents the effect of the span length and girder spacing for an exterior girder moment, and the effect of these parameters in the case of interior girder's moment is shown in Figure 5.42 and 5.43. Similarly, for exterior and interior girder shear results are presented in Figure 5.44 and 5.45, and in Figure 5.46 and 5.47 respectively. The findings are briefly summarized as follows:

- 1) For exterior and interior girder moment in a two and four-lanes bridge configurations, CHBDC equations under-estimate the response when the span was 15 m. However for span greater than 15 m, the CHBDC resulted highly conservative response in comparison to the FEA. Further, it was noticed in Figure 5.41 and 5.43, that with the increase of girder spacing for two-lane and four-lane bridge configurations, it resulted in the increase of the distribution factor. The result showed that with the increase of girder numbers from 3 to 5 in case of two-lane, and 6 to 8 girders in case of 4-lane resulted in a reduction of the distribution factor.
- 2) For exterior and interior girder shear in a two and four-lane bridge configurations, the results of the CHBDC equations were conservative estimate of distribution factors in comparison to the FEA. Further, it was noticed from Figure 5.45 and 5.47, interior girder shear distribution factor were found to be sensitive with the bridge width i.e.

girder spacing (S) x number of girders (N). For two-lane bridge geometry, we observed a decrease of the distribution factor with the increase of the girder spacing. However for four-lane bridge geometry, the distribution factor increases with the increase of girder spacing.

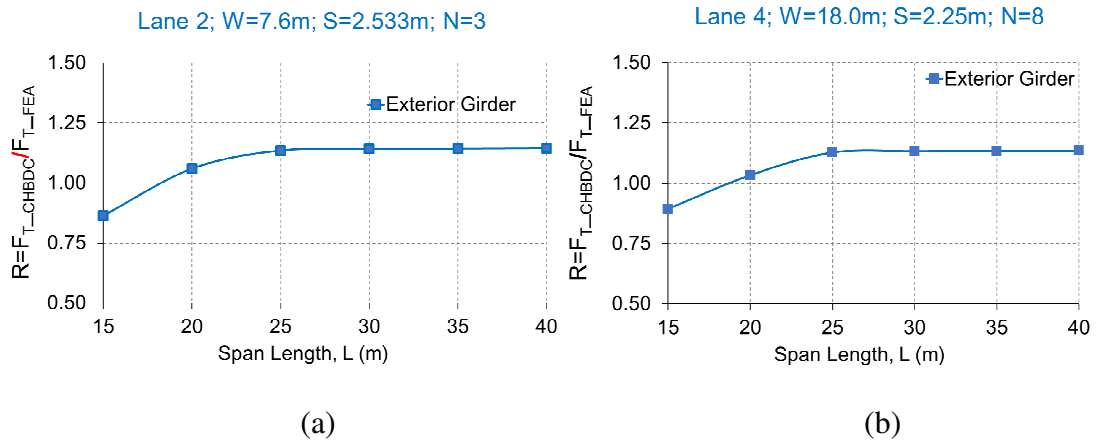


Figure 5.40 Effect of span length on “R” for an exterior girder moment at ULS and SLS for: (a) two-lane, and (b) four-lane

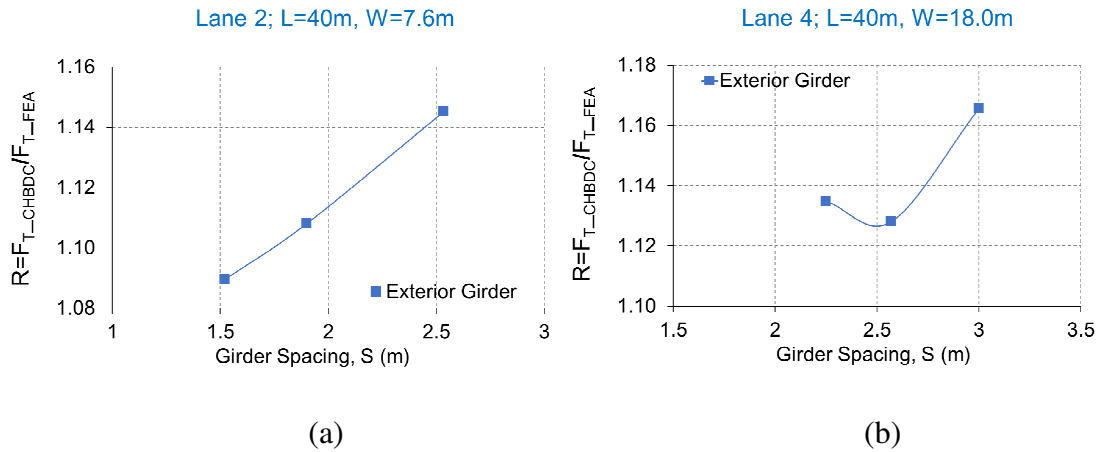


Figure 5.41 Effect of girder spacing on “R” for an exterior girder moment at ULS and SLS for: (a) two-lane, and (b) four-lane

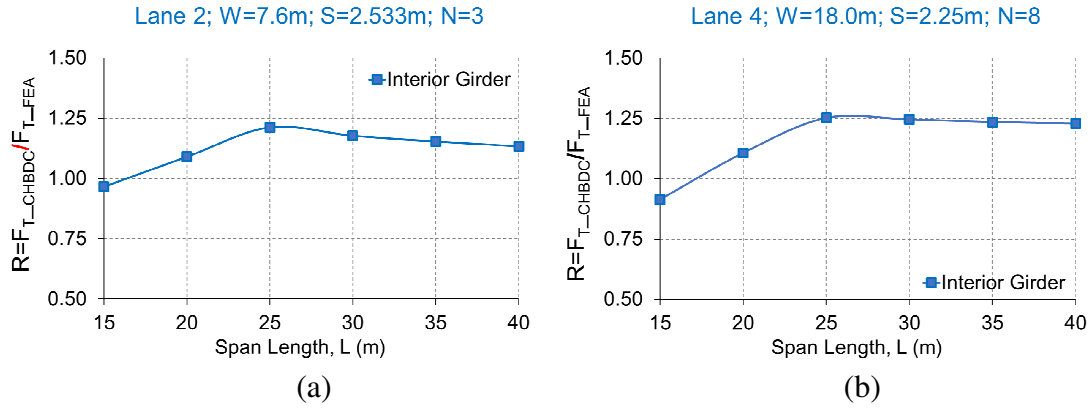


Figure 5.42 Effect of span length on “R” for an interior girder moment at ULS and SLS for: (a) two-lane, and (b) four-lane

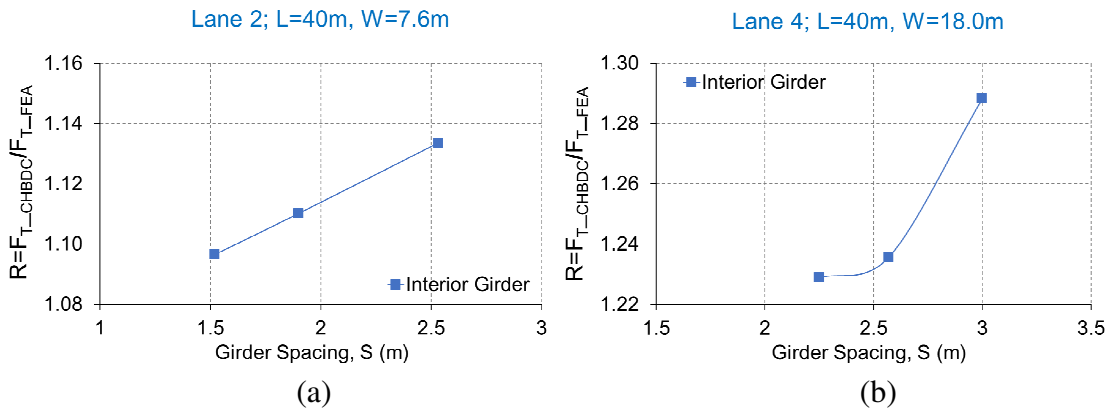


Figure 5.43 Effect of girder spacing on “R” for an interior girder moment at ULS and SLS for: (a) two-lane, and (b) four-lane

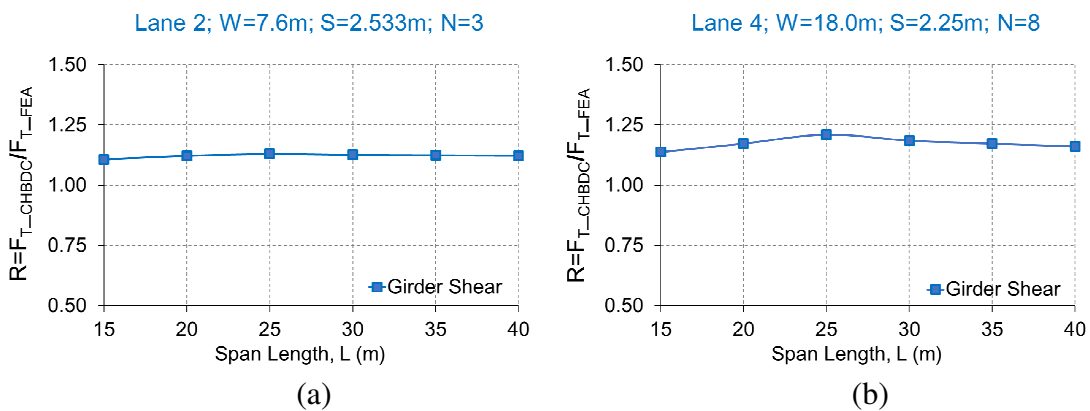


Figure 5.44 Effect of span length on “R” for an exterior girder shear at ULS and SLS for: (a) two-lane, and (b) four-lane

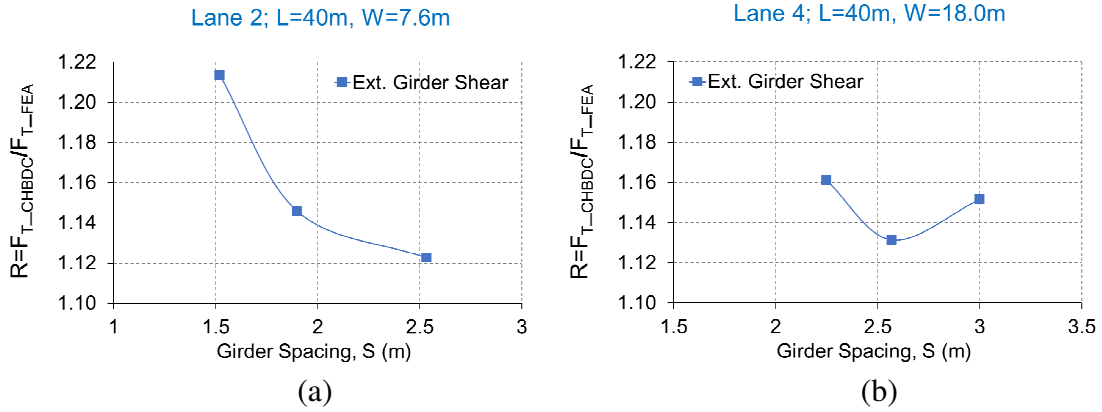


Figure 5.45 Effect of girder spacing on “R” for an exterior girder shear at ULS and SLS for: (a) two-lane, and (b) four-lane

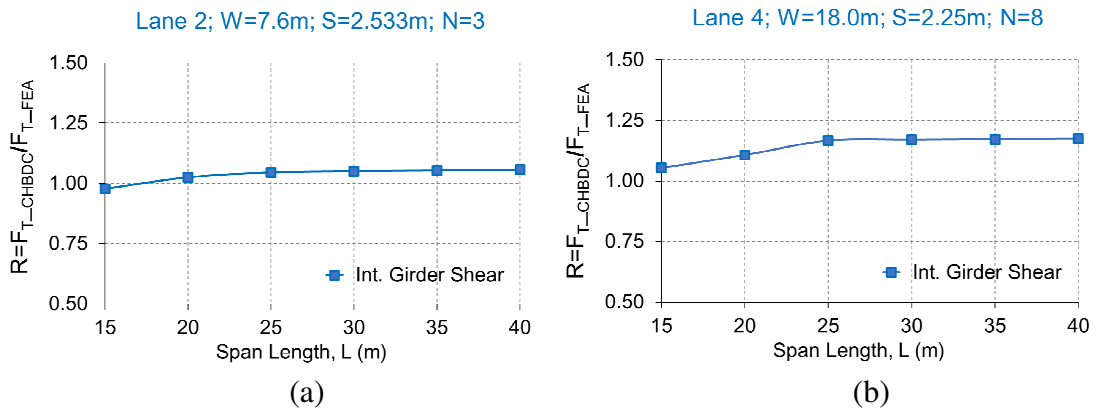


Figure 5.46 Effect of span length on “R” for an interior girder shear at ULS and SLS for: (a) two-lane, and (b) four-lane

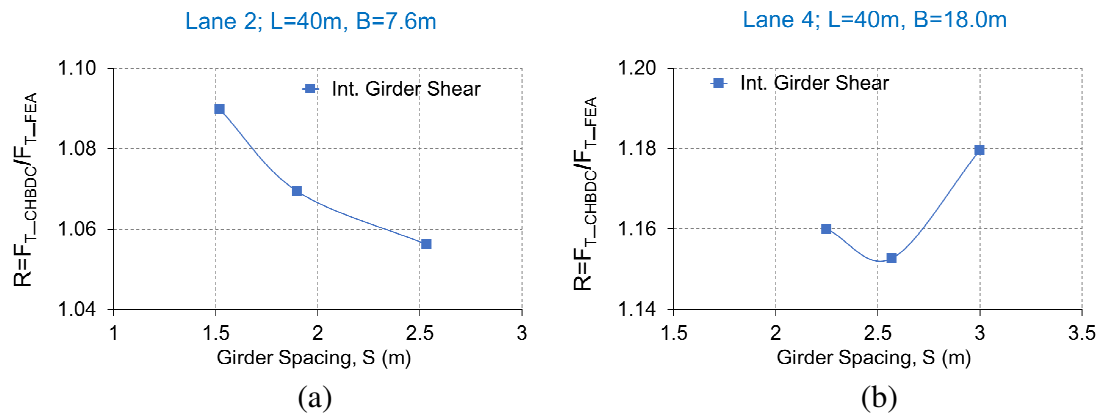


Figure 5.47 Effect of girder spacing on “R” for an interior girder shear at ULS and SLS for: (a) two-lane, and (b) four-lane

From the sensitivity study, it was evident that the CHBDC equations results were conservative estimates of the load effect. It was found that moment and shear distribution factors for a straight slab-on-girder bridge were mainly influenced by few critical parameters, namely: span length, girder spacing, number of girders and number of design lanes. In-order to keep uniformity and simplicity in understanding the distribution factors, it was decided to keep the format of equation same as proposed in the CHBDC code (CSA 2014a), and develop a new equations that replaces CHBDC equations, based on the parametric study results.

To develop new equations for the moment in the exterior and interior girder, three parameters D_T , γ_c and λ as mentioned in Table 5.3 of CHBDC (CSA 2014a) were modified. The general empirical equation of these parameters are written in following form:

$$\begin{aligned} D_T &= (a + bL^c) \times N^d \\ \gamma_c &= S^e \\ \lambda &= \left(f + \frac{g}{L} \right) \end{aligned} \quad (5.9)$$

However, for the shear at the exterior and interior girder location, only two parameters were modified and their empirical expressions are presented below:

$$\begin{aligned} D_T &= (a + bL^c) \times N^d \\ \gamma_c &= \left(\frac{S}{e} \right)^f \end{aligned} \quad (5.10)$$

where, a , b , c , d , e and f are correlation constants, L is the bridge span length in meters; S is the girder spacing in meters; and, N is the number of girders. Using regression analyses, sets of empirical equations for moment and shear distribution factor for the girders under live loading of a straight slab-on girder bridge were deduced and presented in Tables 5.3 to 5.6, respectively.

Table 5.3 Exterior girder moment distribution factors for straight bridge at ULS & SLS under live loading

n	Span (L), m	D_T	λ	γ_c
1	$15 \leq L \leq 40$	$(5.76 - 300L^{-1.89}) \times N^{-0.21}$	$\left(0.05 - \frac{0.10}{L}\right)$	$S^{-0.10}$
2		$(2.21 - 795L^{-2.63}) \times N^{0.27}$	$\left(0.04 - \frac{0.65}{L}\right)$	$S^{0.39}$
3		$(2.66 - 480L^{-2.48}) \times N^{0.13}$	$\left(0.10 - \frac{0.25}{L}\right)$	$S^{0.19}$
4		$(0.14 - 10L^{-2.0}) \times N^{1.27}$	$\left(-0.24 + \frac{1.55}{L}\right)$	$S^{1.31}$

γ_e same as given in Table 5.3 of CHBDC (CSA 2014a)

Table 5.4 Interior girder moment distribution factors for straight bridge at ULS & SLS ULS & SLS under live loading

n	Span (L), m	D_T	λ	γ_c
1	$15 \leq L \leq 40$	$(2.94 - 198L^{-2.0}) \times N^{0.14}$	$\left(0.05 - \frac{0.10}{L}\right)$	$S^{0.90}$
2	$L \leq 25$	$(2.89 - 69.47L^{-1.42}) \times N^{0.28}$	$\left(0.04 - \frac{0.31}{L}\right)$	$S^{0.48}$
	$25 < L \leq 40$	$(1.18 + 110L^{-2.50}) \times N^{0.56}$	$\left(0.07 - \frac{2.76}{L}\right)$	$S^{0.76}$
3 & 4	$L \leq 25$	$(-4.78 + 3.77L^{0.36}) \times N^{-0.25}$	$\left(0.18 - \frac{1.14}{L}\right)$	$S^{-0.10}$
	$25 < L \leq 40$	$(5.48 - 1.21L^{-0.11}) \times N^{-0.10}$	$\left(0.22 - \frac{1.50}{L}\right)$	$S^{0.10}$

γ_e same as given in Table 5.3 of CHBDC (CSA 2014a)

Table 5.5 Exterior girder shear distribution factors for straight bridge at ULS & SLS under live loading

n	Span (L), m	D_T	γ_c
1	$15 \leq L \leq 40$	$(3.68 + 1.68L^{-0.18}) \times N^{-0.11}$	$\left(\frac{S}{1.38}\right)^{-0.21}$
2		$(-0.07 + 3.08L^{0.04}) \times N^{0.10}$	$\left(\frac{S}{2.15}\right)^{0.10}$
3 & 4		$(1.60 + 3.13L^{-0.08}) \times N^{-0.03}$	$\left(\frac{S}{2.77}\right)^{-0.05}$
<i>λ & γ_e same as given in Table 5.3 of CHBDC (CSA 2014a)</i>			

Table 5.6 Interior girder shear distribution factors for straight bridge at ULS & SLS under live loading

n	Span (L), m	D_T	γ_c
1	$15 \leq L \leq 40$	$(0.337 + 0.23L^{0.17}) \times N^{0.18}$	$\left(\frac{S}{0.28}\right)^{0.85}$
2	$L \leq 20$	$(0.285 + 0.29L^{0.38}) \times N^{0.27}$	$\left(\frac{S}{0.28}\right)^{0.36}$
	$20 < L \leq 40$	$(0.54 + 0.47L^{0.09}) \times N^{0.30}$	$\left(\frac{S}{0.39}\right)^{0.42}$
3 & 4	$L \leq 25$	$(-3.274 + 5.28L^{0.11}) \times N^{-0.05}$	$\left(\frac{S}{1.06}\right)^{-0.02}$
	$25 < L \leq 40$	$(1.047 + 1.29L^{0.02}) \times N^{0.02}$	$\left(\frac{S}{0.04}\right)^{0.10}$
<i>λ & γ_e same as given in Table 5.3 of CHBDC (CSA 2014a)</i>			

5.2.7.1 Correlation of FEA Results and Proposed Equations with CHBDC

Based on the results obtained from the parametric study, a series of empirical expressions were developed for the girder moment and shear distribution factors for the prediction of the girder load distribution. Finally, the correlation between the CHBDC (CSA 2014a) equations and the proposed equations based on the parametric study for the moment and shear distribution factors were obtained and compared with the F_{T_m} and F_{T_v} values from the finite element analysis due to live loads, as presented in Figure 5.48 and 5.49, respectively. The result presented good correlation between the values obtained from proposed equations and those calculated results from FEA, and all data points fall within 5% over and under-estimation region, shown by dotted lines in Figure 5.48 and 5.49.

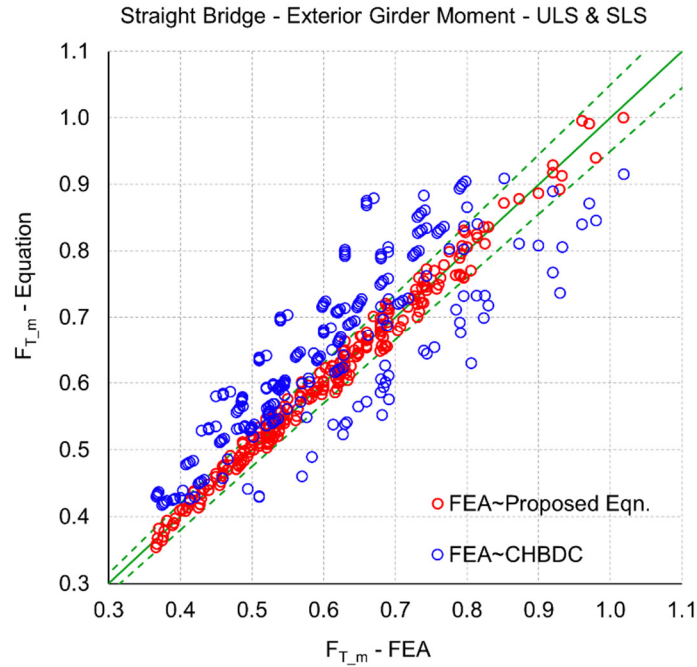
The illustrative example to calculate the moment and shear distribution factors using FEA, proposed equation and the CHBDC (CSA 2014a) for a straight slab-on steel I-girder bridges at ULS and SLS are described in Appendix B. The comparison of results for the moment and shear distribution factors evaluated using FEA, proposed equation and the CHBDC (CSA 2014a) equation are presented in Table 5.7 and 5.8, respectively. The result showed that the proposed equations were sufficiently accurate in predicting the response of a straight bridge behavior. The CHBDC design equations were found conservative for both moment and shear at the exterior and interior girder location. The main reasons for the inadequacy of the design equation to represent the actual behavior of a straight bridge at ULS and SLS are more likely the same as described earlier in section 4.4.7.

Table 5.7 Comparison of moment distribution factors for straight slab-on steel I-girder bridges at ULS and SLS

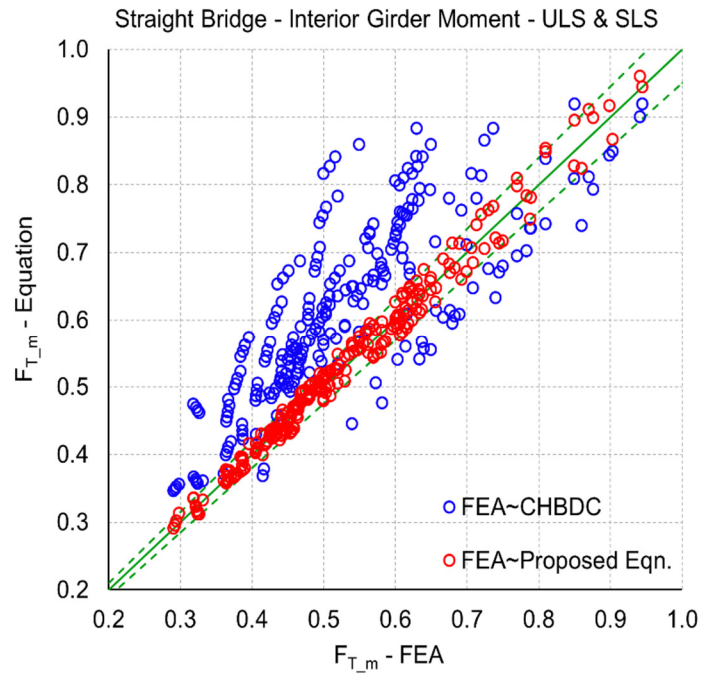
Location of girder	FEA results	Proposed equation	CHBDC (CSA 2014a)
Exterior	0.60	0.59	0.68
Interior	0.50	0.51	0.62

Table 5.8 Comparison of shear distribution factors for straight slab-on steel I-girder bridges at ULS and SLS

Location of girder	FEA results	Proposed equation	CHBDC (CSA 2014a)
Exterior	0.67	0.69	0.76
Interior	0.66	0.67	0.76

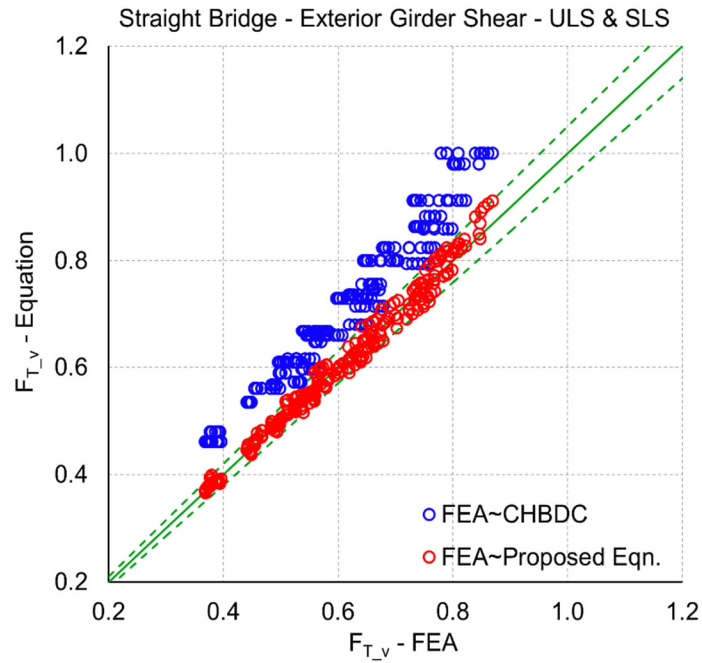


(a)

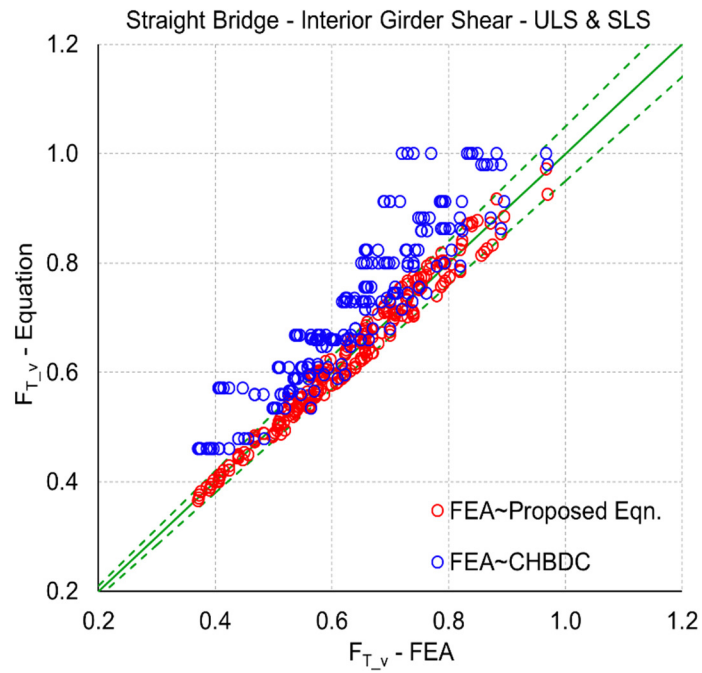


(b)

Figure 5.48 Correlation between moment distribution factors at ULS & SLS obtained from FEA results with proposed equations and CHBDC for straight slab-on-girder bridges for; (a) exterior girder, and (b) interior girder



(a)



(b)

Figure 5.49 Correlation between shear distribution factors at ULS & SLS obtained from FEA results with proposed equations and CHBDC for straight slab-on-girder bridges for; (a) exterior girder, and (b) interior girder

5.2.8 Load Distribution Factors for Straight Bridges at FLS

For FLS, the traffic load includes one CL-W truck that causes maximum effects increased by the dynamic load allowance and placed at the center of one travelled lane, and lane loads are not considered. The parametric study showed that moment and shear distribution factors for a straight slab-on-girder bridge were mainly influenced by few critical parameters, namely: span length, girder spacing, number of girders and number of design lanes. Also, the results of a sensitivity study demonstrates that the CHBDC equations resulted in conservative estimates. So, in-order to keep uniformity and simplicity in developing distribution factors for bridge designers and engineers, it was decided to keep the format of equation same as proposed in the CHBDC code (CSA 2014a), and develop a new equation that replaces CHBDC equations, based on the parametric study results.

To develop new equations for the moment in the exterior and interior girder, three parameters D_T , γ_c and λ mentioned in Table 5.3 of CHBDC (CSA 2014a) were modified for exterior girder, whereas only two parameters, D_T and γ_c were reformed to represent the behavior of interior girder moment. Hence, the general empirical equation of these parameters took the following form, respectively:

For exterior girder:

$$\begin{aligned} D_T &= (a + bL^c) \times N^d \\ \gamma_c &= S^e \\ \lambda &= \left(f + \frac{g}{L} \right) \end{aligned} \quad (5.11)$$

For interior girder:

$$\begin{aligned} D_T &= (a + bL^c) \times N^d \\ \gamma_c &= S^e \times \left(f + \frac{g}{L} \right) \end{aligned} \quad (5.12)$$

Also, for the shear at the exterior and interior girder location at FLS, only two parameters were modified and their empirical expressions are presented below:

$$D_r = (a + bL^c) \times N^d$$

$$\gamma_c = e \times S^f$$
(5.13)

where, a , b , c , d , e and f are equation variables, L is the bridge span length in meters; S is the girder spacing in meters; and, N is the number of girders. Using regression analyses, sets of empirical equations for moment and shear distribution factor for the girders under live loading of a straight slab-on girder bridge were deduced and presented in Tables 5.9 to 5.12, respectively.

Table 5.9 Exterior girder moment distribution factors for straight bridge at FLS under live loading

n	Bridge width (W), m	Span (L), m	D_r	λ	γ_c	γ_e^{*+}
1	All	$15 \leq L \leq 40$	$(0.83 - 250L^{-2.63}) \times N^{1.18}$	0.05*	$S^{1.10}$	Table 5.7 of CHBDC
2	$W \leq 10$ $W > 10$		$(5.62 - 192.22L^{-1.71}) \times N^{-0.12}$ $(0.144 - 0.15L^{-0.08}) \times N^{2.06}$	0.05* 0.05*	$S^{-0.05}$ $S^{1.88}$	
3	All		$(37.42 - 500L^{-1.30}) \times N^{-0.80}$	$(-0.56 + \frac{4.22}{L})$	$S^{-0.74}$	
4	All		$(-29.08 + 26.44L^{0.13}) \times N^{-0.40}$	$(0.27 + \frac{9.59}{L})$	$S^{-0.38}$	

* Same as given in Table-5.3 of CHBDC (CSA 2014a)
+ When the value of $Dve > 3.0$ m, it shall be taken as 3.0 m for the purpose of this clause to calculate γ_e

Table 5.10 Interior girder moment distribution factors for straight bridge at FLS under live loading

n	Bridge width (W), m	Span (L), m	D_T	γ_c
1	All	$15 \leq L \leq 40$	$(5.40 - 82.4L^{-1.26}) \times N^{0.73}$	$S^{0.96} \times \left(0.26 + \frac{2.01}{L}\right)$
2	$W \leq 10$		$(-0.16 + 1.98L^{-0.25}) \times N^{0.05}$	$S^{0.80} \times \left(7.39 - \frac{68.85}{L}\right)$
2	$W > 10$		$(-0.302 + 4.06L^{-0.28}) \times N^{0.66}$	$S^{0.90} \times \left(1.56 - \frac{16.13}{L}\right)$
3	All		$(-4.72 + 7.56L^{-0.07}) \times N^{0.06}$	$S^{0.80} \times \left(4.0 - \frac{37.80}{L}\right)$
4	All		$(0.393 + 3.16L^{-0.23}) \times N^{0.12}$	$S^{0.61} \times \left(2.68 - \frac{23.54}{L}\right)$

λ & γ_e same as given in Table 5.3 of CHBDC (CSA 2014a)

Table 5.11 Exterior girder shear distribution factors for straight bridge at FLS under live loading

n	Bridge width (W), m	Span (L), m	D_T	γ_c^+
1	All	$15 \leq L \leq 40$	$(-0.40 + 0.95L^{-0.06}) \times N^{1.99}$	$0.827S^{1.44}$
2	$W \leq 10$		$(0.152 + 0.14L^{-0.33}) \times N^{2.33}$	$0.227S^{2.05}$
	$W > 10$		$(-0.746 + 0.94L^{-0.04}) \times N^{2.63}$	$0.334S^{2.22}$
3	All		$(-0.152 + 0.30L^{-0.01}) \times N^{3.14}$	$0.02S^{2.90}$
4	$W \leq 16.2$		$(-0.046 + 0.10L^{0.01}) \times N^{2.60}$	$0.085S^{2.43}$
	$W > 16.2$		$(0.08 + 1.82L^{-1.28}) \times N^{2.73}$	$0.074S^{2.02}$

λ & γ_e same as given in Table 5.3 of CHBDC (CSA 2014a)

+ γ_c is applicable to all girder spacing i.e. $S < 2.0m$ & $S \geq 2.0m$

Table 5.12 Interior girder shear distribution factors for straight bridge at FLS under live loading

n	Bridge width (W), m	Span (L), m	D_T	γ_c^+
1	All	$15 \leq L \leq 40$	$(-0.33 + 1.70L^{0.11}) \times N^{0.49}$	$0.84S^{0.45}$
2	$W \leq 10$		$(0.837 - 16.75L^{-1.76}) \times N^{-0.74}$	$14.325S^{0.26}$
	$W > 10$		$(0.029 - 4.72L^{-2.50}) \times N^{0.37}$	$69.565S^{0.47}$
3	All		$(0.831 - 16.62L^{-1.68}) \times N^{-0.70}$	$16.456S^{0.30}$
4	All		$(1.656 - 35.95L^{-1.73}) \times N^{-0.48}$	$8.527S^{0.01}$

λ & γ_e same as given in Table 5.3 of CHBDC (CSA 2014a)
+ γ_c is applicable to all girder spacing i.e. $S < 2.0m$ & $S \geq 2.0m$

5.2.8.1 Correlation of FEA Results and Proposed Equations with CHBDC

The correlation between the CHBDC (CSA 2014a) equations and the proposed equations based on the parametric study for the moment and shear distribution factors at FLS were obtained and compared with the F_{T_m} and F_{T_v} values from the finite element analysis due to live loads, and presented in Figure 5.50 and 5.51, respectively. The correlation presents good correlation between the values obtained from proposed equations and those calculated results from FEA, and all data points fall within 5% over and under-estimation region, shown by dotted lines in Figure 5.50 and 5.51.

The illustrative example to calculate the moment and shear distribution factors using FEA, proposed equation and the CHBDC (CSA 2014a) for a straight slab-on steel I-girder bridges at FLS are described in Appendix C. The comparison of results for the moment and shear distribution factors evaluated using FEA, proposed equation and the CHBDC (CSA 2014a) equation are presented in Table 5.13 and 5.14, respectively. The result showed that the proposed equations were sufficiently accurate in predicting the response of a straight bridge behavior at FLS. The CHBDC design equations were found highly conservative for both moment and shear at the exterior and interior girder location. The

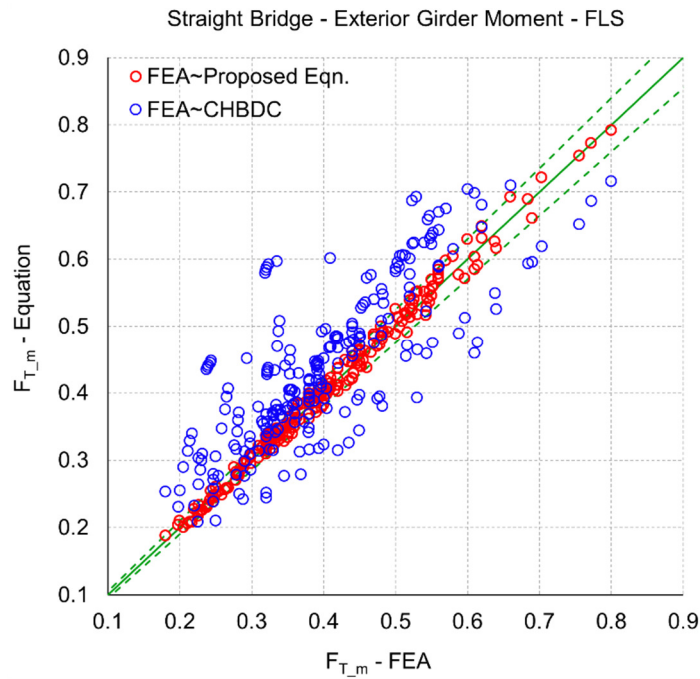
main reasons for the inadequacy of the design equation to represent the actual behavior of a straight bridge at FLS are more likely the same as described earlier in section 4.4.7.

Table 5.13 Comparison of moment distribution factors for straight slab-on steel I-girder bridges at FLS

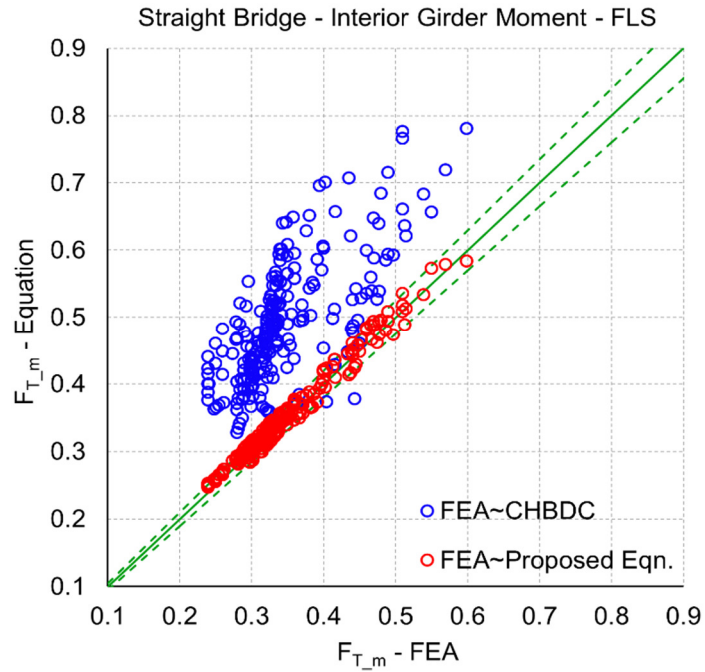
Location of girder	FEA results	Proposed equation	CHBDC (CSA 2014a)
Exterior	0.32	0.33	0.37
Interior	0.30	0.31	0.43

Table 5.14 Comparison of shear distribution factors for straight slab-on steel I-girder bridges at FLS

Location of girder	FEA results	Proposed equation	CHBDC (CSA 2014a)
Exterior	0.27	0.26	0.71
Interior	0.47	0.47	0.71

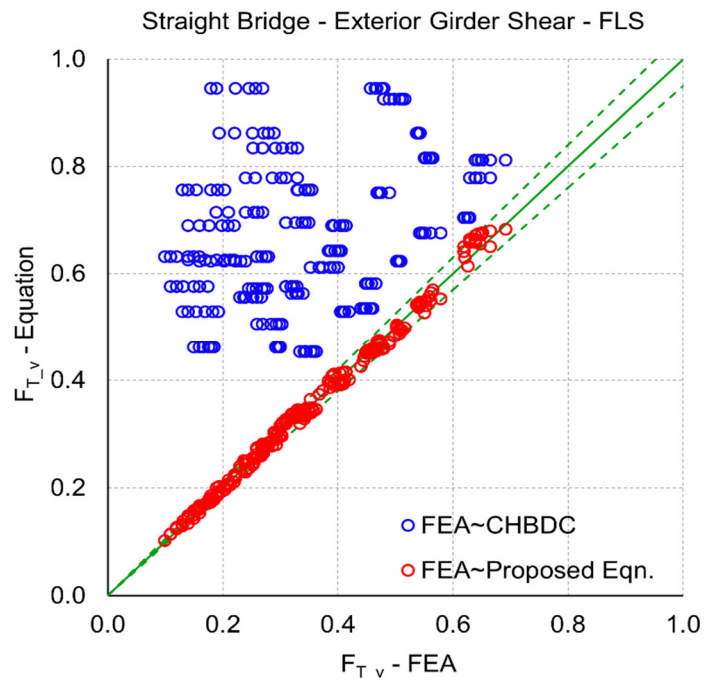


(a)

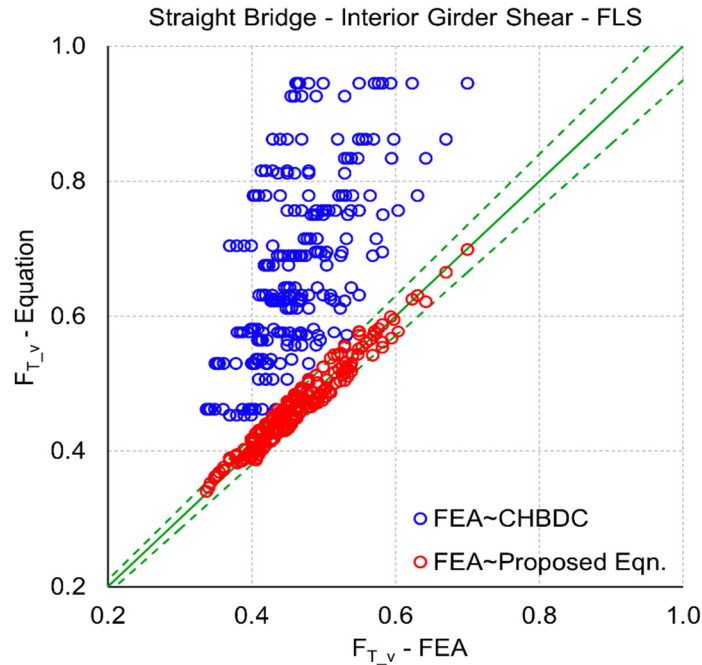


(b)

Figure 5.50 Correlation between moment distribution factors at FLS obtained from FEA results with proposed equations and CHBDC for straight slab-on-girder bridges for; (a) exterior girder, and (b) interior girder



(a)



(b)

Figure 5.51 Correlation between shear distribution factors at FLS obtained from FEA results with proposed equations and CHBDC for straight slab-on-girder bridges for; (a) exterior girder, and (b) interior girder

5.2.9 Load Distribution Factors for Skewed Bridges at ULS and SLS

Skew greatly complicates the behavior of straight slab-on steel I-girder bridges by introducing alternate load paths and causing complex interaction between the main girders and secondary framing members that can lead to significant construction and design problems (Coletti et al. 2011). In skewed bridges, under the influence of live loads longitudinal girders undergo torsional rotation at the supports (Surana and Humar 1984). These rotations are larger at the obtuse corners and they are difficult to predict due to the uneven distribution of loads across the superstructure that increase the skew effects (Choo et al. 2005). As the skew angle increases, the shear and reaction at the obtuse girder corner increases, however for the acute angle a reduction in the shear and reaction can be observed (Fisher 2006, Ozgur et al. 2011, Krupicka and Poellot 1993).

According to clause 5.6.1 of CHBDC (CSA 2014b), in order to take in to account the limitations used in the previous editions of the CHBDC (CSA 2006a) to determine if the

skew effects can be ignored in the analysis or not is inappropriate. Recently, in the current CHBDC (CSA 2014a), the main improvement to the simplified method of bridge analysis is the consideration of skewed slab-on-girder bridge geometries for live load. Based on the parametric study analysis of more than 13,000 skewed slab-on-girder bridges, Theoret and Massicotte (2011) introduced a new parameter F_s to modify the values of F_T to account for skew effects for shear at the obtuse corner. Bridges with skewed geometries up to 45° can now be analyzed with the simplified method. These studies indicates that for slab-on-girder bridges, the main governing parameters to characterize skew effects are: (1) skew angle, (2) span length, and (3) girder spacing. According to clause 5.6.6.2 of CHBDC (CSA 2014a), the shear forces at the girder obtuse corner may be magnified by the skew factor F_s calculated as follows:

$$F_s = 1.2 - \frac{2.0}{(\varepsilon + 10)} \quad (5.14)$$

where,

$$\varepsilon = \left(\frac{L}{S} \right) \tan \psi; \quad \text{for } \psi \leq 45^\circ \quad (5.15)$$

It is stated in the commentary of clause 5.6.6.2 (CSA 2014b) that for the sake of simplicity, the same equation as for dead load (clause 5.6.3) is retained for live load (clause 5.6.6.2). Further, it is stated that the factor F_s is to be applied to all the girders considering that it is a general practice to have the same girder dimensions for the interior and exterior girders.

Based on the current parametric study analysis, it was concluded that it was not only the shear at the obtuse girder corner that was affected with the increase of skew angle but it resulted in the reduction of the shear force at the acute corner and also an increases of shear force at the interior girder was noticed between 30° to 60° skew angle. Further, a reduction in the exterior and interior girder moment distribution factors were noticed with the increase of skew angle. However, no such equation for the moment distribution factor is yet to be proposed in North American highway bridge codes (CSA 2014a, AASHTO-LRFD 2014). Based on the data generated from the parametric study, it was found that

moment and shear distribution factors were mainly influenced by few critical parameters, namely: skew angle, span length, girder spacing, number of girders and number of design lanes. In-order to keep uniformity and simplicity in understanding the distribution factors for bridge designers and engineers, it was decided to preserve the format of equation (5.14) and developed a new equation for the factor “ ε ” that replaces equation (5.15), based on the parametric study results. Hence, the general empirical equation for the moment and shear, the “ ε ” factor is represented as follows:

$$\varepsilon = a \times L^b \times S^c \times N^d \times n^e \times \tan \psi \quad (5.16)$$

where, a, b, c, d and e are correlation constants, L is the bridge span length in meters; S is the girder spacing in meters; N is the number of girders, and n is the number of design lanes. Using regression analyses, a set of empirical equations for the moment and shear distribution factors for the girders under live loading of a skewed slab-on girder bridge were deduced and presented in Table 5.15 and 5.16 for exterior and interior girder moment distribution factor, and Table 5.17, 5.18 and 5.19 for shear distribution factors at girder obtuse, acute and interior corners, respectively.

Table 5.15 Exterior girder moment distribution factors for skewed bridge at ULS & SLS under live load

n	Span (L), m	Skew angle (ψ), deg.	F _s	ε
1 to 4	15 ≤ L ≤ 40	0 < ψ ≤ 30	1.2 - $\frac{2.0}{(\varepsilon + 10)}$ *	$3.06 \times L^{-0.85} \times S^{1.09} \times N^{-0.31} \times n^{0.46} \times \tan \psi$
		30 < ψ ≤ 40		$-11.0 \times L^{-0.02} \times S^{-1.19} \times N^{-1.24} \times n^{1.30} \times \tan \psi$
		40 < ψ ≤ 50		$-29.0 \times L^{-0.04} \times S^{-2.38} \times N^{-1.46} \times n^{1.64} \times \tan \psi$
	15 ≤ L ≤ 25	50 < ψ ≤ 60	$-39.66 \times L^{-0.36} \times S^{-1.19} \times N^{-1.13} \times n^{0.66} \times \tan \psi$	
	25 < L ≤ 40			$-1.97 \times L^{0.03} \times S^{-0.34} \times N^{-0.42} \times n^{0.70} \times \tan \psi$

* Same as given in CHBDC clause 5.6.6.2 (CSA 2014a).

Table 5.16 Interior girder moment distribution factors for skewed bridge at ULS & SLS under live load

n	Span (L), m	Skew angle (ψ), deg.	Fs	ε
1 to 4	$15 \leq L \leq 40$	$0 < \psi \leq 30$	$1.2 - \frac{2.0}{(\varepsilon + 10)}$ *	$-0.40 \times L^{-0.52} \times S^{-0.75} \times N^{2.45} \times n^{-1.60} \times \tan \psi$
		$30 < \psi \leq 40$		$-13.90 \times L^{-1.03} \times S^{0.31} \times N^{0.34} \times n^{0.28} \times \tan \psi$
		$40 < \psi \leq 50$		$-30.0 \times L^{-1.29} \times S^{0.29} \times N^{0.25} \times n^{0.37} \times \tan \psi$
		$50 < \psi \leq 60$		$-1.94 \times L^{-0.18} \times S^{0.50} \times N^{0.40} \times n^{-0.19} \times \tan \psi$
	$15 \leq L \leq 20$			
	$20 < L \leq 40$			$-1.54 \times L^{-0.51} \times S^{1.25} \times N^{0.66} \times n^{-0.13} \times \tan \psi$

* Same as given in CHBDC clause 5.6.6.2 (CSA 2014a).

Table 5.17 Shear distribution factors at girder obtuse corner for skewed bridge at ULS and SLS under live load

n	Span (L), m	Skew angle (ψ), deg.	Fs	ε
1 to 4	$15 \leq L \leq 40$	$0 < \psi \leq 20$	$1.2 - \frac{2.0}{(\varepsilon + 10)}$ *	$0.78 \times L^{0.95} \times S^{-3.18} \times N^{0.23} \times n^{0.02} \times \tan \psi$
		$20 < \psi \leq 30$	$1.115 - \frac{0.20}{(\varepsilon + 0.35)}$	$2.72 \times L^{0.84} \times S^{-2.26} \times N^{-0.18} \times n^{0.13} \times \tan \psi$
		$30 < \psi \leq 40$	$1.412 - \frac{0.80}{(\varepsilon + 1.31)}$	$1.12 \times L^{0.37} \times S^{-1.56} \times N^{-0.02} \times n^{0.39} \times \tan \psi$
	$15 \leq L \leq 20$	$40 < \psi \leq 60$	$1.323 - \frac{1.68}{(\varepsilon + 3.0)}$	$0.50 \times L^{1.28} \times S^{-2.66} \times N^{0.05} \times n^{0.35} \times \tan \psi$
	$20 < L \leq 40$		$1.928 - \frac{0.66}{(\varepsilon + 0.69)}$	$0.02 \times L^{0.71} \times S^{-1.75} \times N^{0.53} \times n^{0.17} \times \tan \psi$

* Same as given in CHBDC clause 5.6.6.2 (CSA 2014a).

Table 5.18 Shear distribution factors at girder acute corner for skewed bridge at ULS and SLS under live load

n	Span (L), m	Skew angle (ψ), deg.	Fs	ε
1 to 4	$15 \leq L \leq 40$	$0 < \psi \leq 20$	$1.2 - \frac{2.0}{(\varepsilon + 10)}$ *	$-18.98 \times L^{-0.25} \times S^{-0.22} \times N^{-0.08} \times n^{0.10} \times \tan \psi$
		$20 < \psi \leq 30$		$-9.28 \times L^{-0.17} \times S^{-0.03} \times N^{0.05} \times n^{0.04} \times \tan \psi$
		$30 < \psi \leq 40$		$-5.0 \times L^{-0.03} \times S^{-0.035} \times N^{0.04} \times n^{0.03} \times \tan \psi$
		$40 < \psi \leq 50$		$-3.65 \times L^{-0.044} \times S^{0.04} \times N^{0.08} \times n^{-0.04} \times \tan \psi$
		$50 < \psi \leq 60$		$-2.15 \times L^{0.01} \times S^{-0.12} \times N^{0.13} \times n^{0.09} \times \tan \psi$

* Same as given in CHBDC clause 5.6.6.2 (CSA 2014a).

Table 5.19 Shear distribution factors at interior girder for skewed bridge at ULS and SLS under live load

n	Span (L), m	Skew angle (ψ), deg.	Fs	ε
1 to 4	$15 \leq L \leq 40$	$0 < \psi \leq 20$	$1.2 - \frac{2.0}{(\varepsilon + 10)}$ *	$0.10 \times L^{2.13} \times S^{-0.09} \times N^{-2.41} \times n^{-3.0} \times \tan \psi$
		$20 < \psi \leq 30$		$0.20 \times L^{1.93} \times S^{-1.74} \times N^{-0.68} \times n^{-5.0} \times \tan \psi$
		$30 < \psi \leq 40$		$0.45 \times L^{2.73} \times S^{0.98} \times N^{-4.17} \times n^{-3.66} \times \tan \psi$
		$40 < \psi \leq 50$		$0.10 \times L^{4.29} \times S^{-0.14} \times N^{-6.90} \times n^{-4.43} \times \tan \psi$
		$50 < \psi \leq 60$		$0.10 \times L^{3.50} \times S^{-0.12} \times N^{-4.84} \times n^{-10.42} \times \tan \psi$

* Same as given in CHBDC clause 5.6.6.2 (CSA 2014a).

5.2.9.1 Correlation of FEA Results and Proposed Equations with CHBDC

The correlation between the CHBDC (CSA 2014a) equations and the proposed equations based on the parametric study for the moment and shear distribution factors for skewed slab-on-girder bridges at ULS and SLS were obtained and compared with the load distribution factors (LDF) from the finite element analysis due to live loads, and presented in Figure 5.52 and 5.53, respectively. First of all the moment and the shear distribution factor for a straight bridge was calculated, and subsequently in order to account the skew

effects a parameter F_s was evaluated and multiplied with the respective moment and shear distribution factors of a straight bridge (F_T). Finally the results showed good correlation between the values obtained from proposed equations and those calculated results from FEA, and all data points fall within 5% over and under-estimation region, shown by dotted lines in Figure 5.52 and 5.53.

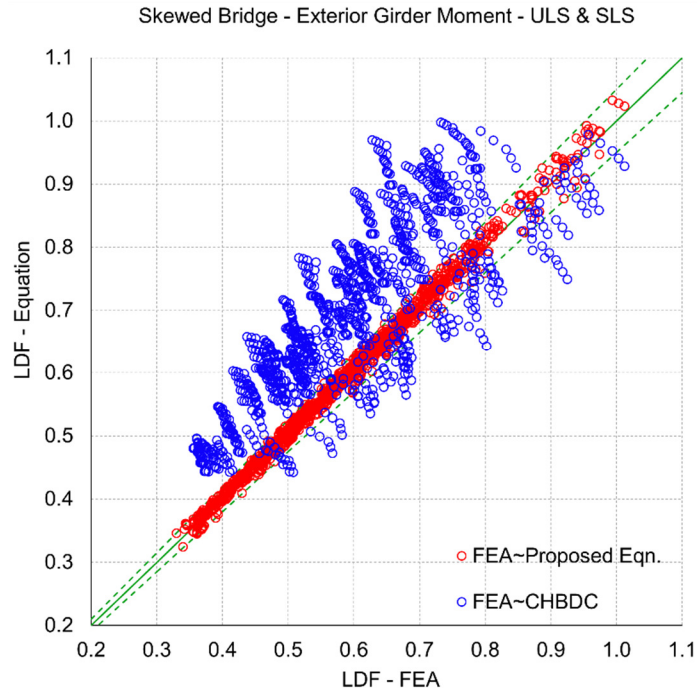
The illustrative example to calculate the moment and shear distribution factors using FEA, proposed equation and the CHBDC (CSA 2014a) for a skewed slab-on steel I-girder bridges at ULS and SLS are described in Appendix D. The comparison of results for the moment and shear distribution factors evaluated using FEA, proposed equation and the CHBDC (CSA 2014a) equation are presented in Table 5.20 and 5.21, respectively. The result showed that the proposed equations were sufficiently accurate in predicting the response of a skewed bridge behavior at ULS and SLS. The CHBDC design equations were found highly conservative for both moment and shear at the exterior and interior girder location. The main reasons for the inadequacy of the design equation to represent the actual behavior of a skewed bridge at ULS and SLS are more likely the same as described earlier in section 4.4.7.

Table 5.20 Comparison of moment distribution factors for skewed slab-on steel I-girder bridges at ULS and SLS

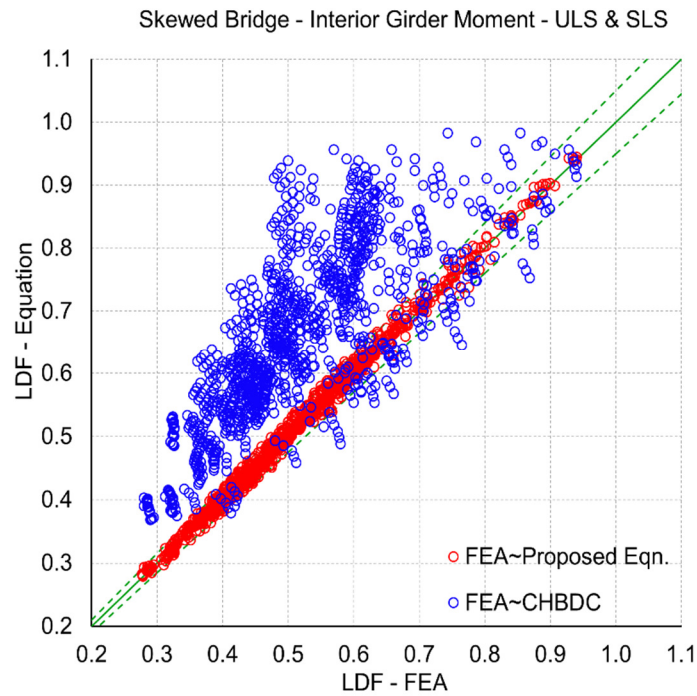
Location of girder	FEA results	Proposed equation	CHBDC (CSA 2014a)
Exterior	0.58	0.57	0.75
Interior	0.48	0.49	0.68

Table 5.21 Comparison of shear distribution factors for skewed slab-on steel I-girder bridges at ULS and SLS

Location of girder	FEA results	Proposed equation	CHBDC (CSA 2014a)
Obtuse corner	0.73	0.76	0.84
Acute corner	0.59	0.59	0.84
Interior girder	0.67	0.67	0.84

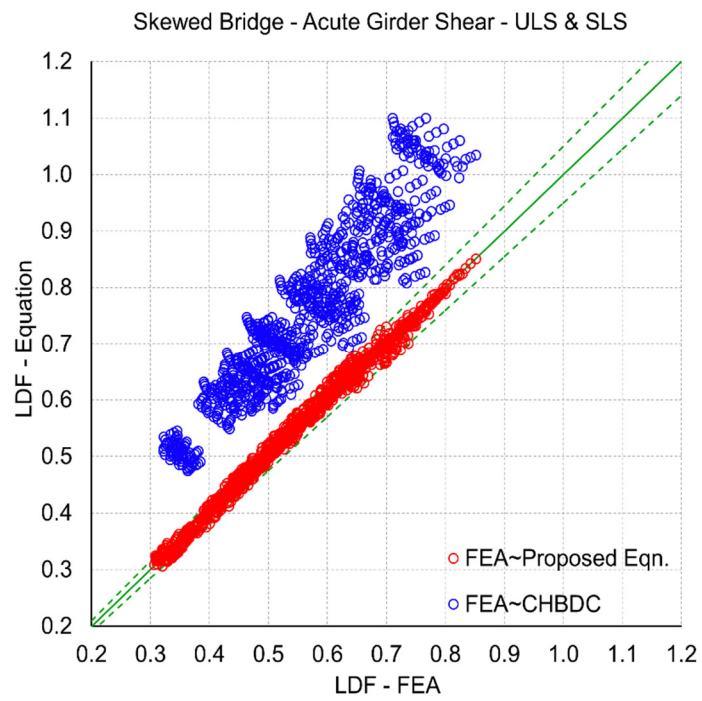
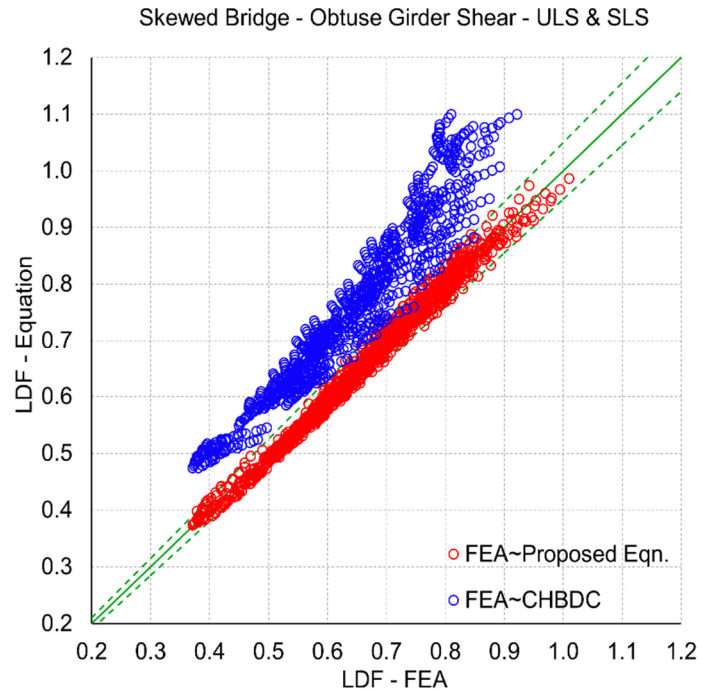


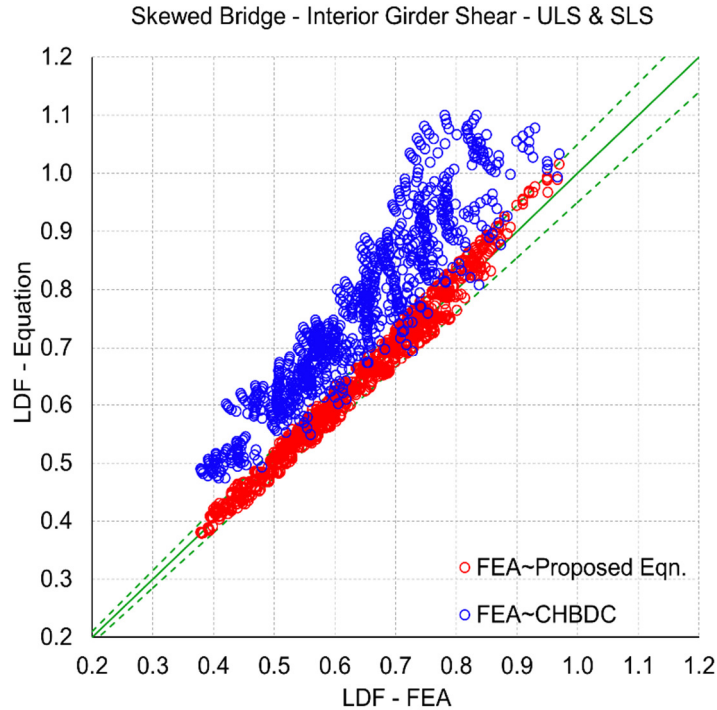
(a)



(b)

Figure 5.52 Correlation between moment distribution factors at ULS & SLS obtained from FEA results with proposed equations and CHBDC for skewed slab-on-girder bridges for; (a) exterior girder, and (b) interior girder





(c)

Figure 5.53 Correlation between shear distribution factors at ULS & SLS obtained from FEA results with proposed equations and CHBDC for skewed slab-on-girder bridges for girders at; (a) obtuse corner, (b) acute corner, and (c) interior

5.2.10 Load Distribution Factors for Skewed Bridges at FLS

Simplified method of analysis at the FLS was treated in a similar fashion to that of ULS and SLS with the exception that only one vehicle was placed on the bridge for the computation of the force effects. Consequently, load distribution factors calculated at FLS were found larger than at ULS and SLS due to lack of uniformity in moment and shear distribution transversely across the bridge. (CSA 2006b, clause 5.7.1.2.2).

Based on the data generated from the parametric study, it was found that moment and shear distribution factors were mainly influenced by few critical parameters, namely: skew angle, span length, girder spacing, number of girders and number of design lanes. In-order to keep uniformity and simplicity in understanding the distribution factors for bridge designers and engineers, it was decided to preserve the format of equation (5.14) and develop a new equation for the factor “ ϵ ” that replaces equation (5.15), based on the parametric study

results. Hence, the empirical equation for the moment and shear at FLS was kept the same as presented in equation (5.16) for ULS and SLS. Subsequently, by using regression analyses a set of empirical equations for the moment and shear distribution factor for the skewed slab-on-girder bridge at FLS were developed and presented in Table 5.22 and 5.23 for exterior and interior girder moment distribution factor, and Table 5.24, 5.25 and 5.26 for shear distribution factors at girder obtuse, acute and interior corners, respectively.

Table 5.22 Exterior girder moment distribution factors for skewed bridge at FLS under live load

N	Span (L), m	Skew angle (ψ), deg.	Fs	ϵ
1 to 4	$15 \leq L \leq 40$	$0 < \psi \leq 30$	$1.2 - \frac{2.0}{(\epsilon + 10)}$ *	$-0.10 \times L^{-0.07} \times S^{1.83} \times N^{1.91} \times n^{-1.52} \times \tan \psi$
		$30 < \psi \leq 50$		$-0.28 \times L^{-0.64} \times S^{2.05} \times N^{2.39} \times n^{-1.58} \times \tan \psi$
	$15 \leq L \leq 20$	$50 < \psi \leq 60$	$-0.22 \times L^{-0.93} \times S^{2.55} \times N^{2.60} \times n^{-1.91} \times \tan \psi$	
	$20 < L \leq 40$	$50 < \psi \leq 60$	$-0.286 \times L^{-0.52} \times S^{1.48} \times N^{2.10} \times n^{-1.16} \times \tan \psi$	

* Same as given in CHBDC clause 5.6.6.2 (CSA 2014a).

Table 5.23 Interior girder moment distribution factors for skewed bridge at FLS under live load

n	Span (L), m	Skew angle (ψ), deg.	Fs	ϵ
1 to 4	$15 \leq L \leq 40$	$0 < \psi \leq 30$	$1.2 - \frac{2.0}{(\epsilon + 10)}$ *	$-0.046 \times L^{0.16} \times S^{1.21} \times N^{1.82} \times n^{-0.67} \times \tan \psi$
		$30 < \psi \leq 40$		$-0.08 \times L^{0.36} \times S^{0.61} \times N^{1.48} \times n^{-0.96} \times \tan \psi$
		$40 < \psi \leq 50$		$-0.12 \times L^{0.41} \times S^{0.75} \times N^{0.40} \times n^{0.18} \times \tan \psi$
	$15 \leq L \leq 20$	$50 < \psi \leq 60$	$-1.19 \times L^{0.24} \times S^{0.17} \times N^{-0.25} \times n^{0.29} \times \tan \psi$	
$20 < L \leq 40$	$50 < \psi \leq 60$	$-1.11 \times L^{-0.57} \times S^{1.74} \times N^{0.60} \times n^{-0.22} \times \tan \psi$		

* Same as given in CHBDC clause 5.6.6.2 (CSA 2014a).

Table 5.24 Shear distribution factors at girder obtuse corner for skewed bridge at FLS under live load

n	Span (L), m	Skew angle (ψ), deg.	F _s	ϵ
1 to 4	$15 \leq L \leq 40$	$0 < \psi \leq 20$	$1.2 - \frac{2.0}{(\epsilon + 10)}^*$	$36.43 \times L^{-0.31} \times S^{-0.71} \times N^{0.23} \times n^{-0.26} \times \tan \psi$
		$20 < \psi \leq 30$		$0.36 \times L^{-0.02} \times S^{0.08} \times N^{3.31} \times n^{-1.83} \times \tan \psi$
		$30 < \psi \leq 40$		$0.30 \times L^{0.60} \times S^{-0.59} \times N^{4.64} \times n^{-2.66} \times \tan \psi$
		$40 < \psi \leq 50$		$5.20 \times L^{1.04} \times S^{0.46} \times N^{1.42} \times n^{-1.34} \times \tan \psi$
		$50 < \psi \leq 60$		$0.10 \times L^{0.01} \times S^{0.25} \times N^{8.54} \times n^{-7.16} \times \tan \psi$

* Same as given in CHBDC clause 5.6.6.2 (CSA 2014a).

Table 5.25 Shear distribution factors at girder acute corner for skewed bridge at FLS under live load

n	Span (L), m	Skew angle (ψ), deg.	F _s	ϵ
1 to 4	$15 \leq L \leq 40$	$0 < \psi \leq 20$	$1.2 - \frac{2.0}{(\epsilon + 10)}^*$	$-6.62 \times L^{-0.10} \times S^{0.35} \times N^{0.08} \times n^{-0.06} \times \tan \psi$
		$20 < \psi \leq 30$		$-5.22 \times L^{-0.11} \times S^{0.57} \times N^{-0.09} \times n^{0.13} \times \tan \psi$
		$30 < \psi \leq 40$		$-2.80 \times L^{-0.14} \times S^{0.83} \times N^{0.29} \times n^{-0.18} \times \tan \psi$
		$40 < \psi \leq 50$		$-2.0 \times L^{-0.08} \times S^{0.61} \times N^{0.29} \times n^{-0.10} \times \tan \psi$
		$50 < \psi \leq 60$		$-1.49 \times L^{-0.10} \times S^{0.79} \times N^{0.38} \times n^{-0.35} \times \tan \psi$

* Same as given in CHBDC clause 5.6.6.2 (CSA 2014a).

Table 5.26 Shear distribution factors at interior girder for skewed bridge at FLS under live load

n	Span (L), m	Skew angle (ψ), deg.	F _s	ϵ
1 to 4	$15 \leq L \leq 40$	$0 < \psi \leq 20$	$1.2 - \frac{2.0}{(\epsilon + 10)}^*$	$15.52 \times L^{2.37} \times S^{-2.59} \times N^{-8.12} \times n^{4.71} \times \tan \psi$
		$20 < \psi \leq 30$		$65.40 \times L^{2.20} \times S^{-3.26} \times N^{-8.57} \times n^{5.94} \times \tan \psi$
		$30 < \psi \leq 40$		$93.50 \times L^{3.75} \times S^{-4.91} \times N^{-14.17} \times n^{10.63} \times \tan \psi$
		$40 < \psi \leq 50$		$97.66 \times L^{3.69} \times S^{-4.94} \times N^{-14.50} \times n^{11.00} \times \tan \psi$
		$50 < \psi \leq 60$		$79.20 \times L^{6.00} \times S^{-10.00} \times N^{-17.00} \times n^{13.94} \times \tan \psi$

* Same as given in CHBDC clause 5.6.6.2 (CSA 2014a).

5.2.10.1 Correlation of FEA Results and Proposed Equations with CHBDC

The correlation between the CHBDC (CSA 2014a) equations and the proposed equations based on the parametric study for the moment and shear distribution factors for skewed slab-on-girder bridges at FLS were obtained and compared with the load distribution factors (LDF) from the finite element analysis results due to live loads, and presented in Figure 5.54 and 5.55, respectively. For this purpose, first of all the moment and the shear distribution factors for a straight bridge at FLS were calculated, and subsequently in order to account the skew effects a parameter F_s was evaluated and multiplied with the respective moment and shear distribution factors of a straight bridge (F_T). Finally the results showed good correlation between the values obtained from proposed equations and those calculated results from FEA, and all data points fall within 5% over and under-estimation region, shown by dotted lines in Figure 5.54 and 5.55.

Table 5.27 Comparison of moment distribution factors for skewed slab-on steel I-girder bridges at FLS

Location of girder	FEA results	Proposed equation	CHBDC (CSA 2014a)
Exterior	0.31	0.32	0.41
Interior	0.28	0.29	0.48

Table 5.28 Comparison of shear distribution factors for skewed slab-on steel I-girder bridges at FLS

Location of girder	FEA results	Proposed equation	CHBDC (CSA 2014a)
Obtuse corner	0.33	0.31	0.79
Acute corner	0.22	0.22	0.79
Interior girder	0.49	0.48	0.79

The illustrative example to calculate the moment and shear distribution factors using FEA, proposed equation and the CHBDC (CSA 2014a) for a skewed slab-on steel I-girder bridges at FLS are described in Appendix E. The comparison of results for the moment and shear distribution factors evaluated using FEA, proposed equation and the CHBDC (CSA 2014a) equation are presented in Table 5.27 and 5.28, respectively. The result showed that the proposed equations were sufficiently accurate in predicting the response of a skewed bridge behavior at FLS. The CHBDC design equations were found highly conservative for both moment and shear at the exterior and interior girder location. The main reasons for

the inadequacy of the design equation are more likely the same as described earlier in section 4.4.7.

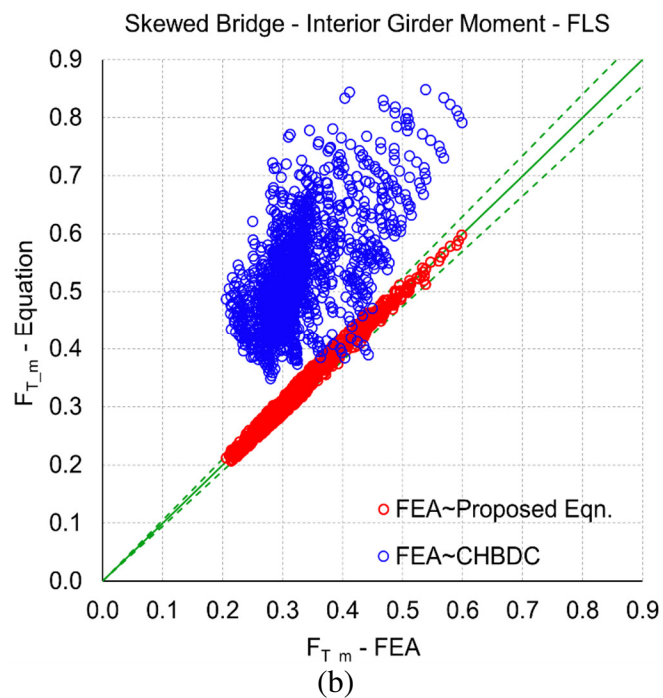
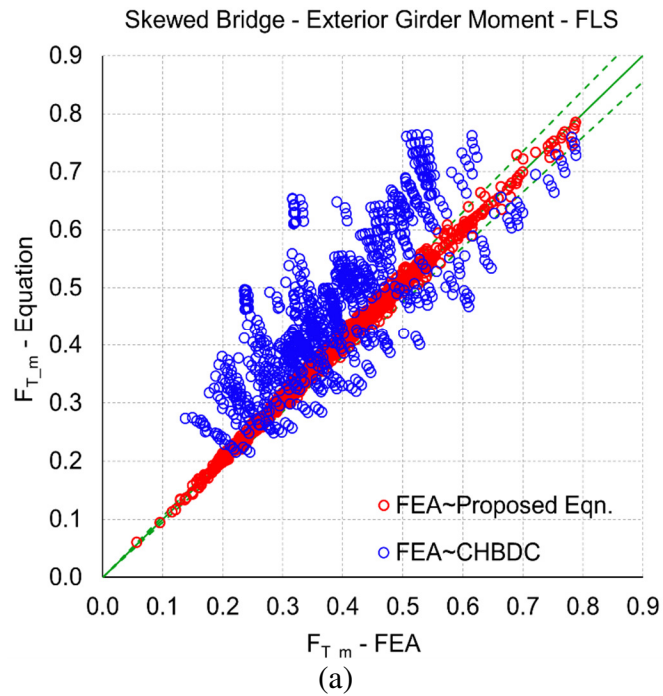
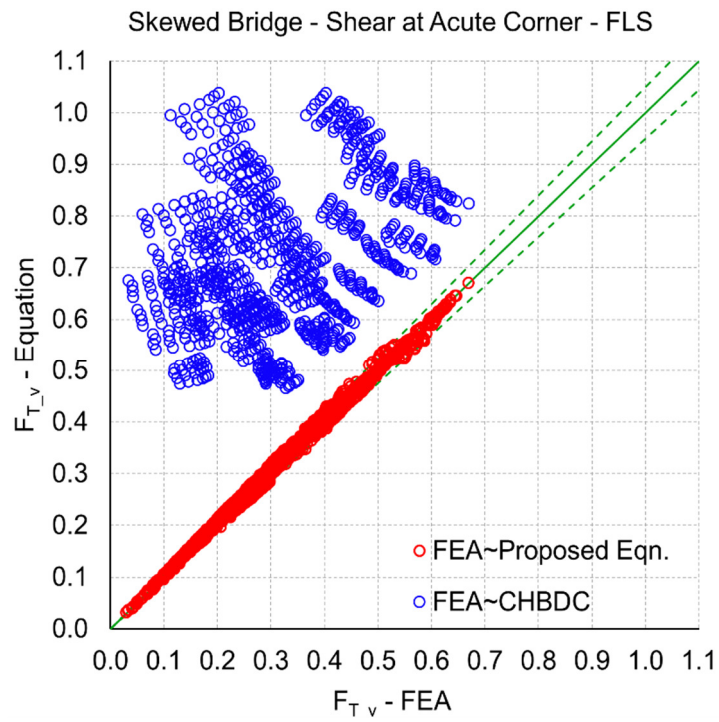
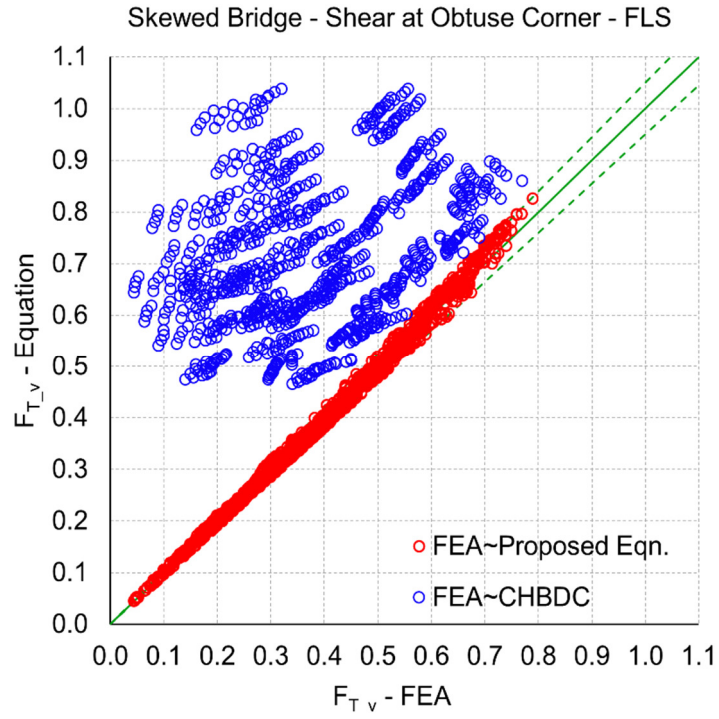
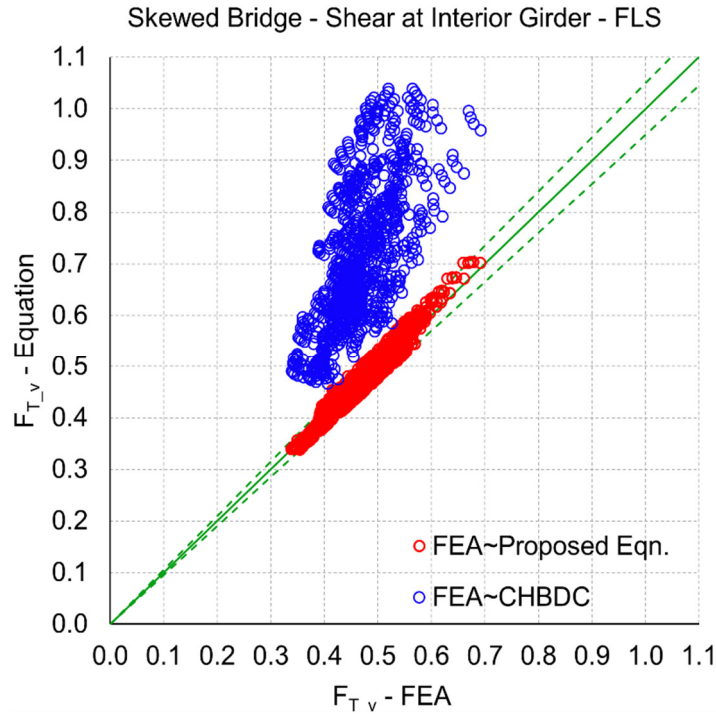


Figure 5.54 Correlation between moment distribution factors at FLS obtained from FEA results with proposed equations and CHBDC for skewed slab-on-girder bridges for; (a) exterior girder, and (b) interior girder





(c)

Figure 5.55 Correlation between shear distribution factors at FLS obtained from FEA results with proposed equations and CHBDC for skewed slab-on-girder bridges for girders at; (a) obtuse corner, (b) acute corner, and (c) interior

5.3 Correlation of Data with Bridge Code Specifications in North America

In this section a comparison of the developed proposed equation, for the skewed slab-on-girder bridge, for the moment and shear distribution factors were made with the existing codes available in North America. For this purpose, AASHTO-LRFD (2014) and the method proposed by Jaeger and Smith (1997) specified in the commentary of CHBDC (CSA 2006b) design specifications were considered. The details about the moment and shear distribution factor equations available in these codes and their comparison with the equations proposed in this study will be presented in the following sub-sections.

5.3.1 AASHTO-LRFD (2014) for Straight Slab-on-Girder Bridges

The AASHTO-LRFD (2014) specification is used throughout the United States as the national standard that engineers are required to follow for bridge design and detailing. Many states include their own amendments and guidelines to this specification, based on

this standard. The specifications have also been adopted by other bridge-owning authorities and agencies in the United States and abroad.

In Section 4-Structural Analysis and Evaluation of the current LRFD bridge design specifications (2014), equations are provided to adjust the live load distribution factors for moment and shears using approximate methods of analysis. The approximate method of analysis involves line girder or one-dimensional analysis of the bridge structure within a set range of applicability for girder design. For two or more design lanes, the moment and shear distribution factor equations specified in AASHTO-LRFD (2014) for the straight slab-on-girder are presented in Table 5.29.

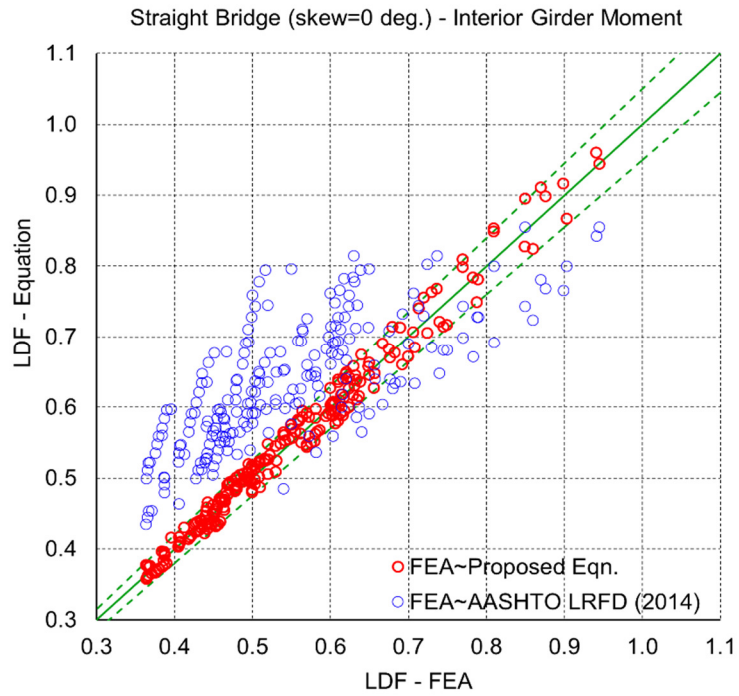
The comparison of LRFD equations for the moment and shear distribution factors for a straight composite slab-on steel I-girder bridge with the FEA results and proposed equations were presented in Figure 5.56 and 5.57 respectively. The comparison revealed that the moments and shear distribution factors predicted using the proposed formulas were close to those from the finite element analysis results that verifies the proposed formulas. However, the following observations were noticed while comparing the finite element analysis results with ASSHTO LRFD (2014) design equations.

- 1) The LRFD equations overestimated the shear live load distribution by 30% when compared with the finite element analysis results for a significant number of cases.
- 2) The LRFD equations overestimated the moment live load distribution to a maximum of 35% when compared with the finite element analysis results for a significant number of cases. However in some cases, the LRFD equations under-estimated the response by 20% when compared to finite elements analysis results. This finding is in agreement with Yousif and Hindi (2007).

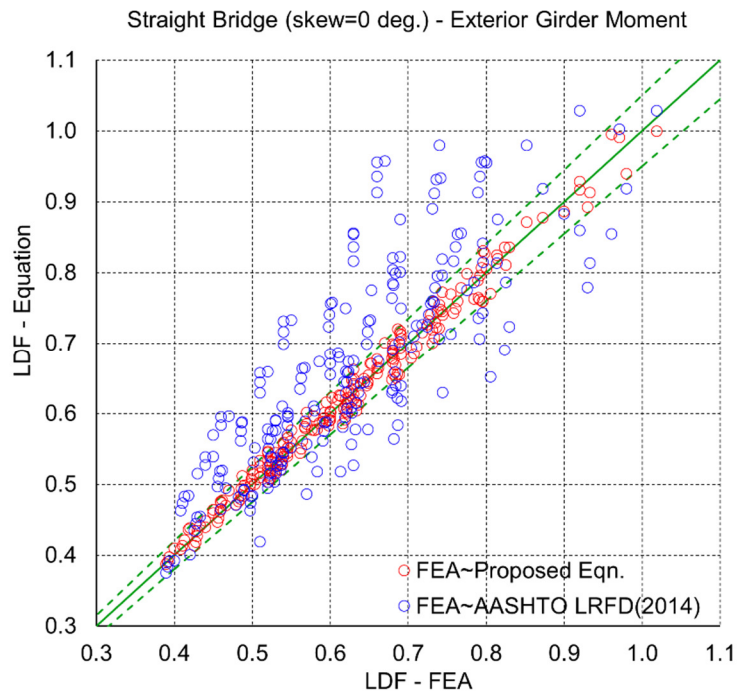
Table 5.29 LRFD load distribution factors for straight slab-on-girder bridges (Customary U.S. Units)

Bridge type	Load effect	Load distribution equations (two- or more design lanes)	Applicability
Slab-on-girder	Moment-Interior (clause 4.6.2.2.2b)	$g_{interior}$ $= 0.075 + \left(\frac{S}{9.5}\right)^{0.6} \left(\frac{S}{L}\right)^{0.2} \left(\frac{Kg}{12.0Lt_s^3}\right)^{0.1}$	$3.5 \leq S \leq 16.0$ $20 \leq L \leq 240$ $4.5 \leq t_s \leq 12.0$ $N_b \geq 4$ $10,000 \leq K_g$ $\leq 7,000,000$
	Moment-Exterior (clause 4.6.2.2.2d)	$g_{exterior} = e \times g_{interior}$ $e = 0.77 + \frac{d_e}{9.1}$	$-1.0 \leq d_e \leq 5.5$
	Shear-Interior (clause 4.6.2.2.3a)	$g_{interior} = 0.2 + \frac{S}{12} - \left(\frac{S}{35}\right)^{2.0}$	$3.5 \leq S \leq 16.0$ $20 \leq L \leq 240$ $4.5 \leq t_s \leq 12.0$ $N_b \geq 4$
	Shear-Exterior (clause 4.6.2.2.3b)	$g_{exterior} = e \times g_{interior}$ $e = 0.6 + \frac{d_e}{10}$	$-1.0 \leq d_e \leq 5.5$

Note: $g_{interior}$ = load-distribution factor for interior girder; $g_{exterior}$ = load-distribution factor for exterior girder; S = girder spacing; L = span length; t_s = deck thickness; K_g = longitudinal stiffness parameter; N_b = number of girders; e = correction factor; and d_e = distance from the exterior web of exterior girder to interior edge of curb or traffic barrier.



(a)



(b)

Figure 5.56 Correlation between moment distribution factors obtained from FEA results with proposed equations and AASHTO-LRFD for straight slab-on-girder bridges for; (a) interior girder, and (b) exterior girder

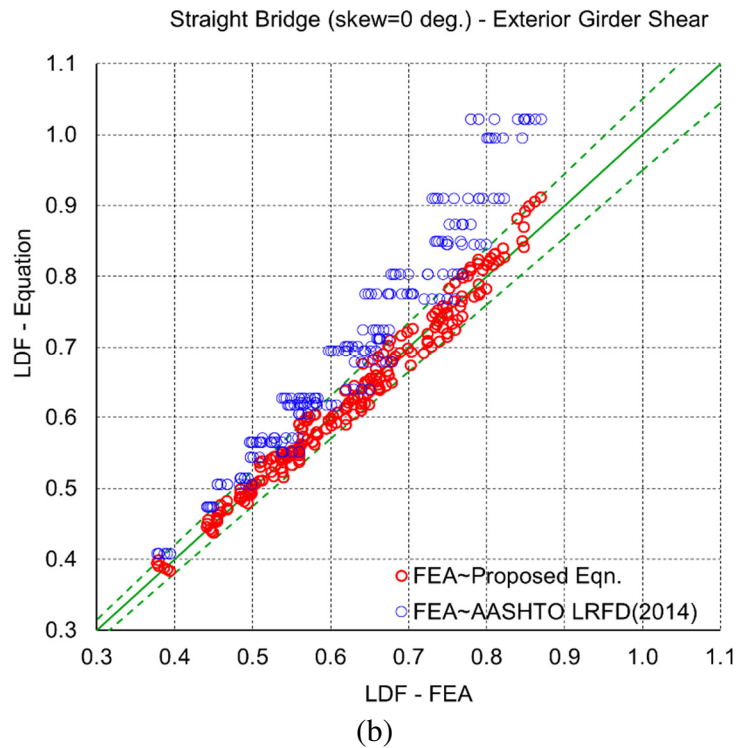
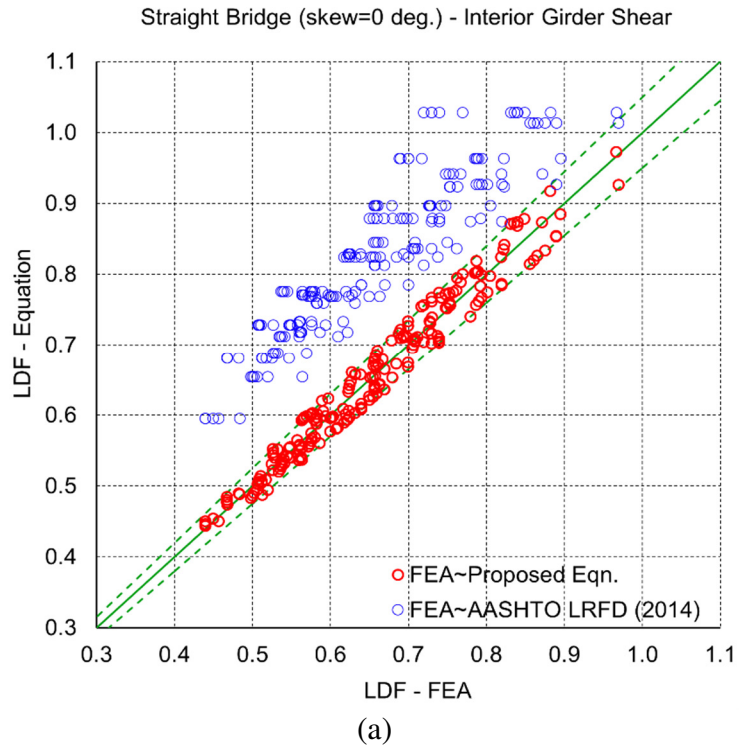


Figure 5.57 Correlation between shear distribution factors obtained from FEA results with proposed equations and AASHTO-LRFD for straight slab-on-girder bridges for; (a) interior girder, and (b) exterior girder

5.3.2 AASHTO-LRFD (2014) for Skewed Slab-on-Girder Bridges

As the national standard, the LRFD specifications are lacking in providing guidelines for designing highly skewed bridges. In the commentary of Section 6-Steel Structures, includes the effects that skewed alignment have on girder and cross-frame deflections, rotations, and potential additional stresses. However, in many cases, it is recommended to perform a more refined analysis to accurately capture the effects of girder skewness and leaves a fair amount to engineering judgment to decide when a refined analysis is necessary.

Correction factors are specified in the LRFD design code for longitudinal moment and shear distribution factors at the obtuse corner to take in to account the variation of skew angle. However, the LRFD code further states that in determining the end shear in deck system bridges, the skew correction at the obtuse corner shall be applied to all the beams. Table 5.30 shows the moment and shear distribution factor equations specified in AASHTO-LRFD (2014) for the skewed slab-on-girder. The comparison of LRFD correction factor equations for the calculation of interior and exterior girder moment distribution factors for a skewed composite slab-on steel I-girder bridge at a skew angle of 40° and 60° with the FEA results and proposed equations are presented in Figure 5.58 and 5.59, respectively. Likewise, the comparison of shear distribution factor at the girder obtuse corner for a skewed bridge at 40° and 60° skew angle are presented in Figure 5.60. The comparison revealed that the moments and shear distribution factors predicted using the proposed formulas were close to those from the finite element analysis results that verifies the proposed formulas. However, the following observations were noticed while comparing the finite element analysis results with ASSHTO LRFD (2014) design equations.

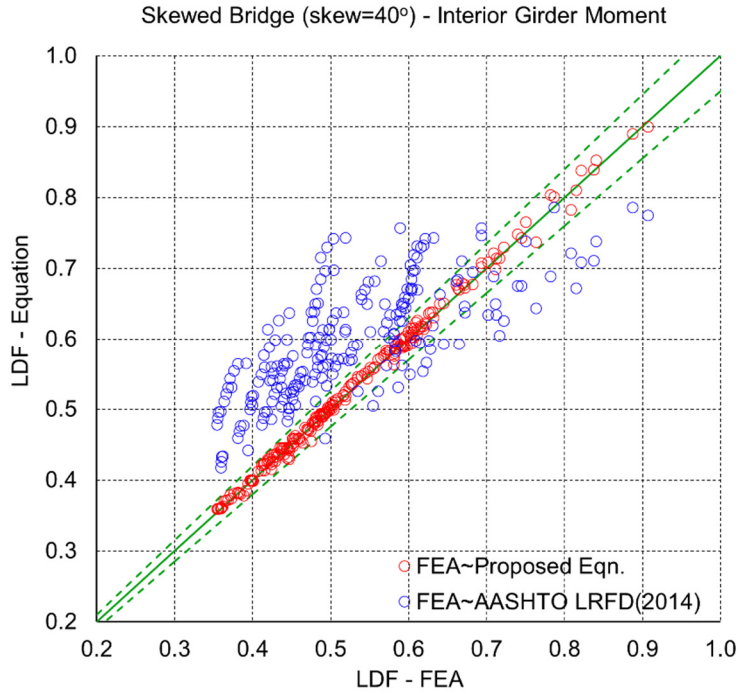
1. Although, AASHTO-LRFD bridge design specifications consider the effect of skew. However, the LRFD method do not consider the effect of secondary elements such as cross bracing and diaphragms. The presence of such structural elements, moment-connected to the longitudinal girders, lead to better load distribution and hence significant reductions in the span moment and support end reactions (Eom and Nowak

- 2001). Furthermore, the LRFD method recommends the same skew-reduction factors for both the exterior and the interior girder moment. As mentioned earlier, the interior girder is much more significantly affected by skew than the exterior girder. For this reason, the span moments predicted using the LRFD method was found extremely conservative for the interior girder. Another shortcoming noticed for both the exterior and interior girders when span was less than 20 m, where it resulted in underestimating the girder response.
2. It was found that the presence of skew always increased the obtuse corner shear distribution factor. In contrast, skew always reduced the acute corner girder shear distribution factor. However, LRFD method recommends the same correction factors for both the exterior and the interior girders.

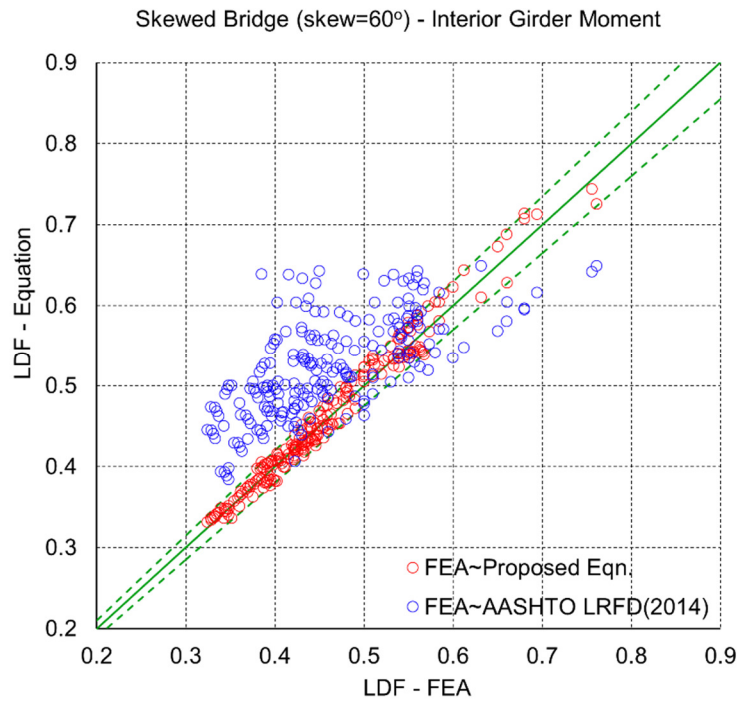
Table 5.30 LRFD Correction factors for skewed slab-on-girder bridges (Customary U.S. Units)

Bridge type	Load effect	Correction factors (Any number of design lanes)	Applicability
Slab-on-girder	Moment <i>(clause 4.6.2.2.2e)</i>	$1 - C_1 (\tan \theta)^{1.5}$ $C_1 = 0.25 \left(\frac{K_g}{12.0 L t_s^3} \right)^{0.25} \left(\frac{S}{L} \right)^{0.5}$ <i>if $\theta < 30^\circ$ then $C_1 = 0.0$</i> <i>if $\theta > 60^\circ$ use $\theta = 60^\circ$</i>	$30^\circ \leq \theta \leq 60^\circ$ $3.5 \leq S \leq 16.0$ $20 \leq L \leq 240$ $N_b \geq 4$
	Shear <i>(clause 4.6.2.2.3c)</i>	$1.0 + 0.20 \left(\frac{12.0 L t_s^3}{K_g} \right)^{0.3} \tan \theta$	$0^\circ \leq \theta \leq 60^\circ$ $3.5 \leq S \leq 16.0$ $20 \leq L \leq 240$ $N_b \geq 4$

Note: C_1 = parameter for skewed supports; S = girder spacing; L = span length; t_s = deck thickness; K_g = longitudinal stiffness parameter; N_b = number of girders; and θ = skew angle (degrees).

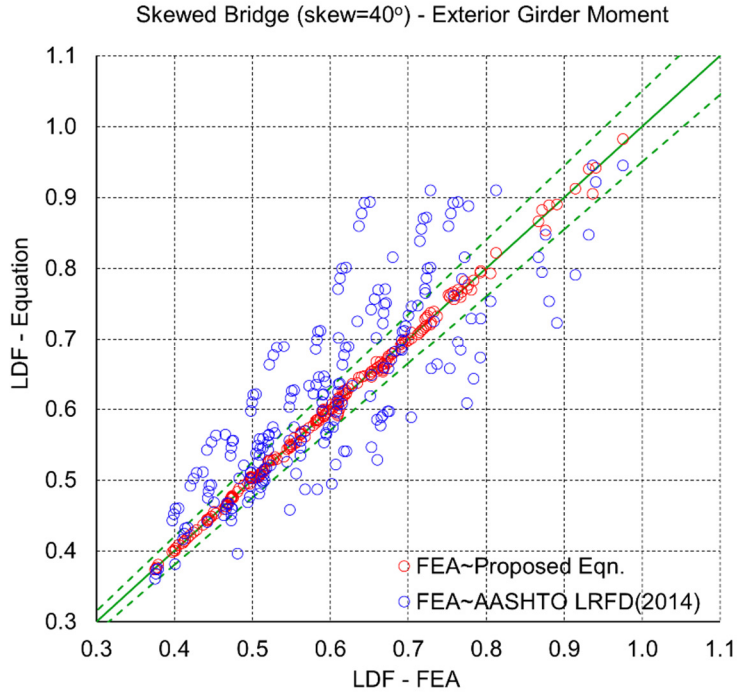


(a)

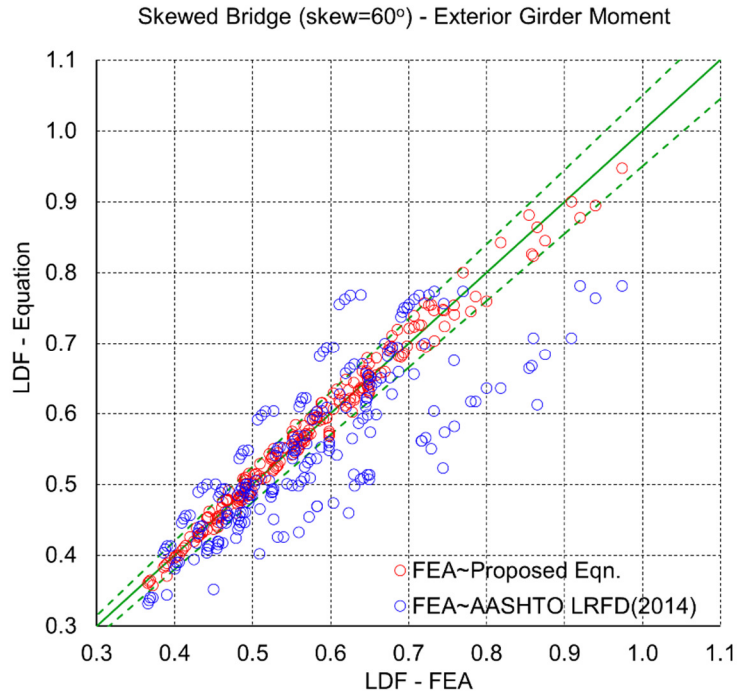


(b)

Figure 5.58 Correlation between interior girder moment distribution factors obtained from FEA results with proposed equations and AASHTO-LRFD for skewed slab-on-girder bridges at skew angle of; (a) 40°, and (b) 60°



(a)



(b)

Figure 5.59 Correlation between exterior girder moment distribution factors obtained from FEA results with proposed equations and AASHTO-LRFD for skewed slab-on-girder bridges at skew angle of; (a) 40°, and (b) 60°

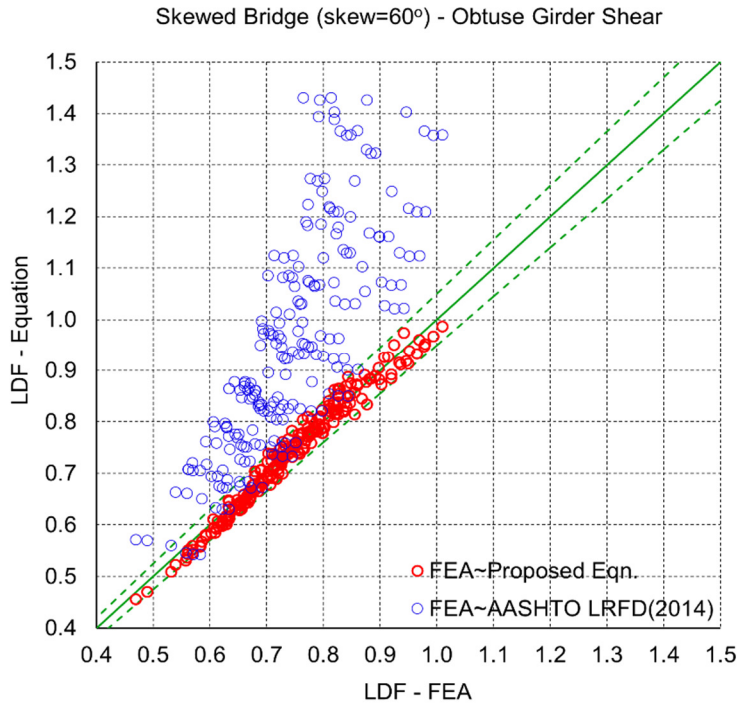
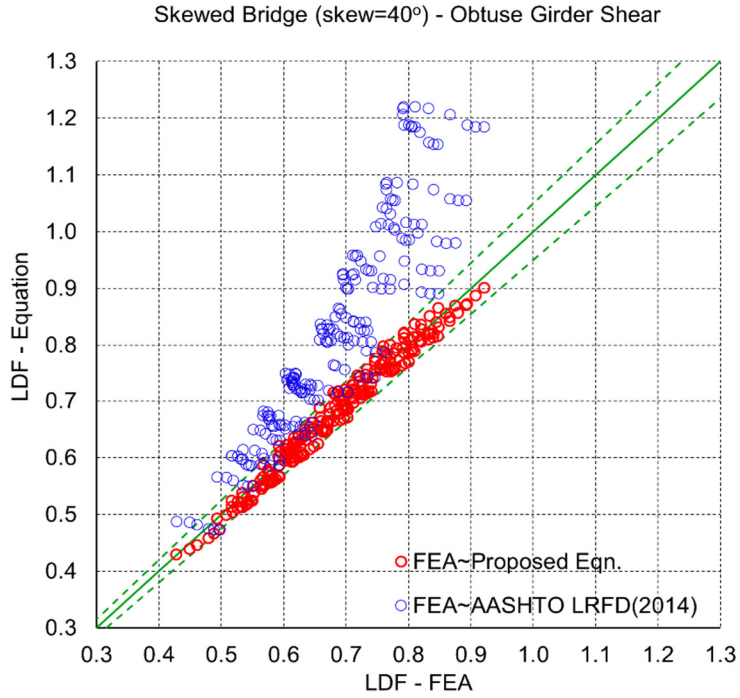


Figure 5.60 Correlation between shear distribution factors at obtuse corners obtained from FEA results with proposed equations and AASHTO-LRFD for skewed slab-on-girder bridges at skew angle of; (a) 40°, and (b) 60°

5.3.3 CHBDC (CSA 2006b) – Jaeger and Smith (1997)

In the commentary of CHBDC (CSA 2006b), Annex CA5.1.3.1-Shallow superstructures on skew spans, the design code has specified a procedure proposed by Jaeger and Smith (1997) for the calculation of longitudinal vertical shear in slab-on-girder bridges with skew geometry. In Jaeger and Smith (1997) method the corresponding bridge without skew, using the skewed span length, needs to be analyzed first for the longitudinal vertical shear in accordance with CHBDC clauses. The shear force thus found in the skewless straight bridge shall be multiplied by a dimensionless parameter C_v , obtained from clause CA-5.1.3.1 (CSA 2006b) for the values of ε and η , which are given by:

$$\begin{aligned}\varepsilon &= \frac{S \tan \psi}{L} \\ \eta &= 0.5 \left(\frac{D_y}{D_x} \right) \left(\frac{L}{S} \right)^4\end{aligned}\tag{5.17}$$

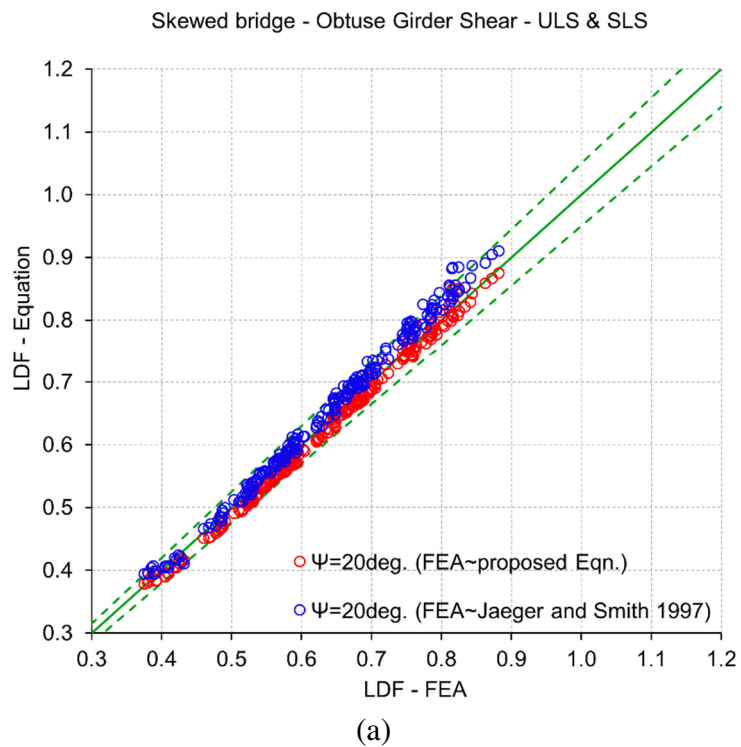
where, D_y = transverse bending stiffness of the bridge superstructure per unit length, D_x = longitudinal bending stiffness per unit width, L = span length, S = girder spacing, and ψ = skew angle.

The comparison of Jaeger and Smith (1997) method for the evaluation of shear distribution factors for a skewed composite slab-on steel I-girder bridge with the FEA results and proposed equations are presented in Figure 5.61 to 5.63 respectively, for three different skew angle (i.e. 20°, 40°, and 60°) at the girder obtuse and acute corners and at the interior girder for ULS and SLS. Figure 5.64 to 5.66 represents the correlation of the shear distribution factors at the obtuse, acute and at the interior girders for FLS, respectively. The comparison revealed that the shear distribution factors predicted using the proposed formulas were close to those from the finite element analysis results that verifies the proposed formulas. However, the following observations were noticed while comparing the finite element analysis results with Jaeger and Smith (1997) design equations.

- 1) Jaeger and Smith (1997) equations showed reasonably comparable results for the girders at the obtuse corners with slight conservative response of girder shear

distribution was noticed beyond 40° skew angle for ultimate and serviceability, and fatigue limit states.

- 2) It was found that the presence of skew angle always reduced the girder shear response at the acute corner. However, Jaeger and Smith (1997) method recommends the same factors for both the obtuse and acute girders. Consequently, resulted in substantial conservative results at the acute corners, that enhances further with the increase of skew angle up to 60°.



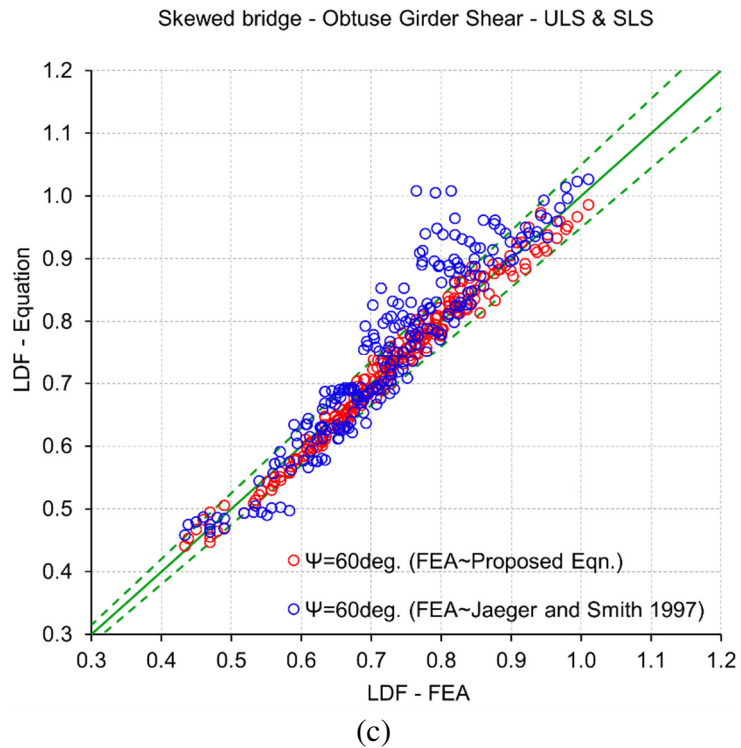
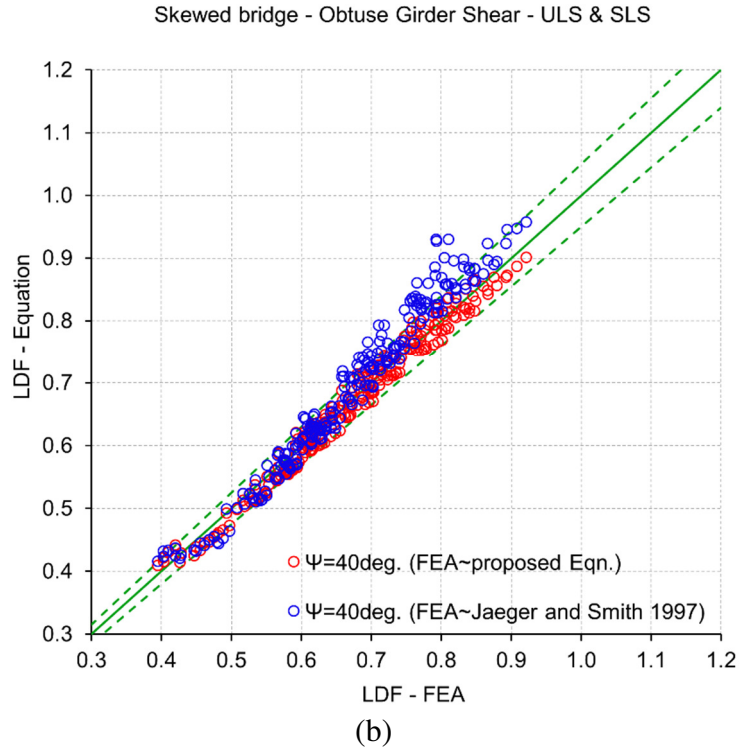
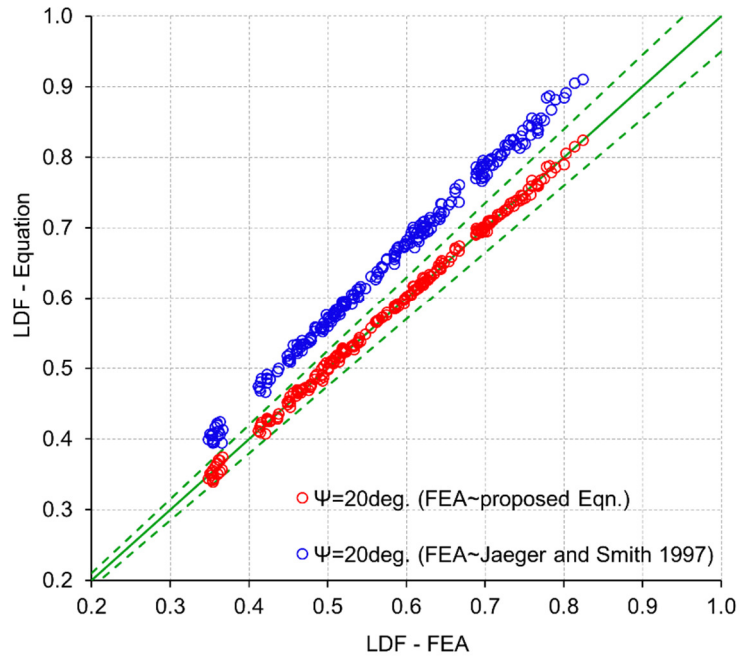


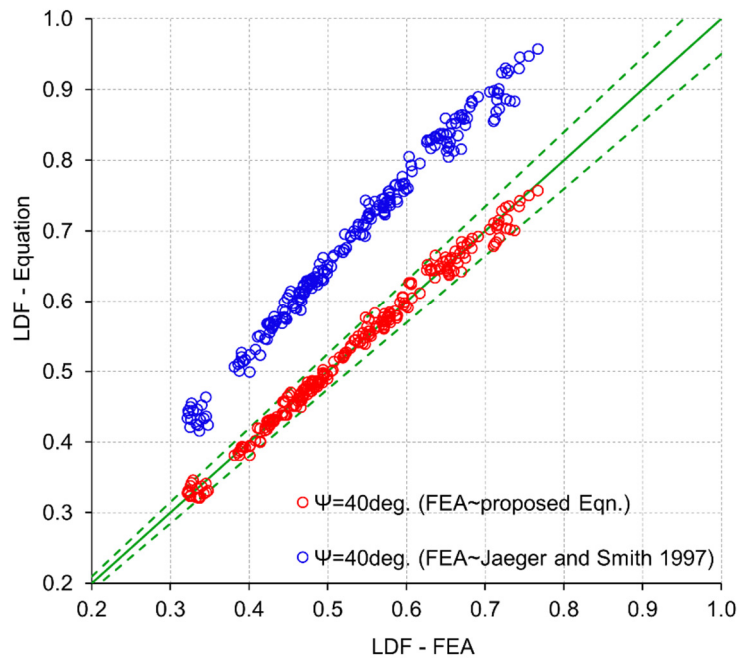
Figure 5.61 Correlation between shear distribution factors at obtuse corners obtained from FEA results with proposed equations and Jaeger and Smith (1997) at ULS & SLS for skewed slab-on-girder bridges at skew angle of; (a) 20°, (b) 40°, and (c) 60°

Skewed bridge - Acute Girder Shear - ULS & SLS



(a)

Skewed bridge - Acute Girder Shear - ULS & SLS



(b)

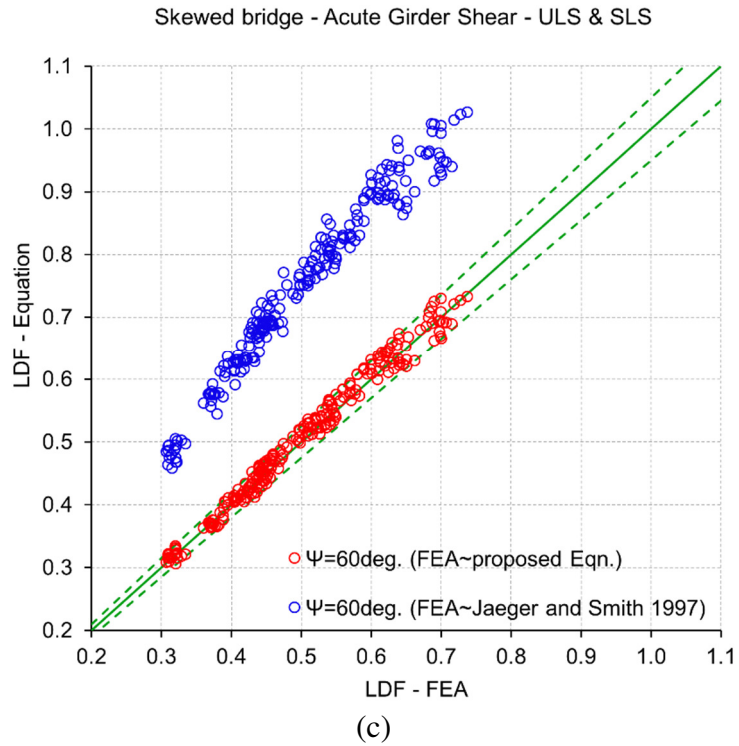
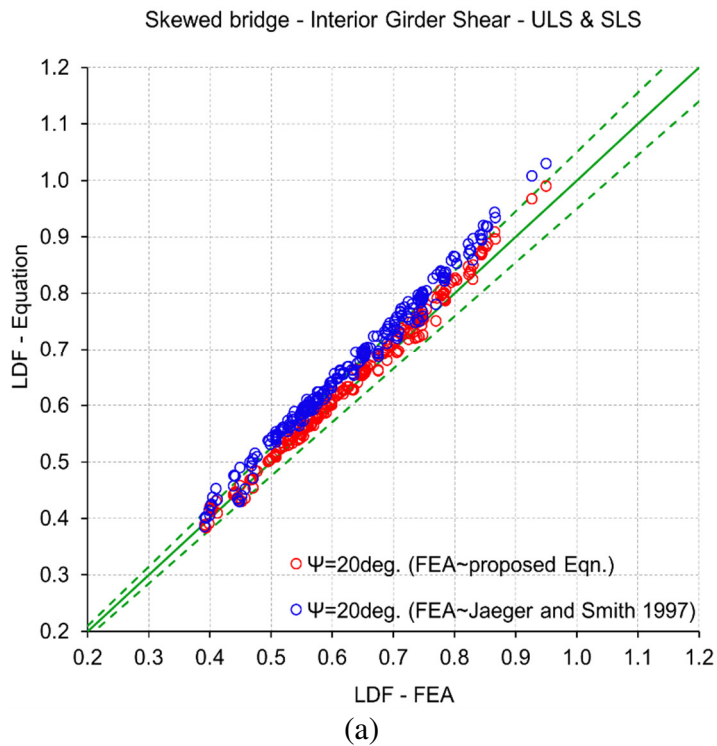


Figure 5.62 Correlation between shear distribution factors at acute corners obtained from FEA results with proposed equations and Jaeger and Smith (1997) at ULS & SLS for skewed slab-on-girder bridges at skew angle of; (a) 20°, (b) 40°, and (c) 60°



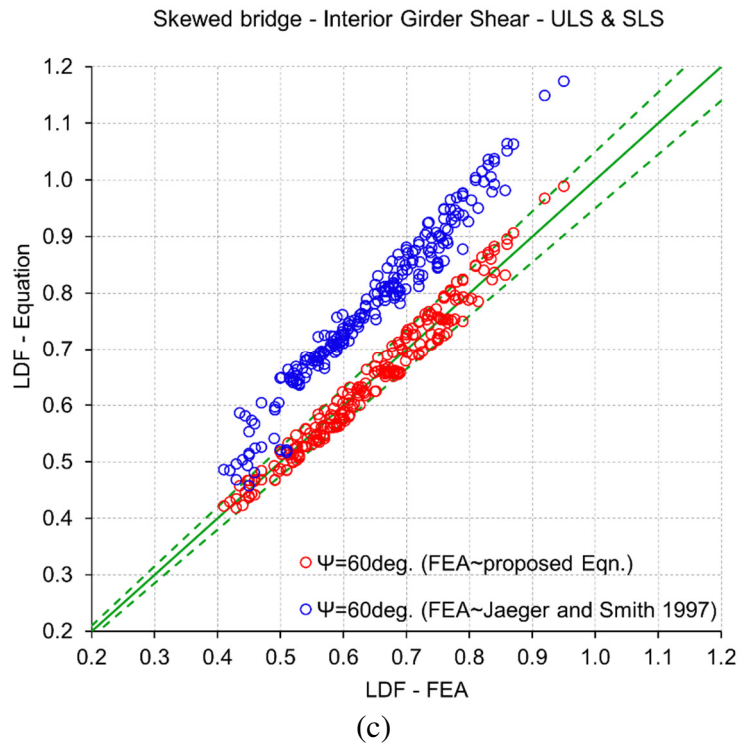
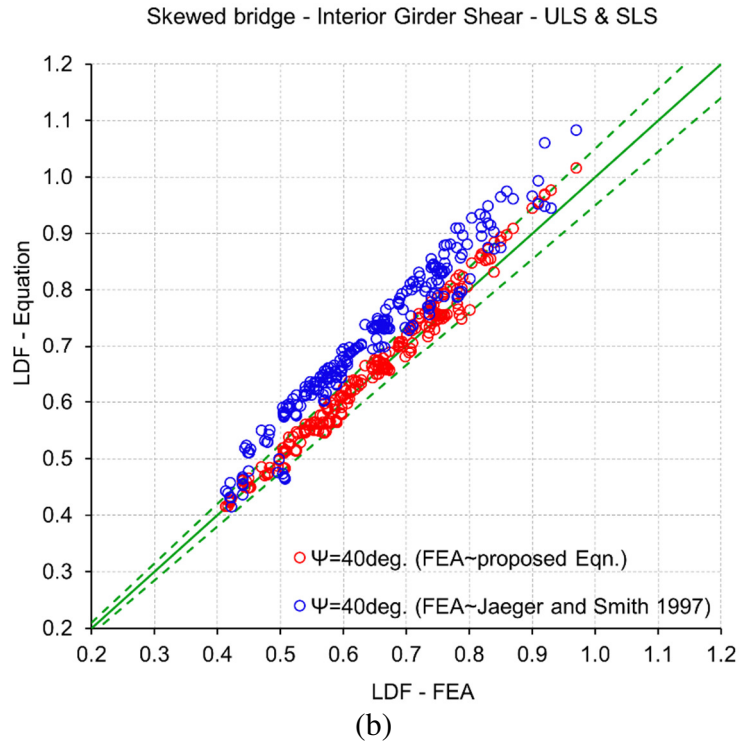
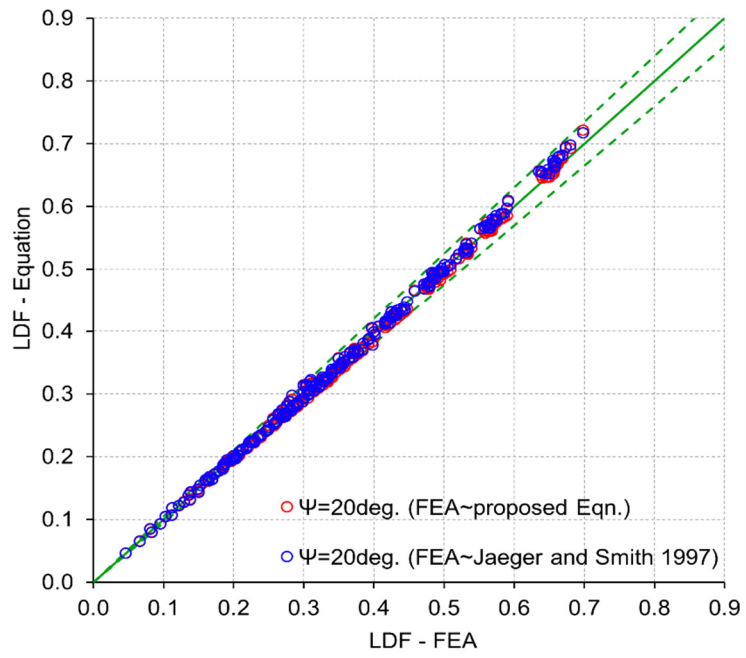


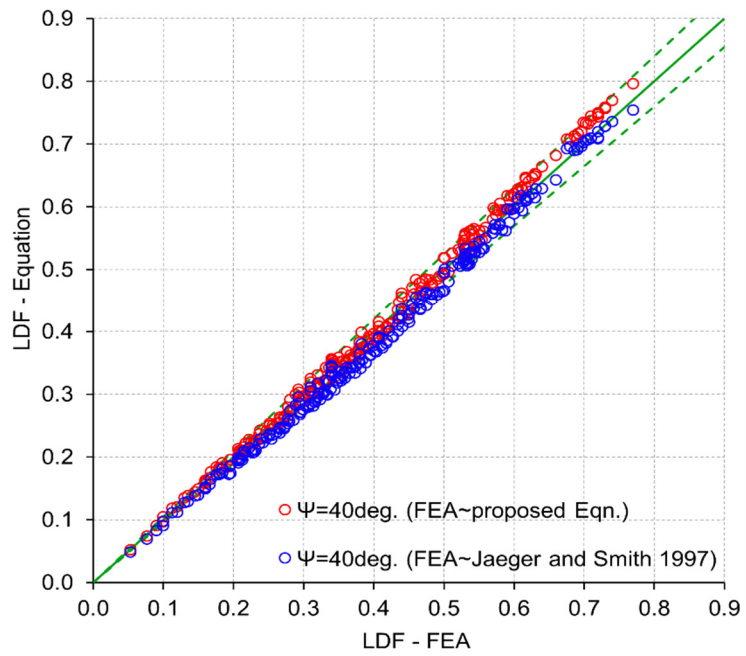
Figure 5.63 Correlation between shear distribution factors at interior girder obtained from FEA results with proposed equations and Jaeger and Smith (1997) at ULS & SLS for skewed slab-on-girder bridges at skew angle of; (a) 20°, (b) 40°, and (c) 60°

Skewed bridge - Obtuse Girder Shear - FLS



(a)

Skewed bridge - Obtuse Girder Shear - FLS



(b)

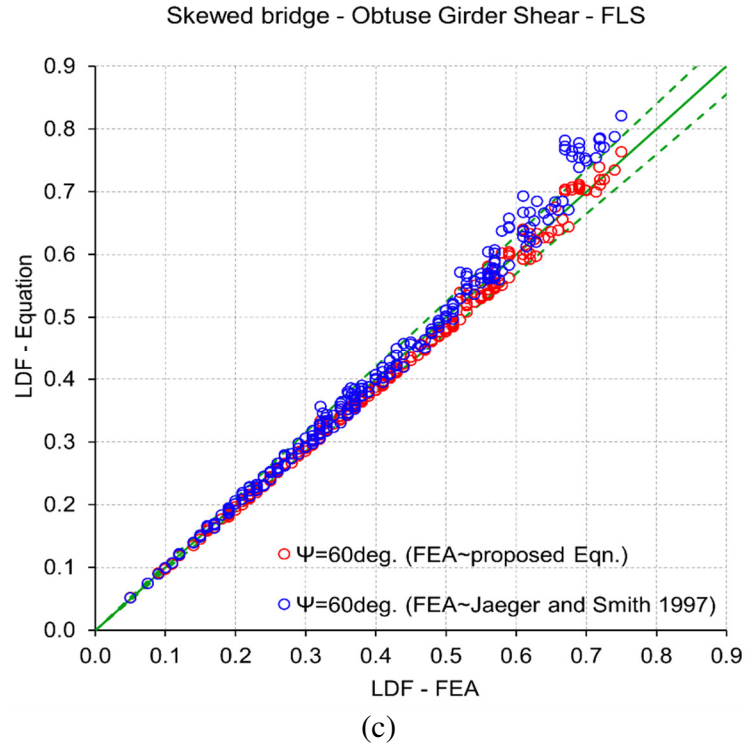
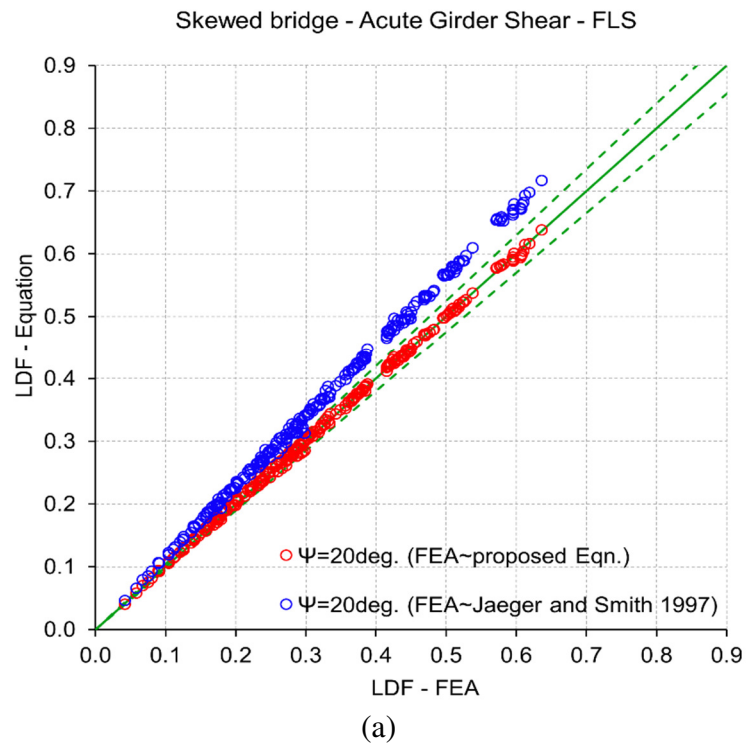
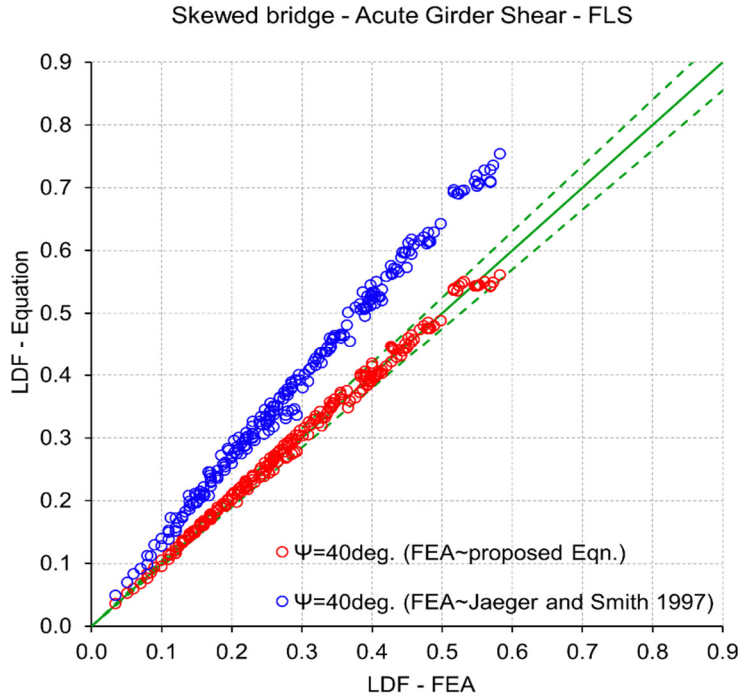
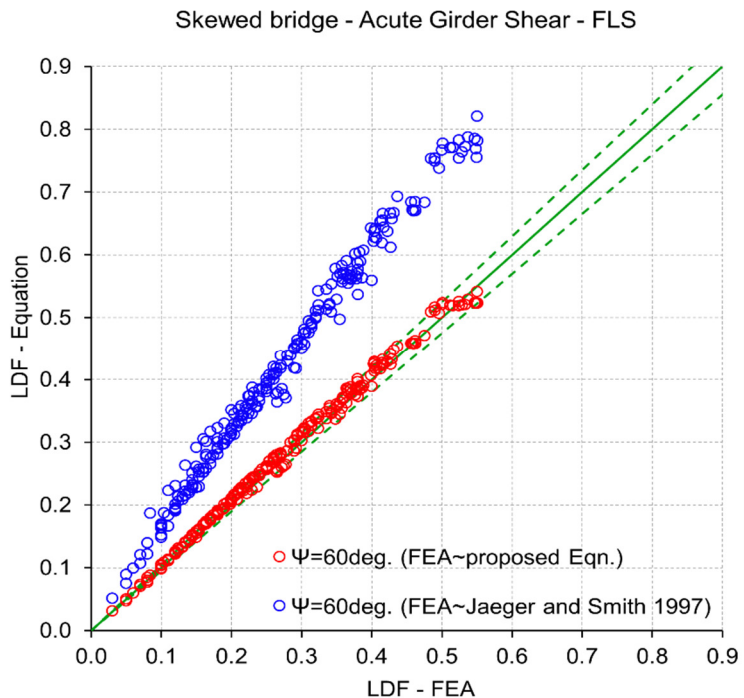


Figure 5.64 Correlation between shear distribution factors at obtuse corners obtained from FEA results with proposed equations and Jaeger and Smith (1997) at FLS for skewed slab-on-girder bridges at skew angle of; (a) 20°, (b) 40°, and (c) 60°





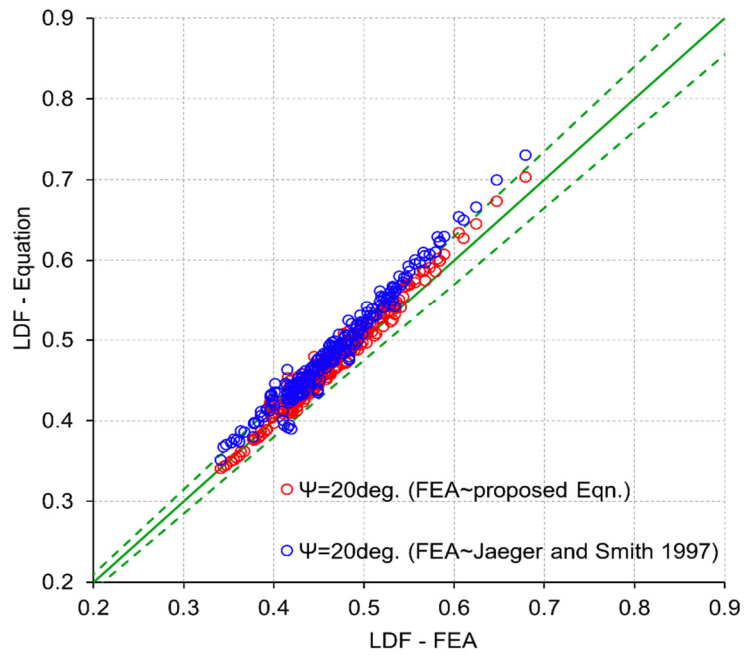
(b)



(c)

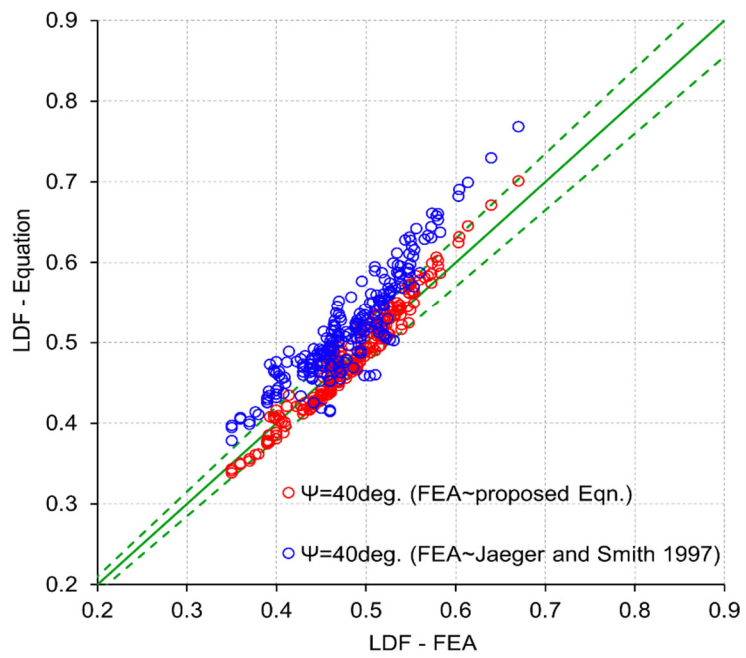
Figure 5.65 Correlation between shear distribution factors at acute corners obtained from FEA results with proposed equations and Jaeger and Smith (1997) at FLS for skewed slab-on-girder bridges at skew angle of; (a) 20°, (b) 40°, and (c) 60°

Skewed bridge - Interior Girder Shear - FLS



(a)

Skewed bridge - Interior Girder Shear - FLS



(b)

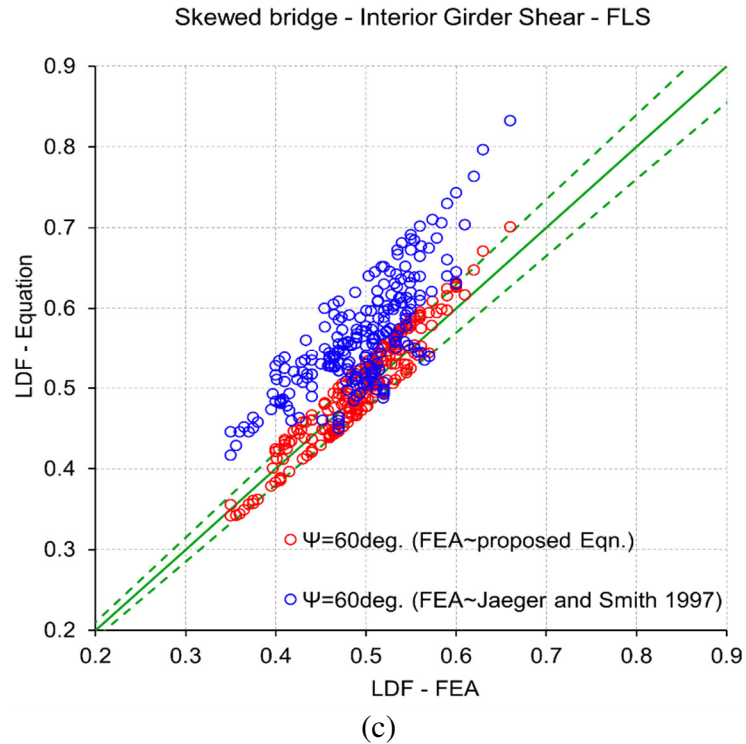


Figure 5.66 Correlation between shear distribution factors at interior girder obtained from FEA results with proposed equations and Jaeger and Smith (1997) at FLS for skewed slab-on-girder bridges at skew angle of; (a) 20°, (b) 40°, and (c) 60°

Table 5.31 Geometry of prototype bridges considered by Al-Hashimy (2005)

Design lanes (n)	Bridge width (W), m	Deck width (Wc), m	Number of girders (N)	Girder spacing (S), m	Deck slab (ts), mm
1	6.0	5.0	3	2.0	225
2	7.5	6.5	3	2.5	225
2	9.0	8.0	3	3.0	225
2	8.0	7.0	4	2.0	225
2	10.0	9.0	4	2.5	225
2 & 3	12.0	11.0	4	3.0	225
2	10.0	9.0	5	2.0	225
2 & 3	12.5	11.5	5	2.5	225
4	15.0	14.0	5	3.0	225
2 & 3	12.0	11.0	6	2.0	225
4	15.0	14.0	6	2.5	225
2 & 3	14.0	13.0	7	2.0	225

5.4 Correlation of Data with Previous Research

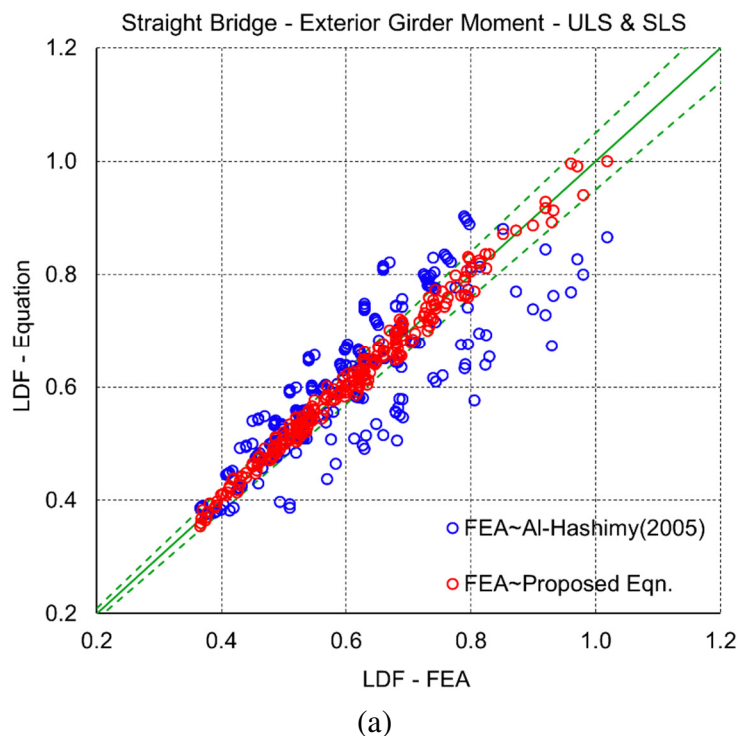
Based on a parametric study analysis, Al-Hashimy (2005) developed empirical equations for the shear and moment distribution factors for straight and curved steel I-girder bridges when subjected to the CHBDC (CSA 2000) truck loading. The parametric study included 256 simply supported straight and curved concrete slab-on-steel I-girder bridge prototypes to investigate the shear distribution factors. In addition to that; another parametric study was conducted on 64 composite bridge prototypes to investigate the moment distribution factors. Details about design parameters considered for this study are presented in Table 5.31, for four different span lengths i.e. 10 m, 15 m, 25 m and 35 m. All the above-mentioned bridge prototypes were analyzed to evaluate their structural response against a total of 48 different combinations of load cases. Further details about the selected bridge prototypes, truck loading and the developed empirical equations for shear and moment distribution factors can be seen elsewhere (Al-Hashimy 2005).

For comparison purposes, Al-Hashimy (2005) shear and moment distribution factor equations developed for straight composite steel-I-girder bridges were considered for all three limit states. Since, the developed equations were based on CHBDC (CSA 2000), that follows the concept of equal distribution of loads among all girder. So, in order to make comparison with the empirical equations proposed in this study that are based on the current CHBDC (CSA 2014a), the shear and moment distribution factors computed from Al-Hashimy's equations were modified.

The comparison of Al-Hashimy (2005) equations for the evaluation of moment distribution factors for a straight composite slab-on steel I-girder bridge with the FEA results and proposed equations are presented in Figure 5.67 to 5.68 respectively, for three limit states. However, Figure 5.69 to 5.70 represents the correlation of the shear distribution factors at the exterior and interior girders respectively for straight slab-on-girder bridge for ULS, SLS and FLS. The comparison revealed that the moment and shear distribution factors predicted using the proposed formulas were close to those from the finite element analysis results that verifies the proposed formulas. However, for some cases Al-Hashimy (2005) design equations presented conservative estimates for the shear and moment distribution

factors, while for other situations the design equations demonstrated under-estimated response. The main cause of disagreement was the limited selection of the parameters used for the formation of design equation for load distribution factors. For-example for all the bridge configurations only three girder spacing were considered (i.e. 2.0 m, 2.5 m and 3.0 m), so it was noticed that most of the bridge geometry outside this girder spacing limit resulted in erroneous results.

It is worth mentioning that the current study was based upon the recent CHBDC code specifications (CSA 2014a). For comparison purposes, no other previous study was identified that devoted toward the estimation of load distribution factors using the current CHBDC design code for the composite slab-on-girder bridges. A substantial amount of work related to the evaluation of shear and moment distribution factors that has been reported in literature is based on the AASHTO standard vehicle and code specifications (Nouri and Ahmadi 2012, Sotelino et al. 2004, Khaloo and Mirzabozorg 2003, Eom and Nowak 2001). In Canada, few studies related to the evaluation of load distribution factors for slab-on-girder bridges were observed in literature, however they are based on different bridge geometry (Wassef 2004, Khalafalla 2009).



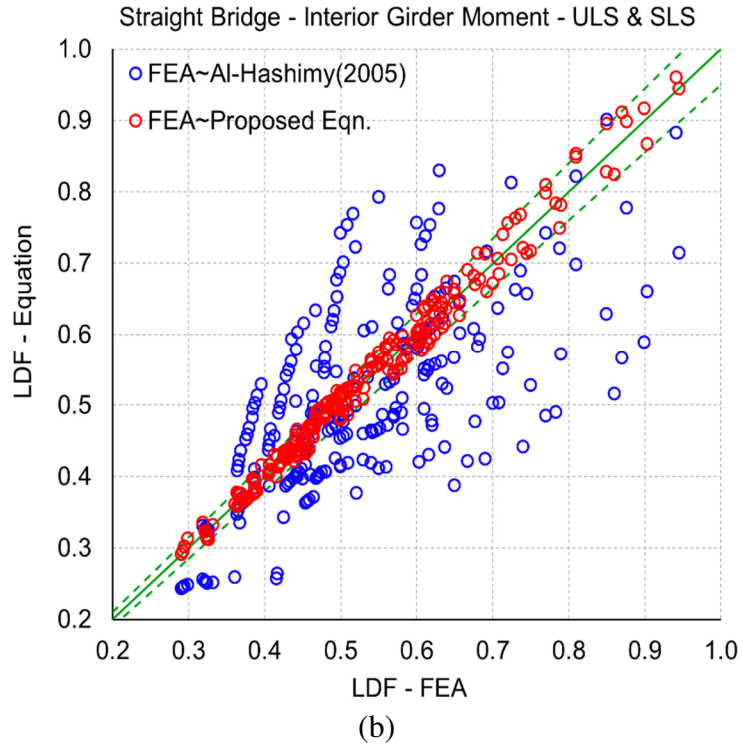
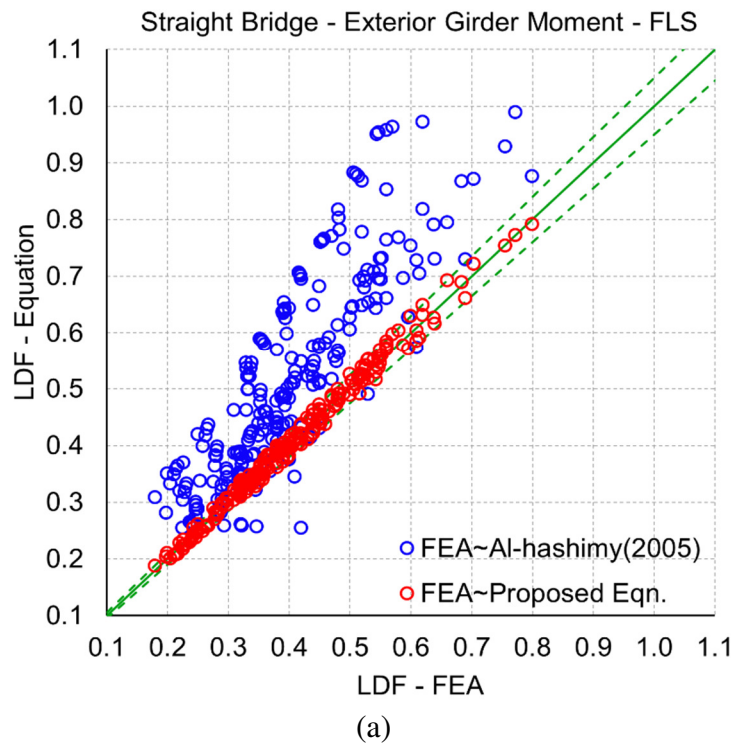


Figure 5.67 Correlation between moment distribution factors obtained from FEA results with proposed equations and Al-Hashimy (2005) equations for ULS & SLS for straight slab-on-girder bridges for; (a) exterior girder, and (b) interior girder



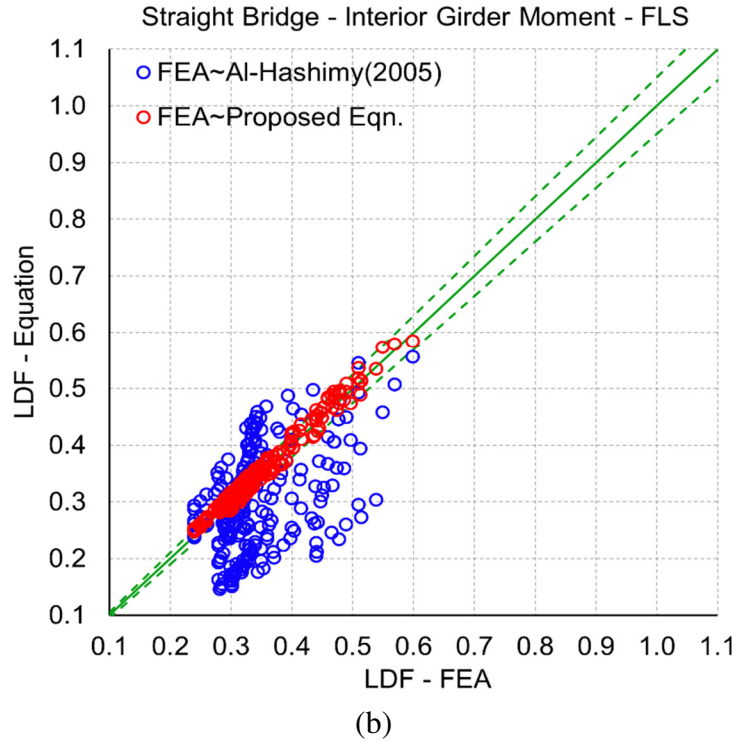
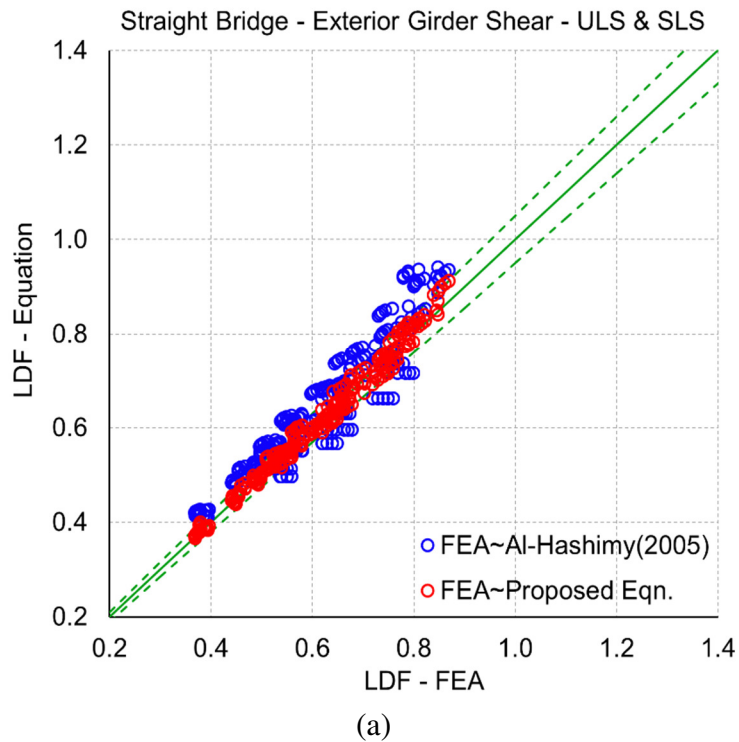


Figure 5.68 Correlation between moment distribution factors obtained from FEA results with proposed equations and Al-Hashimy (2005) equations for FLS for straight slab-on-girder bridges for; (a) exterior girder, and (b) interior girder



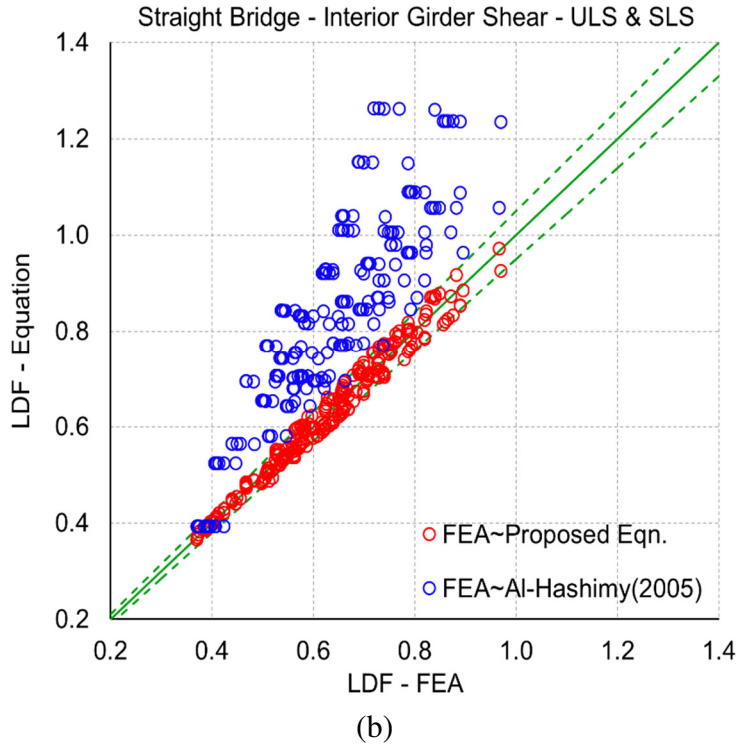
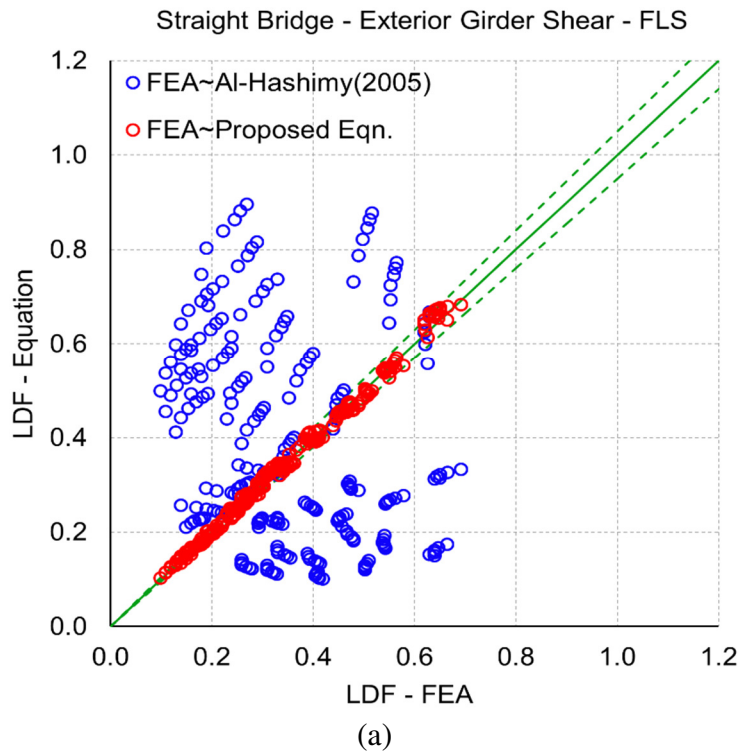


Figure 5.69 Correlation between shear distribution factors obtained from FEA results with proposed equations and Al-Hashimy (2005) equations for ULS & SLS for straight slab-on-girder bridges for; (a) exterior girder, and (b) interior girder



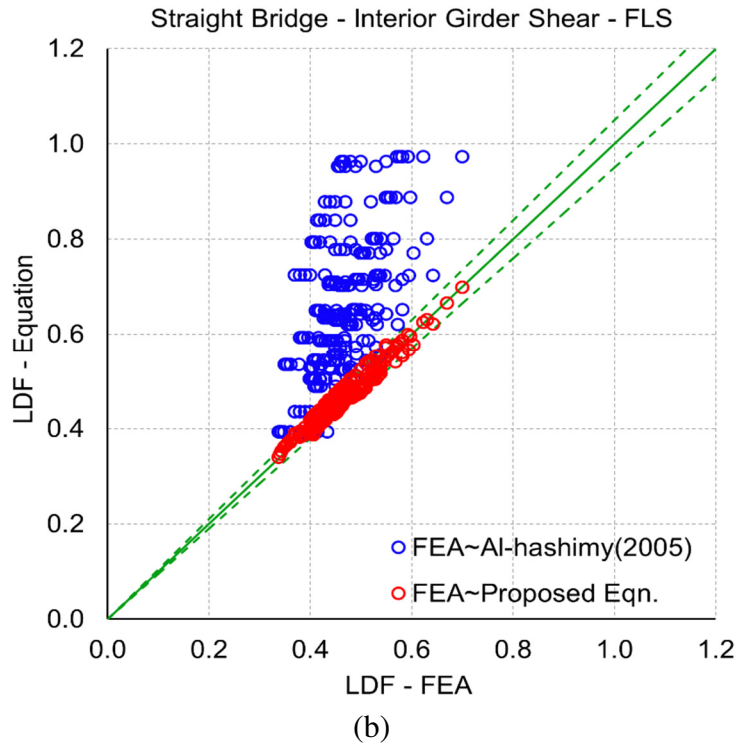


Figure 5.70 Correlation between shear distribution factors obtained from FEA results with proposed equations and Al-Hashimy (2005) equations for FLS for straight slab-on-girder bridges for; (a) exterior girder, and (b) interior girder

5.5 Conclusions

The effect of load distribution in straight and skewed slab-on-girder bridges was investigated by conducting a three-dimensional finite element modeling under CHBDC truck loading for ultimate, serviceability and fatigue limit states (ULS, SLS and FLS). Based on the results obtained from a parametric study, a set of empirical expressions were developed for the girder moment and shear distribution factors for rational prediction of the girder load distribution for ultimate and serviceability limit states, and fatigue limit state, respectively. Further, the load distribution factors for girder moment and shear obtained by FEA for both straight and skewed bridge was correlated with the proposed empirical equations and the CHBDC design guidelines. The results showed that the proposed equations for girder moment and shear distribution factors were in good agreement with the FEA results for both straight and skewed bridge configuration. However for straight bridge, the CHBDC equations given in clause 5.6.4.3 for estimating the load distribution factors under the live loads proved to be ineffective to capture the

behavior of most of the straight slab-on-girder bridge geometries. Also for skewed bridges, the CHBDC equations given in clause 5.6.6.2 for estimating skew effect gave conservative response for certain bridge configurations and for some other bridge geometries it produced highly under-estimated response, yielding to an unsafe design. Finally, to validate the accuracy of the proposed equations, a comparison of the developed proposed equations for the straight and skewed slab-on-girder bridge for the moment and shear distribution factors were made with the existing codes available in North America and also with the previous research work. Result showed the adequacy of the proposed equations in capturing the accurate response of the girders under the truck live loads. Furthermore, the reason of disagreement of the existing bridge code specifications with the proposed equations results were also highlighted. Based on this study, the equations specified in CHBDC needs to be modified to comprehend the shear stresses developing at girder supports under the influence of live loads. Also, it was recommended to include moment distribution equations proposed in this study for accurate assessment of girder flexural stresses. To facilitate bridge engineers and designers, comprehensive design example about the procedure to solve the proposed equations for distribution factors for different limits states were presented herein. The design examples were evaluated for both the straight and skewed bridge geometries. In these illustrative examples the moment distribution factors at the exterior and interior girders were computed and compared with the FEA and the bridge code specified equations. Similarly, the shear distribution factors at the girder obtuse, acute and at the interior girders were calculated by using the proposed equations for the straight and the skewed bridge configurations and the results were correlated with the FEA and the bridge design formulas for comparison purposes. The comparison of results suggested that the bridge design code equations were conservative for a straight bridge geometry. Further, for a bridge geometry at 40° skew angle produced highly conservative results for the moment and shear distribution factors. For-example for skewed bridges at ULS and SLS, the CHBDC design equations were found 30% conservative for both moment and shear distribution factors, and for FLS the code equations produced 42% and 72% conservative results for moment and shear distribution factors, respectively. The results of shear at the acute girders were found significantly affected with the increase of skew angle and the CHBDC equation was found unable to predict shear behavior at this

location. The main reason of difference was that since the design code equation was developed to represent the shear behavior at the girder obtuse corners (clause 5.6.6.2 of CSA 2014a) and according to the commentary of clause 5.6.6.2 (CSA 2014b), the same equation was applied to represent the behavior of the girders at the acute and interior girder locations.

CHAPTER 6

Skew Limitations for Composite Slab-on-Girder Bridges

6.1 General

In the past, highway bridges were placed by determining the most suitable crossing site and little attention was given to the general alignment of the roadway. In recent years, this situation has reversed and now bridges are planned in such a way that they must fit the highway alignment constraints. The growing demands of bridge structures on skewed alignment is presenting real challenges to bridge engineers, especially in the design of cross roadways, waterways, or railways that are not perpendicular to the bridge at the intersection. In North America, about 40% of the total bridge deck area is on skew alignment and about 10% of the total area is on heavy skews, ranging between 40° and 70° (Helba and Kennedy 1994).

Skew greatly complicates the behavior of slab-on steel I-girder bridges by introducing alternate load paths and causing complex interaction between the main girders and secondary framing members that can lead to significant construction and design problems (Coletti et al. 2011). In skewed bridges, under the influence of live loads, longitudinal girders undergo torsional rotation at the supports (Surana and Humar 1984). These rotations are the largest at the obtuse corners and difficult to predict (Choo et al. 2005). Over the past decade, several authors have drawn attention to the potential for steel I-girder twisting on highly skewed supports (AASHTO/NSBA 2003, Beckman et al. 2005, Coletti and Yadlosky (2005, 2007). In addition to girder twisting, skewed bridges can also lead to increased flange lateral bending stresses in the girders, as well as increased girder shears and end reactions for girders framing into the obtuse corners of the bridge and results in subsequent reductions in girder shears and end reactions, and even possibly undesirable uplift in girders, framing into the acute corners of the bridge (Fisher 2006, Ozgur et al. 2011). Furthermore, the presence of skew significantly reduces the longitudinal moment in the girders in comparison to straight bridges, and this effect is more pronounced in interior girders as compared to exterior girders. (Ebeido 1995, Diab et al. 2011).

It is frequently considered safe to ignore the skew angle, if it is less than 20° and analyze the bridge as a straight bridge with a span equal to the skew span, since this approach leads to a conservative estimate of forces in the skew bridge (OHBDC 1979; 1983, Khaloo and Mirzabozorg 2003, Menassa et al. 2007). The implication of this practice is that the angle of skew is considered to be the only necessary measure of the “skewness” of the bridge with respect to its load distribution characteristics. The use of this approximate procedure may lead to significant differences between the skew bridge responses and those of the equivalent straight bridge with larger skew angles. Based on the finite element analysis, numerous research work has been published (e.g., Marx et al. 1986, Khaleel and Itani 1990, Bishara et. al. 1993, Menassa et al. 2007, Mergel and Almansour 2010) indicating the mechanical behavior of skewed bridges being quite different from their straight counterparts.

Treating skewed bridge as straight bridge is one of the recommended method to simplify their analyses and design procedures, given certain limitations of applicability. The North American Bridge Code Specifications (CSA 2006a; 2014a, AASHTO 1996, AASHTO-LRFD 2014), have specified certain limitations to treat skewed bridges as straight ones. Based on the extensive comparative analyses of skew and equivalent right bridges, CHBDC (CSA 2006a) adopted the work of Bakht (1988) and Jaeger and Bakht (1989). This study shows that the angle of skew of the bridge is not the only necessary measure of its skewness but it is also dependent on span length, bridge width and girder spacing (CSA 2006b clause 5.7.1.1). In-order to characterize the skewness of a slab-on-girder bridges, clause 5.6.1.1-c of CHBDC (CSA 2006a) defines a dimensionless parameter as follow:

$$\varepsilon = \frac{S \tan \psi}{L} \leq \frac{1}{18} \quad (6.1)$$

where S , L , and ψ are the girder spacing, bridge span, and angle of skew, respectively. To allow the analysis of a skew bridge as an equivalent right bridge, the 2006 version of CHBDC (CSA 2006a) has imposed the upper limits of 1/18 for ε . This limit ensures that the shear values, in particular, are not in unsafe margin by more than 5%.

The current CHBDC (CSA 2014a) specification has removed these limits as specified in the previous version of CHBDC (CSA 2006a) of treating skew bridges as an equivalent straight bridge. However, CHBDC (CSA 2014a) clause 5.6.2-h(ix) requires that for steel-girder bridges, with skew angle not exceeding 20° , can now be analyzed for the longitudinal load effects using the simplified beam analogy method in accordance with clauses 5.6.3 to 5.6.9, unless some conditions are met as specified in clause 5.6.2. Also, based on the parametric study analysis of skewed slab-on-girder bridges by Theoret and Massicotte (2011), the CHBDC has now introduced a skew magnification factor F_s to modify the values of F_T (clause 5.6.4.1) to account for skew effects for shear at girder obtuse corners up to 45° skew angle (clause 5.6.6.2). Further in the commentary of the clause 5.6.6.2, it is stated that for simplicity, the same equation of shear magnification factor F_s as for dead load was retained for live load. However, based on the three-dimensional finite element modeling of skewed slab-on-girder bridges under dead loads, Razzaq et al. (2016) showed that the CHBDC equation to estimate the shear magnification factor at the obtuse corner results in conservative response for certain bridge configurations and for other bridge geometries it produces highly under-estimated response.

The other North American bridge design guidelines i.e. AASHTO Standard specifications (AASHTO 1996) have limited recommendations for designing skewed bridges. For skewed bridges up to 30° , the AASHTO recommends that the bridge be treated as straight with no modifications. However if the skew angle is greater than 30° , AASHTO suggests the use of an alternative superstructure configuration or to perform a refined analysis, such as, three-dimensional finite element analysis (Menassa et al. 2007, Diab et al. 2011). The limitations in the AASHTO standard specification are adequately addressed in the current LRFD bridge code (AASHTO-LRFD 2014) by including provisions considering skew for slab-on-girder bridges, such as, clause 4.6.2.2.2e and clause 4.6.2.2.3c specifies correction factors to adjust the longitudinal bending moment and shear force at the girder obtuse corner of a skewed bridge, respectively. These clauses are applicable within certain ranges of the design parameters (i.e. skew angle, span length, girder spacing etc.), that are often found too narrow and thus frequently exceeded in a routine design (Bishara et. al. 1993, Barr and Amin 2006, Nouri and Ahmadi 2012, Gheitasi and Harris 2015).

Given the discrepancies in skew limitations in different North American bridge codes, a practical design oriented parametric study was conducted to refine such limitations so that bridge engineers can design such complex structures more accurately and reliably. The following section describes in depth the research methodology we propose for better estimation of bridge skew limitations for the composite slab-on-I-girder bridges.

6.2 Parametric Study

The literature review presented earlier has demonstrated that the presence of skewness in bridge geometry substantially affects girder longitudinal bending moment and shear forces. For this reasons, the North American bridge codes (CSA 2014a, AASHTO-LRFD 2014) have addressed the behavior of a skewed bridge by developing equations for these load effects. In contrast to the AASHTO specifications, the CHBDC (CSA 2006a, 2014a) clause 3.4.4 specifies the deflection limit for serviceability limit state design of girders as a function of the fundamental flexural frequency of the bridge. As such, changes in girder bending moments, shear, and fundamental frequency of a skewed bridge are considered in this study in terms of a magnification factors when the skew angle changes from 0° to 60° .

The objectives of the current research were: (1) to evaluate the magnification factors for a skewed composite slab-on-girder bridge for different load effects (i.e. moment, shear and fundamental frequency), by conducting three-dimensional finite element analysis, and (2) for different load effects, magnification factor values were plotted for different skew angle ranging from 0° to 60° in order to estimate the most critical load case for which the magnification factors values exceed the permissible tolerance limit of $\pm 5\%$, and (3) finally, develop an empirical expression to represent the skew limitations for slab-on-girder bridges. To avoid repetition, the material and geometric properties including the selection of different finite elements and boundary conditions adopted to generate the three dimensional FE model of the bridge prototype have already been explained in chapter 4 and chapter 5 of this dissertation. Further the loading conditions adopted to develop finite element model for the evaluation of magnification factors under dead and live loads have already been explained in section 4.4.4 and section 5.2.5 of this dissertation, respectively.

6.2.1 Evaluation of Magnification Factors

A practical design oriented parametric study was conducted on selected skewed bridge systems to determine (1) the moment magnification factor, (2) the shear magnification factor, and (3) the fundamental flexural frequency magnification factor. These design parameters are explained as follows:

$$\text{Moment magnification factor} = \frac{\sigma_{Skew}}{\sigma_{Straight}} \quad (6.2)$$

where, σ_{Skew} and $\sigma_{Straight}$ are the maximum bending stresses obtained from the finite element modeling for a skewed bridge and a straight bridge of similar geometry and material characteristics, respectively. Since the literature review reveals that the presence of skew significantly reduces the longitudinal moment in the girders in comparison with straight bridges, and this effect is more pronounced in interior girders as compared to exterior girders. (Ebeido and Kennedy 1996c, Diab et al. 2011). Accordingly, the moment magnification factors for both the exterior and interior girders are evaluated using equation 6.2.

$$\text{Shear magnification factor} = \frac{V_{Skew}}{V_{Straight}} \quad (6.3)$$

where, V_{Skew} and $V_{Straight}$ are the maximum shear force obtained from the finite element modeling for a skewed bridge and a straight bridge of similar geometry and material characteristics, respectively. It is concluded from the literature review that the increase of skew angle causes substantial increase of shear force at the girder obtuse corner, and consequently results in the reduction of shear force at the girder acute corners as well as at the interior girders (Ebeido 1995, Ozgur et al. 2011). For this purpose the shear magnification factors at the girder obtuse, acute, and at interior girders are calculated using equation 6.3.

$$\text{Frequency magnification factor} = \frac{f_{Skew}}{f_{Straight}} \quad (6.4)$$

where, f_{Skew} and $f_{Straight}$ are the maximum fundamental flexural frequencies obtained from the finite element modeling for a skewed bridge and a straight bridge of similar geometry and material characteristics, respectively. As per clause 3.4.4 of CHBDC (CSA 2014a), bridge structure shall satisfy the requirements for the serviceability limit states, so that the maximum deflection due to the factored traffic load, including the dynamic load allowance, does not exceed the limit specified in Figure 3.1 of CHBDC (CSA 2014a) for the anticipated degree of pedestrian use. The CHBDC has presented this deflection limit criteria for the bridge structure in terms of first flexural frequency. For this reason, it was required to compute the magnification factors of a skewed slab-on-girder bridges by considering the flexural frequency of the structure.

All bridge configurations considered earlier in chapter 4 and chapter 5 of this dissertation were utilized for the evaluation of magnification factors using equation 6.2, 6.3 and 6.4 for moment, shear and flexural frequency respectively.

6.2.2 Results from the Parametric Study

In order to achieve the second objective of the parametric study, the magnification factor values were plotted against the skew angle ranging from 0° to 60° at an interval of 10° for different span lengths varying from 15 m to 40 m. To identify the limiting skew angle, the critical load cases were selected for which the magnification factor values for a skewed bridge were more susceptible to exceed $\pm 5\%$ tolerance limits when compared to a straight bridge. For load cases where the magnification factor values exceeds the $\pm 5\%$ tolerance limit between two skew angle range, located at 10° skew angle interval, the former skew angle was considered as a limiting skew angle for such load effect as can be seen in Figure 6.1, 6.2 and 6.3 for dead load, ULS and SLS, and FLS respectively. From Figure 6.1, it is clear that the shear force at obtuse corner resulted in limited skew angle of 20° out of all other load effects considered for this study under dead load conditions. Similarly, Figure 6.2 and 6.3 presents a limited skew angle of 10° while considering the shear at the obtuse, acute and interior girder location at ULS and SLS, and FLS respectively. For practical design purposes of treating skewed slab-on-girder bridge as an equivalent straight bridge with different bridge geometries, it was decided to proceed with the magnification factors

values of shear at obtuse, acute corners and interior girder locations at ULS and SLS as critical load condition for the development of skew limitation equation, since it represents the worst loading scenario that the bridge designers consider while designing a new bridge structure or evaluating the existing one (Soliman 1992, Ebeido 1995).

In order to precisely determine the parameters affecting the magnification factors, a sensitivity study was first undertaken to determine the influence of the different bridge parameters that may affect them. It was found that the key parameters that affect the structural response of a skewed bridge system are: (1) skew angle (ψ), (2) span length (L), (3) girder spacing (S), (4) number of girders (N), and (5) number of lanes (n). To avoid repetition, the effect of aforesaid superstructure variables on girder moment and shear distribution factors have already been discussed in section 4.4.5 and section 5.2.6 of this dissertation for dead and live load conditions, respectively. However, for brevity and space limitations the influence of critical parameters on the skewed bridge flexural frequency are presented and discussed in the following sub-section.

6.2.2.1 Effect of Skew Angle

Skew angle is the most critical factor that influences the flexural frequency of the bridge structure. Bapat (2009), based on the finite element modeling of skewed slab-on-girder bridges concluded that in case of a skewed bridge, the first three frequencies of vibration were found lower as compared to a straight aligned bridge. This effect will be more predominant in case of a bridge with higher skew. Figure 6.4, shows the FEA results of a frequency magnification factors for a skewed bridge at dead load, ULS and SLS, and FLS. The result shows that the increase in skew angle resulted in the reduction of the magnification factor. For dead load and at ULS and SLS up to 30° skew angle, the effect of skew angle on the flexural frequency of a bridge structure was found insignificant. Further, between 30° to 60° skew angle the frequency of the bridge shows substantial influence with the change of skew angle, and results in a maximum reduction of 35% and 38% in the response of a four-lane bridge for dead, and ULS and SLS load conditions respectively. However, in FLS this reduction in the response of frequency was more prominent when the skew angle changes from 50° to 60°.

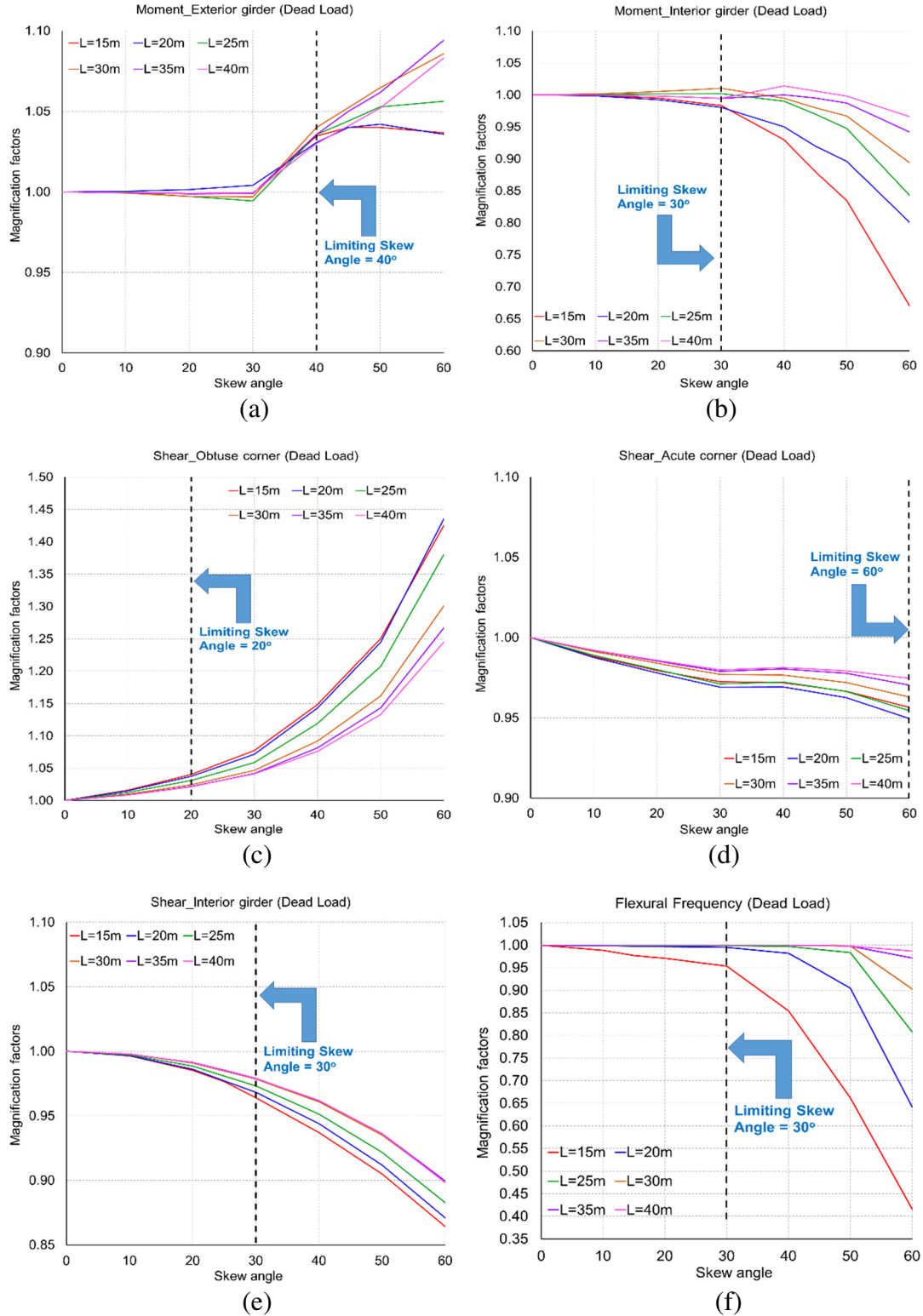


Figure 6.1 Magnification factor with limiting skew angle at dead load condition for: (a) moment for exterior girder, (b) moment for interior girder, (c) shear at obtuse corner, (d) shear at acute corner, (e) shear at interior girder, and (f) flexural frequency

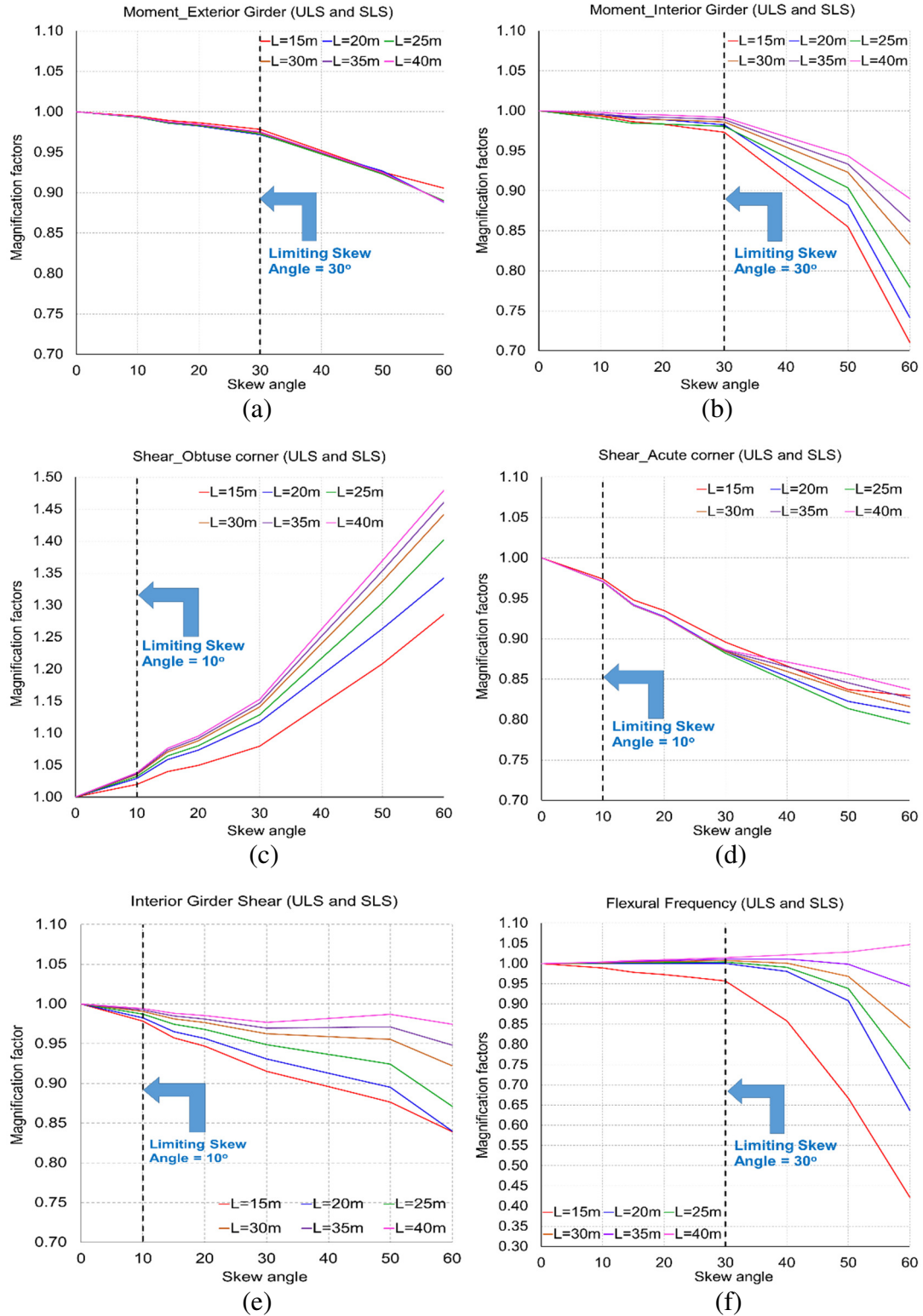


Figure 6.2 Magnification factor with limiting skew angle at ULS and SLS for: (a) moment for exterior girder, (b) moment for interior girder, (c) shear at obtuse corner, (d) shear at acute corner, (e) shear at interior girder, and (f) flexural frequency

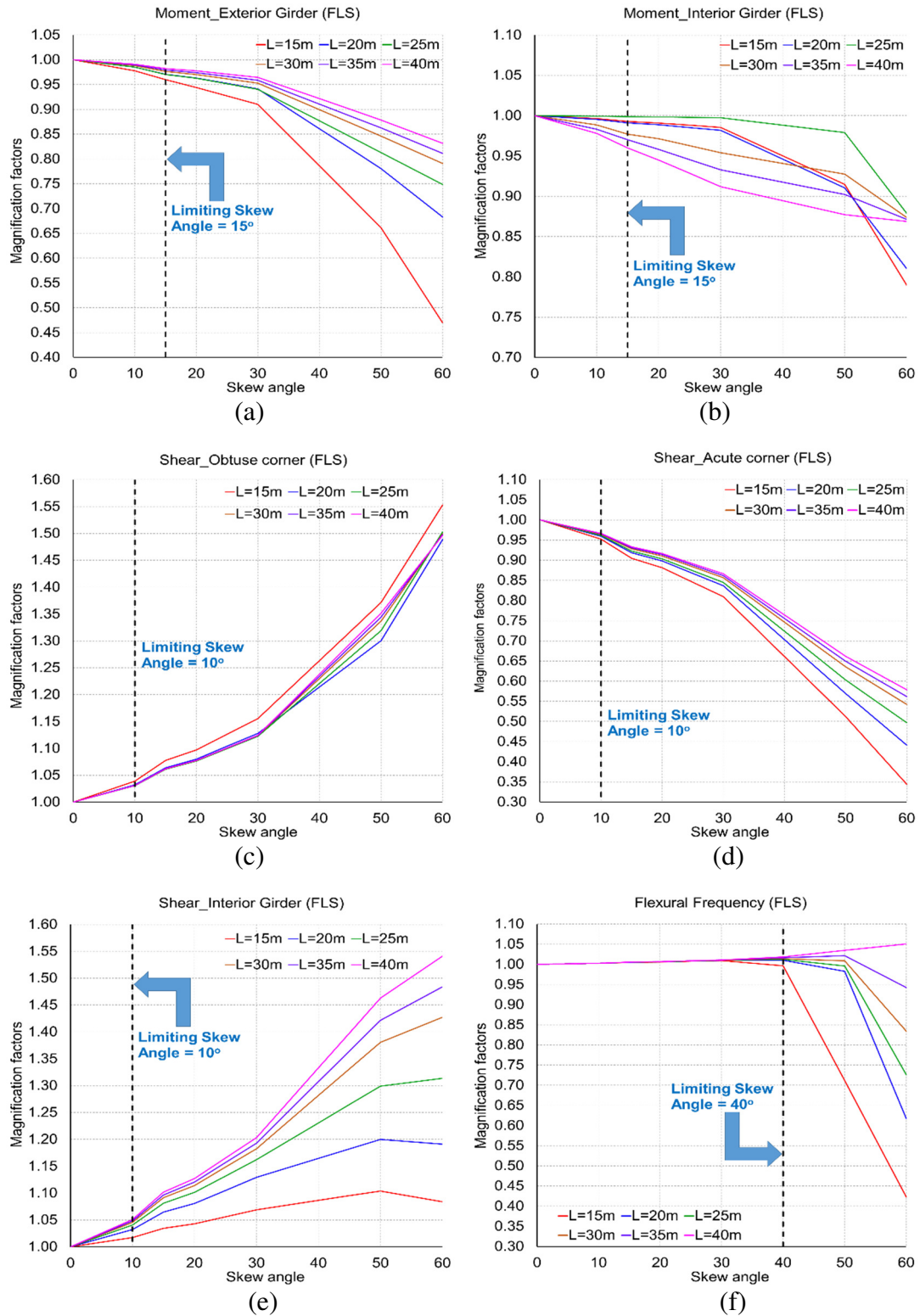
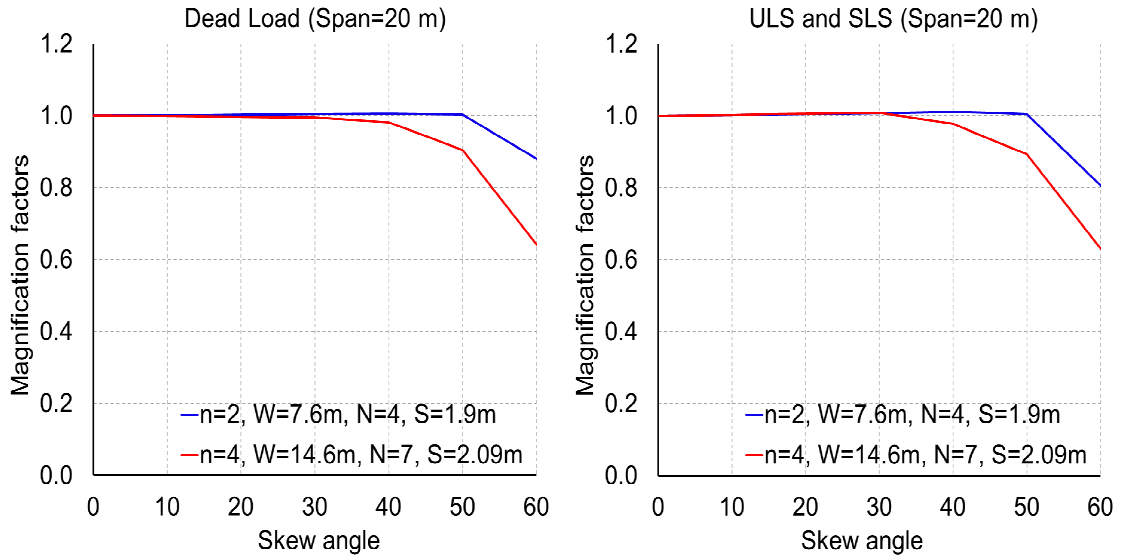
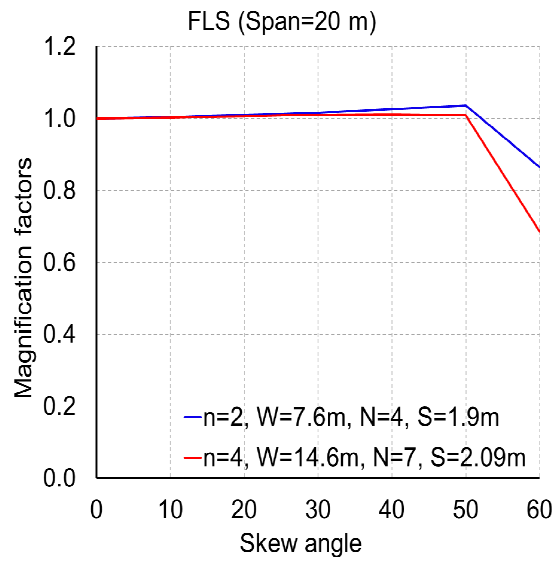


Figure 6.3 Magnification factor with limiting skew angle at FLS for: (a) moment for exterior girder, (b) moment for interior girder, (c) shear at obtuse corner, (d) shear at acute corner, (e) shear at interior girder, and (f) flexural frequency



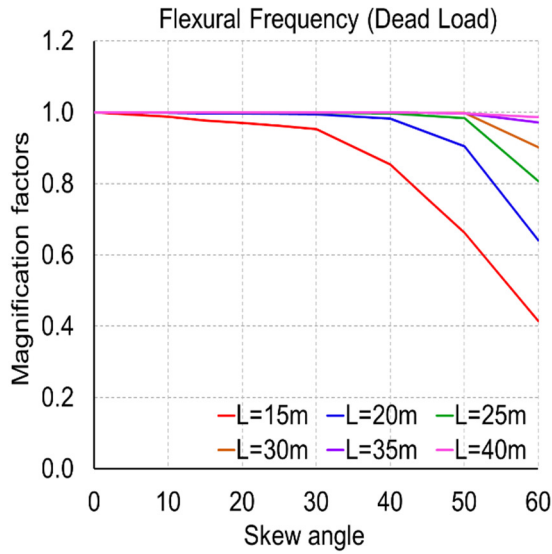
(a)

(b)

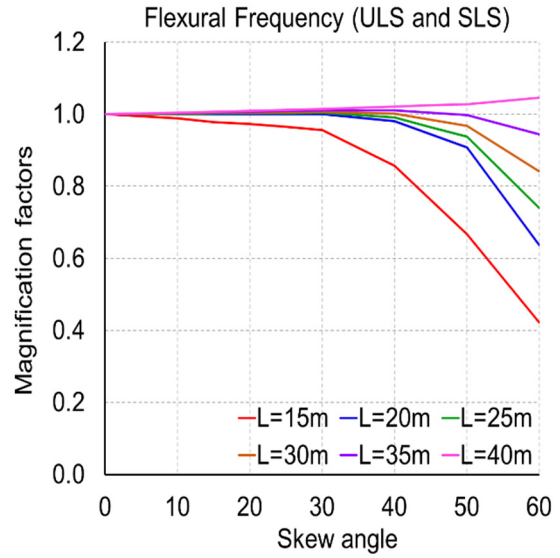


(c)

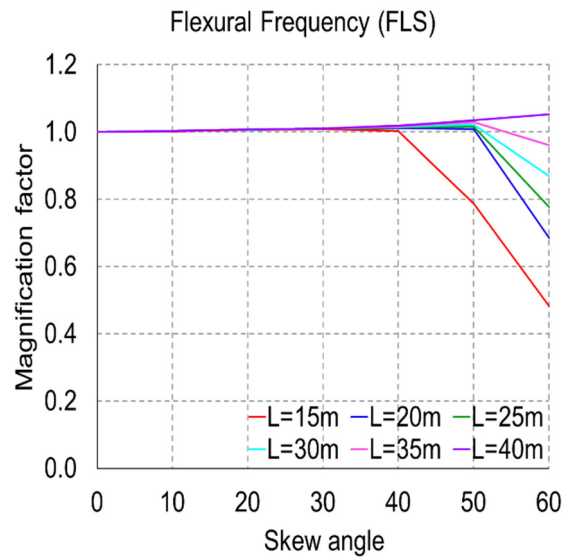
Figure 6.4 Effect of skew angle and bridge width on the flexural frequency of slab-on-girder bridge at: (a) dead load, (b) ULS and SLS, and (c) FLS



(a)



(b)



(c)

Figure 6.5 Effect of span length on the flexural frequency of slab-on-girder bridge at: (a) dead load, (b) ULS and SLS, and (c) FLS

6.2.2.2 Effect of Span Length

The effect of span length on the flexural frequency of a skewed bridge is shown in Figure 6.5. Six different span lengths ranging from 15 m to 40 m at a regular interval of 5 m were compared to evaluate the influence of flexural frequency with the variation of span length. The results showed that the effect is more noticeably in small span length and as the span length increases the effect of change of flexural frequency diminishes.

6.2.2.3 Effect of Bridge Width and Number of Lanes

The girder spacing is related to the bridge width and the number of longitudinal girders. Whereas, bridge width can be considered equal to the number of lanes multiplied by the lane width, which can be assumed to be constant for a given bridge configuration. Therefore the girder spacing could be dependent to the number of girders and the number of lanes. The effect of girder spacing on the frequency magnification factors are presented in Figure 6.4 for dead load, ULS and SLS, and FLS. The result shows that with the increase of number of lanes that is a function of bridge width, results in the reduction of frequency more drastically as compared to the bridge structure having less number of lanes and less bridge width.

6.2.3 Empirical Expression for Magnification Factors

In order to develop empirical expression, the critical data of magnification factors quantified previously in section 6.2.2 from the parametric study under ULS and SLS were used to develop empirical expressions for the magnification factors for shear at obtuse, acute and interior girder locations. Using regression analysis, a set of empirical equations was developed for single-span skewed bridges considered in this study.

Recently, the CHBDC (CSA 2014a) clause 5.6.3(b) has specified equations to compute the shear distribution factor for the skewed slab-on-girder bridges due to dead loads for shored sequence of construction, and for the sake of simplicity the same equation is retained for live load (clause 5.6.6.2). Further, it is stated in the commentary of clause 5.6.6.2 (CSA 2014b) that the factor F_s is to be applied to all the girders considering that it is a general

practice to have the same girder dimensions for the interior and exterior girders. The equation specified in CHBDC codes of practice is as follow:

$$F_s = 1.2 - \frac{2.0}{(\varepsilon + 10)} \quad (6.5)$$

where,

$$\varepsilon = \left(\frac{L}{S}\right) \cdot \tan \psi \quad (6.6)$$

For uniformity and simplicity in understanding the distribution factors for bridge designers and engineers, it was decided to keep the format of equation 6.5 the same as proposed in the code (CSA 2014a), and develop a modification for the “ ε ” factor that replaces equation 6.6, based on the parametric study results. Hence, the general empirical equation for the moment and shear “ ε ” factor took the following form, respectively;

$$\varepsilon = a \times L^b \times S^c \times N^d \times n^e \times \tan \psi \quad (6.7)$$

where, a, b, c, d and e are equation variables, L is the bridge span length in meters; S is the girder spacing in meters; N is the number of girders, and n is the number of design lanes. Using regression analyses sets of empirical equations for shear magnification factor for the girders at obtuse, acute corners and interior location at ULS and SLS of a skewed slab-on girder bridge were deduced and presented in Table 6.1.

Table 6.1 Magnification factor equation for live load at ULS & SLS

Load Effects	Magnification factor	ε
Shear - Obtuse	$1.2 - \frac{2.0}{(\varepsilon + 10)}$	$0.78 \times L^{0.95} \times S^{-3.18} \times N^{0.23} \times n^{0.02} \times \tan \psi$
Shear - Interior girder		$0.10 \times L^{2.13} \times S^{-0.09} \times N^{-2.41} \times n^{-3.0} \times \tan \psi$
Shear - Acute		$-18.98 \times L^{-0.25} \times S^{-0.22} \times N^{-0.08} \times n^{0.10} \times \tan \psi$

6.2.4 Empirical Expression for Skew Limitation

The developed empirical expressions for magnification factors were then extended to establish expressions for skew limitations to treat a skewed bridge as an equivalent straight bridge by setting the magnification factors to $\pm 5\%$ tolerance (i.e., magnification factor

equations were set equal to 1.05 if these factors increases with the increase of skew angle, otherwise it was set equal to 0.95 if these factors decreases with the increase of skew angle to produce skew limitations). The 5% tolerance was used as the basis to develop the skew limitations as specified in clause 5.7.1 of CHBDC (CSA 2006b). In the recent version of CHBDC (CSA 2014a), the skew limitations defined earlier in CHBDC (CSA 2006a) are removed for slab-on-girder bridges. However, the equations in terms of correction factors are introduced to accommodate the skewness in bridge geometry in both North American code specifications (CSA 2014a, AASHTO-LRFD 2014). Table 6.2 summarize the developed expressions for the skew limitations for concrete slab over steel I-girder bridges based on $\pm 5\%$ tolerance in the design parameters, respectively. The developed equations were a function of the span length (L), girder spacing (S), number of girder (N), number of lanes (n), and skew angle (ψ).

Table 6.2 Proposed skew limitations based on $\pm 5\%$ tolerance in design parameters

Magnification factor type	Span (L), m	Proposed Skew Limitation Equation
Shear - Obtuse	$15 \leq L \leq 40$	$L^{0.95} \times S^{-3.18} \times N^{0.23} \times n^{0.02} \times \tan \psi \leq 4.27$
Shear – Interior girder		$L^{2.13} \times S^{-0.09} \times N^{-2.41} \times n^{-3.0} \times \tan \psi \leq 33.33$
Shear - Acute		$L^{-0.25} \times S^{-0.22} \times N^{-0.08} \times n^{0.10} \times \tan \psi \geq 0.105$

6.2.5 Correlation of Proposed Equation with CHBDC (CSA 2006a)

In order to make the design of a skewed bridge more practical and understandable to bridge designers and engineers, a single decisive equation out of the three skew limitation equations presented in Table 6.2 was proposed by considering the shear force at the girder obtuse corners to be the most critical loading that significantly affect the behavior of a skewed bridge. Based on this finding it can be concluded that the proposed equation results in an accurate assessment of skew limitation for all the slab-on steel I-girder bridge configurations, since the developed limitation include additional parameters based on the parametric study analysis, such as, number of girders (N), and number of lanes (n) that do not exist in the 2006 CHBDC equation. Further, the concept of equivalent orthotropic plate theory used to evolve the skew limitation equation specified in CHBDC (CSA 2006a) has

limitation as discussed previously in chapter 2 of this dissertation, which may not be realistic for accurate assessment of skewed bridge behavior. Finally, Table 6.3 shows the correlation of the proposed equation with the CHBDC equations for limiting skew angle, and schematically presented in Figure 6.6. In Figure 6.6 all the bridge configurations were plotted and a comparison of limiting skew angle using the code design equation and the proposed equation was presented. The result shows that a limiting skew of 18° was obtained when considering the proposed equation, while CHBDC design equations resulted in a limiting skew angle of 14°.

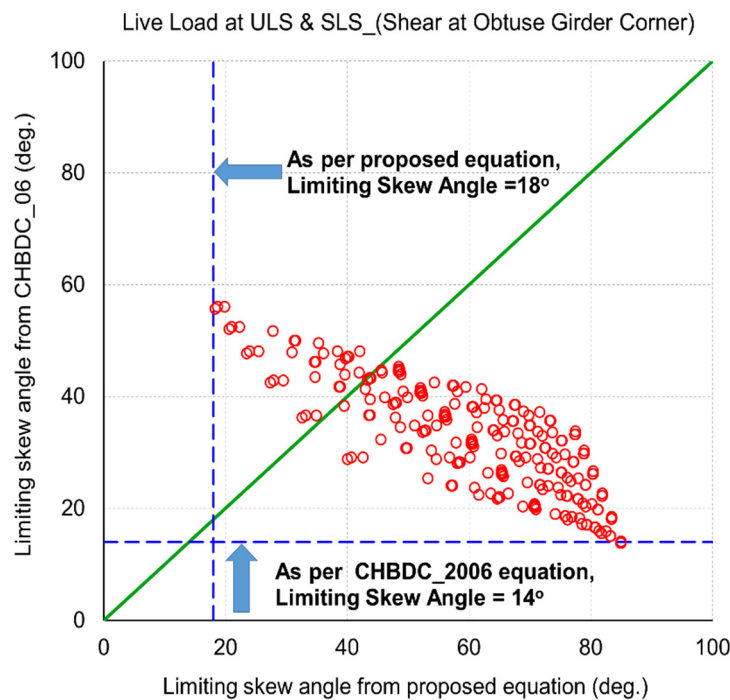


Figure 6.6 Correlation of proposed equation with CHBDC equation for skew limitation

Table 6.3 Correlation of proposed equation with CHBDC equation for skew limitation

Skew Limitation Criteria for Slab-on-girder bridge			
Proposed equation	Limiting skew angle using proposed equation, ψ , (deg.)	CHBDC (CSA 2006a) equation	Limiting skew angle using CHBDC equation, ψ , (deg.)
$L^{0.95} \times S^{-3.18} \times N^{0.23} \times n^{0.02} \times \tan \psi \leq 4.27$	18	$\frac{S \tan \psi}{L} \leq \frac{1}{18}$	14

6.3 Conclusions

To treat the skewed slab-over steel I-girder bridge as an equivalent straight bridge, the skew limitations were evaluated using three-dimensional finite element modeling to investigate the behavior under dead and live load conditions. The major internal forces developed in the members were determined during the parametric study, namely, girder longitudinal bending stresses, vertical shear forces and bridge fundamental flexural frequencies for different degrees of skewness, span length, bridge width, and number of lanes. Based on the results from the parametric study on slab-on-girder bridges, the magnification factors were evaluated for dead loads, ULS and SLS, and FLS respectively. The effect of magnification factor with the change of skew angle was found more predominant for the shear at the obtuse, acute corners and interior girder location at ULS and SLS. For these critical load cases, the magnification factor equations were developed and were set equal to $\pm 5\%$ tolerance error to generate the skew limitation equations for such load effects. Finally based on the most critical loading that significantly affect the behavior of a skewed bridge, the skew limitation equation for the shear force at the girder obtuse corner was proposed to represent the skew limitation criteria for a slab-on steel I-girder bridges.

CHAPTER 7

Load Distribution in Continuous Skewed Bridges

7.1 General

Simply supported structures are effectively utilized for highway bridges up to a certain span lengths, beyond which using continuous structures become inevitable and proved to be cost effective (Amiri 1988). The effect of span continuity results in the development of negative moments at the intermediate supports and consequently causes significant reduction in span moments. Thus for the design of a new continuous skewed slab-on-girder bridges and the evaluation of existing structures require an accurate assessment of girder forces at the span and support locations. The use of load distribution factors specified by codes of practice does simplify the analysis and design of bridges. However, inaccurate prediction of these distribution factors may lead to erroneous design forces especially in case of continuous skewed composite bridges.

The load distribution factors given by North American bridge code specifications (AASHTO-LRFD 2014, CSA 2014a) is limited to simply supported bridges when the skew parameters are less than certain limit specified in the code. The lack of adequate information regarding the load distribution factors for continuous skewed bridges leads to extremely conservative design moments for skewed bridges since the equations given in these bridge codes does not effectively represents the reduction in girder moment due to skewness (Khaleel and Itani 1990, Ebeido and Kennedy 1996a). Furthermore, these codes of practice lead to unsafe support reactions and girder shear forces since the equations does not adequately capture the distribution of such forces with the increase of skew angle (Ebeido and Kennedy 1996b, Modjeski and Masters 2002, Huo and Zhang 2008). In addition, these design specifications does not account for the effect of bridge continuity, nor the presence of intermediate transverse diaphragms are considered during the development of these codes of practice. For this purpose, a better understanding of the behavior of skewed continuous bridge is needed in order to develop an adequate method that proves to be accurate and easy to use for bridge designers.

It is also worth mentioning here that clause 5.6 of the CHBDC has specified equations to calculate the load distribution factors for a simply supported single span slab-on-girder bridges. Further, clause 5.6.4.6 states to use the same set of design equations for the multi-span bridges by considering the effective span length in accordance with Figure 5.1(a) of CHBDC. To address these concerns, the objective of the current study was to check the applicability of the proposed equations developed for moment and shear distribution factors for simply supported straight and skewed bridge geometry under the dead and CHBDC live load conditions to the continuous multi-span bridge structures.

In this chapter, the effect of critical parameters on the shear and moment distribution factors in continuous skewed composite slab-on-girder bridge are presented. The parameters considered for this study were: span length, girder spacing, number of girders, girder stiffness, number of design lanes and skew angle. A detailed parametric study was conducted on prototype continuous composite steel-concrete bridges subjected to CHBDC truck and lane loads, which ever produces the maximum effort, for the three limit states (ULS, SLS and FLS) and under dead load conditions.

7.2 Parametric Study

The basic bridge cross-sectional configurations considered herein are presented in Table 7.1. The number of lanes considered were 1, 2, 3 and 4 lanes with bridge width of 4.5 m for one-lane bridges, 7.6 m for two-lane bridges, 11.2 m for three-lane bridges, and 14.6 m for four-lane bridges. The span length was 15 m and 30 m, with a total bridge length of 30 m and 60 m. The number of girders considered was 3 for one-lane bridges, 4 for two-lane bridges, 5 for three-lane bridges, and 7 for four-lane bridges. For the above bridge widths and number of girders, the girder spacing ranged from 1.5 m to 2.24 m. The angle of skew were taken as 0° and 45° .

To avoid repetition, the material and geometric properties including the selection of different finite elements adopted to generate the three dimensional model of the bridge prototype have already been explained in chapter 4 and chapter 5. Further, section 4.4.5 and section 5.2.2 explicitly explains the procedure adopted to evaluate the moment and shear distribution factors under the dead and live load condition, respectively.

Table 7.1 Geometry of prototype bridges

Span length (L), m	Design lanes (n)	Bridge width (W), m	Number of girders (N)	Girder spacing (S), m	Girder cross-sectional dimensions, mm			
					Girder depth (d)	Flange width (bf)	Flange thickness (t1)	Web thickness (t2)
15	1	4.5	3	1.50	1000	300	20	14
	2	7.6	4	1.90	1000	300	20	14
	3	11.2	5	2.24	1000	300	20	14
	4	14.6	7	2.09	1000	300	20	14
30	1	4.5	3	1.50	1200	550	40	16
	2	7.6	4	1.90	1200	550	40	16
	3	11.2	5	2.24	1200	550	40	16
	4	14.6	7	2.09	1200	550	40	16

The purpose of this parametric study were: (1) to check the applicability of the previously developed equations for moment and shear distribution factors, in chapter 4 and chapter 5, for simply supported straight and skewed slab-on-girder composite bridge under the dead and live load conditions to the continuous bridge structure, and (2) if the proposed equations for simply supported bridge configuration show disagreement for continuous bridge geometries then based on the prototype bridges selected for this study generate a database for both moment and shear distribution factors leading to the formation of empirical equations for the design of continuous skewed composite bridges. The main assumption made in the idealization of the continuous skewed bridge structure suggested that both the reinforced concrete deck slab and the longitudinal steel girders were simply supported at the abutments and continuous over the intermediate piers. This assumption is endorsed by number of researchers (Amiri 1988, Ebeido and Kennedy 1996b, Nouri and Ahmadi 2012). However, other assumptions made for this study remains the same as explained earlier in section 5.2.1 of this dissertation.

7.2.1 Loading Condition

For the evaluation of load distribution factors under live load conditions for continuous bridge structure, Amiri (1988) and Mabsout et al. (1998) found that the AASHTO HS20 truck loading governed when determining the maximum positive bending moments in the girders, while the lane loading (or train of trucks) governed when determining the

maximum negative bending moments. In order to justify the critical loading conditions to generate the maximum load effects at the span and support locations using CHBDC truck and lane loading, a sensitivity study was carried out by considering a one-lane continuous bridge having two equal spans. For the first bridge configuration two equal spans of 15 m was considered, and two equal spans of 30 m were selected for the second bridge geometry. The width of the two span continuous bridge was kept constant (4.5 m) for all prototype bridge selected for this sensitivity study along with the number of girders (3) and girder spacing (1.5 m). The results showed that CL-W truck loading generated the maximum moments both at the span and intermediate support locations when considering first bridge configurations (i.e. two equal spans of 15 m each). However for the second bridge configuration (i.e. two equal spans of 30 m each), the loading arrangements suggested by Amiri (1988) and Mabsout et al. (1998) to generate the maximum load effects at the span and support hold valid. Since no clear indication about the critical loading arrangement was observed during the sensitivity study thus it was decided to proceed with both CL-W truck and lane load, whichever produces the maximum load effect, as per clause 3.8.4.1 of CHBDC (CSA 2014a). However, the application of dead load for the evaluation of distribution factors has already been explained in section 4.4.4 of this dissertation.

7.2.2 Boundary Condition

Appropriate selection of boundary conditions to suit the nature of the problem and type of structure is sometimes a complicated task. In modeling the continuous bridge structure supports, the lower nodes of the girder were restrained against translation in such way to simulate temperature-free bridge superstructure (Lee 1994). For this purpose in case of a two span bridge geometry, at both right and left ends one of the middle supports was restrained against vertical and lateral translations, and at the inner intermediate support one of the middle supports was restrained against all possible translations (vertical, lateral, and longitudinal). The rest of the continuous bridge supports were restrained only against vertical translations. Figure 7.1 shows the typical boundary conditions for two-span bridge configuration considered in this study.

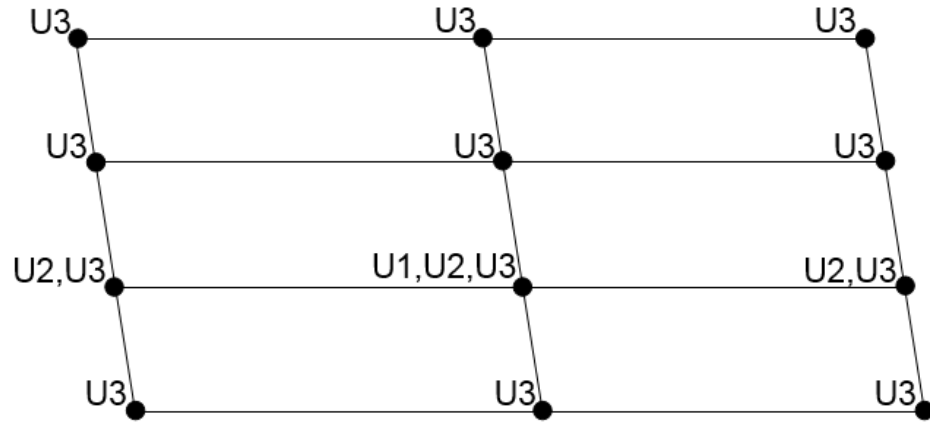


Figure 7.1 Boundary condition for two-span bridge model

7.2.3 Results from the Parametric Study

CHBDC (CSA 2014b) clause 5.6.4.6 states that all the equations for the simplified method were developed for simply supported span bridges, and by considering the equivalent span length (L_e) as shown in Figure 5.1(a) of CHBDC (CSA 2014a) all those equations can be applied to multi-span geometries and support conditions to determine their respective load distribution factors.

In order to achieve the first objective of the parametric study, the proposed load distribution factor equations developed earlier and the CHBDC (CSA 2014a) equations for single span bridges for span moment and shear under the dead load and live load conditions were tested against the load distribution factor data obtained for the two-span skewed bridge geometry. For this purpose, the equivalent span length (L_e) as specified for the use of the beam analogy method in clause 5.6 of CHBDC (CSA 2014a) was considered i.e.

For span load effects (i.e. moment and shear)

$$L_e = 0.75L_1 \quad (7.1)$$

For intermediate support load effects (i.e. moment and shear)

$$L_e = 0.25(L_1 + L_2) \quad (7.2)$$

where, L_e is the equivalent span length (m), and L_1 and L_2 are the clear span lengths (m) for the first and second spans respectively.

It was noticed that for straight single span bridge, the proposed equations developed earlier for dead load conditions showed reasonable correlation with the straight multi-span bridge data. Hence it was retained in this study for the evaluation of load distribution factors of a multi-span bridge at the span and support locations. However for other load conditions at different skew angle, it was observed that for some situations the previous developed proposed equations and the CHBDC simplified equations proved to be unsafe and for other conditions these equations produced conservative results. For comparison purposes, the span moment for the interior girder and the shear at the obtuse girder corners for a straight ($\psi=0^\circ$) and skewed ($\psi=45^\circ$) bridge under the dead and live load conditions are presented in Figure 7.2 to 7.7, respectively.

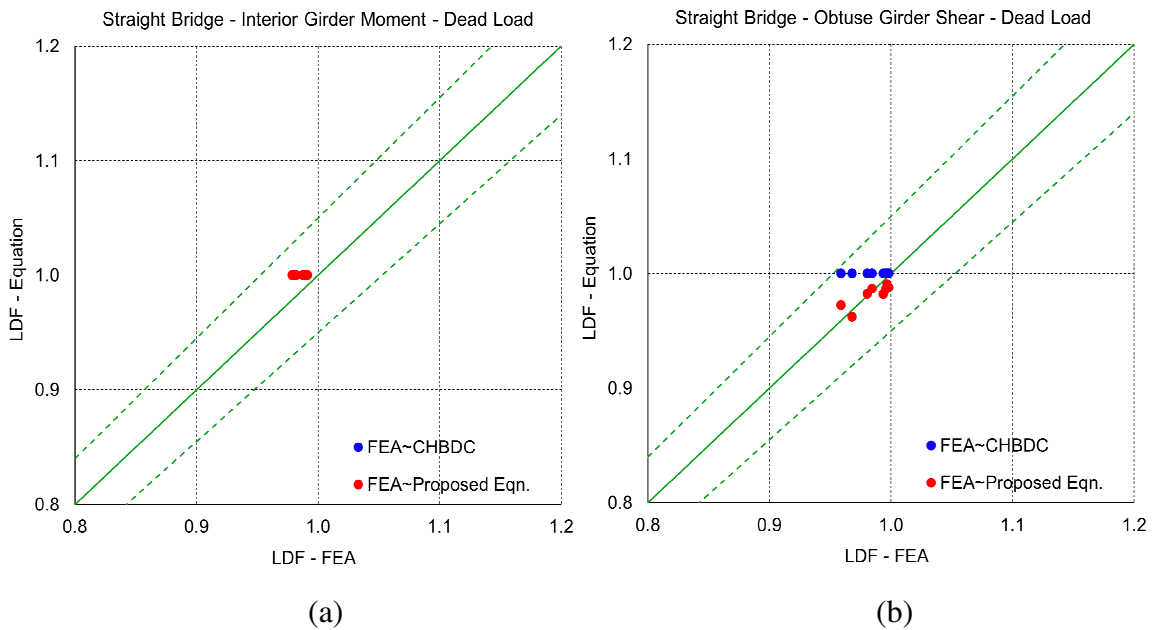


Figure 7.2 Correlation between load distribution factors at dead load obtained from FEA results with proposed equations and CHBDC equations for straight bridges for; (a) interior girder span moment, and (b) obtuse girder span shear

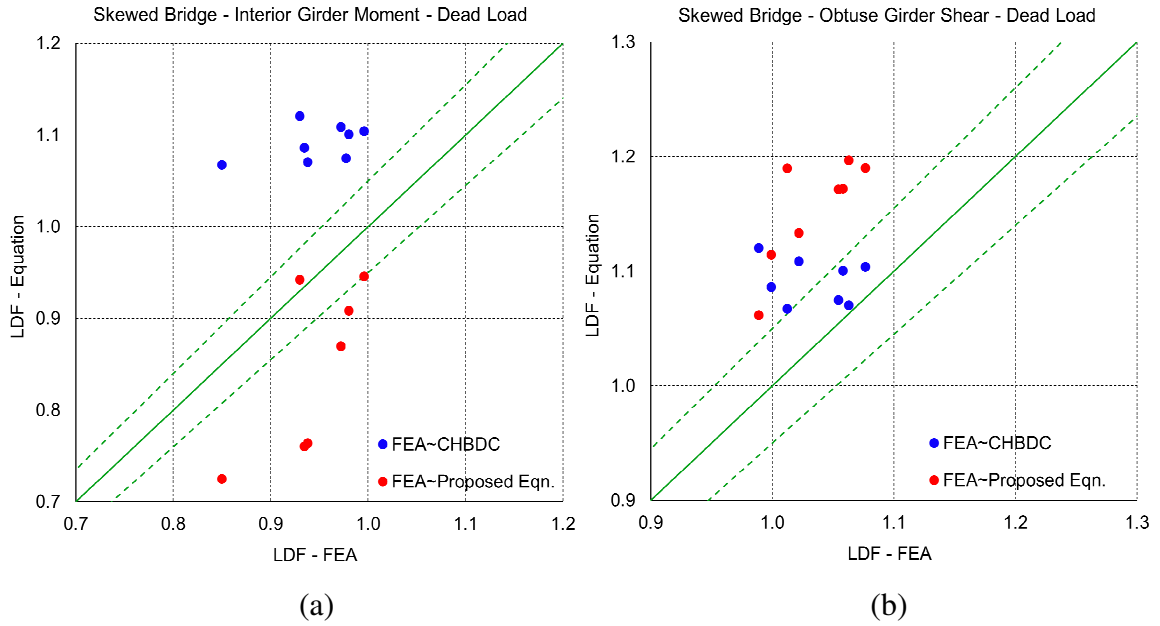


Figure 7.3 Correlation between load distribution factors at dead load obtained from FEA results with proposed equations and CHBDC equations for skewed bridges for; (a) interior girder span moment, and (b) obtuse girder span shear

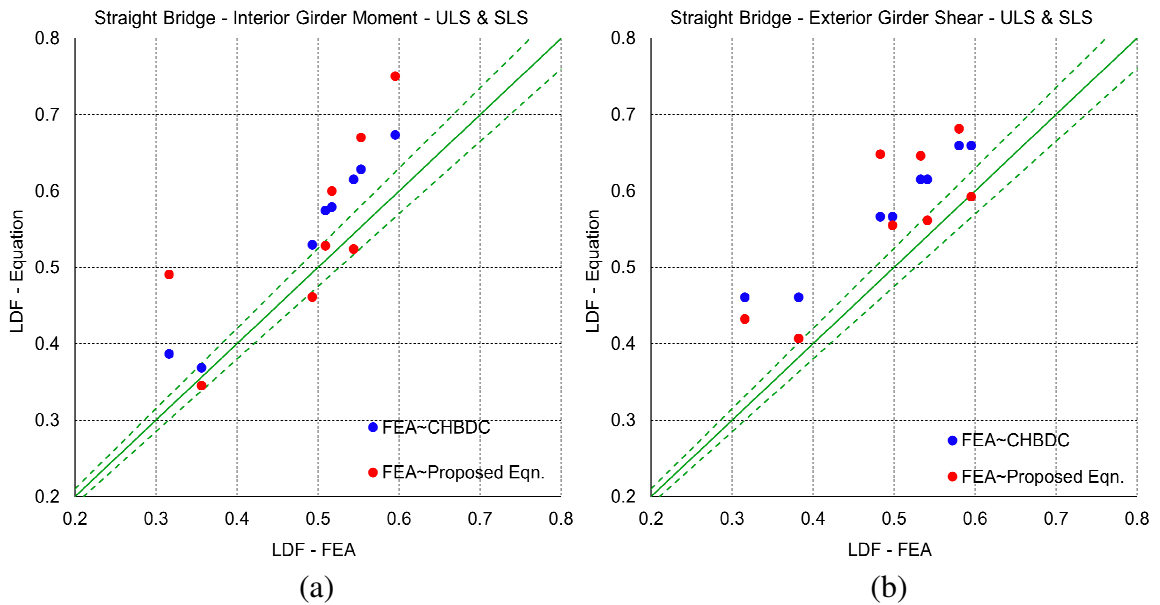


Figure 7.4 Correlation between load distribution factors at ULS and SLS obtained from FEA results with proposed equations and CHBDC equations for straight bridges for; (a) interior girder span moment, and (b) obtuse girder span shear

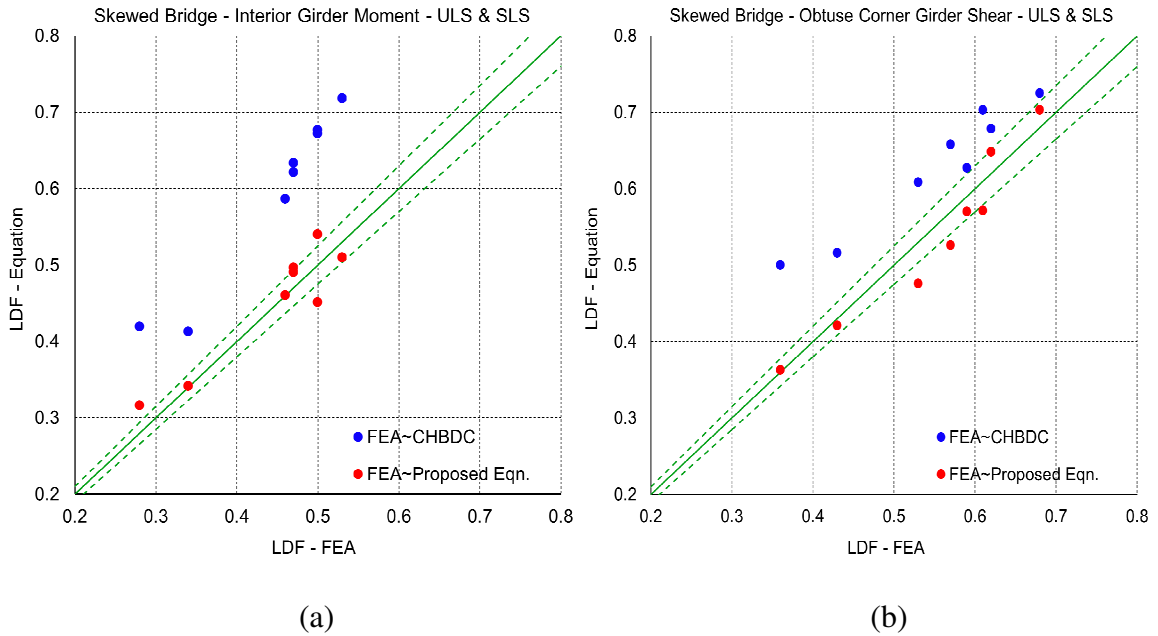


Figure 7.5 Correlation between load distribution factors at ULS and SLS obtained from FEA results with proposed equations and CHBDC equations for skewed bridges for; (a) interior girder span moment, and (b) obtuse girder span shear

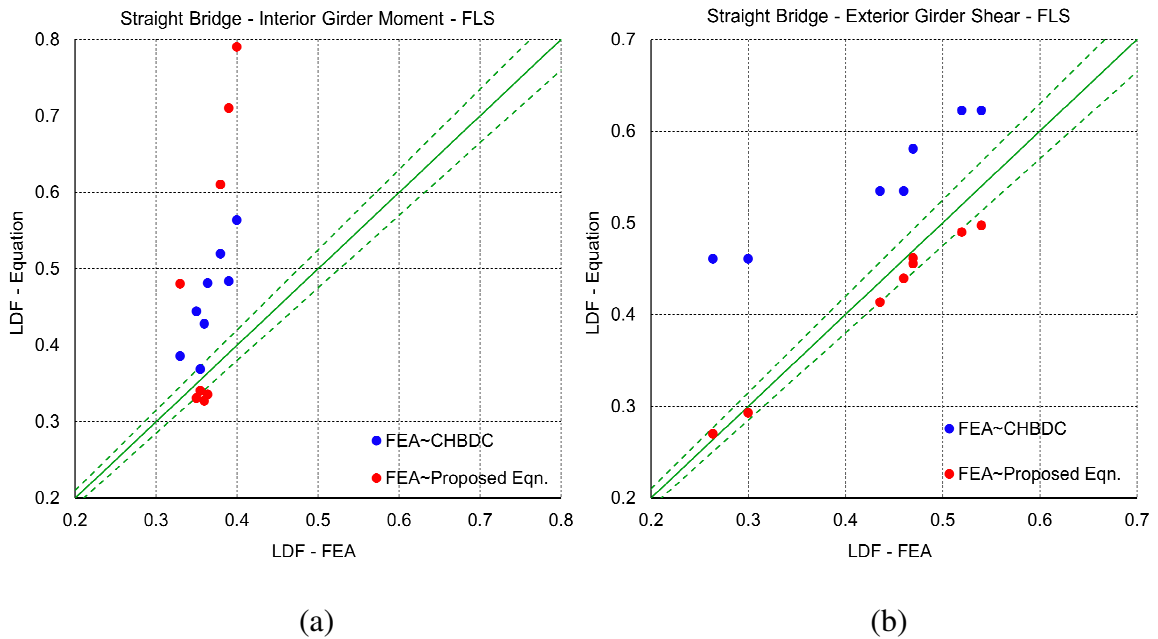


Figure 7.6 Correlation between load distribution factors at FLS obtained from FEA results with proposed equations and CHBDC equations for straight bridges for; (a) interior girder span moment, and (b) obtuse girder span shear

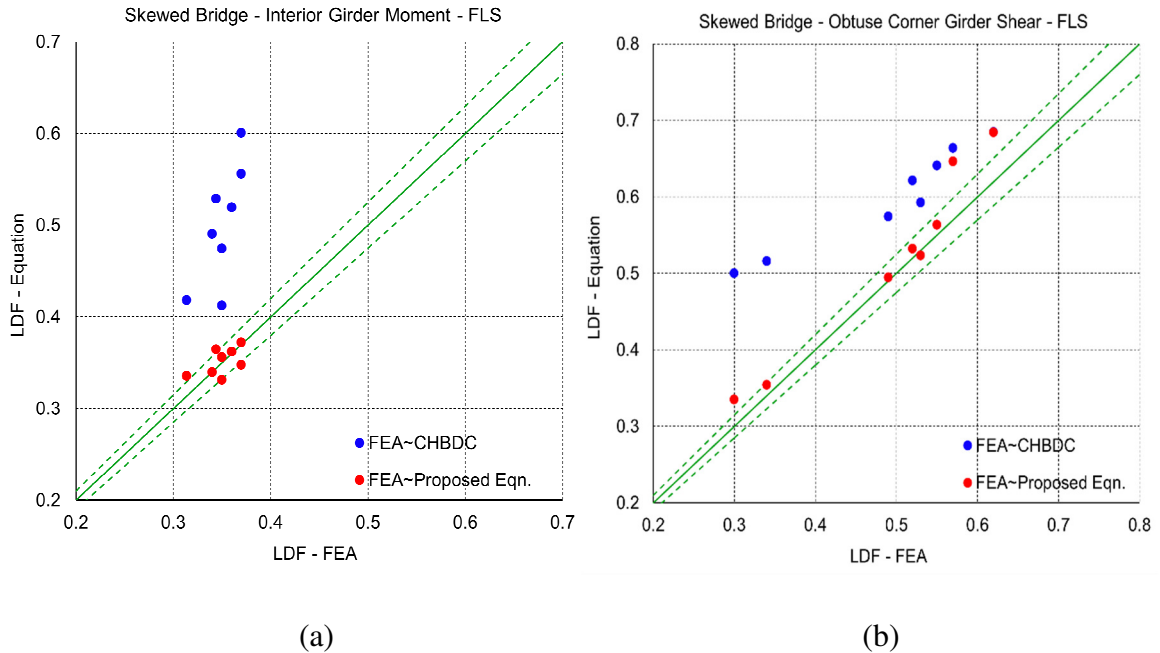


Figure 7.7 Correlation between load distribution factors at FLS obtained from FEA results with proposed equations and CHBDC equations for skewed bridges for; (a) interior girder span moment, and (b) obtuse girder span shear

Based on this finding, it was decided to proceed with the second objective of this study and develop new equations for the span and support load effects in case of two-span skewed bridge geometry. For the development of the new design equations, the effect of different bridge parameters was investigated against the data generated from the parametric study. The study revealed that at span and support locations the moment and shear distribution factors for a two-span straight and skewed slab-on-girder bridge were mainly influenced by few critical parameters, namely: span length, girder spacing, number of girders and number of design lanes. In-order to keep uniformity and simplicity in understanding the distribution factors for bridge designers and engineers, it was decided to keep the format of the equations the same as proposed previously in chapter 4 and chapter 5 for dead and live load conditions, respectively. By using regression analyses a set of empirical equations for moment and shear distribution factor for the straight continuous bridge at dead and live load conditions were developed. In order to take into account the skewness in bridge geometry a parameter F_s was evaluated and subsequently multiplied with the moment and the shear distribution factors for a straight bridge. The equations for a straight continuous bridge at span and support locations for dead load, ULS and SLS, and FLS are presented

in Table 7.2 to 7.7 respectively. Whereas, Table 7.8 to 7.13 represents the skewed continuous bridge at span and support locations for dead load, ULS and SLS, and FLS respectively.

Table 7.2 Span distribution factors under dead loads for straight continuous two-span bridge

Load effect	n	Fs	ϵ
Ext. Girder-Moment	1 to 4	$1.2 - \frac{2.0}{(\epsilon + 10)}$ *	$0.75 \times L_e^{-1.2} \times S^{1.3} \times N^{0.75} \times n^{1.5} \times \tan \psi$
Int. Girder-Moment			$-3.50 \times L_e^{-0.9} \times S^{1.25} \times N^{-0.75} \times n^{1.25} \times \tan \psi$
Obtuse Girder-Shear			$-0.14 \times L_e^{0.38} \times S^{-1.58} \times N^{1.72} \times n^{-1.14} \times \cos \psi$
Acute Girder-Shear			$-0.14 \times L_e^{0.38} \times S^{-1.58} \times N^{1.72} \times n^{-1.14} \times \cos \psi$
Interior Girder-Shear			$0.57 \times L_e^{0.41} \times S^{-0.67} \times N^{1.19} \times n^{-2.85} \times \cos \psi$

Table 7.3 Support distribution factors under dead loads for straight continuous two-span bridge

Load effect	n	Fs	ϵ
Ext. Girder-Moment	1 to 4	$1.2 - \frac{2.0}{(\epsilon + 10)}$ *	$0.75 \times L_e^{-1.2} \times S^{1.3} \times N^{0.75} \times n^{1.5} \times \tan \psi$
Int. Girder-Moment			$-3.50 \times L_e^{-0.9} \times S^{1.25} \times N^{-0.75} \times n^{1.25} \times \tan \psi$
Obtuse Girder-Shear			$-0.14 \times L_e^{0.38} \times S^{-1.58} \times N^{1.72} \times n^{-1.14} \times \cos \psi$
Acute Girder-Shear			$-0.14 \times L_e^{0.38} \times S^{-1.58} \times N^{1.72} \times n^{-1.14} \times \cos \psi$
Interior Girder-Shear			$0.57 \times L_e^{0.41} \times S^{-0.67} \times N^{1.19} \times n^{-2.85} \times \cos \psi$

Table 7.4 Span distribution factors at ULS and SLS for straight continuous two-span bridge

Load effect	n	D_T	λ	γ_c	γ_e
Ext. Girder-Moment	1 to 4	$(2.78 + 2.92L_e^{-0.33}) \times N^{-0.01}$	$\left(0.19 - \frac{0.04}{L_e}\right)$	$S^{-0.11}$	Not Applicable
Int. Girder-Moment		$(1.80 + L_e^{0.31}) \times N^{-0.01}$	$\left(-0.45 + \frac{12.75}{L_e}\right)$	$S^{-0.13}$	Not Applicable
Ext. Girder-Shear		$(1.72 + 14.93L_e^{-1.72}) \times N^{0.07}$	0.0	$\left(\frac{S}{8.30}\right)^{-0.44}$	Not Applicable
Int. Girder-Shear		$(1.897 + 1.95L_e^{0.06}) \times N^{0.06}$	0.0	$\left(\frac{S}{1.11}\right)^{-0.46}$	Not Applicable

Table 7.5 Support distribution factors at ULS and SLS for straight continuous two-span bridge

Load effect	n	D_T	λ	γ_c	γ_e
Ext. Girder-Moment	1 to 4	$(1.42 + 6.13L_e^{-0.47}) \times N^{0.11}$	$\left(-1.19 + \frac{16.33}{L_e}\right)$	$S^{-0.41}$	Not Applicable
Int. Girder-Moment		$(0.40 + 4.20L_e^{-0.10}) \times N^{0.12}$	$\left(-0.87 + \frac{13.97}{L_e}\right)$	$S^{-0.50}$	Not Applicable
Ext. Girder-Shear		$(6.38 + 5.79L_e^{-0.11}) \times N^{0.03}$	0.0	$\left(\frac{S}{0.09}\right)^{-0.354}$	Not Applicable
Int. Girder-Shear		$(4.65 + 0.12L_e^{-0.02}) \times N^{0.10}$	0.0	$\left(\frac{S}{0.92}\right)^{-0.60}$	Not Applicable

Table 7.6 Span distribution factors at FLS for straight continuous two-span bridge

Load effect	n	D_T	λ	γ_c	γ_e
Ext. Girder-Moment	1 to 4	$(-1.0 + 4.71L_e^{0.05}) \times N^{0.02}$	$\left(0.09 + \frac{7.20}{L_e}\right)$	$S^{-0.30}$	Table 5.7 of CHBDC
Int. Girder-Moment		$(1.09 + 1.09L_e^{0.11}) \times N^{0.10}$	0.05	$S^{0.59} \times \left(1.13 + \frac{0.98}{L_e}\right)$	0.0
Ext. Girder-Shear		$(1.76 + 1.77L_e^{-0.83}) \times N^{0.19}$	0.0	$3.12 \times S^{-0.89}$	0.0
Int. Girder-Shear		$(1.56 + 1.92L_e^{0.07}) \times N^{0.04}$	0.0	$0.83 \times S^{0.29}$	0.0

Table 7.7 Support distribution factors at FLS for straight continuous two-span bridge

Load effect	n	D_T	λ	γ_c	γ_e
Ext. Girder-Moment	1 to 4	$(-1.25 + 8.02L_e^{-0.17}) \times N^{0.08}$	$\left(-1.15 + \frac{20.90}{L_e}\right)$	$S^{-0.61}$	Table 5.7 of CHBDC
Int. Girder-Moment		$(1.68 + 2.94L_e^{-0.49}) \times N^{0.08}$	0.05	$S^{0.35} \times \left(1.13 + \frac{1.63}{L_e}\right)$	0.0
Ext. Girder-Shear		$(1.66 - 1.13L_e^{-1.60}) \times N^{0.18}$	0.0	$3.18 \times S^{-0.67}$	0.0
Int. Girder-Shear		$(23.40 - 0.28L_e^{-0.13}) \times N^{0.06}$	0.0	$0.13 \times S^{0.40}$	0.0

Table 7.8 Span distribution factors under dead loads for skewed continuous two-span bridge

Load effect	n	Fs	ε
Ext. Girder-Moment	1 to 4	$1.2 - \frac{2.0}{(\varepsilon + 10)}$ *	$0.02 \times L_e^{0.66} \times S^{0.13} \times N^{1.76} \times n^{-0.08} \times \tan \psi$
Int. Girder-Moment			$-1.545 \times L_e^{-0.60} \times S^{3.20} \times N^{0.25} \times n^{-0.64} \times \tan \psi$
Obtuse Girder-Shear			$3.13 \times L_e^{-0.10} \times S^{-3.28} \times N^{0.18} \times n^{2.10} \times \tan \psi$
Acute Girder-Shear			$-331.75 \times L_e^{0.22} \times S^{-9.48} \times N^{-2.05} \times n^{-1.53} \times \tan \psi$
Interior Girder-Shear			$0.31 \times L_e^{0.96} \times S^{-0.06} \times N^{-0.65} \times n^{-1.17} \times \tan \psi$

Table 7.9 Support distribution factors under dead loads for skewed continuous two-span bridge

Load effect	n	Fs	ε
Ext. Girder-Moment	1 to 4	$1.2 - \frac{2.0}{(\varepsilon + 10)}$ *	$-423.66 \times L_e^{4.72} \times S^{10.0} \times N^{-20.24} \times n^{5.0} \times \tan \psi$
Int. Girder-Moment			$-60.51 \times L_e^{-0.58} \times S^{0.70} \times N^{-2.02} \times n^{1.2} \times \tan \psi$
Obtuse Girder-Shear			$-0.28 \times L_e^{0.34} \times S^{0.34} \times N^{0.12} \times n^{-2.77} \times \tan \psi$
Acute Girder-Shear			$-331.75 \times L_e^{0.22} \times S^{-9.48} \times N^{-2.05} \times n^{-1.53} \times \tan \psi$
Interior Girder-Shear			$0.31 \times L_e^{0.96} \times S^{-0.06} \times N^{-0.65} \times n^{-1.17} \times \tan \psi$

Table 7.10 Span distribution factors at ULS and SLS for skewed continuous two-span bridge

Load effect	n	Fs	ε
Ext. Girder-Moment	1 to 4	$1.2 - \frac{2.0}{(\varepsilon + 10)}$ *	$-29.0 \times L_e^{-0.04} \times S^{-2.38} \times N^{-1.46} \times n^{1.64} \times \tan \psi$
Int. Girder-Moment			$-30.0 \times L_e^{-0.48} \times S^{0.35} \times N^{-0.985} \times n^{0.33} \times \tan \psi$
Obtuse Girder-Shear			$100.0 \times L_e^{1.02} \times S^{-7.10} \times N^{-1.20} \times n^{2.05} \times \tan \psi$
Acute Girder-Shear			$-2.70 \times L_e^{0.01} \times S^{0.92} \times N^{0.02} \times n^{-0.24} \times \tan \psi$
Interior Girder-Shear			$0.11 \times L_e^{3.11} \times S^{-0.14} \times N^{-5.41} \times n^{-2.75} \times \tan \psi$

Table 7.11 Support distribution factors at ULS and SLS for skewed continuous two-span bridge

Load effect	n	Fs	ε
Ext. Girder-Moment	1 to 4	$1.2 - \frac{2.0}{(\varepsilon + 10)}$ *	$0.02 \times L_e^{7.13} \times S^{-11.09} \times N^{-2.95} \times n^{0.04} \times \tan \psi$
Int. Girder-Moment			$0.02 \times L_e^{0.24} \times S^{1.45} \times N^{0.50} \times n^{2.41} \times \tan \psi$
Exterior Girder-Shear			$500.0 \times L_e^{2.38} \times S^{-7.45} \times N^{-5.47} \times n^{4.13} \times \tan \psi$
Interior Girder-Shear			$0.02 \times L_e^{7.17} \times S^{-1.67} \times N^{-7.67} \times n^{5.43} \times \tan \psi$

Table 7.12 Span distribution factors at FLS for skewed continuous two-span bridge

Load effect	n	Fs	ε
Ext. Girder-Moment	1	$1.2 - \frac{2.0}{(\varepsilon + 10)}$ *	$-2.62 \times L_e^{-0.59} \times S^{1.79} \times N^{0.42} \times n^{-0.51} \times \tan \psi$
	to 4		
Int. Girder-Moment			$-0.33 \times L_e^{-0.64} \times S^{7.59} \times N^{-0.27} \times n^{-1.76} \times \tan \psi$
Obtuse Girder-Shear			$92.13 \times L_e^{1.06} \times S^{-12.0} \times N^{0.57} \times n^{3.72} \times \tan \psi$
Acute Girder-Shear			$-0.01 \times L_e^{-0.05} \times S^{6.21} \times N^{3.29} \times n^{-3.56} \times \tan \psi$
Interior Girder-Shear			$8.39 \times L_e^{0.23} \times S^{-1.19} \times N^{-1.85} \times n^{2.07} \times \tan \psi$

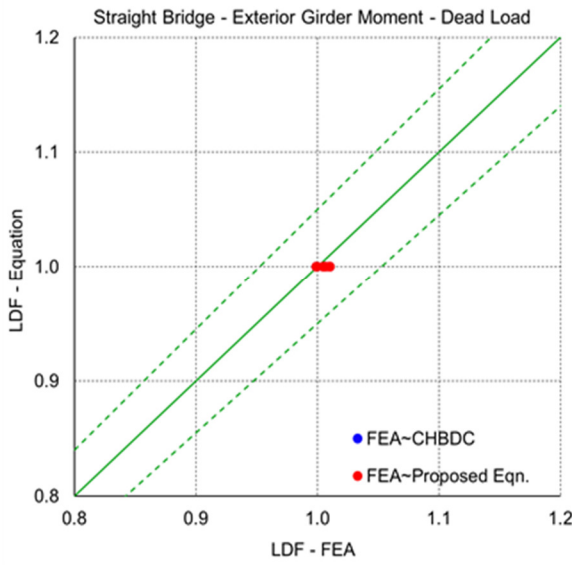
Table 7.13 Support distribution factors at FLS for skewed continuous two-span bridge

Load effect	n	Fs	ε
Ext. Girder-Moment	1	$1.2 - \frac{2.0}{(\varepsilon + 10)}$ *	$0.20 \times L_e^{7.71} \times S^{-10.27} \times N^{-9.33} \times n^{5.10} \times \tan \psi$
	to 4		
Int. Girder-Moment			$95.14 \times L_e^{-0.09} \times S^{-2.93} \times N^{0.85} \times n^{-3.22} \times \tan \psi$
Exterior Girder-Shear			$106.95 \times L_e^{2.54} \times S^{-6.92} \times N^{-3.18} \times n^{2.74} \times \tan \psi$
Interior Girder-Shear			$0.20 \times L_e^{2.36} \times S^{-0.73} \times N^{-1.99} \times n^{1.60} \times \tan \psi$

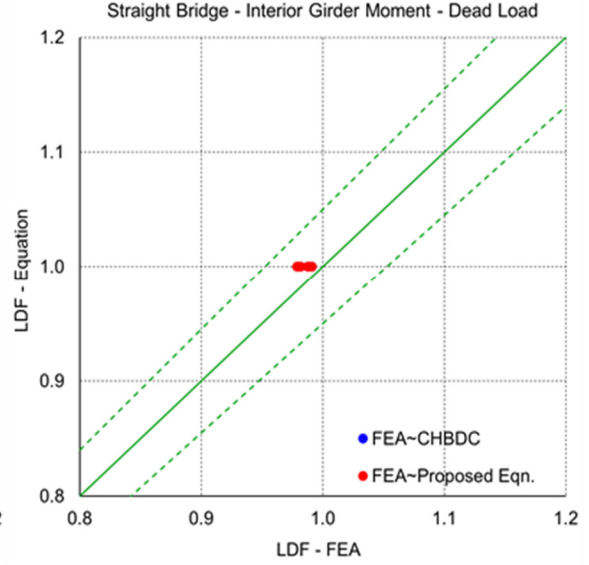
7.2.4 Correlation of FEA Results and Proposed Equations with CHBDC

The correlation between the CHBDC (CSA 2014a) equations and the proposed equations based on the parametric study for the moment and shear distribution factors for straight and skewed two span continuous bridge at dead and live load conditions were evaluated and compared with the load distribution factors (LDF) from the finite element analysis results, and presented in Figure 7.8 to 7.13 for a straight continuous bridge at span and support locations for dead load, ULS and SLS, and FLS respectively. Whereas, Figure 7.14 to 7.19 represents the correlation of a skewed continuous bridge at span and support locations for dead load, ULS and SLS, and FLS respectively. The results shows good correlation between the values obtained from proposed equations and those calculated

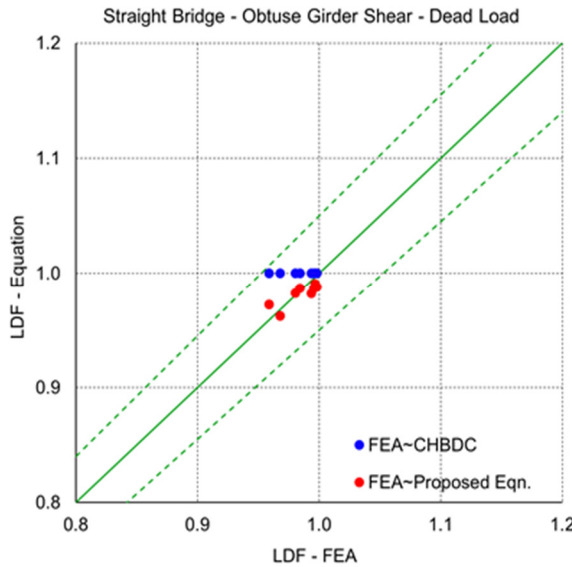
results from FEA, and all the data points fall within $\pm 5\%$ perfect correlation line, shown by dotted lines in Figure 7.8 to 7.19.



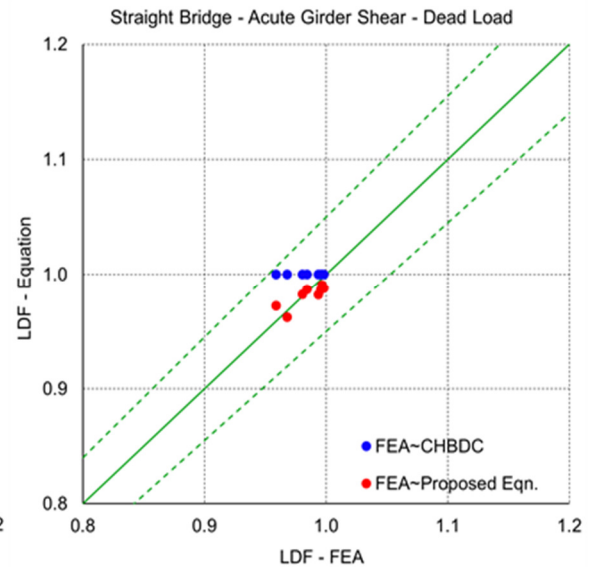
(a)



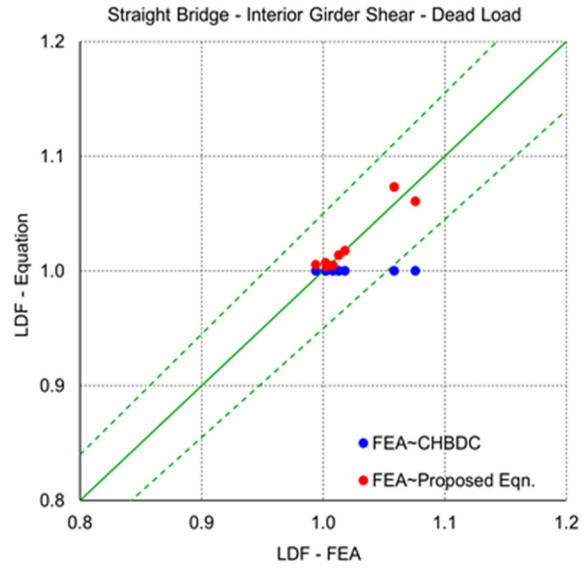
(b)



(c)

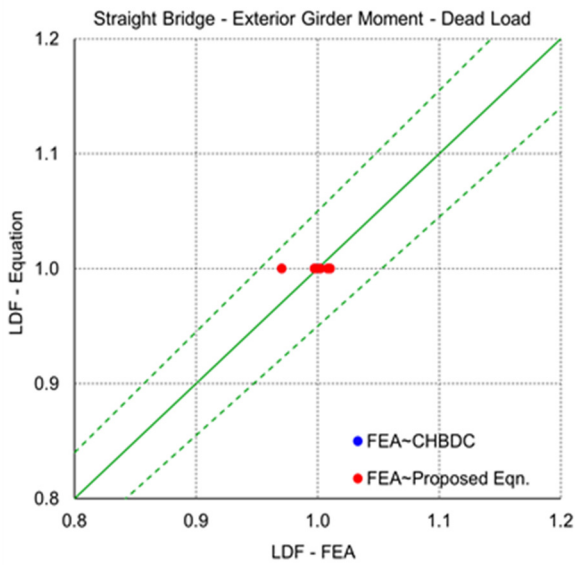


(d)



(e)

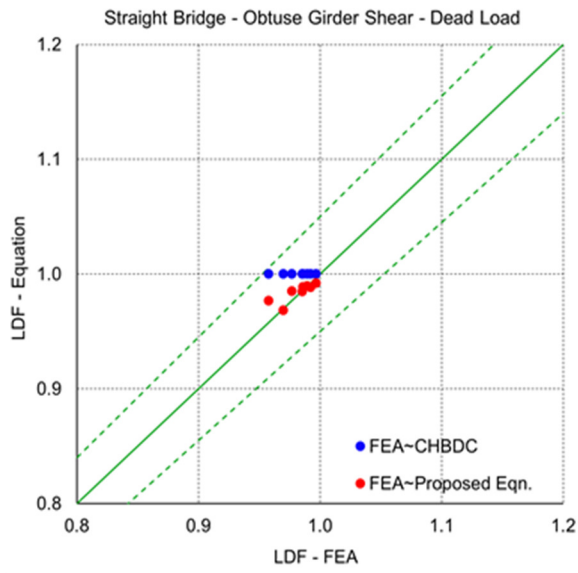
Figure 7.8 Correlation between span load distribution factors at dead load obtained from FEA results with proposed equations and CHBDC equations for straight bridges for; (a) exterior girder moment, (b) interior girder moment, (c) obtuse girder shear, (d) acute girder shear, and (e) interior girder shear



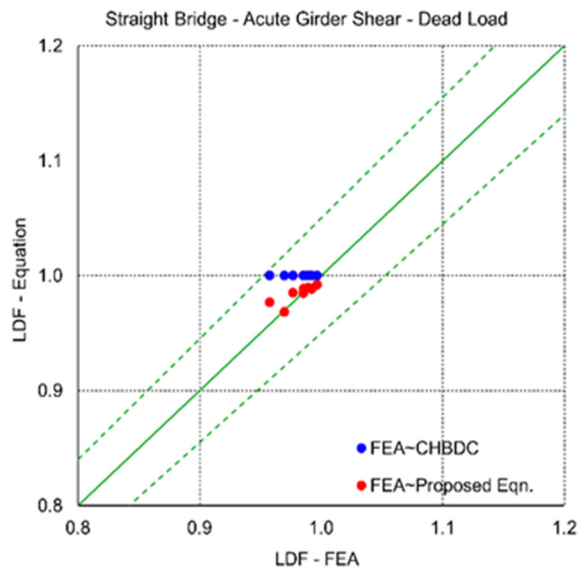
(a)



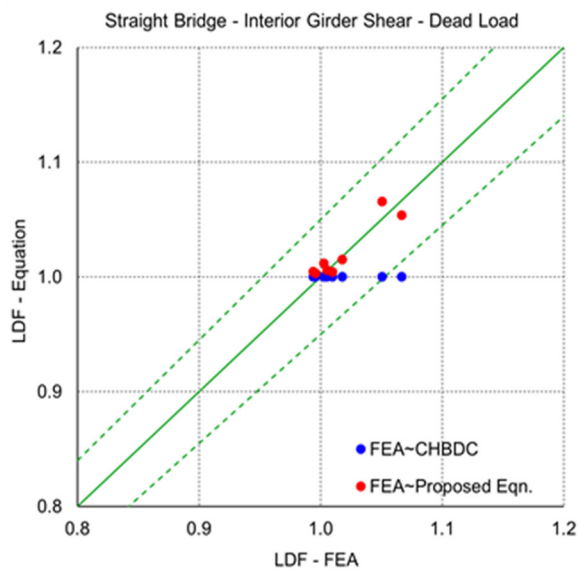
(b)



(c)

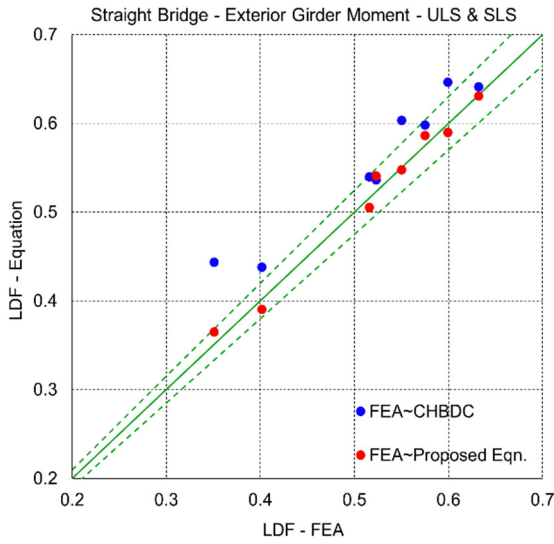


(d)

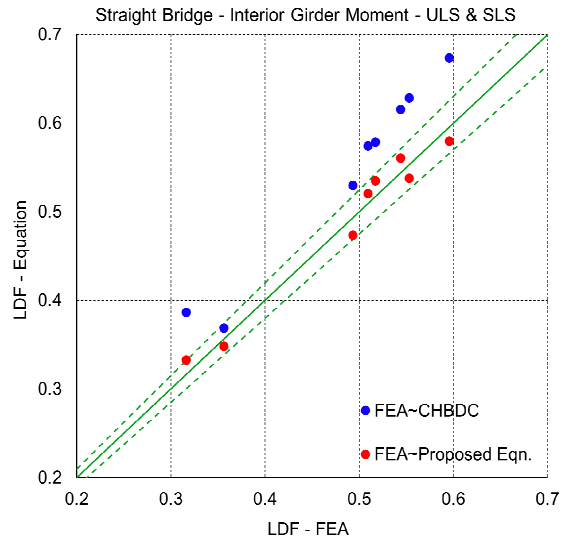


(e)

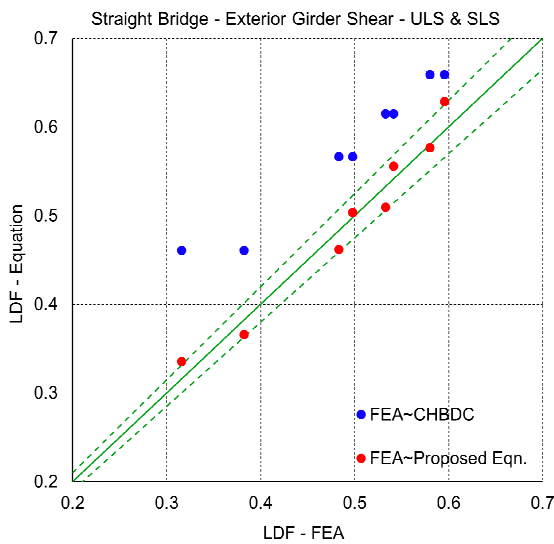
Figure 7.9 Correlation between support load distribution factors at dead load obtained from FEA results with proposed equations and CHBDC equations for straight bridges for; (a) exterior girder moment, (b) interior girder moment, (c) obtuse girder shear, (d) acute girder shear, and (e) interior girder shear



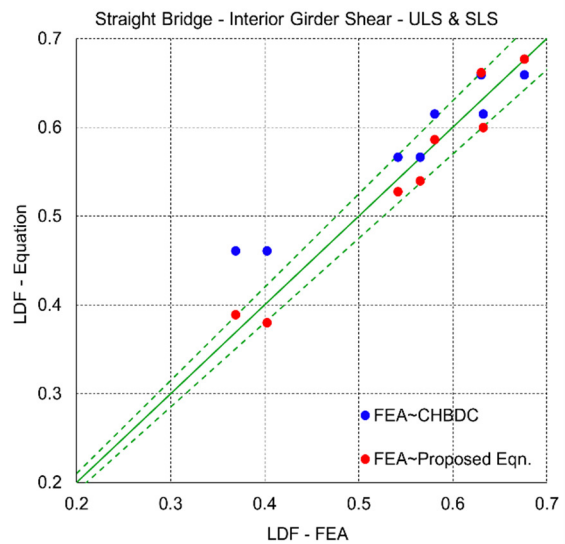
(a)



(b)

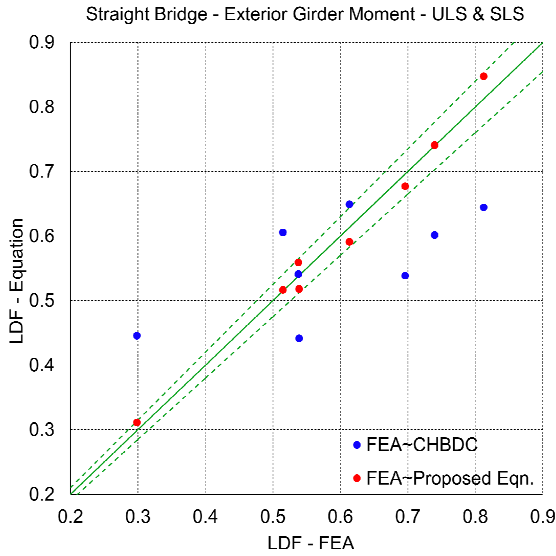


(c)

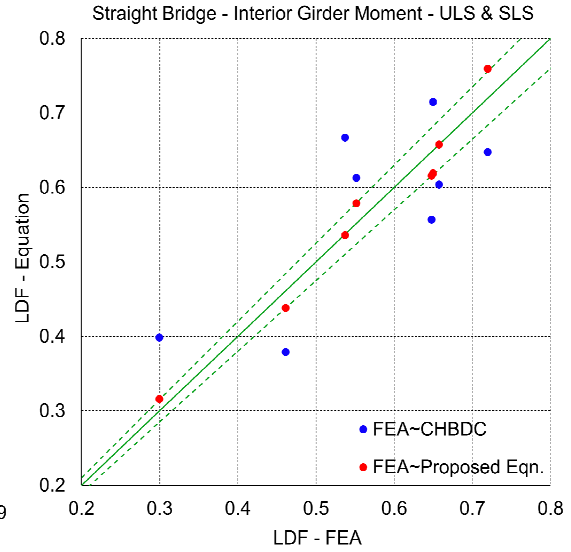


(d)

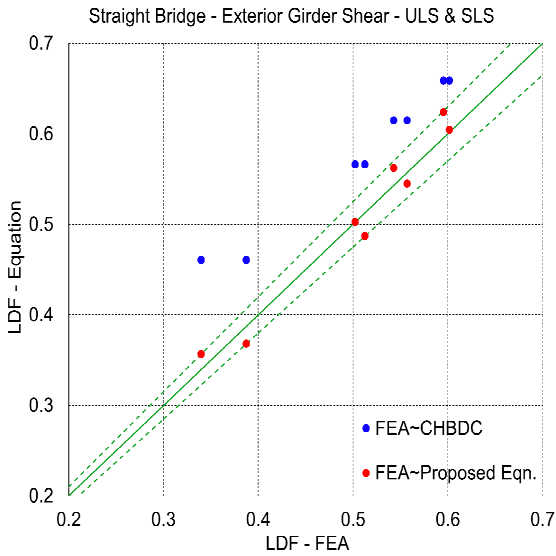
Figure 7.10 Correlation between span load distribution factors at ULS and SLS obtained from FEA results with proposed equations and CHBDC equations for straight bridges for; (a) exterior girder moment, (b) interior girder moment, (c) exterior girder shear, and (d) interior girder shear



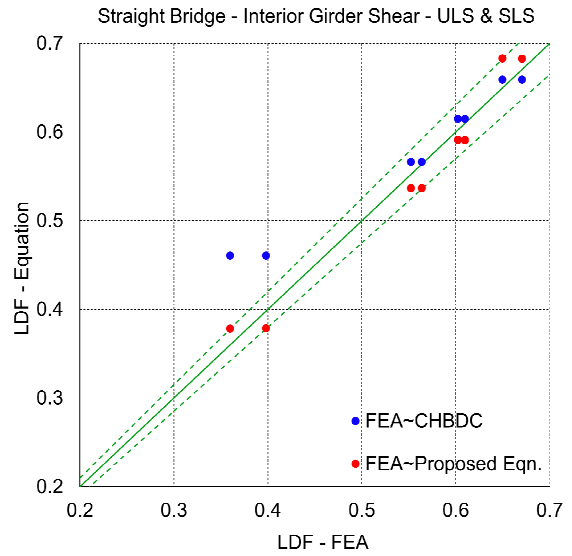
(a)



(b)

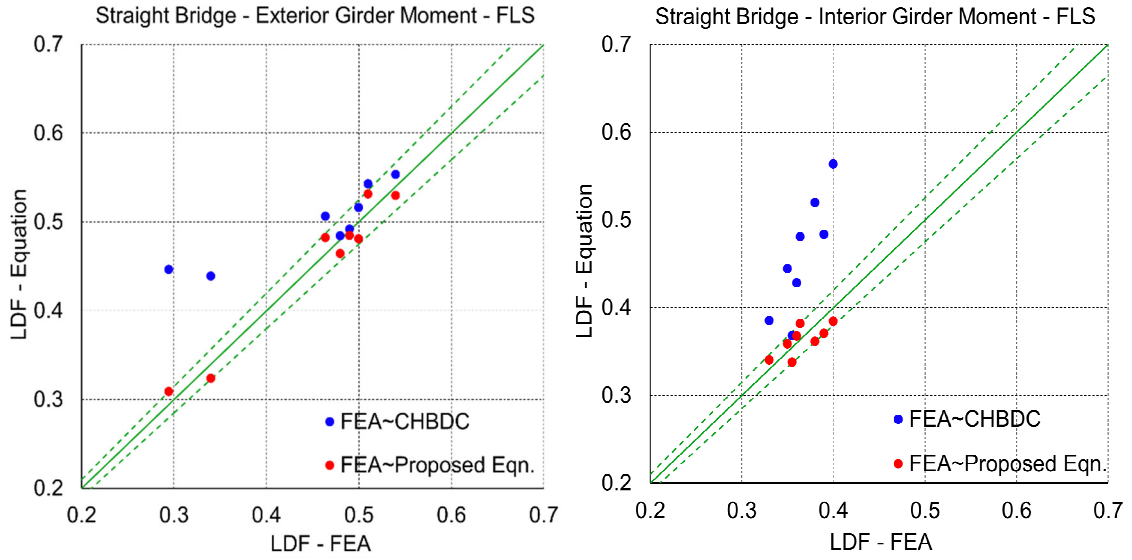


(c)



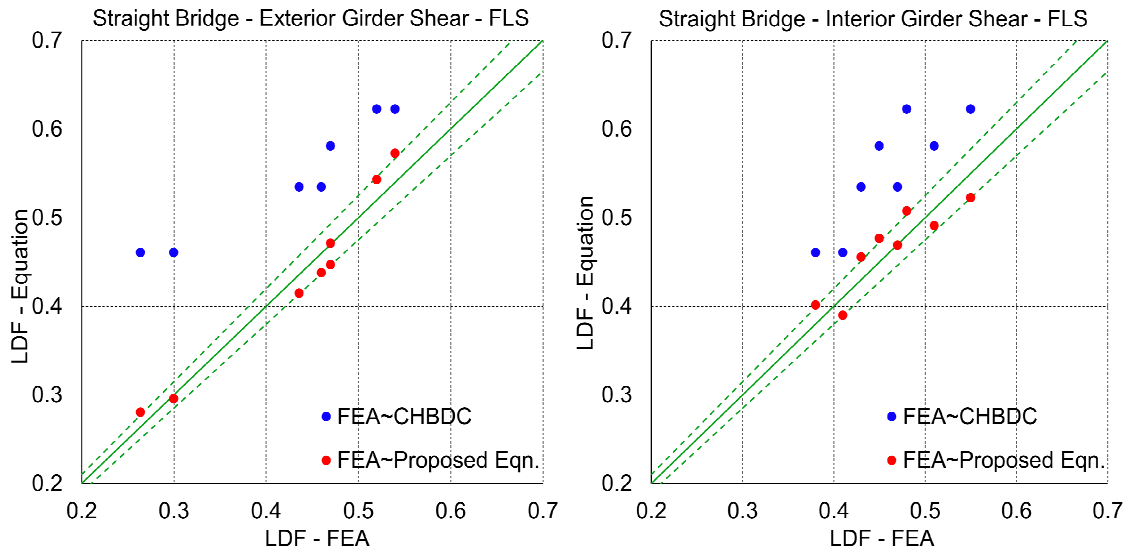
(d)

Figure 7.11 Correlation between support load distribution factors at ULS and SLS obtained from FEA results with proposed equations and CHBDC equations for straight bridges for; (a) exterior girder moment, (b) interior girder moment, (c) exterior girder shear, and (d) interior girder shear



(a)

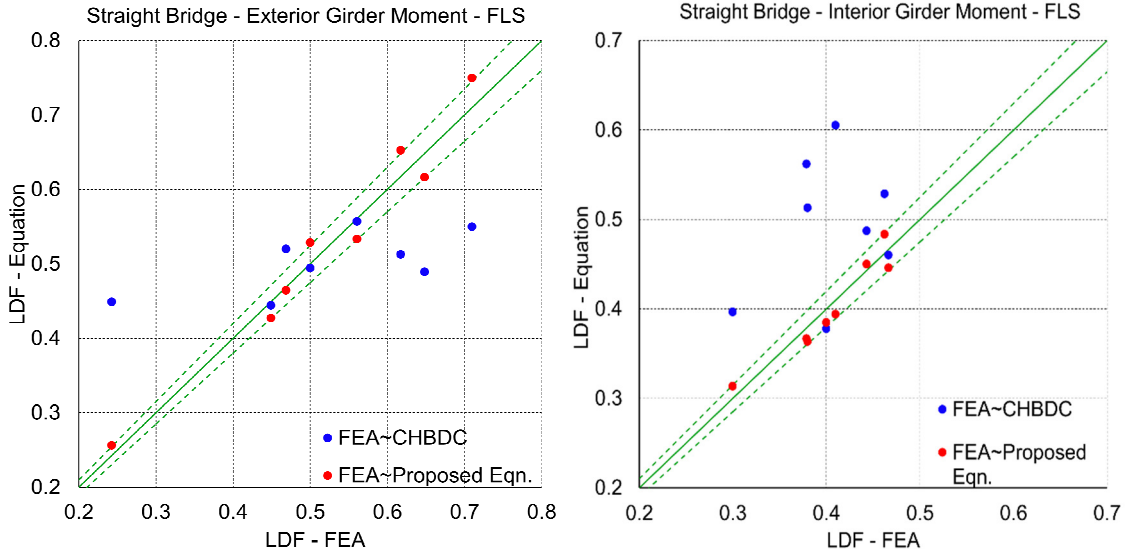
(b)



(c)

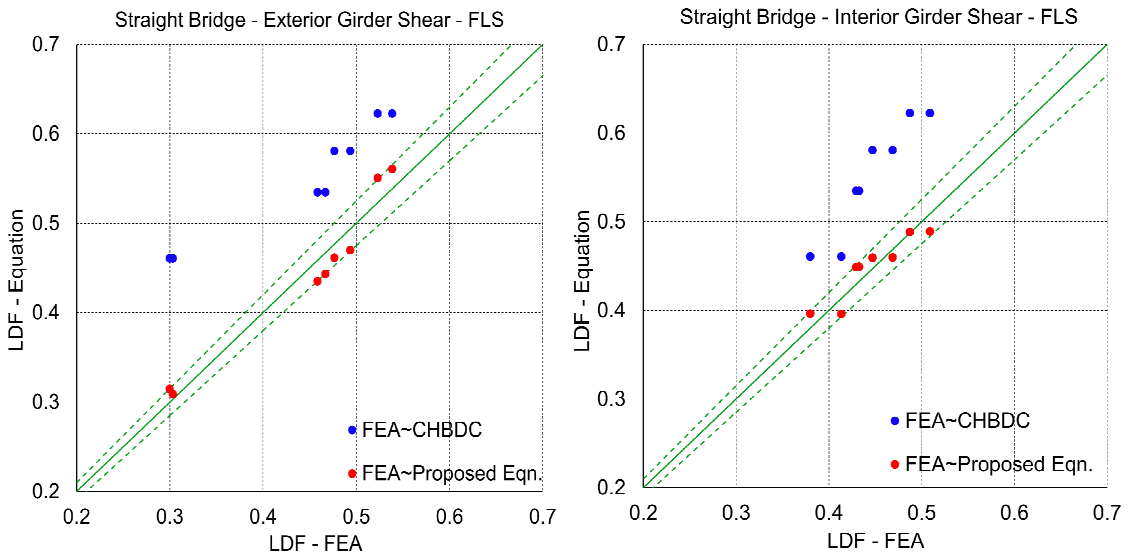
(d)

Figure 7.12 Correlation between span load distribution factors at FLS obtained from FEA results with proposed equations and CHBDC equations for straight bridges for; (a) exterior girder moment, (b) interior girder moment, (c) exterior girder shear, and (d) interior girder shear



(a)

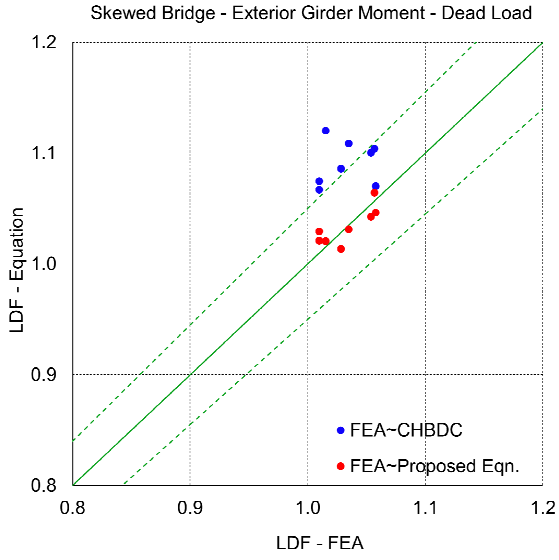
(b)



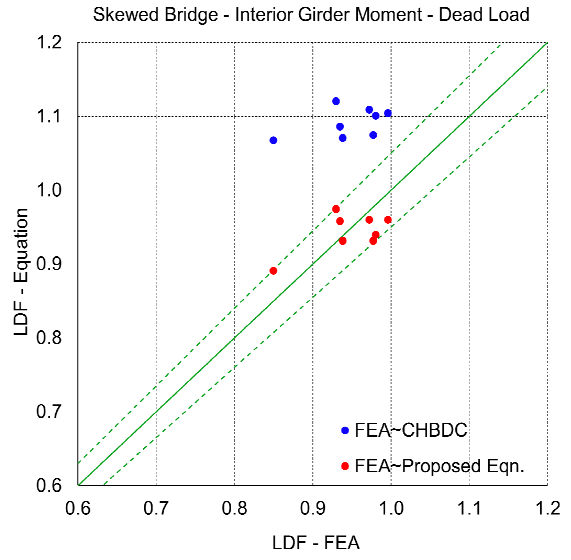
(c)

(d)

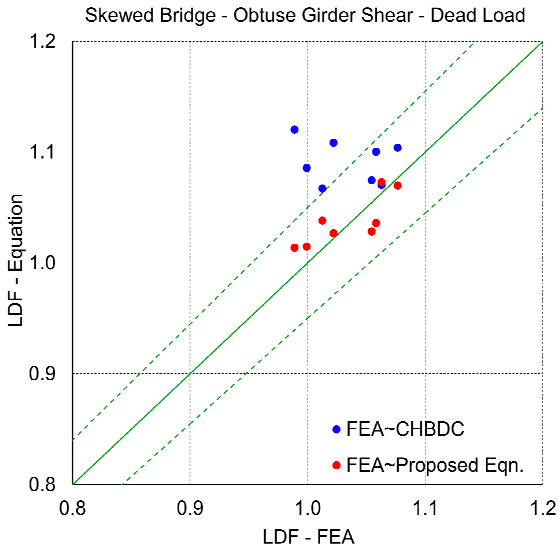
Figure 7.13 Correlation between support load distribution factors at FLS obtained from FEA results with proposed equations and CHBDC equations for straight bridges for; (a) exterior girder moment, (b) interior girder moment, (c) exterior girder shear, and (d) interior girder shear



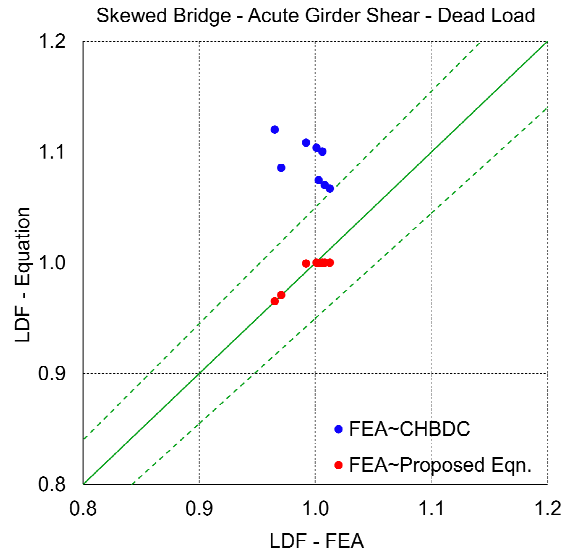
(a)



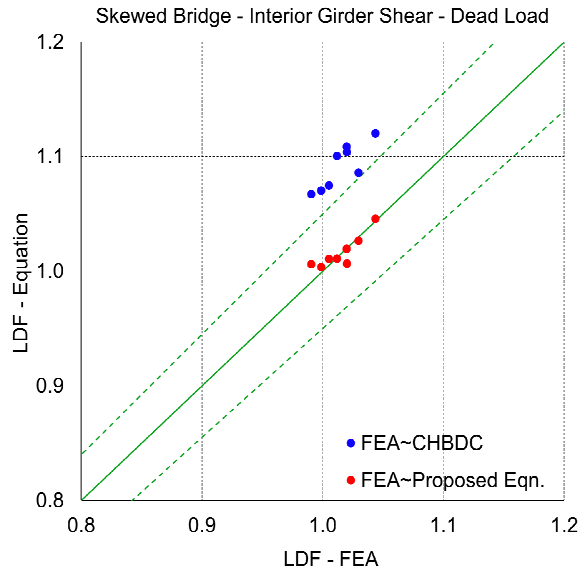
(b)



(c)

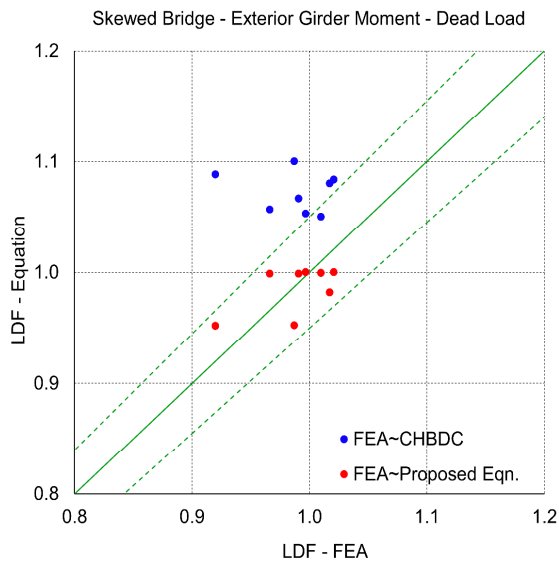


(d)

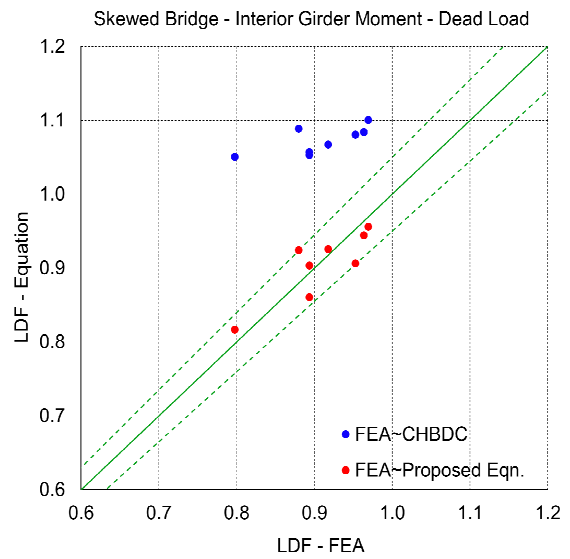


(e)

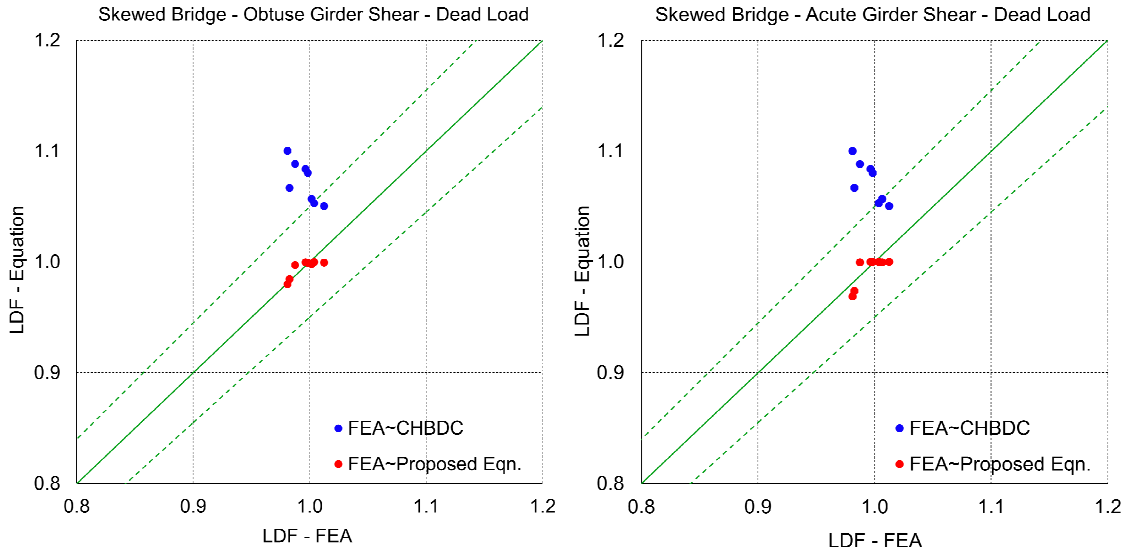
Figure 7.14 Correlation between span load distribution factors at dead load obtained from FEA results with proposed equations and CHBDC equations for skewed bridges for; (a) exterior girder moment, (b) interior girder moment, (c) obtuse girder shear, (d) acute girder shear, and (e) interior girder shear



(a)

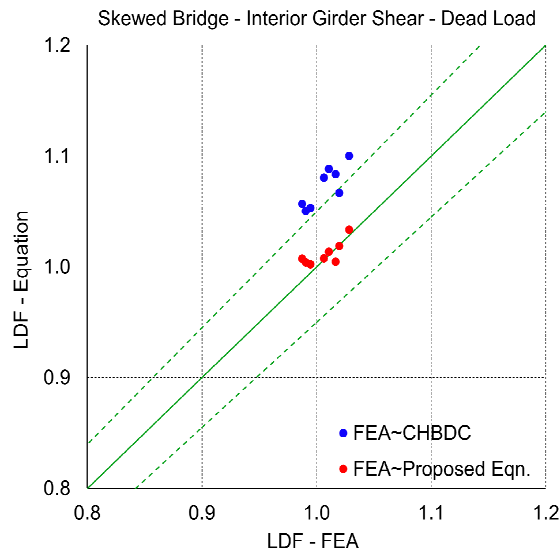


(b)



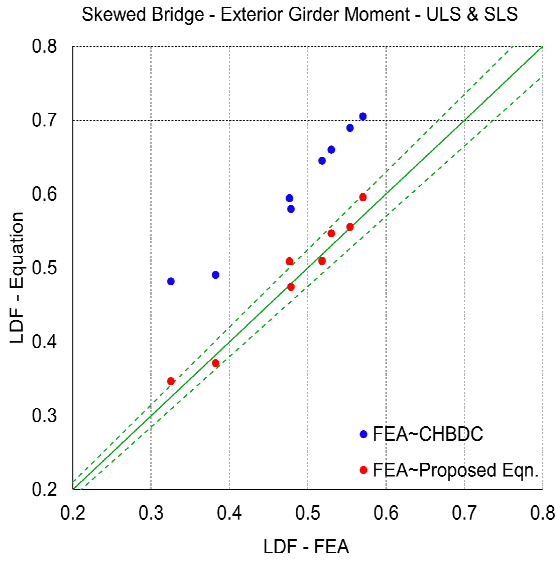
(c)

(d)

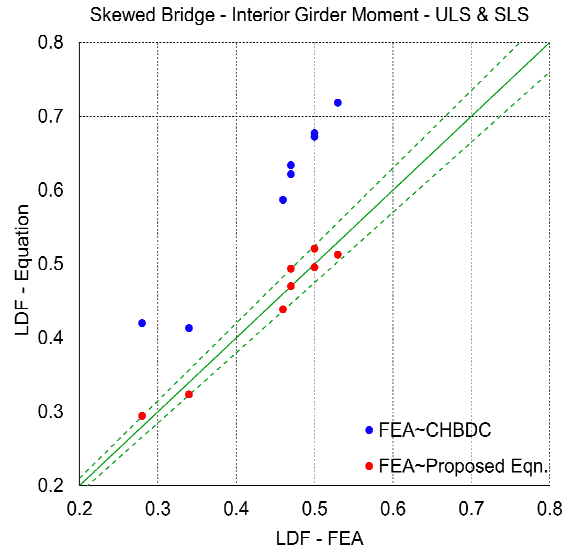


(e)

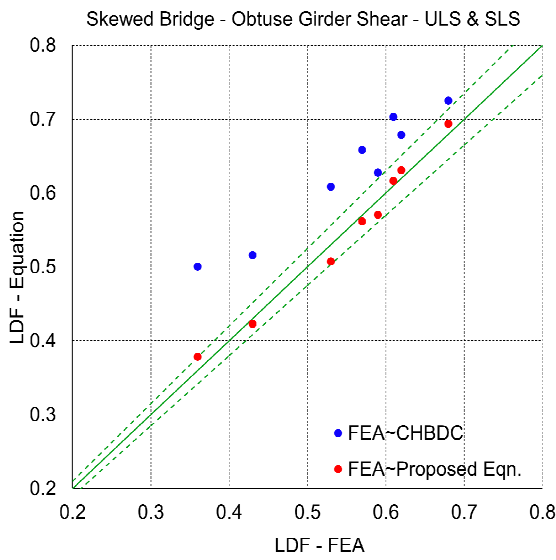
Figure 7.15 Correlation between support load distribution factors at dead load obtained from FEA results with proposed equations and CHBDC equations for skewed bridges for; (a) exterior girder moment, (b) interior girder moment, (c) obtuse girder shear, (d) acute girder shear, and (e) interior girder shear



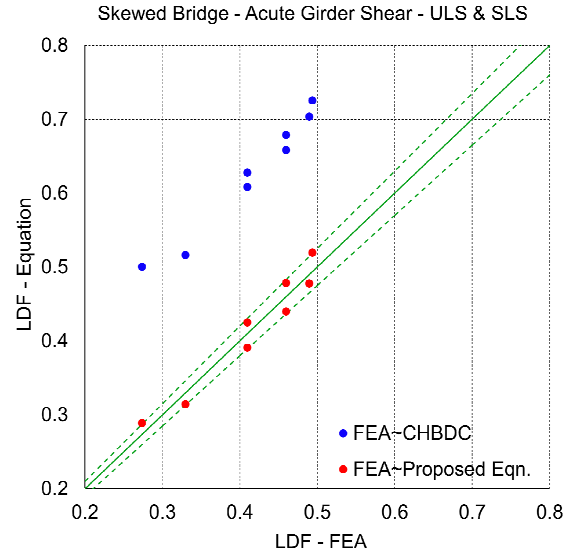
(a)



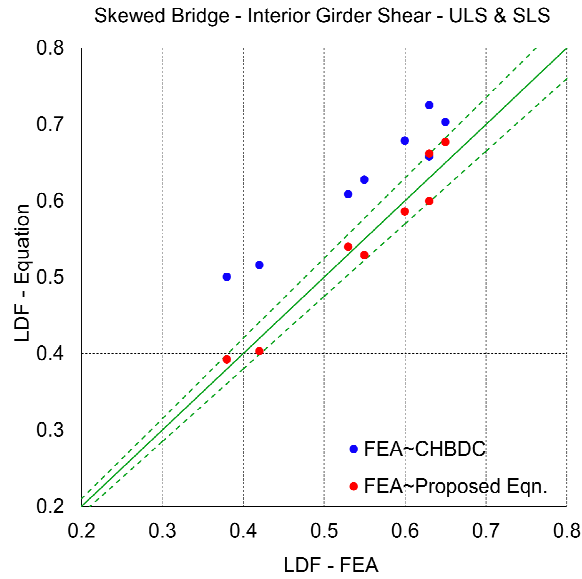
(b)



(c)

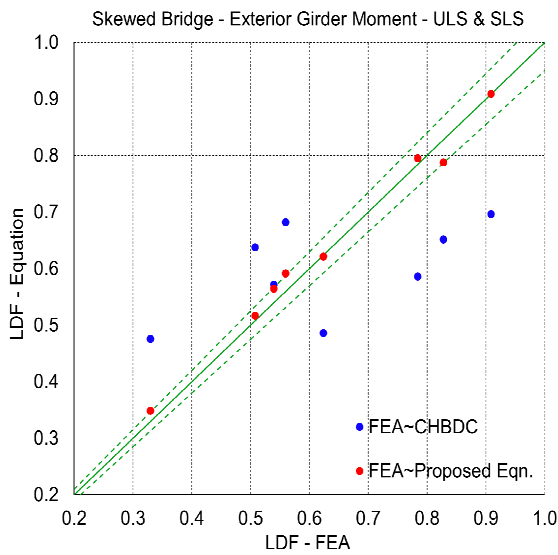


(d)

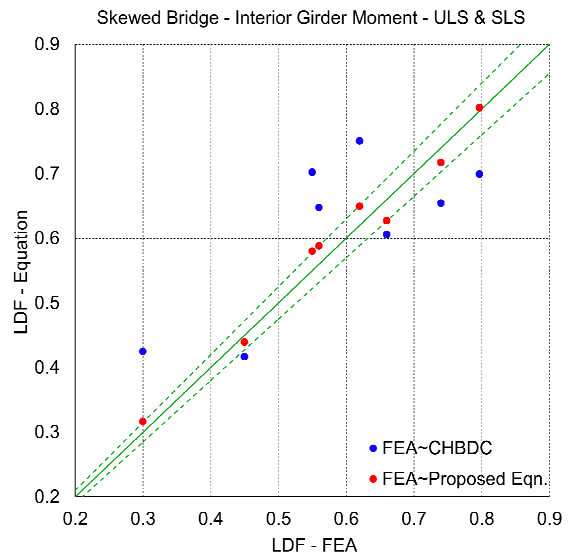


(e)

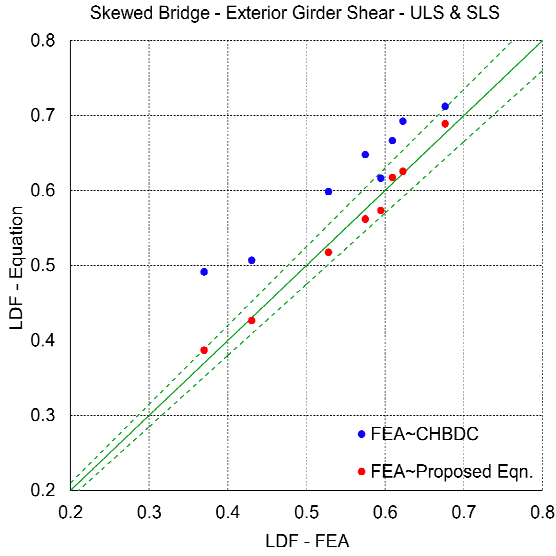
Figure 7.16 Correlation between span load distribution factors at ULS and SLS obtained from FEA results with proposed equations and CHBDC equations for skewed bridges for; (a) exterior girder moment, (b) interior girder moment, (c) obtuse girder shear, (d) acute girder shear, and (e) interior girder shear



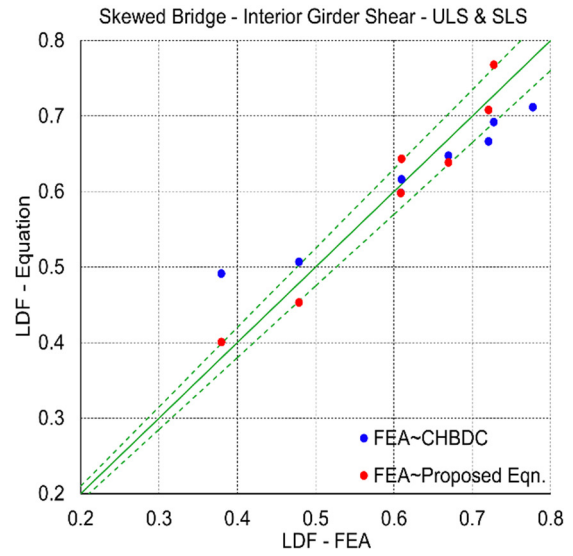
(a)



(b)

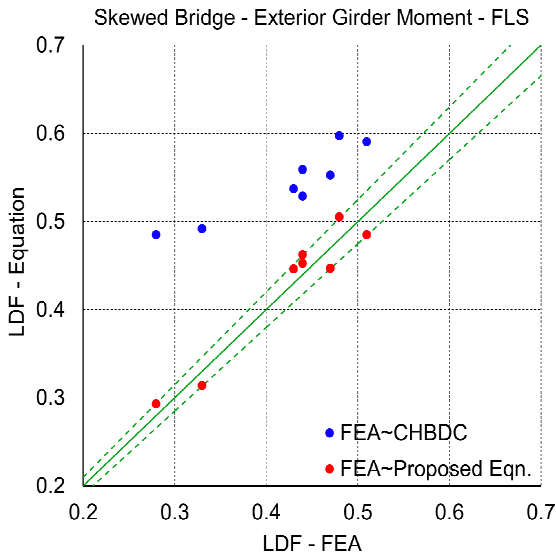


(c)

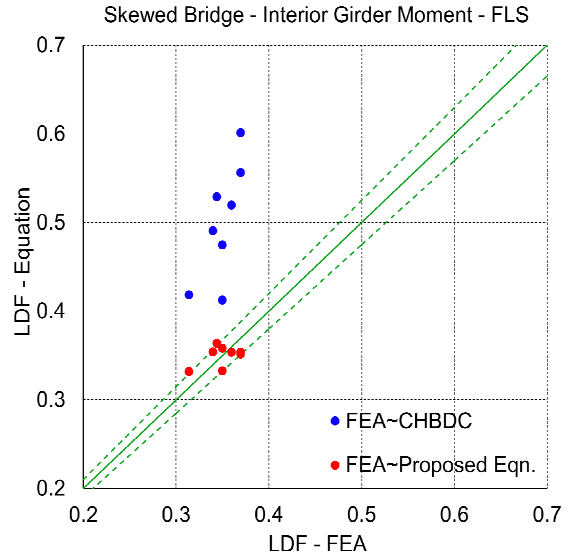


(d)

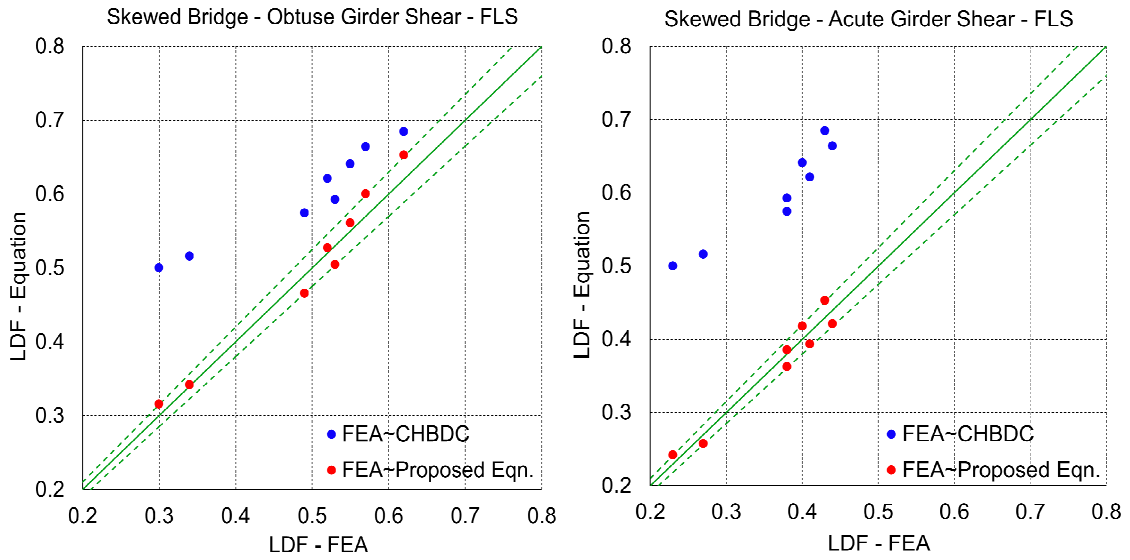
Figure 7.17 Correlation between support load distribution factors at ULS and SLS obtained from FEA results with proposed equations and CHBDC equations for skewed bridges for; (a) exterior girder moment, (b) interior girder moment, (c) exterior girder shear, and (d) interior girder shear



(a)

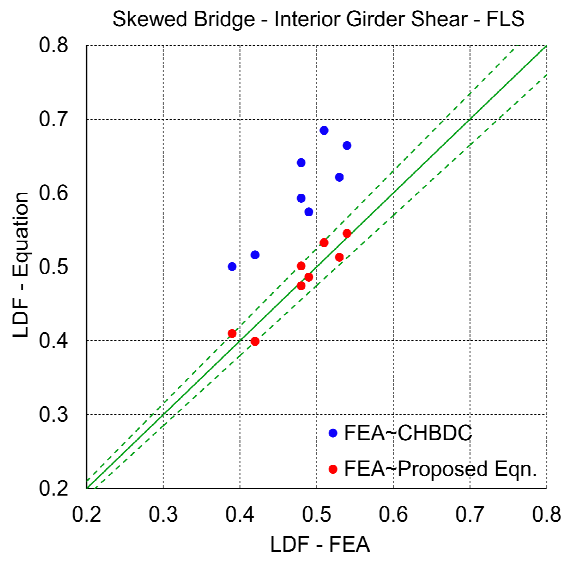


(b)



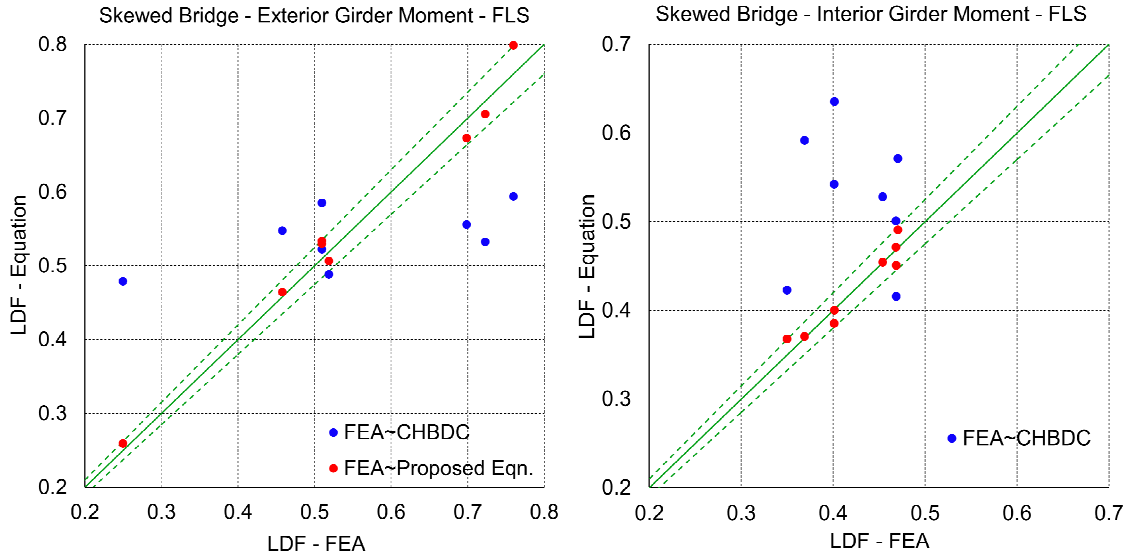
(c)

(d)



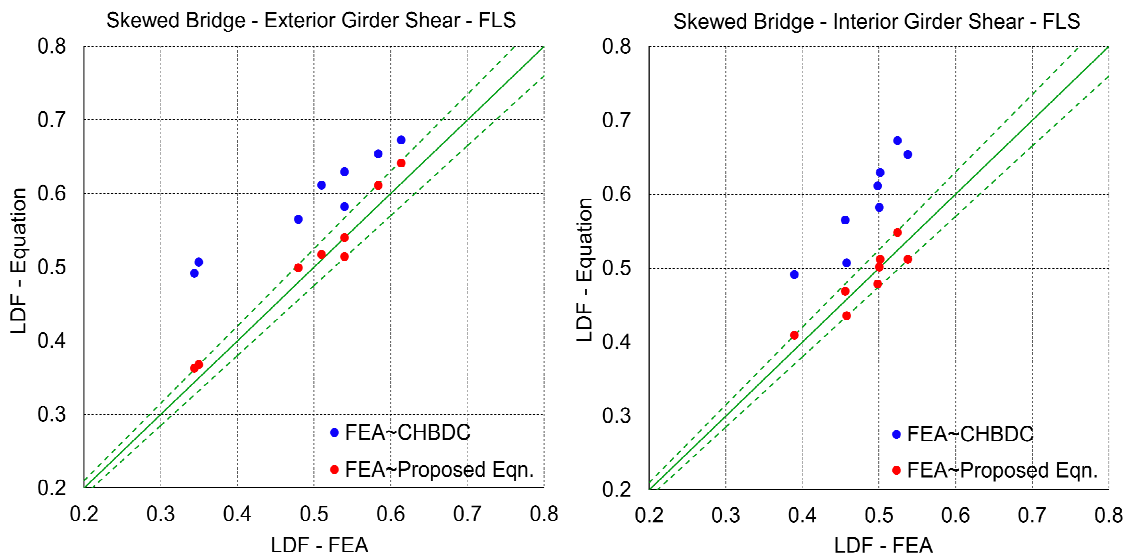
(e)

Figure 7.18 Correlation between span load distribution factors at FLS obtained from FEA results with proposed equations and CHBDC equations for skewed bridges for; (a) exterior girder moment, (b) interior girder moment, (c) obtuse girder shear, (d) acute girder shear, and (e) interior girder shear



(a)

(b)



(c)

(d)

Figure 7.19 Correlation between support load distribution factors at FLS obtained from FEA results with proposed equations and CHBDC equations for skewed bridges for; (a) exterior girder moment, (b) interior girder moment, (c) exterior girder shear, and (d) interior girder shear

The illustrative example to calculate the span and support moment and shear distribution factors using FEA, proposed equation and the CHBDC (CSA 2014a) for a straight slab-on-steel I-girder bridges at dead loads, ULS and SLS, and FLS are described in Appendix F, G and H, respectively. Similarly for the skewed bridge configurations, the illustrative

example to calculate the span and support moment and shear distribution factors using FEA, proposed equation and the CHBDC (CSA 2014a) at dead loads, ULS and SLS, and FLS are presented in Appendix I, J and K, respectively. The result showed that the proposed equations were sufficiently accurate in predicting the response of a straight and skewed bridge behavior at dead and live load conditions. The CHBDC design equations were found highly conservative for both moment and shear at the exterior and interior girder location. The main reasons for the inadequacy of the design equation to represent the actual behavior of a bridge structure are more likely the same as described earlier in section 4.4.7.

7.3 Conclusions

Clause 5.6 of the CHBDC has specified equations to calculate the load distribution factors for a simply supported single span slab-on-girder bridges. Further, it is stated in clause 5.6.4.6 to use the same set of equations for the multi-span bridges by considering the effective span length in accordance with Figure 5.1(a) of CHBDC. The objective of this study was to check the applicability of the proposed equations for moment and shear distribution factors for simply supported straight and skewed bridge geometry under the dead and CHBDC live load conditions to the continuous multi-span bridge structures. The results showed reasonable correlation with the straight multi-span bridge data for the dead load conditions. However for other load conditions at different skew angle the previous developed proposed equations and the CHBDC simplified equations proved to be unsafe, and for other situations resulted in conservative estimates. Based on this finding, new set of equations for the span and support load effects in case of two-span skewed bridge geometry were developed, adequately conforming the results obtained from finite element analysis. Further for better understanding of these proposed equations to the bridge engineers and designers, examples to calculate the load distribution factors at span and support locations of a continuous bridge were quantified and addressed herein. It was noticed that in case of straight continuous bridge, the CHBDC provisions for wheel loads significantly overestimating the design span moments by 33% and 29% for exterior and interior girders respectively. The similar trend of overestimation was also observed for the span shear at the exterior and interior girder location. However, for support design moments, the CHBDC equations resulted in underestimating the response by 23% and 18%

for exterior and interior girders respectively. Whereas, the code design provisions for support design shear resulted in overestimation by 43% and 23% for exterior and interior girders respectively. The addition of skew angle to the bridge geometry further magnified the amount the conservatism that the CHBDC design equations reflected for straight bridges. It is worth mentioning here that since the proposed equations for the continuous straight and skewed bridges at span and support locations were developed based on a limited set of bridge data, hence it would be wise to further investigate the applicability of these equations by considering broad range of bridge parameters for practical design purposes.

CHAPTER 8

Summary and Conclusions

8.1 Dissertation Summary

The presence of skew angle in a composite bridge structure makes the analysis and design much more complex in comparison to a straight bridge. In skewed bridges, the longitudinal girders undergo torsional rotation at the supports under the influence of loads. These rotations are more significant at the obtuse corners and they are difficult to predict. In addition to girder twisting, skewed bridges can also lead to increased girder shears and end reactions for girders framing into the obtuse corners of the bridge and results subsequently in reductions of girder shears and end reactions framing into the acute corners of the bridge. Furthermore, the presence of skew angle causes significantly reduction in the longitudinal bending moment in the girders when compared to straight bridges, and this effect is more noticeable in interior girders as compared to exterior girders.

The concept of load distribution factors enables bridge engineers to consider the longitudinal and transverse wheel load effects as two separate phenomena and thus simplifying the analysis and design of new bridges as well as for the evaluation of the load carrying capacity of existing bridges. Existing bridge design codes do not provide sufficient guidance to bridge engineers for assessment of load distribution factors for skew composite bridges. Recently, the CHBDC has specified equations considering skew for slab-on-girder bridges applicable within certain ranges of design parameters. These limits lead to an extremely conservative design in some cases and to unsafe design in others, since these factors do not represent the actual behavior of the composite bridge structure. Further, the equations in the current design code specifications are developed using the regression of grillage analysis results, which is not always recommended for accurate assessment of skewed bridge behavior. Also, these design guidelines are developed by considering limiting assumptions, such as, as per clause 5.6.2(h)(ix) of CHBDC only bridges with diaphragms and cross-frames parallel to the lines of support or without intermediate diaphragms can be considered. Previous studies revealed that the presence of internal

diaphragms in skewed bridge has a significant effect on the load distribution characteristics.

In order to address the limitations in the CHBDC specifications, the current research was initiated to address these concerns by investigating skew bridges behavior and developing new design guidelines for accurate prediction of load distribution factors for composite skewed bridges. For this purpose, a parametric study was conducted using three-dimensional finite element modeling under dead and CL-W live loads for ultimate, serviceability and fatigue limit states. Based on the results obtained from a parametric study, a set of empirical equations were developed for the girder moment and shear distribution factors. The results showed that the proposed equations for girder moment and shear distribution factors were found in good agreement with the FEA results for both straight and skewed bridge geometries. However, the CHBDC equations proved to be ineffective to capture the accurate behavior of slab-on-girder bridge configurations, thus produced conservative results for certain bridge configurations and for some other bridge geometries predicted highly under-estimated response, yielding to an unsafe design. Finally, an investigation was carried out to check the applicability of the proposed equations developed for simply supported straight and skewed slab-on-girder bridge configurations under dead and live load conditions to the multi-span continuous bridge structure. It was noticed that both the proposed equations and the CHBDC design equations proved to be unsafe for some cases, whereas for other situations resulted in conservative estimates. Based on the limited set of bridge prototypes selected for this study, a new set of design equations for the span and support load effects were proposed, effectively conforming the results obtained from finite element analysis. Further, design guideline to simplify the analysis of a skewed bridge geometry was proposed by treating the skewed bridge as an equivalent straight bridge.

8.2 Principal Contributions

Based on the findings from the sensitivity and parametric studies conducted on selected composite straight and skewed bridge configurations subjected to dead loads and CHBDC live loads, the following conclusions can be drawn:

- 1) For skew angle less than 30° , moment and shear magnification factors have trivial effect with the change of skew angle up to 30° . For that reason, parallel cross-frame layout can be used for skew angles up to 30° . However for skew angles greater than 30° up to 60° perpendicular-discontinuous cross-frame layout provides better load distribution among girders by reducing the girder displacement considerably.
- 2) For highly skewed bridges, equally spaced cross-frame members along the length of the bridge structures and placing them within the prescribed code limitations results in a better load distribution among girders by reducing the support reactions at the obtuse corners.
- 3) The moment magnification factors have insignificant effect on the un-shored sequence of construction for the bridge structure when the skew angle changes from 0° to 60° . Hence it was concluded to set the moment magnification factors equal to 1 for M_d calculation in the design equation.
- 4) For shored sequence of construction, the moment magnification factors resulted in a substantial effect on the girder load distribution characteristics and needs to be considered to develop more realistic design guidelines.
- 5) For short span bridges ranging from 15 m to 40 m span lengths, the CL-W truck load produced dominating girder flexural stresses for a selected bridge configurations when compared with CL-W lane loads.
- 6) To assess the accuracy about modeling the multi-lane truck loading condition on the load distribution among girders in skewed composite steel I-girder bridges, three different truck loading conditions were considered, namely: (i) side-by-side trucks entering the bridges simultaneously, (ii) multi trucks running over the bridge with time lag between them, and (iii) one truck in each lane at a time and with superposition of results. The results showed that for short span bridges, considered in this study, all the three loading arrangements produced an insignificant effect on girder bending and shear stresses.
- 7) It was observed that skew has marginal effect on the exterior and interior girder moment distribution factor (F_m) for skew angles between 0° and 30° under the application of dead loads. However, for skew angle between 30° to 60° , exterior girder

- showed an increase of F_m value with the increase skew angle. This increase in F_m was more noticeable up to two-lane bridge configurations having small span lengths.
- 8) A marginal increase of shear distribution factors (F_v) at the girder obtuse corners were observed under dead loads between 0° and 30° skew angle. With further increase in skew angles from 30° to 60° , the obtuse corners showed a substantial increase in F_v value. This increase in the response of F_v value was more pronounced in bridge structures having small girder spacing.
 - 9) No substantial change in the response of F_m was noticed for both the exterior and interior girders with the increase of span length up to 30° skew angle. However, between 30° to 60° skew angles, a considerable increase in F_m value up to 30 m span length was noticed under dead loads.
 - 10) The girder shear distribution factor at acute corners were found not sensitive to the variation of span length up to 60° skew angle under dead loads. However, a marginal increase of F_v at the bridge obtuse corners was observed; and it increases with span length up to 30° skew angle. However, for skew angle between 30° to 60° , F_v value decreases with the increase of span length. This reduction in the response of F_v value between 30° to 60° skew angles at the obtuse corners were found less significant in case of one-lane and three-lane bridge structures as compared to other bridge configurations.
 - 11) For the skew angle up to 30° , F_m values for both the exterior and interior girders were found unaffected with the change of girder spacing under dead loads. Further increase of skew angle between 30° to 60° causes reduction in the exterior girder F_m value. However, the effect of girder spacing on the interior girder moment distribution factors did not present any clear pattern.
 - 12) For skew angle up to 30° , F_v value showed a marginal change at the obtuse girder supports with the increase of girder spacing. For higher skew angles, increase in girder spacing resulted in the reduction of the obtuse corner F_v value.
 - 13) Based on the results obtained from the parametric study under dead loads, a set of empirical equations were developed for girder moment and shear distribution factors. The correlation between the CHBDC design equations, proposed equations based on the parametric study, and the FEA results was developed. The results showed good correlation between the values obtained from the proposed equations and those

calculated from FEA, However, CHBDC design equation was found conservative for some cases, and for other it resulted in an unsafe design.

- 14) Skew angle was found the most critical factor that influences the moment and shear distribution among girders under live loads. The study showed that the exterior and interior girder moment distribution factors for a composite skewed bridges were always less than those of right bridges. Further, it was noticed that the increase in skew angle resulted in high concentration of shear force in the obtuse girder corners and causes reduction of shear concentration in the girder at the acute corners as well as in the interior girders.
- 15) For both exterior and interior girders under live loads, the effect of span length resulted in the reduction of moment distribution factors when skew angle increases from 0° to 60° . For span length up to 25 m, the sensitivity of span length on the moment distribution factors for the exterior and interior girders was found significant. However, for span length between 25 m to 40 m, the effect of span length on the moment distribution factors was found marginal.
- 16) For straight bridges at ULS and SLS, a marginal decrease in the shear distribution factors were noticed with the increase of span length from 15 m to 40 m. the shear distribution factors at the obtuse girder corner were found not very sensitive to span length. However, the effect of span length on the shear distribution factors were more predominantly evident in skewed bridges. Further, for FLS the increase of span length resulted in the increase of shear distribution factors at the obtuse girder corner. This effect was more significant in skewed bridges as compared to straight bridges.
- 17) Bridge structures having less number of girders at large spacing resulted in higher value of moment distribution factor for both exterior and interior girder at ULS, SLS and FLS, as compared to the bridge geometry comprised of more number of girders arranged at less spacing among them.
- 18) The decrease of number of girders with greater girder spacing between them resulted in higher shear distribution factors for the obtuse, acute and interior girders at ULS, SLS, and FLS.
- 19) For ULS, SLS and FLS, the effect of girder spacing resulted in an increase of shear distribution factor with the increase of skew angle at obtuse girder corner. This effect

- was more significant in bridge configurations having more number of girders with less spacing between them. However, the effect of girder spacing resulted in the decrease of shear distribution factor at acute girder corner with the increase of skew angle. Further, it was noticed that the effect of girder spacing on the shear distribution factors of interior girders at ULS, SLS, and FLS was found to be insignificant.
- 20) For straight bridge configuration under live loads, the CHBDC design equations underestimate the exterior and interior girder moment when a span length of 15 m was considered. However for spans greater than 15 m, the CHBDC equations resulted highly conservative estimates in comparison to the FEA. Further, it was noticed that for exterior and interior girder shear in a two and four-lane bridge configurations, the CHBDC equations produced conservative estimate of distribution factors in comparison to the FEA. Also, it was observed that the interior girder shear distribution factors were found sensitive to the bridge width, that is a function of girder spacing (S) and number of girders (N).
- 21) Based on a parametric study a set of empirical expressions were developed for the girder moment and shear distribution factors for the accurate assessment of the girder load distribution for straight bridges at ULS, SLS and FLS. The correlation between the CHBDC equations, proposed equations, and the FEA results for the moment and shear distribution factors were developed. The result showed that the proposed equations were found sufficiently more accurate in predicting the response of a straight bridge behavior. Whereas, the CHBDC equations for both moment and shear distribution factors were found conservative for the exterior and interior girders.
- 22) The correlation of moment and shear distribution factors evaluated using CHBDC design equations, proposed equations, and the FEA results were developed for skewed bridges at ULS, SLS and FLS. The result showed that the proposed equations predictions were accurate for skewed bridge at ULS, SLS and FLS. The CHBDC design equations for both moment and shear at the exterior and interior girder were found highly conservative.
- 23) With limited set of bridge design parameters, the applicability of the load distribution factor equations proposed for simply supported straight and skewed bridge geometry under the dead and CHBDC live load conditions were investigated by applying them

to the continuous multi-span bridge structures. For a straight bridge configuration under dead load conditions, the results showed reasonable correlation between the single span and multi-span bridge structures. However for skewed bridges at other load conditions the proposed equations and the CHBDC simplified equations proved to be unsafe for some situations, and for others it resulted in conservative estimates. Based on this finding, it is recommended to further investigate the applicability of the proposed equations by considering broader range of bridge parameters for accurate assessment of skewed bridges behavior.

8.3 Future Directions

It is recommended that future research efforts be directed towards the following items:

- 1) The study of the load distribution characteristics of composite skewed multi-span bridges by considering the broader range of bridge design parameters for practical design purposes.
- 2) The study to investigate the load distribution characteristics of a simply supported composite straight and skewed bridge configurations supported by prestressed concrete girders.
- 3) The effect of different slab thickness in a composite skewed bridge on the load distribution factors under CHBDC truck loading need to be investigated.
- 4) The study of the load distribution characteristics for skewed simply supported and continuous multi-span bridges supported by non-parallel support lines.
- 5) The study of the dynamic characteristics for skewed simply supported and continuous multi-span bridges supported by parallel and non-parallel support lines.
- 6) Seismic behavior of the skewed bridges need to be investigated.

REFERENCES

- Al-Hashimy, M. (2005). Load Distribution in Curved Concrete Slab-on-Steel I-Girder Bridges. M.A.Sc. Thesis, Civil Engineering Department, Ryerson University, Toronto, Canada.
- American Association of State Highway and Transportation Officials. (1996). AASHTO Standard specifications for highway bridges. 16th Edition, Washington, D.C.
- American Association of State Highway and Transportation Officials. (2001). AASHTO-A policy on geometric design of highways and streets. 4th Edition, Washington, D.C.
- American Association of State Highway and Transportation Officials. (2014). AASHTO-LRFD Bridge Design Specifications. 7th Edition, Washington, D.C.
- AASHTO/NSBA. (2003). G12.1-2003: Guidelines for Design for Constructability, AASHTO/NSBA Steel Bridge Collaboration.
- AASHTO/NSBA (2011). Guidelines for the Analysis of Steel Girder Bridges, G13.1, AASHTO/NSBA Steel Bridge Collaboration, American Association of State Highway and Transportation Officials, Washington, D.C. and National Steel Bridge Alliance, Chicago, IL.
- Amiri, A., (1988). Behavior of skewed continuous I-beam bridge structures. Ph.D. dissertation. University of Illinois at Urbana-Champaign, Urbana, Illinois.
- Bae, H. U., and Oliva, M. G. (2012). Moment and shear load distribution factors for multigirder bridges subjected to overloads. *J. Bridge Eng.*, 10.1061/(ASCE)BE.1943-5592.0000271, 519–527.
- Bakht, B., and Jaeger, L. G., (1985). *Bridge Analysis Simplified*. McGraw-Hill Book Co., New York.
- Bakht, B. (1988). Analysis of some skew bridges as right bridges. *J.Struct. Eng.*, 114(10), 2307–2322.
- Bakht, B. and Moses, F. (1988). Lateral Distribution Factors for Highway Bridges. *Journal of Structural Engineering*, 114:8, 1785-1803.
- Bakht B. and Jaeger L. G. (1992). Ultimate load test of slab-on-girder bridge. *Journal of Structural Engineering* 118(6):1608–24.
- Bapat, A.V. (2009). Influence of bridge parameters on finite element modeling of slab on girder bridges. Master of Science Thesis, Virginia Polytechnic Institute and State University, Blacksburg, Va.
- Bishara, A. G., Chuan Liu, M., and El-Ali, N. D. (1993). Wheel load distribution on simply supported skew I-beam composite bridges. *J.Struct. Eng.*, 119(2), 399–419.
- Bakht, B. and Moses, F. (1988). Lateral Distribution Factors for Highway Bridges. *Journal of Structural Engineering*, 114:8, 1785-1803.

- Bakht, B. & Jaeger, L.G. (1990). Bridge Testing – A Surprise Every Time. *Journal of Structural Engineering* 116:5, 1370-1383.
- Barker, R. M., Puckett, J. A., (1997). *Design of Highway Bridges: Based on AASHTO LRFD Bridge Design Specifications*. John Wiley & Sons, Inc, NY.
- Barr, P.J., Eberhard, M.O., and Stanton, J.F. (2001). Live-Load Distribution Factors in Prestressed Concrete Girder Bridges. *Journal of Bridge Engineering*, Vol. 6, No. 5, September/October, pp 298-306.
- Barr, P.J., and Amin, N.(2006), Shear Live-Load Distribution Factors for I-Girder Bridges, *Journal of Bridge Engineering*, V. 11, N. 2, March/April 2006, 197-204
- Barth, A. S., and Bowman, M. D. (2001). Fatigue behavior of welded diaphragm-to-beam connections. *Journal of Structural Engineering*, ASCE 127(10), 1145–1152.
- Beckman, F. and Medlock, R.D. (2005). Skewed Bridges and Girder Movements Due to Rotations and Differential Deflections. *Proceedings of the World Steel Bridge Symposium*, Orlando, FL.
- Bell, N. B., (1998). Load Distribution of Continuous Bridges using Field Data and Finite Element Analysis. Master of Science Thesis. Florida Atlantic University, Boca Raton, Florida.
- Bishara, A. G., Chuan Liu, M., and El-Ali, N. D. (1993). Wheel load distribution on simply supported skew I-beam composite bridges. *J.Struct. Eng.*, 119(2), 399–419.
- Canadian Standard Association (2000). CAN/CSA-S6-00. Canadian Highway Bridge Design Code, Etobicoke, ON.
- Canadian Standards Association (2006a). CAN/CSA-S6-06: Canadian Highway Bridge Design Code. CSA, Mississauga, Ontario.
- Canadian Standards Association (2006b). S6.1-06: Commentary on CAN/CSA-S6-06, Canadian Highway Bridge Design Code. CSA, Mississauga, Ontario.
- Canadian Standards Association (2014a). CAN/CSA-S6-14: Canadian Highway Bridge Design Code. CSA, Mississauga, Ontario.
- Canadian Standard Association (2014b). S6.1-14: Commentary Canadian Highway Bridge Design Code, Mississauga, Ontario.
- Castaneda, D. E. (1997). Causes of mechanical damage to Alabama bridge decks. *Transp. Res. Rec.*, 1594, 105–114.
- Chen, Y., and Aswad, A. (1996). Stretching span capability of prestressed concrete bridges under AASHTO-LRFD. *J. Bridge Engrg.*, ASCE, 1(3), 112–120.

- Choo, T., Linzell, D.G., Lee, J. and Swanson, J.A. (2005). Response of a continuous, skewed, steel bridge during deck placement, *Journal of Constructional Steel Research* **61**(5), 567–586.
- Chung, W., Liu, J., and Sotelino, E. D. (2006). Influence of secondary elements and deck cracking on the lateral load distribution of steel girder bridges. *J. Bridge Eng.*, 10.1061/(ASCE)1084-0702(2006)11:2(178), 178–187.
- Coletti, D.A. and J.M. Yadlosky (2005). Behavior and Analysis of Curved and Skewed Steel Girder Bridges. Proceedings of the World Steel Bridge Symposium, Orlando, FL.
- Coletti, D.A. and J.M. Yadlosky (2007). Analysis of Steel Girder Bridges – New Challenges. Proceedings of the World Steel Bridge Symposium, New Orleans, LA.
- Coletti, D., Chavel, B., and Gatti, W. (2011). Challenges of Skew in Bridges with Steel Girders. *Transportation Research Record: Journal of the Transportation Research Board*, 2251(5), 47-56.
- Coletti, D. and Puckett, J. (2012). *Steel Bridge Design Handbook: Structural Analysis*. Technical Report: FHWA-IF-12-052 – Vol. 8, Washington, D.C.
- Computers and Structures, Inc. (CSI). (2015). *CSiBridge user's manual*, CSI, Berkeley, CA, USA.
- Computers and Structures, Inc. (CSI). (2007). *SAP2000 user's manual*, CSI, Berkeley, CA, USA.
- Cook, R. D., Malkus, D. S., and Plesha, M. E. (1989). *Concepts and applications of finite element analysis*, 3rd Ed., Wiley, New York.
- Cross B., Panahshahi N., Vaughn B., Petermeier D., Siow Y. (2006). Investigation of select LRFD design factors through instrumentation of bridge bearings, Report No.: FHWA/IL/HRC.2006-2/152, Southern Illinois Univ. Edwardsville Edwardsville, IL.
- Cross, B., Vaughn, B., Panahshahi, N., Petermeier, D., Siow, Y., and Domagalski, T., (2009). Analytical and Experimental Investigation of Bridge Girder Shear Distribution Factors. *Journal of Bridge Engineering*, 14(3), 154–163.
- Davis, J.M., (2003). Serviceability Field Testing of Hybrid HPS Bridge A-6101, Master's Thesis, University of Missouri, Columbia.
- Deng, K. (1998). *Dynamic Response of Certain Types of Highway Bridges to Moving Vehicles*, PhD Dissertation, Department of Civil and Environmental Engineering, Carleton University, Ottawa, Canada
- Diab, F.B., Mabsout, M., and Tarhini, K. (2011). Influence of skew angle on live load moments in steel girder bridges, *Bridge Structures* 7 (2011) 151–163.
- Dilger, W. H., Ghoneim, G. A., and Tadros, G. S. (1988). Diaphragms in Skew Box Girder Bridges, *Canadian Journal of Civil Engineering*. 15,869-878.

- Ebeido, T.I, (1995), Static and dynamic responses of simply supported and continuous skew composite bridges, Ph.D. Thesis, Civil Engineering Department, University of Windsor, ON, Canada.
- Ebeido, T. and Kennedy, J. B. (1995). Shear distribution in simply supported skew composite bridges. *Can. J. Civ. Engrg.*, Ottawa. Canada. 22(6). 1143-1154.
- Ebeido, T., and Kennedy, J. B. (1996a). Girder moments in continuous skew composite bridges. *J. Bridge Eng.*, 1(1), 37–45.
- Ebeido, T., and Kennedy, J. B. (1996b). Shear and reaction distributions in continuous skew composite bridges. *J. Bridge Eng.*, 1(4), 155–165.
- Ebeido, T., and Kennedy, J. B. (1996c). Girder moments in simply supported skew composite bridges. *Can. J. Civ. Engrg.*, Ottawa. Canada. 23(4), 904-916.
- Eom, J., and Nowak, A. S. (2001). Live Load Distribution for Steel Girder Bridges. *ASCE Journal of Bridge Engineering*, 6(6):489-497.
- Fisher, S.T., (2006). Development of a Simplified Procedure to Predict Dead Load Deflections of Skewed and Non-Skewed Steel Plate Girder Bridges, MS Thesis, North Carolina State University, USA.
- Fraser, R. E. K., Grondin, G. Y., and Kulak, G. L. (2000). Behavior of distortion-induced fatigue cracks in bridge girders. Structural Engineering Report No. 235, Univ. of Alberta, Edmonton, Alberta, Canada.
- Fu, C. C., Elhelbawey, M., Sahin, M. A., & Schelling, D. R. (1996). Lateral Distribution Factor from Bridge Field Testing. *Journal of Structural Engineering*, 122:9, 1106-1109.
- Fu, K.C., Lu, F. (2003). Nonlinear Finite Element Analysis for Highway Bridge Superstructures. *Journal of Bridge Engineering*, ASCE, 8(3), 173-179.
- Fu, G., Zhuang, Y., and Feng, J., (2011). Behavior of Reinforced Concrete Bridge Decks on Skewed Steel Superstructure under Truck Wheel Loads. *J. Bridge Eng.*, 16(2), 219–225
- Gheitasi, A., and Harris, D. K. (2015). Overload Flexural Distribution Behavior of Composite Steel Girder Bridges. *J. Bridge Eng.*, ASCE, ISSN 1084-0702/04014076(15), 20(5).
- Hambly, E. C., (1990). *Bridge Deck Behaviour*. 2nd Edition. E & FN Spon.
- Hartman, A. Hassel, H. Adams, C. Bennett, C. Matamoros, A. and Rolfe, S. (2010). Effects of cross-frame placement and skew on distortion induced fatigue in steel bridges. *Transportation Research Record 2200*, Transportation Research Board, Washington, DC, USA 62–68.
- Helba, A. and Kennedy, J. B. (1994). Collapse Loads of Continuous Skew Composite Bridges. *Journal of Structural Engineering*, Vol. 120, No. 5: 1395-1414.

- Helwig, T. A., Frank, K. H., and Yura, J. A. (1993). Bracing forces in diaphragms and cross-frames. Structural Stability Research Council Conf., Milwaukee, Wis.
- Helwig, T. and Wang, L. (2003). Cross-frame and Diaphragm Behavior for Steel Bridges with Skewed Supports, Report 1772-1, The University of Houston, Texas, 231 p.
- Helwig, T. and Yura, J. (2012). Steel Bridge Design Handbook: Bracing System Design, Report No. FHWA-IF-12-052 - Vol. 13
- Hu, Z. (1996). Simplified analysis method for bridge structures-Lateral live load distribution, People's Transportation, Beijing.
- Huang, H., Shenton, H.W., and Chajes, M.J. (2004). Load Distribution for a Highly Skewed Bridge: Testing and Analysis. *Journal of Bridge Engineering*, ASCE, 9(6), 558-562.
- Huo, X. S., Wasserman, E. P., and Zhu, P. (2004). Simplified method of lateral distribution of live load moment. *J. Bridge Eng.*, 9(4), 382–390.
- Huo, X. S., Wasserman, E. P., and Iqbal, R. A. (2005). Simplified Method for Calculating Lateral Distribution Factors for Live Load Shear. *J. Bridge Eng.*, 10(5), 544–554.
- Huo, X.S., Zhang, Q. (2008). Effect of Skewness on the Distribution of Live Load Reaction at Piers of Continuous Skewed Bridges, *Journal of Bridge Engineering*, Vol. 13, No. 1, pp. 110-114.
- Jaeger, L.G., and Bakht, B. (1982). The Grillage Analogy in Bridge Analysis. *Canadian Journal of Civil Engineering*, Vol. 9, No. 3.
- Jaeger, L.G., and Bakht, B. (1989). *Bridge Analysis by Microcomputer*. McGraw-Hill Book Company, New York.
- Jingjuan Li, and Genmiao Chen (2011). Method to Compute Live-Load Distribution in Bridge Girders. *Practice Periodical on Structural Design and Construction*, ASCE, Vol. 16, No. 4, 191–198.
- Keating, P.B., and Crozier, A.R. (1992). Evaluation and Repair of Fatigue Damage to Midland County Bridges. Report No. TX-92/1313-IF. Texas Department of Transportation. 157 p.
- Khaleel, M. A., and Itani, R. Y. (1990). Live-load moments for continuous skew bridges. *J. Struct. Eng.*, 116(9), 2361–2373.
- Khalafalla, I. (2009). Curvature limitations in bridge codes. M.A.Sc. thesis, Dept. of Civil Engineering, Ryerson University, Toronto.
- Khaloo, A. R., and Mirzabozorg, H. (2003). Load distribution factors in simply supported skew bridges. *J. Bridge Eng.*, 10.1061/(ASCE)1084-0702(2003)8:4(241), 241–244.

- Kim, S., & Nowak, A. S. (1997). Load Distribution and Impact Factors for I-Girders. *ASCE Journal of Bridge Engineering*, 97-104.
- Kocsis, P. (2004). Evaluation of AASHTO live load and line load distribution factors for I-girder bridge decks. *Practice Periodical on Structural Design and Construction*, ASCE, 9(4): 211–215.
- Kupricka, G., and Poellot, B. (1993). Nuisance Stiffness, Bridgeline, HDR Engineering, Inc., 4(1), 3 pp.
- Lee, D. J. (1994). *Bridge Bearings and Expansion Joints*. 2nd ed., E & FN SPON, London, UK.
- Linzell, D.G., Chen, A., Sharafbayani, M., Seo, J., Nevling, D.L., Jaissard, T. and Ashour, O. (2010). Guidelines for analyzing curved and skewed bridges and designing them for construction. Rep. No. FHWA-PA-2010-013-PSU 009, The Thomas D. Larson Transportation Institute, Pennsylvania State University, University Park, PA.
- Logan, D. (2002). *A first course in the finite element method*, 3rd Ed., Brooks/Cole Publisher, Pacific Grove, CA.
- Mabsout, M. E., Tarhini, K. M., Frederick, G. R., & Kobrosly, M. (1997a). Influence of Sidewalks and Railings on Wheel Load Distribution in Steel Girder Bridges. *ASCE Journal of Bridge Engineering*, 88-96.
- Mabsout, M. E., Tarhini, K. M., Frederick, G. R., & Tayar, C. (1997b). Finite Element Analysis of Steel Girder Bridges. *ASCE Journal of Bridge Engineering*, 83-87.
- Mabsout, M. E., Tarhini, K. M., Frederick, G. R., and Kesserwan, A. (1998). Effect of continuity on wheel load distribution in steel girder bridges. *J. Bridge Eng.*, 10.1061/(ASCE)1084-0702(1998)3:3(103), 103–110.
- Marx, H. J., Khachaturian, N., and Gamble, W. L. (1986). Development of design criteria for simply supported skew slab-and-girder bridges. *Structural Research Series No. 522*, University of Illinois, Urbana, Ill.
- Menassa, C., Mabsout, M., Tarhini, K., and Frederick, G. (2007). Influence of Skew Angle on Reinforced Concrete Slab Bridges, *Journal of Bridge Engineering*, Vol. 12, No. 2.
- Mergel, P. R and Almansour, H. H. (2010). Live Load Distribution on a Rigid Frame Concrete Bridge, *Proceedings of 8th International Conference on Short and Medium Span Bridges*, Niagara Falls, ON, Canada.
- Modjeski and Masters, Inc. (2002). *Shear in Skewed Multi-Beam Bridges*, National Cooperative Highway Research Project 20-7/Task 107.
- Mufti, A., Bakht, B., Mahesparan, K., and Jaeger, L. G. (1992). *Semicontinuum method of analysis for bridges (SECAN): A computer program and manual*, Dalhousie Univ., Halifax, Canada.

- Newmark, N. M. (1938). A Distribution Procedure for the Analysis of Slabs Continuous over Flexible Girders. University of Illinois, Engg. Experiment Station Bulletin No. 304, 7-118.
- Newmark, N. M., & Seiss, C. P. (1943). Design of Slab and Stringer Bridges. Public Roads, Vol. 23:7, 157-166.
- Newmark, N. M. (1949). Design of I-beam bridges. Transportation ASC, Vol. 114, 997-1022.
- Norton, E.K., Linzell, D.G., and Laman, J.A. (2003). Examination of Response of a Skewed Steel Bridge Superstructure during Deck Placement, Transportation Research Record, Journal of the Transportation Research Board No. 1845, pp. 66-75.
- Nouri, G. and Ahmadi, Z. (2012). Influence of Skew Angle on Continuous Composite Girder Bridge, Journal of Bridge Engineering, Vol. 17, No. 4.
- Nutt, R. V., Schamber, R. A., and Zokaie, T. (1988). Distribution of wheel loads on highway bridges. Final Rep. No. 83, Imbsen & Associates, Sacramento, Calif.
- Ontario Ministry of Transportation and Communications. (1979). Ontario Highway Bridge Design Code (OHBDC). 1st Edition, Highway Engineering Division, Downsview, Ontario, Canada.
- Ontario Ministry of Transportation and Communications. (1983). Ontario Highway Bridge Design Code (OHBDC). 2nd Edition, Highway Engineering Division, Downsview, Ontario, Canada.
- Ontario Ministry of Transportation and Communications. (1992). Ontario highway bridge design code (OHBDC). 3rd Edition, Highway Engineering Division, Downsview, Ontario.
- Ozgun, C. (2011). Influence of Cross-Frame Detailing on Curved and Skewed Steel I-Girder Bridges, Ph.D. Dissertation, Georgia Institute of Technology, Atlanta, GA. 382 pp.
- Phuvoravan, K., Chung, W., Liu, J., and Sotelino, E. D. (2004). Simplified live load distribution factor equation for steel girder bridges. Transportation Research Record. 1892, Transportation Research Board, Washington, D.C., 88-97.
- Razzaq, M. K., Sennah, K., Ghrib, F., (2015). Effectiveness of Cross-Frame Layout in Skew Composite Concrete Deck-over Steel I-Girder Bridges. 4th International CSCE Specialty Conference of Engineering Mechanics and Materials, May 27-30, 2015, Regina, SK, Canada. (Paper I.D-226)
- Razzaq, M. K., Sennah, K., Ghrib, F., (2016). Effect of Sequence of Construction on the Shear Distribution of Skewed Composite Concrete Deck-Over Steel I-Girder Bridges. CSCE Annual Conference, June 1-4, 2016, London, ON, Canada. (Paper I.D: GEN-252)

- Razaqpur A.G. and Esfandiari A. (2006). Redistribution of longitudinal moments in straight, continuous concrete slab-steel girder composite bridges. *Can J Civ Eng.*, 33:471–88.
- Seo, J., Phares, B. M., and Wipf, T. J., (2014). Lateral Live-Load Distribution Characteristics of Simply Supported Steel Girder Bridges Loaded with Implements of Husbandry. *J. Bridge Eng.*, 19(4). ISSN 1084-0702/04013021(12).
- Shahawy, M., and Huang, D. (2001). Analytical and Field Investigation of Lateral Load Distribution in Concrete Slab-on-Girder Bridges. *ACI Structural Journal*: 590-599.
- Sharafbayani, M., Linzell, D.G. and Chen, C.C., (2011). Web plumb influence on skewed I-girder steel bridges during construction, *Bridge Structures* 7, 115–122
- Soliman, M.H. (1992). Ultimate Behavior of Composite Steel Concrete Bridges with Rigid and Simple Diaphragms Connections, Ph.D. Thesis, Civil Engineering Department, University of Windsor, ON, Canada.
- Sotelino E., Liu Judy, Chung W. and Phuvoravan K. (2004). Simplified Load Distribution Factor for Use in LRFD Design, Final Report, FHWA/IN/JTRP-2004/20, Indiana DOT, Joint Transportation Research Program, Purdue University. West Lafayette, IN.
- Surana, C. S. and Humar, J. L. (1984). Beam-and-slab bridges with small skew, *Canadian Journal of Civil Engineering*. 11, 117-121.
- Tarhini, K. M., & Frederick, G. R. (1992). Wheel Load Distribution in I-Girder Highway Bridges. *ASCE Journal of Structural Engineering*, 118 (5), 1285-1294.
- Theodor, N.C. and Al-Bazi, G. (1997). *Manual of Standard Short-Span Steel Bridges*. Ministry of Transportation, ON, Canada.
- Theoret, P. and Massicotte, B. (2011). Development of a new simplified method of analysis of straight and skewed slab-on-girder bridges for the Canadian Bridge Code. Report SR11-06, Group for Research in Structural Engineering, Polytechnique Montreal, Montreal, Canada.
- Tian, X. (1999). Load Distribution Analyses of Skew Highway Concrete Bridges. Master's Thesis. College of Engineering, Florida Atlantic University Boca Raton, Florida.
- Turer, A. (1997), Stresses and damage predictions of steel stringer bridges using finite element modeling techniques and unit influence line decomposition method. Master's Thesis, Department of Civil and Environmental Engineering, University of Cincinnati, Cincinnati, OH.
- Turer, A. (2000). Condition evaluation and load rating of steel stringer highway bridges using field calibrated 2d-grid and 3D-FE models. Ph.D dissertation, Department of Civil and Environmental Engineering, University of Cincinnati, Cincinnati, USA.

- Vayas, I., Adamakos, T., and Iliopoulos, A. (2011). Three Dimensional Modeling for Steel-Concrete Composite Bridges using Systems of bar elements Modeling of Skewed Bridges. *International Journal of Steel Structures*, March 2011, Vol 11, No 2.
- Walker, W. H. (1987). Lateral Load Distribution in Multi-girder Bridges. *AISC Engg. Journal*, 21-28.
- Wassef, J. (2004). Curved Concrete Slab-on-Steel I-Girder Bridges. M.A.Sc. thesis, Dept. of Civil Engineering, Ryerson University, Toronto.
- Wu, H. (2003). Influence of Live-Load Deflections on Superstructure Performance of Slab on Steel Stringer Bridges. Ph. D. dissertation, Morgantown, West Virginia University, USA.
- Yam, L. C. P., and Chapman, J. C. (1972). The inelastic behavior of continuous composite beams of steel and concrete. *Proceedings, Inst. Civ.Eng., Struct. Build.*, 53, 487–501.
- Yousif, Z. (2005). Live Load Distribution for Highway Bridges based on AASHTO-LRFD and Finite Element Analysis, Master Thesis, Department of Civil Engineering and Construction, Bradley University, Peoria, IL, USA.
- Yousif, Z. and Hindi, R., (2006). Effect of Longitudinal Stiffness on Bridge Live Load Distribution Using the CHBDC, AASHTO-LRFD and Finite Element Analysis, 1st International CSCE Structural Speciality Conference, May 23-26, Calgary, Alberta, Canada
- Yousif, Z. and Hindi, R. (2007). AASHTO-LRFD Live Load Distribution for Beam-and-Slab Bridges: Limitations and Applicability. *Journal of Bridge Engineering*, 12(6): 1084-0702.
- Yura, J. A., Phillips, B. A., Raju, S., and Webb, S. (1992). Bracing of steel beams in bridges. Rep. No. 1239-4F, Center for Transportation Research, The Univ. of Texas at Austin, Austin, Tex., USA.
- Zienkiewicz, O.C., and Taylor, R.L. (1989). *The Finite Element Method*, 4th ed. McGraw-Hill.
- Zokaie, T. (2000). AASHTO-LRFD live load distribution specifications. *Journal of Bridge Engineering*, ASCE, 5(2): 131–138.
- Zokaie, T., and Imbsen, R. A. (1992). Distribution of wheel loads on highway bridges. NCHRP 12-26 Final Rep. Research Results Digest 187, National Cooperative Highway Research Program, Washington, DC.

APPENDIX A

Illustrative Example for Moment and Shear Distribution Factors for Skewed Slab-on Steel I-girder Bridges at Dead Load

For illustrative example, the bridge configuration details are as follows:

Span length (L) = 25 m; Bridge width (W) = 14.6 m; Girder spacing (S) = 2.09 m; Number of girders (N) = 7; Number of lanes (n) = 4, and Skew angle (ψ) = 60°.

1) Moment distribution factor calculation (Fm)

Using FEA: Fm value for exterior girder = 1.08
Fm value for interior girder = 1.17

Using proposed equation: (reference Table 4.2)

i. Exterior girder: $\varepsilon = 0.30 \times (25)^{1.25} \times (2.09)^{-4.6} \times (7)^{-2.5} \times (4)^{4.85} \times \tan(60) = 6.28$

$$Fm = 1.2 - \frac{2.0}{(6.28 + 10)} = \underline{1.08}$$

ii. Interior girder: $\varepsilon = 0.15 \times (25)^{0.28} \times (2.09)^{1.04} \times (7)^{1.16} \times (4)^{-0.82} \times \tan(60) = 4.22$

$$Fm = 5.37 - \frac{60.0}{(4.22 + 10)} = \underline{1.15}$$

2) Shear distribution factor calculation (Fv)

Using FEA: Fv value at obtuse corner = 1.39
Fv value at acute corner = 0.96
Fv value for interior girder = 0.96

Using proposed equation: (reference Table 4.3)

i. Obtuse corner: $\varepsilon = 6.77 \times (25)^{-1.0} \times (2.09)^{-1.0} \times (7)^{2.48} \times (4)^{1.61} \times \cos(60) = 75.27$

$$Fv = 1.4 - \frac{2.35}{(75.27 + 6.52)} = \underline{1.37}$$

ii. Acute corner:

$$\varepsilon = -35 \times (25)^{-0.16} \times (2.09)^{-1.7} \times (7)^{-0.72} \times (4)^{0.38} \times \cos(60) = -1.24$$

$$F_v = 1.2 - \frac{2.0}{(-1.24 + 10)} = \underline{0.97}$$

iii. Interior girder: $\varepsilon = 0.25 \times (25)^{1.15} \times (2.09)^{-1.0} \times (7)^{1.95} \times (4)^{-0.35} \times \cos(60) = 66.32$

$$F_v = 1.0 - \frac{1.4}{(66.32 + 2.5)} = \underline{0.98}$$

For comparison purposes, shear distribution factor using CHBDC (CSA 2014a, clause 5.6.3(b)):

$$\varepsilon = \left(\frac{25}{2.09} \right) \times \tan(60) = 20.72$$

$$F_s = 1.2 - \frac{2.0}{(20.72 + 10)} = \underline{1.13}$$

Comment: CHBDC equation underestimates the girder shear at obtuse corners by 19%, whereas the design equation overestimates the girder shear at acute corners and at interior girder by 15% when compared with FEA.

APPENDIX B

Illustrative Example for Moment and Shear Distribution Factors for Straight Slab-on Steel I-girder Bridges at ULS and SLS

For illustrative example, the straight bridge configuration details are as follows:

Span length (L) = 40 m; Bridge width (W) = 18.0 m; Girder spacing (S) = 2.57 m; Number of girders (N) = 7; Number of lanes (n) = 4, and Design lane width (We) = 4.25 m.

B-1: Moment Distribution Factors

1) Exterior Girder

i. Using FEA:

$$F_{T_m} \text{ value for exterior girder} = \underline{0.60}$$

ii. Using proposed equation (reference Table 5.3):

$$D_T = (0.14 - 10L^{-2.0}) \times N^{1.27} = (0.14 - 10 \times 40^{-2.0}) \times 7^{1.27} = 1.58$$

$$\lambda = -0.24 + \frac{1.55}{L} = -0.24 + \frac{1.55}{40} = -0.20$$

$$\gamma_C = S^{1.31} = 2.57^{1.31} = 3.44$$

$$\mu = \frac{W_e - 3.3}{0.6} \leq 1.0 \Rightarrow \frac{4.25 - 3.3}{0.6} = 1.58 > 1.0 \Rightarrow \text{Take } \mu = 1.0$$

CHBDC clause (5.6.4.3)

$$F_T = \frac{S}{D_T \gamma_C (1 + \mu \lambda)} \geq 1.05 \frac{nR_L}{N} \text{ for ULS \& SLS}$$

$$\therefore F_T = \frac{2.57}{1.58 \times 3.44 (1 + (1) \times (-0.20))} = \underline{0.59}$$

Check :

$$F_T (0.59) \geq 1.05 \frac{nR_L}{N}$$

$$F_T(0.59) \geq 1.05 \times \frac{4 \times 0.70}{7}$$

$$\therefore F_T(0.59) \geq 0.42 \quad (OK)$$

iii. Using CHBDC (CSA 2014a):

From Table - 5.3:

$$D_T = \left(3.40 + \frac{L_e}{500} \right) = \left(3.40 + \frac{40}{500} \right) = 3.48$$

$$\lambda = 0.10 - \frac{0.25}{L_e} = 0.10 - \frac{0.25}{40} = 0.09$$

From Table - 5.5:

$$\gamma_c = 1.0 \quad (\because S_c = 0.5S)$$

$$\mu = \frac{W_e - 3.3}{0.6} \leq 1.0 \Rightarrow \frac{4.25 - 3.3}{0.6} = 1.58 > 1.0 \Rightarrow \text{Take } \mu = 1.0$$

CHBDC clause (5.6.4.3)

$$F_T = \frac{S}{D_T \gamma_c (1 + \mu \lambda)} \geq 1.05 \frac{nR_L}{N} \quad \text{for ULS \& SLS}$$

$$\therefore F_T = \frac{2.57}{3.48 \times 1.0 (1 + (1) \times (0.09))} = \underline{0.68}$$

Check :

$$F_T(0.68) \geq 1.05 \frac{nR_L}{N}$$

$$F_T(0.68) \geq 1.05 \times \frac{4 \times 0.70}{7}$$

$$\therefore F_T(0.68) \geq 0.42 \quad (OK)$$

Comment: CHBDC equations result in conservative estimate (12%) when compared with FEA.

2) Interior girder

i. Using FEA:

$$F_{T_m} \text{ value for interior girder} = \underline{0.50}$$

ii. Using proposed equation (reference Table 5.4):

$$D_T = (5.48 - 1.21L^{-0.11}) \times N^{-0.10} = (5.48 - 1.21 \times 40^{-0.11}) \times 7^{-0.10} = 3.85$$

$$\lambda = 0.22 - \frac{1.50}{L} = 0.22 - \frac{1.50}{40} = 0.18$$

$$\gamma_c = S^{0.10} = 2.57^{0.10} = 1.10$$

$$\mu = \frac{W_e - 3.3}{0.6} \leq 1.0 \Rightarrow \frac{4.25 - 3.3}{0.6} = 1.58 > 1.0 \Rightarrow \text{Take } \mu = 1.0$$

CHBDC clause (5.6.4.3)

$$F_T = \frac{S}{D_T \gamma_c (1 + \mu \lambda)} \geq 1.05 \frac{nR_L}{N} \text{ for ULS \& SLS}$$

$$\therefore F_T = \frac{2.57}{3.85 \times 1.10 (1 + (1) \times (0.18))} = \underline{0.51}$$

Check :

$$F_T(0.51) \geq 1.05 \frac{nR_L}{N}$$

$$F_T(0.51) \geq 1.05 \times \frac{4 \times 0.70}{7}$$

$$\therefore F_T(0.51) \geq 0.42 \quad (\text{OK})$$

iii. Using CHBDC (CSA 2014a):

From Table -5.3:

$$D_T = \left(4.60 - \frac{5.30}{\sqrt{L_e + 5}} \right) = \left(4.60 - \frac{5.30}{\sqrt{40 + 5}} \right) = 3.81$$

$$\lambda = 0.10 - \frac{0.25}{L_e} = 0.10 - \frac{0.25}{40} = 0.09$$

$$\gamma_c = 1.0$$

$$\mu = \frac{W_e - 3.3}{0.6} \leq 1.0 \Rightarrow \frac{4.25 - 3.3}{0.6} = 1.58 > 1.0 \Rightarrow \text{Take } \mu = 1.0$$

CHBDC clause (5.6.4.3)

$$F_T = \frac{S}{D_T \gamma_c (1 + \mu \lambda)} \geq 1.05 \frac{nR_L}{N} \text{ for ULS \& SLS}$$

$$\therefore F_T = \frac{2.57}{3.81 \times 1.0 (1 + (1) \times (0.09))} = \underline{0.62}$$

Check :

$$F_T (0.62) \geq 1.05 \frac{nR_L}{N}$$

$$F_T (0.62) \geq 1.05 \times \frac{4 \times 0.70}{7}$$

$$\therefore F_T (0.62) \geq 0.42 \quad (OK)$$

Comment: CHBDC equations result in conservative estimate (20%) when compared with FEA.

B-2: Shear Distribution Factors

1) Exterior Girder

i. Using FEA:

$$F_{T_v} \text{ value for exterior girder} = \underline{0.67}$$

ii. Using proposed equation (reference Table 5.5):

$$D_T = (1.60 + 3.13L^{-0.08}) \times N^{-0.03} = (1.60 + 3.13 \times 40^{-0.08}) \times 7^{-0.03} = 3.71$$

$$\lambda = 0.0$$

$$\gamma_c = \left(\frac{S}{2.77} \right)^{-0.05} = \left(\frac{2.57}{2.77} \right)^{-0.05} = 1.00$$

$$\mu = \frac{W_e - 3.3}{0.6} \leq 1.0 \Rightarrow \frac{4.25 - 3.3}{0.6} = 1.58 > 1.0 \Rightarrow \text{Take } \mu = 1.0$$

CHBDC clause (5.6.4.3)

$$F_T = \frac{S}{D_T \gamma_c (1 + \mu \lambda)} \geq 1.05 \frac{nR_L}{N} \text{ for ULS \& SLS}$$

$$\therefore F_T = \frac{2.57}{3.71 \times 1.00(1 + (1) \times (0.00))} = \underline{0.69}$$

Check :

$$F_T(0.69) \geq 1.05 \frac{nR_L}{N}$$

$$F_T(0.69) \geq 1.05 \times \frac{4 \times 0.70}{7}$$

$$\therefore F_T(0.69) \geq 0.42 \quad (OK)$$

iii. Using CHBDC (CSA 2014a):

From Table – 5.3:

$$D_T = 3.40$$

$$\lambda = 0.00$$

From Table – 5.6:

$$\gamma_c = 1.0 \quad (\because S \geq 2.0)$$

$$\mu = \frac{W_e - 3.3}{0.6} \leq 1.0 \Rightarrow \frac{4.25 - 3.3}{0.6} = 1.58 > 1.0 \Rightarrow \text{Take } \mu = 1.0$$

CHBDC clause (5.6.4.3)

$$F_T = \frac{S}{D_T \gamma_c (1 + \mu \lambda)} \geq 1.05 \frac{nR_L}{N} \quad \text{for ULS \& SLS}$$

$$\therefore F_T = \frac{2.57}{3.40 \times 1.0(1 + (1) \times (0.00))} = \underline{0.76}$$

Check :

$$F_T(0.76) \geq 1.05 \frac{nR_L}{N}$$

$$F_T(0.76) \geq 1.05 \times \frac{4 \times 0.70}{7}$$

$$\therefore F_T(0.76) \geq 0.42 \quad (OK)$$

Comment: CHBDC equations result in conservative estimate (12%) when compared with FEA.

2) Interior girder

i. Using FEA:

$$F_{T_v} \text{ value for interior girder} = \underline{0.66}$$

ii. Using proposed equation (reference Table 5.6):

$$D_T = (1.047 + 1.29L^{0.02}) \times N^{0.02} = (1.047 + 1.29 \times 40^{0.02}) \times 7^{0.02} = 2.53$$

$$\lambda = 0.0$$

$$\gamma_c = \left(\frac{S}{0.04} \right)^{0.10} = \left(\frac{2.57}{0.04} \right)^{0.10} = 1.52$$

$$\mu = \frac{W_e - 3.3}{0.6} \leq 1.0 \Rightarrow \frac{4.25 - 3.3}{0.6} = 1.58 > 1.0 \Rightarrow \text{Take } \mu = 1.0$$

CHBDC clause (5.6.4.3)

$$F_T = \frac{S}{D_T \gamma_c (1 + \mu \lambda)} \geq 1.05 \frac{nR_L}{N} \text{ for ULS \& SLS}$$

$$\therefore F_T = \frac{2.57}{2.53 \times 1.52 (1 + (1) \times (0.00))} = \underline{0.67}$$

Check :

$$F_T (0.67) \geq 1.05 \frac{nR_L}{N}$$

$$F_T (0.67) \geq 1.05 \times \frac{4 \times 0.70}{7}$$

$$\therefore F_T (0.67) \geq 0.42 \quad (\text{OK})$$

iii. Using CHBDC (CSA 2014a):

From Table - 5.3:

$$D_T = 3.40$$

$$\lambda = 0.00$$

From Table – 5.6 :

$$\gamma_c = 1.0 \quad (\because S \geq 2.0)$$

$$\mu = \frac{W_e - 3.3}{0.6} \leq 1.0 \Rightarrow \frac{4.25 - 3.3}{0.6} = 1.58 > 1.0 \Rightarrow \text{Take } \mu = 1.0$$

CHBDC clause (5.6.4.3)

$$F_T = \frac{S}{D_T \gamma_c (1 + \mu \lambda)} \geq 1.05 \frac{nR_L}{N} \quad \text{for ULS \& SLS}$$

$$\therefore F_T = \frac{2.57}{3.40 \times 1.0 (1 + (1) \times (0.00))} = \underline{0.76}$$

Check :

$$F_T (0.76) \geq 1.05 \frac{nR_L}{N}$$

$$F_T (0.76) \geq 1.05 \times \frac{4 \times 0.70}{7}$$

$$\therefore F_T (0.76) \geq 0.42 \quad \quad \quad (OK)$$

Comment: CHBDC equations result in conservative estimate (13%) when compared with FEA.

APPENDIX C

Illustrative Example for Moment and Shear Distribution Factors for Straight Slab-on Steel I-girder Bridges at FLS

For illustrative example, the straight bridge configuration details are as follows:

Span length (L) = 40 m; Bridge width (W) = 18.0 m; Girder spacing (S) = 2.57 m; Number of girders (N) = 7; Number of lanes (n) = 4, and Design lane width (We) = 3.30 m.

C-1: Moment Distribution Factors

1) Exterior Girder

i. Using FEA:

$$F_{T_m} \text{ value for exterior girder} = \underline{0.32}$$

ii. Using proposed equation (reference Table 5.9):

$$D_T = (-29.08 + 26.44L^{0.13}) \times N^{-0.40} = (-29.08 + 26.44 \times 40^{0.13}) \times 7^{-0.40} = 6.26$$

$$\lambda = 0.27 + \frac{9.59}{L} = 0.27 + \frac{9.59}{40} = 0.51$$

$$\gamma_C = S^{-0.38} = 2.57^{-0.38} = 0.70$$

$$\mu = \frac{W_e - 3.3}{0.6} \leq 1.0 \Rightarrow \frac{3.3 - 3.3}{0.6} = 0.00$$

$$D_{VE} = \frac{\text{lane_width}}{2} - \text{half_truck_axle} + \text{shoulder_width} + \text{barrier}$$

$$\therefore D_{VE} = \frac{3.3}{2} - 0.9 + 1.9 + 0.5 = 3.15 > 3.0; \Rightarrow \therefore \text{Take } D_{VE} = 3.0m$$

From Table – 5.7 of CHBDC

$$\gamma_e = 0.28(D_{VE} - 1.0) \left[1 + \frac{160 \times (D_{VE} - 1.0)^2}{L^2} \right]; \quad \text{for } L > 20m$$

$$\therefore \gamma_e = 0.28(3.0 - 1.0) \left[1 + \frac{160 \times (3.0 - 1.0)^2}{40^2} \right] = 0.78$$

CHBDC clause (5.6.4.3)

$$F_T = \frac{S}{D_T \gamma_c (1 + \mu \lambda + \gamma_e)} \geq 1.05 \frac{1}{N} \quad \text{for FLS}$$

$$\therefore F_T = \frac{2.57}{6.26 \times 0.70 (1 + (0.00) \times (0.51) + 0.78)} = \underline{0.33}$$

Check :

$$F_T(0.33) \geq 1.05 \frac{1}{N}$$

$$F_T(0.33) \geq 1.05 \times \frac{1}{7}$$

$$\therefore F_T(0.33) \geq 0.15 \quad \text{(OK)}$$

iii. Using CHBDC (CSA 2014a):

From Table – 5.3:

$$D_T = \left(3.65 + \frac{L_e}{150} \right) \leq 4.10$$

$$D_T = \left(3.65 + \frac{40}{150} \right) = 3.92 \leq 4.10 \quad \text{(OK)}$$

$$\lambda = 0.00$$

From Table – 5.5:

$$\gamma_c = 1.0 \quad (\because S_c = 0.5S)$$

$$\mu = \frac{W_e - 3.3}{0.6} \leq 1.0 \Rightarrow \frac{3.3 - 3.3}{0.6} = 0.00$$

From Table – 5.7 of CHBDC

$$\gamma_e = 0.28(D_{VE} - 1.0) \left[1 + \frac{160 \times (D_{VE} - 1.0)^2}{L^2} \right]; \quad \text{for } L > 20m$$

$$\therefore \gamma_e = 0.28(3.0 - 1.0) \left[1 + \frac{160 \times (3.0 - 1.0)^2}{40^2} \right] = 0.78$$

CHBDC clause (5.6.4.3)

$$F_T = \frac{S}{D_T \gamma_C (1 + \mu \lambda + \gamma_e)} \geq 1.05 \frac{1}{N} \quad \text{for FLS}$$

$$\therefore F_T = \frac{2.57}{3.92 \times 1.0 (1 + (0.00) \times (0.00) + 0.78)} = \underline{0.37}$$

Check :

$$F_T (0.37) \geq 1.05 \frac{1}{N}$$

$$F_T (0.37) \geq 1.05 \times \frac{1}{7}$$

$$\therefore F_T (0.37) \geq 0.15 \quad \text{(OK)}$$

Comment: CHBDC equations result in conservative estimate (14%) when compared with FEA.

2) Interior girder

i. Using FEA:

$$F_{T_m} \text{ value for interior girder} = \underline{0.30}$$

ii. Using proposed equation (reference Table 5.10):

$$D_T = (0.393 + 3.16L^{-0.23}) \times N^{0.12} = (0.393 + 3.16 \times 40^{-0.23}) \times 7^{0.12} = 2.20$$

$$\lambda = 0.05$$

$$\gamma_C = S^{0.61} \times \left(2.68 - \frac{23.54}{L} \right) = 2.57^{0.61} \times \left(2.68 - \frac{23.54}{40} \right) = 3.72$$

$$\mu = \frac{W_e - 3.3}{0.6} \leq 1.0 \Rightarrow \frac{3.3 - 3.3}{0.6} = 0.00$$

$$\gamma_e = 0.00$$

CHBDC clause (5.6.4.3)

$$F_T = \frac{S}{D_T \gamma_c (1 + \mu \lambda + \gamma_e)} \geq 1.05 \frac{1}{N} \text{ for FLS}$$

$$\therefore F_T = \frac{2.57}{2.20 \times 3.72 (1 + (0.00) \times (0.05) + 0.00)} = \underline{0.31}$$

Check :

$$F_T (0.31) \geq 1.05 \frac{1}{N}$$

$$F_T (0.31) \geq 1.05 \times \frac{1}{7}$$

$$\therefore F_T (0.31) \geq 0.15 \quad (\text{OK})$$

iii. *Using CHBDC (CSA 2014a):*

From Table – 5.3 :

$$D_T = \left(5.15 - \frac{4.00}{\sqrt{L_e}} \right) = \left(5.15 - \frac{4.00}{\sqrt{40}} \right) = 4.52$$

$$\lambda = 0.05$$

$$\gamma_e = 0.00$$

$$\mu = \frac{W_e - 3.3}{0.6} \leq 1.0 \Rightarrow \frac{3.3 - 3.3}{0.6} = 0.00$$

From Table – 5.4 of CHBDC : for : $n \geq 2$; $10m < L_e \leq 50m$; $1.2m < S \leq 3.6m$

$$\gamma_c = 1.0 + (0.3S - 0.36) \left(\frac{L_e - 10}{40} \right) = 1.0 + (0.3 \times 2.57 - 0.36) \times \left(\frac{40 - 10}{40} \right) = 1.31$$

CHBDC clause (5.6.4.3)

$$F_T = \frac{S}{D_T \gamma_C (1 + \mu \lambda + \gamma_e)} \geq 1.05 \frac{1}{N} \text{ for FLS}$$

$$\therefore F_T = \frac{2.57}{4.52 \times 1.31 (1 + (0.00) \times (0.05) + 0.00)} = \underline{0.43}$$

Check :

$$F_T (0.43) \geq 1.05 \frac{1}{N}$$

$$F_T (0.43) \geq 1.05 \times \frac{1}{7}$$

$$\therefore F_T (0.43) \geq 0.15 \quad (OK)$$

Comment: CHBDC equations result in conservative estimate (30%) when compared with FEA.

C-2: Shear Distribution Factors

1) Exterior Girder

i. Using FEA:

$$F_{T_v} \text{ value for exterior girder} = \underline{0.27}$$

ii. Using proposed equation (reference Table 5.11):

$$D_T = (0.08 + 1.82L^{-1.28}) \times N^{2.73} = (0.08 + 1.82 \times 40^{-1.28}) \times 7^{2.73} = 19.51$$

$$\lambda = 0.0$$

$$\gamma_e = 0.0$$

$$\gamma_C = 0.074S^{2.02} = 0.074 \times 2.57^{2.02} = 0.50$$

$$\mu = \frac{W_e - 3.3}{0.6} \leq 1.0 \Rightarrow \frac{3.3 - 3.3}{0.6} = 0.0$$

CHBDC clause (5.6.4.3)

$$F_T = \frac{S}{D_T \gamma_C (1 + \mu \lambda + \gamma_e)} \geq 1.05 \frac{1}{N} \text{ for FLS}$$

$$\therefore F_T = \frac{2.57}{19.51 \times 0.50 (1 + (0.0) \times (0.0) + 0.00)} = \underline{0.26}$$

Check :

$$F_T (0.26) \geq 1.05 \frac{1}{N}$$

$$F_T (0.26) \geq 1.05 \times \frac{1}{7}$$

$$\therefore F_T (0.26) \geq 0.15 \quad (\text{OK})$$

iii. Using CHBDC (CSA 2014a):

From Table - 5.3 of CHBDC :

$$D_T = 3.60$$

$$\lambda = 0.0$$

$$\gamma_e = 0.0$$

From Table - 5.6 :

$$\gamma_C = 1.0 \quad (\because S \geq 2.0)$$

$$\mu = \frac{W_e - 3.3}{0.6} \leq 1.0 \Rightarrow \frac{3.3 - 3.3}{0.6} = 0.0$$

CHBDC clause (5.6.4.3)

$$F_T = \frac{S}{D_T \gamma_C (1 + \mu \lambda + \gamma_e)} \geq 1.05 \frac{1}{N} \text{ for FLS}$$

$$\therefore F_T = \frac{2.57}{3.60 \times 1.0 (1 + (0.0) \times (0.0) + 0.0)} = \underline{0.71}$$

Check :

$$F_T(0.71) \geq 1.05 \frac{1}{N}$$

$$F_T(0.71) \geq 1.05 \times \frac{1}{7}$$

$$\therefore F_T(0.71) \geq 0.15 \quad (\text{OK})$$

Comment: CHBDC equations presents highly conservative results (62%) when compared with FEA.

2) Interior girder

i. Using FEA:

$$F_{T_v} \text{ value for interior girder} = \underline{0.47}$$

ii. Using proposed equation (reference Table 5.12):

$$D_T = (1.656 - 35.95L^{-1.73}) \times N^{-0.48} = (1.656 - 35.95 \times 40^{-1.73}) \times 7^{-0.48} = 0.63$$

$$\lambda = 0.0$$

$$\gamma_e = 0.0$$

$$\gamma_c = 8.527S^{0.01} = 8.527 \times 2.57^{0.01} = 8.61$$

$$\mu = \frac{W_e - 3.3}{0.6} \leq 1.0 \Rightarrow \frac{3.3 - 3.3}{0.6} = 0.0$$

CHBDC clause (5.6.4.3)

$$F_T = \frac{S}{D_T \gamma_c (1 + \mu \lambda + \gamma_e)} \geq 1.05 \frac{1}{N} \text{ for FLS}$$

$$\therefore F_T = \frac{2.57}{0.63 \times 8.61 (1 + (0.0) \times (0.0) + 0.0)} = \underline{0.47}$$

Check :

$$F_T(0.47) \geq 1.05 \frac{1}{N}$$

$$F_T(0.47) \geq 1.05 \times \frac{1}{7}$$

$$\therefore F_T(0.47) \geq 0.15 \quad (OK)$$

iii. Using CHBDC (CSA 2014a):

From Table – 5.3 of CHBDC :

$$D_T = 3.60$$

$$\lambda = 0.0$$

$$\gamma_e = 0.0$$

From Table – 5.6 :

$$\gamma_c = 1.0 \quad (\because S \geq 2.0)$$

$$\mu = \frac{W_e - 3.3}{0.6} \leq 1.0 \Rightarrow \frac{3.3 - 3.3}{0.6} = 0.0$$

CHBDC clause (5.6.4.3)

$$F_T = \frac{S}{D_T \gamma_c (1 + \mu \lambda + \gamma_e)} \geq 1.05 \frac{1}{N} \quad \text{for FLS}$$

$$\therefore F_T = \frac{2.57}{3.60 \times 1.0 (1 + (0.0) \times (0.0) + 0.0)} = \underline{0.71}$$

Check :

$$F_T(0.71) \geq 1.05 \frac{1}{N}$$

$$F_T(0.71) \geq 1.05 \times \frac{1}{7}$$

$$\therefore F_T(0.71) \geq 0.15 \quad (OK)$$

Comment: CHBDC equations presents highly conservative results (34%) when compared with FEA.

APPENDIX D

Illustrative Example for Moment and Shear Distribution Factors for Skewed Slab-on Steel I-girder Bridges at ULS and SLS

For illustrative example, the skewed bridge configuration details are as follows:

Span length (L) = 40 m; Bridge width (W) = 18.0 m; Girder spacing (S) = 2.57 m; Number of girders (N) = 7; Number of lanes (n) = 4; Design lane width (We) = 4.25 m; and Skew angle (ψ) = 40°.

D-1: Moment Distribution Factors

1) Exterior Girder

i. Using FEA:

LDF value for exterior girder = 0.58

ii. Using proposed equation (reference Table 5.15):

For straight bridge: $F_T = 0.59$ (Appendix B)

Now for skewed bridge:

$$\begin{aligned}\varepsilon &= -11.0 \times L^{-0.02} \times S^{-1.19} \times N^{-1.24} \times n^{1.30} \times \tan \psi \\ \varepsilon &= -11.0 \times 40^{-0.02} \times 2.57^{-1.19} \times 7^{-1.24} \times 4^{1.30} \times \tan(40) = -1.51\end{aligned}$$

$$F_S = 1.2 - \frac{2.0}{(\varepsilon + 10)} = 1.2 - \frac{2.0}{(-1.51 + 10)} = 0.96$$

LDF for a skewed bridge = $F_T \times F_S = 0.59 \times 0.96 = \underline{0.57}$

iii. Using CHBDC (CSA 2014a):

For straight bridge: $F_T = 0.68$ (Appendix B)

Now for skewed bridge:

$$\varepsilon = \left(\frac{L}{S}\right) \times \tan \psi = \left(\frac{40}{2.57}\right) \times \tan(40) = 13.06$$

$$F_s = 1.2 - \frac{2.0}{(\varepsilon + 10)} = 1.2 - \frac{2.0}{(13.06 + 10)} = 1.11$$

$$\text{LDF for a skewed bridge} = F_T \times F_s = 0.68 \times 1.11 = \underline{0.75}$$

Comment: CHBDC equations present conservative results (23%) when compared with FEA

2) Interior girder

i. Using FEA:

$$\text{LDF value for interior girder} = \underline{0.48}$$

ii. Using proposed equation (reference Table 5.16):

For straight bridge: $F_T = 0.51$ (Appendix B)

Now for skewed bridge:

$$\varepsilon = -13.90 \times L^{-1.03} \times S^{0.31} \times N^{0.34} \times n^{0.28} \times \tan \psi$$

$$\varepsilon = -13.90 \times 40^{-1.03} \times 2.57^{0.31} \times 7^{0.34} \times 4^{0.28} \times \tan(40) = -1.0$$

$$F_s = 1.2 - \frac{2.0}{(\varepsilon + 10)} = 1.2 - \frac{2.0}{(-1.0 + 10)} = 0.97$$

$$\text{LDF for a skewed bridge} = F_T \times F_s = 0.51 \times 0.97 = \underline{0.49}$$

iii. Using CHBDC (CSA 2014a):

For straight bridge: $F_T = 0.62$ (Appendix B)

Now for skewed bridge:

$$\varepsilon = \left(\frac{L}{S}\right) \times \tan \psi = \left(\frac{40}{2.57}\right) \times \tan(40) = 13.06$$

$$F_S = 1.2 - \frac{2.0}{(\varepsilon + 10)} = 1.2 - \frac{2.0}{(13.06 + 10)} = 1.11$$

$$\text{LDF for a skewed bridge} = F_T \times F_S = 0.62 \times 1.11 = \underline{0.68}$$

Comment: CHBDC equations present conservative results (30%) when compared with FEA

D-2: Shear Distribution Factors

1) Obtuse Corner

i. Using FEA:

$$\text{LDF value for obtuse corner} = \underline{0.73}$$

ii. Using proposed equation (reference Table 5.17):

$$\text{For straight bridge: } F_T = 0.69 \text{ (Appendix B)}$$

Now for skewed bridge:

$$\varepsilon = 1.12 \times L^{0.37} \times S^{-1.56} \times N^{-0.02} \times n^{0.39} \times \tan \psi$$

$$\varepsilon = 1.12 \times 40^{0.37} \times 2.57^{-1.56} \times 7^{-0.02} \times 4^{0.39} \times \tan(40) = 1.39$$

$$F_S = 1.412 - \frac{0.80}{(\varepsilon + 1.31)} = 1.412 - \frac{0.80}{(1.39 + 1.31)} = 1.11$$

$$\text{LDF for a skewed bridge} = F_T \times F_S = 0.69 \times 1.11 = \underline{0.76}$$

iii. Using CHBDC (CSA 2014a):

$$\text{For straight bridge: } F_T = 0.76 \text{ (Appendix B)}$$

Now for skewed bridge:

$$\varepsilon = \left(\frac{L}{S}\right) \times \tan \psi = \left(\frac{40}{2.57}\right) \times \tan(40) = 13.06$$

$$F_s = 1.2 - \frac{2.0}{(\varepsilon + 10)} = 1.2 - \frac{2.0}{(13.06 + 10)} = 1.11$$

$$\text{LDF for a skewed bridge} = F_T \times F_s = 0.76 \times 1.11 = \underline{0.84}$$

Comment: CHBDC equations present conservative results (13%) when compared with FEA

2) Acute Corner

i. Using FEA:

$$\text{LDF value for acute corner} = \underline{0.59}$$

ii. Using proposed equation (reference Table 5.18):

$$\text{For straight bridge: } F_T = 0.69 \text{ (Appendix B)}$$

Now for skewed bridge:

$$\varepsilon = -5.0 \times L^{-0.03} \times S^{-0.035} \times N^{0.04} \times n^{0.03} \times \tan \psi$$

$$\varepsilon = -5.0 \times 40^{-0.03} \times 2.57^{-0.035} \times 7^{0.04} \times 4^{0.03} \times \tan(40) = -4.09$$

$$F_s = 1.20 - \frac{2.0}{(\varepsilon + 10)} = 1.20 - \frac{2.0}{(-4.09 + 10)} = 0.86$$

$$\text{LDF for a skewed bridge} = F_T \times F_s = 0.69 \times 0.86 = \underline{0.59}$$

iii. Using CHBDC (CSA 2014a):

$$\text{For straight bridge: } F_T = 0.76 \text{ (Appendix B)}$$

Now for skewed bridge:

$$\varepsilon = \left(\frac{L}{S}\right) \times \tan \psi = \left(\frac{40}{2.57}\right) \times \tan(40) = 13.06$$

$$F_s = 1.2 - \frac{2.0}{(\varepsilon + 10)} = 1.2 - \frac{2.0}{(13.06 + 10)} = 1.11$$

$$\text{LDF for a skewed bridge} = F_T \times F_s = 0.76 \times 1.11 = \underline{0.84}$$

Comment: CHBDC equations present conservative results (30%) when compared with FEA

3) Interior girder

i. Using FEA:

$$\text{LDF value for interior girder} = \underline{0.67}$$

ii. Using proposed equation (reference Table 5.19):

$$\text{For straight bridge: } F_T = 0.67 \text{ (Appendix B)}$$

Now for skewed bridge:

$$\varepsilon = 0.45 \times L^{2.73} \times S^{0.98} \times N^{-4.17} \times n^{-3.66} \times \tan \psi$$

$$\varepsilon = 0.45 \times 40^{2.73} \times 2.57^{0.98} \times 7^{-4.17} \times 4^{-3.66} \times \tan(40) = 0.04$$

$$F_S = 1.20 - \frac{2.0}{(\varepsilon + 10)} = 1.20 - \frac{2.0}{(0.04 + 10)} = 1.00$$

$$\text{LDF for a skewed bridge} = F_T \times F_S = 0.67 \times 1.00 = \underline{0.67}$$

iii. Using CHBDC (CSA 2014a):

$$\text{For straight bridge: } F_T = 0.76 \text{ (Appendix B)}$$

Now for skewed bridge:

$$\varepsilon = \left(\frac{L}{S} \right) \times \tan \psi = \left(\frac{40}{2.57} \right) \times \tan(40) = 13.06$$

$$F_S = 1.2 - \frac{2.0}{(\varepsilon + 10)} = 1.2 - \frac{2.0}{(13.06 + 10)} = 1.11$$

$$\text{LDF for a skewed bridge} = F_T \times F_S = 0.76 \times 1.11 = \underline{0.84}$$

Comment: CHBDC equations present conservative results (20%) when compared with FEA

APPENDIX E

Illustrative Example for Moment and Shear Distribution Factors for Skewed Slab-on Steel I-girder Bridges at FLS

For illustrative example, the skewed bridge configuration details are as follows:

Span length (L) = 40 m; Bridge width (W) = 18.0 m; Girder spacing (S) = 2.57 m; Number of girders (N) = 7; Number of lanes (n) = 4; Design lane width (We) = 3.3 m; and Skew angle (ψ) = 40°.

E-1: Moment Distribution Factors

1) Exterior Girder

i. Using FEA:

LDF value for exterior girder = 0.31

ii. Using proposed equation (reference Table 5.22):

For straight bridge: $F_T = 0.33$ (Appendix C)

Now for skewed bridge:

$$\begin{aligned}\varepsilon &= -0.28 \times L^{-0.64} \times S^{2.05} \times N^{2.39} \times n^{-1.58} \times \tan \psi \\ \varepsilon &= -0.28 \times 40^{-0.64} \times 2.57^{2.05} \times 7^{2.39} \times 4^{-1.58} \times \tan(40) = -1.80\end{aligned}$$

$$F_S = 1.2 - \frac{2.0}{(\varepsilon + 10)} = 1.2 - \frac{2.0}{(-1.80 + 10)} = 0.96$$

LDF for a skewed bridge = $F_T \times F_S = 0.33 \times 0.96 = \underline{0.32}$

iii. Using CHBDC (CSA 2014a):

For straight bridge: $F_T = 0.37$ (Appendix C)

Now for skewed bridge:

$$\varepsilon = \left(\frac{L}{S}\right) \times \tan \psi = \left(\frac{40}{2.57}\right) \times \tan(40) = 13.06$$

$$F_s = 1.2 - \frac{2.0}{(\varepsilon + 10)} = 1.2 - \frac{2.0}{(13.06 + 10)} = 1.11$$

$$\text{LDF for a skewed bridge} = F_T \times F_s = 0.37 \times 1.11 = \underline{0.41}$$

Comment: CHBDC equations present conservative results (25%) when compared with FEA

2) Interior girder

i. Using FEA:

$$\text{LDF value for interior girder} = \underline{0.28}$$

ii. Using proposed equation (reference Table 5.23):

For straight bridge: $F_T = 0.31$ (Appendix C)

Now for skewed bridge:

$$\varepsilon = -0.12 \times L^{0.41} \times S^{0.75} \times N^{0.40} \times n^{0.18} \times \tan \psi$$

$$\varepsilon = -0.12 \times 40^{0.41} \times 2.57^{0.75} \times 7^{0.40} \times 4^{0.18} \times \tan(40) = -2.59$$

$$F_s = 1.2 - \frac{2.0}{(\varepsilon + 10)} = 1.2 - \frac{2.0}{(-2.59 + 10)} = 0.93$$

$$\text{LDF for a skewed bridge} = F_T \times F_s = 0.31 \times 0.93 = \underline{0.29}$$

iii. Using CHBDC (CSA 2014a):

For straight bridge: $F_T = 0.43$ (Appendix C)

Now for skewed bridge:

$$\varepsilon = \left(\frac{L}{S}\right) \times \tan \psi = \left(\frac{40}{2.57}\right) \times \tan(40) = 13.06$$

$$F_s = 1.2 - \frac{2.0}{(\varepsilon + 10)} = 1.2 - \frac{2.0}{(13.06 + 10)} = 1.11$$

$$\text{LDF for a skewed bridge} = F_T \times F_s = 0.43 \times 1.11 = \underline{0.48}$$

Comment: CHBDC equations present conservative results (42%) when compared with FEA

E-2: Shear Distribution Factors

1) Obtuse Corner

i. Using FEA:

$$\text{LDF value for obtuse corner} = \underline{0.33}$$

ii. Using proposed equation (reference Table 5.24):

$$\text{For straight bridge: } F_T = 0.26 \text{ (Appendix C)}$$

Now for skewed bridge:

$$\varepsilon = 0.30 \times L^{0.60} \times S^{-0.59} \times N^{4.64} \times n^{-2.66} \times \tan \psi$$

$$\varepsilon = 0.30 \times 40^{0.60} \times 2.57^{-0.59} \times 7^{4.64} \times 4^{-2.66} \times \tan(40) = 275.48$$

$$F_s = 1.2 - \frac{2.0}{(\varepsilon + 10)} = 1.2 - \frac{2.0}{(275.48 + 10)} = 1.19$$

$$\text{LDF for a skewed bridge} = F_T \times F_s = 0.26 \times 1.19 = \underline{0.31}$$

iii. Using CHBDC (CSA 2014a):

$$\text{For straight bridge: } F_T = 0.71 \text{ (Appendix C)}$$

Now for skewed bridge:

$$\varepsilon = \left(\frac{L}{S}\right) \times \tan \psi = \left(\frac{40}{2.57}\right) \times \tan(40) = 13.06$$

$$F_s = 1.2 - \frac{2.0}{(\varepsilon + 10)} = 1.2 - \frac{2.0}{(13.06 + 10)} = 1.11$$

$$\text{LDF for a skewed bridge} = F_T \times F_s = 0.71 \times 1.11 = \underline{0.79}$$

Comment: CHBDC equations present highly conservative results (58%) when compared with FEA.

2) Acute Corner

i. Using FEA:

$$\text{LDF value for acute corner} = \underline{0.22}$$

ii. Using proposed equation (reference Table 5.25):

$$\text{For straight bridge: } F_T = 0.26 \text{ (Appendix C)}$$

Now for skewed bridge:

$$\varepsilon = -2.80 \times L^{-0.14} \times S^{0.83} \times N^{0.29} \times n^{-0.18} \times \tan \psi$$

$$\varepsilon = -2.80 \times 40^{-0.14} \times 2.57^{0.83} \times 7^{0.29} \times 4^{-0.18} \times \tan(40) = -4.20$$

$$F_s = 1.20 - \frac{2.0}{(\varepsilon + 10)} = 1.20 - \frac{2.0}{(-4.20 + 10)} = 0.86$$

$$\text{LDF for a skewed bridge} = F_T \times F_s = 0.26 \times 0.86 = \underline{0.22}$$

iii. Using CHBDC (CSA 2014a):

$$\text{For straight bridge: } F_T = 0.71 \text{ (Appendix C)}$$

Now for skewed bridge:

$$\varepsilon = \left(\frac{L}{S}\right) \times \tan \psi = \left(\frac{40}{2.57}\right) \times \tan(40) = 13.06$$

$$F_s = 1.2 - \frac{2.0}{(\varepsilon + 10)} = 1.2 - \frac{2.0}{(13.06 + 10)} = 1.11$$

$$\text{LDF for a skewed bridge} = F_T \times F_S = 0.71 \times 1.11 = \underline{0.79}$$

Comment: CHBDC equations present highly conservative results (72%) when compared with FEA

3) Interior girder

i. Using FEA:

$$\text{LDF value for interior girder} = \underline{0.49}$$

ii. Using proposed equation (reference Table 5.26):

$$\text{For straight bridge: } F_T = 0.47 \text{ (Appendix C)}$$

Now for skewed bridge:

$$\varepsilon = 93.50 \times L^{3.75} \times S^{-4.91} \times N^{-14.17} \times n^{10.63} \times \tan \psi$$

$$\varepsilon = 93.50 \times 40^{3.75} \times 2.57^{-4.91} \times 7^{-14.17} \times 4^{10.63} \times \tan(40) = 2.06$$

$$F_S = 1.20 - \frac{2.0}{(\varepsilon + 10)} = 1.20 - \frac{2.0}{(2.06 + 10)} = 1.03$$

$$\text{LDF for a skewed bridge} = F_T \times F_S = 0.47 \times 1.03 = \underline{0.48}$$

iii. Using CHBDC (CSA 2014a):

$$\text{For straight bridge: } F_T = 0.71 \text{ (Appendix C)}$$

Now for skewed bridge:

$$\varepsilon = \left(\frac{L}{S} \right) \times \tan \psi = \left(\frac{40}{2.57} \right) \times \tan(40) = 13.06$$

$$F_S = 1.2 - \frac{2.0}{(\varepsilon + 10)} = 1.2 - \frac{2.0}{(13.06 + 10)} = 1.11$$

$$\text{LDF for a skewed bridge} = F_T \times F_S = 0.71 \times 1.11 = \underline{0.79}$$

Comment: CHBDC equations present highly conservative results (38%) when compared with FEA.

APPENDIX F

Illustrative Example for Moment and Shear Distribution Factors for Straight Two-span Continuous Slab-on Steel I-girder Bridges at Dead Load

For the evaluation of distribution factors under dead load conditions, the illustrative example of a straight two-span continuous bridge configuration details are as follows:

Two equal spans having clear span length (L_1 & L_2) = 30 m; Bridge width (W) = 4.5 m; Girder spacing (S) = 1.50 m; Number of girders (N) = 3; Number of lanes (n) = 1, and Design lane width (W_e) = 3.5 m.

Span Moment Distribution Factors at Exterior and Interior Girder

For span moment: $L_e = 0.75L_1 = 0.75 \times 30 = 22.5$ m

Using FEA: F_m value for exterior girder = 1.0
 F_m value for interior girder = 0.98

Using proposed equation (reference Table 7.2):

i. Exterior girder: $\varepsilon = 0$ ($\because \psi = 0^\circ$)

$$F_m = 1.2 - \frac{2.0}{(0+10)} = \underline{1.0}$$

ii. Interior girder: $\varepsilon = 0$

$$F_m = 1.2 - \frac{2.0}{(0+10)} = \underline{1.0}$$

Support Moment Distribution Factors at Exterior and Interior Girder

For intermediate support moment: $L_e = 0.25(L_1 + L_2) = 0.25(30 + 30) = 15.0$ m

Using FEA: F_m value for exterior girder = 1.0

Fm value for interior girder = 0.98

Using proposed equation (reference Table 7.3):

- i. Exterior girder: $\varepsilon = 0$

$$Fm = 1.2 - \frac{2.0}{(0+10)} = \underline{1.0}$$

- ii. Interior girder: $\varepsilon = 0$

$$Fm = 1.2 - \frac{2.0}{(0+10)} = \underline{1.0}$$

Span Shear Distribution Factors at Exterior and Interior Girder

For span shear: $L_e = 0.75L_1 = 0.75 \times 30 = 22.5$ m

Using FEA: Fv value for exterior girder = 0.97

Fv value for interior girder = 1.06

Using proposed equation (reference Table 7.2):

- i. Exterior girder:

$$\varepsilon = -0.14 \times (22.5)^{0.38} \times (1.50)^{-1.58} \times (3)^{1.72} \times (1)^{-1.14} \times \cos(0) = -1.59$$

$$Fv = 1.2 - \frac{2.0}{(-1.59+10)} = \underline{0.96}$$

- ii. Interior girder:

$$\varepsilon = 0.57 \times (22.5)^{0.41} \times (1.50)^{-0.67} \times (3)^{1.19} \times (1)^{-2.85} \times \cos(0) = 5.76$$

$$Fv = 1.2 - \frac{2.0}{(5.76+10)} = \underline{1.07}$$

For comparison purposes, shear distribution factor using CHBDC (CSA 2014a, clause 5.6.3(b)):

$$\varepsilon = \left(\frac{22.5}{1.50} \right) \times \tan(0) = 0$$

$$F_s = 1.2 - \frac{2.0}{(0 + 10)} = \underline{1.0}$$

Comment: CHBDC equation underestimates the interior girder shear by 6% when compared with FEA.

Support Shear Distribution Factors at Exterior and Interior Girder

For intermediate support shear: $L_e = 0.25 (L_1 + L_2) = 0.25 (30 + 30) = 15.0 \text{ m}$

Using FEA: F_v value for exterior girder = 0.97

F_v value for interior girder = 1.05

Using proposed equation (reference Table 7.3):

i. Exterior girder:

$$\varepsilon = -0.14 \times (15.0)^{0.38} \times (1.50)^{-1.58} \times (3)^{1.72} \times (1)^{-1.14} \times \cos(0) = -1.37$$

$$F_v = 1.2 - \frac{2.0}{(-1.37 + 10)} = \underline{0.97}$$

ii. Interior girder:

$$\varepsilon = 0.57 \times (15.0)^{0.41} \times (1.50)^{-0.67} \times (3)^{1.19} \times (1)^{-2.85} \times \cos(0) = 4.87$$

$$F_v = 1.2 - \frac{2.0}{(4.87 + 10)} = \underline{1.07}$$

For comparison purposes, shear distribution factor using CHBDC (CSA 2014a, clause 5.6.3(b)):

$$\varepsilon = \left(\frac{15.0}{1.50} \right) \times \tan(0) = 0$$

$$F_s = 1.2 - \frac{2.0}{(0 + 10)} = \underline{1.0}$$

Comment: CHBDC equation underestimates the interior girder shear by 5% when compared with FEA.

APPENDIX G

Illustrative Example for Moment and Shear Distribution Factors for Straight Two-span Continuous Slab-on Steel I-girder Bridges at ULS and SLS

For the evaluation of distribution factors, the illustrative example of a straight two-span continuous bridge configuration details are as follows:

Two equal spans having clear span length (L_1 & L_2) = 15 m; Bridge width (W) = 14.6 m; Girder spacing (S) = 2.09 m; Number of girders (N) = 7; Number of lanes (n) = 4, and Design lane width (W_e) = 3.4 m.

Span Moment Distribution Factors at Exterior and Interior Girder

For span moment at ULS and SLS: $L_e = 0.75L_1 = 0.75 \times 15 = 11.25$ m

1) Exterior Girder

i. Using FEA:

$$F_{T_m} \text{ value for exterior girder} = \underline{0.55}$$

ii. Using proposed equation (reference Table 7.4):

$$D_T = (2.78 + 2.92L_e^{-0.33}) \times N^{-0.01} = (2.78 + 2.92 \times 11.25^{-0.33}) \times 7^{-0.01} = 4.01$$

$$\lambda = 0.19 - \frac{0.04}{L_e} = 0.19 - \frac{0.04}{11.25} = 0.19$$

$$\gamma_C = S^{-0.11} = 2.09^{-0.11} = 0.92$$

$$\mu = \frac{W_e - 3.3}{0.6} \leq 1.0 \Rightarrow \frac{3.4 - 3.3}{0.6} = 0.17$$

CHBDC clause (5.6.4.3)

$$F_T = \frac{S}{D_T \gamma_C (1 + \mu \lambda)} \geq 1.05 \frac{nR_L}{N} \text{ for ULS \& SLS}$$

$$\therefore F_T = \frac{2.09}{4.01 \times 0.92 (1 + (0.17 \times 0.19))} = \underline{0.55}$$

Check :

$$F_T(0.55) \geq 1.05 \frac{nR_L}{N}$$

$$F_T(0.55) \geq 1.05 \times \frac{4 \times 0.70}{7}$$

$$\therefore F_T(0.55) \geq 0.42 \quad (OK)$$

iii. Using CHBDC (CSA 2014a):

From Table - 5.3:

$$D_T = \left(3.40 + \frac{L_e}{500} \right) = \left(3.40 + \frac{11.25}{500} \right) = 3.42$$

$$\lambda = 0.10 - \frac{0.25}{L_e} = 0.10 - \frac{0.25}{11.25} = 0.08$$

From Table - 5.5:

$$\gamma_c = 1.0 \quad (\because S_c = 0.5S)$$

$$\mu = \frac{W_e - 3.3}{0.6} \leq 1.0 \Rightarrow \frac{3.4 - 3.3}{0.6} = 0.17$$

CHBDC clause (5.6.4.3)

$$F_T = \frac{S}{D_T \gamma_c (1 + \mu \lambda)} \geq 1.05 \frac{nR_L}{N} \quad \text{for ULS \& SLS}$$

$$\therefore F_T = \frac{2.09}{3.42 \times 1.0 (1 + (0.17 \times 0.08))} = \underline{0.60}$$

Check :

$$F_T(0.60) \geq 1.05 \frac{nR_L}{N}$$

$$F_T(0.60) \geq 1.05 \times \frac{4 \times 0.70}{7}$$

$$\therefore F_T(0.60) \geq 0.42 \quad (OK)$$

Comment: CHBDC equation overestimates the exterior girder moment by 8%, when compared with FEA.

2) Interior girder

i. Using FEA:

$$F_{T_m} \text{ value for interior girder} = \underline{0.55}$$

ii. Using proposed equation (reference Table 7.4):

$$D_T = (1.80 + 1.00L_e^{0.31}) \times N^{-0.01} = (1.80 + 1.00 \times 11.25^{0.31}) \times 7^{-0.01} = 3.84$$

$$\lambda = -0.45 + \frac{12.75}{L_e} = -0.45 + \frac{12.75}{11.25} = 0.68$$

$$\gamma_C = S^{-0.13} = 2.09^{-0.13} = 0.91$$

$$\mu = \frac{W_e - 3.3}{0.6} \leq 1.0 \Rightarrow \frac{3.4 - 3.3}{0.6} = 0.17$$

CHBDC clause (5.6.4.3)

$$F_T = \frac{S}{D_T \gamma_C (1 + \mu \lambda)} \geq 1.05 \frac{nR_L}{N} \text{ for ULS \& SLS}$$

$$\therefore F_T = \frac{2.09}{3.84 \times 0.91 (1 + (0.17 \times 0.68))} = \underline{0.54}$$

Check :

$$F_T(0.54) \geq 1.05 \frac{nR_L}{N}$$

$$F_T(0.54) \geq 1.05 \times \frac{4 \times 0.70}{7}$$

$$\therefore F_T(0.54) \geq 0.42 \quad (OK)$$

iii. Using CHBDC (CSA 2014a):

From Table -5.3:

$$D_T = \left(4.60 - \frac{5.30}{\sqrt{L_e + 5}} \right) = \left(4.60 - \frac{5.30}{\sqrt{11.25 + 5}} \right) = 3.29$$

$$\lambda = 0.10 - \frac{0.25}{L_e} = 0.10 - \frac{0.25}{11.25} = 0.08$$

$$\gamma_c = 1.0$$

$$\mu = \frac{W_e - 3.3}{0.6} \leq 1.0 \Rightarrow \frac{3.4 - 3.3}{0.6} = 0.17$$

CHBDC clause (5.6.4.3)

$$F_T = \frac{S}{D_T \gamma_c (1 + \mu \lambda)} \geq 1.05 \frac{nR_L}{N} \text{ for ULS \& SLS}$$

$$\therefore F_T = \frac{2.09}{3.29 \times 1.0 (1 + (0.17 \times 0.08))} = \underline{0.63}$$

Check :

$$F_T (0.63) \geq 1.05 \frac{nR_L}{N}$$

$$F_T (0.63) \geq 1.05 \times \frac{4 \times 0.70}{7}$$

$$\therefore F_T (0.63) \geq 0.42 \quad (OK)$$

Comment: CHBDC equation overestimates the exterior girder moment by 13%, when compared with FEA.

Support Moment Distribution Factors at Exterior and Interior Girder

For intermediate support moment at ULS and SLS: $L_e = 0.25(L_1 + L_2) = 0.25(15 + 15) = 7.5$ m

1) Exterior Girder

i. Using FEA:

F_{T_m} value for exterior girder = 0.52

ii. Using proposed equation (reference Table 7.5):

$$D_T = (1.42 + 6.13L_e^{-0.47}) \times N^{0.11} = (1.42 + 6.13 \times 7.5^{-0.47}) \times 7^{0.11} = 4.70$$

$$\lambda = -1.19 + \frac{16.33}{L_e} = -1.19 + \frac{16.33}{7.5} = 0.99$$

$$\gamma_C = S^{-0.41} = 2.09^{-0.41} = 0.74$$

$$\mu = \frac{W_e - 3.3}{0.6} \leq 1.0 \Rightarrow \frac{3.4 - 3.3}{0.6} = 0.17$$

CHBDC clause (5.6.4.3)

$$F_T = \frac{S}{D_T \gamma_C (1 + \mu \lambda)} \geq 1.05 \frac{nR_L}{N} \text{ for ULS \& SLS}$$

$$\therefore F_T = \frac{2.09}{4.70 \times 0.74 (1 + (0.17 \times 0.99))} = \underline{0.51}$$

Check :

$$F_T (0.51) \geq 1.05 \frac{nR_L}{N}$$

$$F_T (0.51) \geq 1.05 \times \frac{4 \times 0.70}{7}$$

$$\therefore F_T (0.51) \geq 0.42 \quad (\text{OK})$$

iii. Using CHBDC (CSA 2014a):

From Table - 5.3:

$$D_T = \left(3.40 + \frac{L_e}{500} \right) = \left(3.40 + \frac{7.5}{500} \right) = 3.42$$

$$\lambda = 0.10 - \frac{0.25}{L_e} = 0.10 - \frac{0.25}{7.5} = 0.07$$

From Table –5.5:

$$\gamma_c = 1.0 \quad (\because S_c = 0.5S)$$

$$\mu = \frac{W_e - 3.3}{0.6} \leq 1.0 \Rightarrow \frac{3.4 - 3.3}{0.6} = 0.17$$

CHBDC clause (5.6.4.3)

$$F_T = \frac{S}{D_T \gamma_c (1 + \mu \lambda)} \geq 1.05 \frac{nR_L}{N} \quad \text{for ULS \& SLS}$$

$$\therefore F_T = \frac{2.09}{3.42 \times 1.0 (1 + (0.17 \times 0.07))} = \underline{0.60}$$

Check :

$$F_T (0.60) \geq 1.05 \frac{nR_L}{N}$$

$$F_T (0.60) \geq 1.05 \times \frac{4 \times 0.70}{7}$$

$$\therefore F_T (0.60) \geq 0.42 \quad \quad \quad (OK)$$

Comment: CHBDC equation overestimates the exterior girder support moment by 16%, when compared with FEA.

2) Interior girder

i. Using FEA:

$$F_{T_m} \text{ value for interior girder} = \underline{0.54}$$

ii. Using proposed equation (reference Table 7.5):

$$D_T = (0.40 + 4.20 L_e^{-0.10}) \times N^{0.12} = (0.40 + 4.20 \times 7.5^{-0.10}) \times 7^{0.12} = 4.84$$

$$\lambda = -0.87 + \frac{13.97}{L_e} = -0.87 + \frac{13.97}{7.5} = 0.99$$

$$\gamma_c = S^{-0.50} = 2.09^{-0.50} = 0.69$$

$$\mu = \frac{W_e - 3.3}{0.6} \leq 1.0 \Rightarrow \frac{3.4 - 3.3}{0.6} = 0.17$$

CHBDC clause (5.6.4.3)

$$F_T = \frac{S}{D_T \gamma_c (1 + \mu \lambda)} \geq 1.05 \frac{nR_L}{N} \text{ for ULS \& SLS}$$

$$\therefore F_T = \frac{2.09}{4.84 \times 0.69 (1 + (0.17 \times 0.99))} = \underline{0.54}$$

Check :

$$F_T(0.54) \geq 1.05 \frac{nR_L}{N}$$

$$F_T(0.54) \geq 1.05 \times \frac{4 \times 0.70}{7}$$

$$\therefore F_T(0.54) \geq 0.42 \quad (OK)$$

iii. Using CHBDC (CSA 2014a):

From Table - 5.3:

$$D_T = \left(4.60 - \frac{5.30}{\sqrt{L_e + 5}} \right) = \left(4.60 - \frac{5.30}{\sqrt{7.5 + 5}} \right) = 3.10$$

$$\lambda = 0.10 - \frac{0.25}{L_e} = 0.10 - \frac{0.25}{7.5} = 0.07$$

$$\gamma_c = 1.0$$

$$\mu = \frac{W_e - 3.3}{0.6} \leq 1.0 \Rightarrow \frac{3.4 - 3.3}{0.6} = 0.17$$

CHBDC clause (5.6.4.3)

$$F_T = \frac{S}{D_T \gamma_c (1 + \mu \lambda)} \geq 1.05 \frac{nR_L}{N} \text{ for ULS \& SLS}$$

$$\therefore F_T = \frac{2.09}{3.10 \times 1.0 (1 + (0.17 \times 0.07))} = \underline{0.67}$$

Check :

$$F_T(0.67) \geq 1.05 \frac{nR_L}{N}$$

$$F_T(0.67) \geq 1.05 \times \frac{4 \times 0.70}{7}$$

$$\therefore F_T(0.67) \geq 0.42 \quad (OK)$$

Comment: CHBDC equation overestimates the interior girder support moment by 20%, when compared with FEA.

Span Shear Distribution Factors at Exterior and Interior Girder

For span shear at ULS and SLS: $L_e = 0.75L_1 = 0.75 \times 15 = 11.25$ m

1) Exterior Girder

i. Using FEA:

$$F_{T_v} \text{ value for exterior girder} = \underline{0.53}$$

ii. Using proposed equation (reference Table 7.4):

$$D_T = (1.72 + 14.93L_e^{-1.72}) \times N^{0.07} = (1.72 + 14.93 \times 11.25^{-1.72}) \times 7^{0.07} = 2.24$$
$$\lambda = 0.0$$

$$\gamma_c = \left(\frac{S}{8.30} \right)^{-0.44} = \left(\frac{2.09}{8.30} \right)^{-0.44} = 1.83$$

$$\mu = \frac{W_e - 3.3}{0.6} \leq 1.0 \Rightarrow \frac{3.4 - 3.3}{0.6} = 0.17$$

CHBDC clause (5.6.4.3)

$$F_T = \frac{S}{D_T \gamma_c (1 + \mu \lambda)} \geq 1.05 \frac{nR_L}{N} \text{ for ULS \& SLS}$$

$$\therefore F_T = \frac{2.09}{2.24 \times 1.83 (1 + (0.17 \times 0.00))} = \underline{0.51}$$

Check :

$$F_T(0.51) \geq 1.05 \frac{nR_L}{N}$$

$$F_T(0.51) \geq 1.05 \times \frac{4 \times 0.70}{7}$$

$$\therefore F_T(0.51) \geq 0.42 \quad (OK)$$

iii. Using CHBDC (CSA 2014a):

From Table – 5.3:

$$D_T = 3.40$$

$$\lambda = 0.00$$

From Table – 5.6:

$$\gamma_C = 1.0 \quad (\because S \geq 2.0)$$

$$\mu = \frac{W_e - 3.3}{0.6} \leq 1.0 \Rightarrow \frac{3.4 - 3.3}{0.6} = 0.17$$

CHBDC clause (5.6.4.3)

$$F_T = \frac{S}{D_T \gamma_C (1 + \mu \lambda)} \geq 1.05 \frac{nR_L}{N} \quad \text{for ULS \& SLS}$$

$$\therefore F_T = \frac{2.09}{3.40 \times 1.0 (1 + (0.17 \times 0.00))} = \underline{0.61}$$

Check :

$$F_T(0.61) \geq 1.05 \frac{nR_L}{N}$$

$$F_T(0.61) \geq 1.05 \times \frac{4 \times 0.70}{7}$$

$$\therefore F_T(0.61) \geq 0.42 \quad (OK)$$

Comment: CHBDC equation overestimates the exterior girder span shear by 13%, when compared with FEA.

2) Interior girder

i. Using FEA:

$$F_{T_v} \text{ value for interior girder} = \underline{0.62}$$

ii. Using proposed equation (reference Table 7.4):

$$D_T = (1.897 + 1.95L_e^{0.06}) \times N^{0.06} = (1.897 + 1.95 \times 11.25^{0.06}) \times 7^{0.06} = 4.67$$

$$\lambda = 0.0$$

$$\gamma_c = \left(\frac{S}{1.11} \right)^{-0.46} = \left(\frac{2.09}{1.11} \right)^{-0.46} = 0.75$$

$$\mu = \frac{W_e - 3.3}{0.6} \leq 1.0 \Rightarrow \frac{3.4 - 3.3}{0.6} = 0.17$$

CHBDC clause (5.6.4.3)

$$F_T = \frac{S}{D_T \gamma_c (1 + \mu \lambda)} \geq 1.05 \frac{nR_L}{N} \text{ for ULS \& SLS}$$

$$\therefore F_T = \frac{2.09}{4.67 \times 0.75 (1 + (0.17 \times 0.00))} = \underline{0.60}$$

Check :

$$F_T (0.60) \geq 1.05 \frac{nR_L}{N}$$

$$F_T (0.60) \geq 1.05 \times \frac{4 \times 0.70}{7}$$

$$\therefore F_T (0.60) \geq 0.42 \quad (OK)$$

iii. Using CHBDC (CSA 2014a):

From Table -5.3:

$$D_T = 3.40$$

$$\lambda = 0.00$$

From Table – 5.6:

$$\gamma_c = 1.0 \quad (\because S \geq 2.0)$$

$$\mu = \frac{W_e - 3.3}{0.6} \leq 1.0 \Rightarrow \frac{3.4 - 3.3}{0.6} = 0.17$$

CHBDC clause (5.6.4.3)

$$F_T = \frac{S}{D_T \gamma_c (1 + \mu \lambda)} \geq 1.05 \frac{nR_L}{N} \quad \text{for ULS \& SLS}$$

$$\therefore F_T = \frac{2.09}{3.40 \times 1.0 (1 + (0.17 \times 0.00))} = \underline{0.61}$$

Check :

$$F_T (0.61) \geq 1.05 \frac{nR_L}{N}$$

$$F_T (0.61) \geq 1.05 \times \frac{4 \times 0.70}{7}$$

$$\therefore F_T (0.61) \geq 0.42 \quad \quad \quad (OK)$$

Comment: CHBDC equation shows good correlation with FEA.

Support Shear Distribution Factors at Exterior and Interior Girder

For intermediate support shear at ULS and SLS: $L_e = 0.25 (L_1 + L_2) = 0.25 (15 + 15) = 7.5$
m

1) Exterior Girder

i. Using FEA:

$$F_{T_v} \text{ value for exterior girder} = \underline{0.56}$$

ii. Using proposed equation (reference Table 7.5):

$$D_T = (6.38 + 5.79 L_e^{-0.11}) \times N^{0.03} = (6.38 + 5.79 \times 7.5^{-0.11}) \times 7^{0.03} = 11.68$$
$$\lambda = 0.0$$

$$\gamma_c = \left(\frac{S}{0.09} \right)^{-0.354} = \left(\frac{2.09}{0.09} \right)^{-0.354} = 0.33$$

$$\mu = \frac{W_e - 3.3}{0.6} \leq 1.0 \Rightarrow \frac{3.4 - 3.3}{0.6} = 0.17$$

CHBDC clause (5.6.4.3)

$$F_T = \frac{S}{D_T \gamma_c (1 + \mu \lambda)} \geq 1.05 \frac{nR_L}{N} \text{ for ULS \& SLS}$$

$$\therefore F_T = \frac{2.09}{11.68 \times 0.33 (1 + (0.17 \times 0.00))} = \underline{0.54}$$

Check :

$$F_T(0.54) \geq 1.05 \frac{nR_L}{N}$$

$$F_T(0.54) \geq 1.05 \times \frac{4 \times 0.70}{7}$$

$$\therefore F_T(0.54) \geq 0.42 \quad (OK)$$

iii. *Using CHBDC (CSA 2014a):*

From Table - 5.3:

$$D_T = 3.40$$

$$\lambda = 0.00$$

From Table - 5.6:

$$\gamma_c = 1.0 \quad (\because S \geq 2.0)$$

$$\mu = \frac{W_e - 3.3}{0.6} \leq 1.0 \Rightarrow \frac{3.4 - 3.3}{0.6} = 0.17$$

CHBDC clause (5.6.4.3)

$$F_T = \frac{S}{D_T \gamma_c (1 + \mu \lambda)} \geq 1.05 \frac{nR_L}{N} \text{ for ULS \& SLS}$$

$$\therefore F_T = \frac{2.09}{3.40 \times 1.0 (1 + (0.17 \times 0.00))} = \underline{0.61}$$

Check :

$$F_T(0.61) \geq 1.05 \frac{nR_L}{N}$$

$$F_T(0.61) \geq 1.05 \times \frac{4 \times 0.70}{7}$$

$$\therefore F_T(0.61) \geq 0.42 \quad (OK)$$

Comment: CHBDC equation overestimates the exterior girder support shear by 8%, when compared with FEA.

2) Interior girder

i. Using FEA:

$$F_{T_v} \text{ value for interior girder} = \underline{0.61}$$

ii. Using proposed equation (reference Table 7.5):

$$D_T = (4.65 + 0.12L_e^{-0.02}) \times N^{0.10} = (4.65 + 0.12 \times 7.5^{-0.02}) \times 7^{0.10} = 5.79$$

$$\lambda = 0.0$$

$$\gamma_c = \left(\frac{S}{0.92} \right)^{-0.60} = \left(\frac{2.09}{0.92} \right)^{-0.60} = 0.61$$

$$\mu = \frac{W_e - 3.3}{0.6} \leq 1.0 \Rightarrow \frac{3.4 - 3.3}{0.6} = 0.17$$

CHBDC clause (5.6.4.3)

$$F_T = \frac{S}{D_T \gamma_c (1 + \mu \lambda)} \geq 1.05 \frac{nR_L}{N} \quad \text{for ULS \& SLS}$$

$$\therefore F_T = \frac{2.09}{5.79 \times 0.61 (1 + (0.17 \times 0.00))} = \underline{0.59}$$

Check :

$$F_T(0.59) \geq 1.05 \frac{nR_L}{N}$$

$$F_T(0.59) \geq 1.05 \times \frac{4 \times 0.70}{7}$$

$$\therefore F_T(0.59) \geq 0.42 \quad (OK)$$

iii. Using CHBDC (CSA 2014a):

From Table – 5.3:

$$D_T = 3.40$$

$$\lambda = 0.00$$

From Table – 5.6:

$$\gamma_C = 1.0 \quad (\because S \geq 2.0)$$

$$\mu = \frac{W_e - 3.3}{0.6} \leq 1.0 \Rightarrow \frac{3.4 - 3.3}{0.6} = 0.17$$

CHBDC clause (5.6.4.3)

$$F_T = \frac{S}{D_T \gamma_C (1 + \mu \lambda)} \geq 1.05 \frac{nR_L}{N} \quad \text{for ULS \& SLS}$$

$$\therefore F_T = \frac{2.09}{3.40 \times 1.0 (1 + (0.17 \times 0.00))} = \underline{0.61}$$

Check :

$$F_T(0.61) \geq 1.05 \frac{nR_L}{N}$$

$$F_T(0.61) \geq 1.05 \times \frac{4 \times 0.70}{7}$$

$$\therefore F_T(0.61) \geq 0.42 \quad (OK)$$

Comment: CHBDC equation shows good correlation with FEA.

APPENDIX H

Illustrative Example for Moment and Shear Distribution Factors for Straight Two-span Continuous Slab-on Steel I-girder Bridges at FLS

For the evaluation of distribution factors, the illustrative example of a straight two-span continuous bridge configuration details are as follows:

Two equal spans having clear span length (L_1 & L_2) = 15 m; Bridge width (W) = 14.6 m; Girder spacing (S) = 2.09 m; Number of girders (N) = 7; Number of lanes (n) = 4, and Design lane width (W_e) = 3.4 m.

Span Moment Distribution Factors at Exterior and Interior Girder

For span moment at FLS: $L_e = 0.75L_1 = 0.75 \times 15 = 11.25$ m

1) Exterior Girder

i. Using FEA:

$$F_{T_m} \text{ value for exterior girder} = \underline{0.50}$$

ii. Using proposed equation (reference Table 7.6):

$$D_T = (-1.0 + 4.71L_e^{0.05}) \times N^{0.02} = (-1.0 + 4.71 \times 11.25^{0.05}) \times 7^{0.02} = 4.49$$

$$\lambda = 0.09 + \frac{7.20}{L_e} = 0.09 + \frac{7.20}{11.25} = 0.73$$

$$\gamma_C = S^{-0.30} = 2.09^{-0.30} = 0.80$$

$$\mu = \frac{W_e - 3.3}{0.6} \leq 1.0 \Rightarrow \frac{3.4 - 3.3}{0.6} = 0.17$$

$$D_{VE} = \frac{\text{lane_width}}{2} - \text{half_truck_axle} + \text{shoulder_width} + \text{barrier}$$

$$\therefore D_{VE} = \frac{3.4}{2} - 0.9 + 0 + 0.5 = 1.30$$

From Table-5.7 of CHBDC

$$\gamma_e = 0.28(D_{VE} - 1.0) \left[1 + 0.40 \times (D_{VE} - 1.0)^2 \right] \quad \text{for } n \geq 2; L \leq 20m$$
$$\therefore \gamma_e = 0.28(1.30 - 1.0) \left[1 + 0.40 \times (1.30 - 1.0)^2 \right] = 0.087$$

CHBDC clause (5.6.4.3)

$$F_T = \frac{S}{D_T \gamma_c (1 + \mu \lambda + \gamma_e)} \geq 1.05 \frac{1}{N} \quad \text{for FLS}$$
$$\therefore F_T = \frac{2.09}{4.49 \times 0.80 (1 + (0.17 \times 0.73) + 0.087)} = \underline{0.48}$$

Check :

$$F_T (0.48) \geq 1.05 \frac{1}{N}$$
$$F_T (0.48) \geq 1.05 \times \frac{1}{7}$$
$$\therefore F_T (0.48) \geq 0.15 \quad (OK)$$

iii. Using CHBDC (CSA 2014a):

From Table-5.3:

$$D_T = \left(3.65 + \frac{L_e}{150} \right) \leq 4.10$$
$$D_T = \left(3.65 + \frac{11.25}{150} \right) = 3.73 \leq 4.10 \quad (OK)$$
$$\lambda = 0.00$$

From Table-5.5:

$$\gamma_c = 1.0 \quad (\because S_c = 0.5S)$$
$$\mu = \frac{W_e - 3.3}{0.6} \leq 1.0 \Rightarrow \frac{3.4 - 3.3}{0.6} = 0.17$$

From Table-5.7 of CHBDC

$$\gamma_e = 0.28(D_{VE} - 1.0) \left[1 + 0.40 \times (D_{VE} - 1.0)^2 \right] \quad \text{for } n \geq 2; L \leq 20m$$

$$\therefore \gamma_e = 0.28(1.30 - 1.0) \left[1 + 0.40 \times (1.30 - 1.0)^2 \right] = 0.087$$

CHBDC clause (5.6.4.3)

$$F_T = \frac{S}{D_T \gamma_C (1 + \mu \lambda + \gamma_e)} \geq 1.05 \frac{1}{N} \quad \text{for FLS}$$

$$\therefore F_T = \frac{2.09}{3.73 \times 1.0 (1 + (0.17 \times 0.00) + 0.087)} = \underline{0.52}$$

Check :

$$F_T (0.52) \geq 1.05 \frac{1}{N}$$

$$F_T (0.52) \geq 1.05 \times \frac{1}{7}$$

$$\therefore F_T (0.52) \geq 0.15 \quad (OK)$$

Comment: CHBDC equation shows good correlation with FEA.

2) Interior girder

i. Using FEA:

$$F_{T_m} \text{ value for interior girder} = \underline{0.38}$$

ii. Using proposed equation (reference Table 7.6):

$$D_T = (1.09 + 1.09 L_e^{0.11}) \times N^{0.10} = (1.09 + 1.09 \times 11.25^{0.11}) \times 7^{0.10} = 3.05$$

$$\lambda = 0.05$$

$$\gamma_C = S^{0.59} \times \left(1.13 + \frac{0.98}{L_e} \right) = 2.09^{0.59} \times \left(1.13 + \frac{0.98}{11.25} \right) = 1.88$$

$$\mu = \frac{W_e - 3.3}{0.6} \leq 1.0 \Rightarrow \frac{3.4 - 3.3}{0.6} = 0.17$$

$$\gamma_e = 0.00$$

CHBDC clause (5.6.4.3)

$$F_T = \frac{S}{D_T \gamma_c (1 + \mu \lambda + \gamma_e)} \geq 1.05 \frac{1}{N} \text{ for FLS}$$

$$\therefore F_T = \frac{2.09}{3.05 \times 1.88 (1 + (0.17 \times 0.05) + 0.00)} = \underline{0.36}$$

Check :

$$F_T (0.36) \geq 1.05 \frac{1}{N}$$

$$F_T (0.36) \geq 1.05 \times \frac{1}{7}$$

$$\therefore F_T (0.36) \geq 0.15 \quad (\text{OK})$$

iii. Using CHBDC (CSA 2014a):

From Table – 5.3 :

$$D_T = \left(5.15 - \frac{4.00}{\sqrt{L_e}} \right) = \left(5.15 - \frac{4.00}{\sqrt{11.25}} \right) = 3.96$$

$$\lambda = 0.05$$

$$\gamma_e = 0.00$$

$$\mu = \frac{W_e - 3.3}{0.6} \leq 1.0 \Rightarrow \frac{3.4 - 3.3}{0.6} = 0.17$$

From Table – 5.4 of CHBDC : for : $n \geq 2$; $10m < L_e \leq 50m$; $1.2m < S \leq 3.6m$

$$\gamma_c = 1.0 + (0.3S - 0.36) \left(\frac{L_e - 10}{40} \right) = 1.0 + (0.3 \times 2.09 - 0.36) \times \left(\frac{11.25 - 10}{40} \right) = 1.01$$

CHBDC clause (5.6.4.3)

$$F_T = \frac{S}{D_T \gamma_c (1 + \mu \lambda + \gamma_e)} \geq 1.05 \frac{1}{N} \text{ for FLS}$$

$$\therefore F_T = \frac{2.09}{3.96 \times 1.01 (1 + (0.17 \times 0.05) + 0.00)} = \underline{0.52}$$

Check :

$$F_T(0.52) \geq 1.05 \frac{1}{N}$$

$$F_T(0.52) \geq 1.05 \times \frac{1}{7}$$

$$\therefore F_T(0.52) \geq 0.15 \quad (OK)$$

Comment: CHBDC equation shows overestimates the interior girder span moment by 27% when compared with FEA.

Support Moment Distribution Factors at Exterior and Interior Girder

For intermediate support moment at FLS: $L_e = 0.25 (L_1 + L_2) = 0.25 (15 + 15) = 7.5$ m

1) Exterior Girder

i. Using FEA:

$$F_{T_m} \text{ value for exterior girder} = \underline{0.47}$$

ii. Using proposed equation (reference Table 7.7):

$$D_T = (-1.25 + 8.02L_e^{-0.17}) \times N^{0.08} = (-1.25 + 8.02 \times 7.5^{-0.17}) \times 7^{0.08} = 5.19$$

$$\lambda = -1.15 + \frac{20.90}{L_e} = -1.15 + \frac{20.90}{7.5} = 1.64$$

$$\gamma_C = S^{-0.61} = 2.09^{-0.61} = 0.64$$

$$\mu = \frac{W_e - 3.3}{0.6} \leq 1.0 \Rightarrow \frac{3.4 - 3.3}{0.6} = 0.17$$

$$D_{VE} = \frac{\text{lane_width}}{2} - \text{half_truck_axle} + \text{shoulder_width} + \text{barrier}$$

$$\therefore D_{VE} = \frac{3.4}{2} - 0.9 + 0 + 0.5 = 1.30$$

From Table-5.7 of CHBDC

$$\gamma_e = 0.28(D_{VE} - 1.0) \left[1 + 0.40 \times (D_{VE} - 1.0)^2 \right] \quad \text{for } n \geq 2; L \leq 20m$$

$$\therefore \gamma_e = 0.28(1.30 - 1.0) \left[1 + 0.40 \times (1.30 - 1.0)^2 \right] = 0.087$$

CHBDC clause (5.6.4.3)

$$F_T = \frac{S}{D_T \gamma_C (1 + \mu \lambda + \gamma_e)} \geq 1.05 \frac{1}{N} \quad \text{for FLS}$$

$$\therefore F_T = \frac{2.09}{5.19 \times 0.64 (1 + (0.17 \times 1.64) + 0.087)} = 0.46$$

Check :

$$F_T (0.46) \geq 1.05 \frac{1}{N}$$

$$F_T (0.46) \geq 1.05 \times \frac{1}{7}$$

$$\therefore F_T (0.46) \geq 0.15 \quad \quad \quad (OK)$$

iii. Using CHBDC (CSA 2014a):

From Table-5.3:

$$D_T = \left(3.65 + \frac{L_e}{150} \right) \leq 4.10$$

$$D_T = \left(3.65 + \frac{7.5}{150} \right) = 3.70 \leq 4.10 \quad (OK)$$

$$\lambda = 0.00$$

From Table-5.5:

$$\gamma_C = 1.0 \quad (\because S_C = 0.5S)$$

$$\mu = \frac{W_e - 3.3}{0.6} \leq 1.0 \Rightarrow \frac{3.4 - 3.3}{0.6} = 0.17$$

From Table-5.7 of CHBDC

$$\gamma_e = 0.28(D_{VE} - 1.0) \left[1 + 0.40 \times (D_{VE} - 1.0)^2 \right] \quad \text{for } n \geq 2; L \leq 20m$$

$$\therefore \gamma_e = 0.28(1.30 - 1.0) \left[1 + 0.40 \times (1.30 - 1.0)^2 \right] = 0.087$$

CHBDC clause (5.6.4.3)

$$F_T = \frac{S}{D_T \gamma_C (1 + \mu \lambda + \gamma_e)} \geq 1.05 \frac{1}{N} \quad \text{for FLS}$$

$$\therefore F_T = \frac{2.09}{3.70 \times 1.0 (1 + (0.17 \times 0.00) + 0.087)} = \underline{0.52}$$

Check :

$$F_T (0.52) \geq 1.05 \frac{1}{N}$$

$$F_T (0.52) \geq 1.05 \times \frac{1}{7}$$

$$\therefore F_T (0.52) \geq 0.15 \quad \quad \quad (OK)$$

Comment: CHBDC equation shows overestimates the exterior girder support moment by 10% when compared with FEA.

2) Interior girder

i. Using FEA:

$$F_{T_m} \text{ value for interior girder} = \underline{0.38}$$

ii. Using proposed equation (reference Table 7.7):

$$D_T = (1.68 + 2.94 L_e^{-0.49}) \times N^{0.08} = (1.68 + 2.94 \times 7.5^{-0.49}) \times 7^{0.08} = 3.24$$

$$\lambda = 0.05$$

$$\gamma_C = S^{0.35} \times \left(1.13 + \frac{1.63}{L_e} \right) = 2.09^{0.35} \times \left(1.13 + \frac{1.63}{7.5} \right) = 1.74$$

$$\mu = \frac{W_e - 3.3}{0.6} \leq 1.0 \Rightarrow \frac{3.4 - 3.3}{0.6} = 0.17$$

$$\gamma_e = 0.00$$

CHBDC clause (5.6.4.3)

$$F_T = \frac{S}{D_T \gamma_c (1 + \mu \lambda + \gamma_e)} \geq 1.05 \frac{1}{N} \text{ for FLS}$$

$$\therefore F_T = \frac{2.09}{3.24 \times 1.74 (1 + (0.17 \times 0.05) + 0.00)} = \underline{0.37}$$

Check :

$$F_T(0.37) \geq 1.05 \frac{1}{N}$$

$$F_T(0.37) \geq 1.05 \times \frac{1}{7}$$

$$\therefore F_T(0.37) \geq 0.15 \quad (\text{OK})$$

iii. *Using CHBDC (CSA 2014a):*

From Table -5.3:

$$D_T = \left(5.15 - \frac{4.00}{\sqrt{L_e}} \right) = \left(5.15 - \frac{4.00}{\sqrt{7.5}} \right) = 3.69$$

$$\lambda = 0.05$$

$$\gamma_e = 0.00$$

$$\mu = \frac{W_e - 3.3}{0.6} \leq 1.0 \Rightarrow \frac{3.4 - 3.3}{0.6} = 0.17$$

From Table -5.4 of CHBDC: for : $n \geq 2$; $L_e \leq 10m$;

$$\gamma_c = 1.0$$

CHBDC clause (5.6.4.3)

$$F_T = \frac{S}{D_T \gamma_c (1 + \mu \lambda + \gamma_e)} \geq 1.05 \frac{1}{N} \text{ for FLS}$$

$$\therefore F_T = \frac{2.09}{3.69 \times 1.0 (1 + (0.17 \times 0.05) + 0.00)} = 0.56$$

Check :

$$F_T(0.56) \geq 1.05 \frac{1}{N}$$

$$F_T(0.56) \geq 1.05 \times \frac{1}{7}$$

$$\therefore F_T(0.56) \geq 0.15 \quad (OK)$$

Comment: CHBDC equation shows overestimates the interior girder support moment by 32% when compared with FEA.

Span Shear Distribution Factors at Exterior and Interior Girder

For span shear at FLS: $L_e = 0.75L_1 = 0.75 \times 15 = 11.25$ m

1) Exterior Girder

i. Using FEA:

$$F_{T_v} \text{ value for exterior girder} = \underline{0.47}$$

ii. Using proposed equation (reference Table 7.6):

$$D_T = (1.76 + 1.77L_e^{-0.83}) \times N^{0.19} = (1.76 + 1.77 \times 11.25^{-0.83}) \times 7^{0.19} = 2.89$$

$$\lambda = 0.0$$

$$\gamma_e = 0.0$$

$$\gamma_c = 3.12S^{-0.89} = 3.12 \times 2.09^{-0.89} = 1.62$$

$$\mu = \frac{W_e - 3.3}{0.6} \leq 1.0 \Rightarrow \frac{3.4 - 3.3}{0.6} = 0.17$$

CHBDC clause (5.6.4.3)

$$F_T = \frac{S}{D_T \gamma_c (1 + \mu \lambda + \gamma_e)} \geq 1.05 \frac{1}{N} \text{ for FLS}$$

$$\therefore F_T = \frac{2.09}{2.89 \times 1.62 (1 + (0.17 \times 0.0) + 0.00)} = \underline{0.45}$$

Check :

$$F_T(0.45) \geq 1.05 \frac{1}{N}$$

$$F_T(0.45) \geq 1.05 \times \frac{1}{7}$$

$$\therefore F_T(0.45) \geq 0.15 \quad (OK)$$

iii. Using CHBDC (CSA 2014a):

From Table – 5.3 of CHBDC :

$$D_T = 3.60$$

$$\lambda = 0.0$$

$$\gamma_e = 0.0$$

From Table – 5.6 :

$$\gamma_C = 1.0 \quad (\because S \geq 2.0)$$

$$\mu = \frac{W_e - 3.3}{0.6} \leq 1.0 \Rightarrow \frac{3.4 - 3.3}{0.6} = 0.17$$

CHBDC clause (5.6.4.3)

$$F_T = \frac{S}{D_T \gamma_C (1 + \mu \lambda + \gamma_e)} \geq 1.05 \frac{1}{N} \quad \text{for FLS}$$

$$\therefore F_T = \frac{2.09}{3.60 \times 1.0 (1 + (0.17 \times 0.0) + 0.0)} = \underline{0.58}$$

Check :

$$F_T(0.58) \geq 1.05 \frac{1}{N}$$

$$F_T(0.58) \geq 1.05 \times \frac{1}{7}$$

$$\therefore F_T(0.58) \geq 0.15 \quad (OK)$$

Comment: CHBDC equation shows overestimates the exterior girder shear by 19% when compared with FEA.

2) Interior girder

i. Using FEA:

$$F_{T_v} \text{ value for interior girder} = \underline{0.51}$$

ii. Using proposed equation (reference Table 7.6):

$$D_T = (1.56 + 1.92L_e^{0.07}) \times N^{0.04} = (1.56 + 1.92 \times 11.25^{0.07}) \times 7^{0.04} = 4.14$$

$$\lambda = 0.0$$

$$\gamma_e = 0.0$$

$$\gamma_c = 0.83S^{0.29} = 0.83 \times 2.09^{0.29} = 1.03$$

$$\mu = \frac{W_e - 3.3}{0.6} \leq 1.0 \Rightarrow \frac{3.4 - 3.3}{0.6} = 0.17$$

CHBDC clause (5.6.4.3)

$$F_T = \frac{S}{D_T \gamma_c (1 + \mu \lambda + \gamma_e)} \geq 1.05 \frac{1}{N} \text{ for FLS}$$

$$\therefore F_T = \frac{2.09}{4.14 \times 1.03 (1 + (0.17 \times 0.0) + 0.0)} = \underline{0.49}$$

Check :

$$F_T (0.49) \geq 1.05 \frac{1}{N}$$

$$F_T (0.49) \geq 1.05 \times \frac{1}{7}$$

$$\therefore F_T (0.49) \geq 0.15 \quad (OK)$$

iii. Using CHBDC (CSA 2014a):

From Table -5.3 of CHBDC :

$$D_T = 3.60$$

$$\lambda = 0.0$$

$$\gamma_e = 0.0$$

From Table -5.6:

$$\gamma_c = 1.0 \quad (\because S \geq 2.0)$$

$$\mu = \frac{W_e - 3.3}{0.6} \leq 1.0 \Rightarrow \frac{3.4 - 3.3}{0.6} = 0.17$$

CHBDC clause (5.6.4.3)

$$F_T = \frac{S}{D_T \gamma_c (1 + \mu \lambda + \gamma_e)} \geq 1.05 \frac{1}{N} \text{ for FLS}$$

$$\therefore F_T = \frac{2.09}{3.60 \times 1.0 (1 + (0.17 \times 0.0) + 0.0)} = \underline{0.58}$$

Check :

$$F_T (0.58) \geq 1.05 \frac{1}{N}$$

$$F_T (0.58) \geq 1.05 \times \frac{1}{7}$$

$$\therefore F_T (0.58) \geq 0.15 \quad (OK)$$

Comment: CHBDC equation shows overestimates the interior girder shear by 12% when compared with FEA.

Support Shear Distribution Factors at Exterior and Interior Girder

For intermediate support shear at FLS: $L_e = 0.25 (L_1 + L_2) = 0.25 (15 + 15) = 7.5 \text{ m}$

1) Exterior Girder

i. Using FEA:

$$F_{T_v} \text{ value for exterior girder} = \underline{0.49}$$

ii. Using proposed equation (reference Table 7.7):

$$D_T = (1.66 - 1.13 L_e^{-1.60}) \times N^{0.18} = (1.66 - 1.13 \times 7.5^{-1.60}) \times 7^{0.18} = 2.29$$

$$\lambda = 0.0$$

$$\gamma_e = 0.0$$

$$\gamma_c = 3.18 S^{-0.67} = 3.18 \times 2.09^{-0.67} = 1.94$$

$$\mu = \frac{W_e - 3.3}{0.6} \leq 1.0 \Rightarrow \frac{3.4 - 3.3}{0.6} = 0.17$$

CHBDC clause (5.6.4.3)

$$F_T = \frac{S}{D_T \gamma_C (1 + \mu \lambda + \gamma_e)} \geq 1.05 \frac{1}{N} \text{ for FLS}$$

$$\therefore F_T = \frac{2.09}{2.29 \times 1.94 (1 + (0.17 \times 0.0) + 0.00)} = \underline{0.47}$$

Check :

$$F_T(0.47) \geq 1.05 \frac{1}{N}$$

$$F_T(0.47) \geq 1.05 \times \frac{1}{7}$$

$$\therefore F_T(0.47) \geq 0.15 \quad (\text{OK})$$

iii. *Using CHBDC (CSA 2014a):*

From Table - 5.3 of CHBDC :

$$D_T = 3.60$$

$$\lambda = 0.0$$

$$\gamma_e = 0.0$$

From Table - 5.6:

$$\gamma_C = 1.0 \quad (\because S \geq 2.0)$$

$$\mu = \frac{W_e - 3.3}{0.6} \leq 1.0 \Rightarrow \frac{3.4 - 3.3}{0.6} = 0.17$$

CHBDC clause (5.6.4.3)

$$F_T = \frac{S}{D_T \gamma_C (1 + \mu \lambda + \gamma_e)} \geq 1.05 \frac{1}{N} \text{ for FLS}$$

$$\therefore F_T = \frac{2.09}{3.60 \times 1.0 (1 + (0.17 \times 0.0) + 0.0)} = \underline{0.58}$$

Check :

$$F_T(0.58) \geq 1.05 \frac{1}{N}$$

$$F_T(0.58) \geq 1.05 \times \frac{1}{7}$$

$$\therefore F_T(0.58) \geq 0.15 \quad (OK)$$

Comment: CHBDC equation shows overestimates the exterior girder support shear by 16% when compared with FEA.

2) Interior girder

i. Using FEA:

$$F_{T_v} \text{ value for interior girder} = \underline{0.47}$$

ii. Using proposed equation (reference Table 7.7):

$$D_T = (23.40 - 0.28L_e^{-0.13}) \times N^{0.06} = (23.40 - 0.28 \times 7.5^{-0.13}) \times 7^{0.06} = 26.06$$

$$\lambda = 0.0$$

$$\gamma_e = 0.0$$

$$\gamma_c = 0.13S^{0.40} = 0.13 \times 2.09^{0.40} = 0.17$$

$$\mu = \frac{W_e - 3.3}{0.6} \leq 1.0 \Rightarrow \frac{3.4 - 3.3}{0.6} = 0.17$$

CHBDC clause (5.6.4.3)

$$F_T = \frac{S}{D_T \gamma_c (1 + \mu \lambda + \gamma_e)} \geq 1.05 \frac{1}{N} \text{ for FLS}$$

$$\therefore F_T = \frac{2.09}{26.06 \times 0.17 (1 + (0.17 \times 0.0) + 0.0)} = \underline{0.47}$$

Check :

$$F_T(0.47) \geq 1.05 \frac{1}{N}$$

$$F_T(0.47) \geq 1.05 \times \frac{1}{7}$$

$$\therefore F_T(0.47) \geq 0.15 \quad (OK)$$

iii. Using CHBDC (CSA 2014a):

From Table –5.3 of CHBDC :

$$D_T = 3.60$$

$$\lambda = 0.0$$

$$\gamma_e = 0.0$$

From Table –5.6:

$$\gamma_C = 1.0 \quad (\because S \geq 2.0)$$

$$\mu = \frac{W_e - 3.3}{0.6} \leq 1.0 \Rightarrow \frac{3.4 - 3.3}{0.6} = 0.17$$

CHBDC clause (5.6.4.3)

$$F_T = \frac{S}{D_T \gamma_C (1 + \mu \lambda + \gamma_e)} \geq 1.05 \frac{1}{N} \quad \text{for FLS}$$

$$\therefore F_T = \frac{2.09}{3.60 \times 1.0 (1 + (0.17 \times 0.0) + 0.0)} = \underline{0.58}$$

Check :

$$F_T (0.58) \geq 1.05 \frac{1}{N}$$

$$F_T (0.58) \geq 1.05 \times \frac{1}{7}$$

$$\therefore F_T (0.58) \geq 0.15 \quad (OK)$$

Comment: CHBDC equation shows overestimates the interior girder support shear by 19% when compared with FEA.

APPENDIX I

Illustrative Example for Moment and Shear Distribution Factors for Skewed Two-span Continuous Slab-on Steel I-girder Bridges at Dead Load

For the evaluation of distribution factors at dead load conditions, the illustrative example of a skewed two-span continuous bridge configuration details are as follows:

Two equal spans having clear span length (L_1 & L_2) = 30 m; Bridge width (W) = 4.5 m; Girder spacing (S) = 1.50 m; Number of girders (N) = 3; Number of lanes (n) = 1; Design lane width (W_e) = 3.5 m, and Skew angle (ψ) = 45°.

Span Moment Distribution Factors at Exterior and Interior Girder

For span moment: $L_e = 0.75L_1 = 0.75 \times 30 = 22.5$ m

Using FEA: F_m value for exterior girder = 1.02

F_m value for interior girder = 0.94

Using proposed equation (reference Table 7.8):

i. Exterior girder: $\varepsilon = 0.02 \times 22.5^{0.66} \times 1.5^{0.13} \times 3^{1.76} \times 1^{-0.08} \times \tan(45) = 1.14$

$$F_m = 1.2 - \frac{2.0}{(1.14 + 10)} = \underline{1.02}$$

ii. Interior girder: $\varepsilon = -1.545 \times 22.5^{-0.60} \times 1.5^{3.2} \times 3^{0.25} \times 1^{-0.64} \times \tan(45) = -1.15$

$$F_m = 1.2 - \frac{2.0}{(-1.15 + 10)} = \underline{0.97}$$

Support Moment Distribution Factors at Exterior and Interior Girder

For intermediate support moment: $L_e = 0.25(L_1 + L_2) = 0.25(30 + 30) = 15.0$ m

Using FEA: F_m value for exterior girder = 0.98

Fm value for interior girder = 0.97

Using proposed equation (reference Table 7.9):

i. Exterior girder: $\varepsilon = -423.66 \times 15.0^{4.72} \times 1.5^{10.0} \times 3^{-20.24} \times 1^{5.0} \times \tan(45) = -1.91$

$$Fm = 1.2 - \frac{2.0}{(-1.91 + 10)} = \underline{0.95}$$

ii. Interior girder: $\varepsilon = -60.51 \times 15.0^{-0.58} \times 1.5^{0.70} \times 3^{-2.02} \times 1^{1.2} \times \tan(45) = -1.82$

$$Fm = 1.2 - \frac{2.0}{(-1.82 + 10)} = \underline{0.96}$$

Span Shear Distribution Factors at Exterior and Interior Girder

For span shear: $L_e = 0.75L_1 = 0.75 \times 30 = 22.5$ m

Using FEA: Fv value for exterior girder = 0.99

Fv value for interior girder = 1.04

Using proposed equation (reference Table 7.8):

i. Exterior girder:

$$\varepsilon = 3.13 \times (22.5)^{-0.10} \times (1.50)^{-3.28} \times (3)^{0.18} \times (1)^{2.10} \times \tan(45) = 0.74$$

$$Fv = 1.2 - \frac{2.0}{(0.74 + 10)} = \underline{1.01}$$

ii. Interior girder:

$$\varepsilon = 0.31 \times (22.5)^{0.96} \times (1.50)^{-0.06} \times (3)^{-0.65} \times (1)^{-1.17} \times \tan(45) = 2.94$$

$$Fv = 1.2 - \frac{2.0}{(2.94 + 10)} = \underline{1.05}$$

For comparison purposes, shear distribution factor using CHBDC (CSA 2014a, clause 5.6.3(b)):

$$\varepsilon = \left(\frac{22.5}{1.50} \right) \times \tan(45) = 15.0$$

$$F_s = 1.2 - \frac{2.0}{(15 + 10)} = \underline{1.12}$$

Comment: CHBDC equation overestimates the exterior and interior girder span shear by 12% and 7%, respectively when compared with FEA.

Support Shear Distribution Factors at Exterior and Interior Girder

For intermediate support shear: $L_e = 0.25 (L_1 + L_2) = 0.25 (30 + 30) = 15.0 \text{ m}$

Using FEA: F_v value for exterior girder = 0.98

F_v value for interior girder = 1.03

Using proposed equation (proposed Table 7.9):

i. Exterior girder:

$$\varepsilon = -0.28 \times (15.0)^{0.34} \times (1.50)^{0.34} \times (3)^{0.12} \times (1)^{-2.77} \times \tan(45) = -0.92$$

$$F_v = 1.2 - \frac{2.0}{(-0.92 + 10)} = \underline{0.98}$$

ii. Interior girder:

$$\varepsilon = 0.31 \times (15.0)^{0.96} \times (1.50)^{-0.06} \times (3)^{-0.65} \times (1)^{-1.17} \times \tan(45) = 2.0$$

$$F_v = 1.2 - \frac{2.0}{(2.0 + 10)} = \underline{1.03}$$

For comparison purposes, shear distribution factor using CHBDC (CSA 2014a, clause 5.6.3(b)):

$$\varepsilon = \left(\frac{15.0}{1.50} \right) \times \tan(45) = 10.0$$

$$F_s = 1.2 - \frac{2.0}{(10 + 10)} = \underline{1.10}$$

Comment: CHBDC equation overestimates the exterior and interior girder shear by 11% and 7%, respectively when compared with FEA.

APPENDIX J

Illustrative Example for Moment and Shear Distribution Factors for Skewed Two-span Continuous Slab-on Steel I-girder Bridges at ULS and SLS

For the evaluation of distribution factors, the illustrative example of a skewed two-span continuous bridge configuration details are as follows:

Two equal spans having clear span length (L_1 & L_2) = 15 m; Bridge width (W) = 14.6 m; Girder spacing (S) = 2.09 m; Number of girders (N) = 7; Number of lanes (n) = 4; Design lane width (W_e) = 3.4 m, and Skew angle (ψ) = 45°.

Span Moment Distribution Factors at Exterior and Interior Girder

For span moment: $L_e = 0.75L_1 = 0.75 \times 15 = 11.25$ m

1) Exterior Girder

i. Using FEA:

LDF value for exterior girder = 0.52

ii. Using proposed equation (reference Table 7.10):

For the same bridge configuration with skew angle = 0°; $F_T = 0.55$

Now for skewed bridge:

$$\varepsilon = -29.0 \times L_e^{-0.04} \times S^{-2.38} \times N^{-1.46} \times n^{1.64} \times \tan \psi$$

$$\varepsilon = -29.0 \times 11.25^{-0.04} \times 2.09^{-2.38} \times 7^{-1.46} \times 4^{1.64} \times \tan(45) = -2.58$$

$$F_S = 1.2 - \frac{2.0}{(\varepsilon + 10)} = 1.2 - \frac{2.0}{(-2.58 + 10)} = 0.93$$

LDF for a skewed bridge = $F_T \times F_S = 0.55 \times 0.93 = \underline{0.51}$

iii. Using CHBDC (CSA 2014a):

For non-skewed bridge using clause 5.6.6.1 of CHBDC (CSA 2014a); $F_T = 0.60$

Now for skewed bridge:

$$\varepsilon = \left(\frac{L_e}{S} \right) \times \tan \psi = \left(\frac{11.25}{2.09} \right) \times \tan(45) = 5.38$$

$$F_S = 1.2 - \frac{2.0}{(\varepsilon + 10)} = 1.2 - \frac{2.0}{(5.38 + 10)} = 1.07$$

$$\text{LDF for a skewed bridge} = F_T \times F_S = 0.60 \times 1.07 = \underline{0.64}$$

2) Interior girder

i. Using FEA:

$$\text{LDF value for interior girder} = \underline{0.50}$$

ii. Using proposed equation (reference Table 7.10):

For the same bridge configuration with skew angle = 0° ; $F_T = 0.54$

Now for skewed bridge:

$$\varepsilon = -30.0 \times L^{-0.48} \times S^{0.35} \times N^{-0.985} \times n^{0.33} \times \tan \psi$$

$$\varepsilon = -30.0 \times 11.25^{-0.48} \times 2.09^{0.35} \times 7^{-0.985} \times 4^{0.33} \times \tan(45) = -2.82$$

$$F_S = 1.2 - \frac{2.0}{(\varepsilon + 10)} = 1.2 - \frac{2.0}{(-2.82 + 10)} = 0.92$$

$$\text{LDF for a skewed bridge} = F_T \times F_S = 0.54 \times 0.92 = \underline{0.50}$$

iii. Using CHBDC (CSA 2014a):

For non-skewed bridge using clause 5.6.6.1 of CHBDC (CSA 2014a); $F_T = 0.63$

Now for skewed bridge:

$$\varepsilon = \left(\frac{L_e}{S} \right) \times \tan \psi = \left(\frac{11.25}{2.09} \right) \times \tan(45) = 5.38$$

$$F_S = 1.2 - \frac{2.0}{(\varepsilon + 10)} = 1.2 - \frac{2.0}{(5.38 + 10)} = 1.07$$

$$\text{LDF for a skewed bridge} = F_T \times F_S = 0.63 \times 1.07 = \underline{0.67}$$

Comment: CHBDC equation overestimates the exterior and interior girder moment by 18% and 25%, respectively when compared with FEA.

Support Moment Distribution Factors at Exterior and Interior Girder

For intermediate support moment: $L_e = 0.25 (L_1 + L_2) = 0.25 (15 + 15) = 7.5 \text{ m}$

1) Exterior Girder

i. Using FEA:

$$\text{LDF value for exterior girder} = \underline{0.51}$$

ii. Using proposed equation (reference Table 7.11):

For the same bridge configuration with skew angle = 0°; $F_T = 0.52$

Now for skewed bridge:

$$\varepsilon = 0.02 \times L_e^{7.13} \times S^{-11.09} \times N^{-2.95} \times n^{0.04} \times \tan \psi$$

$$\varepsilon = 0.02 \times 7.5^{7.13} \times 2.09^{-11.09} \times 7^{-2.95} \times 4^{0.04} \times \tan(45) = 0.03$$

$$F_S = 1.2 - \frac{2.0}{(\varepsilon + 10)} = 1.2 - \frac{2.0}{(0.03 + 10)} = 1.00$$

$$\text{LDF for a skewed bridge} = F_T \times F_S = 0.52 \times 1.00 = \underline{0.52}$$

iii. Using CHBDC (CSA 2014a):

For non-skewed bridge using clause 5.6.6.1 of CHBDC (CSA 2014a); $F_T = 0.61$

Now for skewed bridge:

$$\varepsilon = \left(\frac{L_e}{S} \right) \times \tan \psi = \left(\frac{7.5}{2.09} \right) \times \tan(45) = 3.59$$

$$F_s = 1.2 - \frac{2.0}{(\varepsilon + 10)} = 1.2 - \frac{2.0}{(3.59 + 10)} = 1.05$$

$$\text{LDF for a skewed bridge} = F_T \times F_s = 0.61 \times 1.05 = \underline{0.64}$$

2) Interior girder

i. Using FEA:

$$\text{LDF value for interior girder} = \underline{0.55}$$

ii. Using proposed equation (reference Table 7.11):

For the same bridge configuration with skew angle = 0°; $F_T = 0.54$

Now for skewed bridge:

$$\varepsilon = 0.02 \times L_e^{0.24} \times S^{1.45} \times N^{0.50} \times n^{2.41} \times \tan \psi$$

$$\varepsilon = 0.02 \times 7.5^{0.24} \times 2.09^{1.45} \times 7^{0.50} \times 4^{2.41} \times \tan(45) = 7.06$$

$$F_s = 1.2 - \frac{2.0}{(\varepsilon + 10)} = 1.2 - \frac{2.0}{(7.06 + 10)} = 1.08$$

$$\text{LDF for a skewed bridge} = F_T \times F_s = 0.54 \times 1.08 = \underline{0.58}$$

iii. Using CHBDC (CSA 2014a):

For non-skewed bridge using clause 5.6.6.1 of CHBDC (CSA 2014a); $F_T = 0.67$

Now for skewed bridge:

$$\varepsilon = \left(\frac{L_e}{S} \right) \times \tan \psi = \left(\frac{7.5}{2.09} \right) \times \tan(45) = 3.59$$

$$F_s = 1.2 - \frac{2.0}{(\varepsilon + 10)} = 1.2 - \frac{2.0}{(3.59 + 10)} = 1.05$$

$$\text{LDF for a skewed bridge} = F_T \times F_S = 0.67 \times 1.05 = \underline{0.70}$$

Comment: CHBDC equation overestimates the support exterior and interior girder moment by 20% and 21%, respectively when compared with FEA.

Span Shear Distribution Factors at Exterior and Interior Girder

For span shear: $L_e = 0.75L_1 = 0.75 \times 15 = 11.25 \text{ m}$

1) Exterior Girder

i. Using FEA:

$$\text{LDF value for exterior girder} = \underline{0.57}$$

ii. Using proposed equation (reference Table 7.10):

For the same bridge configuration with skew angle = 0° ; $F_T = 0.51$

Now for skewed bridge:

$$\varepsilon = 100.0 \times L_e^{1.02} \times S^{-7.1} \times N^{-1.2} \times n^{2.05} \times \tan \psi$$

$$\varepsilon = 100.0 \times 11.25^{1.02} \times 2.09^{-7.1} \times 7^{-1.2} \times 4^{2.05} \times \tan(45) = 10.45$$

$$F_S = 1.2 - \frac{2.0}{(\varepsilon + 10)} = 1.2 - \frac{2.0}{(10.45 + 10)} = 1.10$$

$$\text{LDF for a skewed bridge} = F_T \times F_S = 0.51 \times 1.10 = \underline{0.56}$$

iii. Using CHBDC (CSA 2014a):

For non-skewed bridge using clause 5.6.6.1 of CHBDC (CSA 2014a); $F_T = 0.61$

Now for skewed bridge:

$$\varepsilon = \left(\frac{L_e}{S} \right) \times \tan \psi = \left(\frac{11.25}{2.09} \right) \times \tan(45) = 5.38$$

$$F_s = 1.2 - \frac{2.0}{(\varepsilon + 10)} = 1.2 - \frac{2.0}{(5.38 + 10)} = 1.07$$

$$\text{LDF for a skewed bridge} = F_T \times F_s = 0.61 \times 1.07 = \underline{0.65}$$

2) Interior girder

i. Using FEA:

$$\text{LDF value for interior girder} = \underline{0.63}$$

ii. Using proposed equation:

For the same bridge configuration with skew angle = 0°; $F_T = 0.60$

Now for skewed bridge:

$$\varepsilon = 0.11 \times L_e^{3.11} \times S^{-0.14} \times N^{-5.41} \times n^{-2.75} \times \tan \psi$$

$$\varepsilon = 0.11 \times 11.25^{3.11} \times 2.09^{-0.14} \times 7^{-5.41} \times 4^{-2.75} \times \tan(45) = 0.0001$$

$$F_s = 1.2 - \frac{2.0}{(\varepsilon + 10)} = 1.2 - \frac{2.0}{(0.0001 + 10)} = 1.0$$

$$\text{LDF for a skewed bridge} = F_T \times F_s = 0.60 \times 1.0 = \underline{0.60}$$

iii. Using CHBDC (CSA 2014a):

For non-skewed bridge using clause 5.6.6.1 of CHBDC (CSA 2014a); $F_T = 0.61$

Now for skewed bridge:

$$\varepsilon = \left(\frac{L_e}{S} \right) \times \tan \psi = \left(\frac{11.25}{2.09} \right) \times \tan(45) = 5.38$$

$$F_s = 1.2 - \frac{2.0}{(\varepsilon + 10)} = 1.2 - \frac{2.0}{(5.38 + 10)} = 1.07$$

$$\text{LDF for a skewed bridge} = F_T \times F_s = 0.61 \times 1.07 = \underline{0.65}$$

Comment: CHBDC equation overestimates the span exterior and interior girder shear by 12% and 3%, respectively when compared with FEA.

Support Shear Distribution Factors at Exterior and Interior Girder

For intermediate support shear: $L_e = 0.25 (L_1 + L_2) = 0.25 (15 + 15) = 7.5 \text{ m}$

1) Exterior Girder

i. *Using FEA:*

LDF value for exterior girder = 0.58

ii. *Using proposed equation (reference Table 7.11):*

For the same bridge configuration with skew angle = 0°; $F_T = 0.54$

Now for skewed bridge:

$$\begin{aligned}\varepsilon &= 500.0 \times L_e^{2.38} \times S^{-7.45} \times N^{-5.47} \times n^{4.13} \times \tan \psi \\ \varepsilon &= 500.0 \times 7.5^{2.38} \times 2.09^{-7.45} \times 7^{-5.47} \times 4^{4.13} \times \tan(45) = 1.82\end{aligned}$$

$$F_S = 1.2 - \frac{2.0}{(\varepsilon + 10)} = 1.2 - \frac{2.0}{(1.82 + 10)} = 1.03$$

LDF for a skewed bridge = $F_T \times F_S = 0.54 \times 1.03 = \underline{0.56}$

iii. *Using CHBDC (CSA 2014a):*

For non-skewed bridge using clause 5.6.6.1 of CHBDC (CSA 2014a); $F_T = 0.61$

Now for skewed bridge:

$$\varepsilon = \left(\frac{L_e}{S} \right) \times \tan \psi = \left(\frac{7.5}{2.09} \right) \times \tan(45) = 3.59$$

$$F_S = 1.2 - \frac{2.0}{(\varepsilon + 10)} = 1.2 - \frac{2.0}{(3.59 + 10)} = 1.05$$

LDF for a skewed bridge = $F_T \times F_S = 0.61 \times 1.05 = \underline{0.64}$

2) Interior girder

i. Using FEA:

$$\text{LDF value for interior girder} = \underline{0.67}$$

ii. Using proposed equation:

For the same bridge configuration with skew angle = 0°; $F_T = 0.59$

Now for skewed bridge:

$$\begin{aligned}\varepsilon &= 0.02 \times L_e^{7.17} \times S^{-1.67} \times N^{-7.67} \times n^{5.43} \times \tan \psi \\ \varepsilon &= 0.02 \times 7.5^{7.17} \times 2.09^{-1.67} \times 7^{-7.67} \times 4^{5.43} \times \tan(45) = 6.73\end{aligned}$$

$$F_S = 1.2 - \frac{2.0}{(\varepsilon + 10)} = 1.2 - \frac{2.0}{(6.73 + 10)} = 1.08$$

$$\text{LDF for a skewed bridge} = F_T \times F_S = 0.59 \times 1.08 = \underline{0.64}$$

iii. Using CHBDC (CSA 2014a):

For non-skewed bridge using clause 5.6.6.1 of CHBDC (CSA 2014a); $F_T = 0.61$

Now for skewed bridge:

$$\varepsilon = \left(\frac{L_e}{S} \right) \times \tan \psi = \left(\frac{7.5}{2.09} \right) \times \tan(45) = 3.59$$

$$F_S = 1.2 - \frac{2.0}{(\varepsilon + 10)} = 1.2 - \frac{2.0}{(3.59 + 10)} = 1.05$$

$$\text{LDF for a skewed bridge} = F_T \times F_S = 0.61 \times 1.05 = \underline{0.64}$$

Comment: CHBDC equation overestimates the exterior girder support shear by 10%, and underestimates the interior girder support shear by 5%, respectively when compared with FEA.

APPENDIX K

Illustrative Example for Moment and Shear Distribution Factors for Skewed Two-span Continuous Slab-on Steel I-girder Bridges at FLS

For the evaluation of distribution factors, the illustrative example of a skewed two-span continuous bridge configuration details are as follows:

Two equal spans having clear span length (L_1 & L_2) = 15 m; Bridge width (W) = 14.6 m; Girder spacing (S) = 2.09 m; Number of girders (N) = 7; Number of lanes (n) = 4; Design lane width (W_e) = 3.4 m, and Skew angle (ψ) = 45°.

Span Moment Distribution Factors at Exterior and Interior Girder

For span moment: $L_e = 0.75L_1 = 0.75 \times 15 = 11.25$ m

1) Exterior Girder

i. Using FEA:

LDF value for exterior girder = 0.47

ii. Using proposed equation (reference Table 7.12):

For the same bridge configuration with skew angle = 0°; $F_T = 0.48$

Now for skewed bridge:

$$\begin{aligned}\epsilon &= -2.62 \times L_e^{-0.59} \times S^{1.79} \times N^{0.42} \times n^{-0.51} \times \tan \psi \\ \epsilon &= -2.62 \times 11.25^{-0.59} \times 2.09^{1.79} \times 7^{0.42} \times 4^{-0.51} \times \tan(45) = -2.62\end{aligned}$$

$$F_S = 1.2 - \frac{2.0}{(\epsilon + 10)} = 1.2 - \frac{2.0}{(-2.62 + 10)} = 0.93$$

LDF for a skewed bridge = $F_T \times F_S = 0.48 \times 0.93 = \underline{0.45}$

iii. Using CHBDC (CSA 2014a):

For non-skewed bridge using clause 5.6.6.1 of CHBDC (CSA 2014a); $F_T = 0.52$

Now for skewed bridge:

$$\varepsilon = \left(\frac{L_e}{S} \right) \times \tan \psi = \left(\frac{11.25}{2.09} \right) \times \tan(45) = 5.38$$

$$F_S = 1.2 - \frac{2.0}{(\varepsilon + 10)} = 1.2 - \frac{2.0}{(5.38 + 10)} = 1.07$$

$$\text{LDF for a skewed bridge} = F_T \times F_S = 0.52 \times 1.07 = \underline{0.56}$$

2) Interior girder

i. Using FEA:

$$\text{LDF value for interior girder} = \underline{0.37}$$

ii. Using proposed equation (reference Table 7.12):

For the same bridge configuration with skew angle = 0° ; $F_T = 0.36$

Now for skewed bridge:

$$\varepsilon = -0.33 \times L_e^{-0.64} \times S^{7.59} \times N^{-0.27} \times n^{-1.76} \times \tan \psi$$

$$\varepsilon = -0.33 \times 11.25^{-0.64} \times 2.09^{7.59} \times 7^{-0.27} \times 4^{-1.76} \times \tan(45) = -0.97$$

$$F_S = 1.2 - \frac{2.0}{(\varepsilon + 10)} = 1.2 - \frac{2.0}{(-0.97 + 10)} = 0.98$$

$$\text{LDF for a skewed bridge} = F_T \times F_S = 0.36 \times 0.98 = \underline{0.35}$$

iii. Using CHBDC (CSA 2014a):

For non-skewed bridge using clause 5.6.6.1 of CHBDC (CSA 2014a); $F_T = 0.52$

Now for skewed bridge:

$$\varepsilon = \left(\frac{L_e}{S} \right) \times \tan \psi = \left(\frac{11.25}{2.09} \right) \times \tan(45) = 5.38$$

$$F_S = 1.2 - \frac{2.0}{(\varepsilon + 10)} = 1.2 - \frac{2.0}{(5.38 + 10)} = 1.07$$

$$\text{LDF for a skewed bridge} = F_T \times F_S = 0.52 \times 1.07 = \underline{0.56}$$

Comment: CHBDC equation overestimates the exterior and interior girder span moment by 16% and 34%, respectively when compared with FEA.

Support Moment Distribution Factors at Exterior and Interior Girder

For, intermediate support moment: $L_e = 0.25 (L_1 + L_2) = 0.25 (15 + 15) = 7.5 \text{ m}$

1) Exterior Girder

i. Using FEA:

$$\text{LDF value for exterior girder} = \underline{0.46}$$

ii. Using proposed equation (reference Table 7.13):

For the same bridge configuration with skew angle = 0°; $F_T = 0.46$

Now for skewed bridge:

$$\varepsilon = 0.20 \times L_e^{7.71} \times S^{-10.27} \times N^{-9.33} \times n^{5.10} \times \tan \psi$$

$$\varepsilon = 0.20 \times 7.5^{7.71} \times 2.09^{-10.27} \times 7^{-9.33} \times 4^{5.10} \times \tan(45) = 0.009$$

$$F_S = 1.2 - \frac{2.0}{(\varepsilon + 10)} = 1.2 - \frac{2.0}{(0.009 + 10)} = 1.00$$

$$\text{LDF for a skewed bridge} = F_T \times F_S = 0.46 \times 1.00 = \underline{0.46}$$

iii. Using CHBDC (CSA 2014a):

For non-skewed bridge using clause 5.6.6.1 of CHBDC (CSA 2014a); $F_T = 0.52$

Now for skewed bridge:

$$\varepsilon = \left(\frac{L_e}{S} \right) \times \tan \psi = \left(\frac{7.5}{2.09} \right) \times \tan(45) = 3.59$$

$$F_s = 1.2 - \frac{2.0}{(\varepsilon + 10)} = 1.2 - \frac{2.0}{(3.59 + 10)} = 1.05$$

$$\text{LDF for a skewed bridge} = F_T \times F_s = 0.52 \times 1.05 = \underline{0.55}$$

2) Interior girder

i. Using FEA:

$$\text{LDF value for interior girder} = \underline{0.37}$$

ii. Using proposed equation (reference Table 7.13):

For the same bridge configuration with skew angle = 0°; $F_T = 0.37$

Now for skewed bridge:

$$\varepsilon = 95.14 \times L_e^{-0.09} \times S^{-2.93} \times N^{0.85} \times n^{-3.22} \times \tan \psi$$

$$\varepsilon = 95.14 \times 7.5^{-0.09} \times 2.09^{-2.93} \times 7^{0.85} \times 4^{-3.22} \times \tan(45) = 0.55$$

$$F_s = 1.2 - \frac{2.0}{(\varepsilon + 10)} = 1.2 - \frac{2.0}{(0.55 + 10)} = 1.01$$

$$\text{LDF for a skewed bridge} = F_T \times F_s = 0.37 \times 1.01 = \underline{0.37}$$

iii. Using CHBDC (CSA 2014a):

For non-skewed bridge using clause 5.6.6.1 of CHBDC (CSA 2014a); $F_T = 0.56$

Now for skewed bridge:

$$\varepsilon = \left(\frac{L_e}{S} \right) \times \tan \psi = \left(\frac{7.5}{2.09} \right) \times \tan(45) = 3.59$$

$$F_s = 1.2 - \frac{2.0}{(\varepsilon + 10)} = 1.2 - \frac{2.0}{(3.59 + 10)} = 1.05$$

$$\text{LDF for a skewed bridge} = F_T \times F_s = 0.56 \times 1.05 = \underline{0.59}$$

Comment: CHBDC equation overestimates the exterior and interior girder support moment by 16% and 37%, respectively when compared with FEA.

Span Shear Distribution Factors at Exterior and Interior Girder

For span shear: $L_e = 0.75L_1 = 0.75 \times 15 = 11.25$ m

1) Exterior Girder

i. Using FEA:

LDF value for exterior girder = 0.52

ii. Using proposed equation (reference Table 7.12):

For the same bridge configuration with skew angle = 0° ; $F_T = 0.45$

Now for skewed bridge:

$$\varepsilon = 92.13 \times L_e^{1.06} \times S^{-12.0} \times N^{0.57} \times n^{3.72} \times \tan \psi$$

$$\varepsilon = 92.13 \times 11.25^{1.06} \times 2.09^{-12.0} \times 7^{0.57} \times 4^{3.72} \times \tan(45) = 90.83$$

$$F_S = 1.2 - \frac{2.0}{(\varepsilon + 10)} = 1.2 - \frac{2.0}{(90.83 + 10)} = 1.18$$

LDF for a skewed bridge = $F_T \times F_S = 0.45 \times 1.18 = \underline{0.53}$

iii. Using CHBDC (CSA 2014a):

For non-skewed bridge using clause 5.6.6.1 of CHBDC (CSA 2014a); $F_T = 0.58$

Now for skewed bridge:

$$\varepsilon = \left(\frac{L_e}{S} \right) \times \tan \psi = \left(\frac{11.25}{2.09} \right) \times \tan(45) = 5.38$$

$$F_S = 1.2 - \frac{2.0}{(\varepsilon + 10)} = 1.2 - \frac{2.0}{(5.38 + 10)} = 1.07$$

LDF for a skewed bridge = $F_T \times F_S = 0.58 \times 1.07 = \underline{0.62}$

2) Interior girder

i. Using FEA:

LDF value for interior girder = 0.53

ii. Using proposed equation:

For the same bridge configuration with skew angle = 0°; $F_T = 0.49$

Now for skewed bridge:

$$\begin{aligned}\varepsilon &= 8.39 \times L_e^{0.23} \times S^{-1.19} \times N^{-1.85} \times n^{2.07} \times \tan \psi \\ \varepsilon &= 8.39 \times 11.25^{0.23} \times 2.09^{-1.19} \times 7^{-1.85} \times 4^{2.07} \times \tan(45) = 2.93\end{aligned}$$

$$F_S = 1.2 - \frac{2.0}{(\varepsilon + 10)} = 1.2 - \frac{2.0}{(2.93 + 10)} = 1.05$$

$$\text{LDF for a skewed bridge} = F_T \times F_S = 0.49 \times 1.05 = \underline{0.51}$$

iii. Using CHBDC (CSA 2014a):

For non-skewed bridge using clause 5.6.6.1 of CHBDC (CSA 2014a); $F_T = 0.58$

Now for skewed bridge:

$$\begin{aligned}\varepsilon &= \left(\frac{L_e}{S} \right) \times \tan \psi = \left(\frac{11.25}{2.09} \right) \times \tan(45) = 5.38 \\ F_S &= 1.2 - \frac{2.0}{(\varepsilon + 10)} = 1.2 - \frac{2.0}{(5.38 + 10)} = 1.07\end{aligned}$$

$$\text{LDF for a skewed bridge} = F_T \times F_S = 0.58 \times 1.07 = \underline{0.62}$$

Comment: CHBDC equation overestimates the exterior and interior girder shear by 16% and 15%, respectively when compared with FEA.

Support Shear Distribution Factors at Exterior and Interior Girder

For intermediate support shear: $L_e = 0.25 (L_1 + L_2) = 0.25 (15 + 15) = 7.5 \text{ m}$

1) Exterior Girder

i. Using FEA:

$$\text{LDF value for exterior girder} = \underline{0.51}$$

ii. Using proposed equation (reference Table 7.13):

For the same bridge configuration with skew angle = 0°; $F_T = 0.47$

Now for skewed bridge:

$$\begin{aligned}\varepsilon &= 106.95 \times L_e^{2.54} \times S^{-6.92} \times N^{-3.18} \times n^{2.74} \times \tan \psi \\ \varepsilon &= 106.95 \times 7.5^{2.54} \times 2.09^{-6.92} \times 7^{-3.18} \times 4^{2.74} \times \tan(45) = 9.97\end{aligned}$$

$$F_S = 1.2 - \frac{2.0}{(\varepsilon + 10)} = 1.2 - \frac{2.0}{(9.97 + 10)} = 1.10$$

$$\text{LDF for a skewed bridge} = F_T \times F_S = 0.47 \times 1.10 = \underline{0.52}$$

iii. Using CHBDC (CSA 2014a):

For non-skewed bridge using clause 5.6.6.1 of CHBDC (CSA 2014a); $F_T = 0.58$

Now for skewed bridge:

$$\varepsilon = \left(\frac{L_e}{S} \right) \times \tan \psi = \left(\frac{7.5}{2.09} \right) \times \tan(45) = 3.59$$

$$F_S = 1.2 - \frac{2.0}{(\varepsilon + 10)} = 1.2 - \frac{2.0}{(3.59 + 10)} = 1.05$$

$$\text{LDF for a skewed bridge} = F_T \times F_S = 0.58 \times 1.05 = \underline{0.61}$$

2) Interior girder

i. Using FEA:

$$\text{LDF value for interior girder} = \underline{0.50}$$

ii. Using proposed equation (reference Table 7.13):

For the same bridge configuration with skew angle = 0°; $F_T = 0.46$

Now for skewed bridge:

$$\varepsilon = 0.20 \times L_e^{2.36} \times S^{-0.73} \times N^{-1.99} \times n^{1.60} \times \tan \psi$$

$$\varepsilon = 0.20 \times 7.5^{2.36} \times 2.09^{-0.73} \times 7^{-1.99} \times 4^{1.60} \times \tan(45) = 2.60$$

$$F_s = 1.2 - \frac{2.0}{(\varepsilon + 10)} = 1.2 - \frac{2.0}{(2.60 + 10)} = 1.04$$

$$\text{LDF for a skewed bridge} = F_T \times F_s = 0.46 \times 1.04 = \underline{0.48}$$

iii. Using CHBDC (CSA 2014a):

For non-skewed bridge using clause 5.6.6.1 of CHBDC (CSA 2014a); $F_T = 0.58$

Now for skewed bridge:

$$\varepsilon = \left(\frac{L_e}{S} \right) \times \tan \psi = \left(\frac{7.5}{2.09} \right) \times \tan(45) = 3.59$$

$$F_s = 1.2 - \frac{2.0}{(\varepsilon + 10)} = 1.2 - \frac{2.0}{(3.59 + 10)} = 1.05$$

$$\text{LDF for a skewed bridge} = F_T \times F_s = 0.58 \times 1.05 = \underline{0.61}$$

Comment: CHBDC equation overestimates the exterior and interior girder shear by 16% and 18%, respectively when compared with FEA.

VITA AUCTORIS

Name: Muhammad Kashif Razzaq

Place of Birth: Lahore, Pakistan

Education: University of Engineering and Technology
Lahore, Pakistan 1995-2000
B.Sc. Civil Engineering

Saitama University
Saitama, Japan 2008-2010
MS Civil Engineering

University of Windsor
Windsor, Canada 2012-2017
Ph.D. Civil Engineering